Open File Envelope No. 8426

COOPER BASIN

SOURCE ROCK STUDIES

REPORTS AND DATA

Submitted by

Delhi Petroleum Pty Ltd, Santos Ltd, the University of Adelaide, CSIRO, Amdel Ltd and Shell Development (Australia) Pty Ltd
1995

© 4/6/91

This report was supplied as part of the requirement to hold a mineral or petroleum exploration tenement in the State of South Australia. PIRSA accepts no responsibility for statements made, or conclusions drawn, in the report or for the quality of text or drawings. This report is subject to copyright. Apart from fair dealing for the purposes of study, research, criticism or review as permitted under the Copyright Act, no part may be reproduced without written permission of the Chief Executive of Primary Industries and Resources South Australia, GPO Box 1671, Adelaide, SA 5001.

Enquiries: Customer Services
Ground Floor
101 Grenfell Street, Adelaide 5000

Telephone: (08) 8463 3000
Facsimile: (08) 8204 1880

PRIMARY INDUSTRIES AND RESOURCES SA

NUMBER 8426

COOPER BASIN

SOURCE ROCK STUDIES

REPORTS

Submitted by

Amdel Ltd, CSIRO, University of Adelaide and Shell Development (Aust.) Pty Ltd
1987

© 4/6/91

ENVELOPE 8426

TENEMENT: Not applicable

TENEMENT HOLDER: Not applicable

CONTENTS OF VOLUME ONE

		MESA NO.	
REPORT:	**McKirdy, D.M. and Cox, R.E., 1987.** Role of CO_2 in origin of oil and condensate, Cooper Basin, South Australia (Amdel Ltd consultant's report no. F 6846/87 [Part 1] for SADME, 30/6/87).	**8426 R 1** Pgs 3-19	
APPENDIX 1:	Analytical methods.	Pgs 20-21	
REPORTS:	**Smyth, M., 1979.** Results of maceral analyses of the organic matter in selected drill cuttings samples, from sediments below the Patchawarra Formation, in Mudrangie 1, Moorari 2 and Coonatie 1 (CSIRO, Institute of Earth Resources, Fuel Geoscience Unit, report for SADME, 19/2/79). [Note: These reports have been microfilmed separately as part of the respective well test report Envelopes].	Not Scanned	
	Saxby, J.D. and Raphael, N.M., 1979. Crude oils from Gidgealpa in the Cooper Basin, South Australia (CSIRO, Institute of Earth Resources, Fuel Geoscience Unit, Restricted Investigation Report no. 1022 R for Delhi Petroleum Pty Ltd, April 1979).	**8426 R 2** Pgs 22-27	
	Smyth, M., 1979. Cooper Basin, Patchawarra Trough. Petrology of coals and dispersed organic matter from the Tirrawarra, Merrimelia and un-named formations (CSIRO, Minerals Research Laboratories, Fuel Geoscience Unit, Restricted Investigation Report no. 1026 R for the joint SADME / CSIRO / Delhi Petroleum Pty Ltd research program on hydrocarbon generation in the Cooper Basin, May 1979).	**8426 R 3** Pgs 28-56	
	Lonergan, T., 1979. Aspects of coal type and rank variation, and their bearing on hydrocarbon potential in seven wells from the southern Cooper Basin (University of Adelaide, Department of Geology and Geophysics, Honours thesis, November 1979). [Note: Pg. 105 now plan 8426-1].	**8426 R 4** Pgs 57-128	
PLAN			
Fig. 10	Isorank profile of the seven wells.	8426-1	*A2*
APPENDIX 1:	Sampling.	Pgs 129-131	
APPENDIX 2:	Analytical techniques.	Pgs132-150	
APPENDIX 3:	Data.	Pgs 151-160	
REPORT:	**Higgs, M.D., 1984.** Source rock investigation of samples from wells Brolga 1, Dullingari 1, Dullingari North 1, Murteree 1, Tinga Tingana 1 and Toolachee 1 (Shell Exploratorie en Produktie Laboratorium, Rijswijk, The Netherlands, November 1984).	**8426 R 5** Pgs 161-201	

CONTENTS OF VOLUME TWO

REPORTS:

Shibaoka, M., 1972. Hydrocarbons in coals from Moorari and Tirrawarra, Cooper Basin, South Australia (CSIRO, Division of Mineralogy, Minerals Research Laboratories, Restricted Investigation Report no. 460 R for Delhi International Oil Corp., 14/2/72). **8426 R 6** [6 pages]

Gould, K.W. and Shibaoka, M., 1972. Gas chromatographic analysis of Tirrawarra oil and chemical analysis of Tirrawarra and Moorari coals (CSIRO, Division of Mineralogy, Minerals Research Laboratories, Restricted Investigation Report no. 507 R for Delhi International Oil Corp., October 1972). **8426 R 7** [8 pages]

Bennett, A.J.R. and Shibaoka, M., 1973. Reflectance of coals from Gidgealpa 3 and Tinga Tingana 1 wells, Cooper Basin, South Australia (CSIRO, Division of Mineralogy, Minerals Research Laboratories, Restricted Investigation Report no. 577 R for Delhi International Oil Corp., December 1973). **8426 R 8** [5 pages]

Smyth, M., 1974. Petrographic composition of coals from Gidgealpa 3, Innamincka 1 and Tinga Tingana 1 wells, Cooper Basin, South Australia (CSIRO, Division of Mineralogy, Minerals Research Laboratories, Restricted Investigation Report no. 620 R for Delhi International Oil Corp., May 1974). **8426 R 9** [8 pages]

Rigby, D. and Smith, J.W., 1980. Carbon dioxide in natural gas from the Cooper Basin (CSIRO, Institute of Earth Resources, Fuel Geoscience Unit, Restricted Investigation Report no. 1131 R for Delhi Petroleum Pty Ltd, May 1980). **8426 R 10** [10 pages]

Philp, R.P. and Gilbert, T., 1983. Geochemical prospecting for natural gas in the Cooper Basin, South Australia, 1980 (CSIRO, Institute of Energy and Earth Resources, Div. of Fossil Fuels, Restricted Investigation Report no. 1377 R for SADME, January 1983). **8426 R 11** [20 pages]

END OF CONTENTS

amdel
technology and enterprise
Amdel Limited - Inc. in S.A.

Amdel
31 Flemington Street,
Frewville, S.A. 5063

Telephone: (08) 372 2700

Address all correspondence to:
P.O. Box 114,
Eastwood, S.A. 5063

Telex: AA82520
Facsimile: (08) 79 6623

OPEN FILE
4/6/91
Date Released
Initials

30 June 1987

F 1/1/291
F 6846/87 - Part 1

The Director-General
South Australian Department of Mines and Energy
PO Box 151
EASTWOOD SA 5063

Attention: Dr D.I. Gravestock

REPORT F 6846/87

YOUR REFERENCE: SR 28/1/57/5 DG:DG

TITLE: Role of CO_2 in origin of oil and condensate, Cooper Basin, S.A.

MATERIAL: Condensates

LOCALITIES: BIG LAKE-2&3, BROLGA-1, BURKE-1, FLY LAKE-1, KANOWANA-1, MOOMBA-9&36

IDENTIFICATION: As in Table 1 of report

DATE RECEIVED: 25 June 1987

WORK REQUIRED: Thin layer chromatography. GC-MS analysis of di- and triaromatic hydrocarbons. Determination of methylphenanthrene index (MPI) and calculated vitrinite reflectance.

Investigation and Report by: Dr David M. McKirdy and
Dr Robert E. Cox

Manager-Petroleum Services Section: Dr Brian G. Steveson

Brian G Steveson

for Dr William G. Spencer
General Manager
Applied Sciences Group

cap

8426 R1

1. INTRODUCTION

A heavy (15° API), low sulphur, aromatic crude oil is associated with CO_2 production from the Late Cretaceous Waarre Sandstone in Caroline-1, Otway Basin (McKirdy, 1986; McKirdy and Chivas, 1987). Although itself not of economic significance, this unusual crude has important implications for the origin of petroleum in other non-marine basins where oil and condensate occur in association with CO_2-rich gas.

The aromatic composition of the Caroline-1 crude is similar to that of solvent-extracts of coals and clastic sediments containing poor quality terrestrial organic matter. Highly aromatic condensates are produced from the Moomba and Big Lake gas fields in the Nappamerri Trough, Cooper Basin (Fig. 1). In marked contrast, condensates produced with CO_2-rich gas from the Patchawarra Trough are more paraffinic in composition (Fig. 2).

Problems addressed by the present study include the following:

1. Did the Caroline-1 oil originate by CO_2 extraction of low-grade carbonaceous matter within the reservoir (Waarre Sandstone), or instead from the underlying fine-grained clastics of the Eumeralla Formation (a more conventional source rock unit)?

2. Is the difference in composition of the Nappamerri Trough and Patchawarra Trough condensates (Figs. 1 and 2) a function of source quality or maturity (or both)?

3. What role does CO_2-rich gas (CO_2 >20% mole vol.) play in the origin and migration of oil and condensate in the Patchawarra Trough?

This interim report presents aromatic maturity data on a suite of eight condensates, five from the Nappamerri Trough (Fig. 1) and three from the Patchawarra Trough (Fig. 2).

2. ANALYTICAL METHODS

Details of the analytical procedure are given in Appendix 1.

3. RESULTS

Analytical data are summarised and presented herein as follows:

	Table	Figure
C_{12+} aromatic/saturates ratio of condensate and CO_2 content of associated gas	-	1,2
GC-MS of aromatics	2	3A-3H
Calculated vitrinite reflectance	2	-

4. REFERENCES

BOREHAM, C.J. and POWELL, T.G., 1987. Recalibration of the methylphenanthrene index : application to maturity measurements on oils and Proterozoic rocks. Unpublished manuscript.

McKIRDY, D.M., 1982. Petroleum geochemistry and source-rock potential of the Arrowie, Pedirka, Cooper and Eromanga Basins, central Australia. Part 4 : Cooper Basin and superjacent Eromanga Basin. *Report for Delhi Petroleum Pty Limited* (unpubl.).

McKIRDY, D.M., 1986. Geochemistry of oil from Caroline-1, Otway Basin, South Australia. *AMDEL Report F6433/86 for South Australian Department of Mines & Energy* (unpubl.).

McKIRDY, D.M. and CHIVAS, A.R., 1987. Nonbiodegraded aromatic crude oil of land plant origin associated with volcanic CO_2. *13th International Meeting on Organic Geochemistry, Venice, Sept. 21-25, 1987, Abstract.*

RADKE, M. and WELTE, D.H., 1983. The methylphenanthrene index (MPI) : a maturity parameter based on aromatic hydrocarbons. In : *Advances in Organic Geochemistry 1981* (eds. BJORØY, M. *et al.*), Wiley, Chichester, pp. 504-512.

RADKE, M., LEYTHAEUSER, D. and TEICHMULLER, M., 1984. Relationship between rank and composition of aromatic hydrocarbons for coals of different origins. *Org. Geochem.*, 6, 423-430.

TABLE 1: COOPER BASIN CONDENSATES* SELECTED FOR GC-MS ANALYSIS OF THEIR AROMATIC HYDROCARBONS

Well	Depth m	Reservoir Formation
Big Lake-2	2274.1-2341.8	Toolachee
Big Lake-3	2342.4-2365.8	Toolachee
Brolga-1	2769.1-2798.1	Patchawarra
Burke-1	2168.7-2199.1	Toolachee
Fly Lake-1	2618.5-2795.0	Patchawarra
Kanowana-1	2834.6-2850.2	Patchawarra
Moomba-9	2461.0-2468.0	Daralingie
Moomba-36	2304.6-2422.9	Toolachee-Daralingie

*Analytical data plotted in Figures 1 and 2 are taken from McKirdy (1982).

TABLE 2: CONDENSATE MATURITY BASED ON AROMATIC HYDROCARBON DISTRIBUTIONS*, COOPER BASIN, S.A.

Well	Formation	MPI	MPR	DNR	VR_{calc} (a)	(b)	(c)	(d)	(e) ✓
Big Lake-2	Toolachee	1.47	2.55	nd	1.28	1.42	1.34	nd	1.25
Big Lake-3	Toolachee	1.42	2.24	nd	1.25	1.45	1.29	nd	1.22
Brolga-1	Patchawarra	1.22	1.80	nd	1.13	1.57	1.19	nd	1.07
Burke-1	Toolachee	1.05	1.43	nd	1.03	1.67	1.09	nd	0.96
Fly Lake-1	Patchawarra	1.14	1.42	nd	1.09	2.03	1.09	nd	1.02
Kanowana-1	Patchawarra	1.08	1.59	nd	1.05	1.65	1.14	nd	0.97
Moomba-9	Daralingie	1.80	3.21	nd	1.48	1.22	1.44	nd	1.48
Moomba-36	Toolachee-Daralingie	1.66	3.03	nd	1.39	1.30	1.42	nd	1.38

*See key (next page) for derivation of listed parameters

✓ = preferred value

nd = not determined

KEY TO AROMATIC MATURITY INDICATORS

Methylphenanthrene index (MPI), methylphenanthrene ratio (MPR), dimethylnaphthalene ratio (DNR) and calculated vitrinite reflectance (VR_{calc}) are derived from the following equations (after Radke and Welte, 1983; Radke *et al.*, 1984):

$$MPI = \frac{1.5\ (2\text{-MP} + 3\text{-MP})}{P + 1\text{-MP} + 9\text{-MP}}$$

$$VR_{calc}\ (a) = 0.6\ MPI + 0.4\ (\text{for } VR < 1.35\%)$$

$$VR_{calc}\ (b) = -0.6\ MPI + 2.3\ (\text{for } VR > 1.35\%)$$

$$MPR = \frac{2\text{-MP}}{1\text{-MP}}$$

$$VR_{calc}\ (c) = 0.99 \log_{10} MPR + 0.94\ (\text{for } VR = 0.5\text{-}1.7\%)$$

$$DNR = \frac{2,6\text{-DMN} + 2,7\text{-DMN}}{1,5\text{-DMN}}$$

$$VR_{calc}\ (d) = 0.046\ DNR + 0.89\ (\text{for } VR = 0.9\text{-}1.5\%)$$

Where P = phenanthrene
1-MP = 1-methylphenanthrene
2-MP = 2-methylphenanthrene
3-MP = 3-methylphenanthrene
9-MP = 9-methylphenanthrene
1,5-DMN = 1,5-dimethylnaphthalene
2,6-DMN = 2,6-dimethylnaphthalene
2,7-DMN = 2,7-dimethylnaphthalene

Peak areas measured from m/z 156 (dimethylnaphthalene), m/z 169+170 (trimethylnaphthalene), m/z 178 (phenanthrene) and m/z 191+192 (methylphenanthrene) mass fragmentograms of diaromatic and triaromatic hydrocarbon fraction isolated by thin layer chromatography.

Recalibration of the methylphenanthrene index using data from a suite of Australian coals has given rise to another equation for calculated vitrinite reflectance (after Boreham and Powell, 1987):

$$VR_{calc}\ (e) = 0.7\ MPI + 0.22\ (\text{for } VR < 1.7\%)$$

FIGURE 1

RELATIONSHIP BETWEEN CO2 CONTENT OF GAS AND COMPOSITION OF ASSOCIATED LIQUIDS, NAPPAMERRI TROUGH, COOPER BASIN

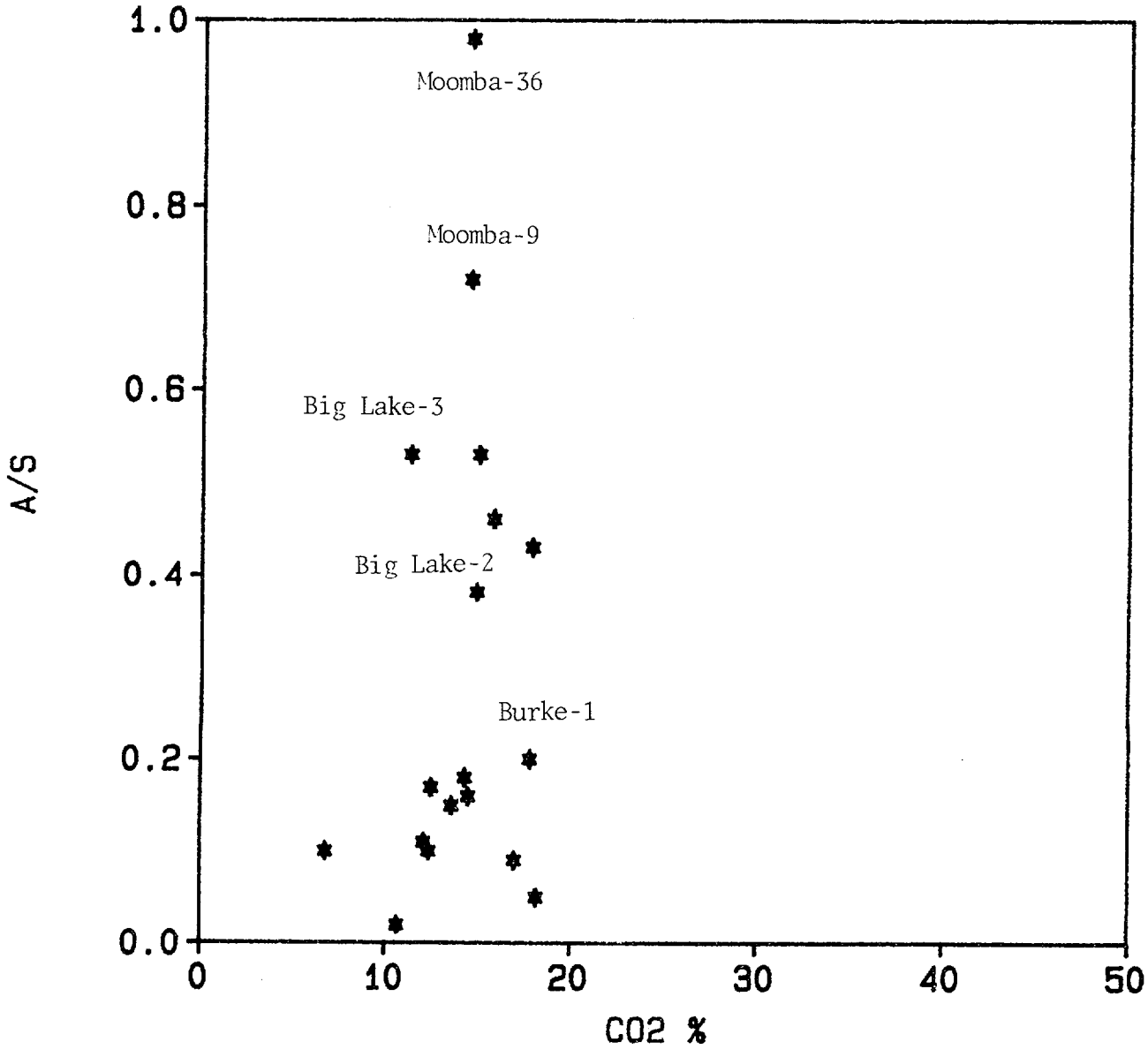

FIGURE 2

RELATIONSHIP BETWEEN CO2 CONTENT OF GAS AND COMPOSITION OF ASSOCIATED LIQUIDS, PATCHAWARRA TROUGH, COOPER BASIN

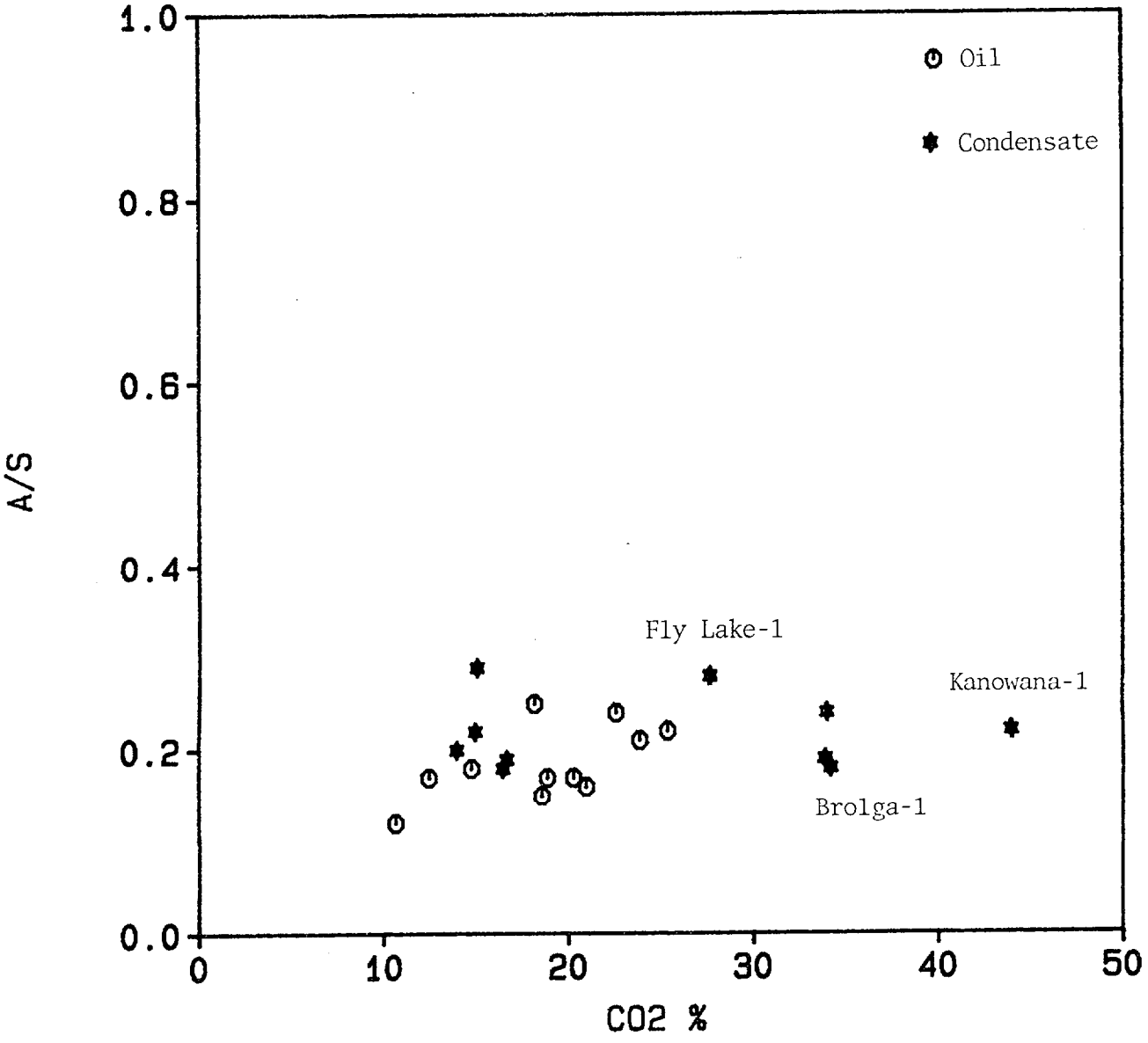

FIGURE 3

MASS FRAGMENTOGRAMS OF TRIAROMATIC HYDROCARBONS IN PERMIAN CONDENSATES FROM THE COOPER BASIN, S.A.

m/z 178 phenanthrene

m/z 191+192 methylphenanthrenes

A.	Big Lake-2	(Toolachee)
B.	Big Lake-3	(Toolachee)
C.	Brolga-1	(Patchawarra)
D.	Burke-1	(Toolachee)
E.	Fly Lake-1	(Patchawarra)
F.	Kanowana-1	(Patchawarra)
G.	Moomba-9	(Daralingie)
H.	Moomba-36	(Toolachee-Daralingie)

FIGURE 3A

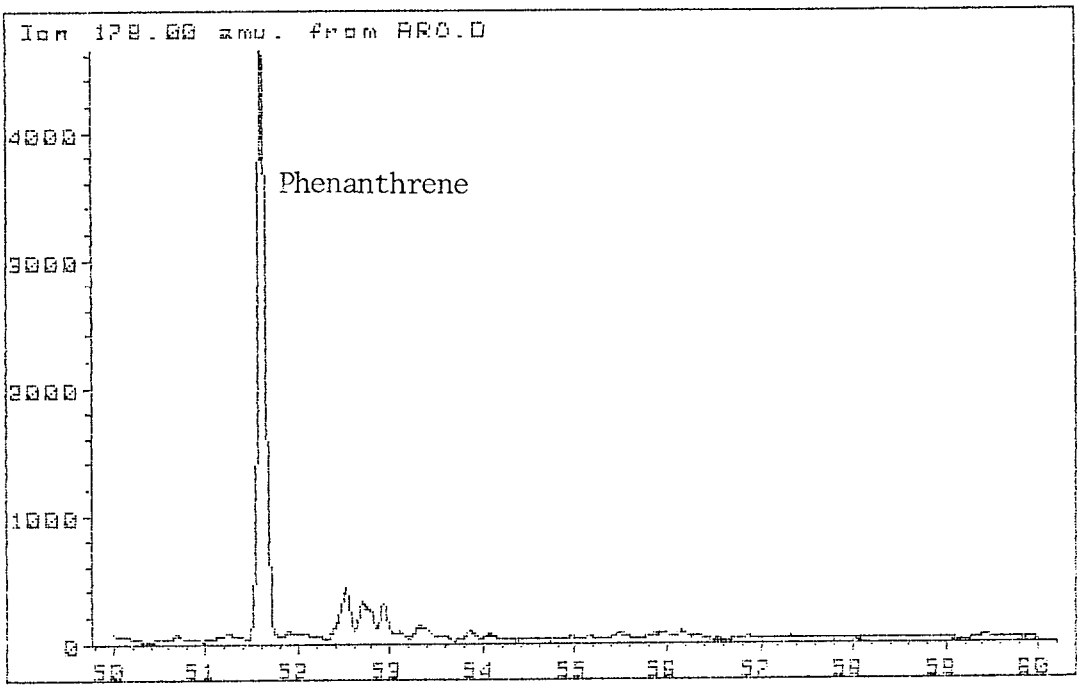

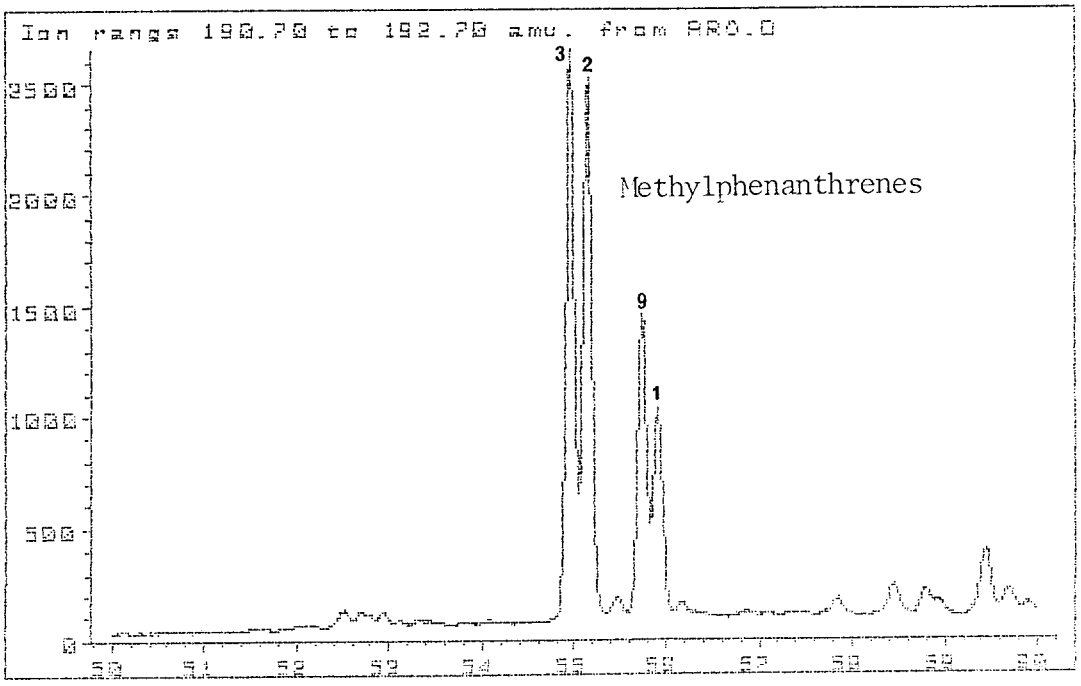

amdel

FIGURE 3B

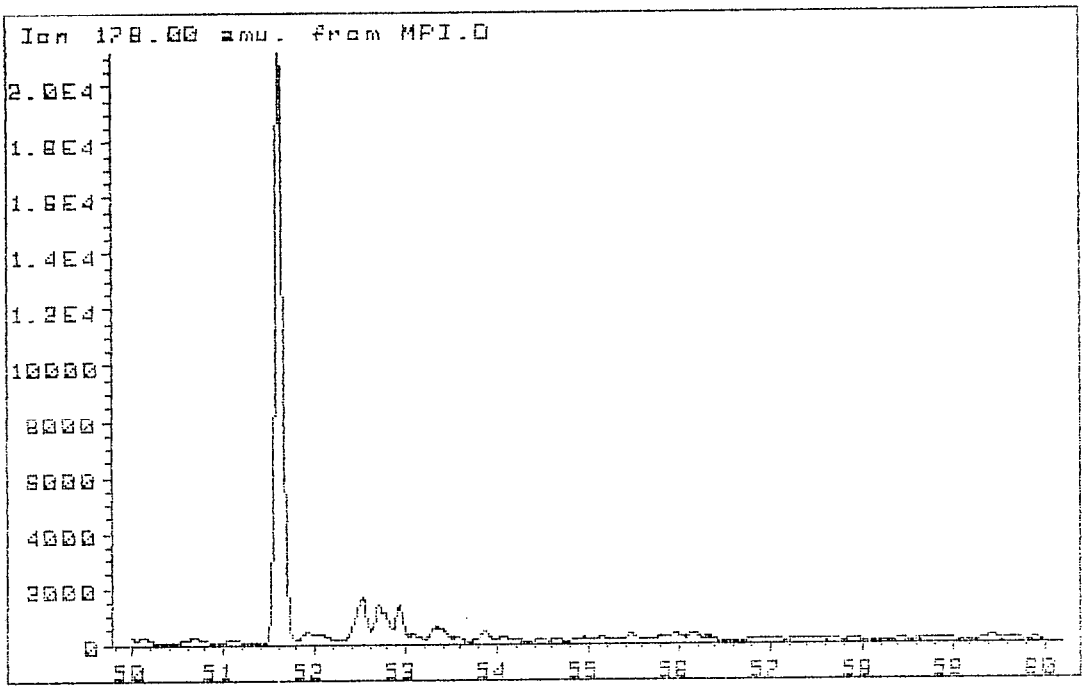
Ion 178.00 amu. from MPI.D
2.0E4
1.8E4
1.6E4
1.4E4
1.2E4
10000
8000
6000
4000
2000
0
50
51
52
53
54
55
56
57
58
59
60

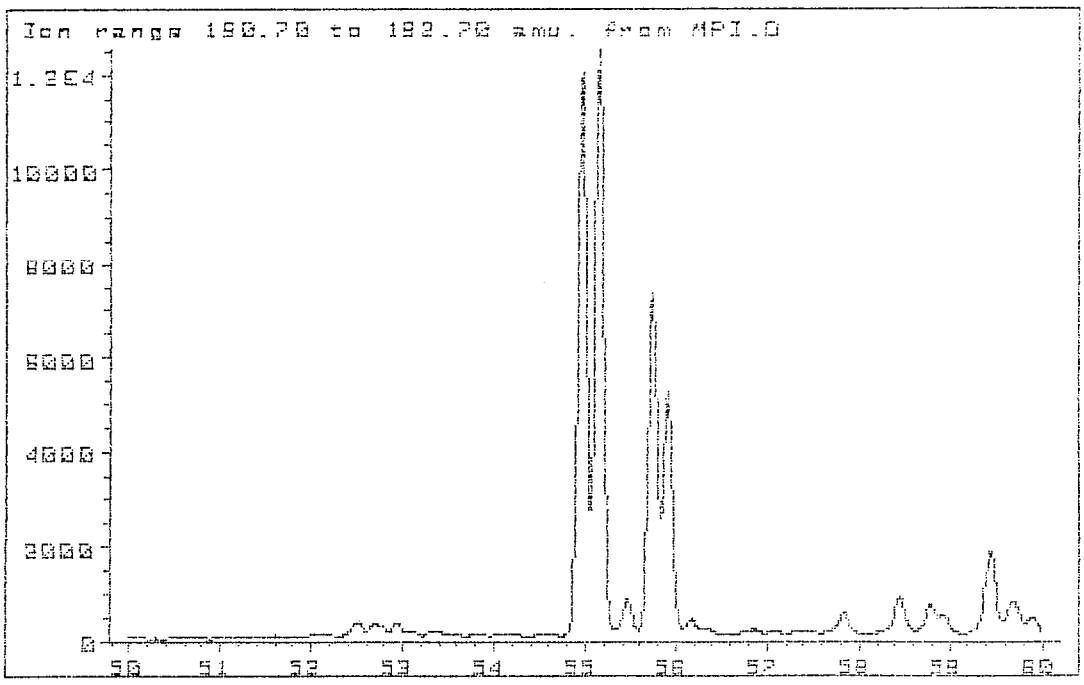
Ion range 190.20 to 192.20 amu. from MPI.D
1.2E4
10000
8000
6000
4000
2000
0
50
51
52
53
54
55
56
57
58
59
60

FIGURE 3C

0014

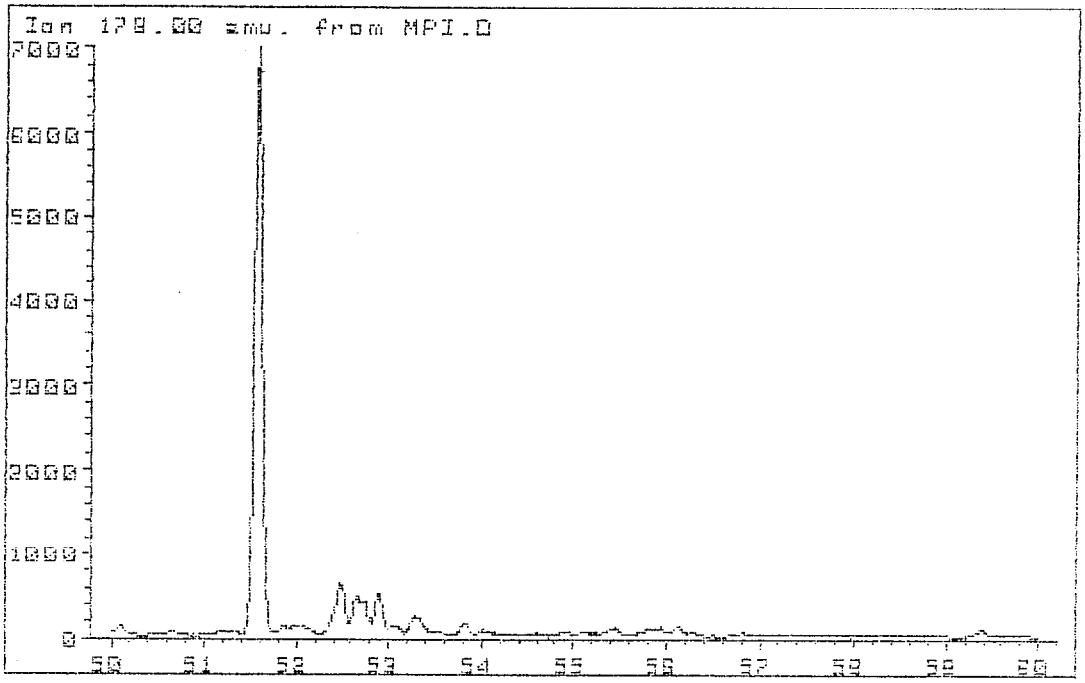

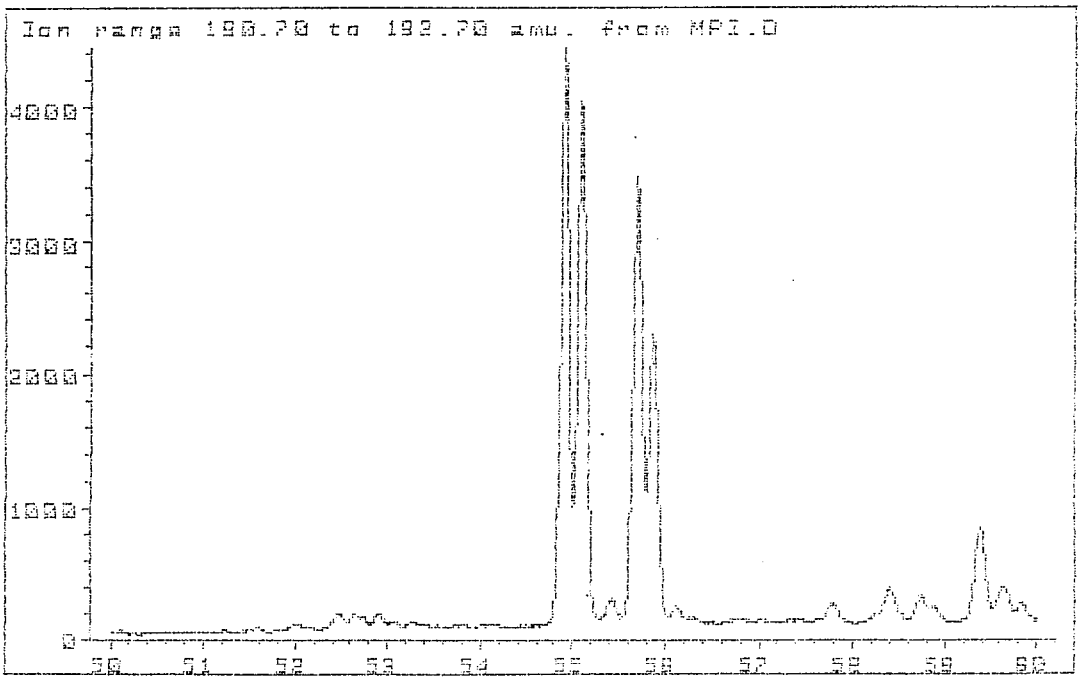

FIGURE 3D

0015

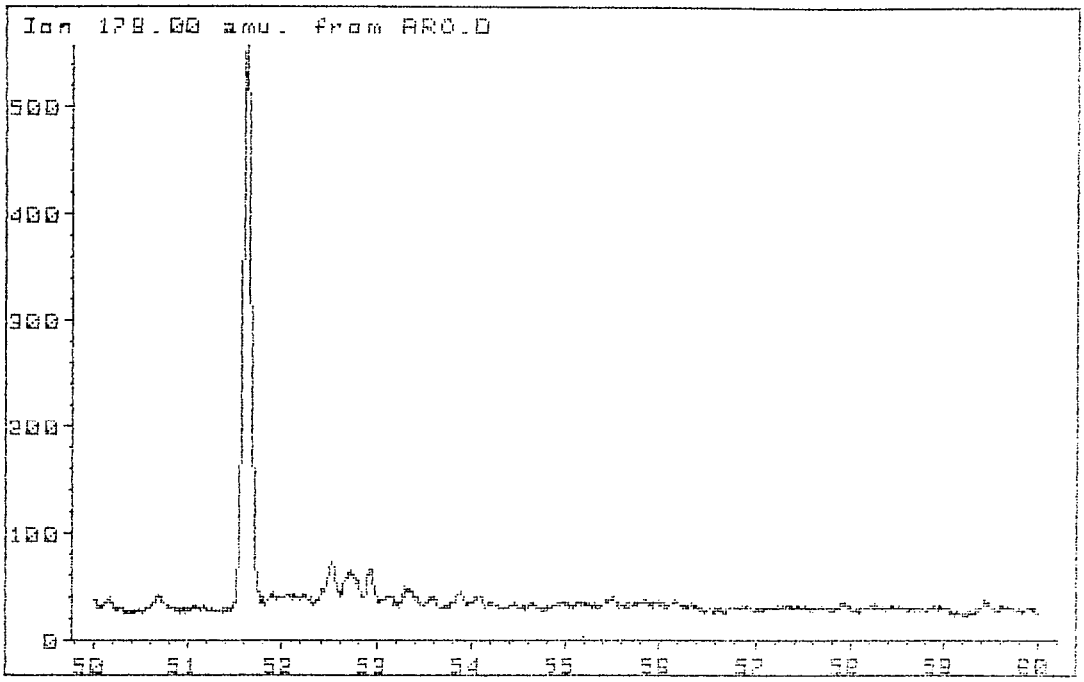

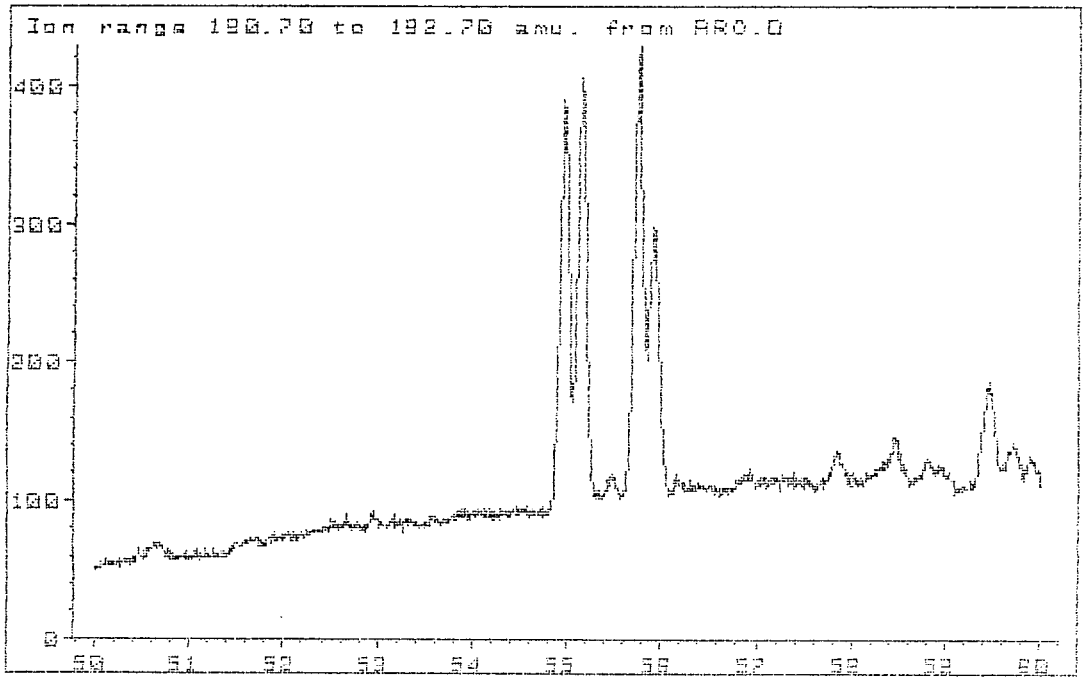

amdel

FIGURE 3E

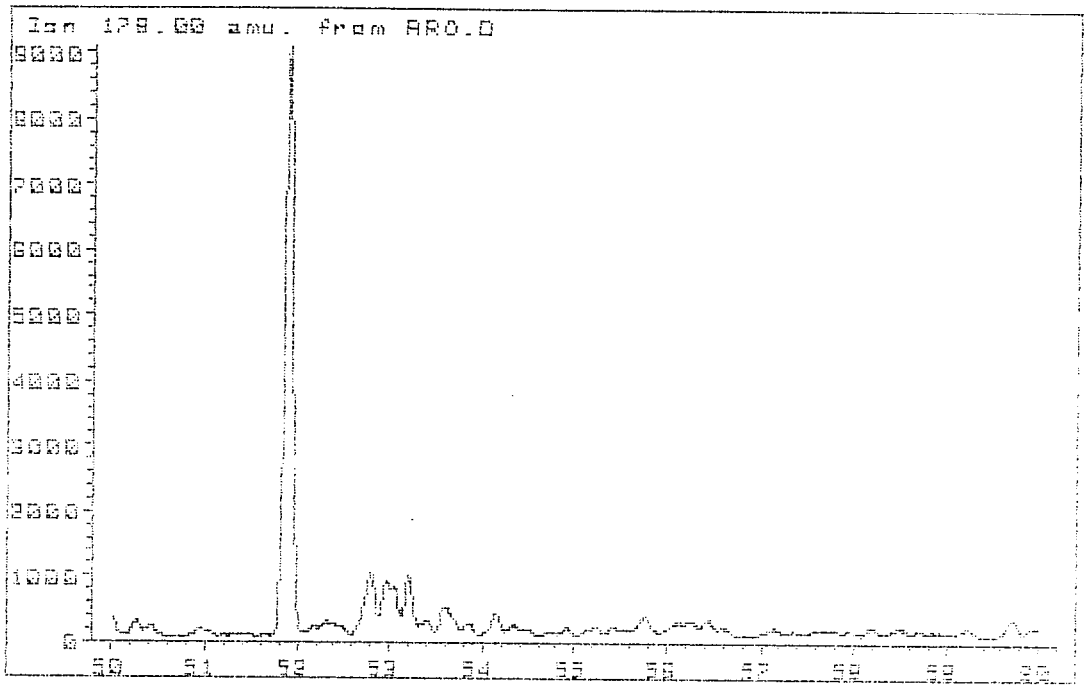

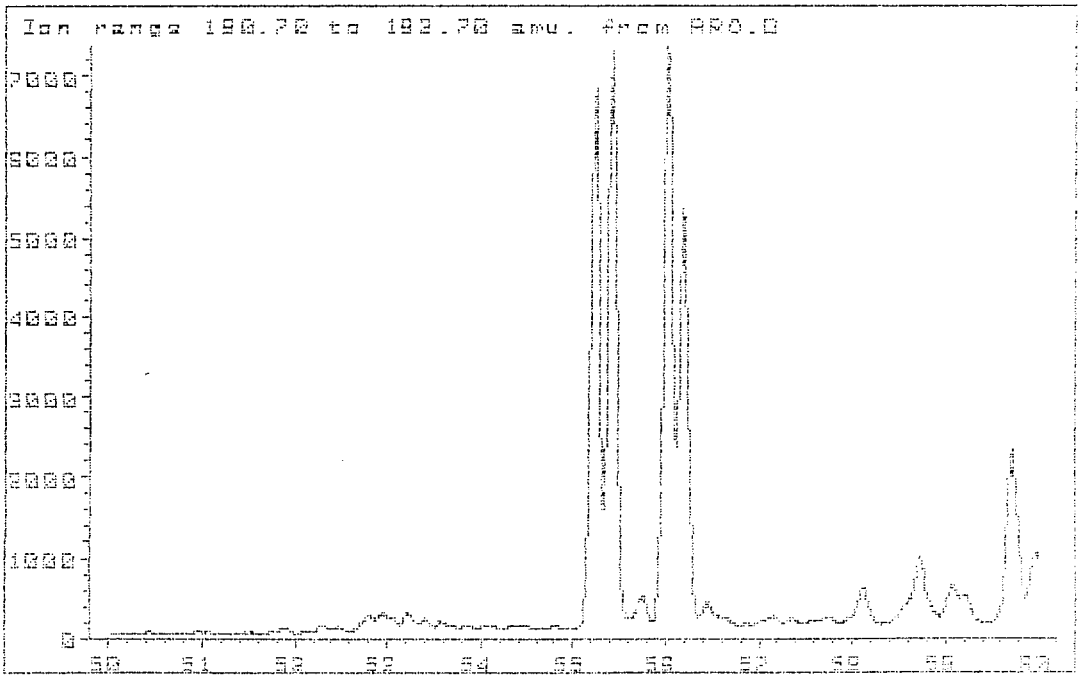

amdel

FIGURE 3F

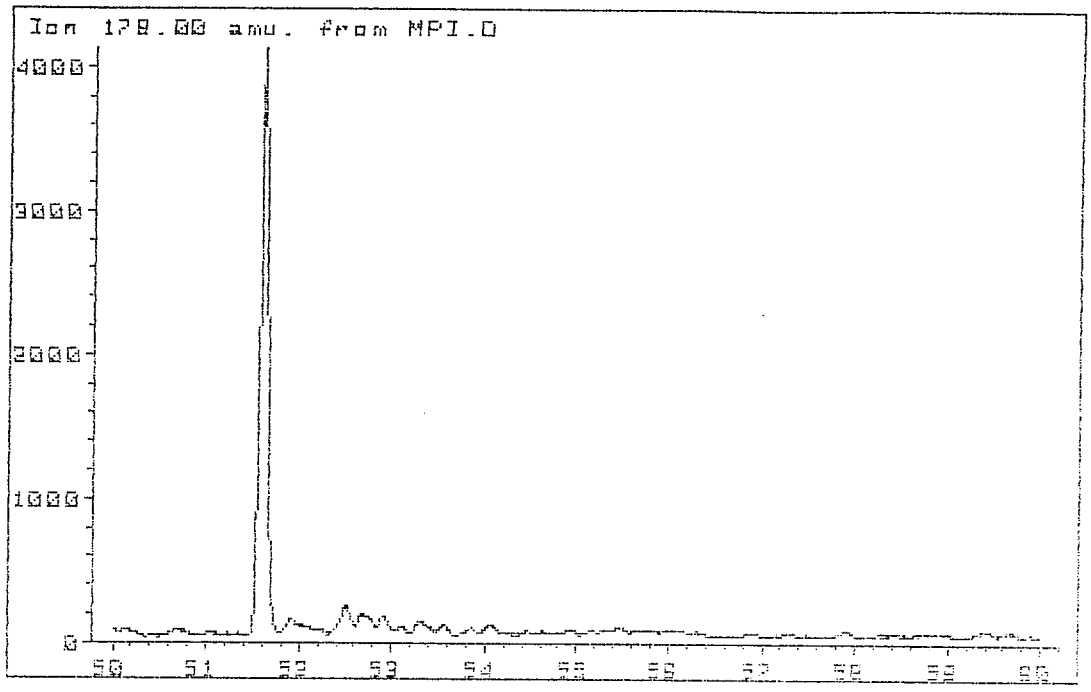

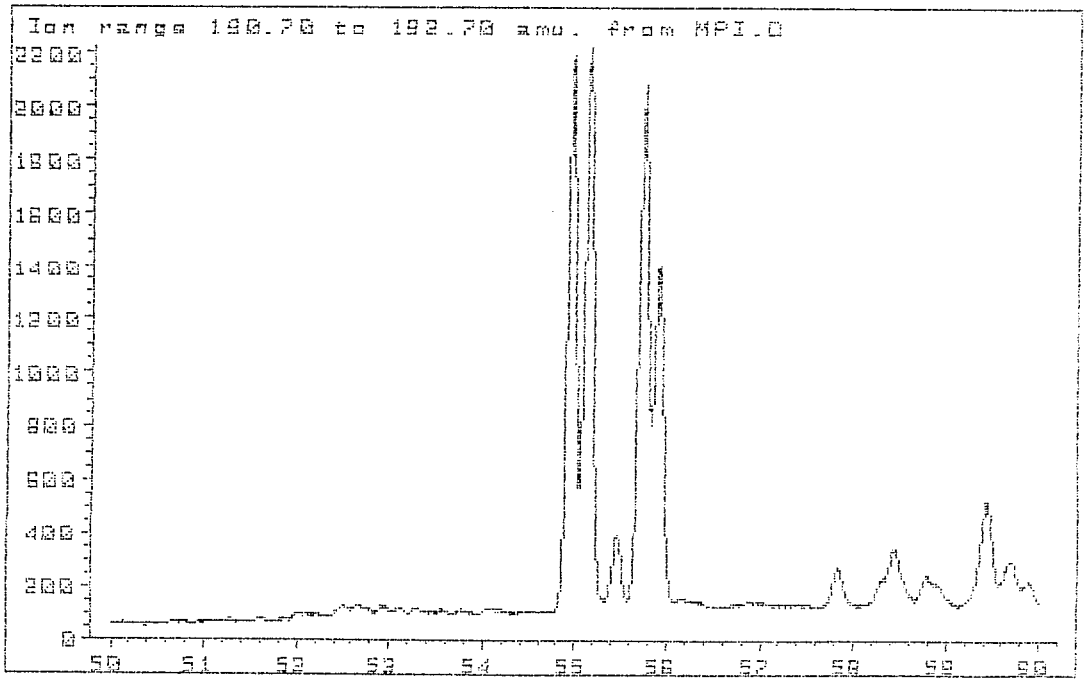

amdel

FIGURE 3G

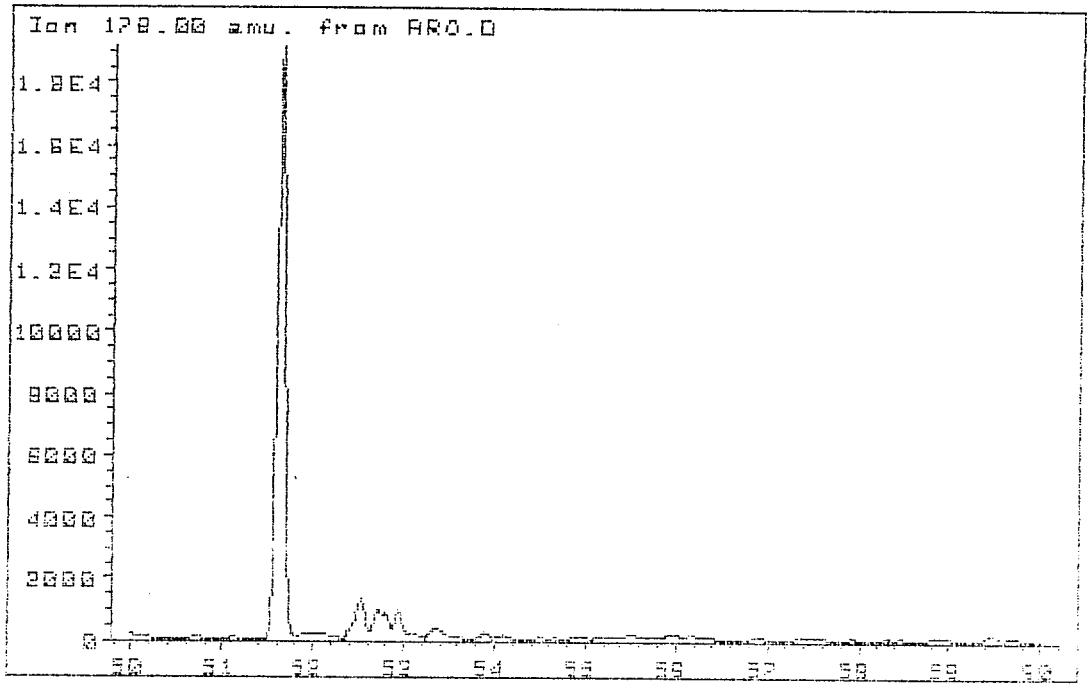

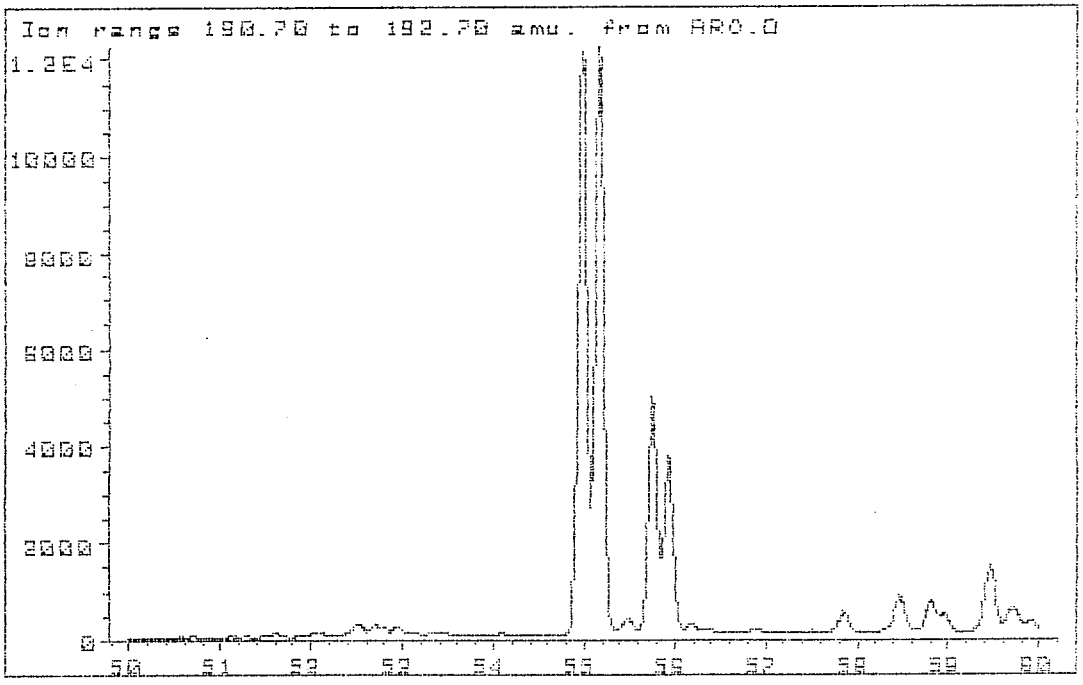

amdel

FIGURE 3H

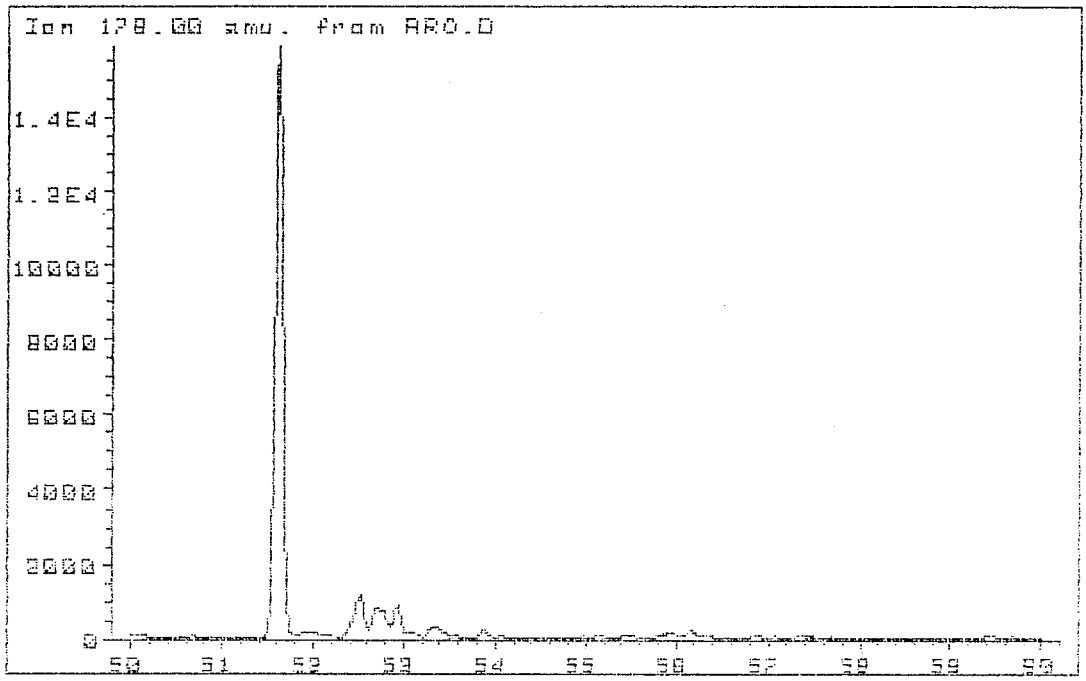

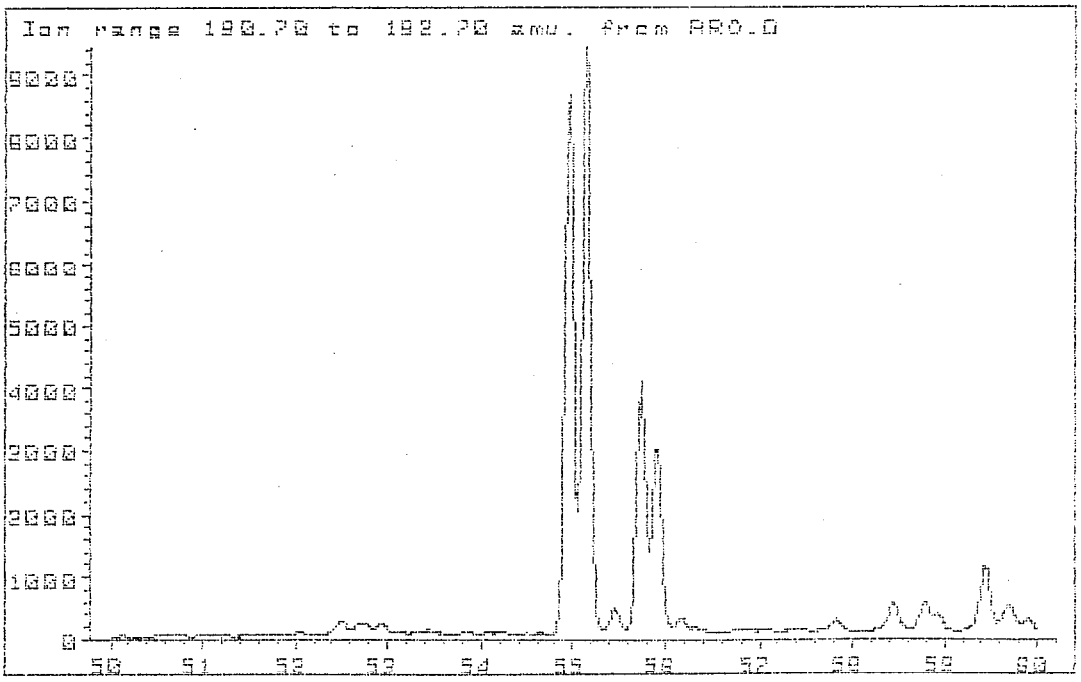

amdel

APPENDIX 1

ANALYTICAL METHODS

1. ISOLATION OF C_{12+} FRACTION

Two condensates (Big Lake-3, Moomba-36) were topped to 210°C by distillation prior to analysis. The remainder were analysed neat.

2. THIN LAYER CHROMATOGRAPHY (TLC)

Aromatic hydrocarbons were isolated from the condensates by preparative TLC using Merck GF_{254} silica plates and distilled AR grade n-pentane as eluent. Naphthalene and anthracene were employed as reference standards for the diaromatic and triaromatic hydrocarbons, respectively. These two bands, visualised under UV light, were scraped from the plate and the aromatic hydrocarbons redissolved in dichloromethane.

3. GAS CHROMATOGRAPHY-MASS SPECTROMETRY (GC-MS)

GC-MS analysis of the aromatic hydrocarbons was undertaken in the selected ion detection (SID) mode. The instrument and its operating parameters were as follows:

System:	Hewlett Packard (HP) 5790 GC coupled with a HP5970A mass selective detector and HP9816S data system
Column:	50 m x 0.2 mm i.d. HP PONA cross-linked methylsilicone phase fused silica, interfaced directly to source of mass spectrometer
Injector:	Split injection (40:1)
Carrier gas:	He at 1.2 kg/cm^2 head pressure
Column temperature:	50-260°C @ 4°/min
Mass spectrometer conditions:	70 eV EI; 9-ion selected ion monitoring, 70 millisec dwell time for each ion

The following mass fragmentograms were recorded:

m/z	Compound Type
156	dimethylnaphthalenes
169+170	trimethylnaphthalenes
178	phenanthrene
191+192	methylphenanthrenes

The area of the phenanthrene peak was multiplied by a response factor of 0.667 when calculating the methylphenanthrene index (MPI).

00022

RESTRICTED INVESTIGATION REPORT 1022R

CSIRO

INSTITUTE OF EARTH RESOURCES

FUEL GEOSCIENCE UNIT

OPEN FILE

23/3/93 dlg

Date Released | Initials

CRUDE OILS FROM GIDGEALPA IN THE COOPER BASIN (SOUTH AUSTRALIA)

J.D. SAXBY AND N.M. RAPHAEL

RECEIVED
4 MAY 1979
DEPT. OF MINES AND ENERGY SECURITY

P.O. Box 136
NORTH RYDE, NSW
AUSTRALIA 2113

APRIL, 1979

00023

1. INTRODUCTION

Following a discussion with Jack Mulready of Delhi Petroleum Pty. Ltd., a sample of oil from Gidgealpa No. 16, DST No. 2, was supplied to CSIRO. This sample was recovered from the Toolachee Formation and it was of interest to compare this oil with that found in the older Tirrawarra Formation in the nearby well Gidgealpa No. 7.

2. METHOD AND RESULTS

A small representative sample of each oil was placed on a 5 x 1cm column of florisil and eluted with petroleum ether. Evaporation of the solvent under a stream of nitrogen gave the aliphatic fraction. The column was then eluted with benzene and the resulting solution evaporated under nitrogen giving the aromatic fraction. The same procedure was followed for methanol to give the polar fraction. Table 1 shows results for this separation. Thus:

total original sample taken (%)	= aliphatic fraction (%)	+ aromatic fraction (%)	+ polar fraction (%)	+ volatile material lost during evaporation and material remaining on the column (%)

The aliphatic fractions were analyzed by gas chromatography for hydrocarbons in the n-C_{15} to n-C_{35} range. The resulting chromatograms are shown in Fig. 1. Data from these chromatograms are shown in Fig. 2 and 3 (J.D. Saxby, Geochim. Cosmochim. Acta, 1978, 42, 215-217). These diagrams enable a visual comparison to be made of the high boiling aliphatic fractions from different crude oils.

3. DISCUSSION AND CONCLUSIONS

(i) The Toolachee oil in Gidgealpa 16 and the Tirrawarra oil in Gidgealpa 7 appear to have come from the same source rock. Differences can be attributed to fractionation during migration and within reservoirs.

(ii) The Gidgealpa 16 oil can be formed from the Gidgealpa 7 oil by loss of more volatile components possibly through a slightly more permeable cap rock. This more volatile material may have been

00024

trapped elsewhere in the basin or been lost at the surface.

(iii) Bacterial alteration of these oils has been small or non-existent and both oils are similarly abundant in normal alkanes.

TABLE 1. Data on Gidgealpa Oils

CSIRO Lab No.	78731	60851
Well	Gidgealpa 16	Gidgealpa 7
Test/Depth (m)	DST 2	2204-2223
Aliphatic fraction (%)	65.7	66.8
Aromatic Fraction (%)	22.0	6.4
Polar fraction (%)	1.1	1.3
Low-boiling material (%)*	11.2	25.5

* Corresponds to total material lost during evaporation of aliphatic, aromatic and polar fractions (plus a small amount of material which is not eluted from the florisil column).

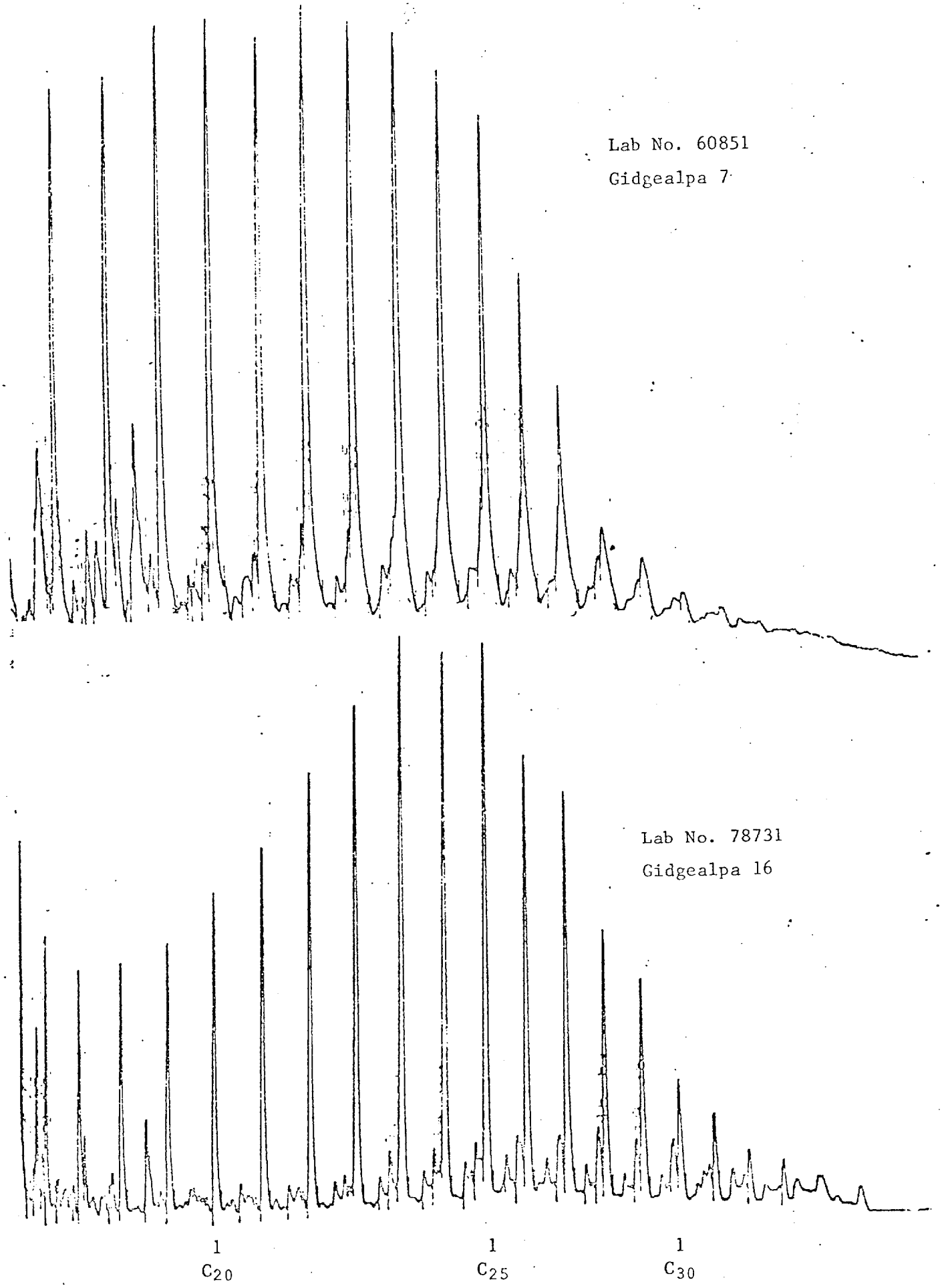

Fig. 1 Gas chromatograms of aliphatic fractions separated from Gidgealpa crude oils.

	Saturated hydrocarbons having M.W.>~150 (% of original crude)	
dgealpa	16	65.7
dgealpa	7	66.8

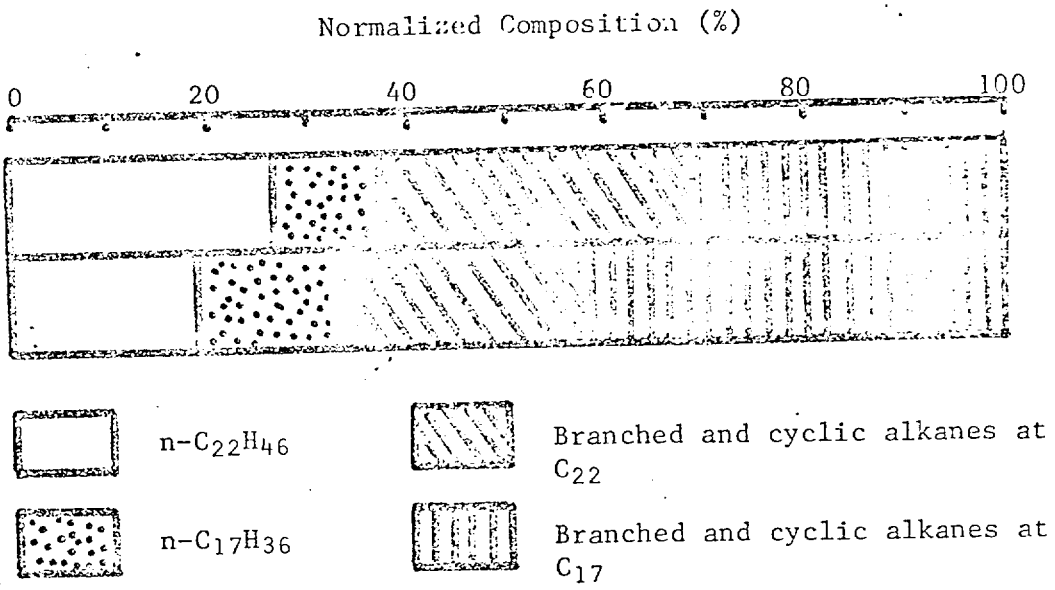

Fig. 2 Distribution of hydrocarbons in Gidgealpa crude oils

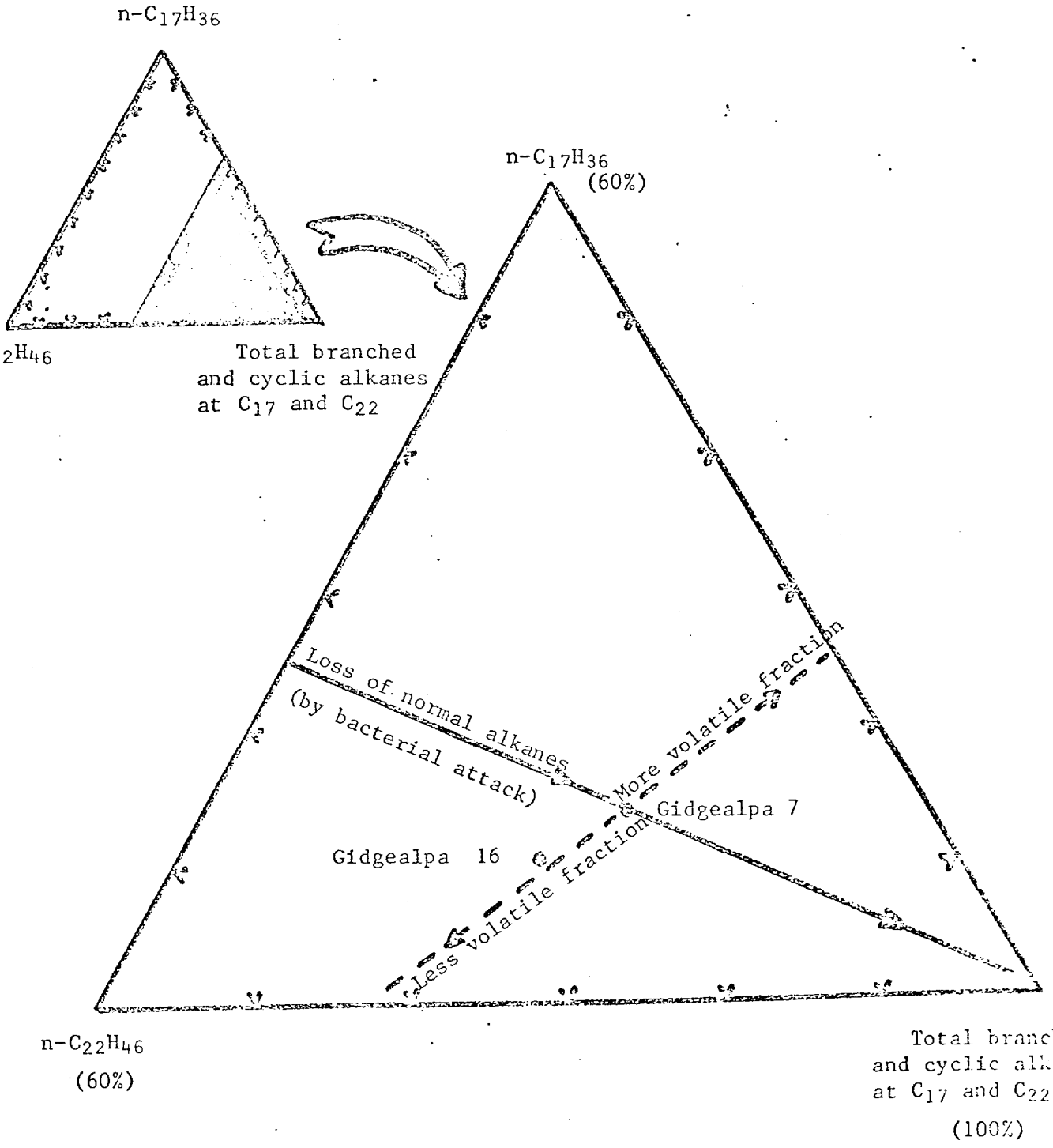

Fig. 3 Compositions and possible alteration pathways of Gidgealpa crude oils.

06025

RESTRICTED INVESTIGATION REPORT 1026R

RESTRICTED
CIRCULATION

CSIRO

MINERALS RESEARCH LABORATORIES

FUEL GEOSCIENCE UNIT

OPEN FILE
23/3/93 Initials
Date Released

COOPER BASIN : PATCHAWARRA TROUGH
PETROLOGY OF COALS AND DISPERSED ORGANIC MATTER FROM THE TIRRAWARRA, MERRIMELIA AND UNNAMED FORMATIONS

MICHELLE SMYTH

RECEIVED
31 MAY 1979
DEPT. OF MINES AND ENERGY SECURITY
3344

FUEL GEOSCIENCE UNIT
P.O. BOX 136
NORTH RYDE, NSW
AUSTRALIA, 2113

MAY 1979

06023

1. INTRODUCTION

In November 1978, a collaborative program on hydrocarbon generation in the Cooper Basin was discussed by the South Australian Department of Mines and Energy, Delhi International Oil Corporation and CSIRO Fuel Geoscience Unit.

SADME and CSIRO have agreed to carry out specific investigations within the Cooper Basin project, so that the work of the two bodies is complimentary and not overlapping. One of the topics to be covered by CSIRO is the petrographic evaluation of the hydrocarbon source potential of the Permian shales in certain wells in the Patchawarra Trough.

The first phase of this petrographic program has been to look at the coals and dispersed organic matter (d.o.m.) in the sediments below the Patchawarra Formation, i.e. in the Tirrawarra, Merrimelia and unnamed formations.

The wells which are included in this report are Tirrawarra No. 2, Mudrangie No. 1, Moorari No. 2, Coonatie No. 1, Yanpurra No. 1 and Tindilpie No. 1 (Fig. 1).

2. ANALYSES

Grain mounts were made from any ditch cuttings which appeared to contain carbonaceous material. In some wells the cuttings are very coaly, and this coal is most likely to be cavings from the overlying Patchawarra Formation. Whether the carbonaceous shales are in situ or cavings cannot be determined.

Maceral analyses have been carried out on 50 samples from the six wells, following the recommendations of the International Committee for Coal Petrology.

3. RESULTS

The results for each well are presented in two ways: the first showing the vitrinite, exinite and inertinite contents of the samples as a whole, including the total d.o.m. content of the sample. These results are

in Tables 1, 3, 5, 7, 9 and 11 for the wells Tirrawarra No. 2, Mudrangie No. 1, Moorari No. 2, Coonatie No. 1, Yarpurra No. 1 and Tindilpie No. 1, respectively. The second set of tables is a breakdown of the organic matter into the maceral species for each of the groups, vitrinite, exinite and inertinite. The proportion of the organic matter which is in coal grains and that which occurs as d.o.m. is given. These are Tables 2, 4, 6, 8, 10 and 12, in the same order as above.

The information from the tables has also been plotted in Figs. 2 and 3.

4. DISCUSSION

All of the organic matter is low in exinite (Fig. 2) and most of it is rich in inertinite. The amount of d.o.m. in the sediments varies between a trace and 7%, but is most often 1% or less (Fig. 4).

The coals contain some exinite, the d.o.m. virtually none (Fig. 3). Many of the samples contain so little d.o.m. that the compositions plotted are not statistically significant, but merely indicate trends.

A substance listed in Tables 7 and 8, (Coonatie No. 1) as mobile organic matter, is most probably remnants of drilling mud. It has a reflectivity of 0.03%, does not fluoresce with blue light excitation and was found only in the one sample at the bottom of the well. The drilling fluid used in Coonatie No. 1 was "Black Magic" an oil base mud concentrate. 5% by weight of a substance was extracted from the cuttings with chloroform. In a simple liquid chromatographic separation most of this material appeared in the polar fraction eluted with methanol rather than in the aliphatic and aromatic fractions eluted with petroleum ether and benzene respectively.

5. CONCLUSIONS

In the 50 samples of cuttings examined, most contained only 1% or less of d.o.m. It is assumed that the shaly sediments containing this d.o.m. are in situ. Coaly fragments are most probably cavings, as coal seams are not reported from below the Patchawarra Formation.

00631

The organic matter is inertinite-rich, with low exinite contents. Coal fragments contain some exinite, the d.o.m. virtually none.

The low percentage of d.o.m. in most cuttings, and its inertinite-rich nature, suggest that these sediments are unlikely to be good potential source rocks for the generation of hydrocarbons, particularly liquid hydrocarbons.

Another topic in the collaborative program which is to be covered by CSIRO is the relationship between the isotopic composition of natural gases from the Cooper Basin and the organic matter in the source rocks. Because of the small quantity of d.o.m. in the sediments studied here, its intertinite-rich composition and the contamination from overlying coals, no isotopic analysis will be done on these cuttings at present.

TABLE 1

COOPER BASIN: PATCHAWARRA TROUGH

TIRRAWARRA No 2 WELL

MACERAL ANALYSES OF CUTTINGS

(Results are given as percentages by volume unless otherwise stated)

	Lab. No. Depth Feet	Depth (metres)	Vitrinite	Exinite	Iner-tinite	Mineral Matter	Total d.o.m.	Total Organic Matter
Merrimelia Formation	78181 9895-9900	3016.0-3017.5	1	tr	1	98	1	2
	78182 9885-9890	3012.9-3914.5	2	-	3	95	1	5
	78183 9865	3006.9	1	-	4	95	2	5
Tirrawarra Formation	78184 9855	3003.8	2	-	1	97	1	3
	78185 9825	2994.7	1	tr	2	97	1	3
	78186 9820	2993.1	3	tr	4	93	1	7
	78187 9815	2991.6	6	1	12	81	2	19
	78188 9800	2987.0	3	tr	4	93	1	7
	78189 9795	2985.5	4	tr	10	86	1	14
	78190 9755	2973.3	1	-	5	94	1	6
	78191 9750	2971.8	4	-	3	93	3	7
	78192 9740	2968.8	10	tr	11	79	3	21

tr - Trace

TABLE 2

COOPER BASIN: PATCHAWARRA TROUGH

TIRRAWARRA No 2 WELL

MACERAL ANALYSES OF THE ORGANIC MATTER

(Results are given as percentages by volume unless otherwise stated)

	Lab. No. Depth (feet)	Depth (metres)	Vitr-inite	Resinite	Micr-inite	Semi-Fus-inite	Fus-inite	Inerto-detrinite	%coal grains	%d.o.m.
Merrimelia Formation	78181 9895-9900	3016.0 3017.5	33	11	-	-	11	45	56	44*
	78182 9885-9890	3012.9 3014.5	32	-	4	28	-	36	84	16
	78183 9865	3006.9	13	-	-	27	-	60	67	33*
	78184 9855	3003.8	50	-	6	13	-	31	81	19*
	78185 9825	2994.7	18	Sporinite 6	-	35	-	46	77	23*
	78186 9820	2993.1	38	Resinite 3	5	27	3	24	89	11
	78187 9815	2991.6	31	3	2	27	2	35	90	10
	78188 9800	2987.0	47	6	-	26	-	21	90	10
Tirrawarra Formation	78189 9795	2985.5	25	Sporinite 1	-	38	-	36	91	9
	78190 9755	2973.3	14	-	-	36	4	46	79	21
	78191 9750	2971.8	60	-	-	9	-	31	51	49
	78192 9740	2968.8	46	+ Resinite 2	1	9	1	41	84	16

* Actual figures are not statistically significant - too few points counted (<25)

TABLE 3

COOPER BASIN: PATCHAWARRA TROUGH

MUDRANGIE No 1 WELL

MACERAL ANALYSES OF CUTTINGS

(Results are given as percentages by volume unless otherwise stated)

	Lab. No. Depth Feet	Depth (metres)	Vitrinite	Exinite	Inertinite	Mineral Matter	Total d.o.m.	Total Organic Matter
Unnamed	78267 10420-30	3176.0-3179.1	-	-	1	99	tr	1
	78268 10380-90	3163.8-3166.9	tr	-	2	98	1	2
	78269 10350-60	3154.7-3157.7	1	-	2	97	1	3
	78270 10320-30	3145.5-3148.6	1	-	5	94	tr	6
	78271 10260-70	3127.2-3130.3	3	-	tr	97	2	3
	78272 10180-90	3102.9-3105.9	1	-	3	96	3	4
Tirrawarra Formation	78273 10100-10	3078.5-3081.5	3	tr	9	88	7	12
	Coal		40	-	60	mmf		
	d.o.m.		16	4	80	mmf		

tr - trace
mmf - mineral matter free

TABLE 4

COOPER BASIN: PATCHAWARRA TROUGH

MUDRANGIE No 1 WELL

MACERAL ANALYSES OF THE ORGANIC MATTER

(Results are given as percentages by volume unless otherwise stated)

	Lab. No. Depth (feet)	Depth (metres)	Vitrinite	Resinite	Micrinite	Semi-Fusinite	Fusinite	Inertodetrinite	% coal grains	% d.o.
Unnamed	78267 10420-30	3176.0-3179.1	-	-	-	-	-	100	75	25*
	78268 10380-90	3163.8-3166.9	25	-	-	-	-	75	63	37*
	78269 10350-60	3154.7-3157.7	33	-	-	11	-	56	56	44*
	78270 10320-30	3145.5-3148.6	15	-	8	15	8	54	100	tr*
	78271 10260-70	3127.2-3130.3	91	-	-	-	-	9	45	55*
	78272 10180-90	3102.9-3105.9	22	-	-	28	6	44	17	83*
Tirrawarra Formation	78273 10100-10	3078.5-3081.5	26+	2	-	25	-	47	44	56
	Coal		40	-	-	20	-	40*		
	d.o.m.		16	4	-	28	-	52		

tr - trace

+ 22% vitrinite
4% resinous vitrinite

* actual figures are not statistically significant - too few counts (<25)

TABLE 5

COOPER BASIN: PATCHAWARRA TROUGH

MOORARI No 2 WELL

MACERAL ANALYSES OF CUTTINGS

(Results are given as percentages by volume unless otherwise stated)

	Lab. No. / Depth Feet	Depth (metres)	Vitrinite	Exinite	Inertinite	Mineral Matter	Total d.o.m.	Total Organic Matter
Formation	78379 / 10150	3093.7	2	-	2	96	1	4
	Coal		53	-	47	mmf		
	d.o.m.		17	-	83	mmf		
Tirrawarra	78380 / 10040	3060.2	9	-	4	87	1	13
	Coal		71	-	29	mmf		
	d.o.m.		50	-	50	mmf		

tr - trace
mmf - mineral matter free

TABLE 6

80037

COOPER BASIN: PATCHAWARRA TROUGH

MOORARI No 2 WELL

MACERAL ANALYSES OF THE ORGANIC MATTER

(Results are given as percentages by volume unless otherwise stated)

	Lab. No. Depth (feet)	Depth (metres)	Vitrinite	Resinite	Micrinite	Semi-Fusinite	Fusinite	Inertodetrinite	% coal grains	% d.o.
Tirrawarra Formation	78379 10150	3093.7	42	-	5	31	11	11	68	32*
	Coal		53	-	8	23	8	8		
	d.o.m.		17	-	-	50	16	16		
	78380 10040	3060.2	69	-	4	18	2	7	91	9
	Coal		71	-	5	20	2	2		
	d.o.m.		50	-	-	-	-	50*		

* actual figures are not statistically significant - too few counts (<25)

TABLE 7

COOPER BASIN: PATCHAWARRA TROUGH

COONATIE No 1 WELL

MACERAL ANALYSES OF CUTTINGS

(Results are given as percentages by volume unless otherwise stated)

	Lab. No. Depth Feet	Depth (metres)	Vitrinite	Exinite	Iner- tinite	Mineral Matter	Total d.o.m.	Total Organic Matter
Merrimelia Formation	78417 (10370-80)	3160.8-3063.7	tr	5*	1	94	5	6
Tirrawarra Formation	78418 (10140-50)	3090.7-3093.7	3	-	17	80	3	20
	Coal		15	-	85			
	d.o.m.		18	-	82			

tr - trace

* mobile organic matter

TABLE 8

COOPER BASIN: PATCHAWARRA TROUGH

COONATIE No 1 WELL

MACERAL ANALYSES OF THE ORGANIC MATTER

(Results are given as percentages by volume unless otherwise stated)

	Lab. No. Depth (feet)	Depth (metres)	Vitrinite	Resinite	Micrinite	Semi-Fusinite	Fusinite	Inertodetrinite	% coal grains	% d.o.
Merrimelia Formation	78417 10370-80	3160.8-3163.8	8	77+	-	15	-	-	23	77*
	Coal		33	-	-	67	-	-		
	d.o.m.		-	100+	-	-	-	-		
Tirrawarra Formation	78418 10140-50	3090.7-3093.7	16	-	-	25	-	59	86	14
	Coal		15	-	-	22	-	63		
	d.o.m.		18	-	-	46	-	36*		

+mobile organic matter

*actual figures are not statistically significant - too few counts (<25)

TABLE 9

COOPER BASIN: PATCHAWARRA TROUGH

YANPURRA NO.1

MACERAL ANALYSES OF CUTTINGS

(Results are given as percentages by volume unless otherwise stated)

	Lab. No. Depth Feet	Depth (metres)	Vitrinite	Exinite	Inertinite	Mineral Matter	Total d.o.m.	Total Organic Matter
Unnamed	78336 9700-10	2956.6-2959.6	12	tr	30	58	1	42
	Coal		29	tr	71	mmf		
	d.o.m.		50	-	50	mmf		
	78337 9690-9700	2956.5-2959.6	14	2	30	54	1	46
	Coal		31	3	66	mmf		
	d.o.m.		17	-	83	mmf		
	78338 9680-90	2950.5-2953.5	3	2	7	88	tr	12
	Coal		28	8	64	mmf		
	d.o.m.		-	-	100	mmf		
	78339 9650-60	2941.3-2944.4	4	tr	10	86	tr	14
	Coal		28	1	71	mmf		
	78340 9630-40	2935.2-2938.3	28	1	48	23	2	77
	Coal		35	1	64	mmf		
	d.o.m.		88	-	12	mmf		

tr = trace

mmf = mineral matter free

TABLE 9 Cont'd

COOPER BASIN: PATCHAWARRA TROUGH

YANPURRA NO.1

MACERAL ANALYSES OF CUTTINGS

(Results are given as percentages by volume unless otherwise stated)

	Lab. No. Depth Feet	Depth (metres)	Vitrinite	Exinite	Inertinite	Mineral Matter	Total d.o.m.	Total Organic Matter
Merrimelia Formation	78341 9610-20	2929.1-2932.2	12	1	21	66	tr	34
	Coal		36	3	61	mmf		
	d.o.m.		-	-	100	mmf		
	78342 9606-10	2927.9-2929.1	17	1	44	38	1	62
	Coal		28	1	71	mmf		
	d.o.m.		33	-	67	mmf		
	78343 9580-90	2920.0-2923.0	15	1	37	47	3	53
	Coal		29	1	70	mmf		
	d.o.m.		17	-	83	mmf		
	78344 9560-70	2913.9-2916.9	8	tr	17	75	4	25
	Coal		35	1	64	mmf		
	d.o.m.		29	-	71	mmf		

tr = trace

mmf - mineral matter free

TABLE 9 Cont'd

COOPER BASIN: PATCHAWARRA TROUGH

YANPURRA NO 1 WELL

MACERAL ANALYSES OF CUTTINGS

(Results are given as percentages by volume unless otherwise stated)

	Lab. No. Depth Feet	Depth (metres)	Vitrinite	Exinite	Inertinite	Mineral Matter	Total d.o.m.	Total Organic Matter
Tirrawarra Formation	78345 9540-50	2907.8-2910.8	13	1	19	67	6	33
	Coal		36	5	59	mmf		
	d.o.m.		52	-	48	mmf		
	78346 9530-40	2904.7-2907.8	13	tr	29	58	1	42
	Coal		30	1	69	mmf		
	d.o.m.		50	-	50	mmf		
	78347 9510-20	2898.6-2901.7	9	1	33	57	2	43
	Coal		20	2	78	mmf		
	d.o.m.		27	-	73	mmf		
	78348 9490-9500	2892.6-2895.6	11	1	32	56	2	44
	Coal		25	3	72	mmf		
	d.o.m.		33	-	67	mmf		

tr - trace
mmf - mineral matter free

TABLE 10

COOPER BASIN: PATCHAWARRA TROUGH

YANPURRA NO 1

MACERAL ANALYSES OF THE ORGANIC MATTER

(Results are given as percentages by volume unless otherwise stated)

	Lab. No. Depth (feet)	Depth (metres)	Vitrinite	Sporinite	Micrinite	Semi-Fusinite	Fusinite	Inertodetrinite	% coal grains	% d.o.m
	78336 9700-10	2956.6-2959.6	29	tr	4	40	4	23	97	3
	Coal		29	tr	4	41	4	22		
	d.o.m.		50	-	-	17	-	33*		
	78337 9690-9700	2953.5-2956.6	30	3=	2	40	3	22	97	3
	Coal		31	3=	2	41	3	20		
	d.o.m.		17	-	-	-	-	83*		
Unnamed	78338 9680-90	2950.5-2953.5	28	8†	3Ø	19	6	36	97	3
	Coal		29	8†	3	19	6	35		
	d.o.m.		-	-	-	-	-	100*		
	78339 9650-60	2941.3-2944.4	28	1	1	33	1Ø	36	100	-
	78340 9630-40	2935.2-2938.3	36	2	3	28	3	28	98	2
	Coal		35	2	3	28	3	29		
	d.o.m.		88	-	-	12	-	- *		

= - 1% each of sporinite, cutinite, resinite

† - 4% each of sporinite, resinite

Ø - macrinite

tr - trace

* actual figures not statistically significant - too few counts (<25)

TABLE 10 Cont'd

COOPER BASIN: PATCHAWARRA TROUGH

YANPURRA NO.1

MACERAL ANALYSES OF THE ORGANIC MATTER

(Results are given as percentages by volume unless otherwise stated)

Lab. No. Depth (feet)	Depth (metres)	Vitrinite	Sporinite	Micrinite	Semi-Fusinite	Fusinite	Inertodetrinite	Macrinite	% coal grains	% d.o.m
78341 9610-20	2929.1-2932.2	12	1	1	9	tr	11		100	tr
Coal		36	3+	2	28	1	30			
d.o.m.		-	-	-	-	-	100*			
78342 9606-10	2927.9-2929.1	28	1	2	32	6	30		98	2
Coal		28	1	2	32	6	30	1		
d.o.m.		33	-	-	-	-	67*			
343 9580-90	2920.0-2923.0	28	1	2	35	4	27	3	95	5
Coal		29	1	2	36	4	25	3		
d.o.m.		17	-	8	-	-	75*			
78344 9560-70	2913.9-2916.9	34	1	4	24	8	26	3	85	15
Coal		35	1	5	24	9	23	3		
d.o.m.		29	-	-	24	-	47*			

tr -- trace

+ 2% sporinite
1% resinite

* actual figures are not statistically significant - too few counts (<25)

TABLE 10 Cont'd

COOPER BASIN: PATCHAWARRA TROUGH

YANPURRA NO.1 WELL

MACERAL ANALYSES OF THE ORGANIC MATTER

(Results are given as percentages by volume unless otherwise stated)

Lab. No. Depth (feet)	Depth (metres)	Vitrinite	Sporinite	Micrinite	Semi-Fusinite	Fusinite	Inertodetrinite	Macrinite	% coal grains	% d.o.m
78345 9540-50	2907.8-2910.8	39	3+	2	24	4	26	2	82	18
Coal		36	5+	2	25	4	26	2		
d.o.m.		52	-	-	18	4	26			
78346 9530-40	2904.7-2907.8	30	1	1	26	3	38	1	97	3
Coal		30	1	1	26	3	38	1		
d.o.m.		50	-	-	-	-	50*			
78347 9510-20	2898.6-2901.7	20	2	5	31	4	35	3	95	5
Coal		20	2	5	32	4	34	3		
d.o.m.		27	-	-	13	-	60*			
78348 9490-9500	2892.6-2895.6	25	3+	3	31	5	30	3	95	5
Coal		25	3+	3	31	5	30	3		
d.o.m.		33	-	-	33	7	27*			

Patchawarra Formation

tr - trace

- includes sporinite
cutinite
resinite

* actual figures are not statistically significant - too few counts (<25)

TABLE 11

COOPER BASIN: PATCHAWARRA TROUGH

TINDILPIE NO.1 WELL

MACERAL ANALYSES OF CUTTINGS

(Results are given as percentages by volume unless otherwise stated)

		Lab. No. Depth (feet)	Depth (metres)	Vitrinite	Exinite	Inertinite	Mineral Matter	Total d.o.m.	Total organic matter
Merrimelia Formation	1	77901 11160-70	3401.6-3404.6	3	tr	11	86	1	14
		Coal		21	1	78	mmf		
		d.o.m.		17	–	83	mmf		
	2	77903 11130-40	3392.4-3395.5	2	tr	3	95	1	5
		Coal		38	3	59	mmf		
		d.o.m.		25	–	75	mmf		
	3	77904 11110-20	3386.3-3389.4	8	1	21	70	1	30
		Coal		29	2	69	mmf		
		d.o.m.		–	25	75	mmf		
	4	77907 11080-90	3377.2-3380.2	tr	–	1	99	tr	1
		Coal		29	–	71	mmf		
		d.o.m.		–	–	100	mmf		
	5	77910 11030-40	3361.9-3365.0	tr	tr	3	97	tr	3
		Coal		12	6	82	mmf		
		d.o.m.		–	–	100	mmf		
	6	77913 11000-10	3352.8-3355.8	1	–	3	96	1	4
		Coal		14	–	86	mmf		
		d.o.m.		40	–	60	mmf		
	7	77916 10950-60	3337.6-3340.6	tr	–	1	99	tr	1
		Coal		40	–	60	mmf		
		d.o.m.		–	–	100	mmf		

TABLE 11 Cont'd

COOPER BASIN: PATCHAWARRA TROUGH

TINDILPIE NO.1 WELL

MACERAL ANALYSES OF CUTTINGS

(Results are given as percentages by volume unless otherwise stated)

		Lab. No. Depth (feet)	Depth (metres)	Vitrinite	Exinite	Inertinite	Mineral Matter	Total d.o.m.	Total organic matter
Merrimelia Formation		77920 10890-10900	3319.3-3322.3	4	-	10	86	tr	14
	8	Coal		28	-	72	mmf		
		d.o.m.		-	-	100	mmf		
Tirrawarra Formation		77923 10820-30	3297.9-3301.0	1	tr	2	97	tr	3
	9	Coal		40	7	53	mmf		
		d.o.m.		-	-	100	mmf		
		77924 10780-90	3285.7-3288.8	2	-	3	95	tr	5
	10	Coal		33	-	67			
		d.o.m.		-	-	100	mmf		
		77925 10770-80	3282.7-3285.7	4	-	11	85	tr	15
	11	Coal		28	-	72	mmf		
		d.o.m.		-	-	100	mmf		
		77928 10720-30	3267.5-3270.5	2	tr	3	95	1	5
	12	Coal		38	6	56	mmf		
		d.o.m.		25	-	75	mmf		
		77931 10640-50	3243.1-3246.1	2	-	4	94	tr	6
	13	Coal		35	-	65	mmf		
		d.o.m.		50	-	50	mmf		

TABLE 11 Cont'd

COOPER BASIN: PATCHAWARRA TROUGH

TINDILPIE NO.1 WELL

MACERAL ANALYSES OF CUTTINGS

(Results are given as percentages by volume unless otherwise stated)

Tirrawarra Formation

Lab. No. Depth (feet)	Depth (metres)	Vitrinite	Exinite	Inertinite	Mineral Matter	Total d.o.m.	Total organic matter
77935 10580-90	3224.8-3227.8	3	-	5	92	4	8
Coal		40	-	60	mmf		
d.o.m.		18	-	82	mmf		

tr - trace
mmf - mineral matter free

TABLE 12

COOPER BASIN: PATCHAWARRA TROUGH

TINDILPIE NO.1 WELL

MACERAL ANALYSES OF ORGANIC MATTER

(Results are given as percentages by volume unless otherwise stated)

	Lab. No. Depth (feet)	Depth (metres)	Vitrinite	Sporinite	Micrinite	Semi-fusinite	Fusinite	Inertodetrinite	Macrinite	% coal grains	% d.o.m
Merrimelia Formation	77901 11160-70	3401.6-3404.6	21	1	3	40	6	29		93	7
1	Coal		21	1	4	42	6	26			
	d.o.m.		17	–	–	17	–	66*			
	77903 11130-40	3392.4-3395.5	35	Resinite 3	–	30	–	32		78	22
2	Coal		38	3	–	31	–	28			
	d.o.m.		25	–	–	25	–	50*			
	77904 1110-20	3386.3-3389.4	28	Resinite 2 & Cutinite	3	30	4	29	4	97	3
3	Coal		28	2	3	31	4	28	4		
	d.o.m.		–	Cutinite 25	–	–	–	75*			
	77907 11080-90	3377.2-3380.2	20	–	–	10	10	60		70	30
4	Coal		29	–	–	14	14	43			
	d.o.m.		–	–	–	–	–	100			
	77910 11030-40	3361.9-3365.0	11	Sporinite 5	–	79	–	5		89	11
5	Coal		12	6	–	82	–	–			
	d.o.m.		–	–	–	50	–	50			
	77913 11000-10	3352.8-3355.8	21	–	–	37	5	32		74	26
6	Coal		14	–	–	43	7	29	7		
	d.o.m.		40	–	–	20	–	40			

* actual figures not statistically significant – too few counts (<25)

TABLE 12 Cont'd

COOPER BASIN: PATCHAWARRA TROUGH

TINDILPIE NO.1 WELL

MACERAL ANALYSES OF ORGANIC MATTER

(Results are given as percentages by volume unless otherwise stated)

		Lab. No. Depth (feet)	Depth (metres)	Vitr-inite	Spor-inite	Micr-inite	Semi-fus-inite	Fus-inite	Inerto-detrinite	Macr-inite	% coal grains	% d.o.m
Merrimelia Formation		77916 10950-60	3337.6-3340.6	25	–	–	50	–	25		63	37*
	7	Coal		40	–	–	40	–	20			
		d.o.m.		–	–	–	67	–	33			
		77920 10890-10900	3319.3-3322.3	27	–	–	33	3	37		99	1
	8	Coal		28	–	–	32	3	37			
		d.o.m.		–	–	–	100	–	– *			
Tirrawarra Formation		77923 10820-30	3297.9-3301.0	35	6	–	35	–	24		88	12*
	9	Coal		40	7	–	33	–	20			
		d.o.m.		–	–	–	50	–	50			
		77924 10780-90	3285.7-3288.8	31	–	–	19	27	23		92	8
	10	Coal		33	–	–	17	25	25*			
		d.o.m.		–	–	–	50	50	– *			
		77925 10770-80	3282.7-3285.7	28	–	3	32	3	31	3	98	2
	11	Coal		28	–	3	33	3	30	3		
		d.o.m.		–	–	–	–	–	100*			
		77928 10720-30	3267.5-3270.5	35	5	–	20	15	25	–	80	20
	12	Coal		38	6	–	19	12	25			
		d.o.m.		25	–	–	25	25	25			

* actual figures not statistically significant - too few counts (<25)

TABLE 12 Cont'd

COOPER BASIN: PATCHAWARRA TROUGH

TINDILPIE NO.1 WELL

MACERAL ANALYSES OF ORGANIC MATTER

(Results are given as percentages by volume unless otherwise stated)

	Lab. No. Depth (feet)	Depth (metres)	Vitr-inite	Spor-inite	Micr-inite	Semi-fus-inite	Fus-inite	Inerto-detrinite	Macr-inite	% coal grains	% d.o.m
Tirrawarra Formation 13	77931 10640-50	3143.1-3246.1	36	-	-	20	4	40		92	8
	Coal		35	-	-	22	4	39*			
	d.o.m.		50	-	-	-	-	50*			
14	77935 10580-90	3224.8-3227.8	31	-	-	23	4	42		58	42
	Coal		40	-	-	20	7	33*			
	d.o.m.		18	-	-	27	-	55*			

* actual figures are not statistically significant - too few counts (<25)

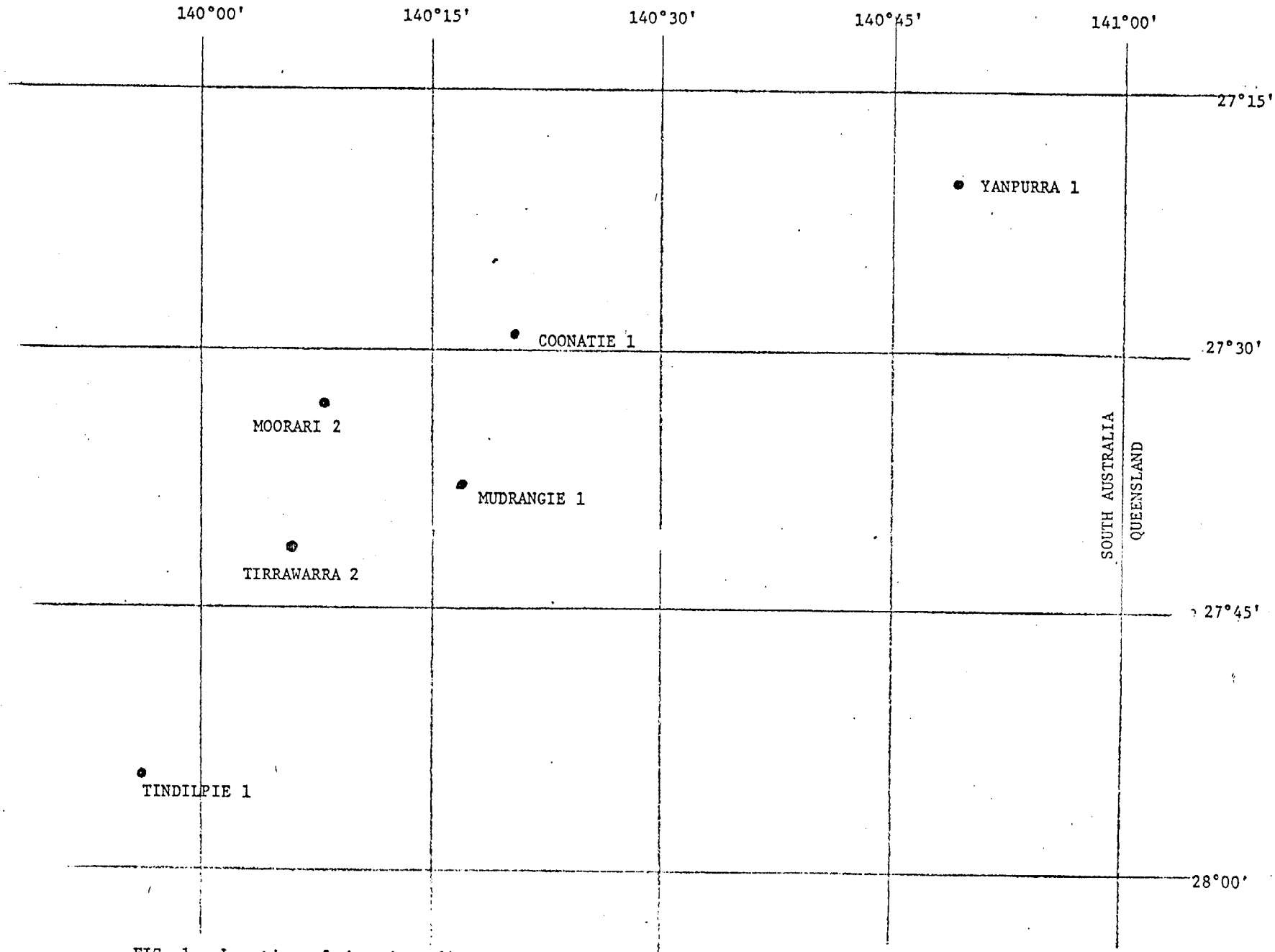

FIG. 1 Location of the six wells in the Patchawarra Trough of the Cooper Basin

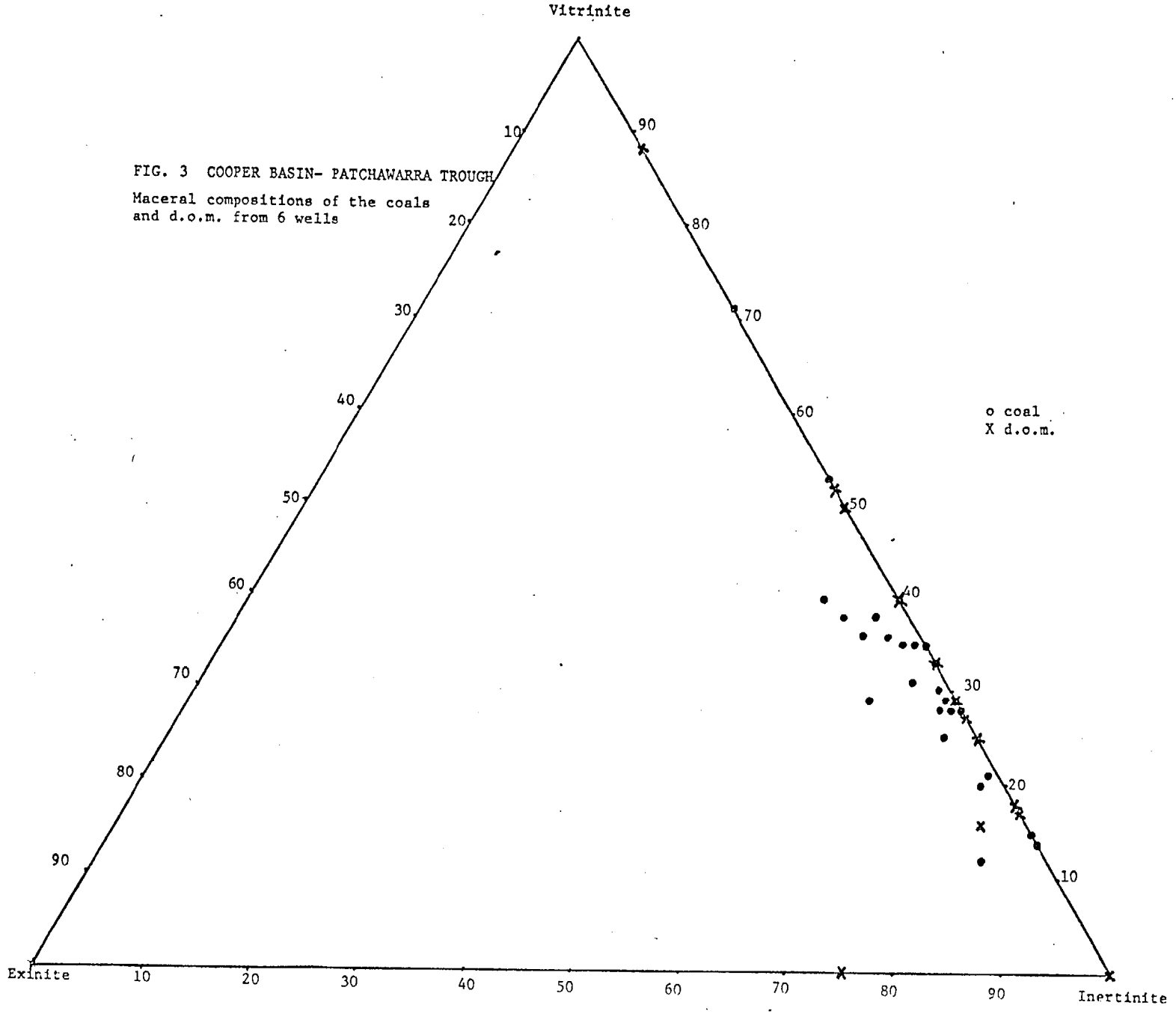

FIG. 3 COOPER BASIN- PATCHAWARRA TROUGH

Maceral compositions of the coals and d.o.m. from 6 wells

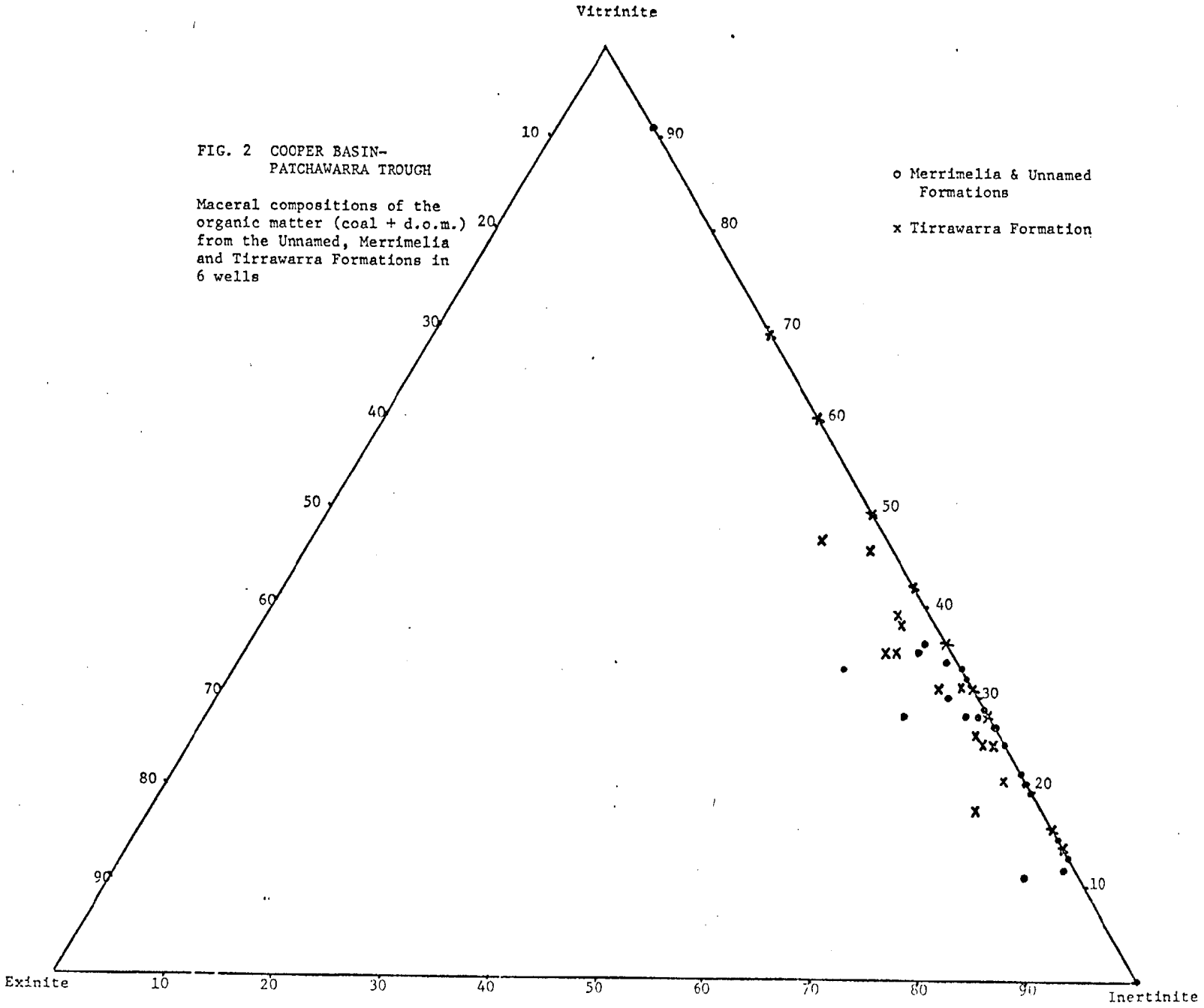

FIG. 2 COOPER BASIN-
PATCHAWARRA TROUGH

Maceral compositions of the organic matter (coal + d.o.m.) from the Unnamed, Merrimelia and Tirrawarra Formations in 6 wells

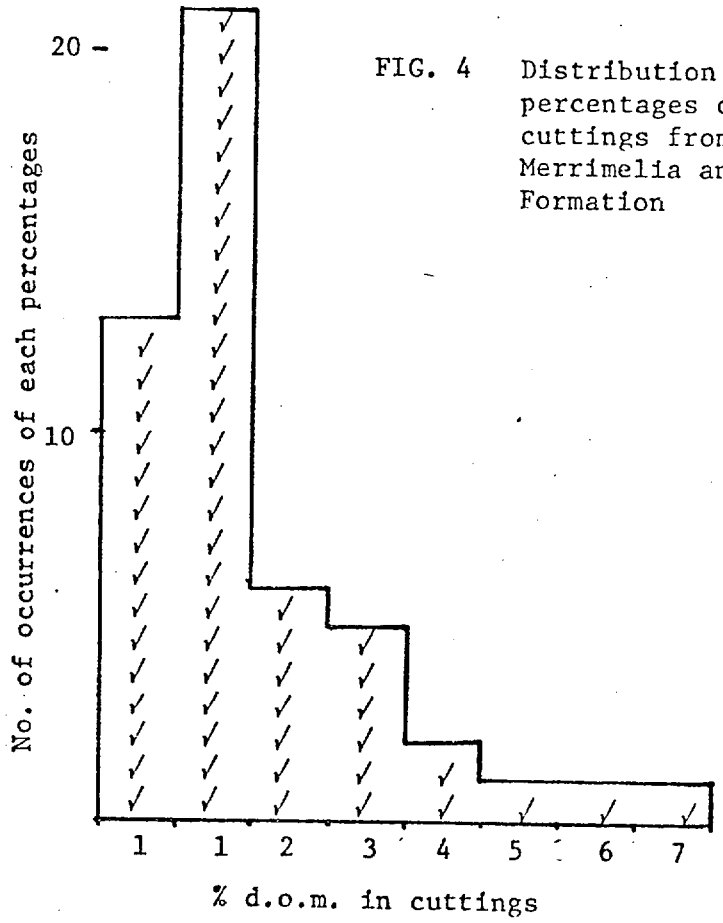

FIG. 4 Distribution of percentages of d.o.m. in cuttings from Unnamed, Merrimelia and Tirrawarra Formation

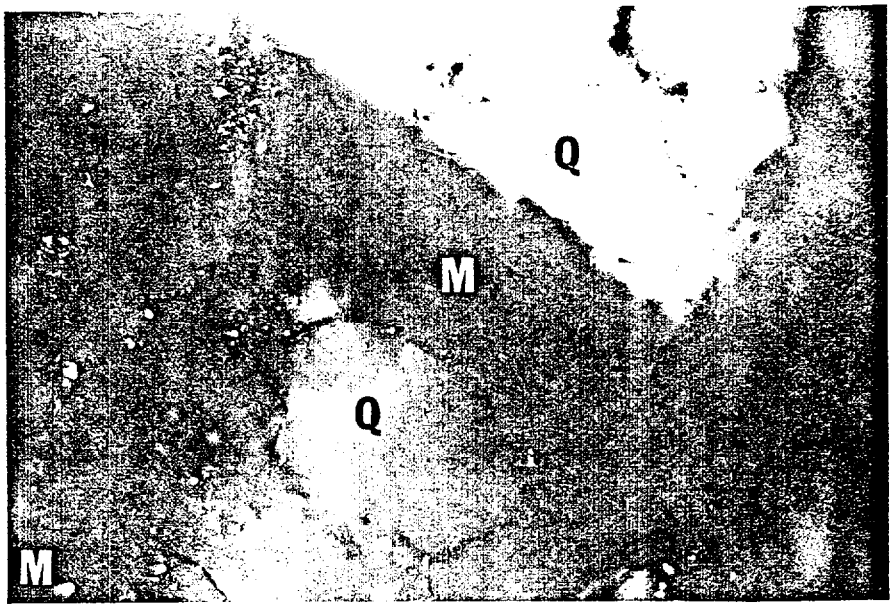

"Mobile organic matter" (M) between quartz grains (Q). Reflected light, oil immersion. Magnification x400.

00057

ASPECTS OF COAL TYPE AND RANK VARIATION, AND THEIR BEARING ON HYDROCARBON POTENTIAL IN SEVEN WELLS FROM THE SOUTHERN COOPER BASIN

BY

Tom Lonergan, B.Sc.

This thesis is submitted as partial fulfilment of the requirements for the Honours Degree of Bachelor of Science in Geology at The University of Adelaide.

November, 1979.

PAGE

CONTENTS

ABSTRACT

INTRODUCTION, AIMS

1. GEOLOGY 1

1.1 Regional Setting

1.2 Structural Control

1.3 Stratigraphy

2. WELLS 4

2.1 Wells Status

2.2 Sampling

2.3 Reflectance

2.4 Possible Sampling Bias

3. LITHOFACIES OF PRINCIPAL COAL-BEARING FORMATIONS 6

3.1 Permian

3.2 Jurassic

4. MACERAL CONTENT 10

4.1 Vitrinite

4.2 Inertinite

4.3 Exinite

5. COAL MICROLITHOTYPES 13

5.1 Jurassic

5.2 Permian

5.2.1 Toolachee Formation

5.2.2 Patchawarra Formation

6. VITRINITE REFLECTANCE 17

6.1 Techniques

6.2 Depth-Reflectance Profiles

6.2.1 Post-Triassic

6.2.2 Permo-Triassic

6.3 Lateral Rank Trends; South West Cooper Basin

6.3.1 Post-Jurassic

6.3.2 Permo-Triassic

7. BOTTOM HOLE TEMPERATURES AND PRESENT DAY GEOTHERMAL GRADIENTS 21

CONTENTS (Cont.)

		PAGE
8.	INTERPRETATION	22
8.1	Coal Microlithotypes	
8.1.1	Permian	
8.1.2	Jurassic	
8.2	Coal Maceral Groups	
8.2.1	Jurassic	
8.2.2	Permian	
8.3	Vitrinite Reflectance and Geothermal History	
8.3.1	Present Day Geothermal Gradients	
8.3.2	Rank Variation and Geothermal History	
8.3.3	Triassic Unconformity	
9.	HYDROCARBON ORIGIN, MIGRATION AND ENTRAPMENT	29
10.	HYDROCARBON POTENTIAL	31
10.1	Permo-Triassic	
10.2	Jurassic	
CONCLUSIONS		33
REFERENCES		34, 35, 36

FIGURES, TABLES, PLATES AND APPENDICES

FIGURE 1 -	Location and Structural Map	
2 -	Well Location Map	
3 -	Generalized Stratigraphy	
4 -	Stratigraphic Section and Coal Maceral Group Occurrence	Gidgealpa-7
5 -	Stratigraphic Section and Coal Maceral Group Occurrence	Moomba-2
6 -	Stratigraphic Section and Coal Maceral Group Occurrence	Big Lake-4
7 -	Stratigraphic Section and Coal Maceral Group Occurrence	Big Lake-3
8 -	Stratigraphic Section and Coal Maceral Group Occurrence	Murteree-1
9 -	Stratigraphic Section and Coal Maceral Group Occurrence	Toolachee-8
10 -	Stratigraphic Section and Coal Maceral Group Occurrence	Toolachee-3
11 -	Vitrinite, Exinite, Inertinite Content in Selected Formations	
12 -	Depth-Reflectance Gradients	Gidgealpa-7
13	Depth-Reflectance Gradients	Moomba-2
14 -	Depth-Reflectance Gradients	Big Lake-4
15 -	Depth-Reflectance Gradients	Big Lake-3
16 -	Depth-Reflectance Gradients	Murteree-1
17 -	Depth-Reflectance Gradients	Toolachee-8
18 -	Depth-Reflectance Gradients	Toolachee-3
19 -	Rank Profile of the Line of Section	
TABLE 1 -	Well Data	
2 -	Summary of vitrinite reflectance data	
3 -	Present Day Geothermal Temperatures	

FIGURES, TABLES, PLATES AND APPENDICES (cont.)

PLATE 1a - Vitrinite
b - Vitrinite
c - Vitrinite
2a - Clarite
- Duroclarite
- Duroclarite
3a - Vitrinertite
b - Duroclarite
c - Duroclarite

APPENDICES I - Sampling
II - Analytical Techniques
III - Data

Abstract

Seven wells along a line of section in the south Cooper Basin were studied. Examination of coals in Permian and Triassic sequences revealed marked vertical and lateral trends in vitrinite, inertinite and exinite content and their microlithotypes. Vitrinite content in the coals increases from the Permian to the Jurassic whilst exinite content increases over the major anticlinal trends. Variations in coal-sediment associations, maceral groups and microlithotypes suggest a complex and varying depositional environment.

Vitrinite depth-reflectance gradients indicated that coalification in the Permian and Jurassic was influenced by time of deposition, stratigraphic position, depth from basement, type of basement and extraneous geothermal influences. The inferred geothermal history of the basin varies complexly both in space and time.

Evidence suggests the coal in the presently producing Permian formations (Toolachee and Patchawarra Formations) is the source of commercial hydrocarbons found; being well placed for hydrocarbon generation.

Potential for further commercial hydrocarbon discoveries in the Permian is very good. Future small commercial hydrocarbon discoveries from Jurassic reservoirs appear likely with the Jurassic sediments, in many areas having attained suitable maturation stages for hydrocarbon generation and the coals and shales containing suitable hydrocarbon precursors.

Introduction and Aims

In this thesis seven wells (Figure 2) in the southern Cooper Basin, South Australia have been investigated using well completion reports, log data, core and rock cuttings and relevant papers in print. Emphasis has been placed upon examination of coal contained in cores and cuttings from the wells.

The wells studied (Table 1) are located along a line of section (Figure 2) which trends roughly south-east across the south western Cooper Basin.

Polished sections of particulate and cored coal were examined in detail using reflected white and U.V. light microscopy.

Vitrinite, exinite, inertinite content, microlithotypes present and depth-reflectance profiles were determined. Due to the abundance of coal in all wells there was no need to resort to using disseminated carbonaceous matter.

Measured vitrinite reflectances (% $\bar{R}_o$(max)) were used in conjunction with formation depth, present temperature gradients and stratigraphy; attempting to relate geothermal history with time, and depth of burial.

Vitrinite, inertinite and exinite content of the coals and their microlithotypes from the Jurassic and selected Permian Formations (Patchawarra Formation, Toolachee Formation) were investigated. Lateral and vertical variation of vitrinite, inertinite, exinite content and microlithotypes across the line of section was used to determine possible hydrocarbon source rock and its influence on hydrocarbon origin and potential in the Cooper Basin.

TABLE 1

WELL	CO-ORDINATES	SPONSOR	STATUS	DATE DRILLED
Gidgealpa-7	140° 00' 09.5"E 28° 02' 18.7"S	Delhi-Santos	Oil, Gas	1964-65
Moomba-2	140° 13' 37.36"E 28° 10' 56.85"S	Delhi-Santos	Gas	1966
Big Lake-3	140° 19' 00"E 28° 13' 14"S	Delhi-Santos-Vamgas	Gas	1972
Big Lake-4	140° 14' 18"E 28° 15' 29"S	Delhi-Santos-Vamgas	Gas	1972
Murteree-1	140° 34' 22"E 28° 23' 48"S	Pursuit Oil N.L.	Dry	1970
Toolachee-8	140° 47' 59"E 28° 23' 43"S	Delhi-Santos-Vamgas	Dry	1972
Toolachee-3	140° 46' 46.3"E 28° 27' 52.1"S	Delhi-Santos-Vamgas	Gas	1971

1. GEOLOGY

1.1 REGIONAL SETTING

The Cooper Basin (Figure 1) is a Permo-Triassic basin, lying in the north-east corner of South Australia and extends into south western Queensland. The Cooper Basin is oriented north east-south west and covers an area of approximately 127,000 sq. km. It is a Permo-Triassic intrabasin unconformably overlying earlier Palaeozoic basins and is in turn unconformably overlain by the Jurassic and Cretaceous sediments of the Eromanga Basin, part of the Great Artesian Basin.

The geology of the area has been described by Battersby (1976). The following brief outline relies heavily upon this work.

1.2 STRUCTURAL CONTROL

Sedimentation in the Cooper Basin has been influenced by four prominent structural highs (Figure 1). The basin is bounded by three prominent structural highs (Figure 1). The southern limit is an irregular boundary controlled by Proterozoic rocks of the Kopperamanna-Naryilco High. The Kopperamana-Warbreccan High,consisting of Proterozoic rocks forms the western boundary of the basin. The north eastern boundary of the basin is controlled by the Cannaway Ridge. The major basement ridge within the Cooper Basin is the Arrabury-Karmona Anticlinal Trend. This trend running approximately east-west divides the basin in two and separates the southern part of the basin, an area of thick Permian sedimentation from the northern part of the basin, an area of thick Triassic sedimentation.

The southern area of the basin which outlines the seven wells investigated is discussed in detail in this thesis. The structure of the southern part of the Cooper Basin is controlled by two prominent anticlinal trends (Figure 1,2) Gidgealpa-Merrimelia-Innaminicka Trend and the Murteree-Nappacoongee Trend which divide the basin into three major depositional troughs; the Patchawarra Trough, Nappamerri Trough and the Tenneppera Trough. The two anticlinal trends are sinuous and give rise to additional trends of generally similar northeast-southwest attitude.

The tectonic history has been detailed by Battersby (1976) and his summary of the tectonic history of the Cooper Basin is given:

1. deposition of marine Cambrian and Ordovician sediments.
2. major orogeny in Late Silurian to Early Devonian.
3. a period of folding, faulting and erosion.
4. epeirogenic downwarping in Late Carboniferous to Early Permian.
5. deposition of continental Permo-Triassic with contemporaneous faulting along major pre-Permian structural trends.
6. uplift and erosion in Middle-Late Triassic.
7. epeirogenic downwarping of most of Eastern Australia.
8. continental Jurassic deposition.
9. marine transgression in the Early Cretaceous and regression in the Late Cretaceous.
10. regional folding (monocline formation) and faulting in the Tertiary.

1.3 STRATIGRAPHY

The stratigraphy of the Cooper Basin has been extensively documented by Gatehouse (1972), Battersby (1976) and Thornton (1978) and the Eromanga Basin by Nugent (1968). A generalized stratigraphic column is presented in Figure 3. The stratigraphy of the major Permian coal-bearing formations and the Jurassic formations is briefly outlined, based, primarily, upon discussion by the aforementioned authors.

Patchawarra Formation

The Patchawarra Formation conformably overlies the Tirrawarra Sandstone. It is the thickest formation in the Gidgealpa Group (Figure 3).

The Patchawarra Formation consists of sandstones and shales, containing abundant coal and minor conglomerate. It is widespread throughout the Cooper Basin being thickest in the Patchawarra Trough. Evidence suggests that the Patchawarra Formation sediments were deposited by a northward flowing deltaic-fluvial system (Thornton 1978, Battersby 1976). Facies studies (Thornton 1978) indicate a central area dominated by channel deposits with surrounding areas dominated by overbank and swamp deposits. The uppermost Patchawarra Formation sediments indicate a senile topography incapable of supplying sufficient sediment to prevent inundation of the subsiding basin.

00066

Toolachee Formation

The Toolachee Formation consists of fine grained grey sandstones, shales and abundant coal deposited under a fluvial regime. The Toolachee Formation is a thick (Figure 3), widespread unit which has little thickness variation indicating deposition on a peneplaned erosion surface (Battersby 1976). Some areas of the anticlinal trend may have escaped mantling by Toolachee sediments.

Two lithological units have been delineated in the Toolachee Formation (Gatehouse 1972). The lower unit is dominantly point bar and channel sands whilst the upper unit contains coals and shales. This suggests a deltaic sequence ranging from a river dominated basal unit to a ponded lacustrine upper unit (Battersby 1976).

Jurassic

Jurassic sedimentation marked resumed subsidence in the area and formation of the Eromanga Basin. The sediments are typically thick clean sandstone units with minor interbedded shales and minor, often lenticular coal seams. The sediments indicate a fluvial depositional environment (Nugent 1968).

COOPER BASIN

STRUCTURAL ELEMENTS

FIGURE 1

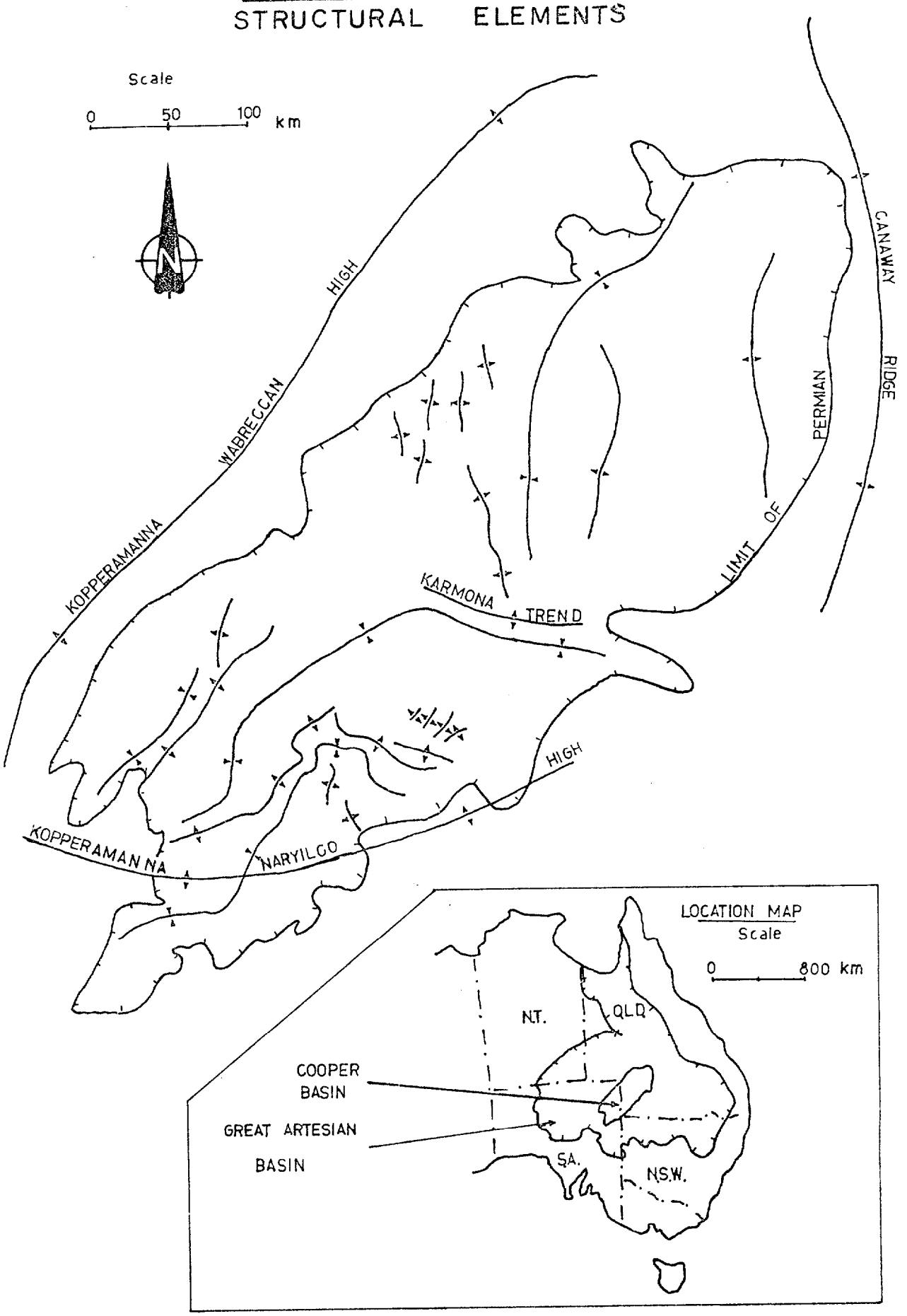

FIGURE 2

SOUTH COOPER BASIN

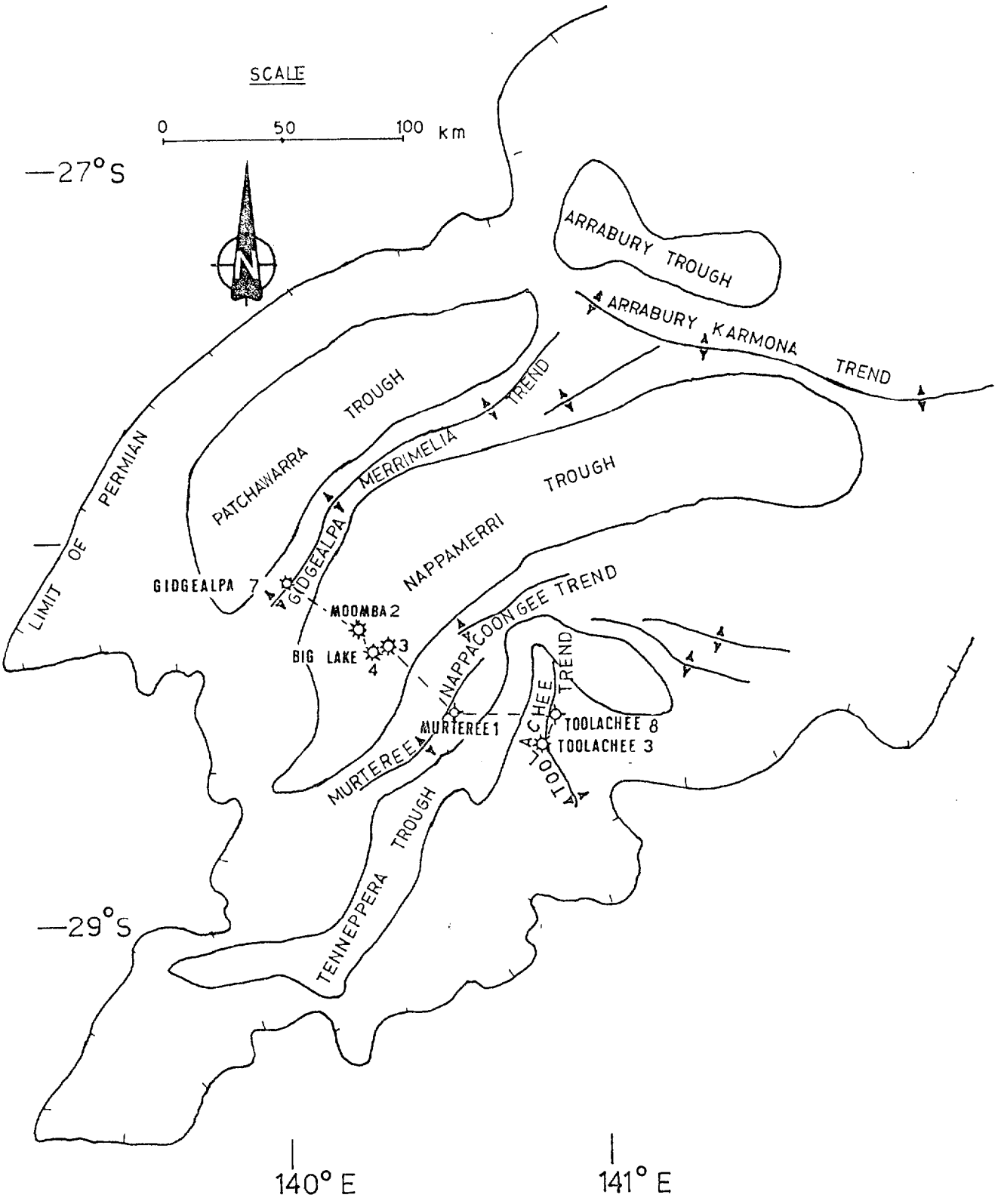

FIGURE 3

COOPER BASIN

GENERALIZED STRATIGRAPHY

PERIOD	EPOCH	STAGE	FORMATION (MAX. THICKNESS IN m)	HYDRO-CARBONS	ENVIRONMENTS
QUATERNARY & TERTIARY			UNNAMED		
CRETACEOUS	UPPER	CENOMANIAN	WINTON FM		FLUVIAL – LACUSTRINE
	LOWER	ALBIAN	TAMBO FM		SHALLOW MARINE
		APTIAN	ROMA FM		SHALLOW MARINE
		NEOCOMIAN	TRANSITION BEDS		SHALLOW MARINE
JURASSIC	UPPER		MOOGA FM		FLOOD PLAIN
	MIDDLE		BIRKHEAD FM	☼ ⊖	LACUSTRINE
	LOWER		HUTTON SS	⊙ ☼	FLUVIAL
TRIASSIC	MIDDLE TO LOWER		NAPPAMERRI FM 494	☼	LACUSTRINE – FLUVIAL
PERMIAN	UPPER	TARTARIAN	GIDGEALPA GROUP: TOOLACHEE FM 158	☼	FLUVIAL
		KAZANIAN			
	LOWER	ARTINSKIAN	DARALINGIE BEDS 95		DELTAIC
			ROSENEATH SH 81		LACUSTRINE
			EPSILON FM 88	☼	DELTAIC
			MURTEREE SH 79	☼	LACUSTRINE
			PATCHAWARRA FM 681	☼	UPPER-DELTAIC
			MOORARI BEDS	☼	FLOOD PLAIN
		ARTINSKIAN TO SAKMARIAN	TIRRAWARRA SS 122	⊙	FLUVIAL
		SAKMARIAN	MERRIMELIA FM 396		PERIGLACIAL
CARBONIFEROUS			GRANITE INTRUSION		
DEVONIAN			INNAMINCKA RED BEDS		
PRE-DEVONIAN			UNNAMED		

Beddoes 1973

00070

2. WELLS

Seven wells (see introduction) formed the basis of coal maceral and reflectance study. The wells follow a line from the Gidgealpa Field to the Toolachee Field, (Figure 2). All wells were drilled on structure within the Permian -

Gidgealpa-7	Gidgealpa-Merrimelia Trend
Moomba-2	Nappamerri Trough
Big Lake-4	Nappamerri Trough
Big Lake-3	Nappamerri Trough
Murteree-1	western flank of the Tennappera Trough
Toolachee-8	Toolachee Trend
Toolachee-3	Toolachee Trend

The selection of the wells was intended to give a sufficiently good coverage of the anticlines and troughs in the Cooper Basin and to extend information already obtained from other wells.

2.1 WELL STATUS

Gidgealpa-7	wet gas and oil production from the Toolachee Formation and Patchawarra Formation and Tirrawarra Formation.
Moomba-2	gas production from the Toolachee Formation.
Big Lake-4	dry gas production from the Toolachee Formation.
Big Lake-3	dry gas production from the Toolachee Formation.
Murteree-1	dry hole with minor gas shows in Toolachee Formation
Toolachee-8	dry hole with minor gas shows in the Toolachee Formation.
Toolachee-3	suspended producer, gas from the Patchawarra Formation.

The principal gas producing formations within the Permian of the Cooper Basin are the Toolachee Formation and the Patchawarra Formation. Minor gas production has come from the Daralingie Beds, Epsilon Formation and rarely the Tirrawarra Sandstone and Nappamerri Formation. Gidgealpa, Big Lake and Moomba in the southern area of the Cooper Basin are at present the only producing fields.

Jurassic and Cretaceous sediments have in the past been neglected in consideration of oil and gas potential. However recent exploration has discovered good oil occurrences in the Jurassic at Strzlecki-3 and Dullingari North-1.

2.2 SAMPLING

Coal was found in all wells studied from Permian to Tertiary sediments (where available), being particularly abundant in the Permian and Jurassic sequences. The Toolachee and Patchawarra Formations contained the best coal seams in the Permian, while all the Jurassic formations contained some coal seams.

00071

Sampling of the wells was restricted by availability of cuttings (APPENDIX I). Only Murteree-1 was sampled to total depth. In the other wells, sampling was commenced at any interval between the basal Cretaceous and the Triassic.

Examination of the coals was done using samples from cuttings and in a few cases, coal cut from core. Polished sections were used exclusively, with a total of 175 polished sections being examined.

Sampling was subject to availability of sufficient coal in the cuttings and all polished samples were examined for microlithotype content and associations. Because the coal analyses were carried out on particulate samples the coal petrology is based on microlithotypes only, see APPENDIX II for nomenclature.

2.3 REFLECTANCE

Reflectance Measurements were made subject to polish, suitability, etc. (see APPENDIX II) and the coverage of the wells varied accordingly, thus:

	No. of Polished Sections	No. of sections suitable for reflectance measurements
Gidgealpa-7	25	21
Moomba-2	27	20
Big Lake-4	33	26
Big Lake-3	35	26
Murteree-1	16	12
Toolachee-8	21	21
Toolachee-3	18	8

2.4 POSSIBLE SAMPLING BIAS

During examination of polished sections a potential selective bias emerged when vitrinite, inertinite and exinite content were being determined (APPENDIX I). Examination of closely spaced cuttings and core yielded a 15-30% greater relative content of vitrinite in the core samples. This feature can probably be attributed to the generally lower density of vitrinite compared to inertinite and the greater fracturing ability of vitrinite. Thus vitrinite is likely to be concentrated in the finer fractions of the cuttings, which float off in the drilling mud and are lost.

00072

3. LITHOFACIES OF PRINCIPAL COAL-BEARING FORMATIONS

The macroscopic relationships of the coals and minerogenic sediments found in the Cooper Basin have been based principally upon well completion reports and well log data. Study of the few cores taken assisted in determining such relationships.

Permian and Triassic sediments in the Cooper Basin were logged in detail and control is very good. The Jurassic to Recent lithologies were not described in similar detail and as such control is not as good as in the Permo-Triassic.

The coal petrography of the Permian Tirrawarra Sandstone, Patchawarra Formation and Toolachee Formation and Jurassic sediments was examined because of the suspected hydrocarbon potential of these sediments.

3.1 PERMIAN

A. Tirrawarra Sandstone

The Tirrawarra Sandstone in all wells where it occurs (Gidgealpa-7) contains only rare coals associated with the sandstones. The coals are lenticular in occurrence.

B. Patchawarra Formation

The Patchawarra Formation contains abundant coals in the sediments. The thickest and most numerous coal seams occur in Big Lake-3 and Big Lake-4 which also contain the thickest Patchawarra Formation.

Gidgealpa-7
- contains approximately 9m of coal (total thickness) in 4 seams.
- all coal seams are surrounded by sandstone and silty-sandstone.

Moomba-2
- contains 4m of coal (total thickness) in 4 seams of similar thickness.
- all coal seams have a sandy-siltstone base and a shale top.

Big Lake-4
- contains approximately 60m of coal (total thickness) in many seams .
- coal seams are thickest in the upper and middle Patchawarra Formation.
- upper-formation coals have sandy-siltstone bases and thin shale tops grading into sandstone.
- middle-formation coals have sandy-siltstone bases and sandstone tops.
- lower-formation coals have siltstone-shale bases and tops.

99073

Big Lake-3
- contains approximately 60m of coal (total thickness) in many seams.
- coal seams are thickest in the central Patchawarra Formation with 15m seam at 2866m.
- sediment-coal relationships vary; however the thickest seams have a shale base and sandstone top.

Murteree-1
- contains approximately 16m of coal (total thickness) in 15 seams with 4 major seams.

Toolachee-3
- contains approximately 8m of coal in 10-12 seams (thickest seam 3m).
- coals occur throughout the formation.
- most seams have sandstone bases and shale tops while 2-3 seams have a reverse sequence to this and 3 minor seams; shale tops and bottoms.

Toolachee-8
- contains approximately 12m of coal in many seams (thickest seam 3.5m).
- coals occur in the middle and lower part of the formation.
- almost all seams excepting very minor upper coal seams have shale tops and bottoms.

C. Toolachee Formation

The Toolachee Formation contains abundant coal in the sediments. The thickest coal seams occur in Big Lake-3 and Big Lake-4 in the Nappamerri Trough.

Gidgealpa-7
- contains approximately 9m of coal in 4 principal seams.
- major seams have sandstone or silty-sandstone bases and tops.

Moomba-2
- contains 20-30m of coal in many seams.
- the majority of the seams occur in the middle and upper part of the formation.
- the upper seams have siltstone and sandy siltstone bases and tops.
- the middle seams generally have shale bases and tops.

Big Lake-4
- contains approximately 15m of coal in 16 seams (thickest 6m).
- principal seams occur in the middle and Upper Toolachee Formation.
- all major seams have shale bases and sandstone-siltstone tops.

00074

Big Lake-3
- contains 20-25m of coal in 15 seams.
- coals occur throughout the formation.
- sedimentary environment of the coal is variable, however the major seams usually have siltstone bases sandy-siltstone tops.

Murteree-1
- contains approximately 10 seams up to 3m thick.
- coals occur throughout the formation.
- major seams have shale bases and sandstone tops with the smaller seams having shale bases and tops.

Toolachee-8
- contains 15 main seams with seams up to 6m in thickness.
- the best coal seams occur in the middle and lower part of the formation.
- most of the best seams have shale tops and bottoms with minor seams generally having a shale base and sandstone-siltstone top.

Toolachee-3
- contains 10-11 coal seams up to 8m thick.
- coal occurs throughout the formation with the upper and lower part of the formation containing the best coal seams.
- the upper seams (including the 8m seam) have a shale base and sandstone top or a sandstone top and base.
- the lower seams have a shale base and a thin siltstone top grading into sandstone.

3.2 JURASSIC

From electric log data and well completion reports the Jurassic sediments do not contain thick coal seams. The seams are generally less than 1m and are often lenticular. The Mooga Formation and Hutton Sandstone contain most of the coal seams present in the sequence.

Gidgealpa-7
- contains minor coal, generally lenticular in occurrence, throughout the Jurassic.
- the coals are generally associated with shales except in the Mooga Formation where the coals have a sandstone top and base.

Moomba-2
- contains many coal seams throughout the Hutton Sandstone and Mooga Formation with minor coals in other formations.
- the seams are generally thin; 0.5m or less.
- the upper coal seams of the upper Mooga Formation are surrounded by shales whilst the coal seams in the lower Mooga Formation have sandstone or sandy-siltstone bases and tops.

Moomba-2 (cont.)	-	the Hutton Sandstone contains coals with siltstone-shale bases and siltstone tops.
Big Lake-4	-	minor coal seams occur throughout the Hutton Sandstone, Birkhead Formation and Mooga Formation. Seams are up to 0.5m thick.
	-	in the Birkhead Formation and Mooga Formation most seams are associated with shales, whilst in the Hutton sandstone seams have sandstone tops and shale bases or vice versa.
Big Lake-3	-	contains very minor coal which appears to be lenticular.
Murteree-1	-	the electric logs indicate little coal. However lithological descriptions of the cuttings record 5% of Mooga Formation as coal and the upper Hutton Sandstone containing 10% coal.
	-	the Birkhead Formation contains only very minor coal seams.
	-	the Mooga Formation and Hutton Sandstone coals are thin and have siltstone-sandstone bases and tops.
Toolachee-8	-	contains minor, thin coal seams in all formations which appear related to shales and siltstones.
Toolachee-3	-	contains minor, thin coal seams in the Mooga Formation and Hutton Sandstone.
	-	the coal seams are associated with sandstones and siltstones.

The Permian coal seams of the Patchawarra Formation and Toolachee Formation are numerous, generally thick and continuous. The coal seams in the Jurassic are generally thin and lenticular, with the Mooga Formation and Hutton Sandstone containing the most numerous coal occurrences.

The coal seams observed in the Patchawarra Formation, Toolachee Formation and the Jurassic are generally associated with sandstone-sandy-siltstone-siltstone minerogenic sediments.

00076

4. MACERAL CONTENT

The coals in the seven wells were analysed and histograms (Figures 4-10) showing vitrinite, inertinite and exinite content produced. Triangular plots of these three coal maceral groups (Figure 11) were prepared for coals from Patchawarra Formation, Toolachee Formation and the sampled Jurassic.

The individual maceral groups - vitrinite, inertinite, exinite varied considerably in their abundance in each of the polished sections. Despite this several broad trends were observed in all wells.

4.1 VITRINITE

Vitrinite is the dominant maceral group found in the coals of all wells. Tellocollinite (vitrinite A) (Plate 2, A) and desmocollinite (Plate 3, B) are the dominant vitrinite macerals. Other vitrinite macerals which occur are tellinite (Plate 1, A,B), vitrodetrinite (Plate 3, C) and rare collinite (Plate 1, A). Tellocollinite constitutes the structureless (apparent) thicker bands of vitrinite and is found in all wells studied. Tellinite and collinite are generally associated. Tellinite outlines the original cellular structure and is often filled with collinite (Plate 1, A) and more rarely resinite (Plate A6). Desmocollinite occurs as the groundmass in many of the clarites, duroclarites and clarodurites. Original plant structures in the vitrinite are progressively destroyed or masked during burial, such that often the Permian coals, particularly those in the Nappamerri Trough, no longer show original lumen.

There is a general tendency for vitrinite content to increase from the Permian to Jurassic in all the wells examined. Tellocollinite is the most abundant vitrinite sub-maceral, although in the Permian (upper Toolachee Formation and Patchawarra Formation) of the Nappamerri Trough, desmocollinite is the dominant form of vitrinite. This observed increase in the vitrinite content of the coals with decreasing age could reflect the greater compaction in response to load, of vitrinite as compared to inertinite. The Nappamerri Trough is the focus of the greatest Permo-Triassic sedimentation and consequently the Permian coals experience high load pressures.

4.2 INERTINITE

Inertinite content generally decreases from the Permian (20-50%) to the Jurassic (5-30%). Fusinite (Plate 2, C) semifusinite (Plate 3, A) and inertodetrinite (Plate 3, C) are the most dominant inertinite macerals. Scloterinite does occur but is rare. In the Jurassic and Cretaceous, inertodetrinite and semifusinite are the most common inertinite macerals.

00077

Fusinite content increases to 20-30% of total inertinite content in the Permian sediments at the expense of semifusinite. The high percentage (up to 70%) of fusinite versus semifusinite in the Permian of the Big Lake wells indicates a higher degree of oxidative degradation of the original plant tissue (Stack 1975, p.98).

4.3 EXINITE

Exinite occurs throughout the coals of the seven wells. Sporinite (Plates 2, C; 6, C), resinite (Plates 2, B; A3, A, B,C), cutinite (Plates 2, A,B) and minor liptodetrinite (Plate 3,C) were recognised. Sporinite was the dominant exinite maceral, generally comprising 60% - 90% of the total exinite. The spores, almost without exception, were small (microspores) and thin walled (tenuispores). Above 1.2-1.4% vitrinite reflectance, exinite becomes difficult to distinguish from vitrinite. Hence no attempt was made to determine exinite percentages in the higher rank coals. The changing reflectances of the three maceral groups with increasing rank has been examined in Murteree-1 and the results gave a good correlation with the work of G. Smith (1979) (Appendix II).

The fluorescence of exinites when examined in ultra-violet light is a very useful tool for locating exines in polished sections of coal (Appendix II). This fluorescence was useful in determining the exinite content of cuttings sample with a high clay content, and in recognising the presence of resinite in vitrinite (tellinite) lumens (Appendix II).

Exinites are most common in the Jurassic formations and in the Permian Toolachee Formation constituting up to 20% at 1686m in Toolachee-8 (Figure 9), but generally 3%-5%. Exinite content is highest over major anticlinal structures as represented by Gidgealpa-7, Murteree-1, Toolachee-3 and 8 (Figure 19). Exinite content is 3-5% in these wells with only a marginal decrease with depth. The eastern wells Murteree-1, Toolachee-3 and 8 have the highest exinite content. In these wells resinite and cutinite are often the dominant exinite macerals. Resinite constitutes 40-50% of total exinite in some of the coals in the Toolachee Formation at Murteree-1, Toolachee 3 and 8. A cutinite content of 10-20% of total exinite is common in the Jurassic Hutton Sandstone and Birkhead Formation and in the Permian Toolachee Formation and Patchawarra Formation of Toolachee-8, Toolachee-3 and Murteree-1. Cutinite in samples from 1821m and 2068m in Murteree-1 comprises up to 40% of total exinite.

00073

Gidgealpa-7 is the only other well in which coals have a significant cutinite content (up to 20% of total exines). As in the eastern wells, the cutinite is concentrated in the lower Jurassic and in the Toolachee Formation and Patchawarra Formation. A high resinite content commonly coincides with a relatively high cutinite content.

The pattern of exinite occurrence which emerges for the south western Cooper Basin is one of enhanced exinite concentration over the major anticlinal trends, with coals in the Nappamerri Trough being generally exinite-poor. Pre-Jurassic coals in the Nappamerri Trough appear to contain less exinite than those on the anticlinal trends and in the Tenneperra Trough, bearing in mind that the original exinite content of Permian coals for which vitrinite reflectance is >1.2%-1.4% is not known.

00079

5. COAL MICROLITHOTYPES

The associations of the maceral groups is extremely variable, both within the same formations and throughout the basin. Microlithotypes (Appendix II) and their mode of occurrence were examined in the Jurassic formations and the Permian Toolachee Formation and Patchawarra Formation. Coal samples from the Toolachee and Patchawarra Formations were sufficiently numerous to permit a meaningful analysis of microlithotypes. The Jurassic formations do not have good control due to paucity of samples, but nonetheless have been considered because of the good petroleum source rock potential of Jurassic sediments in the Cooper Basin (D.M. McKirdy pers. comm. 1979).

The results of microlithotype analysis of Jurassic and Permian (Toolachee and Patchawarra Formations) coals are outlined on a well by well basis.

5.1 JURASSIC

Gidgealpa-7 (complete section)

- vitrite (Plate A1, A ,B) and clarite (v) (Plate 2, A) with duroclarite (Plate 2, C) common in the Walloon C.M. and Hutton Sandstone.
- carbargilite content low in the middle and lower Jurassic. It constitutes up to 50% of the sample cuttings in the upper Mooga Formation.
- pyrite present in the upper Mooga Formation.
- detrital, granular "degrado" textures (Plate 1,C) towards the upper Jurassic.

00080

Moomba-2 (complete section)	-	vitrinite, clarite (v) with minor durite and duroclarite in the Hutton Sandstone and lower Mooga Formation.
	-	vitric carbargilite (10%) occurs in the Mooga Formation and the lower Hutton Sandstone.
	-	detrital textures increase toward the basal Hutton Sandstone.
Big Lake-3 (basal Hutton Sandstone)	-	duroclarite (v) and cannel coal (Plate 3, C) in the basal Hutton Sandstone.
	-	vitric carbargilite is present throughout the coals.
	-	detrital, "degrado" textures increase towards the basal Hutton Sandstone.
Murteree-1 (complete sequence)	-	vitrite, clarite (v) and duroclarite (v).
	-	vitritic carbargilite present throughout.
	-	carbonate (siderite) and minor pyrite in the Hutton Sandstone.
	-	"degrado" - detrital textures appear to increase in the basal Hutton Sandstone.
Toolachee-8 (basal Hutton)	-	vitrite and clarite (v).
	-	few detrital textures.

5.2 PERMIAN

6.2.1 Toolachee Formation

Gidgealpa-7	-	duroclarite (v) and minor vitrite.
	-	vitric and minor duritic carbargilite.
	-	granular detrital textures increase toward the upper Toolachee Formation.
	-	carbonate is common in the central Toolachee Formation.
	-	granular, detrital, "degrado" textures increase towards the upper Toolachee Formation.
Big Lake-3	-	clarodurite, duroclarite (v) and minor vitrinertite (Plate 3, A) in the upper Toolachee Formation and duroclarite (v) and clarite (v) in the lower Toolachee Formation.
	-	minor vitritic and duric carbargilite occurs in the upper Toolachee Formation.
	-	granular detrital textures increase toward the upper Toolachee Formation.

00081

Murteree-1
- duroclarite (v) and vitrinertite.
- minor carbonate and pyrite is present.
- insufficient samples for textural trends, but possibly detrital textures increase towards the basal Toolachee Formation.

Toolachee-8
- vitrite, clarite (v) and duroclarite (v) in the upper Toolachee Formation and duroclarite (v) and clarite (v) in the lower Toolachee Formation.
- minor pyrite in the upper Toolachee Formation.
- textural trends indicate detrital textures in the coals in the mid-Toolachee Formation.

Toolachee-3
- duroclarite (v) and minor clarite (v).
- rare carbonate (siderite) present in the mid-Toolachee Formation.
- detrital textures increase towards the upper Toolachee Formation.

5.2.2 Patchawarra Formation.

Gidgealpa-7
- vitrite, clarodurite in the upper Patchawarra Formation and clarite (v) and duroclarite (v) in the lower Patchawarra Formation.
- vitric carbosilicite and vitritic and duritic carbargilites occur in the upper Patchawarra Formation

Moomba-2
- vitrinertinite.
- vitric and duritic carbargilite in the central and upper Patchawarra Formation.
- granular, detrital textures increase toward the upper Patchawarra Formation.

Big Lake-4
- vitrinertite with minor inertite in the lower Patchawarra Formation.
- vitric and duritic carbargilite occurs in the central and upper Patchawarra Formation.
- detrital textures increase toward the upper Patchawarra Formation.

Big Lake-3
- vitrinertite and minor cannel coals in the upper Patchawarra Formation.
- minor carbonate.
- detrital and "degrado" textures increase toward the upper Patchawarra Formation.

00082

Murteree-1	-	clarite (v), duroclarite (v) and minor vitrinertite in the basal Patchawarra Formation.
	-	detrital textures decrease from the basal Patchawarra Formation.
Toolachee-8	-	clarite (v) and duroclarite (v) and minor durite.
	-	carbonate in the central and lower Patchawarra Formation.
	-	detrital "degrado" textures increase towards the upper Patchawarra Formation.
Toolachee-3	-	duroclarite (v) and minor vitrite.
	-	carbonate in the basal Patchawarra Formation.
	-	detrital textures increase toward the upper Patchawarra Formation.

In conclusion the dominant microlithotypes are vitrite, clarite and duroclarite with lesser vitrinertite and clarodurite. Where there was sufficient sampling there was a broad increase or decrease in the detrital aspect of the coal and/or naturally oxidized coal content in each of the sequences examined.

The Jurassic coals consist principally of vitrite and clarite. Where clarite occurs the exinite content in the clarite is usually high. The Permian coals consist principally of duroclarite and vitrinertite. The Permian coals of Moomba-2 and Big Lake 3 and 4 in the Nappamerri Trough have a considerably higher vitrinertite content than the other wells examined.

Pyrite and carbonate occurs at several intervals in the Jurassic and Permian in all wells. However percentage content of total cuttings was small.

FIGURES - 4-10

STRATIGRAPHIC SECTION

AND VITRINITE, INERTINITE, EXINITE

AS PERCENTAGE OF TOTAL COAL CONTENT OF

SELECTED POLISHED SECTIONS.

GIDGEALPA NO.7

FIGURE 4

STRATIGRAPHIC SECTION

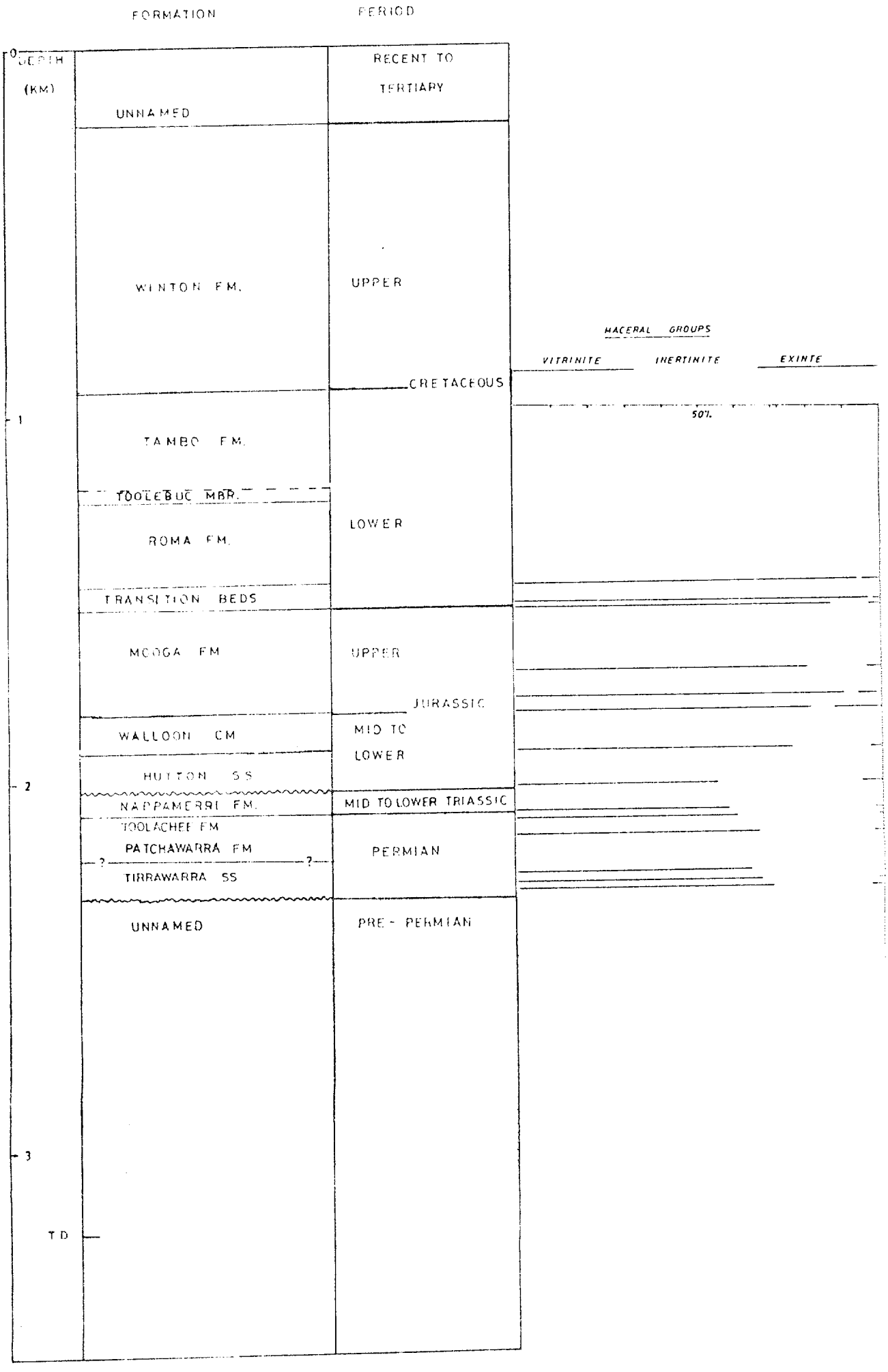

MOOMBA NO 2 FIGURE 5

STRATIGRAPHIC SECTION

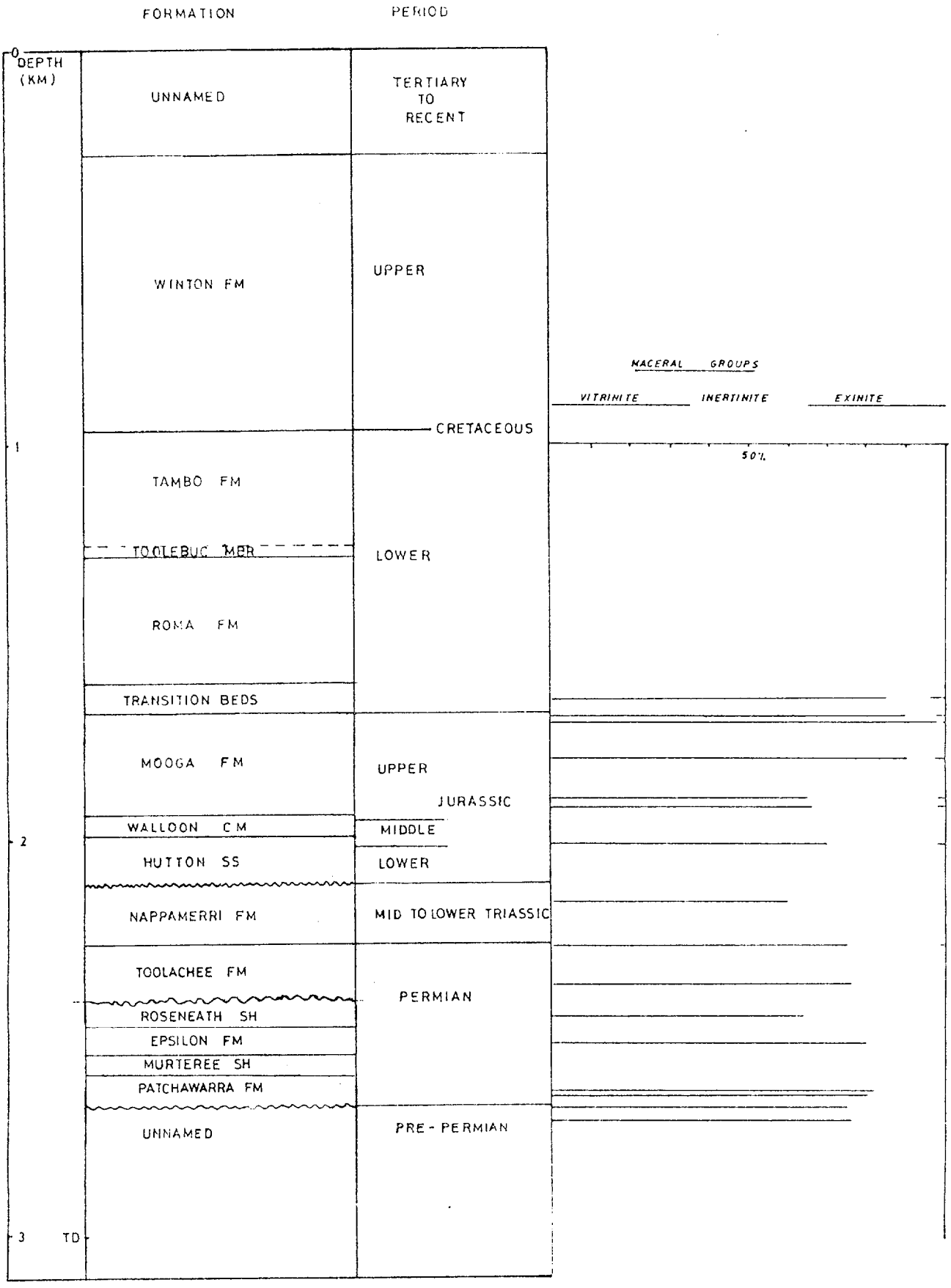

BIG LAKE NO 4

FIGURE 6

STRATIGRAPHIC SECTION

00086

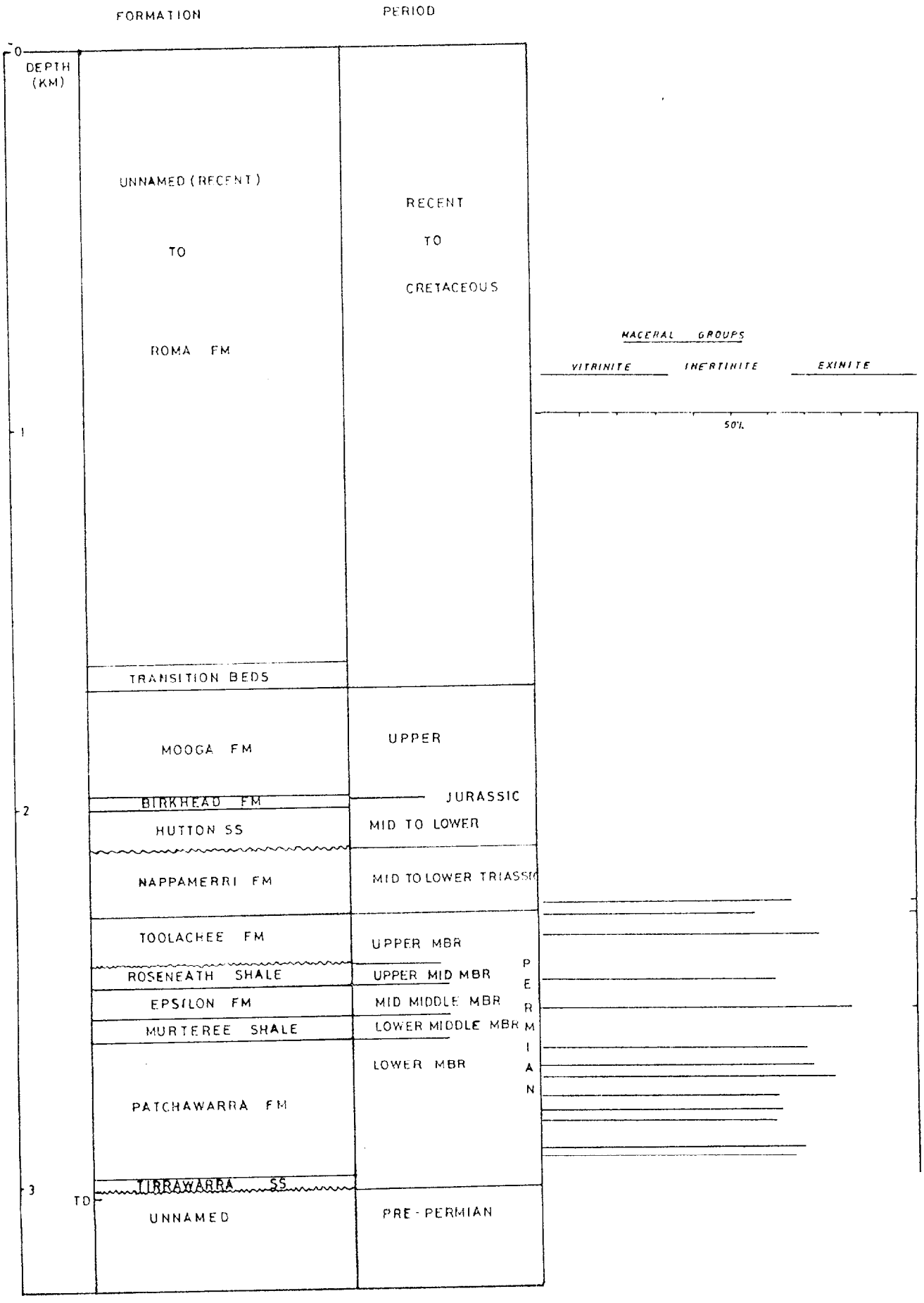

BIG LAKE NO 3

FIGURE 7

00087

STRATIGRAPHIC SECTION

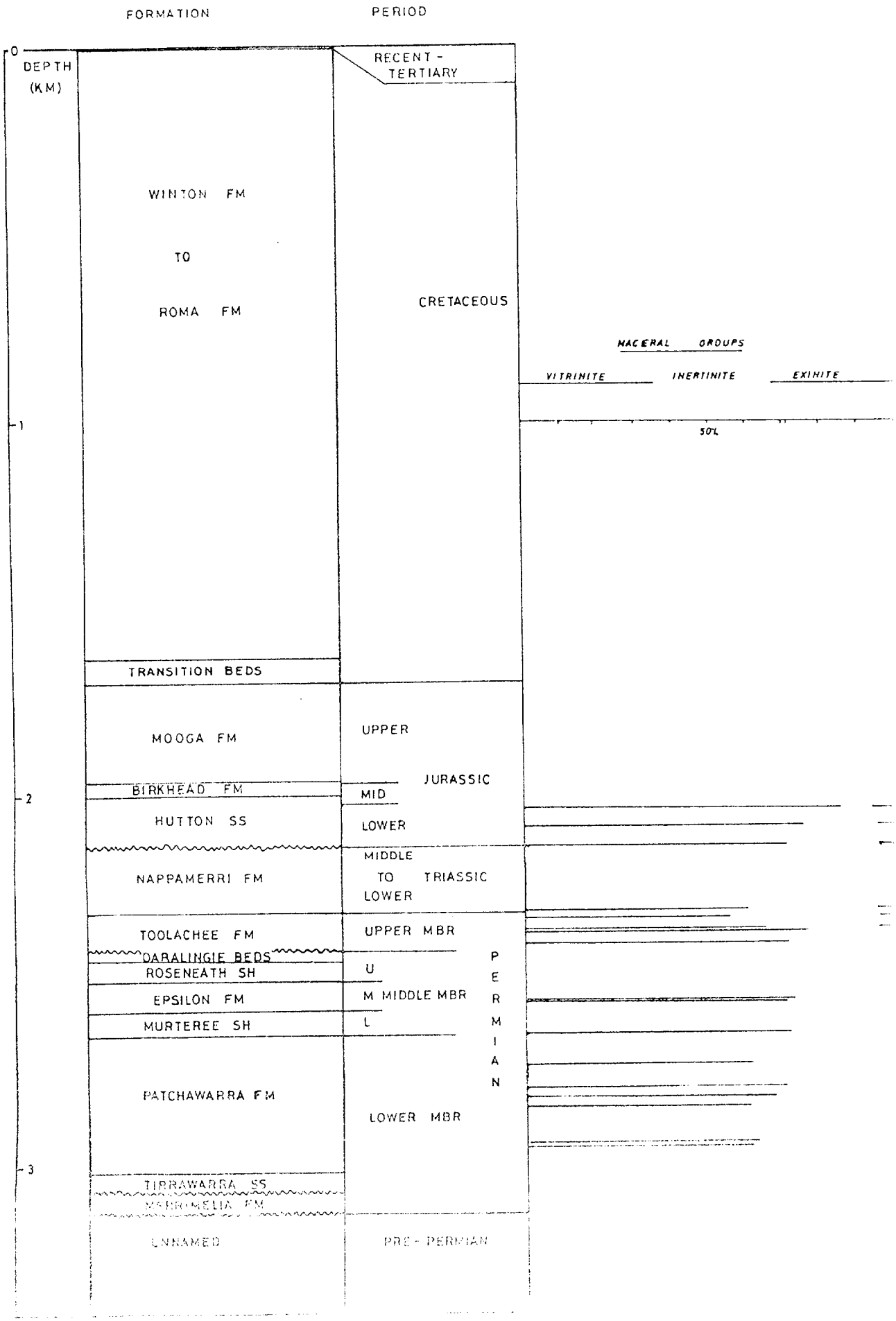

MURTEREE NO 1 FIGURE 8

STRATIGRAPHIC COLUMN

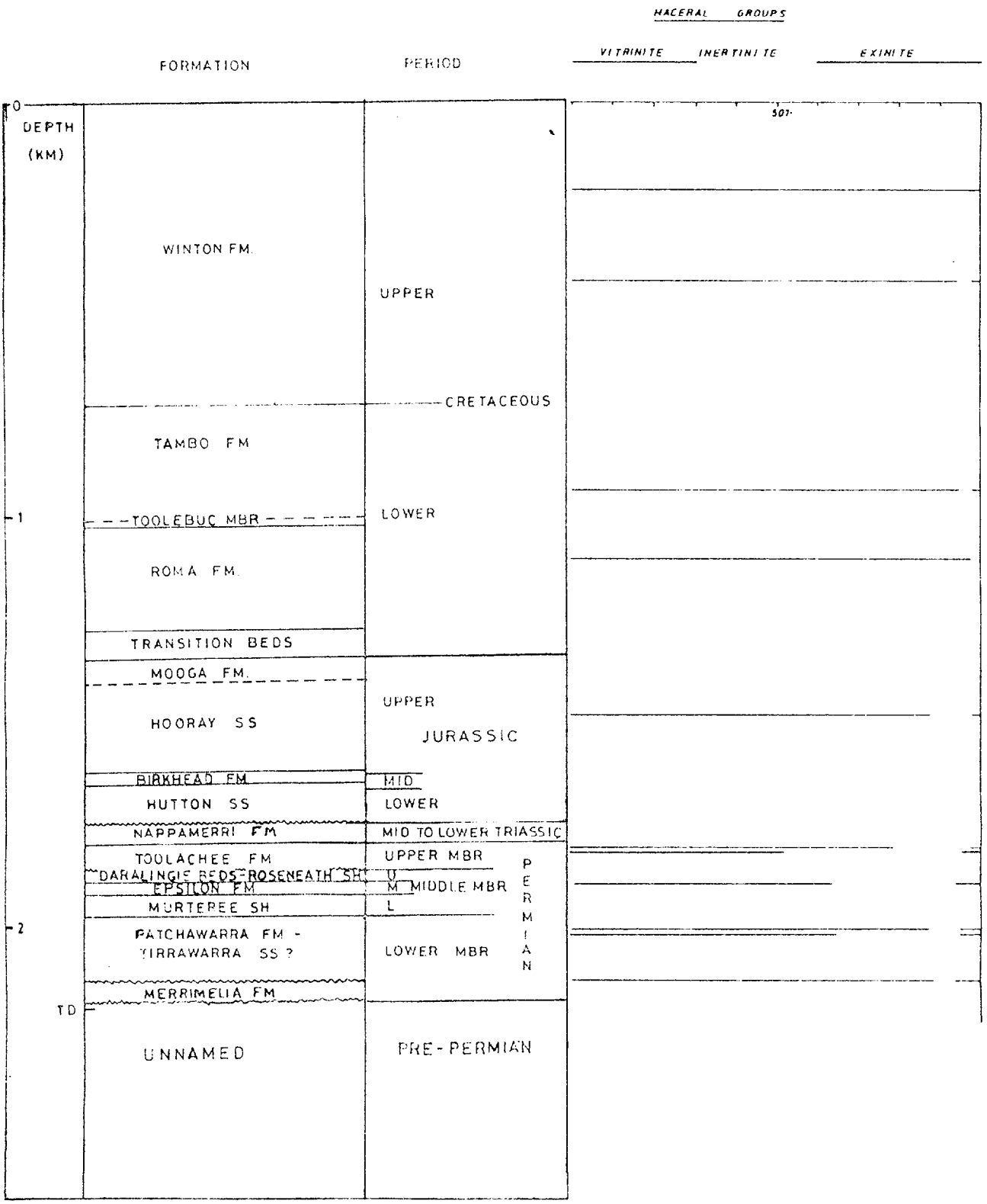

TOOLACHEE NO 8.

FIGURE 9

STRATIGRAPHIC COLUMN

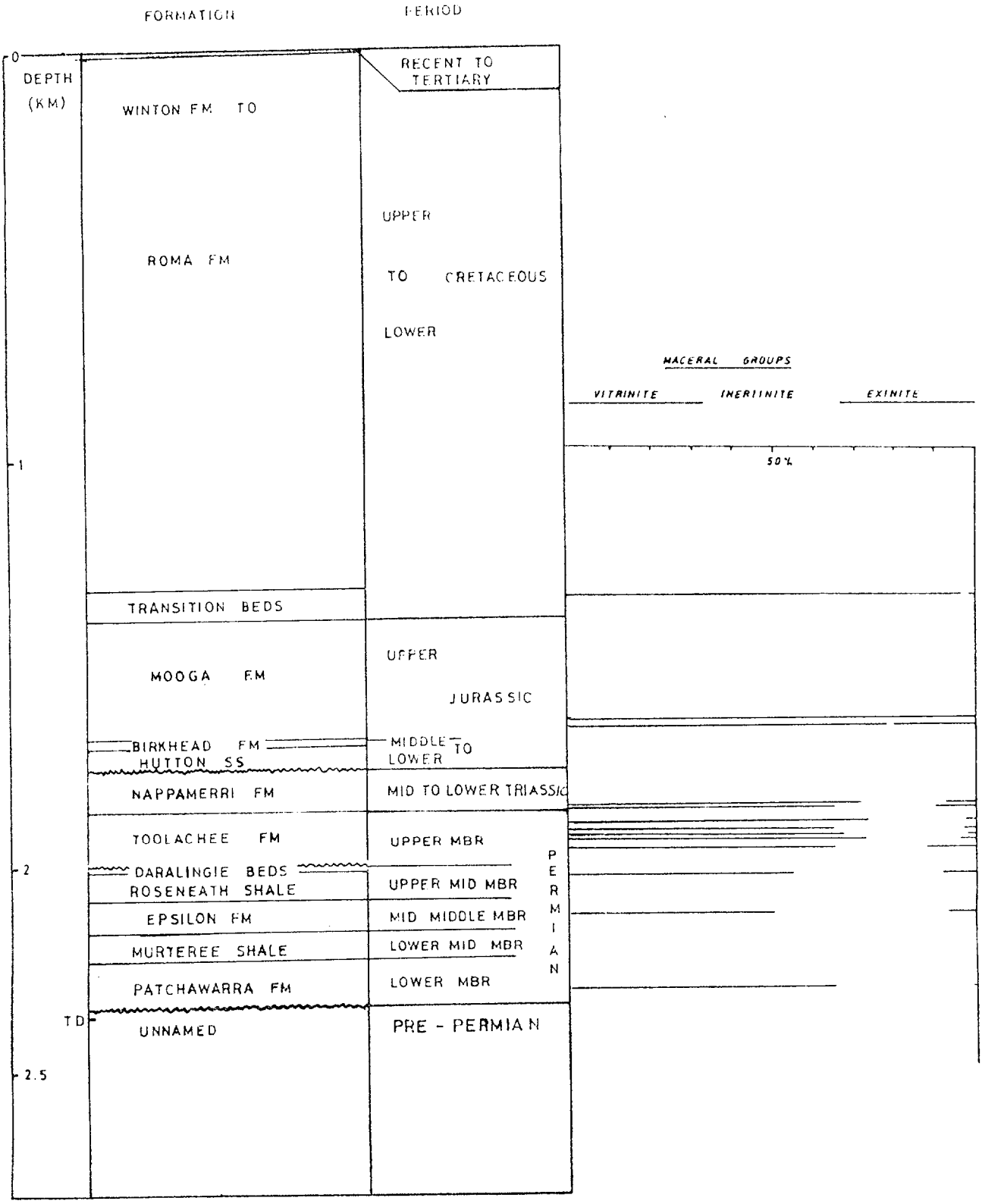

TOOLACHEE NO 3

FIGURE 10

STRATIGRAPHIC COLUMN

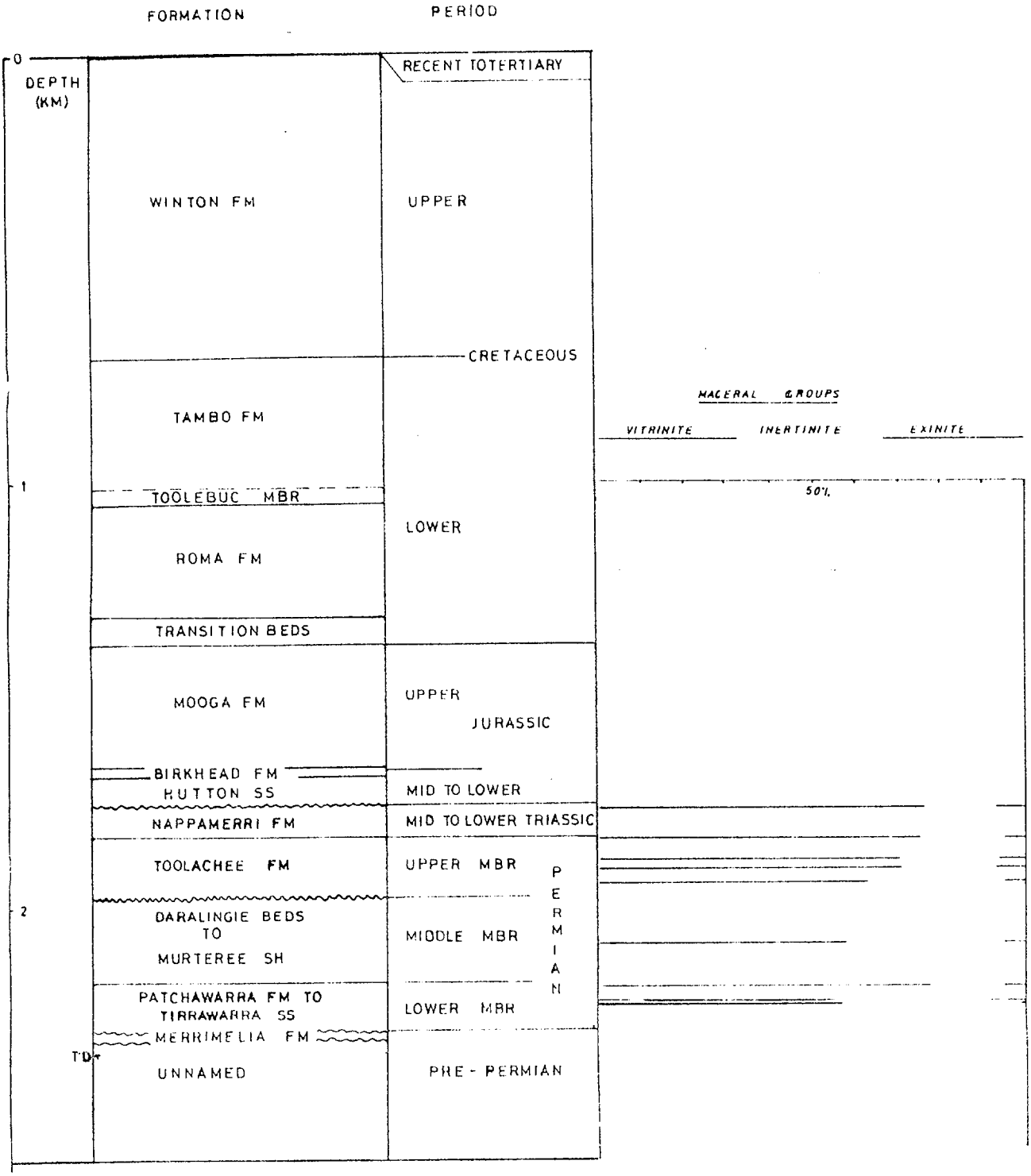

FIGURE 11

Vitrinite, Exinite, Inertinite Percentage of Total Coal Content from Selected Polished Sections.

A - JURASSIC
B - TOOLACHEE FORMATION
C - PATCHAWARRA FORMATION

WELLS

• - GIDGEALPA-7
o - MOOMBA-2
□ - BIG LAKE-4
▣ - BIG LAKE-3
+ - MURTEREE-1
▲ - TOOLACHEE-8
△ - TOOLACHEE-3

FIGURE 11

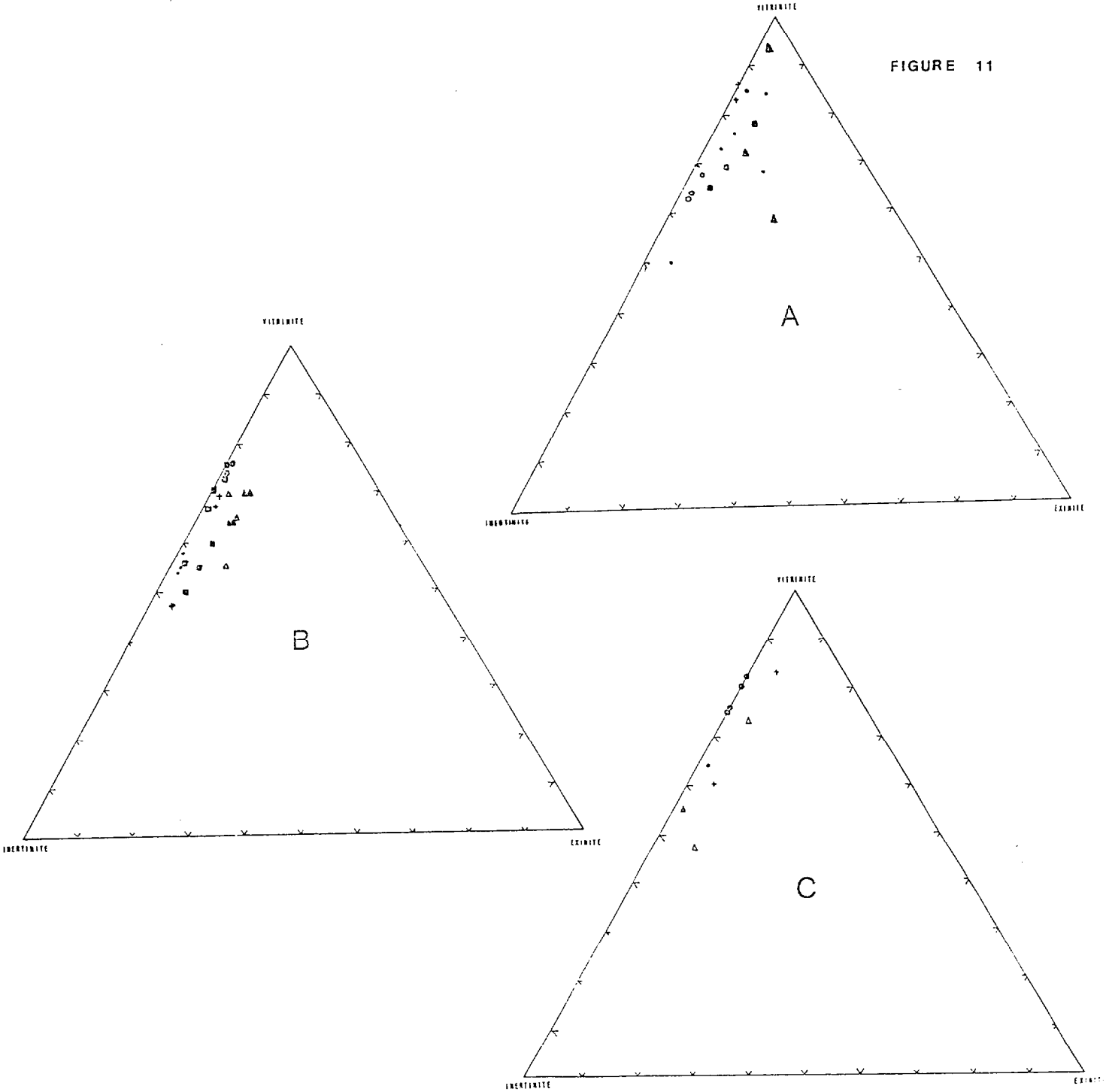
VITRINITE
A
EXINITE
VITRINITE
B
INERTINITE
EXINITE
VITRINITE
C
INERTINITE

6. VITRINITE REFLECTANCE

6.1 TECHNIQUES

Vitrinite reflectance measurements were made on polished sections from all wells. Paucity of coal cuttings in the post-Triassic meant that in several wells reflectance curves and their slopes were obtained from only 300-500 metres of sequence thickness (Toolachee-8, Figu. 17; Big Lake-3, Fig. 15).

Reflectance measurements were made using a Lietz reflecting microscope (Appendix II) with a standard deviation of .01%. Measurements were made under oil using a 32x objective. Between 40 and 100 individual reflectance measurements were made on suitable vitrinite grains in the polished sections. By convention, tellocollinite (vitrinite A) is the maceral used for reflectance measurements. All reflectance values quoted represent percentage, maximum, mean vitrinite reflectance (i.e. % $\overline{R}_o$(max)), because the orientation of the coal cuttings in the cold-setting epoxy resin mount was random.

Reflectance variations found in individual polished sections was generally $\pm$ 0.2% $\overline{R}_o$(max). This allowed reflectance curves for individual wells to be constructed with reasonable accuracy. However some polished sections of post-Triassic coals exhibited individual variations of up to $\pm$0.4% $\overline{R}_o$(max) (Moomba-2 Figure 13 and Big Lake-3 Figure 15). This somewhat greater variation of reflectance values meant that more than one reflectance curve could be constructed in some cases e.g. Moomba-2.

Four factors probably contribute to this wide variation in reflectance values (see Appendix 1,)

1. Down hole contamination of cavings,
2. Extreme heat involved in drying well cuttings,
3. Sedimentary reworking of older coals, and
4. Movement of hot connate waters through lower Jurassic aquifers.

6.2 DEPTH-REFLECTANCE PROFILES

6.2.1 POST-TRIASSIC

Post-Triassic vitrinite reflectance values at the surface range from 0.10% $\overline{R}_o$(max) at Moomba-2 (Figure 13) to .35% $\overline{R}_o$(max) in Toolachee-8 (Figure 17). The somewhat higher value for the latter surface intercept is considered unreliable because of the small number of data points through which the reflectance curve was drawn. Basal Jurassic reflectance values range from 0.45% $\overline{R}_o$(max) in Murteree-1 (Figure 16) to 1% $\overline{R}_o$(max) in Moomba-2 (Figure 13, curve B). The post-Triassic reflectance curves (Figures 12-18) are all linear with gradients ranging from 0.011% $\overline{R}_o$(max) per 100 metres in Toolachee-8 (Figure 18) to approximately 0.032 to 0.040% $\overline{R}_o$(max) per 100 metres in Moomba 2.

The Gidgealpa-7 (Figure 12) vitrinite reflectance values allow a single curve to be constructed of intermediate (relative to the other wells) gradient namely, 0.024% $\overline{R}_o$(max) per 100 metres.

Moomba-2 (Figure 13) reflectance values have a wide spread of values allowing two possible curves (A and B) to be constructed. Down hole contamination of Jurassic cuttings has been found in other wells in the central Nappamerri Trough (A.J. Kantsler pers. comm. 1979) and it is reasonable to postulate some degree of down hole contamination in Moomba-2. Many coal cuttings in Moomba 2 (Plate A1; A,B) show the effects of extreme heat, "frypanning" during drying, desiccation cracks and oxidation rims. Anomalously high reflectance values therefore would be expected.

Elevated vitrinite reflectance values in Jurassic sediments of the Eromanga Basin can be attributed to hot artesian waters moving through aquifers of the Hutton Sandstone (A.J. Kantsler pers. comm. 1979) in the Nappamerri Trough. It is concluded that curve A in Moomba-2 is probably a result of down-hole contamination. Curve B, however, has a wider range of reflectance values and is probably at least partly a result of heating effect of hot waters moving through the basal Jurassic.

Jurassic coals in Big Lake-3 yielded a wide range of vitrinite reflectance values (0.6% to 0.95% $\overline{R}_o$(max), Figure 15) over the 200 metres of section sampled. Three clusters of vitrinite reflectance values were found with mean $\overline{R}_o$(max) values of 0.63%, 0.73% and 0.9% respectively. The basal Jurassic coals comprise microlithotypes of a detrital nature (i.e. reworked, see Section 5.1). The higher reflectance values obtained from these vitrinites (0.7-0.9% $\overline{R}_o$(max)) are very similar to reflectances anticipated in coals from the upper Triassic on the basis of the extrapolated pre-Jurassic curve (Figure 16). Reworking of older coals at Big Lake-3 would therefore explain the higher reflectance values obtained. Down-hole contamination was a recognised problem in Big Lake-3. Down-hole coal cavings yielded .45%-.5% $\overline{R}_o$(max) vitrinite reflectance values and were discarded. The .55%-.6% $\overline{R}_o$(max) vitrinite reflectance values were accepted as a valid indication of basal Jurassic coal rank.

Post-Triassic vitrinite reflectance values obtained for Murteree-1 allowed a curve to be constructed over the complete Jurassic-Cretaceous sequence penetrated by the well. The basal reflectance intercept of 0.5% $\overline{R}_o$(max) was the lowest of all wells in this study. The reflectance gradient was also low (Figure 16, 0.19% $\overline{R}_o$(max) per 100 metres).

The Toolachee-8 post-Triassic vitrinite depth-reflectance curve (Figure 17) is based on only 5 points. Consequently, the very low reflectance gradient of 0.11% $\overline{R}_o$(max) per 100 metres could well be higher than interpreted herein.

The post-Triassic reflectance data are summarized in Table 2.

6.2.2 PERMO-TRIASSIC

Coal samples were available throughout the Permo-Triassic sequence in the seven wells studied, facilitating determination of the lateral variation in vitrinite reflectance between the well localities. Triassic reflectance values range from 0.65% $\overline{R}_o$(max) in Toolachee-8 (Figure 17) to 1.1% $\overline{R}_o$(max) in Moomba-2 (Figure 13). Basal Permian reflectance values range from 0.95% $\overline{R}_o$(max) in Gidgealpa-7 to 2.80% $\overline{R}_o$(max) in Big Lake-3 and 4 (Figures 15 and 14).

The Permo-Triassic depth-reflectance curves with the probable exception of Big Lake-4 are all linear. They are offset from the post-Triassic reflectance curves by up to 0.25% $\overline{R}_o$(max). Permo-Triassic vitrinite reflectance-depth gradients ranges from 0.058% $\overline{R}_o$(max) per 100 metres in Toolachee-3 to 0.25% $\overline{R}_o$(max) per 100 metres in Big Lake-4.

TABLE 2: SUMMARY OF VITRINITE REFLECTANCE DATA; SOUTHWEST COOPER BASIN

	$\overline{R}_o$(max)%			$\overline{R}_o$(max)%		
	Top Jurassic	Basal Jurassic	Post-Triassic Rank Gradient*	Triassic	Basal Permian	Permo-Triassic Rank Gradient*
Gidgealpa-7	0.35	0.58	0.024	0.68	0.95	0.094
Moomba-2	0.10	1.00	0.032-0.042 (curve B)	1.10	1.81	0.13
Big Lake-4	n.d.	n.d.	n.d.	0.80	2.80	0.25**
Big Lake-3	0.15	0.65	≈0.03	0.85	2.80	0.21
Murteree-1	0.13	0.45	0.019	0.68	1.02	0.067
Toolachee-8	0.35	0.60	(0.011)	0.65	1.15	0.087
Toolachee-3	n.d.	n.d.	n.d.	0.72		0.058

* % $\overline{R}_o$(max) per 100m

n.d. not determined

(**) depth-reflectance curve non-linear; gradient determined for basal Permian from logarithmic plot.

( ) unreliable value.

00096

6.3 LATERAL RANK TRENDS; SOUTHWEST COOPER BASIN

6.3.1 POST-TRIASSIC

Depth-reflectance gradients in post-Triassic sediments are steepest in the Nappamerri Trough, as represented by Big Lake-3, 4 and Moomba-2 (Table 2). Reflectance gradients decrease to the northwest and southeast away from the Nappamerri Trough. Post-Triassic isorank surfaces (Figure 19) are generally concordant with stratigraphic boundaries. Departures from this are evident at Moomba-2 and Murteree-1 (Figure 19). At Moomba-2 the isorank surfaces are markedly convex upward, following the pre-Permian basement so that the 0.5% $\overline{R}_o$(max) and 0.7% $\overline{R}_o$(max) surfaces occur at a considerably shallower depth than elsewhere along the line of section. By contrast, at Murteree-1, the 0.5% $\overline{R}_o$(max) surface is convex downward. For the wells studied the 0.5% $\overline{R}_o$(max) isorank surface is deepest at Murteree-1.

6.3.2 PERMO-TRIASSIC

Figure 19 shows that in the Permian and Triassic sediments within the central Nappamerri Trough at Moomba-2 and Big Lake-3 and 4 appear to be broadly concordant with the stratigraphy. Toward the margins of the Nappamerri Trough (A.J. Kantsler pers. comm. 1979) they become notably diachronous. Hence the overall shape of the 1.3% and 2.0% $\overline{R}_o$(max) in the thick Permian sequence of the Nappamerri Trough is upwardly convex.

The configurations of the isorank surfaces in Gidgealpa-7, Murteree-1, Toolachee-3 and Toolachee-8 (Figure 19) indicate that there is a return to stratigraphic concordance away from the central Nappamerri Trough. In the Tennappera Trough and across the flanking Nappacoongee-Murteree and Toolachee Anticlinal Trends, the 0.7% and 0.9% $\overline{R}_o$(max) isorank surfaces lie entirely within the Triassic and Permian respectively.

FIGURES 12-18

DEPTH REFLECTANCE GRADIENTS

GIDGEALPA-7
MOOMBA-2
BIG LAKE-4
BIG LAKE-3
MURTEREE-1
TOOLACHEE-8
TOOLACHEE-3

FIGURE 12

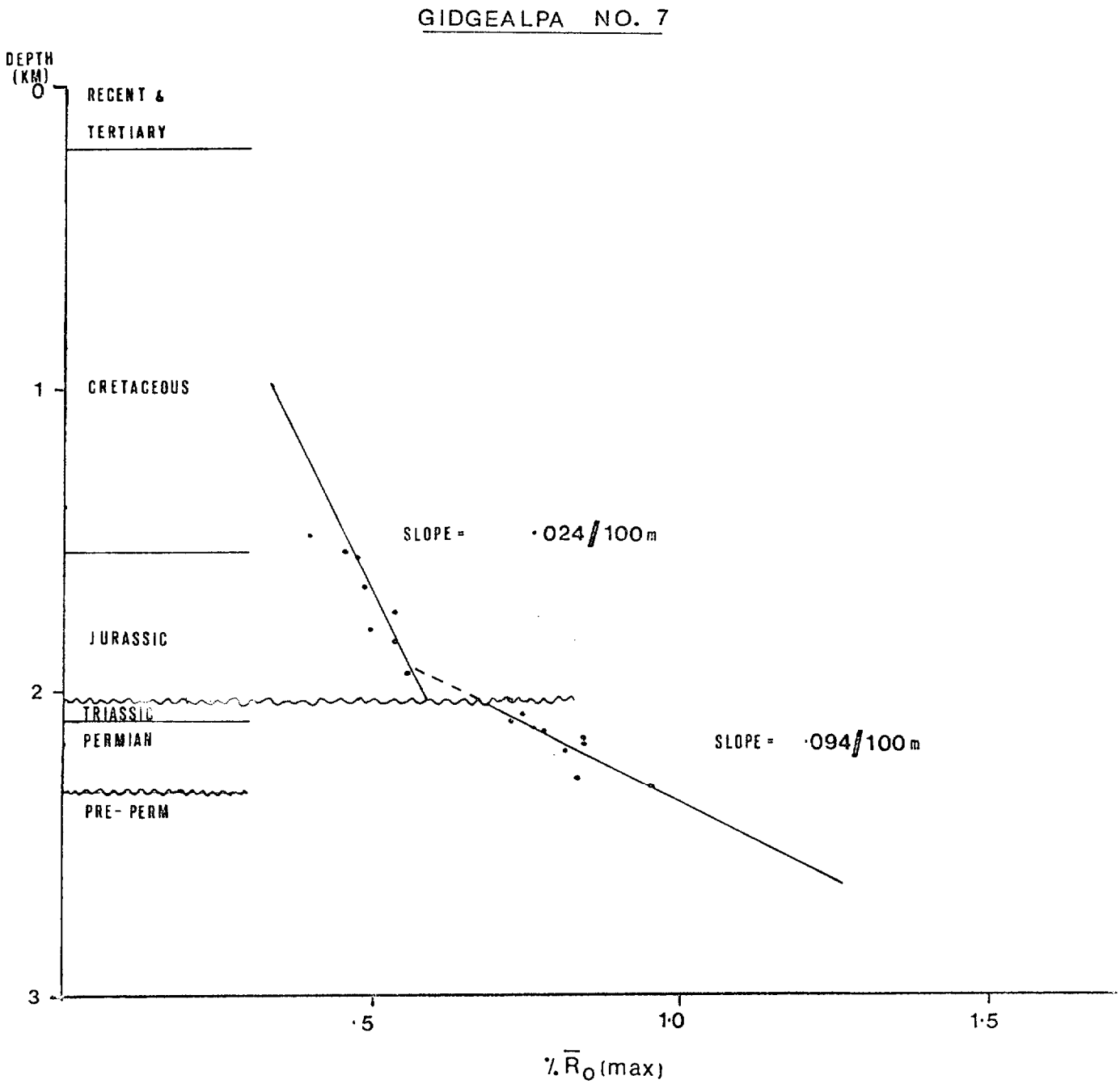
GIDGEALPA NO. 7
DEPTH (KM)
0
1
2
3
RECENT & TERTIARY
CRETACEOUS
JURASSIC
TRIASSIC
PERMIAN
PRE-PERM
SLOPE = ·024/100m
SLOPE = ·094/100m
·5
1·0
1·5
% $\bar{R}_o$ (max)

FIGURE 13

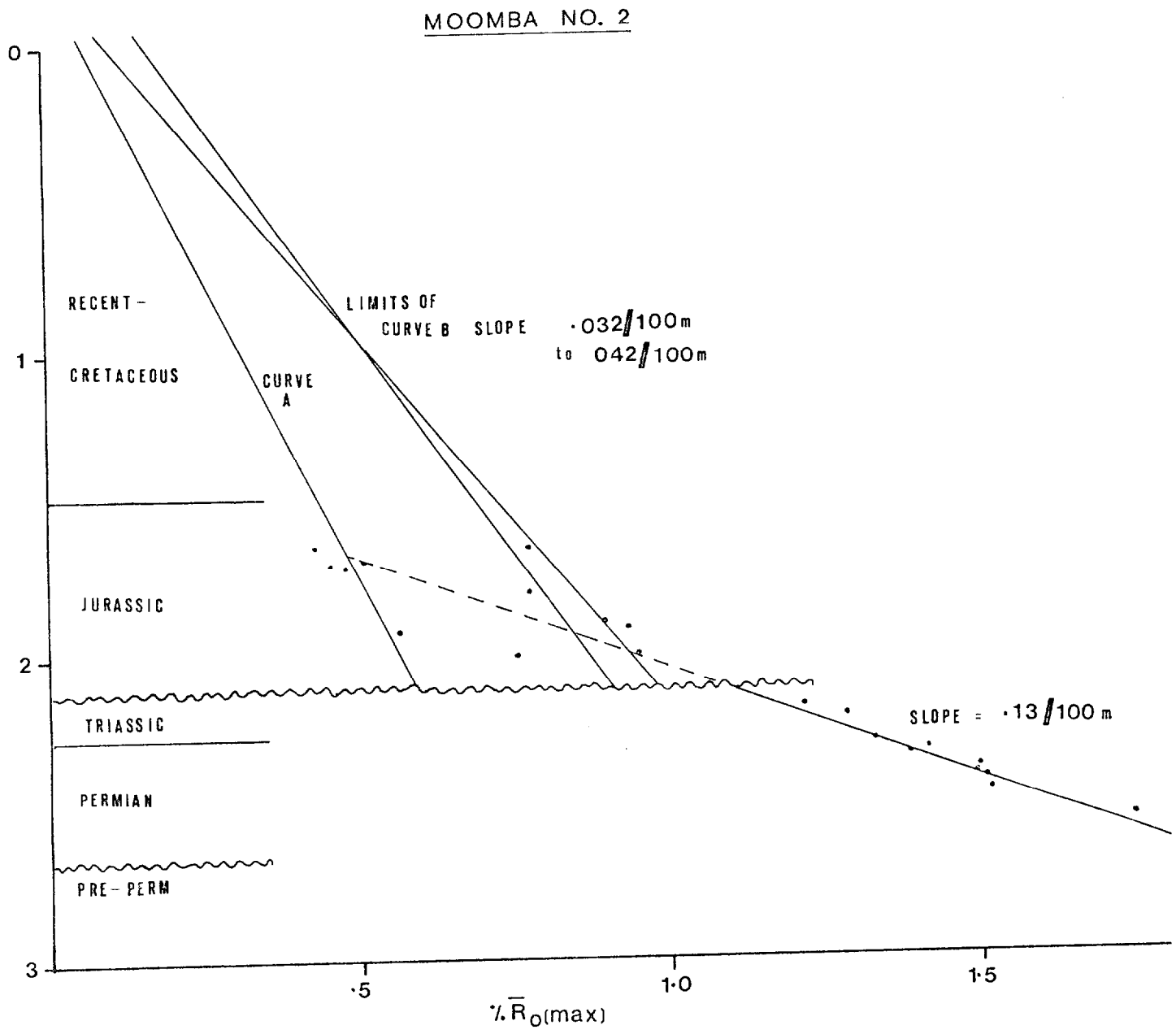
MOOMBA NO. 2
0
1
2
3
RECENT –
CRETACEOUS
JURASSIC
TRIASSIC
PERMIAN
PRE – PERM
CURVE A
LIMITS OF CURVE B SLOPE ·032/100m to 042/100m
SLOPE = ·13/100m
·5
1·0
1·5
% $\bar{R}_{O(max)}$

FIGURE 14

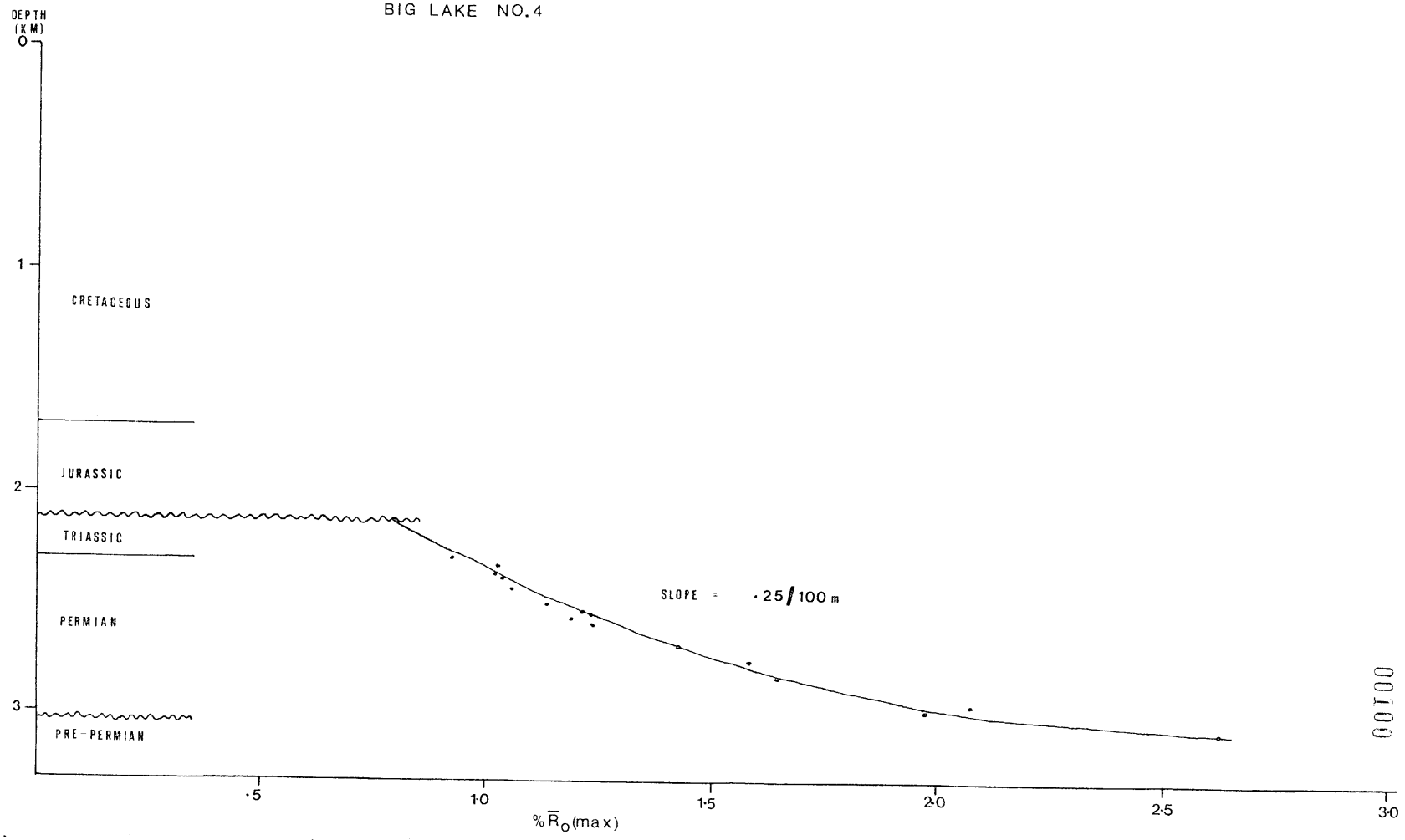

00100

BIG LAKE NO. 3

FIGURE 15

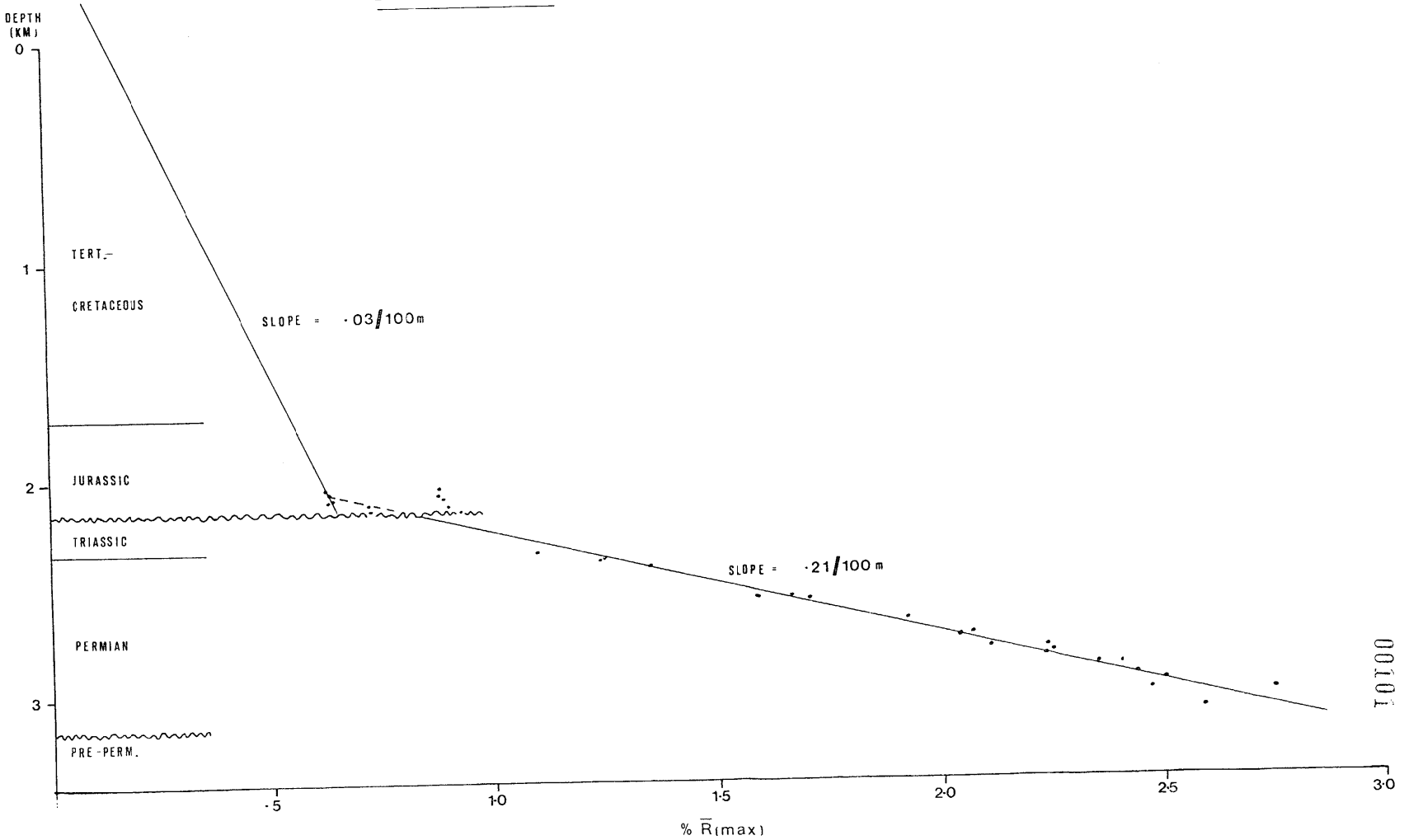

10100

FIGURE 16

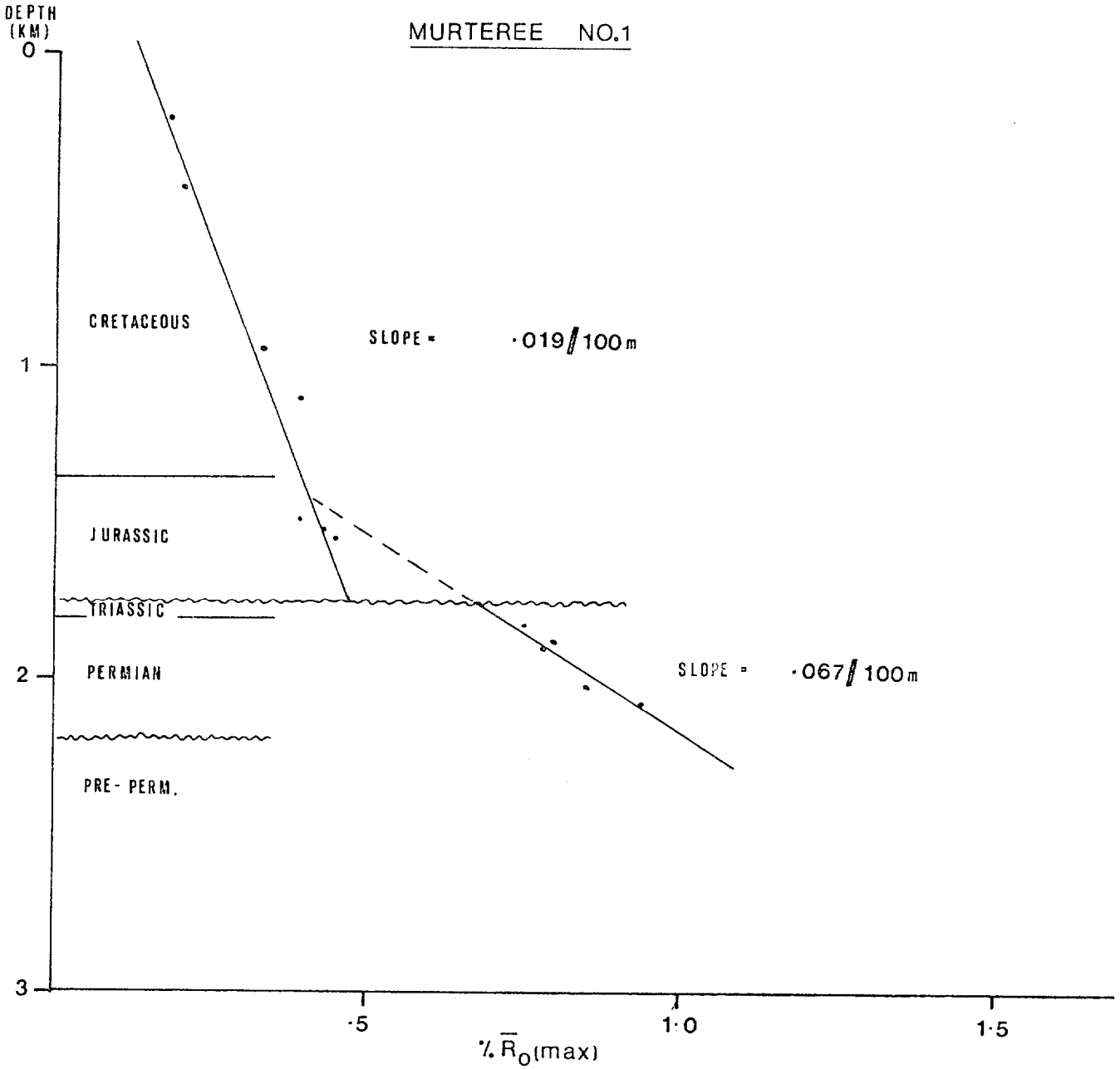
DEPTH (KM)
0
1
2
3
MURTEREE NO.1
CRETACEOUS
JURASSIC
TRIASSIC
PERMIAN
PRE-PERM.
SLOPE = ·019/100m
SLOPE = ·067/100m
·5
1·0
1·5
% $\bar{R}_o$(max)

FIGURE 17

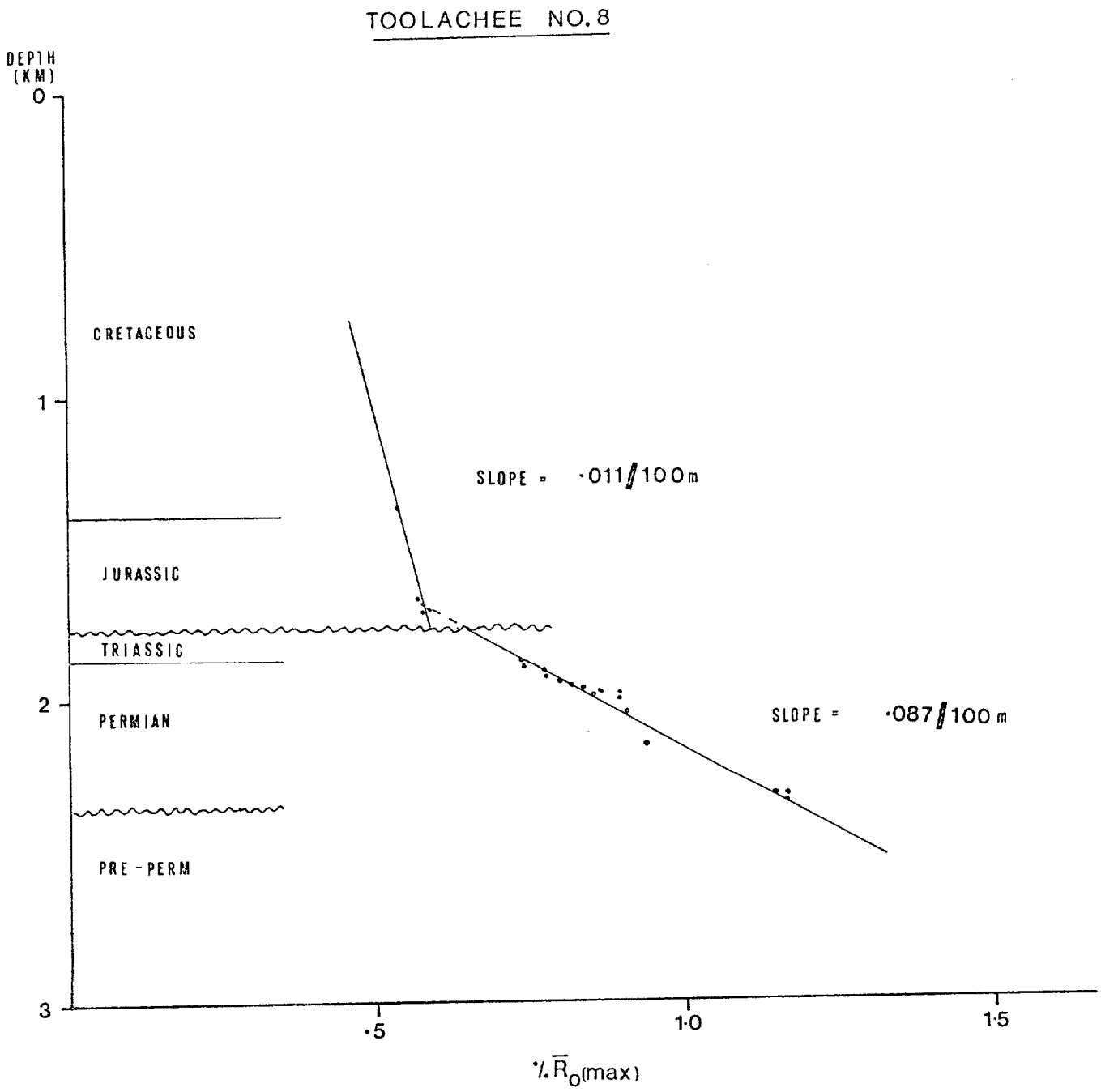
TOOLACHEE NO. 8
DEPTH (KM)
0
1
2
3
CRETACEOUS
JURASSIC
TRIASSIC
PERMIAN
PRE-PERM
SLOPE = ·011/100m
SLOPE = ·087/100m
·5
1·0
1·5
%$\bar{R}_o$(max)

FIGURE 18

TOOLACHEEE NO. 3

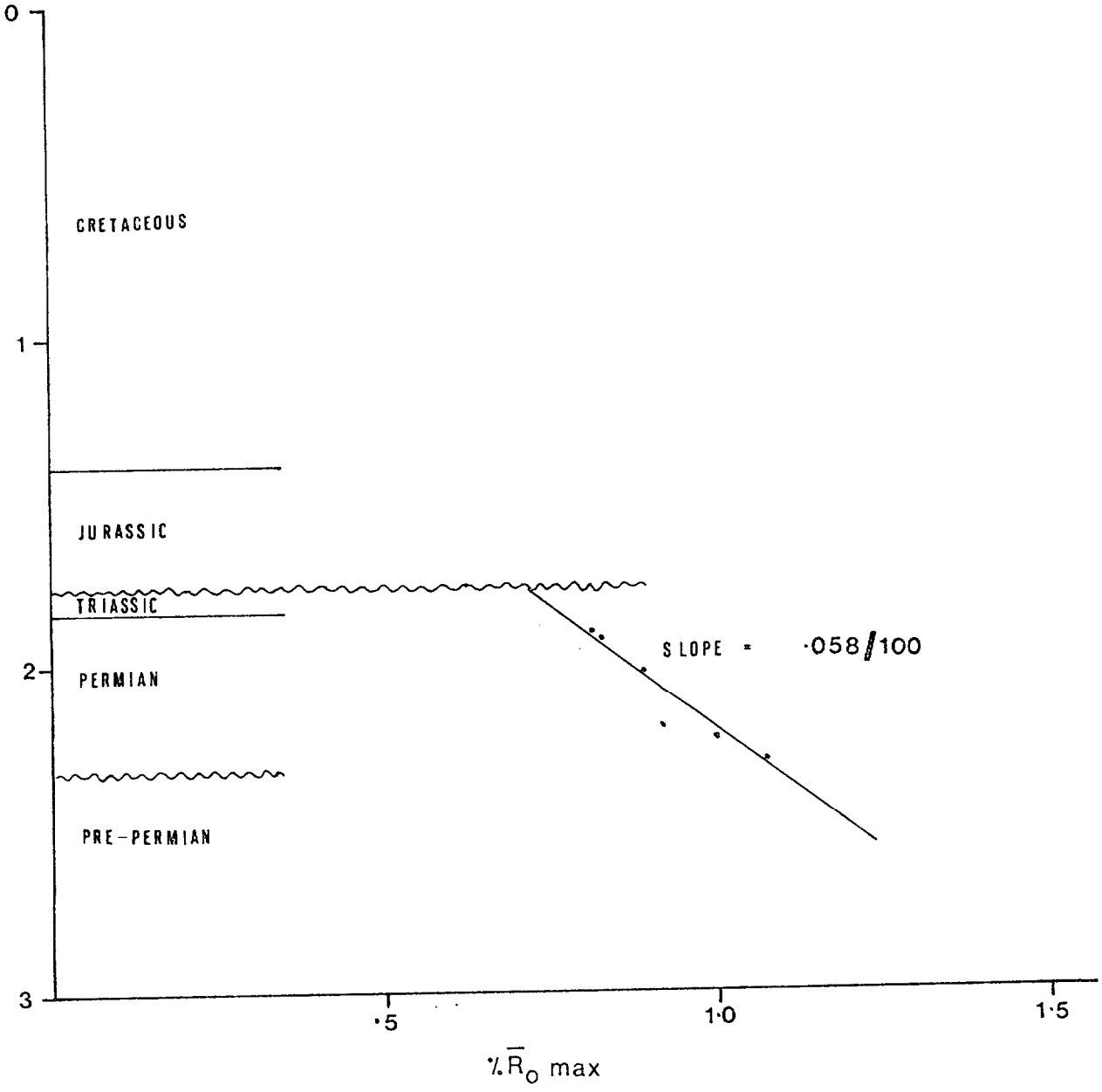

PLATE 1

A Vitrinite (TOOLACHEE-8, 2055 m)

T - Tellocollinite

C - Collinite

B Vitrinite (TOOLACHEE-8, 1923 m)

T - Tellocollinite with clay filling lumens and some crushed lumens.

C Vitrinite (MOOMBA-2, 2648m)

V - Granular vitrinite.

PLATE I

a

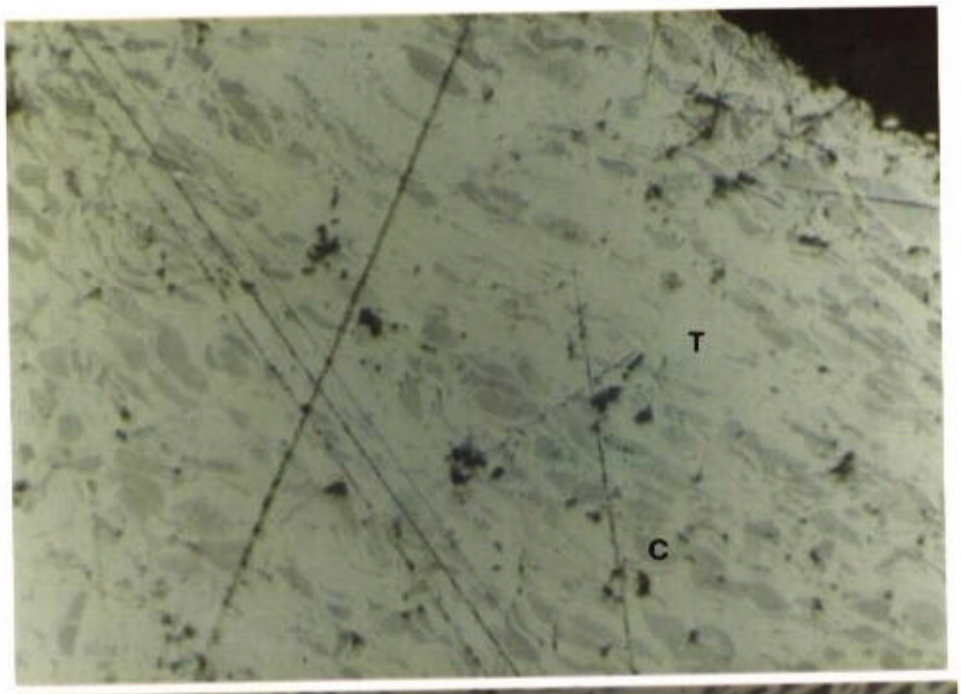

b

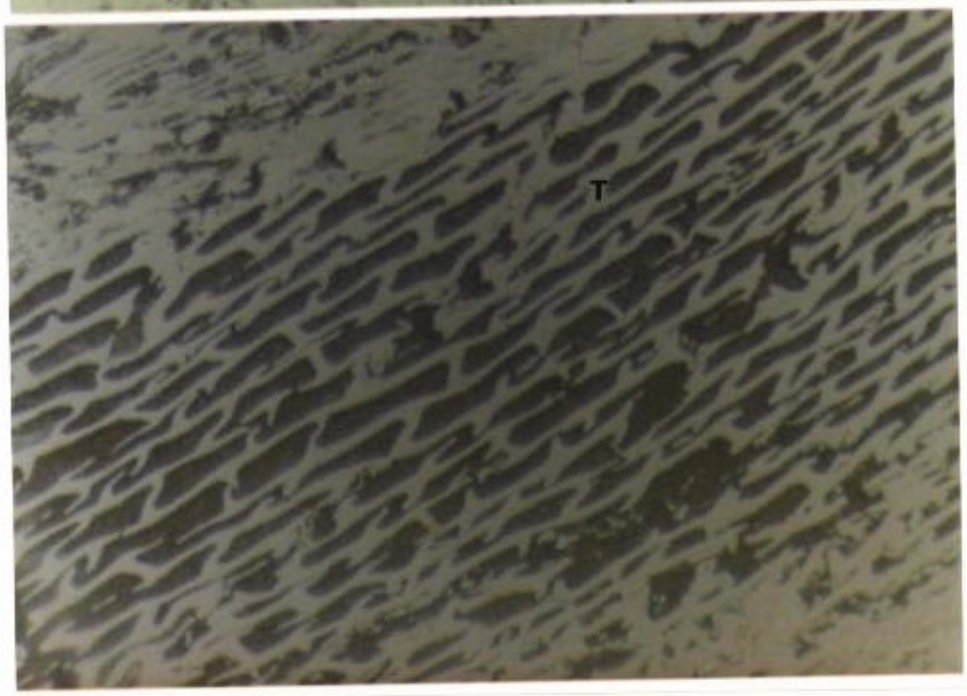

c

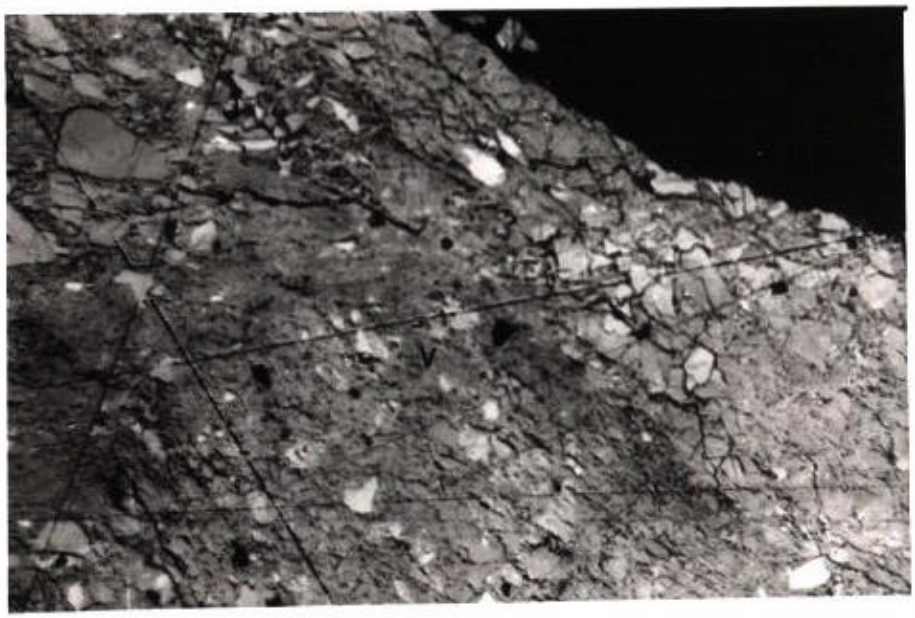

PLATE 2

A Clarite (MURTEREE-1, 2016m)

V - Vitrinite (tellocollinite and desmocollinite)

C - Cutinite

- also resinite

B Duroclarite (MURTEREE-1, 2016m)

V - Vitrinite (tellocollinite)

R - Resinite (pod)

F - fusinite

- cutinite is also present

C Duroclarite (TOOLACHEE-3, 1890m)

V - Vitrinite (tellocollinite)

S - Spore

F - Fusinite

00109

a

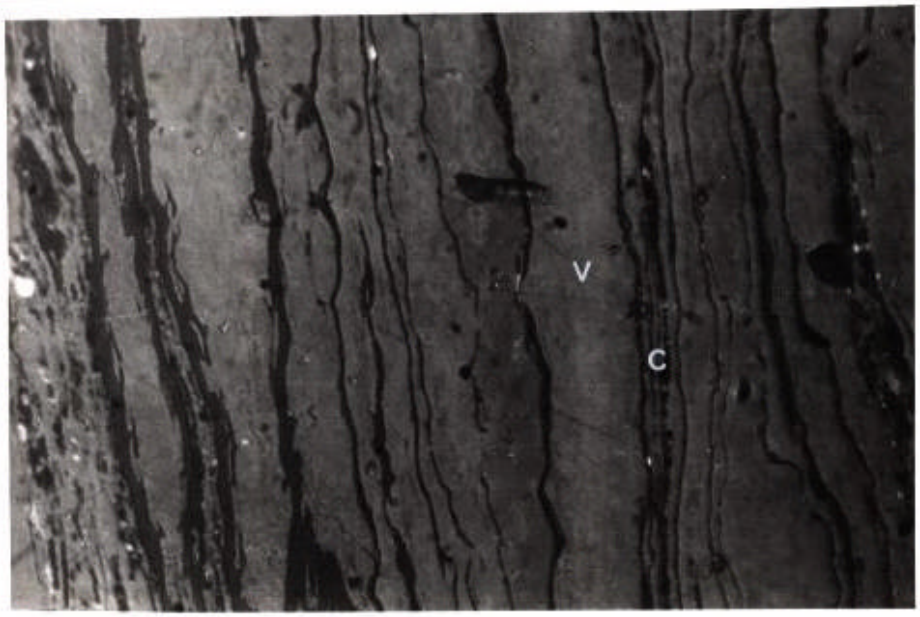

b

c

PLATE 3

A Vitrinertite (MURTEREE-1, 2125m)

V - Vitrinite (tellocollinite)

F - Fusinite

SF - Semifusinite

B Duroclarite (MURTEREE-1, 1905.5m)

D - Vitrinite (desmocollinite)

R - Resinite

C Duroclarite (MURTEREE-1, 1905.5m)
contains

- inertodetrinite
- resinite
- sporinite
- vitrodetrinite
- desmocollinite

a

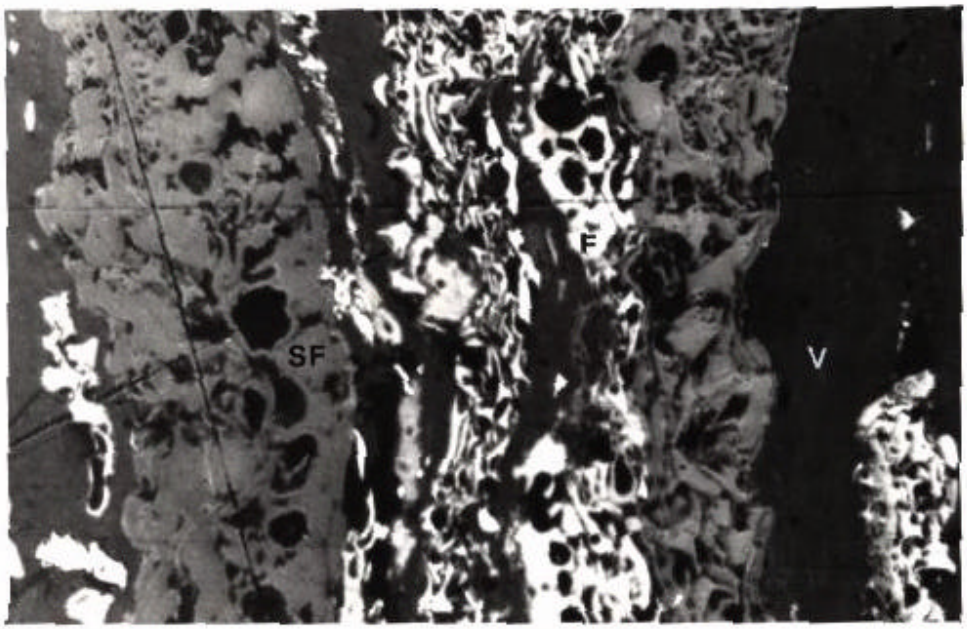

b

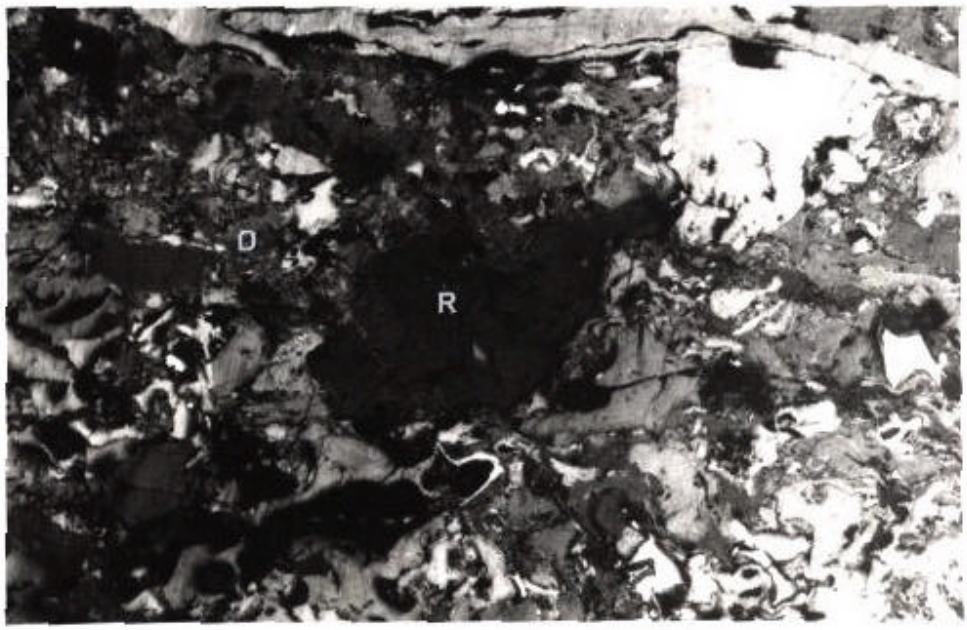

c

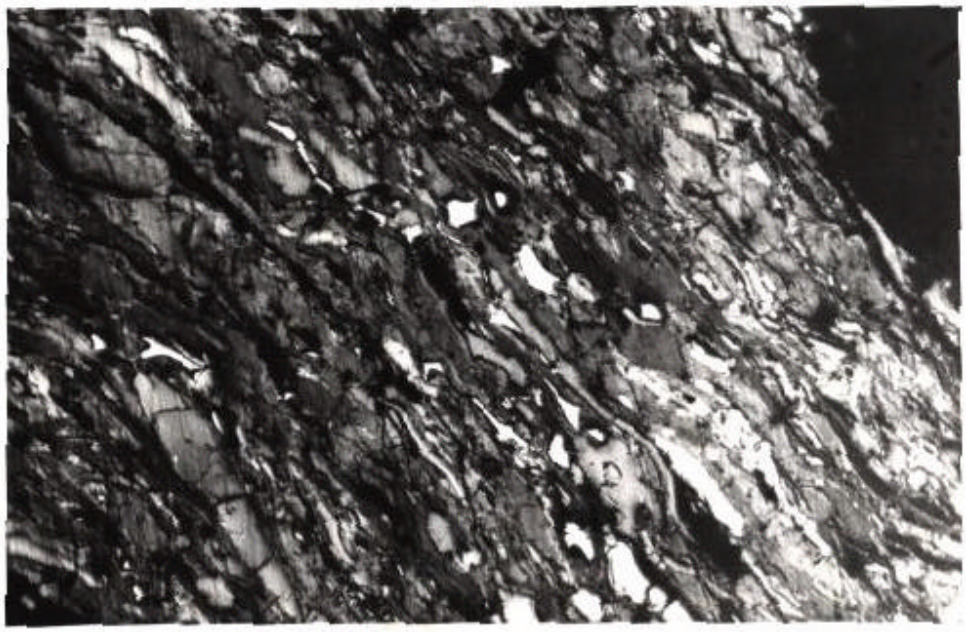

00112

7. BOTTOM HOLE TEMPERATURES AND PRESENT DAY GEOTHERMAL GRADIENTS

Present day bottom hole temperatures and geothermal gradients have been calculated for the seven wells under study by Schwebel and Riley (1978) using the method of Fertl and Wichmann (1977). These data are listed in Table 3.

TABLE 3

Well	Temperature Top of Permian (^{o}C)	Temperature Top of Basement (^{o}C)	Geothermal Gradient*
Gidgealpa-7	>75.2	82.4	> 2.2
Moomba-2	>115.2	134.7	> 3.3
Big Lake-4	116.3	131.9	3.3
Big Lake-3	126.3	168	3.5
Murteree-1	86.9	103.6	> 3.0
Toolachee-8	96.9	120.2	2.1
Toolachee-3	91.3	113.6	3.3

* ^{o}C/100m

8. INTERPRETATION

8.1 COAL MICROLITHOTYPES

8.1.1 PERMIAN

Coals were common in the Permian section of the seven wells studied. Coal was particularly abundant in the Toolachee Formation and Patchawarra Formation. Total thickness of coal as a proportion of thickness of the formation was relatively constant in the Toolachee and Patchawarra Formations, indicating that, in the Permian, total coal content in a formation was a function of subsidence.

The thickness of individual Permian coal seams varies considerably. The Toolachee Formation and Patchawarra Formation contain several seams of 4 metres or greater thickness. The wells located in the Nappamerri Trough, particularly Big Lake-3 and 4, contain the thickest coal seams. A 20 metre seam is present in the Patchawarra Formation at Big Lake-3. The presence of many thick coal seams indicates that stable environment conditions existed for long periods during the deposition of the Patchawarra and Toolachee Formations.

The coal seams vary considerably in their environment of deposition in that the classical clay, shale coal seat (E. Stack 1975) is rarely present. Where this sedimentary sequence does occur multiple coal seams separated by shale are developed. The majority of the coal seams in the Toolachee Formation and Patchawarra Formation have a sandstone or siltstone top and/or base indicating abrupt changes in sedimentation.

These sharp changes in sedimentary regime are characteristic of the fluvio-deltaic environment which has been proposed by Thornton (1978) for the Patchawarra Formation and Toolachee Formation.

Most of the coal is autochthonous although some allochthonous coals are present. Cannel coal and fine grained, well sorted, stratified duroclarite cuttings (Plate 3, C) are common in the coals sampled, especially those in Big Lake-3 and 4.

8.1.2 JURASSIC

Post-Triassic coal seams are generally thin (i.e. of the order of 1m thick). The coal in many cases appears to be lenticular. Adequate lithological description were available for Murteree-1. and the Mooga Formation and the Hutton Sandstone contain many minor seams and this could be the case in other southern wells in Toolachee-3 and 8 where lithological description is not as good. Geophysical logs of the other six wells examined indicate that coal

00114

is present in only a few thin seams. However the Jurassic cuttings which were available for examination contained more coal than was indicated by the well completion reports, especially for Toolachee-8. Coal seams are generally thin and lenticular and appear to be more common in the Tenneppera Trough than in the Nappamerri Trough. The Jurassic coals analysed appeared to be wholly autochthonous.

8.2 COAL MACERAL GROUPS

8.2.1 JURASSIC

The prominance of vitrinite and exinite maceral groups in the Jurassic coals examined compared to the Permian coals could reflect a fundamental change in type of flora present in the Cooper Basin. However in several wells (Gidgealpa-7, Murteree-1) vitrinite and exinite content varies little through the Jurassic and Permo-Triassic sequence.

Despite limited sampling lateral influences appear to affect exinite content with the anticlinal trends having a somewhat higher exinite content in the coals than is the case in the troughs (Nappamerri Trough).

8.2.2. PERMIAN

A broad trend of increasing detrital textures (granular vitrinite, oxidized rims etc.), and often an increase in carbonaceous shales and silts, toward the upper or lower boundaries of the Toolachee and Patchawarra Formations was found in the wells with adequate sample coverage. Gidgealpa-7, Moomba-2, Big Lake-3 and 4 and Toolachee-3 show a general upward increase in detrital content in both formations.

An upward decrease in vitrinite content of the coals in each formation (excepting the Patchawarra Formation at Big Lake-3 and 4) is evident in these wells. The Toolachee and Patchawarra Formations at Murteree-1 and Toolachee-8 contain a downward increase in detrital coal content and a corresponding downward decrease in total vitrinite content.

These vertical and lateral variations in coal and argillic content can be related to the sedimentary environment prevailing in the basin during organic matter deposition. Increasing dessication of coal forming swamps on a relatively stable basement may influence vitrinite content in the deposited organic matter (Smyth 1970).

The exinite content of the coals was found to decrease as trimacerite microlithotype groups, i.e. clarodurite and duroclarite, became more dominant. Greater mechanical and chemical weathering of the precursor plant materials preferentially destroyed much of the reactive exinites, i.e. resinite and cutinite.

8.3 VITRINITE REFLECTANCE AND GEOTHERMAL HISTORY

8.3.1 PRESENT DAY GEOTHERMAL GRADIENTS

Wells in and around the Nappamerri Trough (Gidgealpa-7, Moomba-2, Big Lake-3 and 4) show evidence of a relationship between vitrinite reflectance and present-day geothermal gradients. Big Lake-3 and 4 and Moomba-2 have high basal Permian vitrinite reflectances and high bottom hole temperatures; whereas Gidgealpa-7 has low reflectances and a low bottom hole temperature.

Murteree-1, Toolachee-3 and 8 show a different relationship, having high geothermal gradients and low basal Permian reflectances.

These present-day geothermal gradients cannot have been operative throughout the Cooper Basin's history because

1. Coals in the Tenneppera Trough would show a higher degree of coalification in the Tenneppera Trough than is in fact seen; and
2. The present geothermal are sufficient to produce the observed coal ranks present in a far shorter time (Kantsler et al. 1978).

Thus present-day geothermal gradients may be a relatively recent phenomenon possibly dating from the Tertiary (Kantsler pers. comm. 1979).

8.3.2 RANK VARIATION AND GEOTHERMAL HISTORY

A. PERMO-TRIASSIC

Isorank depth variations across the southwestern Cooper Basin (Figure 19) indicate a complex geothermal gradient history. The isorank surface to basement depths decrease south eastwards and north westwards away from the central Nappamerri Trough, indicating a higher heat flow in the central Nappamerri Trough.

Nappamerri Trough

Moomba-2 and Big Lake-3 and 4 exhibit stratigraphically diachronous coalification (reflectance) haloes. Drilling in the central Nappamerri Trough in the vicinity of these wells has penetrated radiogenic granitic intrusions in the basement (Battersby 1976). The elevated thermal input from these granitic intrusions would explain the high Permo-Triassic reflectance values and high Permo-Triassic and Jurassic reflectance gradients in these wells (Middleton, 1979).

00116

The Permo-Triassic vitrinite reflectance curves of Big Lake-3 and 4 (Figures 14, 15) suggests possible differences between the two localities in sediment type (and hence thermal conductivity) and/or thermal flux, particularly during the early Permian. The first possibility pre-supposes that the Big Lake-4 reflectance curve is due to variations in sediment type, porosity or compaction resulting in a non-linear coalification (reflectance) curve. This alternative is not supported by close examination of the evidence. The sediments in Big Lake-4 are very similar to those at Big Lake-3 in thickness, type, grainsize and porosity. The sonic logs run for both Big Lake-3 and Big Lake-4 indicate a similar interval transit time (viz. 0.2-0.23m per micro second) and therefore a similar degree of compaction. Compaction history is unknown. Hence differences in the degree of sediment compaction in the two wells during the Permian may well have exerted a controlling influence on geothermal gradients. It is also possible that the radiogenic mineral content of the basal Permian (Merrimelia Formation) differs between the two wells. These radiogenic sediments would have been derived via glacial erosion of the pre-Permian basement. This could result in a raised geothermal gradient in Big Lake-4 relative to Big Lake-3.

The second alternative requires a higher geothermal input to the Big Lake-4 area than was operating in the Moomba-2 and Big Lake-3 areas. This higher thermal flux resulted in an exponential depth-reflectance pattern. No significant difference in reflectance was found in the basal Permian of Big Lake-3 and 4. Thus Big Lake-4 would have to be near a localized hot spot. This elevated geothermal regime would only be transient but sufficient to imprint an exponential reflectance curve on the Permo-Triassic coals.

In assuming an early anomalous and transient heat flow in the vicinity of Big Lake-4, it is important to realize that subsequent coalification would be expected to eventually mask the initially inhomogeneous coalification pattern and replace it with a more linear trend similar to that now seen at Big Lake-3 and Moomba-2. Whereas, an anomalous heat flow at Big Lake-4 cannot be discounted, the inhomogeneous coalification pattern across the Big Lake field appears most likely to be related to primary sedimentary differences with extraneous influence (e.g. radiogenic sediments, or movement of hot basin waters through the Permian sediments), possibly also being responsible.

00117

Finally, observed variation in reflectance gradients within a relatively small portion of the Nappamerri Trough partly account for the upwardly convex isorank surfaces associated with Moomba-2.

Tenneppera Trough and Gidgealpa-Merrimelia Anticlinal Trend.

Permo-Triassic isorank surfaces at Murteree-1 and Toolachee-3 and 8 are largely stratigraphically concordant, whilst Gidgealpa-7 on the flank of the Gidgealpa-Merrimelia Anticlinal Trend indicates a westward return to concordance. The isorank surfaces show that Permo-Triassic coalification in these areas was primarily a function of depth and duration of burial.

Depth-reflectance curves for the Permo-Triassic sediments of all the above wells suggest that coalification and therefore geothermal gradients throughout the Permo-Triassic were relatively stable, or varied sufficiently slowly to give rise to linear coalification trends.

B. JURASSIC-CRETACEOUS

Post-Triassic isorank surfaces are reasonably concordant with formation boundaries and tend to parallel the basement. Only at Murteree-1 and Moomba-2 (Figure 19) are there marked departures from this pattern of coalification.

Nappamerri Trough

The shallow depths at which the 0.5% and 0.7% $\overline{R}_0$(max) isorank surfaces occur in the Moomba-2 area is in marked contrast to the situation elsewhere along the line of section (Figure 17). Around Moomba-2 these isorank surfaces are markedly convex upward. This feature can probably be attributed to one or more of several causes:

(a) the large thickness of Permian sediment in the Nappamerri Trough inhibiting heat flow.

(b) variation in basement lithology and topography.

(c) the previously mentioned movement of hot waters along faults and through the lower Jurassic aquifers.

Moomba-2 has a thin Permian sequence, relative to Big Lake-3 and 4. The consequent closer proximity of the post-Triassic sediments to granitic basement no doubt contributed to the raised 0.5% and 0.7% $\overline{R}_0$(max) isorank surfaces.

From similar studies of other wells in the area, it has been proposed (Kantsler et al. 1978) that possible movement of hot connate waters from underlying sediments up deep seated faults associated with some of the structural trends were responsible for the enhanced Jurassic-Cretaceous coalification found in several wells located on or adjacent to these highs. This also may partly account for the upwardly convex isorank surfaces associated with Moomba-2.

00118

Movement of hot waters out of the Nappamerri Trough via lower Jurassic aquifers could also be expected to raise lower Jurassic coal rank.

The downward convex 0.7 $\overline{R}_0$(max) isorank surface at Big Lake-3 contrasts the upward convex 1.3% and 2.0% $\overline{R}_0$(max) isorank surfaces. The downward convex Jurassic isorank surfaces could be attributed to the thickness of Permian sedimentation inhibiting heat flow and migration of hot waters in the lower Jurassic, transferring thermal input to the margins of the basin. Tenneppera Trough and Gidgealpa-Merrimelia Anticlinal Trend.

Toolachee-3 and 8 show a slightly upward convex 0.5% $\overline{R}_0$(max) isorank surface, suggesting the movement of Eromanga Basin formation waters over the anticlinal trends as a means of heat transfer.

Murteree-1, located on the western flank of the Tenneppera Trough, has a depressed 0.5% $\overline{R}_0$(max) isorank surface indicating that coalification ranks are a function simply of depth and duration of burial, without any modifying influences.

Gidgealpa-7 - located on the flank of the Gidgealpa-Merrimelia Anticlinal Trend (Figure 19) has isorank surfaces at depth typical of the Patchawarra Trough (Kantsler et al. 1978).

Conclusions

Rank and geothermal gradients vary in a complex fashion along the line of section examined. Rank of the coal has changed in response to increasing depth of burial, thermal input from the basement (in part granitic), and extraneous intrabasinal thermal influences. Thus, the thermal input to the basin has varied markedly in space and time.

8.3.3 TRIASSIC UNCONFORMITY

All wells show a marked offset in reflectance of about 0.2-0.3% $\overline{R}_0$(max) between the Permo-Triassic and the Jurassic sequences (Figures 12-18). This break is due to the erosion and non-deposition of Nappamerri Formation sediments. The unconformity also marks a significant change in reflectance gradient and indicates that a somewhat lower thermal regime was operating in the post-Triassic than operating in the Permo-Triassic.

From the offset in the reflectance versus depth curves minimum erosion of the Nappamerri Formation can be estimated. Gidgealpa-7 (Figure 12), Toolachee-8 (Figure 17), Big Lake-3 (Figure 15) and Moomba-2 (Figure 13) have had a minimum of 100-150 metres of the Nappamerri Formation removed, whilst at Murteree-1 (Figure 16) at least 200 of section has been lost by erosion. Estimation of sediment erosion is difficult. For example, in an area of non-erosion and non-deposition, coalification would continue, albeit very slowly, such that a reflectance "break" would still occur. Similarly

00119

there is no way of knowing the Permian reflectance gradient during Jurassic time.

The Gidgealpa-Merrimelia Anticlinal Trend and the Murteree-Nappacoongee Trend appear to have suffered the most extensive erosion during the Triassic.

00120

9. HYDROCARBON ORIGIN MIGRATION AND ENTRAPMENT

The Permo-Triassic hydrocarbons present in the Cooper Basin have been derived from Permian sediments (Battersby, 1976). Pre-Permian sediments have been discounted as a source (Battersby, 1976) because of their very low content of carbonaceous matter and indurated nature.

Land-plant organic material is the source of hydrocarbons found in the Permo-Triassic reservoir rocks because there are no marine sediments found in the sequence. Geochemical studies (Brooks et al. 1971) of the gaseous hydrocarbons and the paraffinic base of the oils (and some condensates) present, (Powell and McKirdy, 1976) also support land plant organic material as the hydrocarbon source.

Carbonaceous shales (Murteree Shale, Roseneath Shale and shales in the other formations) and coals from the Tirrawarra Sandstone, Patchawarra Formation, Epsilon Formation and Toolachee Formation are possible source rocks. Vitrinite and exinites, particularly cutinite and resinite, during coalification yield light oils gas and condensate (Stack 1975, Powell 1979). The prominence of vitrinite and low but significant concentrations of exinite in the Permian coals makes it likely that they have been an important source of hydrocarbons.

Migration of the hydrocarbons from Permian source beds has been assumed to have taken place relatively soon after the end of Triassic deposition (Battersby, 1976), with migration of hydrocarbons from lower Permian sediments possibly occurring during late Permian time. Economic reserves of hydrocarbons occur in Permian structures. However there is a deterioration of reservoir quality with increasing depth of burial again indicating early migration of hydrocarbons. The presence of wet gas in the Patchawarra Formation and often dry gas in the Toolachee Formation of many wells suggest upward diffusion of lighter hydrocarbons which supports early migration.

The Cooper Basin generally subsided slowly during the Permian. The large thicknesses of peat (latter coal) deposited would have resulted in considerable vertical and lateral differential compaction of the peats, whereas the minerogenic sediments would be somewhat less affected.

00121

Maximum hydrocarbon generation from land plant remains undergoing coalification during burial occur for woody herbaceous material between 0.7% and 1.3% $\bar{R}_o$(max) vitrinite reflectance (Powell et al. 1979). Depth-reflectance curves (Figures 12-18) obtained from the wells studied indicate that the lower limit of this reflectance was first reached in the coals and interseam sediments during the late Permian, particularly in the Nappamerri Trough. Hydrocarbon generation probably commenced soon after.

With increasing temperatures due to increasing depth of burial, minerogenic sediments would alter in response to the higher thermal regime. Clays are most susceptible to such alteration. Correlations of clay alteration and vitrinite reflectance (M. and R. Teichmüller 1966) have found that the major clay transformations occur at vitrinite reflectances of 1.4-2.0%. Montmorillonite-rich clays undergo structural transformations at .4-.6% $\bar{R}_o$(max) vitrinite reflectance, well before the period of major hydrocarbon generation period. The presence of water and suitable ions and lower pH accelerate the major clay transformations and correspondingly lowers the temperature and time required. Even so, hydrocarbons forming in carbonaceous shales would be severely restricted in their ability to move into more permeable sands if clay dewatering is necessary for their migration (c.f. Powell et al. 1978).

Hydrocarbons generated in the coals must eventually find their way into permeable sands if they are to form economic accumulations. Thus, the presence of a sandstone or sandy-siltstone top and/or base for the majority of coal seams present and compaction from sediment loading, would allow hydrocarbons being formed to migrate into the surrounding sands.

Whilst the evidence is not conclusive, coal from the productive horizons appears to be the major source of hydrocarbons in the south western Cooper Basin. The Toolachee Formation and Patchawarra Formation both contain abundant coal and also are the two major hydrocarbon reservoir formations.

Detailed petrographic investigation of dispersed organic matter in the shales of the various Permo-Triassic formations would assist in clarifying their source rock potential.

00122

10. HYDROCARBON POTENTIAL

10.1 PERMO-TRIASSIC

Prospects for further commercial hydrocarbon discoveries in the Permo-Triassic formations of the Cooper Basin are very promising. The vitrinite and exinite content of the coals throughout the Permian sediments ensures hydrocarbon generation during coalification. Available conduits for migration (sandstones) are present (as evidenced by present producing fields) in the Permian sediments of the Cooper Basin.

Production and development wells are sufficiently numerous to enable reasonably confident subsurface geological extrapolation of new areas. Major discoveries to date are mostly located on the margins of the main depositional troughs. These fields occur on Permian structural closures; the Toolachee and Patchawarra Formations are the major producing horizons.

10.2 JURASSIC

From the nature and rank of the organic matter in Jurassic coals of the wells studied, and the results of recent drilling, the Jurassic appears very promising for further hydrocarbon discoveries. The Jurassic coals contain very high exinite contents (generally 3-5% of total coal and rarely 20% of total coal). The coals are vitrite and clarite . Exinite content in the coals is highest in the wells adjacent to the Tenneppera Trough. These south eastern wells also contain the thickest Jurassic coals. In terms of their rank, the carbonaceous shales and siltstones in the sequence are well placed for hydrocarbon generation. Vitrinite reflectances in the Jurassic coals are generally within the reflectance range associated with oil generation. The maceral content of the coals is likely to reflect the composition of the organic matter in adjacent shales and siltstones; moreover exinite tends to be enhanced in the sediments (Smyth, 1979). The potential for hydrocarbon generation , particularly light oils, is therefore very good in this area of the Cooper Basin.

Jurassic sands are generally quite porous (e.g. Mooga Formation is an aquifer) with few impermeable horizons. The Birkhead Formation and Westbourne Formation form reasonable barriers to hydrocarbon escape (Nugent 1968). Stratigraphic traps from draping of Jurassic sediments over the Permo-Triassic highs, and possibly structural traps from late-Tertiary folding (Battersby, 1976) are the best sites for potential hydrocarbon accumulation. The

00123

necessary conditions for such economic hydrocarbons are:-

- impermeable cap rock
- suitable conduit for migration of hydrocarbons
- minimal flushing by artesian waters.

These constraints mean that the hydrocarbon producing structures will be relatively small and occur irregularly. The best potential hydrocarbon reservoirs would be located in the Mooga Formation and Birkhead Formation or their equivalents (Hooray Sandstone, Walloon Coal Measures).

00124

CONCLUSIONS

1. In the south western Cooper Basin there are definite trends in coal maceral composition, both vertically and laterally, and knowledge of such trends would greatly assist further exploration of the basin.
2. The rank profiles of the wells studied (Figure 19) are complex and indicate coalification in the Cooper Basin is dependent upon several factors including:
   - age of the coal
   - stratigraphic position
   - depth from basement
   - structural location within the basin i.e. whether in a trough or on a high
   - movement of formation waters.
3. Reflectance data combined with present day geothermal gradients indicate:
   - a stable Permo-Triassic geothermal gradient, enhanced in the central Nappamerri Trough and declining in the late Triassic-early Jurassic
   - with cessation of Permo-Triassic sedimentation a lower (relative to the Permo-Triassic) geothermal gradient in the Jurassic, Cretaceous.
   - and a post Cretaceous rise in geothermal gradient possibly in the late Tertiary.
4. Jurassic hydrocarbon potential is very promising and deserves further investigation. Good potential is shown by sediments within or adjacent to the Tenneppera Trough and particularly on the stratigraphic traps associated with the major anticlinal trends.

REFERENCES

Baker, E.G. (1960): A Hypothesis Concerning the Accumulation of Sediment Hydrocarbons to crude oil. Geochimica et Cosmochimica Acta, Vol. 19, pp.309-317.

Battersby, D.G. (1976): Cooper Basin Gas and Oil Fields. Economic Geology of Australia and Papua New Guinea, Part 3, Petroleum Section: Australian Institute of Mining and Metallurgy pp. 321-368.

Beddoes, L.R. (1973): Oil and Gas Fields of Australia, Papua New Guinea and New Zealand. Tracer Petroleum and Mining Publications, Sydney, Aust.

Bennet, A.J.R. (1968): The Reflectance and Coking Behaviour of Vitrinite-Semifusinite Transition Material. Fuel, 47, pp.51-62.

Bostick, N.H., Foster, J.N. (1975): Comparison of Vitrinite Reflectance in Coal and in Kerogen of Sandstones, Shales and Limestones in the Same Part of a Sedimentary Section. Petrographie de la Matiere Organique des Sediments, CNRS, Paris, pp.13-25.

Brooks, J.D. (1970): The Use of Coals as Indicators of the Occurrence of Oil and Gas. APEA J., 10(2), pp.35-40.

Brooks, J.D., Hesp, W.R., Rigby, D. (1971): The Natural Conversion of oil to gas in sediments in the Cooper Basin. APEA J., 11(1), pp.121-125.

Brown, H.R., Cook, A.C., Taylor, G.H. (1964): Variations in the Properties of Vitrinite in Isometamorphic Coal. Fuel, 43, London, pp.111-124.

Castano, J.R. (1975): Comparative Study of Burial Using Vitrinite Reflectance and Anthigenic Minerals. Colloque International Petrographie de la Matiere Organique des Sediments, Paris.

Castano, J.R., Sparks, D.M. (1974): Interpretation of Vitrinite Reflectance Measurements in Sedimentary Rocks and Determination of Burial History Using Vitrinite Reflectance and Authigenic Minerals. Geol. Soc. of America, Special Paper 153, pp.31-52.

Chandra, D. (1958): Reflectance of Oxidized Coals. Economic Geology, 53(2), pp.102-108.

Cordell, R.J. (1972): Depths of Oil Origin and Primary Migration: A Review and Critique: Am. Assoc. Petroleum Geologists Bull, Vol. 56, 10, pp.2029-2067.

Demaison, G.J. (1975): Relationship of Coal Rank to Palaeotemperatures in Sedimentary Rocks. Petrographie de la Matiere Organique des Sediments. CNRS Paris. pp.217-224.

Devine, S.B., (1975): An Assessment of the Onshore Petroleum Potential of Central and South Australia. Aust. Petrol. Explor. Ass. J., 15(2), pp.60-71.

Dow, W.G., (1977): Kerogen Studies and Geological Interpretations. Journ. of Geochem. Explor., 7 (1977), pp.79-99.

Fertl, Wichmann, (1977): Static Temperature Temp. from Well Logs. Dresser, Atlas Technical Memorandum 7 (3).

Gatehouse, C.G., (1972): Formations of the Gidgealpa Group in the Cooper Basin. Australas. Oil, Gas Review, 18(12), pp.10-15.

Kantsler, A.J., Smith, G.C., Cook, A.C. (1978): Lateral and Vertical Rank Variation in the Cooper Basin: Implications for Hydrocarbon Exploration. A.P.E.A.J., Vol. 18 (1).

Kapel, A.J. (1966): Geol.of the Patchawarra Area, Cooper Basin. Aust. Pet. Explor. Assoc. J., 12(1), pp.53-57.

Karweil, J., (1975): The Determination of Palaeotemperatures From Optical Reflectance of Coaly Particles in Sediments. In Petrographie de la Matiere Organiques de Sediments CNRS, Paris, 1975. pp.196-203.

Kisch, H.J. (1975): Coal Rank and "Very Low-Stage" Metamorphic Mineral Facies in Associated Sedimentary Rocks: An Introduction. Colloque International, Petrographie de la Matiere Organiques des Sediments. Paris, pp.117-121.

Middleton, M.F. (1979): Heat Flow in the Moomba, Big Lake and Toolachee Gas Fields of the Cooper Basin and Implications of Hydrocarbon Maturations. Bull. Aust. Soc. Explor. Geophys., Vol. 10(2).

Nugent, O.W. (1969): Sedimentation and Petroleum Potential of the Jurassic Sequence in the South-Western Great Artesian Basin, APEA, J., 9, pp.97-107.

Maxwell, J.C. (1964): Influence of Depth, Temperature and Geological Age on Porosity of Quartzose Sandstone. Bull. Am. Assoc. Petrol Geologists, Vol. 48, No. 5, pp.697-709.

Powell, T.G., Fosiolos, A.E., Gunther, P.R. and Snowdon, L.R. (1978): Diagenesis of Organic Matter and Fine Clay Minerals: A Comparative Study. (Inst. Sed. and Petrol. Geol.; Geol. Survey of Canada). Geochimica et Cosmochimica Acta, Vol. 42, pp.1181-1197.

Powell, T.G. and McKirdy, D.M. (1976): Geochemical Character of Crude Oils from Australia and Papua New Guinea. Econ. Geology of Aust. Papua New Guinea. Australas. Institute of Mining and Metallurgy. Vol. 3, Petroleum pp.18-29.

Powell, T.G., McKirdy, D.M. (1975): Geologic Factors Controlling Crude Oil Composition in Australia on Papua New Guinea. Am. Ass. of Pet. Geologists Bull. Vol. 59, No. 7.

Schwebel, D., Riley, M., (1978): Temperature Study of the Cooper Basin. Unpublished report of S.A. Oil and Gas Corp. Ltd.

Shibaoka, M. and Bennett, A.J., (1977): Patterns of Diagenesis in Some Australian Sedimentary Basins. APEA J., 1977, pp.58-63.

Smith, G., Cook, A.C. (1979): Coalification Paths of Exinite, Vitrinite and Inertinite. To be published (submitted) - Fuel, London.

Smyth, M., (1970): Type Seam Sequences from some Permian Australian Coals. Proc. Australas. Institute of Mining and Metallurgy, No. 233, pp7-15.

Smyth, M., (1979): Hydrocarbon Generation in the Fly Lake-Brolga Area of the Cooper Basin. APEA Journal Vol. 19, Part 1, pp.108-115.

Stack, E. (1975): Stack's Textbook of Coal Petrology. 2nd Edition. Gebruder Borntraeger, Berlin.

Steveson, B.G., and Spry, A.H. (1973): Nature of Porosity in Some Indurated Permian Sandstones from the Cooper Basin. APEA Journal 1973, pp.86-90.

Teichmuller, M. and R. (1966): Geological Causes of Coalification. Coal Science. Adv. Chem. Ser. 55, Washington D.C., pp.133-155.

Thompson, R., R., and Benedict, L.G. (1974): Vitrinite Reflectance as an Indicator of Coal Metamorphism for Cokemaking. Geol. Soc. of America. Special Paper 153, pp.95-108.

Thornton, R.C.N., (1978): Regional Lithofacies and Palaeography of the Gidgealpa Group. APEA Journal, pp.52-63.

Tissot, B., Durand, B., Espilitalie, J. and Combaz, A. (1974): Influence of Nature and Diagenesis of Organic Matter in Formation of Petroleum. Am. Assoc. Pet. Geol. Bull. 58, pp.499-506.

Wopfner, H. (1972): Climate and deposition in Permian and Early Triassic in South Australia. Abstracts 44th ANZAAS Congress Sydney, pp.95-96.

ACKNOWLEDGEMENTS

I wish to thank Professor P. Ypma of the University of Adelaide and Dr. D. McKirdy of the South Australian Department of Mines and Energy for their supervision and debate throughout the development of this paper.

Thanks are extended to: the South Australian Department of Mines and Energy for its support in providing polished sections and colour plates; Delhi Oil for approval to consult well completion reports and other input data; A.M.D.E.L. for the generous use of the reflectance microscope and Dr. B. Steveson and Ms. L. Day for their advice and technical assistance; Professor A. Cook of the University of Wollongong for facilitating my attendance at a coal microscopy course and Mr. A.J. Kantsler for his essential assistance and correspondence during the year and the Economic Geology Department of the University of Adelaide for providing financial assistance for various undertakings during the year.

I would also like to thank: Mr. J. Armstrong for his help and discussion; the laboratory staff of the Geology Department in particular Wayne Mussared for his tireless efforts; Sue Brockhouse for typing this thesis; my fellow honours students for their interest and debate and finally I would like to thank my parents for their unerring faith.

8426-1

ISORANK PROFILE OF THE SEVEN WELLS

FIG. 19

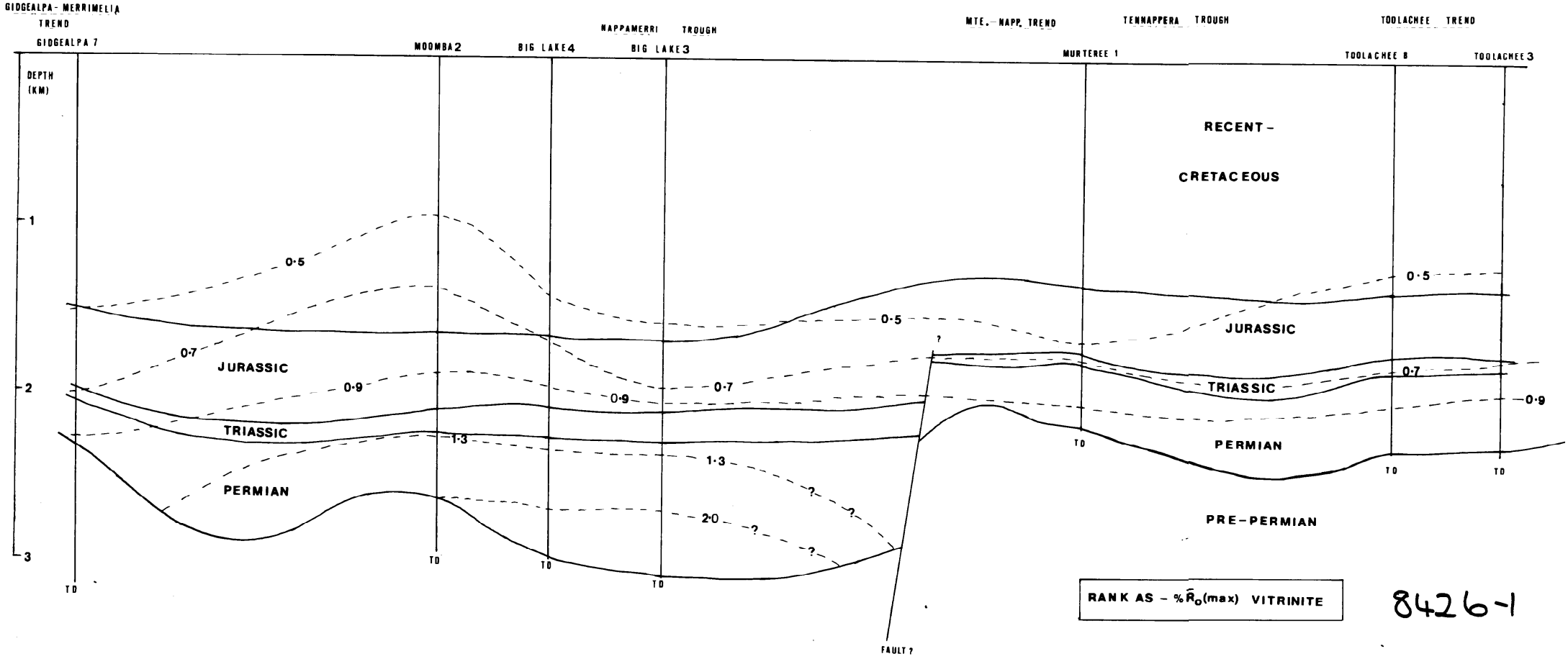

8426-1

T Lonergan 1979

APPENDIX I

A. Sampling.

Sampling of the seven wells under study was as comprehensive as possible. Sample intervals were selected from the electric logs and sequence descriptions (Triassic and Permian) available from well completion reports.

The well samples available consisted almost exclusively of rock-cuttings. The amount of core available was extremely limited with core being taken in the Permian and Triassic sequences and only then in limited quantities (order of 100 metres per well).

The intervals over which the cuttings were taken were 9.15 metres (30 feet) in the post-Triassic and 3.05 metres (10 feet) in the Triassic and Permian sequences. All cuttings were skeletonized before being deposited at the S. Aust. Mines and Energy Dept. Core Library.

To obtain good control in the wells, particularly near the Triassic unconformity, the skeletonized cuttings were all progressively sampled for even minor amounts of coal.

Well cuttings Available for Sampling

	Total Depth	Depth sampling commenced	Rock Unit
Gidgealpa No. 7	3226m (10582')	Transition beds (unspecified)	Transition beds (L. Cret)
Moomba No. 2	3005m (9858')	1616m (5300')	Transition beds (L. Cret)
Big Lake No. 3	3122m (10242')	2034m (6670')	Hutton S.S. (L.-Jurassic)
Big Lake No. 4	3028m (9933')	2113m (6929')	Nappamerri Fm. (M-L. Triassic)
Murteree No. 1	2205m (7232')	0m (0')	Unnamed (Recent)
Toolachee No. 8	2367m (7763')	1646m (5400')	Mooga Fm. (U. Jurassic)
Toolachee No. 3	2351m (7710')	1677m (5500')	Birkhead Fm. (U-M Jurassic)

B. Problems Associated with Sampling

1. A serious problem encountered in sampling the wells was the lack of rock cuttings in the post-Triassic. Rock cuttings of the post-Triassic sequences from wells drilled in established fields e.g. Toolachee Field and Big Lake Field, appear as a rule to have not been collected for future reference. This procedure has only recently been changed for obvious reasons.

APPENDIX 1 (cont.)

2. Down hole cavings, contaminating lower intervals could be expected, particularly from coal sampled in intervals with a very low coal content. Definitive evidence of down well contamination was found in several wells. In Big Lake No. 4 coal cuttings were found at 3061 metres, some 45 metres below the basal Permian sediments.

   Down hole contamination has been found to be a problem in several wells in the Nappamerri Trough and has been interpreted as a contributing cause of the wide vitrinite reflectance variations found in the lower Jurassic coal samples from Big Lake No. 3 (fig. 13) and Moomba No. 2 (fig. 11). In both wells coal sampled in the lower Jurassic yielded vitrinite reflectances ranging from .45% $\overline{R}_o$(max) to 1.00% $\overline{R}_o$(max). The vitrinite reflectances of approximately .45% $\overline{R}_o$(max) were interpreted as down hole contamination (supported by A. Kantsler pers. comment.).

   Down hole contamination in other wells examined in this study and in the Permo-Triassic samples of Big Lake No. 3 and Moomba No. 2 was minimal and easily recognised and as such measurements were discarded.

3. Particulate coal samples from two wells, Moomba No. 2 and Big Lake No. 3 when polished exhibited the effects of extreme artificial drying ("fry-panning"). The Moomba No. 2 samples (plate A1) were seriously affected, exhibiting oxidation rims and dessication cracks due to drying at high temperatures.

   This oxidation is most pronounced in the Jurassic coals of Moomba No. 2 and despite avoidance of such oxidized vitrinite for reflectance measurements it is probably responsible for many of the higher reflectance values obtained in the Jurassic coals of Moomba No. 2.

C. Sample Preparation

The coal samples to be used for research are set in the standard resin or fibreglass mounts for polished sections. The softer astic is preferred due to its similarity to maceral hardness. Having a mount of similar hardness to coal considerably reduces relief. Obtaining an acceptable degree of polish has been found to be a process of trial and error. A problem encountered was that a high relief was often associated with a high polish.

Because the majority of the samples were particulate there was no preferred orientation for the polished sections. The polished sections of core samples, allowed preferred orientations to be examined.

APPENDIX 1 (cont.)

The mounted sample was polished using suitable abrasive papers of 400, 600, 1200 grade. The final polish was obtained on a lap plate using Magnesium oxide, bromium sesquioxide and diamond paste (down to quarter micron) or a combination of the three. The lubricating agent was generally water although some of the coals required an oil or glycerine lubricating agent. Kerosene proved a very poor lubricating agent giving a smeared, discoloured polish to the coal.

D. Influence of Coal Sample Type on Total Maceral Type Content

During examination of polished sections a potential selective bias emerged when vitrinite, inertinite and exinite content were being determined.

In Murteree-1 coal cuttings and core in close depth proximity were prepared and compared for variation in vitrinite, inertinite and exinite content. Core samples cut approximately perpendicular to bedding contained approximately 15-30% greater relative vitrinite content than did the particulate samples.

Polished Sections

Toolachee Formation	1821m core
	1829m particulate sample
Patchawarra Formation	2016m core
	2027m particulate sample

Whilst closely similar results would not necessarily be expected the difference is sufficient to introduce some error into the use of cuttings for maceral content determination, particularly in those cases when vitrinite is low.

This problem can probably be related to the generally lower density of vitrinite compared to inertinite and exinite (Stack 1975 p.117) and the greater fracturing ability of vitrinite resulting in grains breaking up during drilling and the finer cuttings often being lost in the drilling mud. Thus size of coal cuttings probably have some bearing on total vitrinite content in the sample.

Analysis of polished sections containing finer cuttings (Toolachee-3, Toolachee Formation) indicated that the finer cuttings were almost exclusively vitrinite.

APPENDIX II

1. The reflectance of coal macerals has been found to increase as coalification progresses. This reflectance variation has been found to be a very useful and easily recognized indicator of coalification. This change in reflectance is a direct result of the altering and rearrangement of constitutent molecules in the coal.

Of the three coal maceral types: vitrinite, inertinite and exinite, vitrinite alone varies in any uniform way as coalification progresses. Vitrinite experiences, to a close approximation, a linear increase in reflectance versus coalification through the brown coal to bituminous-anthracite coal stages. Because coalification is related to depth of burial, prevailing temperature and time, reflectance and depth can be related.

The comparative reflectance trends of exinite and inertinite versus increasing vitrinite reflectance as found in Murteree No. 1 are shown in figure A1.

The vitrinite maceral group consists of several maceral types. These macerals differ in origin and in appearance in polished section (Plates An abridged table of the various coal maceral types is listed in Figure A2.

Tellocollinite or vitrinite A (Brown et al. 1964) is the agreed upon vitrinite maceral for determining vitrinite reflectance. Tellocollinite occurs in thicker layers and is generally pure although minor inertinite or exinite macerals may occur within the tellocollinite. Tellocollinite is derived from humic substances in plants originating from trunks, branches, stems, leaves and roots.

2. Coal is anisotropic and distinctly so with increasing rank. As such, in plane polarized light, accurate maximum, mean and minimum reflectances can be determined from samples examined perpendicular to bedding. However, because of the particulate nature of the bulk of the coal examined in this study, the maximum mean reflectance % $\overline{R}_o$(Max) is used because the minimum reflectance cannot be measured.

Reflectance values of vitrinite can vary from less than .2% $\overline{R}_o$(max) in lignites to greater than 6% $\overline{R}_o$(max) in anthracites. The majority of sub-bituminous to semi-anthracites have reflectance values between .5% $\overline{R}_o$(max) and 2% $\overline{R}_o$(max). Because reflectance values are so low extreme accuracy and reproducibility of results are essential.

3. The microscope used for obtaining the reflectance measurements in this paper was a Leitz Ortholux II Pol BK. The microscope (figure A3) consists of a phototube for receiving the reflected light and a photomultiplier with digital readout. The photomultiplier was calibrated against a glass standard of 1.23% $\bar{R}_o$. By convention reflectance measurements are determined in green light of 546 n.m.

There are two light sources in the microscope. The "observation" light source (A in figure A3) is a standard tungsten light of suitable intensity. The "observation" light was replaced by the "measurement" light (B in figure A3) when measurements were being made. The "reflected" light source is a tungsten lamp equipped with an extremely sensitive voltage stabilizer to maintain a continuous light intensity. The reproducibility of measurements made was within .01%.

The maceral to be measured is located within the "measurement" light illuminated area. The illuminated area of the maceral actually measured is approximately 3μ metres^2.

All examination of the macerals was done under immersion oil. The oil used was a Ziess non-fluorescing oil. The reflectance measurements were made using a 32x magnification objective. Maceral identification and examinations were made using 25x to 125x objectives. Point counts were made using a 25x objective.

The microscope is also equipped with a U.V. lamp allowing the macerals to be viewed and photographed under U.V. light.

4. The three maceral groups, vitrinite, inertinite and exinite fluoresce to some extent, however exinites fluoresce much more strongly than do the vitrinite and inertinite groups. This feature allows exinite macerals to be clearly seen in U.V. light whilst often being undetectable in white light.

From figure A1 it can be seen that above 1.2-1.4% mean maximum vitrinite reflectance exinite reflectance is similar or greater than that of vitrinite and as such disappears into the groundmass of the coal. Coalification stage and type of exinite under examination in ultra-violet light greatly affect fluorescence strength and colour. Exinite loses its fluorescence with coalification. Resinite and sporinite fluoresce strongly whilst in this study cutinite and liptodetrinite lacked marked fluorescence. The exines fluorescence colours range from pale yellow and orange through to red and brown-black. Due to chemical restribution of maceral constituents the fluorescence colours decrease in intensity and become progressively darker (eventually black) as coalification increases.

Ultra-violet microscopy is a very useful technique for recognising exinites which would otherwise be difficult to see.

1. Resinite and sporinite content when associated with a high argillic content.
   - plate A2, photo A under U.G. (photo B) indicated that spores and resinite macerals and not clay were present.
   - plate A3, photo A. under U.V. (photo B) indicated resinite macerals and not clay were present.
   - plate A3, photo C indicated a much higher resinite content than seen in white light.
   - plate A4 photo A under U.V. (photo B) indicated alginite? and sporinite was present amongst the argillic content.
   - plate A5, photo A. under U.V. (photo B) indicated little resinite was present.
2. Resinite content in vitrinite lumen.
   - plate A6, photo A under U.V. (photo B) indicated some resinite was present within the cell lumen.
   - plate 1 photo 1 under U.V. light indicated gellocollinite and not resinite present in the lumen.
3. Resinite and sporinite in cannel coal and detrital coals.
   - plate A6 photo C indicated that sporinite content was higher than expected from study under white light.

5. A. Samples for reflectivity measurements were selected from each of the seven wells. However the intervals at which reflectivity values were taken were dependent upon availability of coal cuttings, polish of sample when taken and suitability of vitrinite in the polished section. The samples selected give the most uniform coverage of the wells with depth. The number of polished sections used for obtaining reflectance values varied from polished sections in Toolachee No. 3 to 26 polished sections in Big Lake No. 3. In all polished sections were used for obtaining reflectance values.

The reflectivity of each polished section was calculated from 20-40 measurements on tellocollonite (Vitrinite A) macerals and then averaged. Because of the anisotrophy of the coal and the fact that the microscope is not perfectly centred; after the calculation of the maximum reflectance, rotation of the stage by approximately 180^{0} the maximum reflectance of another point can be determined. Thus some 40-80 reflectance values could be calculated. Mathematically 40-80 such readings give as accurate a value as 100 readings (Kantsler 1979). It is only when 300-400 readings are made, that accuracy is improved and then only marginally.

B. All samples polished (175) were used for determining the gross percentages of vitrinite, inertinite and exinite and the association of the macerals. Visual estimation was the method of determining microlithotype groups and associations. Point counting methods were used for determining vitrinite, inertinite and exinite percentages. The percentages obtained were based on 100-700 counts for each polished section and correlation with the visual estimate was found to be good.

Identification of exinite group macerals in coal above 1.2-1.4% $\bar{R}_o$(max) vitrinite reflectance was difficult and determining exinite percentage in samples was not attempted. The use of U.V. reflected light allowed some exinite to be identified in some of the samples which would otherwise have escaped detection.

FIG. A1

Summary of the microlithotypes*

Maceral composition (mineral-free)		Microlithotype	Maceral-group composition (mineral-free)	Microlithotype group
Monomaceral				
Co	> 95%	(Collite)*	V > 95%	Vitrite
T	> 95%	(Telite)*		
VD	> 95%			
S	> 95%	Sporite		
Cu	> 95%	(Cutite)*		
R	> 95%	(Resite)*	E (L) > 95%	Liptite
A	> 95%	Algite		
LD	> 95%			
Sf	> 95%	Semifusite		
F	> 95%	Fusite	I > 95%	Inertite
Sc	> 95%	(Sclerotite)*		
ID	> 95%	Inertodetrite		
M	> 95%	(Macroite)*		
Bimaceral				
V + S	> 95%	Sporoclarite		
V + Cu	> 95%	Cuticoclarite	V + E (L) > 95%	Clarite
V + R	> 95%	(Resinoclarite)*		V, E(L)
V + LD	> 95%			
V + M	> 95%			
V + Sf	> 95%			
V + F	> 95%		V + I > 95%	Vitrinertite
V + Sc	> 95%			V, I
V + ID	> 95%			
I + S	> 95%	Sporodurite		
I + Cu	> 95%	(Cuticodurite)*		
I + R	> 95%	(Resinodurite)*	I + E (L) > 95%	Durite
I + LD	> 95%			I, E(L)
Trimaceral				
V, I, E	> 5%	Duroclarite	V > I, E (L)	Trimacerite
		Vitrinertoliptite	E > I, V	V, I, E(L)
		Clarodurite	I > V, E (L)	

* The terms in parentheses are not at present in use.

Co = Collinite; T = Telinite; VD = Vitrodetrinite; S = Sporinite; Cu = Cutinite; R = Resinite; A = Alginite; LD = Liptodetrinite; M = Macrinite; Sf = Semifusinite; F = Fusinite; Sc = Sclerotinite; ID = Inertodetrinite; V = Vitrinite; F = Fusinite; L = Liptinite; I = Inertinite.

FIG. 2

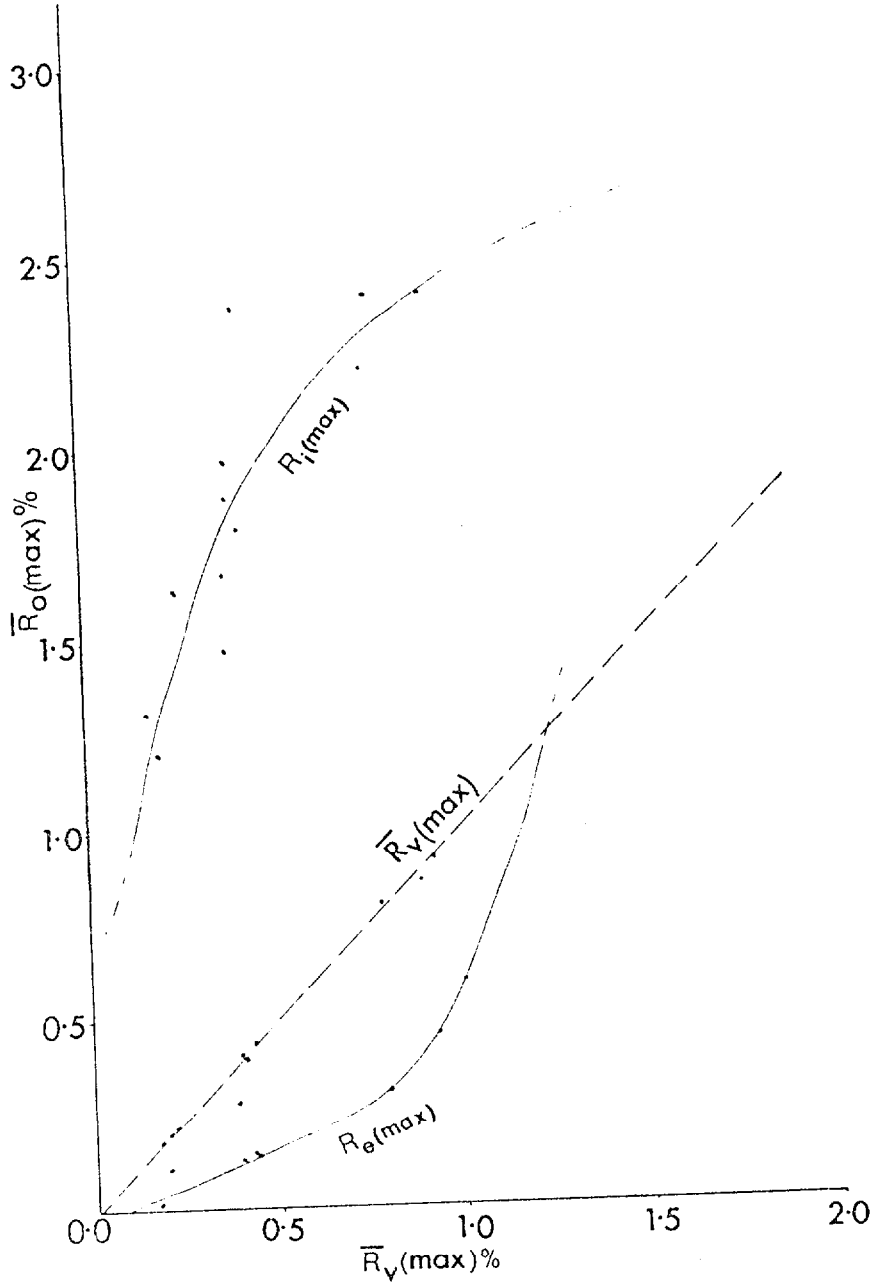
3·0
2·5
2·0
1·5
1·0
0·5
0·0
0·5
1·0
1·5
2·0
$\overline{R}_o(max)\%$
$\overline{R}_v(max)\%$
$R_i(max)$
$\overline{R}_v(max)$
$R_e(max)$

FIG. 3

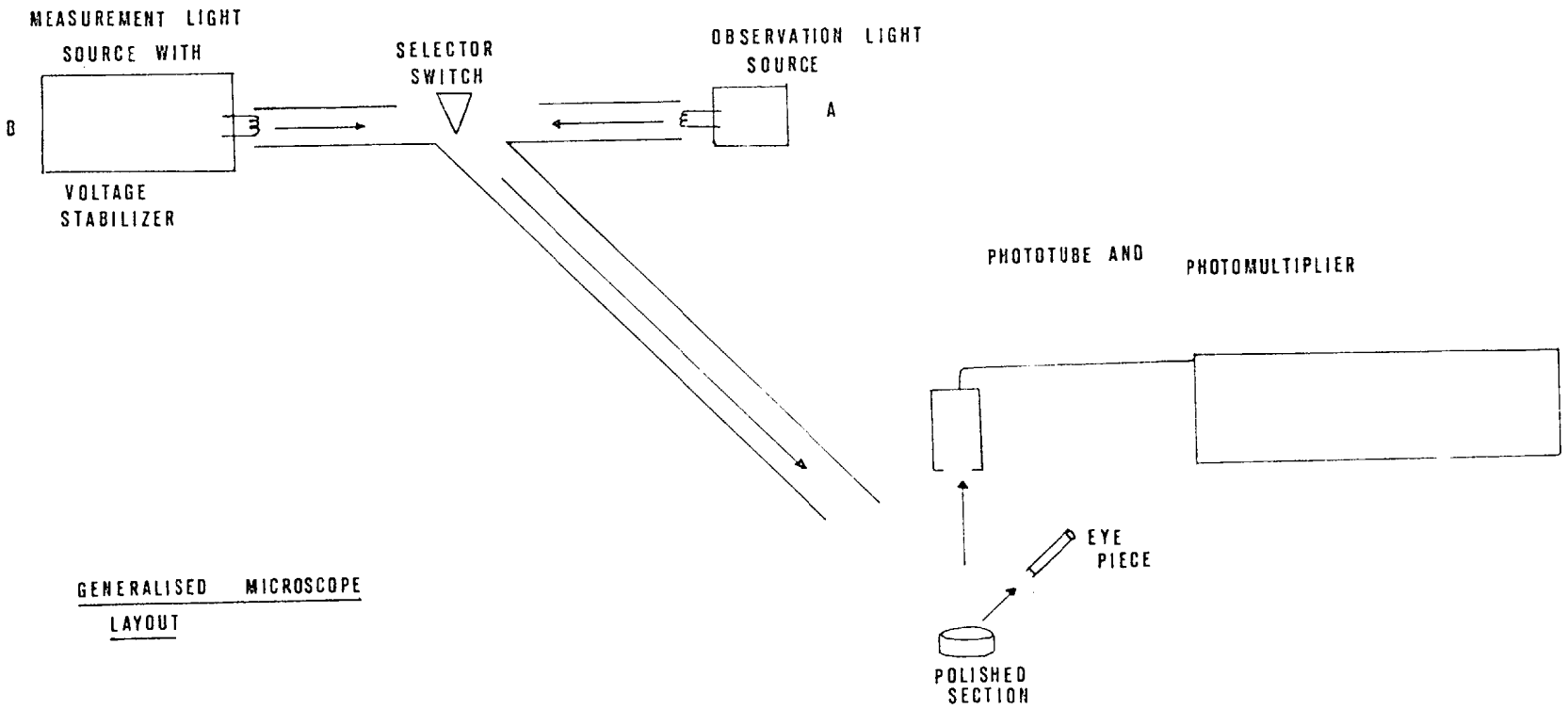

GENERALISED MICROSCOPE
LAYOUT

001138

PLATE A1

A - oxidation rim in vitrinite
(MOOMBA No. 2 1704m)

B - oxidation and dessication cracks in vitrinite
(MOOMBA No. 2 1899m)

PLATE A1

a

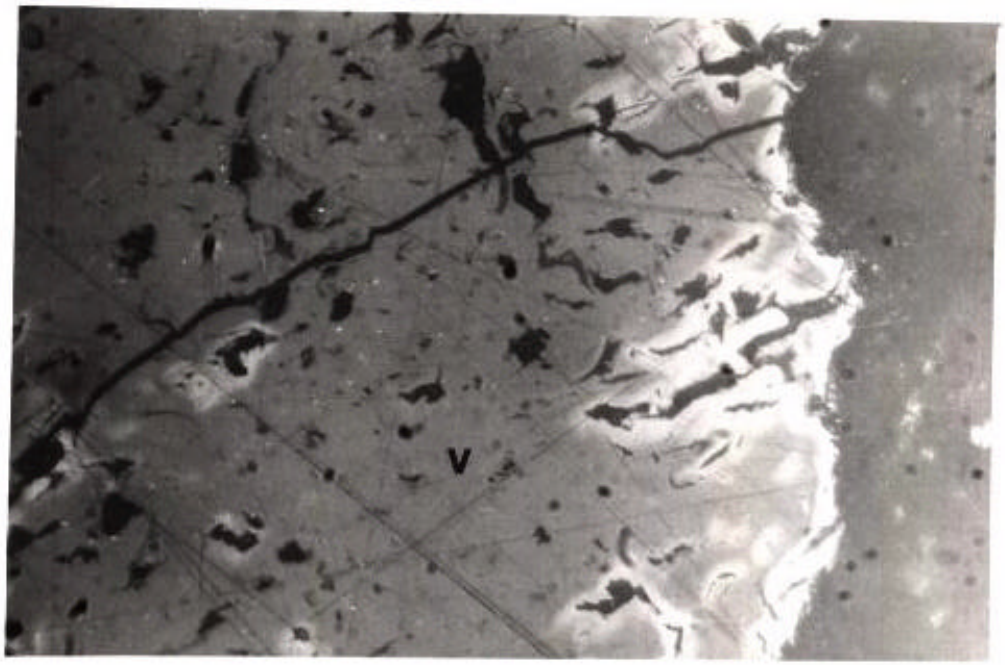

b

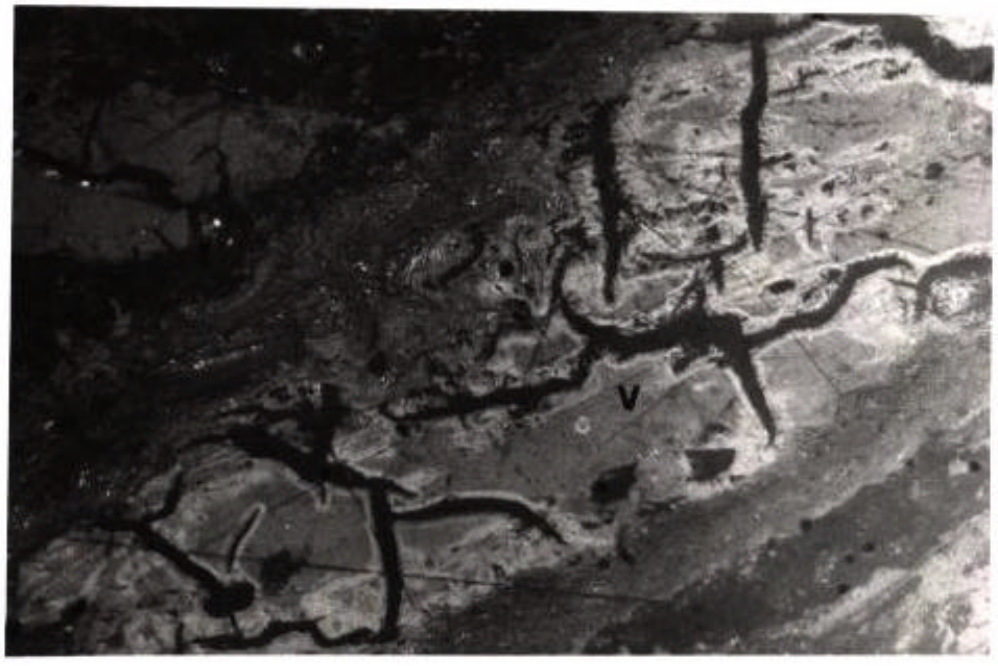

PLATE A2

A - Duroclarite (TOOLACHEE-8, 1887m)

B - Under U.V. light the well stratified nature of the exinite (sporinite, cutinite resinite) is apparent.

PLATE A2

a

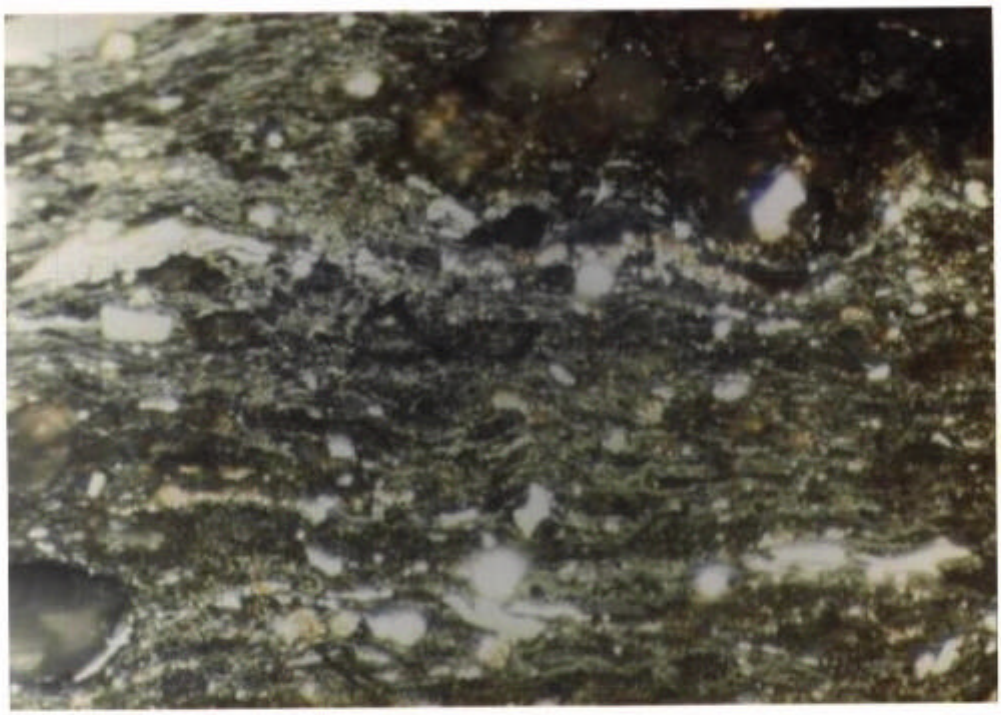

b

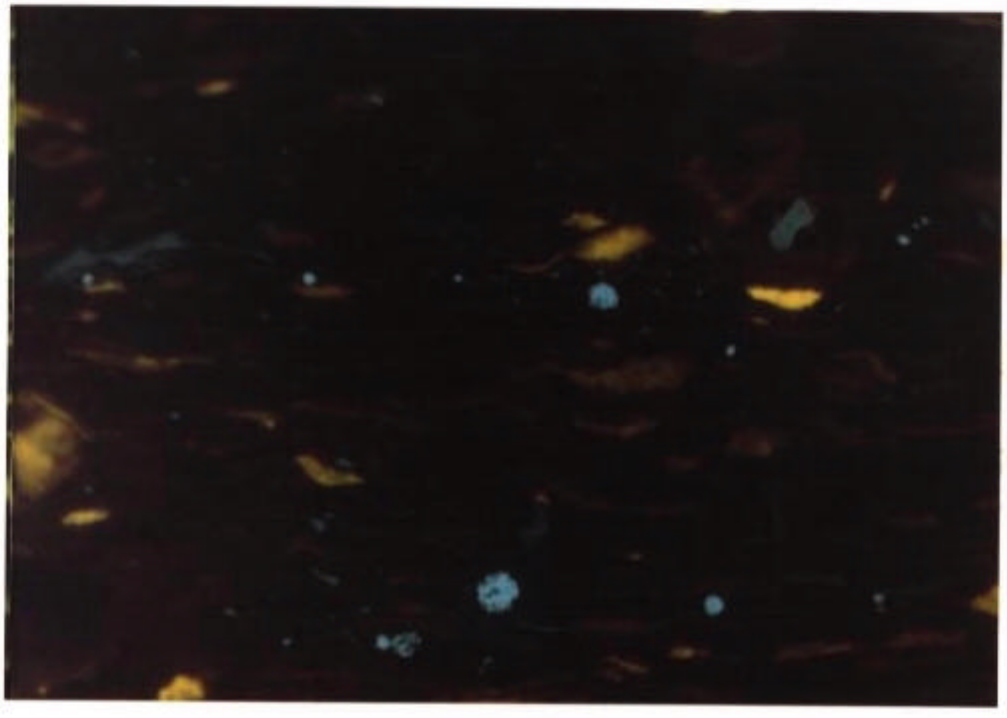

PLATE A3

A - Clarite (MURTEREE-1, 1490.8)

B - Under U.V. light the coal is seen to contain pods of resinite, minor spores and cutinite.

C - Clarite (TOOLACHEE-8, 1887m)
Under U.V. light resinite (yellow) is seen to be abundant.

00144

a

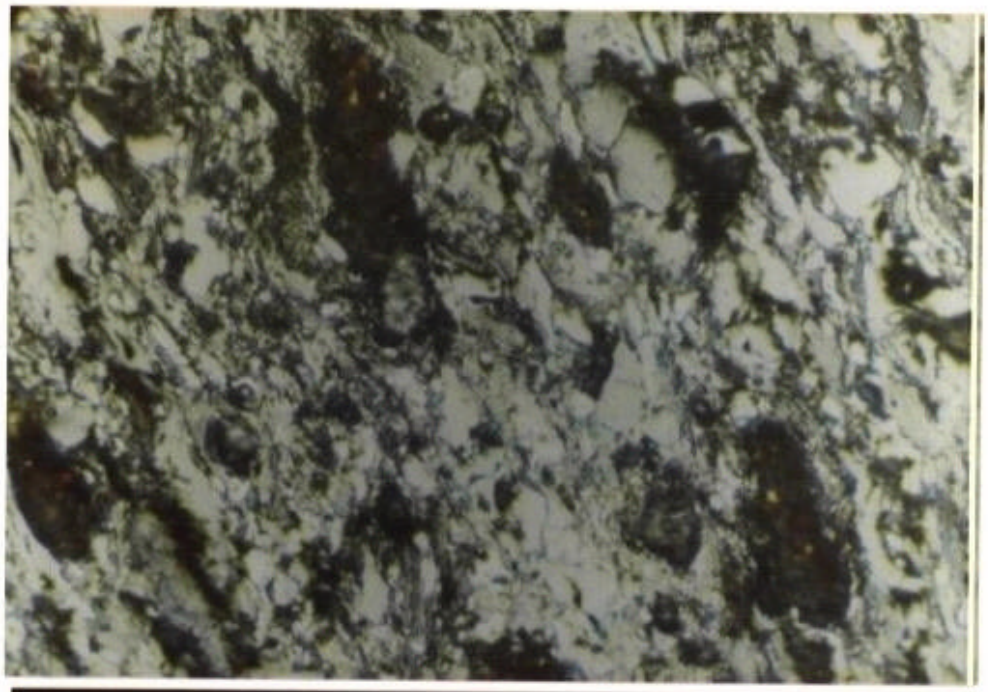

b

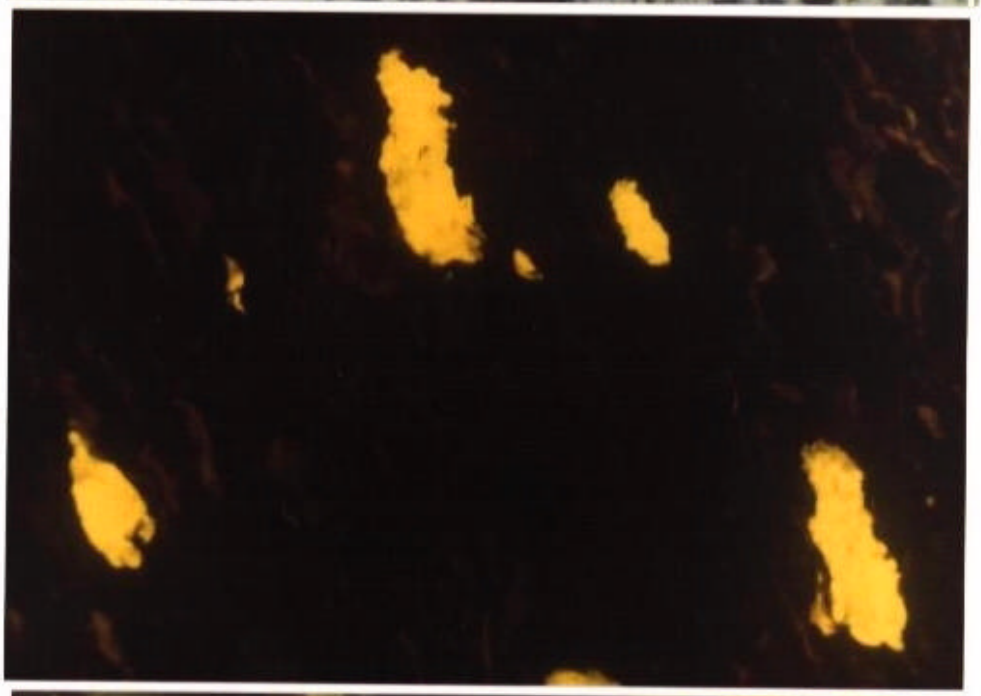

c

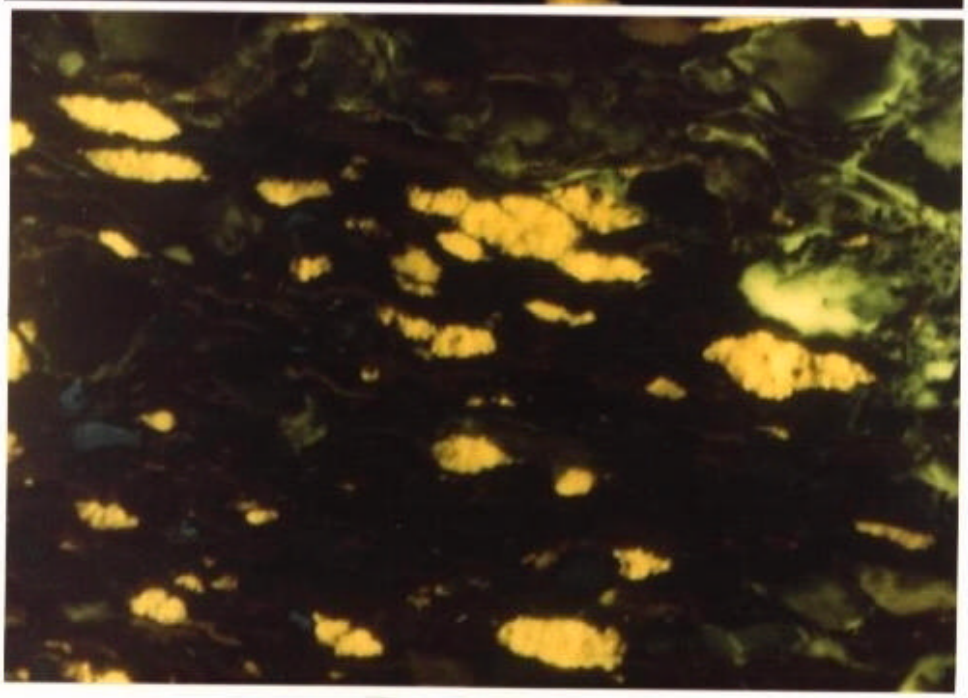

PLATE A4

A - Clarite-vitric carbargilite (GIDGEALPA-7, 1829m)

B - Under U.V. light exinite (yellow-brown) is seen to be abundant.

PLATE A4

a

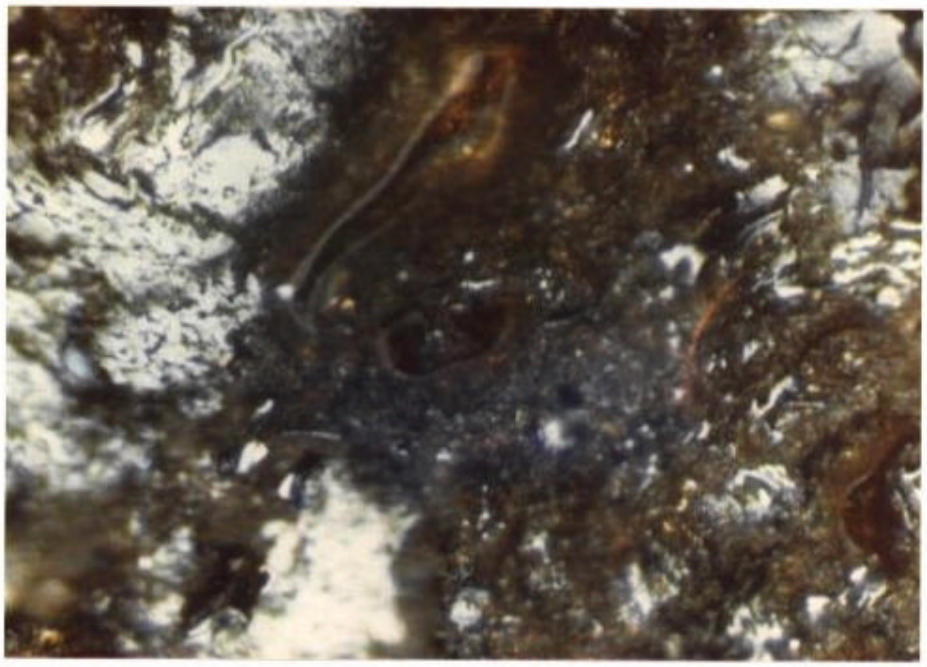

b

PLATE 5

A - Clarite (MOOMBA-2, 1689m)

B - Under U.V. light the cutinite bands fluoresic dull orange whilst possible resinite pods do not fluoresce and are therefore argilite.

PLATE A 5

a

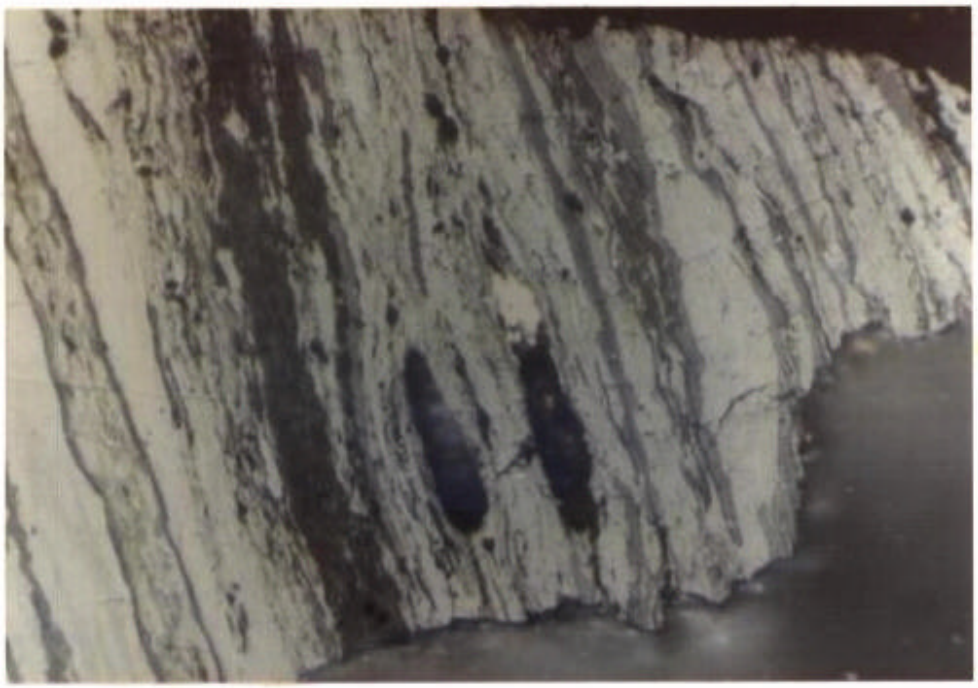

b

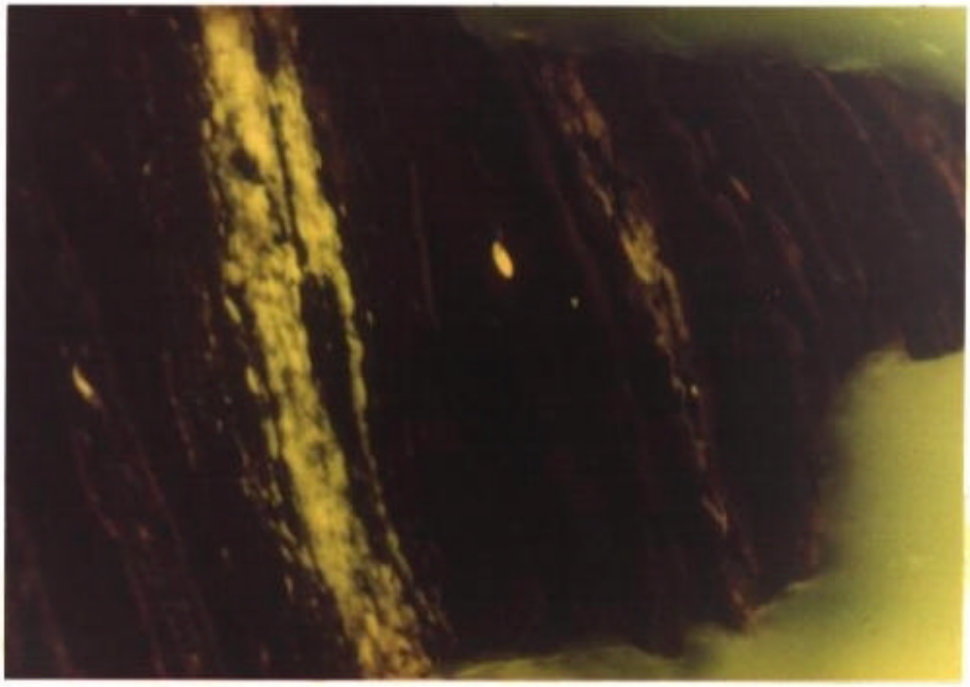

PLATE 6

A - Duroclarite (Big Lake-3, 2094.5m)
Vitrinite cell lumens visible.

B - Under U.V. light the lumens are seen
to contain resinite (orange-yellow).

C - Duroclarite (Toolachee-8, 2152.4m)
Under U.V. light the well stratified nature
of the coal can be seen. Exinite (sporinite)
content is very high, typical of cannel coal.

PLATE A6

a

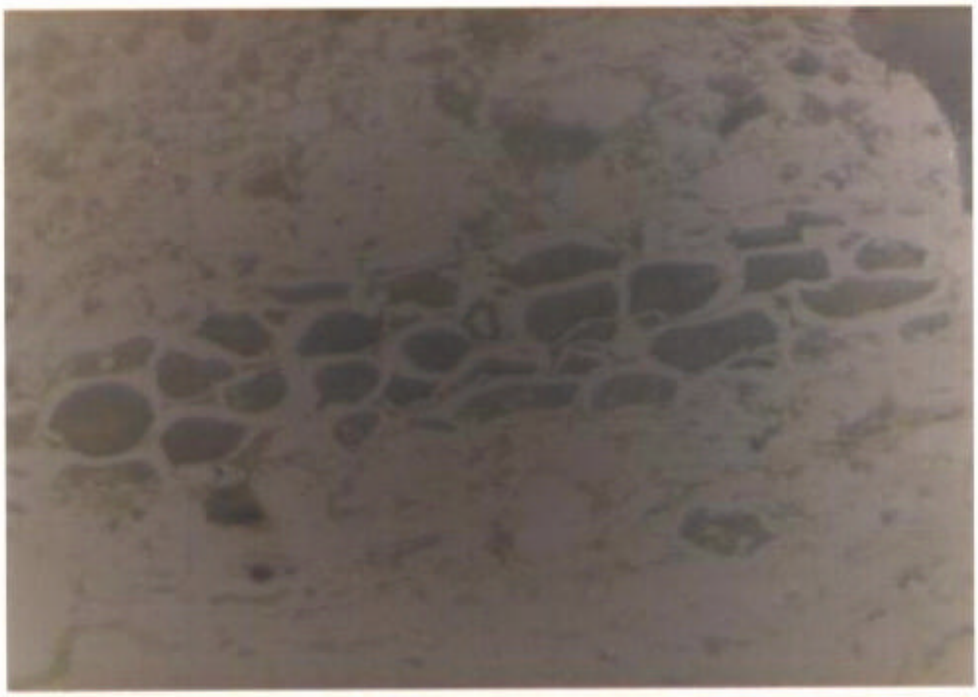

b

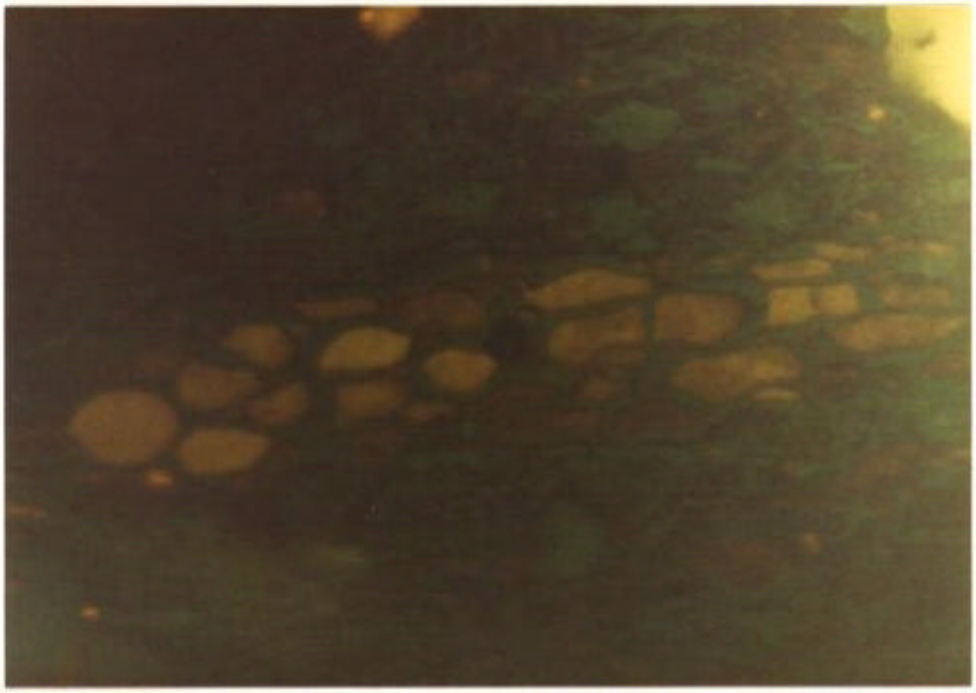

c

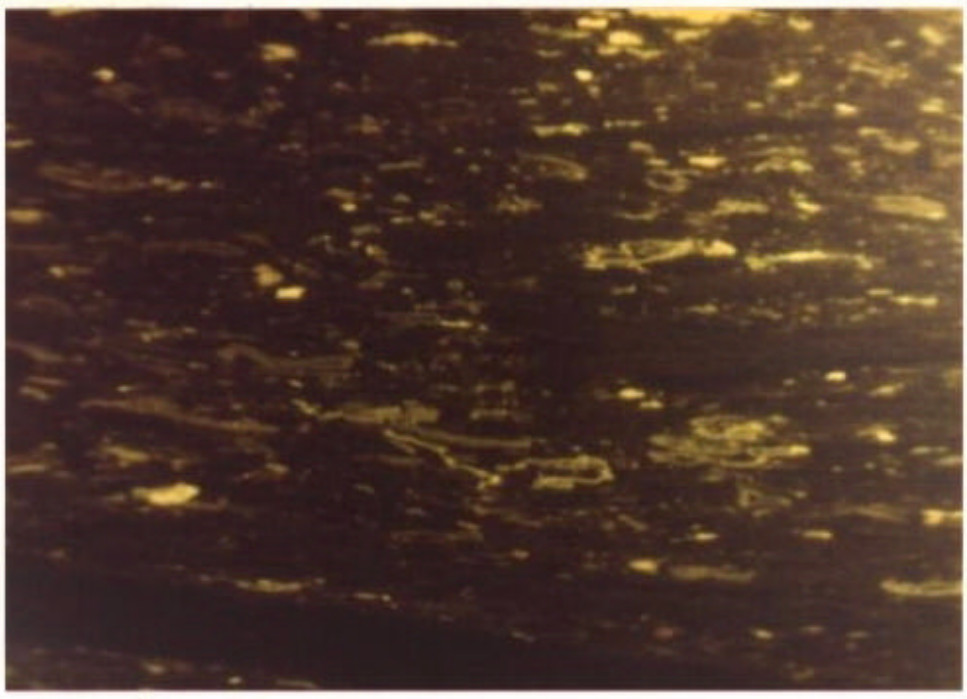

APPENDIX III - DATA

COAL SAMPLES USED FOR DATA COMPILATION

GIDGEALPA No. 7

Depth (m)	% $\bar{R}_{o(max)}$ Vit.
1475	.40% ± .02
1530	.46% ± .06
1550	.48% ± .05
1649	.49% ± .05
1716.5	.54% ± .06
1792.7	.50% ± .05
1829.3	.54% ± .04
1936	.56% ± .08
2033.5	.73% ± .04
2043	
2073	.75% ± .04
2097	.73% ± .04
2119.5	.77% ± .07
2121	.78% ± .04
2134	
2155	.85% ± .05
2165	.85% ± .04
2184	.82 ± .04
2268	
2299	.84% .03
2317	.96% .06

MOOMBA No. 2

Depth (m)	% $\bar{R}_{o(max)}$ Vit.
1646	.43% ± .03
1689	(.51% ± .02
	(.35% ± .02
1704	.48% ± .02
1799	(.77% ± .04
	(.42% ± .02
1899	
1923.8	(.95% ± .05
	(.60% ± .05
2018	(.77% ± .06
	(.97% ± .08
2164.6	1.22% ± .09
2207	1.29% ± .09
2280	
2296	
2298.8	1.29% ± .10
2320	1.42% ± .04
2326	
2330.8	1.39% ± .04
2381	1.50% ± .05
2387	1.31% ± .10
2421	1.51% ± .08
2460	1.52% ± .08
2491	
2531	1.91% ± .07
2564	1.85% ± .07
2648	
2661.6	2.01% ± .08
2689	
2724	
2789.6	2.00% ± .07

BIG LAKE No. 4

Depth (m)	% $\bar{R}_{o(max)}$ Vit.
2296	.93% ± .05
2304.8	
2329	
2332	1.03% ± .07
2371.9	1.03% ± .08
2384	1.04% ± .05
2390	
2439	1.06% ± .05
2503	
2506	1.14% ± .07
2530	
2543	
2596	1.19% ± .04
2600.6	
2606.7	1.24% ± .05
2683	
2695	
2698	1.43% ± .05
2728.6	
2762.2	
2768.3	1.59% ± .11
2789.6	
2810.9	
2844.5	1.65% ± .10
2847.6	
2875	
2948.1	2.08% ± .10
2972.6	
2987.8	1.98% ± .06
3060.9	2.53% ± .06

BIG LAKE No. 3

Depth (m)	% $\bar{R}_{o(max)}$ Vit.
2042.7	(.61% ± .06
	(.88% ± .09
2088.4	.87% ± .04
2094.5	(.63% ± .05
	(.87% ± .06
2122	(.72% ± .04
	(.90% ± .04
2140	(.73% ± .06
	(.99% ± .05
2323.2	
2338.4	1.10% ± .07
2365.9	1.25% ± .06
2372	1.24% ± .08
2375	
2408.5	1.35% ± .07
2558	1.59% ± .08
2560.9	1.67% ± .05
2564	1.71% ± .06
2649.4	1.93% ± .06
2734.7	2.07% ± .09
2744	2.04% ± .09
2756.1	
2759.1	
2798.8	2.11% ± .15
2801.8	2.23% ± .1
2820.1	2.25% ± .06
2823.2	
2838.4	2.23% ± .04
2850.6	2.35% ± .07
2878	2.40% ± .10
2905.5	
2923.8	2.44% ± .06
2936	2.40% ± .09
2954.3	
2960.3	2.50% ± .08
2996.9	2.75% ± .13
3000	2.47% ± .15
3082.3	2.59% ± .06

MURTEREE No. 1

Depth (m)	% $\overline{R}_{o(max)}$ Vit.
210.4	.18% ± .04
429.9	.20% ± .05
942.1	.33% ± .05
1106.7	
1490.8	.39% ± .02
1527.4	.43% ± .06
1554.9	.45% ± .01
1821	
1829.26	.75% ± .03
1884	.80% ± .03
1905.5	.78% ± .04
2016	
2027.4	.85% ± .03
2076.2	.94% ± .03
2143	

TOOLACHEE No. 8

Depth (m)	% $\overline{R}_{o(max)}$ Vit.
1365.9	.54% ± .06
1670.7	.57% ± .04
1686	(.56% ± .02
	(.53% ± .03
1704.3	.59% ± .02
1710.4	.58% ± .06
1878	.74% ± .05
1887.2	.74% ± .03
1923.8	.78% ± .05
1926.8	.78% ± .06
1942.1	.80% ± .03
1945	.83% ± .06
1954.3	.82% ± .05
1963.4	.84% ± .03
1966.5	.87% ± .05
1987.8	.90% ± .07
1994	.90% ± .05
2054.9	.91% ± .04
2152.5	.94% ± .04
2323.2	1.15% ± .07
2329.3	1.17% ± .08
2332.3	1.17% ± .05

TOOLACHEE No. 3

Depth (m)	% $\bar{R}_{o(max)}$ Vit.
1768.3	.66% ± .05
1838.4	
1890.2	
1908.5	.82% ± .04
1932.9	
1981.7	.86% ± .07
2088.4	
2192	.92% ± .05
2231.7	1.00% ± .06
2223	
2271.6	1.08% ± .03

SELECTED POLISHED SECTION DESCRIPTIONS

GIDGEALPA No.7

Depth (m)	
1550 (5100')	VITRITE, CLARITE (V) 1. 80% - tellocollinite with some lumen filled with collinite. 2. <20% - tellocollinite with minor resinite rodlets. 3. 1-2% - semifusinite, fusinite, pyrite in 90% clay.
1792.7 (5880')	VITRITE, CLARITE (V) 1. 60% - tellocollinite with some lumen, clay and resinite filled. 2. 40% - desmocollinite and tellocollinite with sporinite, resinite and 20% clay.
2097 (6878')	CLARITE (V) VITRITE 1. 20% - tellocollinite grains with minor clay, resinite. 2. 30% - oxidized granular desmocollinite, fusinite, semifusinite and inertodetrinite and rare spores. 3. 40% - banded vitrinite A with minor inertinite and spores. 4. 10% - grains of semivitrinite.
2119.5 (6952')	CLARODURITE 1. 20% - pure tellocollinite bands. 2. 80% - macrinite, desmocollinite, semifusinite and sporinite grains.
2155.5 (7070')	VITRINERTITE (V), DUROCLARITE (V) 1. 40% - semifusinite grains and Fe argilite. 2. 40% - clay (Fe) with desmocollinite, inertodetrinite sporinite. 3. 20% - desmocollinite, inertodetrinite, spores.
2165 (7100')	VITRITE 1. 95% - Vitrinite A bands with minor cutinite. 2. 5% - grains of semifusinite.

MOOMBA No. 2

Depth	
1689 (5540')	VITRITE 1. 50% - vitrinite with lumen and minor clay and quartz grains. 2. 50% - minor desmocollinite, inertodetrinite in argilite.
1799 (5900')	VITRITE, CLARITE (V) 1. Vitrinite with cutinite, resinite, sporinite. 2. Argilite with minor inertodetrinite and pyrite and carbonate (siderite).
1924 (6310')	VITRITE, CLARITE (V) 1. 80% - oxidized, dessicated vitrinite. 2. 20% - oxidized desmocollinite, inertodetrinite and minor sporinite and resinite and carbonate (siderite).
2280 (7479')	DUROCLARITE (V) 1. 5% - inertodetrinite with 90% argilite. 2. 65% - granular vitrinite grains. 3. 30% - granular well compacted, degrado-vitrinite, inertodetrinite and minor spores.
2298.8 (7540')	VITRINERTITE (V) 1. 50% - granular vitrinite and inertodetrinite. 2. 50% - granular vitrinite and inertodetrinite >30% and carbonate.
2330.8 (7645')	VITRINERTITE (V) 1. 90% - vitrinite A/B with minor inertodetrinite. 2. 10% - granular vitrodetrinite and inertodetrinite and carbonate.
2648 (8687')	VITRINERTITE (V) 1. 40% - banded tellocollinite, semifusinite and minor inertodetrinite. 2. 60% - granular, compacted, stratified vitrinite, inertodetrinite.
2661.5 (8730')	VITRINERTITE (V) 1. 55% - tellocollinite with minor fusinite bands and inertodetrinite. 2. 15% - cannel coal, vitrinite, inertodetrinite and relict spores. 3. 30% - fusinite grains (bogens.) - carbonate present throughout.

MOOMBA No. 2 (cont.)

2789.6 (9150')
VITRINERTITE (V)
1. 20-10% - granular vitrinite, semifusinite and inertodetrinite with argilite.
2. 80-90% - banded vitrinite A (tellocollinite) and fusinite, semifusinite and minor inertodetrinite.

BIG LAKE No. 4

2295.7 (7530')
DUROCLARITE (V)
1. 80% - elongate, stratified well compacted vitrinite, inertodetrinite, sporinite cannel type.
2. 20% - tellocollinite bands and desmocollinite and semifusinite with clay.

2332 (7650')
CLARODURITE (V), VITRINERTITE (V)
1. 60% - vitrinite bands with fusinite bands and minor sporinite, resinite.
2. 40% - desmocollinite with inertodetrinite, carbonate.

2384 (7820')
VITRITE, DUROCLARITE (V), MINOR CARBOSILICITE
1. 25% - vitrinite, some lumen clay filled and sporinite.
2. 60% - desmocollinite with inertodetrinite and sporinite.
3. 15% - vitrinite and quartz grains with minor sclerotinite.

2682.9 (8800')
VITRINERTITE (V)
1. 50% - granular vitrinite with minor inertodetrinite.
2. 40% - desmocollinite with carbonate, fusinite inertodetrinit and argilite.
3. 10% - vitric carbargilite.

2810.9 (9220')
VITRINERTITE (V), INERTITE
1. 15% - detrovitrinite in clay, shale.
2. 85% - granular vitrinite, inertodetrinite and argilite.

2875
VITRINERTITE (V), INERTINITE
1. 70% - tellocollinite and desmocollinite with inertodetrinite, fusinite.
2. 20% - fusinite and semifusinite bands and vitrinite grains.
3. 5-10%- vitrinite B and argilite.

2810.9 (9220')
VITRINERTITE (V)
1. 10-15%-vitrinite B in shales.
2. 85% - banded vitrinite A, fusinite, semifusinite with inertodetrinite and desmocollinite, tightly packed.

BIG LAKE No. 3

2042.7 (6700')
CLARITE (V), DUROCLARITE (V)
1. 25% - vitrinite A and B with sporinite resinite and inertodetrinite.
2. 65% - vitrinite B with minor cutinite, resinite, sporinite wrapped around clay.
3. 10% - vitrinite grains in argilite.

2094.5 (6870')
VITRIC CARBARGILITE, DUROCLARITE (V)
1. 55% - VITRIC and DURIC carbargilite.
2. 45% - vitrinite A and B bands with clay, quartz grains, cutinite and inertodetrinite.

2122 (6960')
VITRIC CARBARGILITE, CLARITE (V)
1. 60% - VITRIC and minor DURIC carbargilite.
2. 40% - vitrinite B (desmocollinite) with sporinite, clay, inertodetrinite, all exhibiting folds.

2338.4 (7670')
VITRINERTITE, DUROCLARITE (V)
oxidized, granular and detrital, vitrinite inertodetrinite, rare sporinite, resinite with clay 0 → 40%.

2365.9 (7760')
DUROCLARITE (V)
1. 100% - vitrinite A and B with fusinite, semifusinite, inertodetrinite and minor sporinite.

2375 (7790')
VITRINERTITE (V)
1. 60% - banded vitrinite A and B with semifusinite bands and inertodetrinite.
2. 40% - desmocollinite with inertodetrinite, micrinite.

2734.7 (8970')
VITRINERTITE (V), VITRIC AND DURITIC CARBARGILITE.
1. 50% - vitric and duritic carbargilite.
2. <30% - granular vitrinite.
3. ~25% - banded vitrinite A and B

2868.9 (9410')
VITRINERTITE (V)
1. 20% - granular vitrinite.
2. 80% - banded vitrinite A and B, fusinite and semifusinite with minor clay and inertodetrinite.

2960.3 (9710')
VITRINERTITE (V)
1. 70% - banded vitrinite A and B, fusinite and semifusinite and minor inertodetrinite.
2. 30% - cannel type vitrinite, inertodetrinite.

MURTEREE No. 1

1490.8 (4890')	CLARITE, DUROCLARITE (V) Vitrinite B with clay, sporinite, resinite and inertodetrinite.
1554.9 (5100')	VITRITE Vitrinite with cellular structure and minor resinite sporinite and argilite.
1821 (5972')	VITRINERTITE, CLARITE (V) banded vitrinite A and B, semifusinite and sporinite, inertodetrinite, cutinite, resinite and carbonate (siderite).
1829.26 (6000')	DUROCLARITE (V) vitrinite with lumen. desmocollinite with inertodetrinite, semifusinite, resinite sporinite and cutinite.
2016 (6613')	CLARITE (V) vitrinite A (tellocollinite) with abundant cutinite.
2027.4 (6650')	DUROCLARITE (V) vitrinite A and B, fusinite, semifusinite bands with inertodetrinite, sporinite, cutinite.

TOOLACHEE No. 8

1365.9 (4480')	CLARITE (V), VITRITE 1. 50% - vitrinite A and B with resinite and cutinite. 2. 10% - vitrinite with 20% clay (Fe). 3. 40% - desmocollinite with resinite.
1704.3 (5590')	VITRITE, CLARITE (V) 1. 90% - tellinite with collinite in lumen; resinite sporinite and minor cutinite. 2. 5-10%- desmocollinite with minor inertodetrinite, sporinite, resinite.
1878 (6160')	VITRITE, CLARITE (V) 1. 70% - tellocollinite with abundant cutinite. 2. 30% - desmocollinite with sporinite, resinite inertodetrinite.
1923.8 (6310')	DUROCLARITE (V) 1. 2-3 grains - vitrodetrinite and argilite. 2. 40% - tellocollinite with cutinite. 3. 15% - tellocollinite with minor sporinite. 4. 45% - desmocollinite with semifusinite, fusinite, inertodetrinite and sporinite.

TOOLACHEE No. 8 (cont.)

1954.3 (6410')
DUROCLARITE (V), VITRINERTITE (V)
1. 10% - clay with vitrodetrinite, inertodetrinite and minor spores.
2. 10% - tellocollinite with cutinite, sporinite, resinite.
3. 30% - vitric carbargilite.
4. 50% - desmocollinite with fusinite, semifusinite, inertodetrinite, resinite and sporinite.

2329.3 (7640')
CLARODURITE (V), DUROCLARITE (V)
1. 70% - banded vitrinite with sporinite, resinite, fusinite, semifusinite.
2. 30% - clay with vitrinite, sporinite and inertodetrinite.

2332.3 (7650')
CLARITE (V), DUROCLARITE (V)
1. 30% - vitrinite A and B with sporinite, fusinite, semifusinite and inertodetrinite.
2. 45% - desmocollinite, fusinite inertodetrinite and sporinite.
3. 25% - vitrinite and carbonate (siderite) in argilite.

TOOLACHEE No. 3

1908.5 (6260')
DUROCLARITE (V)
1. 30% - desmocollinite with fusinite sporinite, inertodetrinit
2. 70% - banded vitrinite A and B with fusinite, semifusinite, resinite, sporinite and inertodetrinite.

1932.9 (6340')
DUROCLARITE (V)
1. 30% - granular vitrinite, inertodetrinite and minor sporinite.
2. 70% - banded vitrinite A and B, fusinite semifusinite, sporinite, resinite.

2192 (7190')
DUROCLARITE (V), VITRIC CARBARGILITE
1. 85% - banded vitrinite A and B, fusinite, semifusinite and inertodetrinite, resinite, cutinite.
2. 15% - vitric carbargilite, carbonate.

2223 (7291'6")
DUROCLARITE (V)
banded vitrinite A and B, fusinite, semifusinite and minor inertodetrinite, sporinite, resinite, cutinite.

2271.6 (7451')
VITRITE
1. 100% - tellocollinite.

00161

November 1984

RKER.84.191

SOURCE ROCK INVESTIGATION OF SAMPLES FROM WELLS BROLGA-1, DULLINGARI-1, DULLINGARI NORTH-1, MURTEREE-1, TINGA TINGANA-1 AND TOOLÉCHEE-1

by

M.D. Higgs

Investigation 9.5.5500

With co-operation of
Mrs. A.A. van Adrichem-Wustefeld, J.M. Buiskool Toxopeus
R.F.M. Hofland

This **CONFIDENTIAL** report is made available subject to the condition that the recipient will neither use or disclose the contents except as agreed in writing with the sponsoring party.

Neither the whole nor any part of this document may be reproduced, stored in any retrieval system or transmitted in any form or by any means (electronic, mechanical, reprographic, recording or otherwise) without the prior written consent of the copyright owner.

Neither Royal Dutch Petroleum Company nor The **"SHELL"** Transport and Trading Company p.l.c. nor any company of the Royal Dutch/Shell Group will accept any liability for loss or damage originating from the use of the information contained therein.

Although **SHELL** companies have their own separate identities the expressions **"SHELL"** and **"GROUP"** are used for convenience to refer to companies of the Royal Dutch/Shell Group in general, or to one or more such companies as the context may require.

Copyright is vested in Shell Internationale Research Mij. B.V., The Hague.

KONINKLIJKE/SHELL EXPLORATIE EN PRODUKTIE LABORATORIUM

RIJSWIJK, THE NETHERLANDS

(Shell Research B.V.)

00161

November 1984

RKER.84.191

SOURCE ROCK INVESTIGATION OF SAMPLES FROM WELLS BROLGA-1, DULLINGARI-1, DULLINGARI NORTH-1, MURTEREE-1, TINGA TINGANA-1 AND TOOLÆCHEE-1

by

M.D. Higgs

Investigation 9.5.5500

With co-operation of
Mrs. A.A. van Adrichem-Wustefeld, J.M. Buiskool Toxopeus
R.F.M. Hofland

This **CONFIDENTIAL** report is made available subject to the condition that the recipient will neither use or disclose the contents except as agreed in writing with the sponsoring party.

Neither the whole nor any part of this document may be reproduced, stored in any retrieval system or transmitted in any form or by any means (electronic, mechanical, reprographic, recording or otherwise) without the prior written consent of the copyright owner.

Neither Royal Dutch Petroleum Company nor The **"SHELL"** Transport and Trading Company p.l.c. nor any company of the Royal Dutch/Shell Group will accept any liability for loss or damage originating from the use of the information contained therein.

Although **SHELL** companies have their own separate identities the expressions **"SHELL"** and **"GROUP"** are used for convenience to refer to companies of the Royal Dutch/Shell Group in general, or to one or more such companies as the context may require.

Copyright is vested in Shell Internationale Research Mij. B.V., The Hague.

KONINKLIJKE/SHELL EXPLORATIE EN PRODUKTIE LABORATORIUM

RIJSWIJK, THE NETHERLANDS

(Shell Research B.V.)

CONTENTS

	Page
1. Introduction	1
2. Results	1

SOURCE ROCK INVESTIGATION OF SAMPLES FROM WELLS BROLGA-1, DULLINGARI-1, DULLINGARI NORTH-1, MURTEREE-1, TINGA TINGANA-1 AND TOOLACHEE-1

1. INTRODUCTION

A source rock analysis has been done on Permian core and cuttings samples from ~~five~~ six wells in the Cooper Basin obtained from the South Australian Department of Mines and Energy. The 33 samples analysed (28 core and 5 cuttings samples) come from the the Toolachee, Roseneath, Patchwarra, and Merrimelia formations.

2. RESULTS

The results are listed in Table 1 (total organic carbon and vitrinite reflectance, Tables 2-7 (maceral descriptions) and Figs. 1-29 (vitrinite reflectance histograms).

Well	Sample Depth (m)	Sample type	Formation	Org. Carbon (%)	VR (%)
Brolga-1	2664-2676	cuttings	Toolachee	41.4	0.83
	2758-2767	"	Patchawarra	46.1	0.92
	2817	core	"	73.0	0.94
	2828.6	"	"	76.3	1.02
	2842.9	"	"	82.4	0.97
	2917.9	"	"	81.2	0.99
	2927	"	"	65.6	1.00
Dullingari-1	2197.3	"	Toolachee	9.3	1.28 *
	2408.1	"	Patchawarra	3.4	1.51 *
	2522.6	"	"	3.9	1.33 *
	2708.6	"	"	78.5	1.72
Dullingari North-1	2215.6	"	Toolachee	77.9	1.03
	2307-2310	cuttings	Roseneath	5.1	1.10
	2531.8	core	Patchawarra	30.4	1.60 *
	2532.2	"	"	29.3	1.53 *
	2614.3	"	"	79.9	1.52
Murteree-1	1808.4	"	Toolachee	74.9	0.77 *
	1819.1	"	"	73.6	0.78
	1844-1856	cuttings	"	38.4	0.76
	1986.3	core	Patchawarra	18.0	0.91
	2011.1	"	"	78.3	0.93
	2017.2	"	"	74.6	0.94
	2025.7	"	"	6.9	0.78 *
	2136-2148	cuttings	"	23.7	1.08
Tinga Tingana-1	1474.6	core	"	30.3	0.51 *
	1482.7	"	"	61.2	0.47 *
	1586.4	"	"	3.5	nd
	1687.7	"	"	1.7	nd
Toolachee-1	1849	"	Toolachee	6.3	0.77 *
	1978	"	Roseneath	2.7	nd
	2106.7	"	Patchawarra	54.0	1.00
	2109.7	"	"	83.0	1.06
	2182.8	"	Merrimelia	0.3	nd

* unreliable measurements due to quality of vitrinite
nd not done due to absence of suitable vitrinite

Table 1 : Organic carbon content and vitrinite reflectance measurements

00164

REFLECTANCE HISTOGRAM

COUNTRY : AUSTRALIA
WELL/OUTCROP : BROLGA-1
DEPTH/SAMPLE NR. : 2664 M
SAMPLE TYPE : CUTTING SAMPLE

MEAN : 0.83
DEVIATION : 0.02
MODE : 0.83
MEASUREMENTS : 50

ANALYST: BTX D.D. : 26-OCT-84

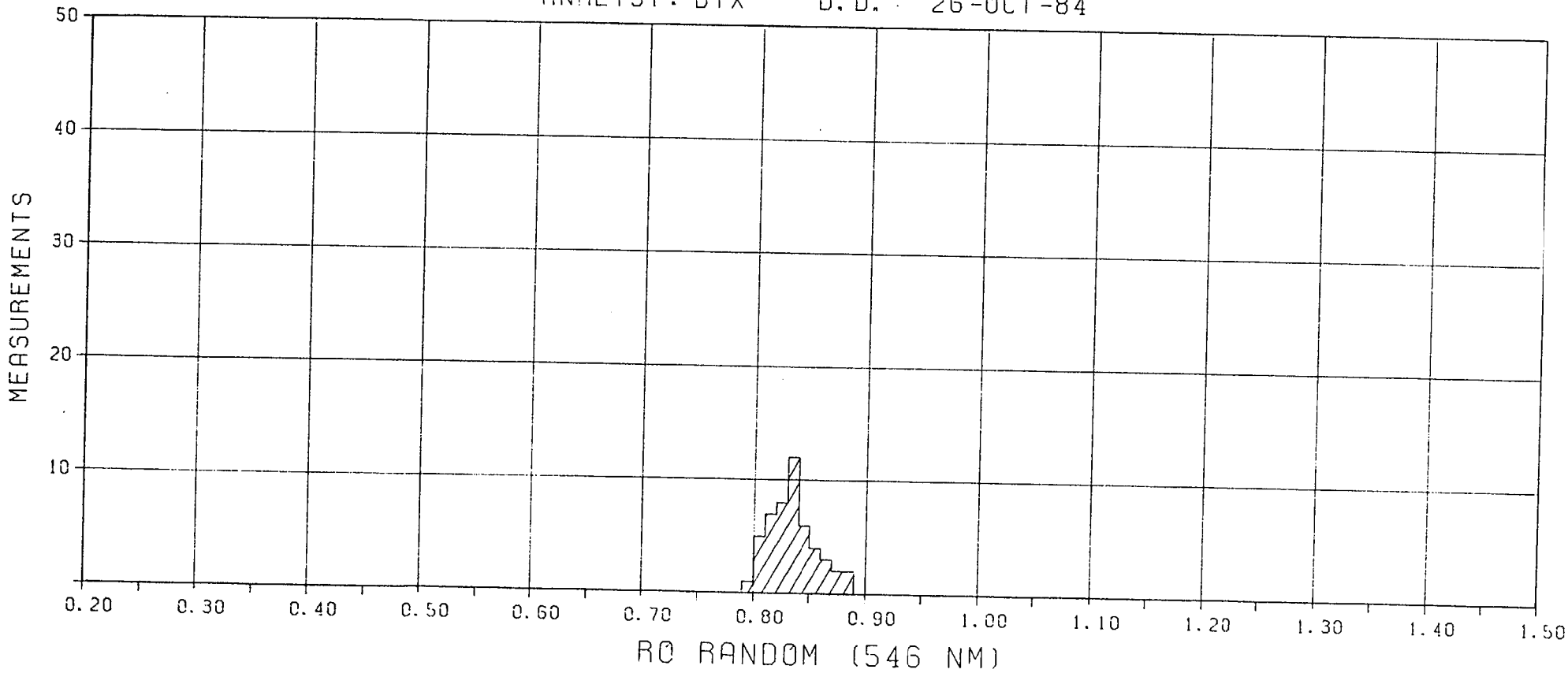

Fig. 1

TELOCOLLINITE (SLIGHTLY SCRATCHED)

00165

REFLECTANCE HISTOGRAM

COUNTRY	: AUSTRALIA	MEAN	: 0.92
WELL/OUTCROP	: BROLGA-1	DEVIATION	: 0.04
DEPTH/SAMPLE NR.	: 2758 M	MODE	: 0.94
SAMPLE TYPE	: CUTTING SAMPLE	MEASUREMENTS	: 75

ANALYST: BTX D.D.: 30-AUG-84

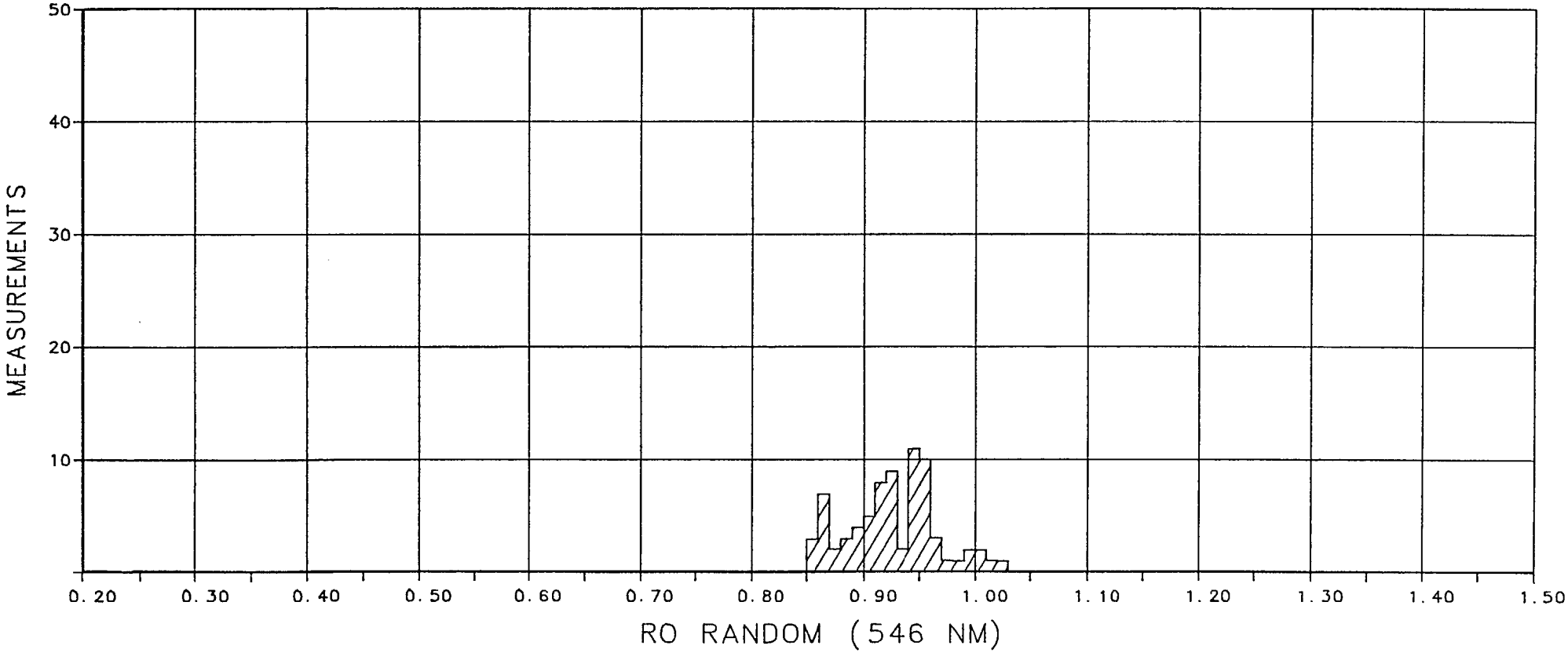

Fig. 2

TELOCOLLINITE

00166

REFLECTANCE HISTOGRAM

COUNTRY : AUSTRALIA
WELL/OUTCROP : BROLGA-1
DEPTH/SAMPLE NR. : 2817 M
SAMPLE TYPE : CORE SAMPLE

MEAN : 0.94
DEVIATION : 0.05
MODE : 0.93
MEASUREMENTS : 50

ANALYST: ROD D.D. : 22-OCT-84

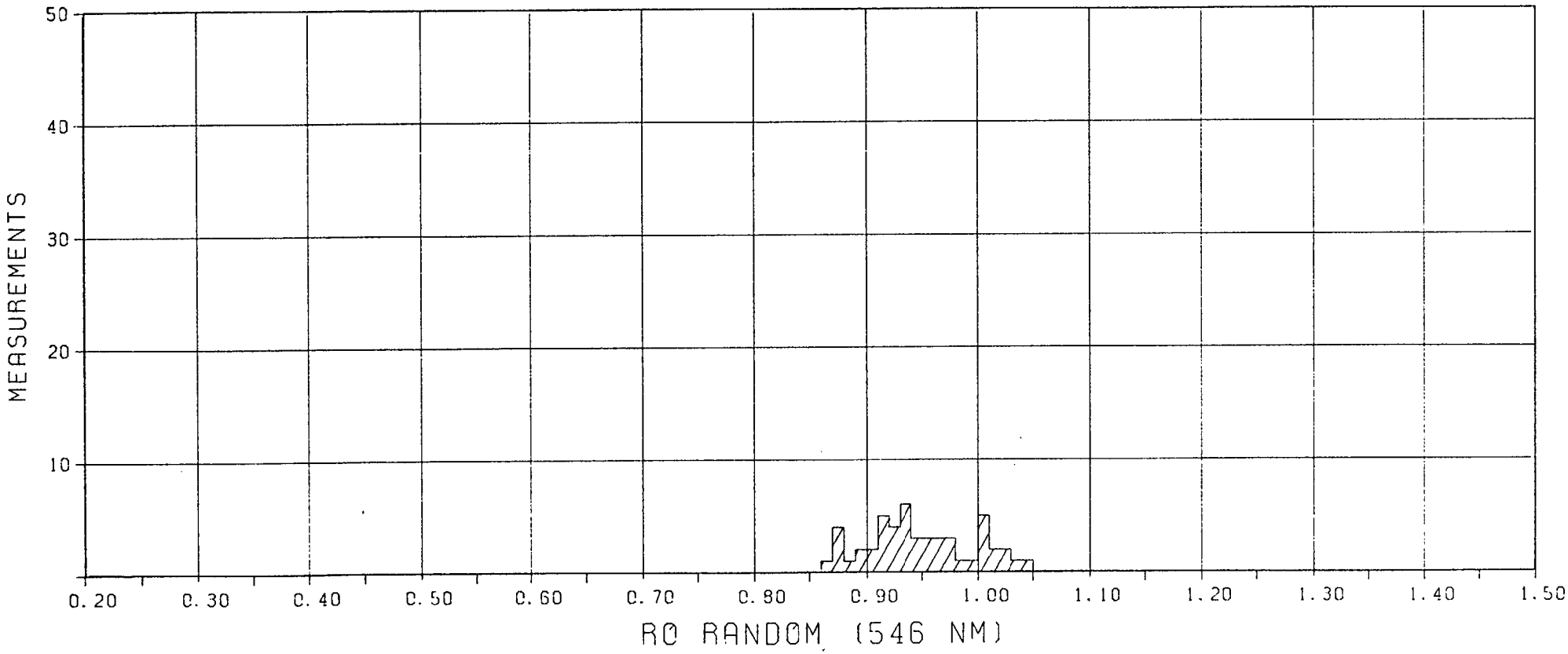

Fig. 3

TELOCOLLINITE

REFLECTANCE HISTOGRAM

COUNTRY : AUSTRALIA
WELL/OUTCROP : BROLGA-1
DEPTH/SAMPLE NR. : 2828 M
SAMPLE TYPE : CORE SAMPLE

MEAN : 1.02
DEVIATION : 0.05
MODE : 1.05
MEASUREMENTS: 50

ANALYST: BTX D.D.: 30-AUG-84

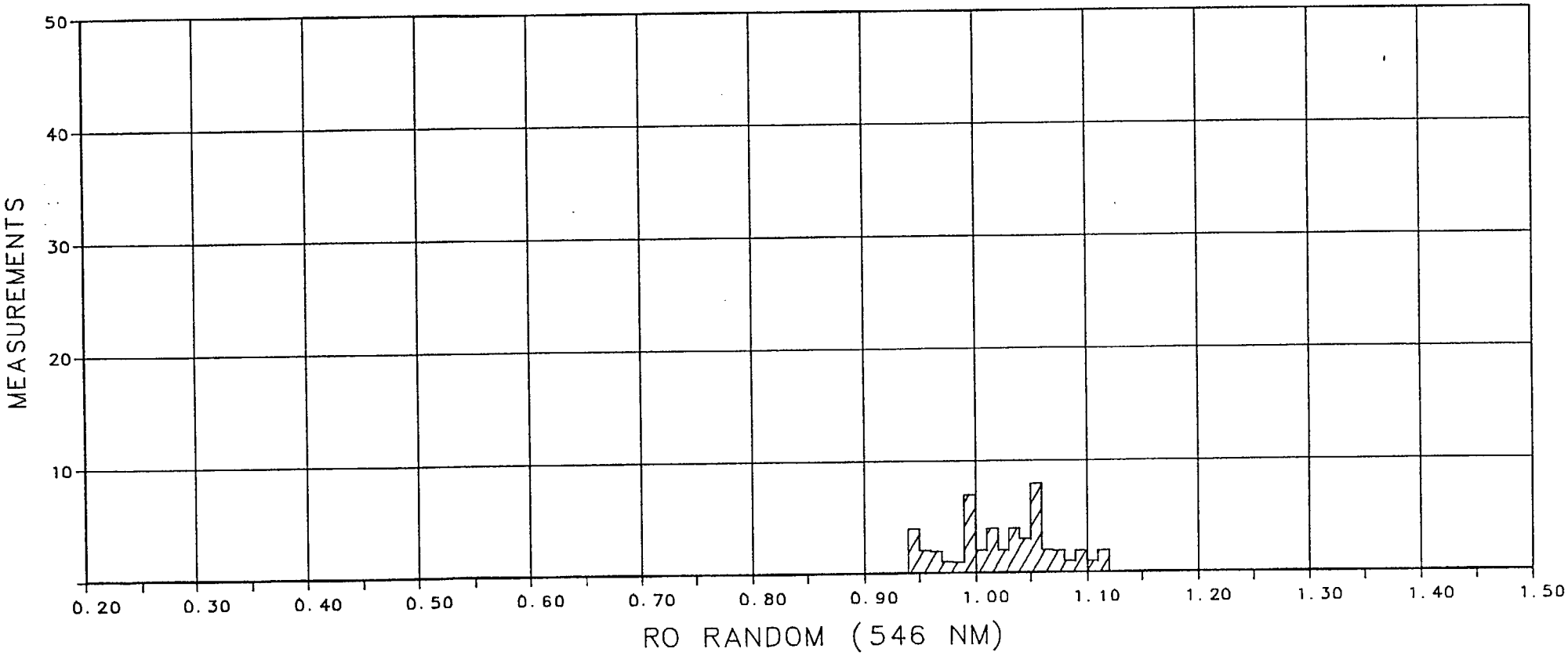

Fig. 4

TELOCOLLINITE; SAMPLE 2828.6 M

00168

REFLECTANCE HISTOGRAM

COUNTRY : AUSTRALIA
WELL/OUTCROP : BROLGA-1
DEPTH/SAMPLE NR. : 2842 M
SAMPLE TYPE : CORE SAMPLE

MEAN : 0.97
DEVIATION : 0.04
MODE : MULTI
MEASUREMENTS : 50

ANALYST: BTX D.D.: 30-AUG-84

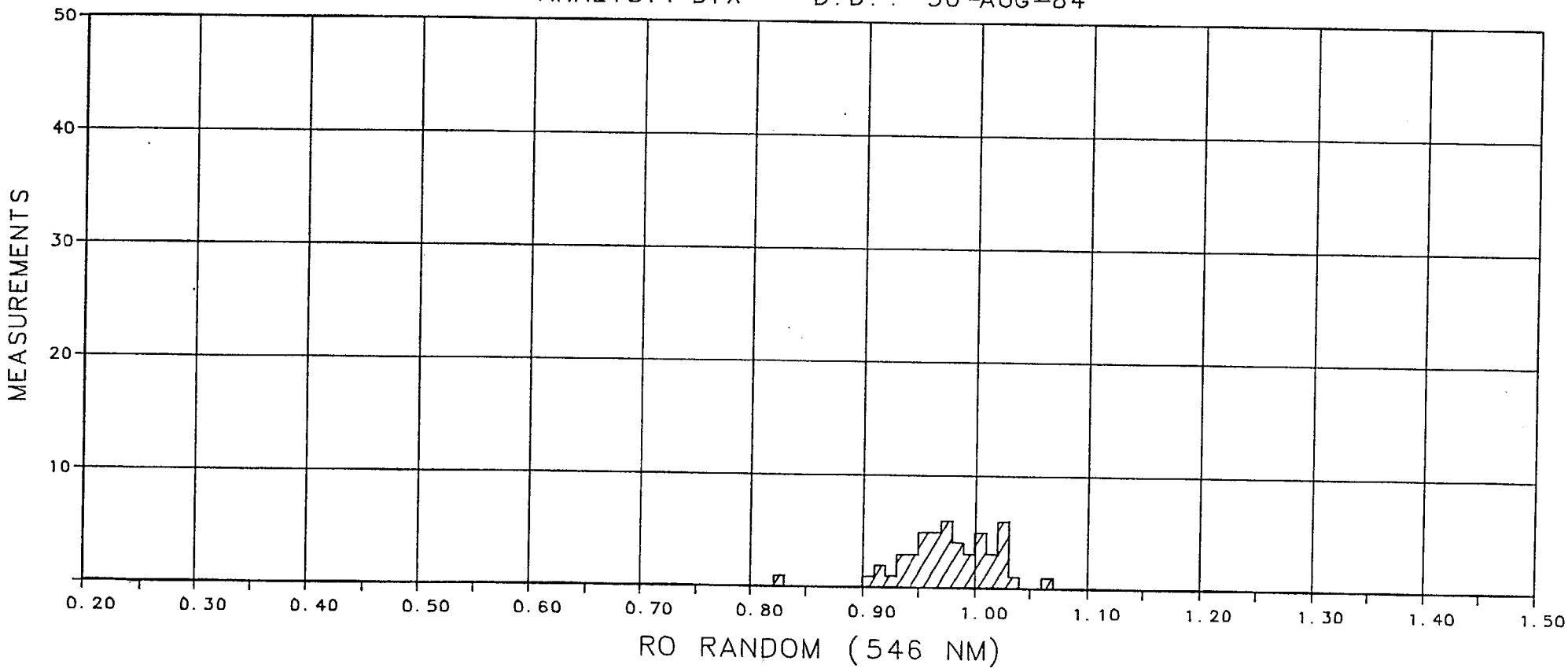

Fig. 5

TELOCOLLINITE; SAMPLE 2842.9 M

00169

REFLECTANCE HISTOGRAM

COUNTRY	: AUSTRALIA	MEAN	: 0.99
WELL/OUTCROP	: BROLGA-1	DEVIATION	: 0.02
DEPTH/SAMPLE NR.	: 2917 M	MODE	: 0.97
SAMPLE TYPE	: CORE SAMPLE	MEASUREMENTS	: 74

ANALYST: ROD D.D. : 23-OCT-84

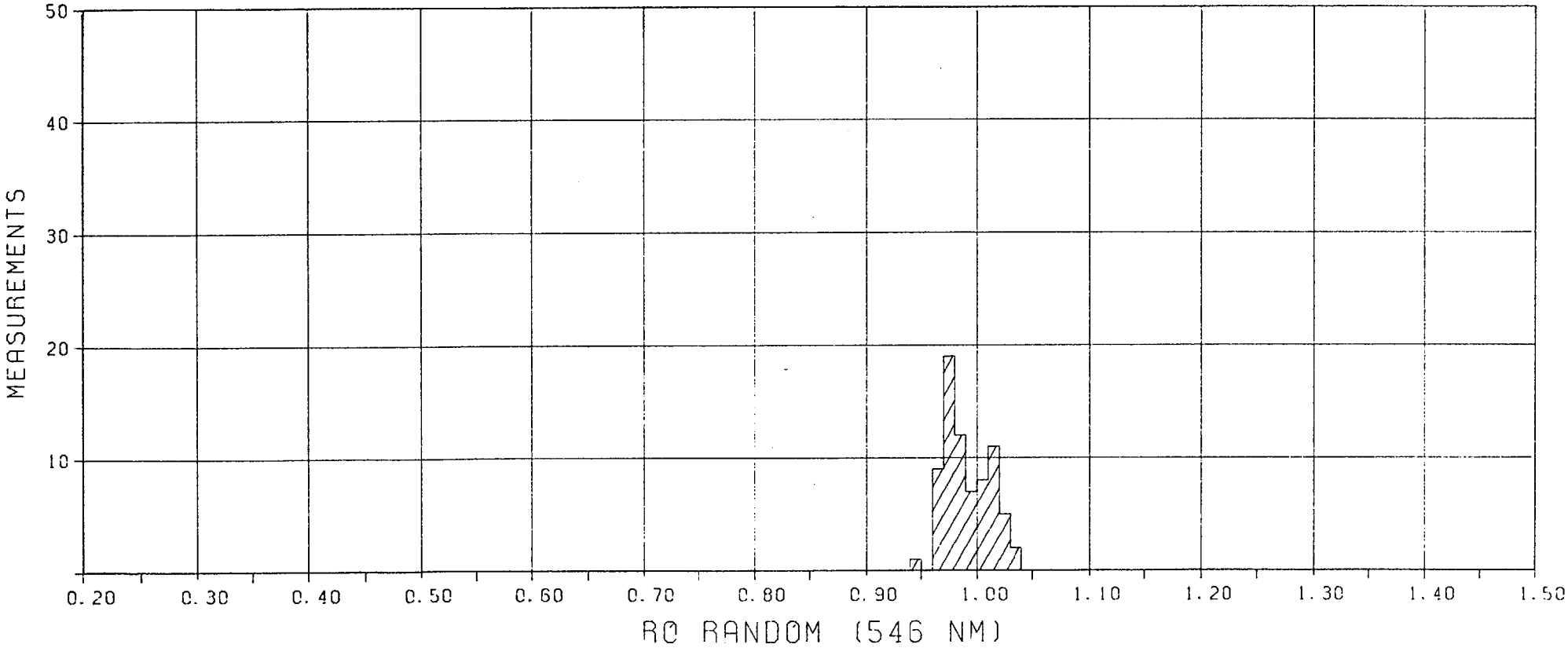

Fig. 6

SAMPLE 2917.9 M; TELOCOLLINITE (SLIGHTLY SCRATCHED)

REFLECTANCE HISTOGRAM

COUNTRY : AUSTRALIA
WELL/OUTCROP : BROLGA-1
DEPTH/SAMPLE NR. : 2927 M
SAMPLE TYPE : CORE SAMPLE

MEAN : 1.00
DEVIATION : 0.02
MODE : 1.00
MEASUREMENTS : 25

ANALYST: BTX D.D. 26-OCT-84

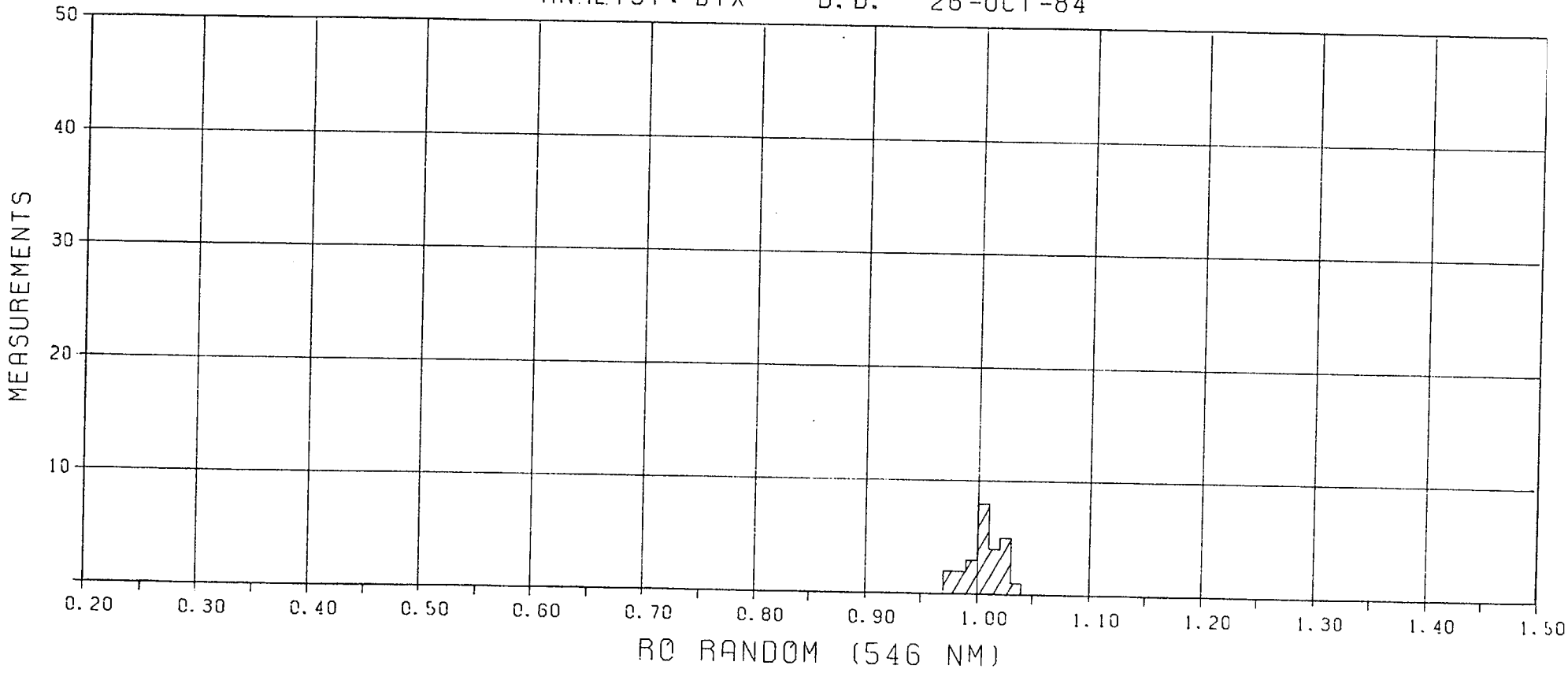

Fig. 7

TELOCOLLINITE

REFLECTANCE HISTOGRAM

COUNTRY	: AUSTRALIA	MEAN	: 1.28
WELL/OUTCROP	: DULLINGARI-1	DEVIATION	: 0.14
DEPTH/SAMPLE NR.	: 2197 M	MODE	: 1.27
SAMPLE TYPE	: CORE SAMPLE	MEASUREMENTS	: 44

ANALYST: BTX D.D.: 24-OCT-84

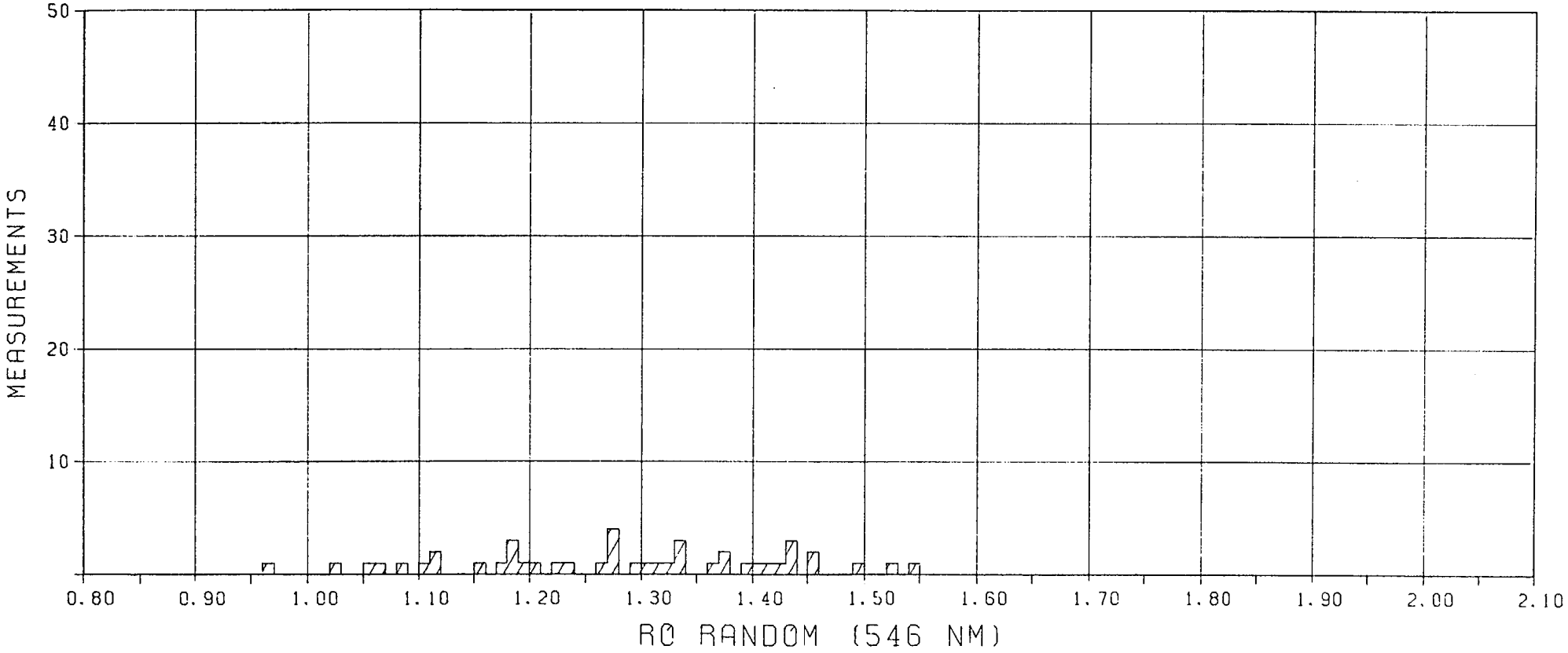

Fig. 8

SAMPLE 2197.3 M; VITRINITE-2 GRADING INTO (SEMI-)FUSINITE

REFLECTANCE HISTOGRAM

COUNTRY	: AUSTRALIA	MEAN	: 1.51
WELL/OUTCROP	: DULLINGARI-1	DEVIATION	: 0.16
DEPTH/SAMPLE NR.	: 2408 M	MODE	: MULTI
SAMPLE TYPE	: CORE SAMPLE	MEASUREMENTS	: 19

ANALYST: BTX D.D.: 24-OCT-84

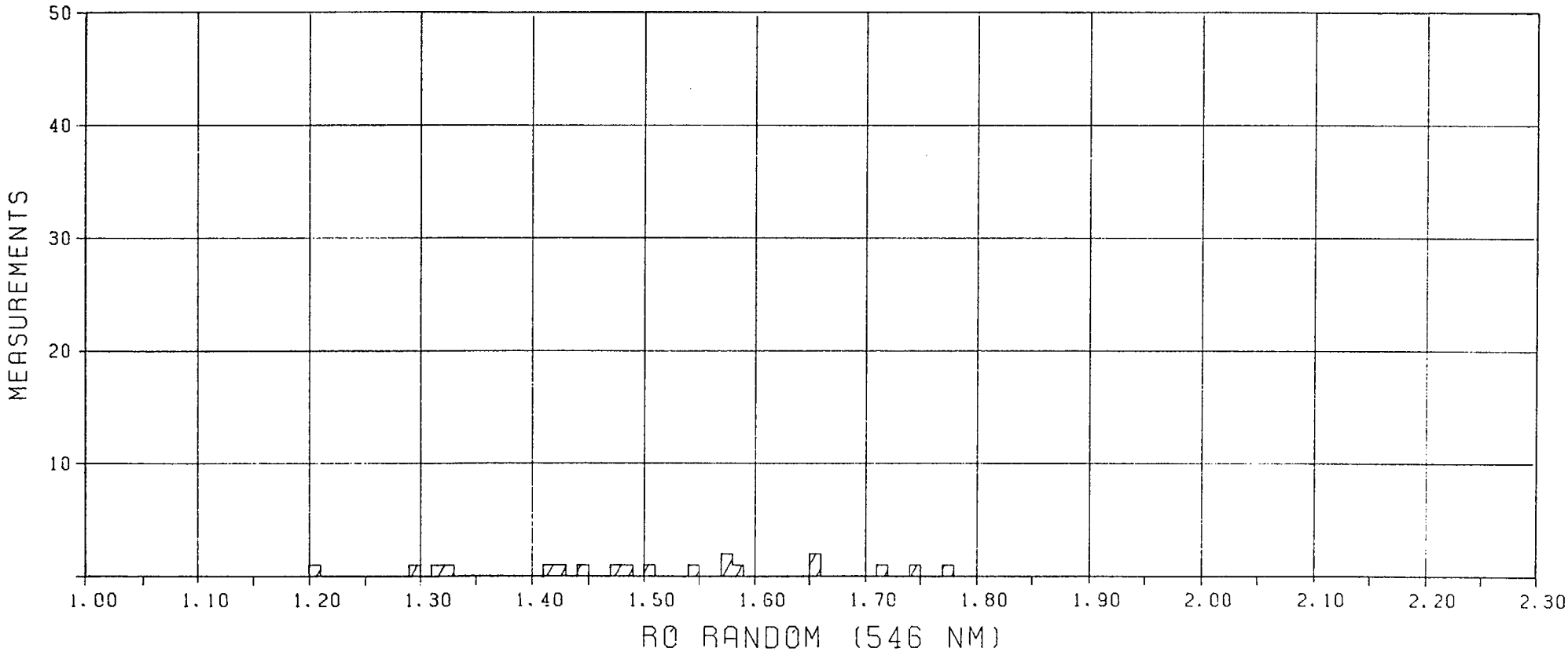

Fig. 9

SAMPLE 2408.1 M; DETRITAL VITRINITE-2 GRADING INTO (SEMI-) FUSINITE

REFLECTANCE HISTOGRAM

COUNTRY	: AUSTRALIA	MEAN	: 1.33
WELL/OUTCROP	: DULLINGARI-1	DEVIATION	: 0.06
DEPTH/SAMPLE NR.	: 2522 M	MODE	: 1.38
SAMPLE TYPE	: CORE SAMPLE	MEASUREMENTS	: 25

ANALYST: BTX D.D. : 24-OCT-84

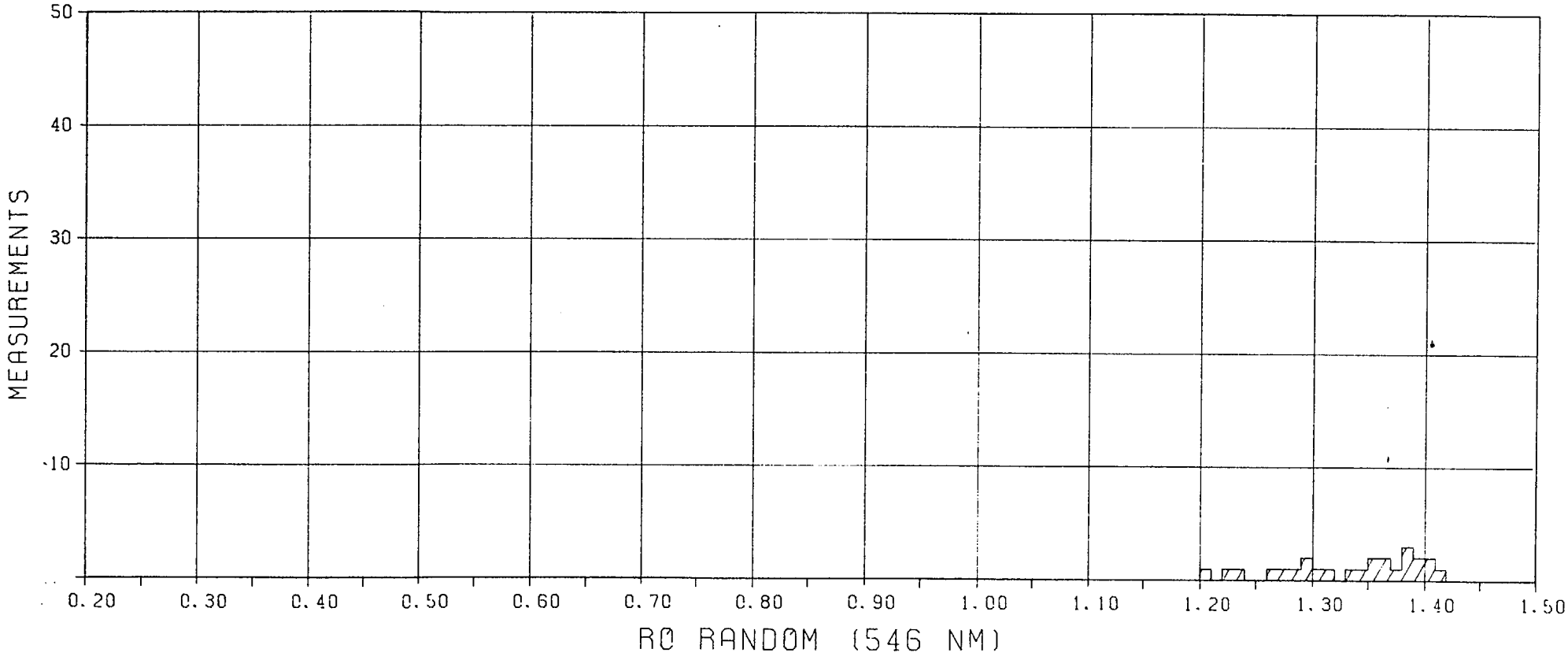

SAMPLE 2522.6 M; VITRINITE-2

Fig. 10

REFLECTANCE HISTOGRAM

COUNTRY	: AUSTRALIA	MEAN	: 1.72
WELL/OUTCROP	: DULLINGARI-1	DEVIATION	: 0.03
DEPTH/SAMPLE NR.	: 2708 M	MODE	: 1.73
SAMPLE TYPE	: CORE SAMPLE	MEASUREMENTS	: 100

ANALYST: ROD D.D. : 23-OCT-84

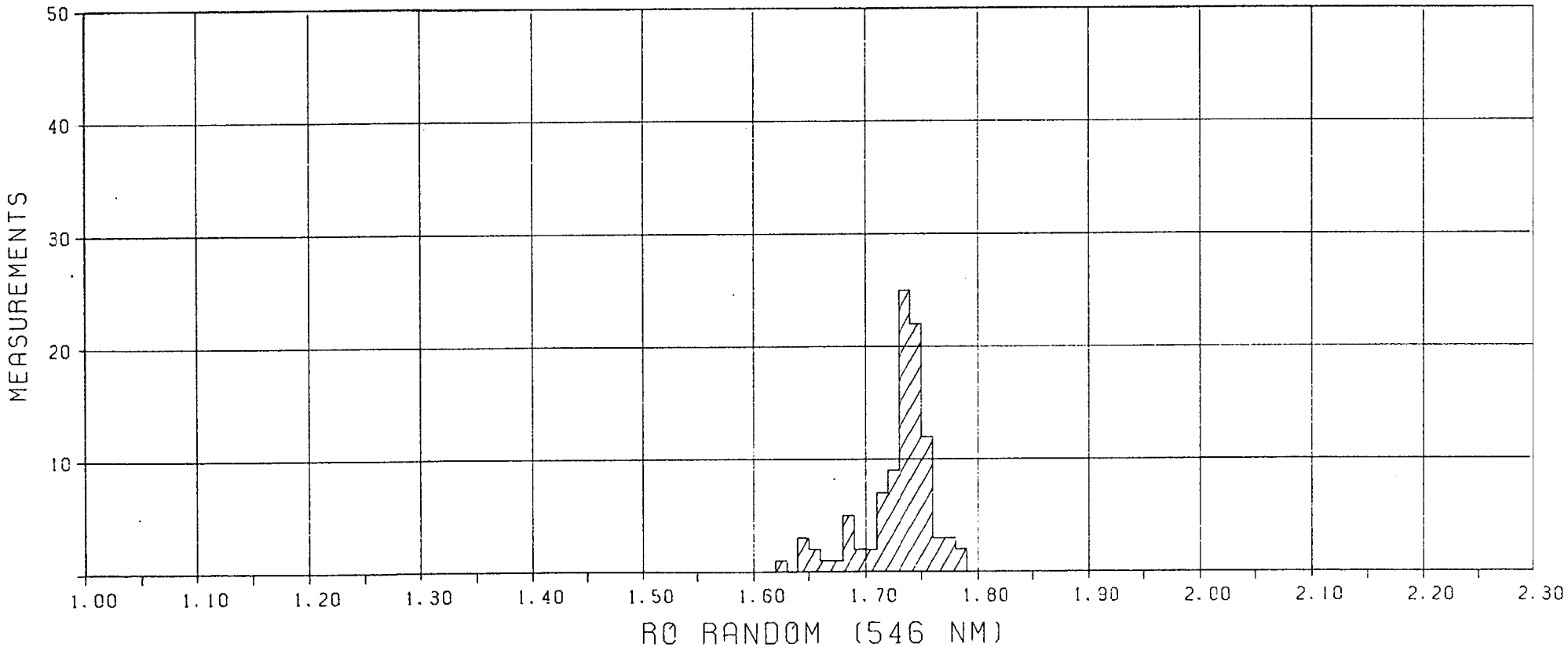

Fig. 11

SAMPLE 2708.6 M; TELOCOLLINITE

REFLECTANCE HISTOGRAM

COUNTRY	: AUSTRALIA	MEAN	: 1.03
WELL/OUTCROP	: DULLINGARI NORTH-1	DEVIATION	: 0.01
DEPTH/SAMPLE NR.	: 2215 M	MODE	: 1.02
SAMPLE TYPE	: CORE SAMPLE	MEASUREMENTS	: 56

ANALYST: ROD D.D. : 24-OCT-84

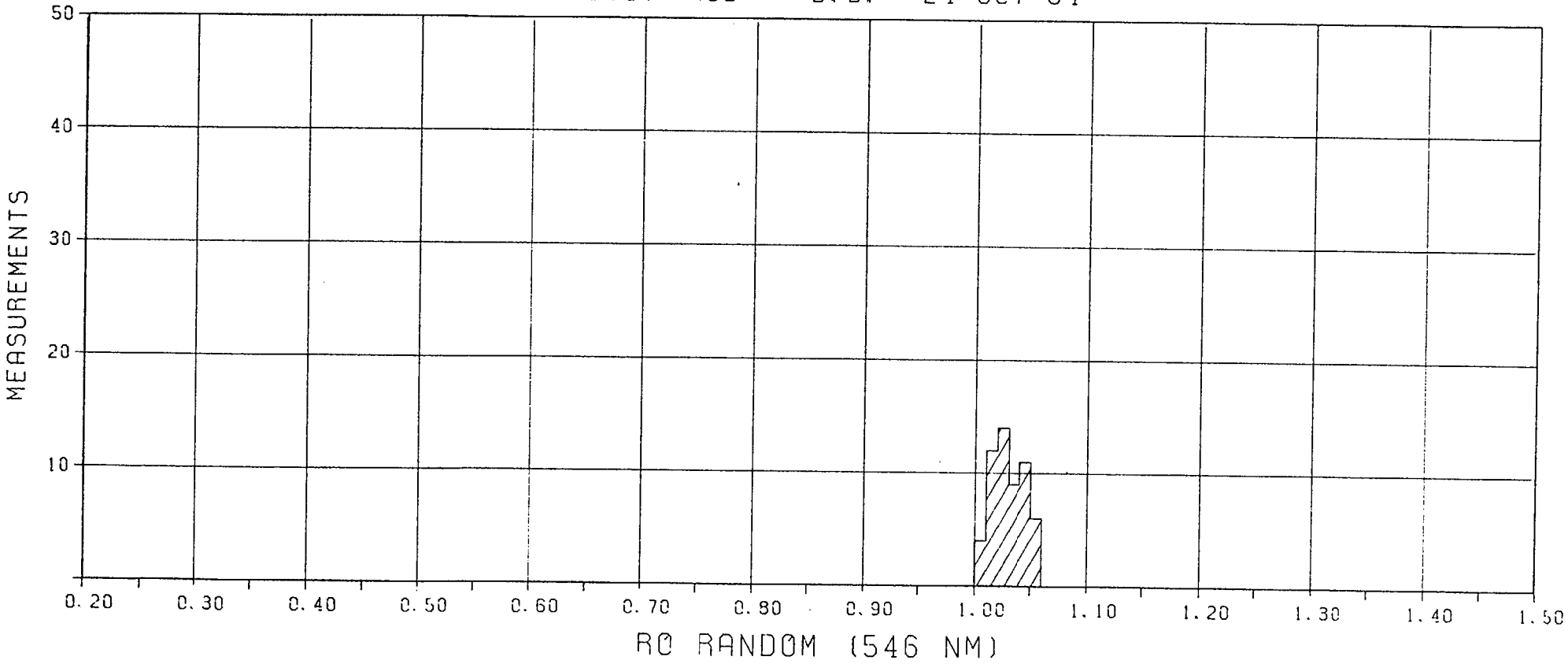

SAMPLE 2215.6M , TELOCOLLINITE

Fig. 12

REFLECTANCE HISTOGRAM

COUNTRY : AUSTRALIA
WELL/OUTCROP : DULLINGARI NORTH-1
DEPTH/SAMPLE NR. : 2307 M
SAMPLE TYPE : CUTTING SAMPLE

MEAN : 1.10
DEVIATION : 0.04
MODE : 1.06
MEASUREMENTS : 27

ANALYST: BTX D.D. : 26-OCT-84

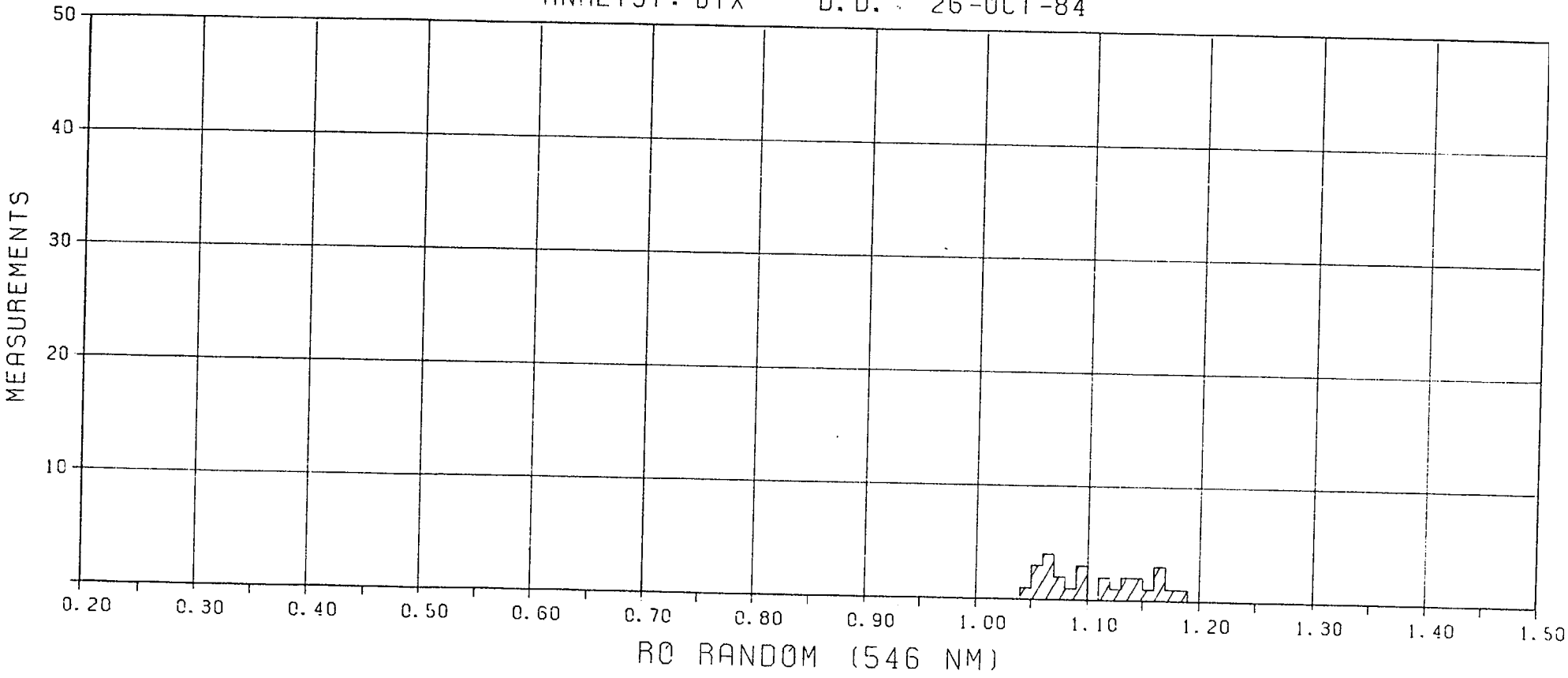

Fig. 13

TELOCOLLINITE

REFLECTANCE HISTOGRAM

COUNTRY	: AUSTRALIA	MEAN	: 1.60
WELL/OUTCROP	: DULLINGARI NORTH-1	DEVIATION	: 0.10
DEPTH/SAMPLE NR.	: 2531 M	MODE	: MULTI
SAMPLE TYPE	: CORE SAMPLE	MEASUREMENTS	: 50

ANALYST: BTX D.D. 24-OCT-84

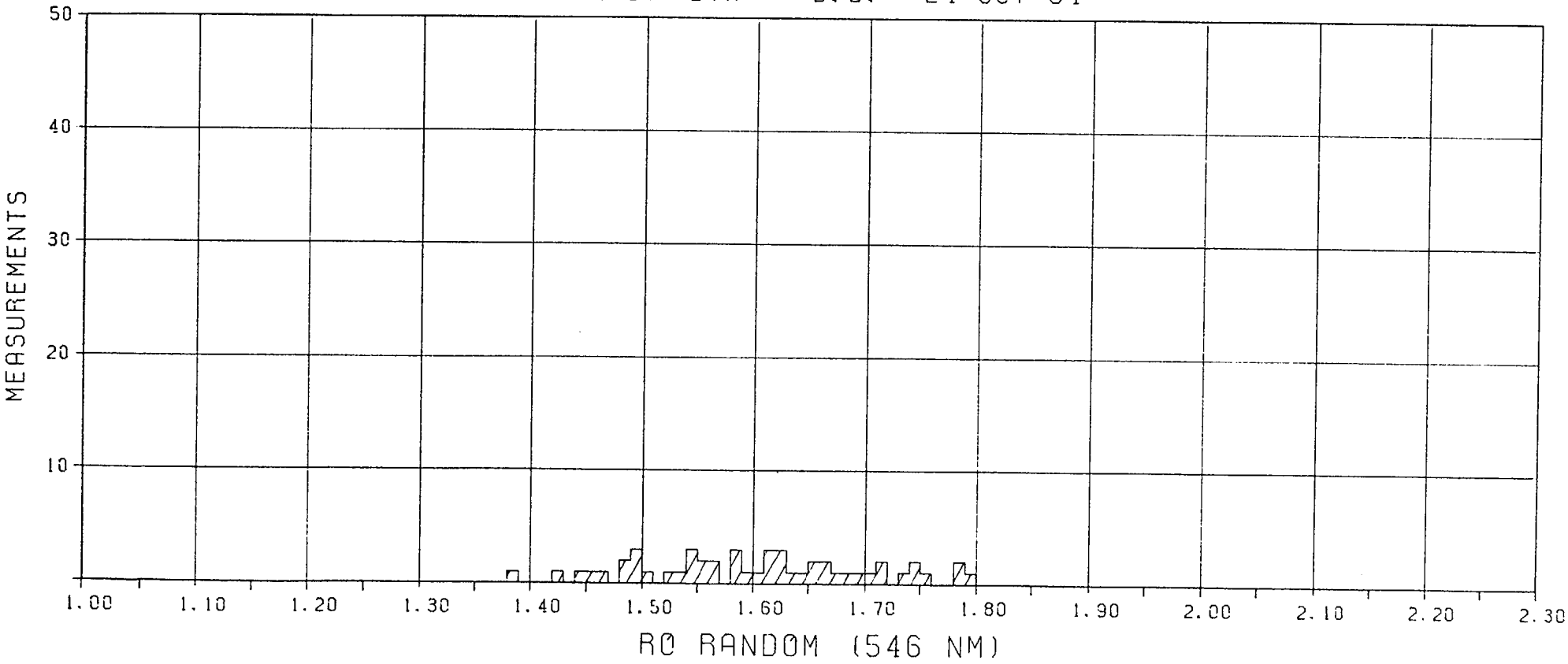

Fig. 14

SAMPLE 2531.8 M; VITRINITE-2 GRADING INTO (SEMI-)FUSINITE

REFLECTANCE HISTOGRAM

COUNTRY	: AUSTRALIA	MEAN	: 1.53
WELL/OUTCROP	: DULLINGARI NORTH-1	DEVIATION	: 0.15
DEPTH/SAMPLE NR.	: 2532 M	MODE	: 1.35
SAMPLE TYPE	: CORE SAMPLE	MEASUREMENTS	: 50

ANALYST: BTX D.D. : 24-OCT-84

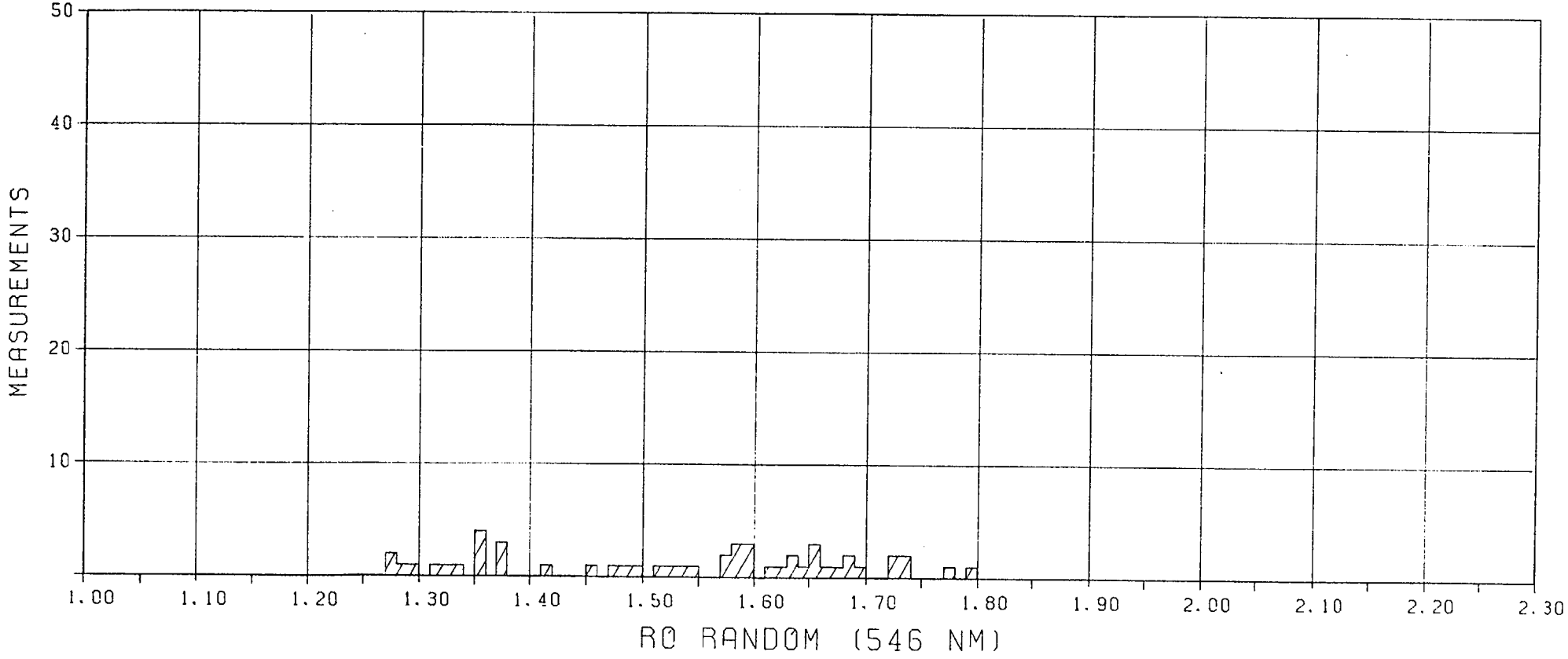

SAMPLE 2532.2 M; VITRINITE-2 GRADING INTO (SEMI-)FUSINITE

Fig. 15

REFLECTANCE HISTOGRAM

COUNTRY	: AUSTRALIA	MEAN	: 1.52
WELL/OUTCROP	: DULLINGARI NORTH-1	DEVIATION	: 0.02
DEPTH/SAMPLE NR.	: 2614 M	MODE	: 1.53
SAMPLE TYPE	: CORE SAMPLE	MEASUREMENTS	: 73

ANALYST: BTX D.D.: 24-OCT-84

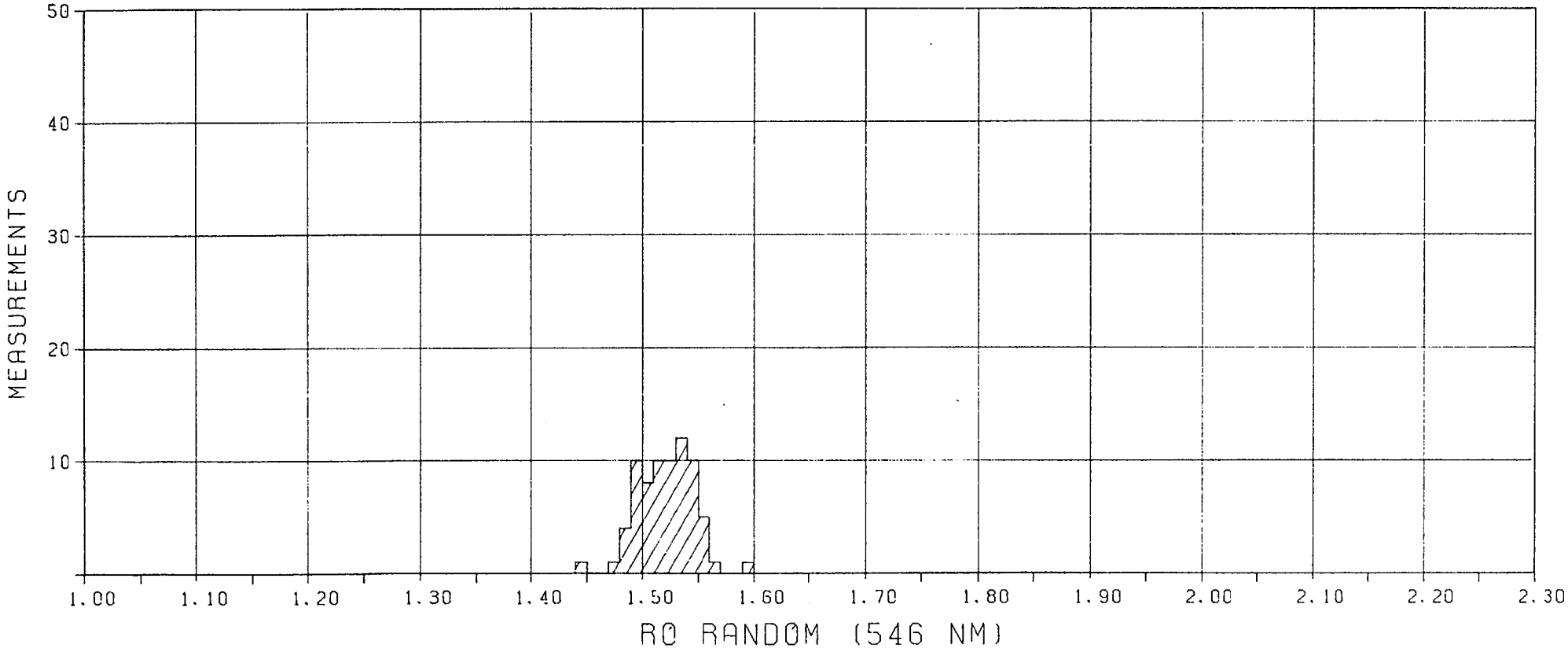

Fig. 16

SAMPLE 2614.3M;TELOCOLLINITE

REFLECTANCE HISTOGRAM

COUNTRY : AUSTRALIA
WELL/OUTCROP : MURTEREE-1
DEPTH/SAMPLE NR. : 1808 M
SAMPLE TYPE : CORE SAMPLE

MEAN : 0.77
DEVIATION : 0.03
MODE : MULTI
MEASUREMENTS : 45

ANALYST: BTX D.D. : 26-OCT-84

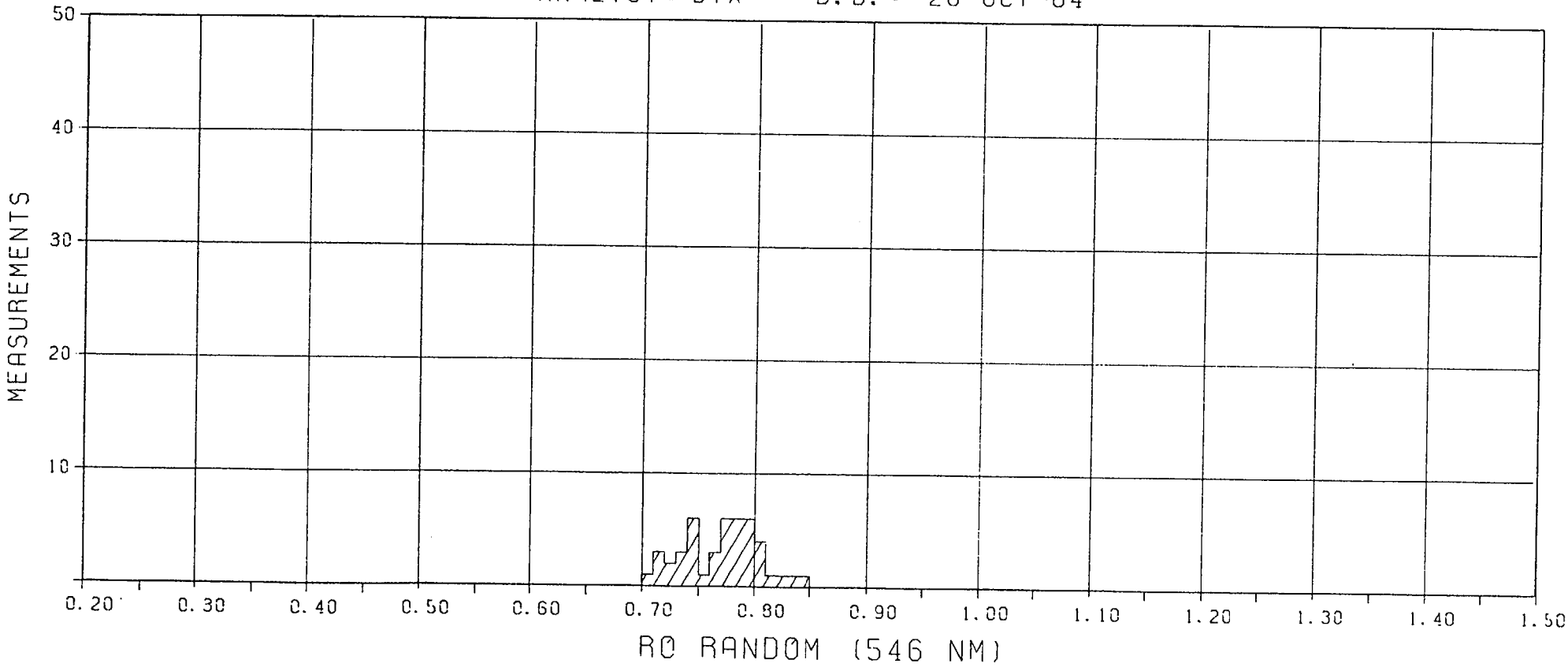

SAMPLE 1808.4 M; DETRITAL VITRINITE-2/(SEMI-)FUSINITE

Fig. 17

REFLECTANCE HISTOGRAM

COUNTRY : AUSTRALIA
WELL/OUTCROP : MURTEREE-1
DEPTH/SAMPLE NR. : 1819 M
SAMPLE TYPE : CORE SAMPLE

MEAN : 0.78
DEVIATION : 0.03
MODE : 0.77
MEASUREMENTS : 100

ANALYST: ROD D.D. : 29-OCT-84

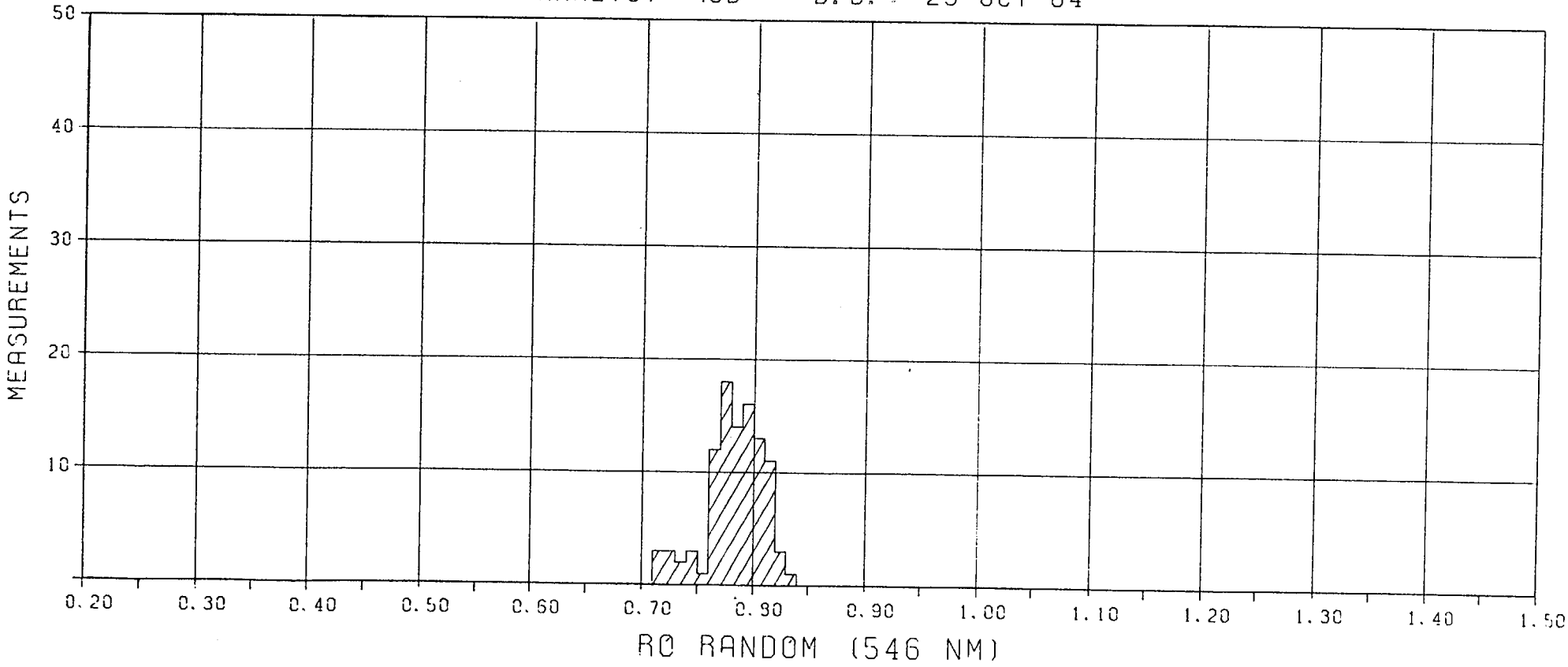

SAMPLE 1819.1M ; TELOCOLLINITE

Fig. 18

REFLECTANCE HISTOGRAM

COUNTRY	: AUSTRALIA	MEAN	: 0.76
WELL/OUTCROP	: MURTEREE-1	DEVIATION	: 0.03
DEPTH/SAMPLE NR.	: 1844 M	MODE	: 0.76
SAMPLE TYPE	: CUTTING SAMPLE	MEASUREMENTS	: 100

ANALYST: BTX D.D. : 29-OCT-84

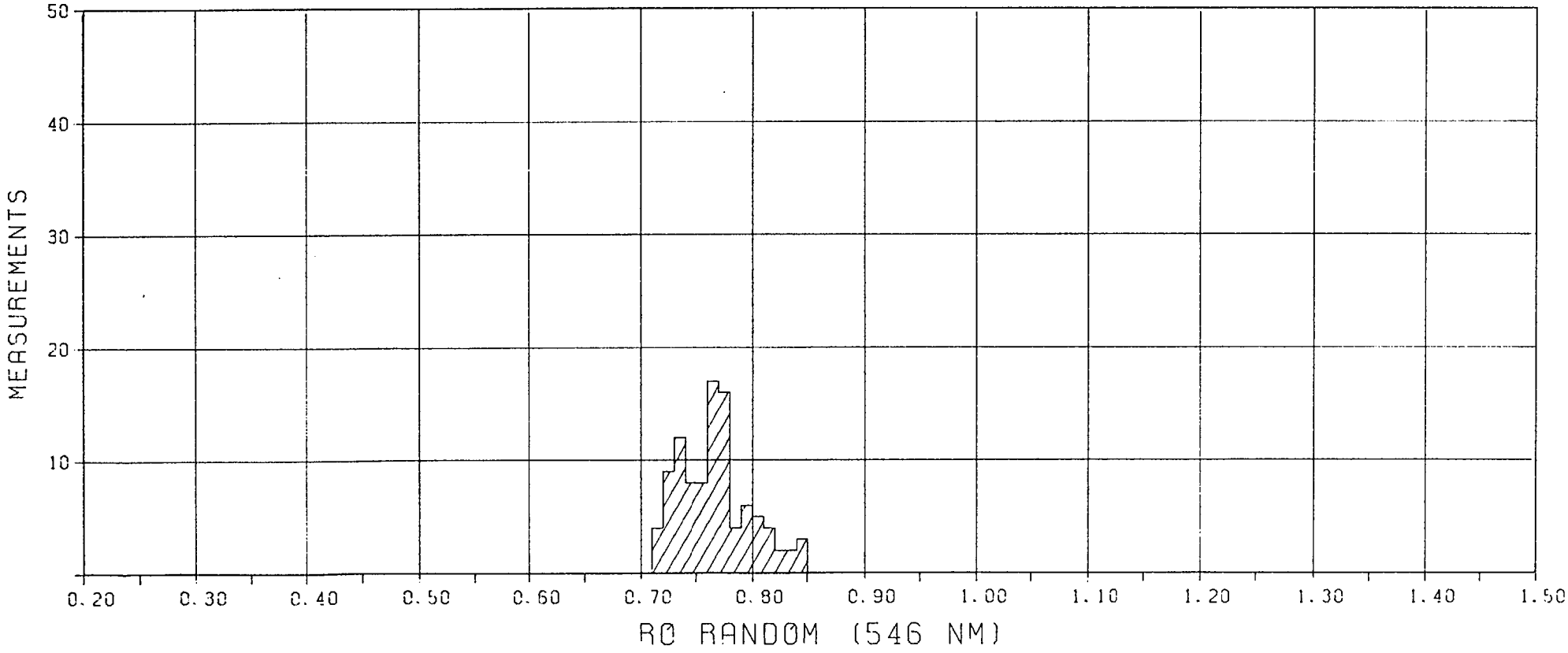

Fig. 19

TELOCOLLINITE

001863

REFLECTANCE HISTOGRAM

COUNTRY	: AUSTRALIA	MEAN	: 0.91
WELL/OUTCROP	: MURTEREE-1	DEVIATION	: 0.02
DEPTH/SAMPLE NR.	: 1986 M	MODE	: 0.91
SAMPLE TYPE	: CORE SAMPLE	MEASUREMENTS	: 99

ANALYST: ROD D.D.: 29-OCT-84

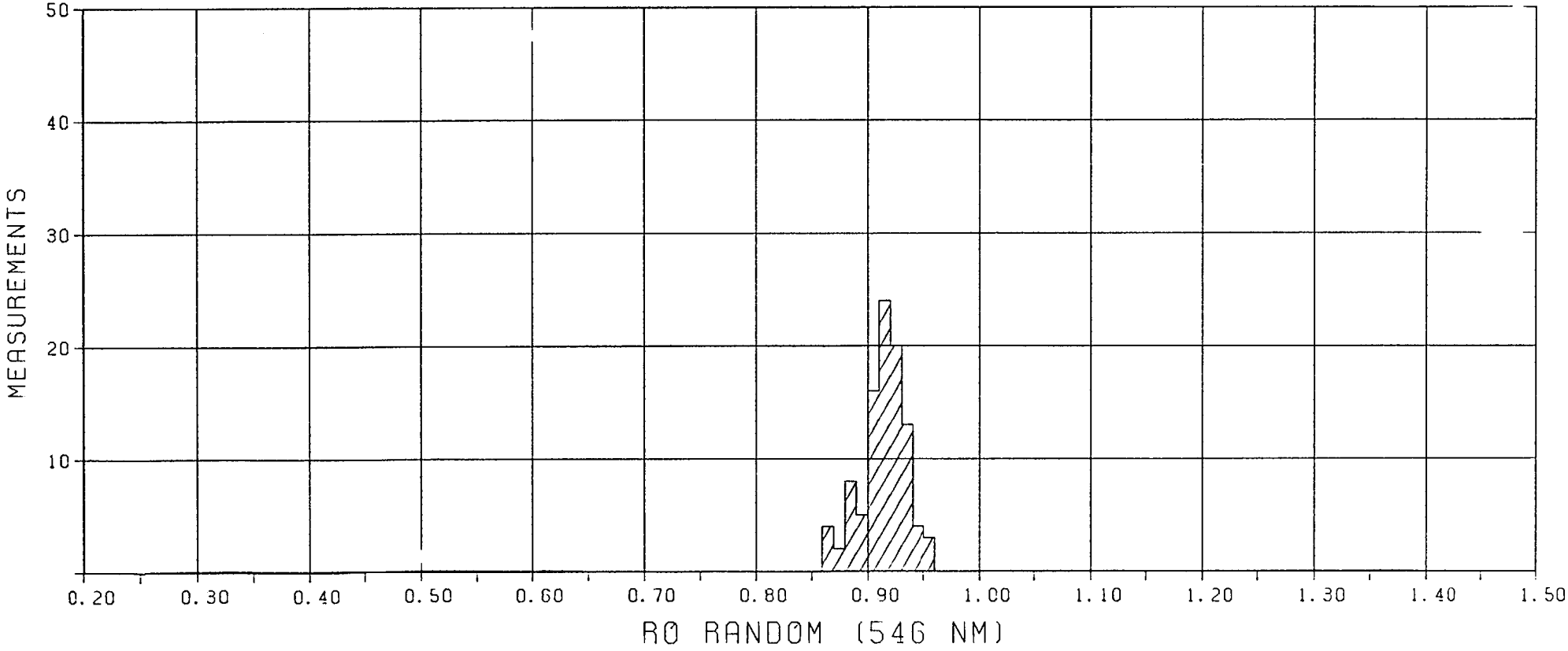

Fig. 20

SAMPLE 1986.3 M ; TELOCOLLINITE

REFLECTANCE HISTOGRAM

COUNTRY	: AUSTRALIA	MEAN	: 0.93
WELL/OUTCROP	: MURTEREE-1	DEVIATION	: 0.03
DEPTH/SAMPLE NR.	: 2011 M	MODE	: 0.92
SAMPLE TYPE	: CORE SAMPLE	MEASUREMENTS	: 100

ANALYST: ROD D.D. : 29-OCT-84

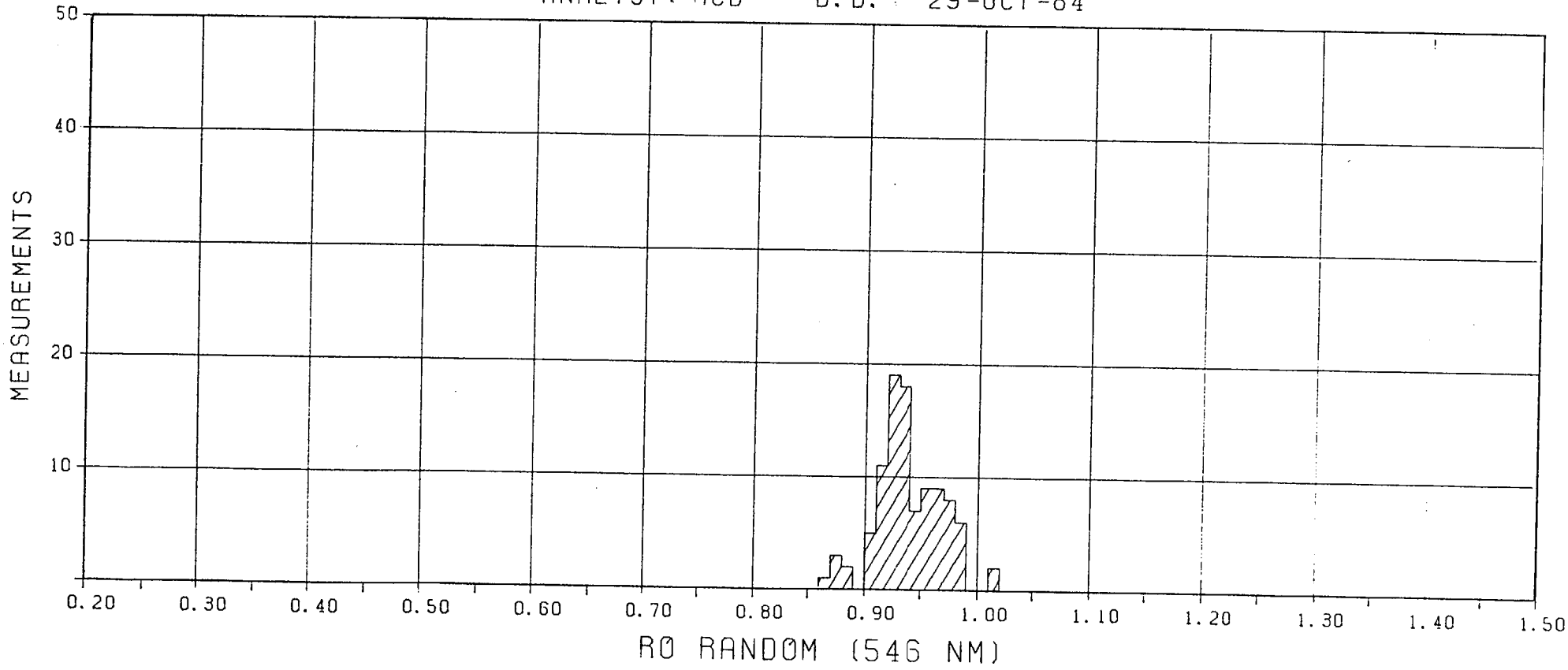

SAMPLE 2011.1 M ; TELECOLLINITE

Fig. 21

REFLECTANCE HISTOGRAM

COUNTRY : AUSTRALIA
WELL/OUTCROP : MURTEREE-1
DEPTH/SAMPLE NR. : 2017 M
SAMPLE TYPE : CORE SAMPLE

MEAN : 0.94
DEVIATION : 0.02
MODE : 0.92
MEASUREMENTS : 100

ANALYST: ROD D.D. : 29-OCT-84

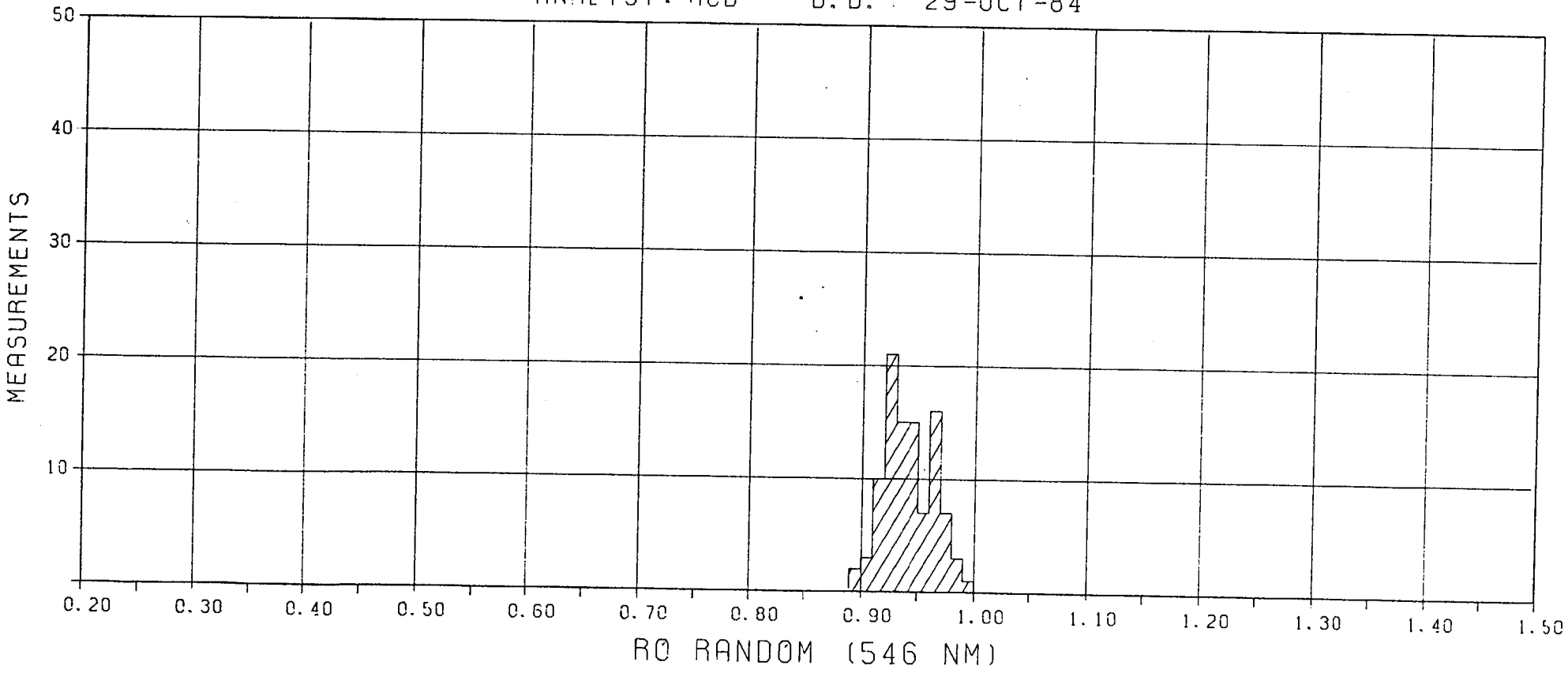

SAMPLE 2017.2 M ; TELOCOLLINITE

Fig. 22

REFLECTANCE HISTOGRAM

COUNTRY : AUSTRALIA
WELL/OUTCROP : MURTEREE-1
DEPTH/SAMPLE NR. : 2025 M
SAMPLE TYPE : CORE SAMPLE

MEAN : 0.78
DEVIATION : 0.03
MODE : 0.80
MEASUREMENTS : 52

ANALYST: BTX D.D. : 26-OCT-84

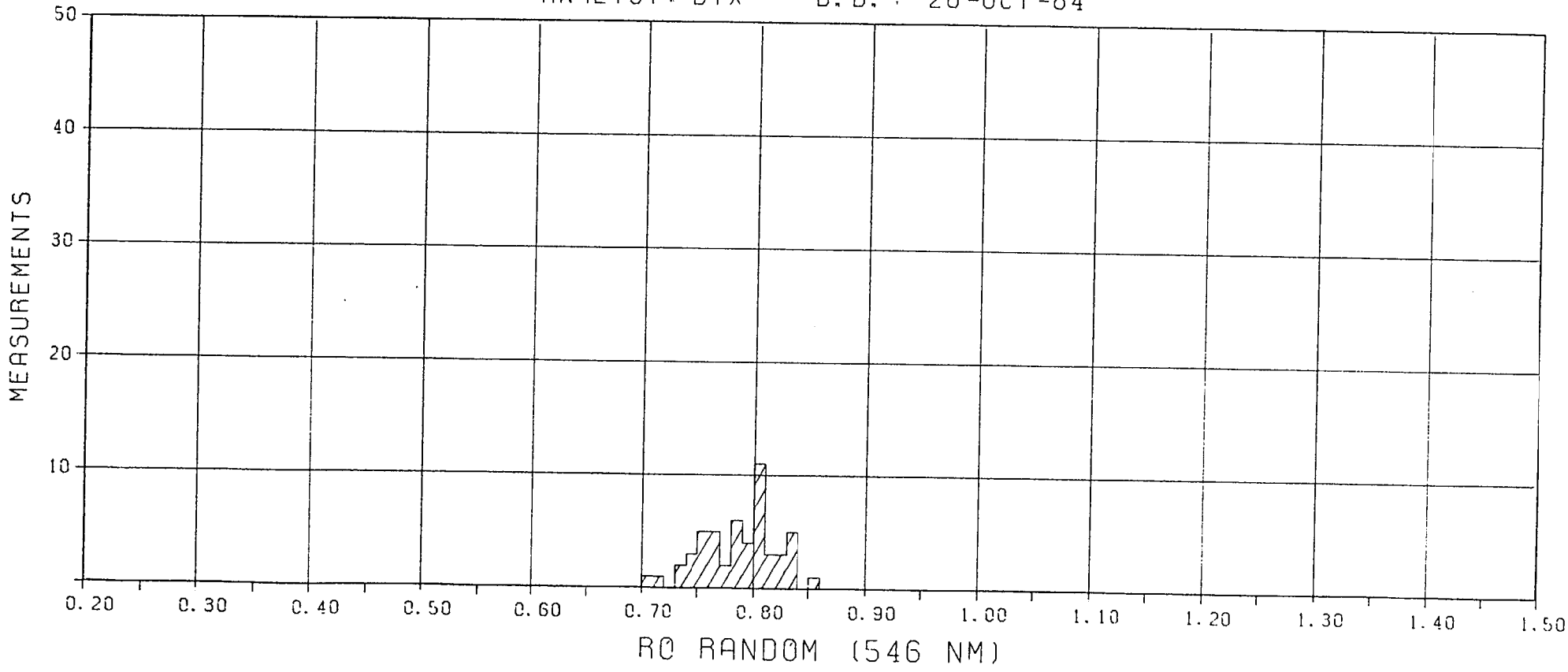

SAMPLE 2025.7 M; VITRINITE-2/(SEMI-)FUSINITE

Fig. 23

REFLECTANCE HISTOGRAM

COUNTRY	: AUSTRALIA	MEAN	: 1.08
WELL/OUTCROP	: MURTEREE-1	DEVIATION	: 0.05
DEPTH/SAMPLE NR.	: 2136 M	MODE	: 1.02
SAMPLE TYPE	: CUTTING SAMPLE	MEASUREMENTS	: 37

ANALYST: BTX D.D.: 29-OCT-84

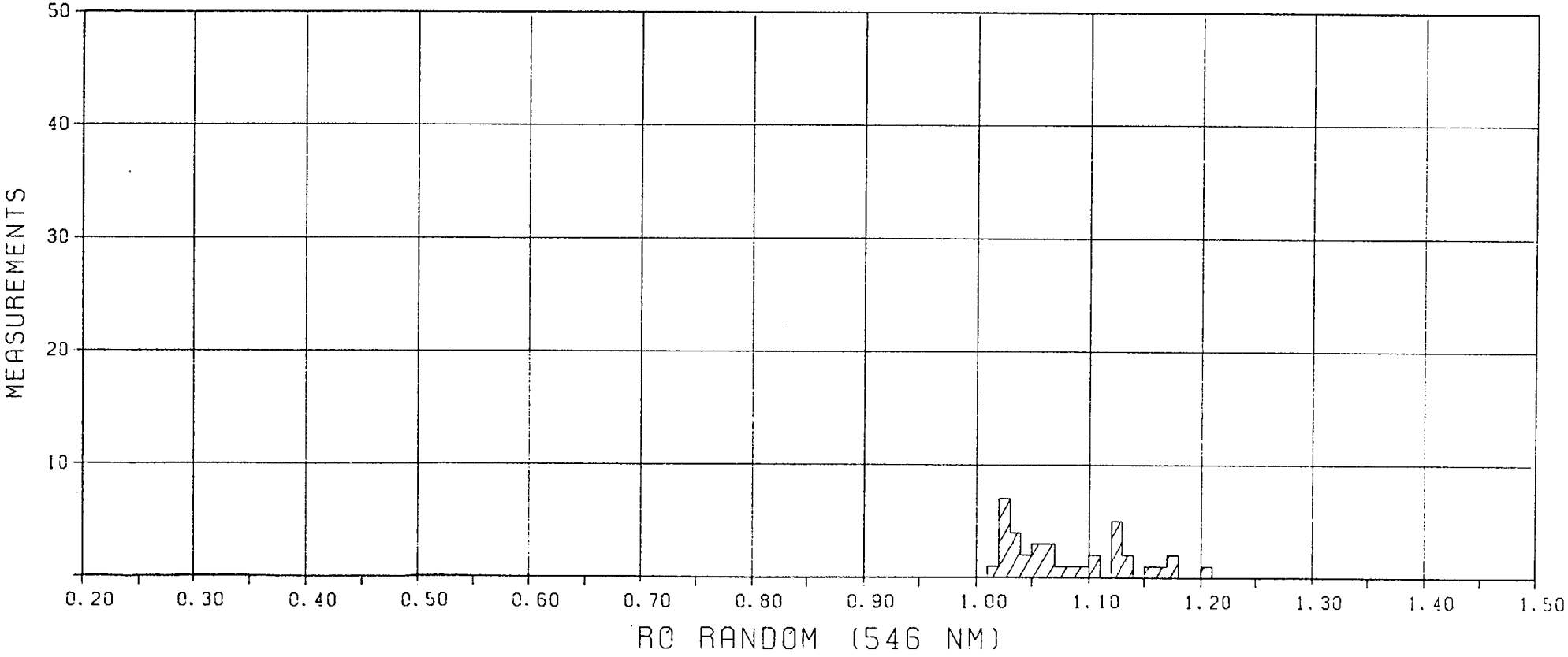

Fig. 24

TELOCOLLINITE

00183

REFLECTANCE HISTOGRAM

COUNTRY	: AUSTRALIA	MEAN	: 0.51
WELL/OUTCROP	: TINGA TINGANA-1	DEVIATION	: 0.05
DEPTH/SAMPLE NR.	: 1474 M	MODE	: 0.51
SAMPLE TYPE	: CORE SAMPLE	MEASUREMENTS	: 50

ANALYST: BTX · D.D.: 26-OCT-84

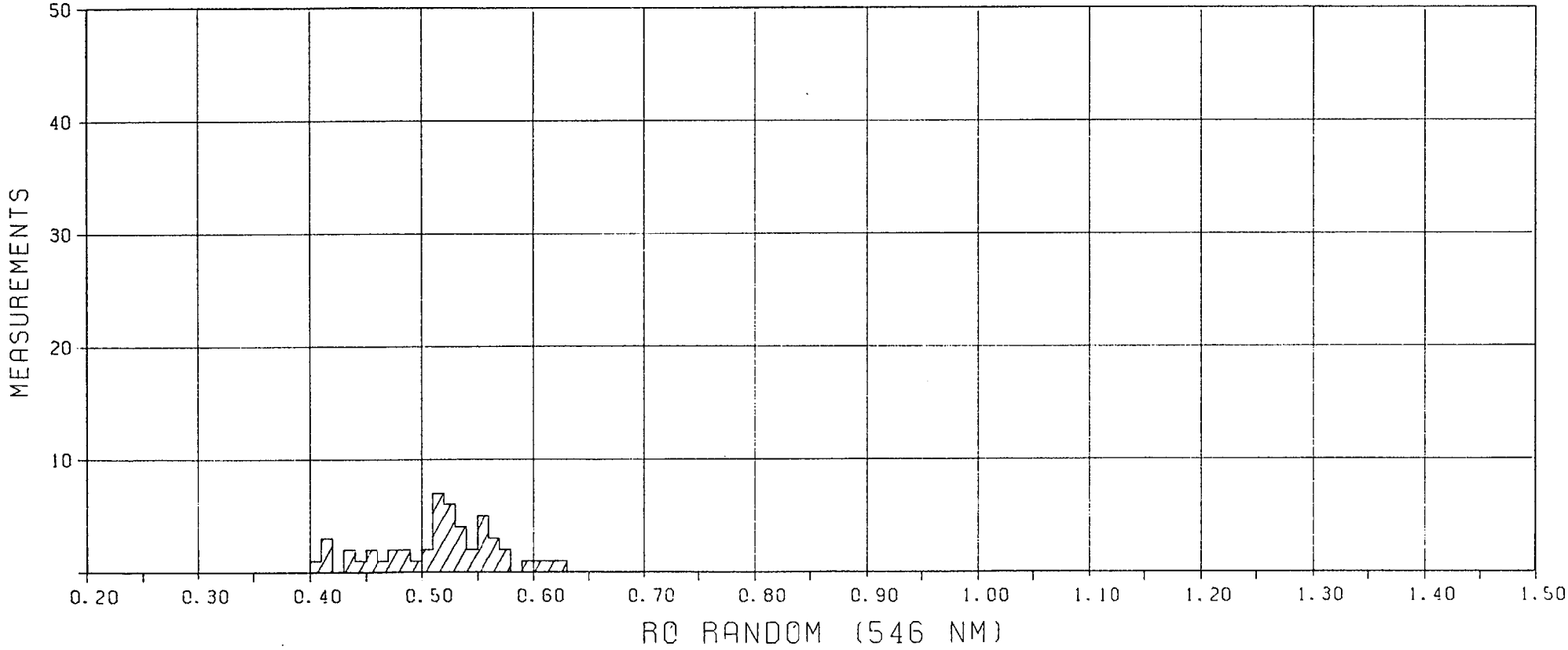

Fig. 25

SAMPLE 1474.6 M; VITRINITE-2 GRADING INTO SEMI-FUSINITE

REFLECTANCE HISTOGRAM

COUNTRY : AUSTRALIA
WELL/OUTCROP : TINGA TINGANA-1
DEPTH/SAMPLE NR. : 1482 M
SAMPLE TYPE : CORE SAMPLE

MEAN : 0.47
DEVIATION : 0.03
MODE : MULTI
MEASUREMENTS : 75

ANALYST : BTX D.D. : 24-OCT-84

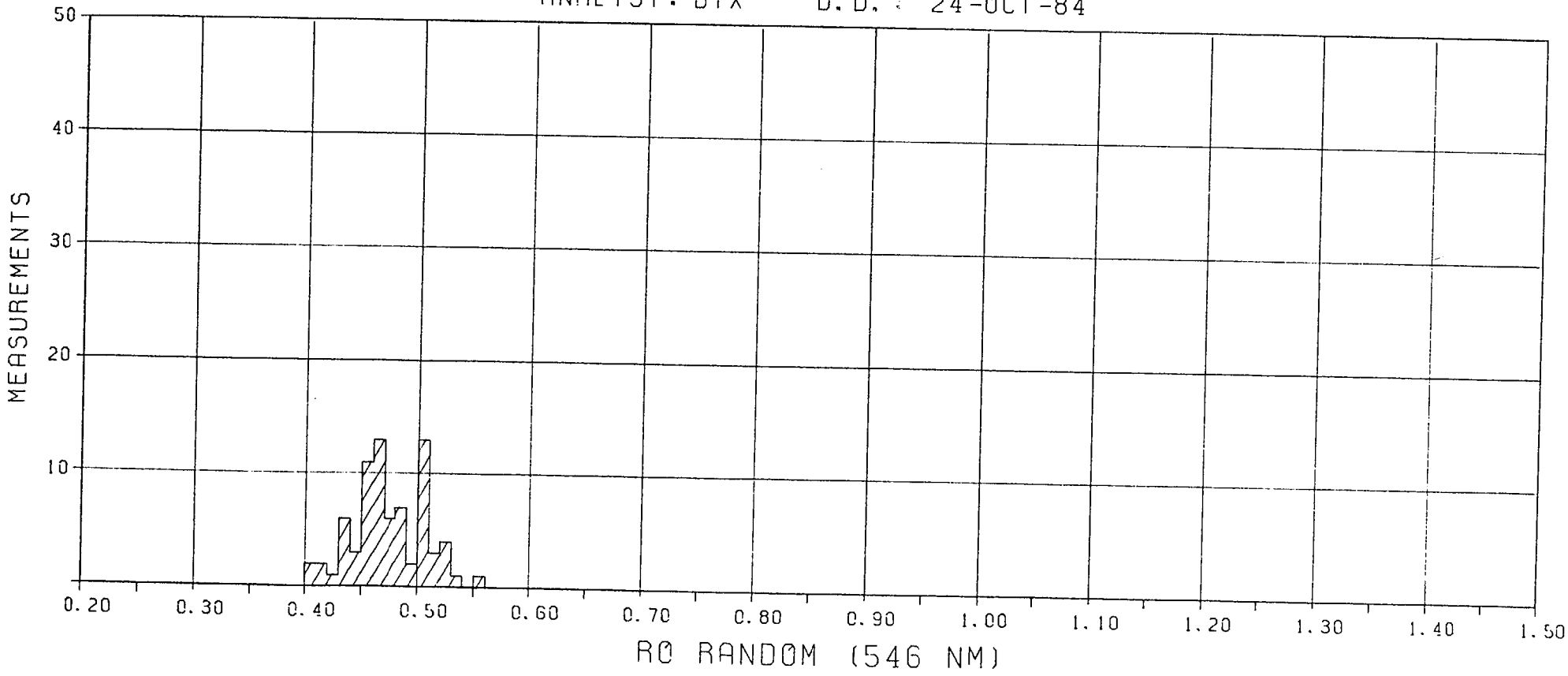

Fig. 26

SAMPLE 1482.7 M; TELINITE

REFLECTANCE HISTOGRAM

COUNTRY	: AUSTRALIA	MEAN	: 0.77
WELL/OUTCROP	: TOOLACHEE-1	DEVIATION	: 0.04
DEPTH/SAMPLE NR.	: 1849 M	MODE	: MULTI
SAMPLE TYPE	: CORE SAMPLE	MEASUREMENTS	: 50

ANALYST: BTX D.D. : 26-OCT-84

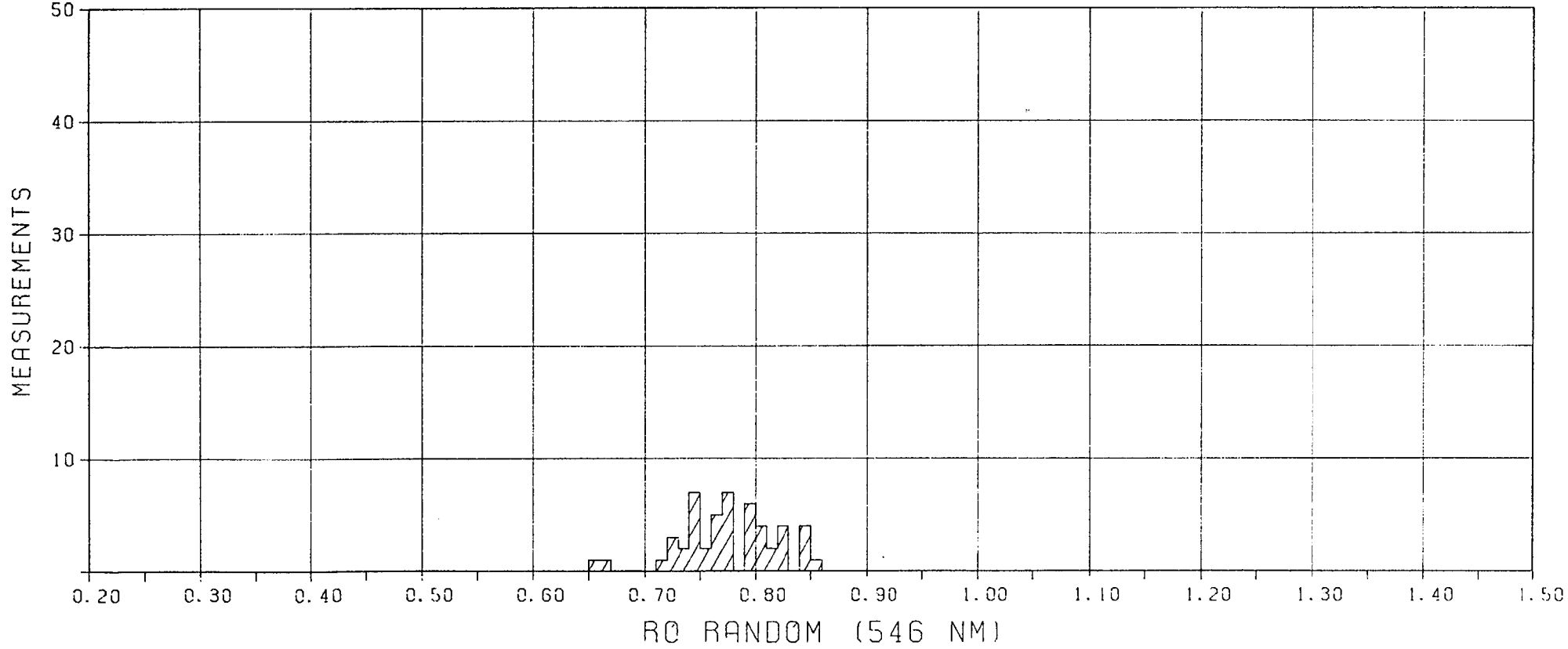

Fig. 27

DETRITAL VITRINITE-2 (OXIDISED ?)

REFLECTANCE HISTOGRAM

COUNTRY : AUSTRALIA
WELL/OUTCROP : TOOLACHEE-1
DEPTH/SAMPLE NR. : 2106 M
SAMPLE TYPE : CORE SAMPLE

MEAN : 1.00
DEVIATION : 0.04
MODE : 1.02
MEASUREMENTS : 75

ANALYST: ROD D.D. : 26-OCT-84

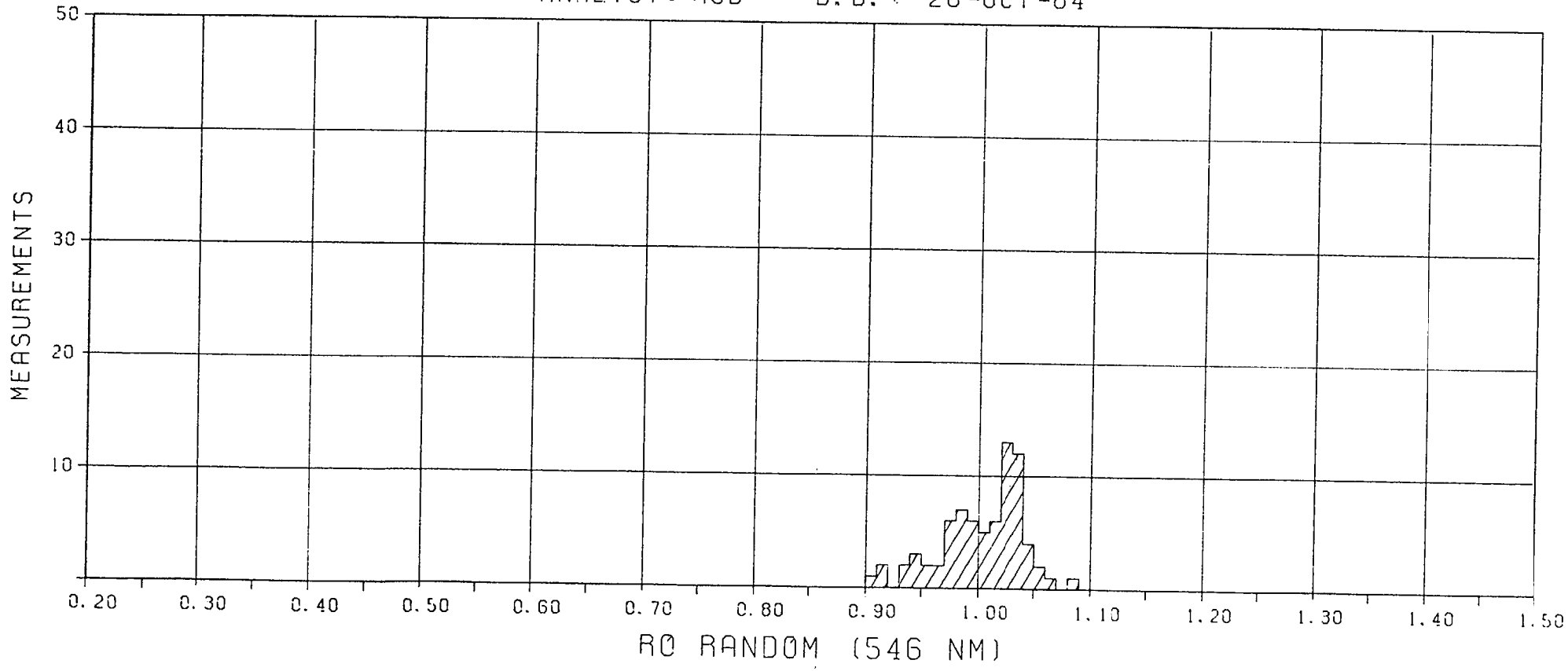

Fig. 28

SAMPLE 2106.7M; TELOCOLLINITE

REFLECTANCE HISTOGRAM

COUNTRY	: AUSTRALIA	MEAN	: 1.06
WELL/OUTCROP	: TOOLACHEE-1	DEVIATION	: 0.03
DEPTH/SAMPLE NR.	: 2109 M	MODE	: 1.06
SAMPLE TYPE	: CORE SAMPLE	MEASUREMENTS	: 100

ANALYST: ROD D.D. : 26-OCT-84

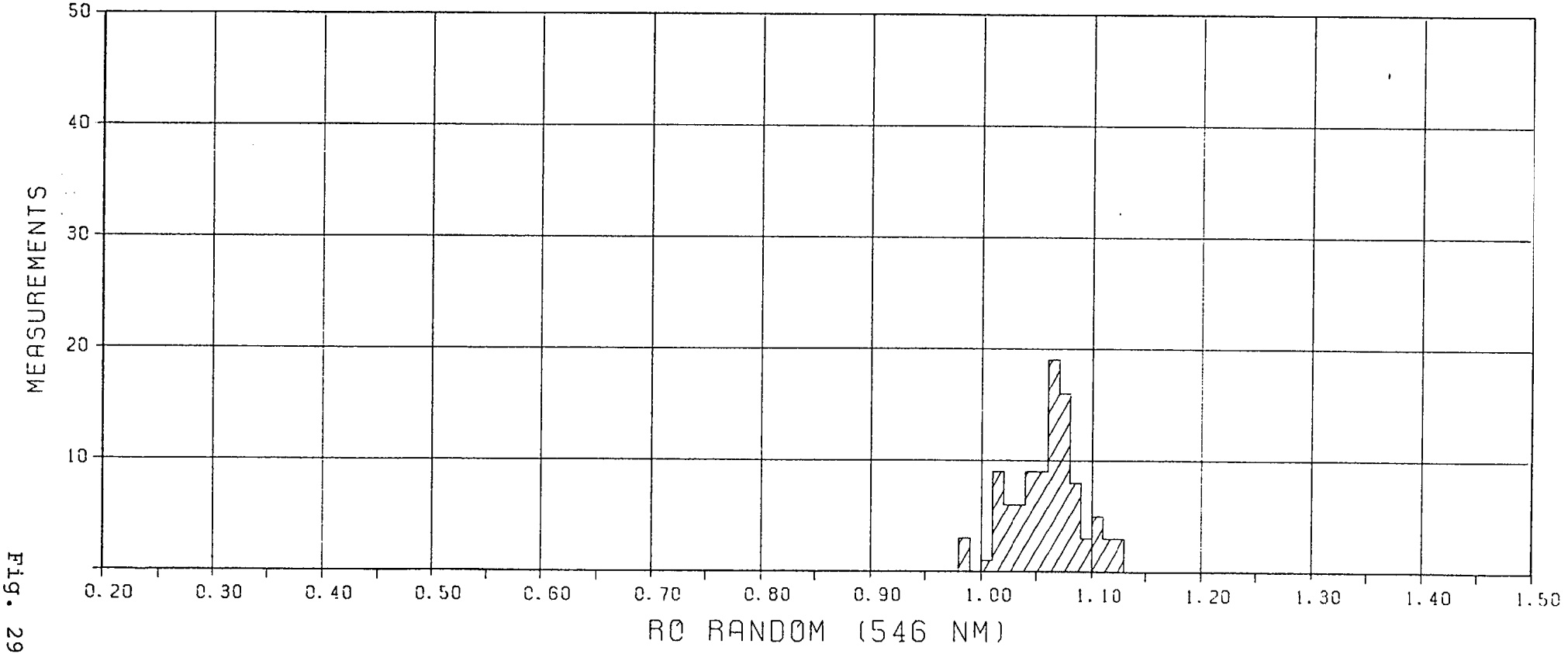

Fig. 29

SAMPLE 2109.7 ; TELOCOLLINITE

00193

MACERAL DESCRIPTION OF 6 SAMPLES FROM WELL BROLGA-1

DEPTH IN M	SAMPLE TYPE	ORGANIC: SAPROPELIC ORG. MATTER	VITR.: TELOCOLLINITE	VITR.: TELINITE	VITR.: DESMOCOLLINITE	LIPTINITE: SPORINITE	LIPTINITE: CUTINITE	LIPTINITE: RESINITE	LIPTINITE: LIPTODETRINITE	ALGAE: BOTRYOCOCCUS	ALGAE: TASMANITES	ALGAE: OTHER ALGAE	MICROPLANKTON	EXSUDATINITE	INERT.: SCLEROTINITE	INERT.: FUSINITE	INERT.: MACRINITE	INERT.: MICRINITE	INORG.: UNDIFFINED MINERALS	INORG.: FRAMBOIDAL PYRITE	INORG.: AGGREGATES OF PYRITE	INORG.: CRYSTALS OF PYRITE
2664.0	CTGS	-	/		+	+	-		+					-		*		/	+			-
2758.0	CTGS	-	+		*	+	-		+					-		+		/	/			-
2817.0	CORE		+		*	/	/		/					-		+		/				
2828.6	CORE	/	+		*				/				/	/		*		/	/		-	-
2917.9	CORE		*		+				-					/		+			-			
2927.0	CORE		/		+									/		*			-			

LEGEND	
*	ABUNDANT
+	COMMON
/	FEW
-	RARE

Table 2: Maceral descriptions of Brologa-1 samples

MACERAL DESCRIPTION OF 19 SAMPLES FROM WELL DULLINGARI-1

DEPTH IN M	SAMPLE TYPE
1773.3	CORE
1847.1	CTGS
2087.9	CTGS
2196.4	CORE
2197.3	CORE
2278.1	CORE
2319.8	CORE
2331.7	CTGS
2408.1	CORE
2408.2	CORE
2426.2	CTGS
2468.9	CTGS
2594.8	CORE
2651.8	CTGS
2708.6	CORE
2849.9	CTGS
2965.7	CTGS

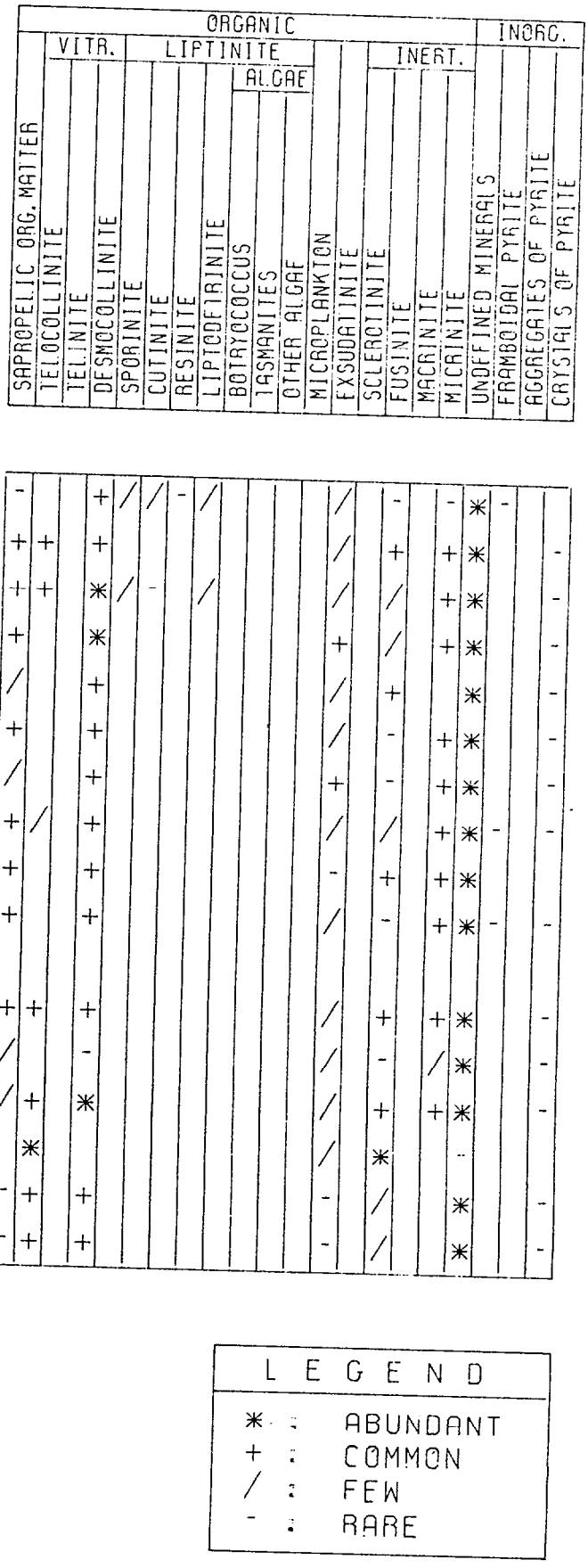

LEGEND	
*	ABUNDANT
+	COMMON
/	FEW
-	RARE

Table 3: Maceral descriptions of Dullingari-1 samples

DEPTH IN M	SAMPLE TYPE
3261.4	CTGS
9522.6	CORE

	ORGANIC																		INORG.			
	VITR.			LIPTINITE				ALGAE					INERT.									
SAPROPELIC ORG. MATTER	TELOCOLLINITE	TELINITE	DESMOCOLLINITE	SPORINITE	CUTINITE	RESINITE	LIPTODETRINITE	BOTRYOCOCCUS	TASMANITES	OTHER ALGAE	MICROPLANKTON	EXSUDATINITE	SCLEROTINITE	FUSINITE	MACRINITE	MICRINITE	UNDEFINED MINERALS	FRAMBOIDAL PYRITE	AGGREGATES OF PYRITE	CRYSTALS OF PYRITE
-	+		*									-		/			*			-
+			/									-		+		+	*			-

LEGEND	
*	: ABUNDANT
+	: COMMON
/	: FEW
-	: RARE

Table 3: Continued

MACERAL DESCRIPTION OF 5 SAMPLES FROM WELL DULLINGARI NORTH-1

DEPTH IN M	SAMPLE TYPE	SAPROPELIC ORG.MATTER	VITR.			LIPTINITE				ALGAE				INERT.				INORG.			
			TELOCOLLINITE	TELINITE	DESMOCOLLINITE	SPORINITE	CUTINITE	RESINITE	LIPTODETRINITE	BOTRYOCOCCUS	TASMANITES	OTHER ALGAE	MICROPLANKTON	EXSUDATINITE	SCLEROTINITE	FUSINITE	MACRINITE	MICRINITE	UNDEFINED MINERALS	FRAMBOIDAL PYRITE	AGGREGATES OF PYRITE	CRYSTALS OF PYRITE
2215.6	CORE		+		+				/					/		*			/			-
2307.0	CTGS		/		*				-					-		+		+	*			-
2531.8	CORE				*									/		+		+	*			-
2532.2	CORE				*									/		/		+	*			-
2614.3	CORE		+											-		*			-			-

LEGEND	
*	ABUNDANT
+	COMMON
/	FEW
-	RARE

Table 4: Maceral descriptions of Dullingari North-1 SAmples

MACERAL DESCRIPTION OF 8 SAMPLES FROM WELL MURTEREE-1

DEPTH IN M	SAMPLE TYPE	ORGANIC: SAPROPELIC ORG. MATTER	VITR.: TELOCOLLINITE	VITR.: TELINITE	VITR.: DESMOCOLLINITE	LIPTINITE: SPORINITE	LIPTINITE: CUTINITE	LIPTINITE: RESINITE	LIPTINITE: LIPTODETRINITE	LIPTINITE: ALGAE: BOTRYOCOCCUS	LIPTINITE: ALGAE: TASMANITES	LIPTINITE: ALGAE: OTHER ALGAE	MICROPLANKTON	EXSUDATINITE	INERT.: SCLEROTINITE	INERT.: FUSINITE	INERT.: MACRINITE	INERT.: MICRINITE	INORG.: UNDEFINED MINERALS	FRAMBOIDAL PYRITE	AGGREGATES OF PYRITE	CRYSTALS OF PYRITE
1808.4	CORE				+	+	-		/					-		*		/	/			-
1819.1	CORE		+		*	+	-		/					-		*			/			-
1844.0	CTGS	/	+		*	+	-		+					-		*		/	+			-
1986.3	CORE	+	+		+	+			+	-				-		-		+	*			-
2011.1	CORE		*		*	+			+					-		+			-			-
2017.2	CORE		*		+	/	+		+					-		-			-			-
2025.7	CORE	+			/	/			+					/		+		+	*			
2136.0	CTGS	/	/		+	/			/					/		*			*			-

LEGEND	
*	ABUNDANT
+	COMMON
/	FEW
-	RARE

Table 5: Maceral descriptions of Murteree-1 samples

MACERAL DESCRIPTION OF 4 SAMPLES FROM WELL TINGA TINGANA-1

DEPTH IN M	SAMPLE TYPE
1474.6	CORE
1482.7	CORE
1586.4	CORE
1687.7	CORE

ORGANIC																					INORG.			
	VITR.			LIPTINITE					ALGAE					INERT.										
SAPROPELIC ORG. MATTER	TELOCOLLINITE	TELINITE	DESMOCOLLINITE	SPORINITE	CUTINITE	RESINITE	LIPTODETRINITE	BOTRYOCOCCUS	TASMANITES	OTHER ALGAE	MICROPLANKTON	EXSUDATINITE	SCLEROTINITE	FUSINITE	MACRINITE	MICRINITE	UNDEFINED MINERALS	FRAMBOIDAL PYRITE	AGGREGATES OF PYRITE	CRYSTALS OF PYRITE
+		/	+	-		+	-							*		+	*			-
	*		+	/		+	/							/			+			
-		-	/	-		/	-							+		/	*			-
-		-	/			/						-		+			*			

LEGEND	
*	: ABUNDANT
+	: COMMON
/	: FEW
-	: RARE

Table 6: Maceral descriptions of Tinga Tingana-1

MACERAL DESCRIPTION OF 5 SAMPLES FROM WELL TOOLACHEE-1

DEPTH IN M	SAMPLE TYPE	ORGANIC																				INORG.			
			VITR.		LIPTINITE					ALGAE						INERT.									
		SAPROPELIC ORG. MATTER	TELOCOLLINITE	TELINITE	DESMOCOLLINITE	SPORINITE	CUTINITE	RESINITE	LIPTODETRINITE	BOTRYOCOCCUS	TASMANITES	OTHER ALGAE	MICROPLANKTON	EXSUDATINITE	SCLEROTINITE	FUSINITE	MACRINITE	MICRINITE	UNDEFINED MINERALS	FRAMBOIDAL PYRITE	AGGREGATES OF PYRITE	CRYSTALS OF PYRITE
1849.0	CORE	/			/	-			/					/		+		+	*			-
1978.0	CORE	/			/	-			/					-		+		/	*			-
2106.7	CORE		*		/	-			+					-		/			-			-
2109.7	CORE		*		/	/			+					-		+			-			-
2182.8	CORE	/																/	*		/	-

LEGEND	
*	ABUNDANT
+	COMMON
/	FEW
-	RARE

Table 7: Maceral descriptions of Toolachee-1 samples

INITIAL DISTRIBUTION

3 copies	Shell Perth EXH
3 copies	SIPM The Hague EP/11/13

RESTRICTED INVESTIGATION
REPORT 460R

CSIRO

MINERALS RESEARCH LABORATORIES

DIVISION OF MINERALOGY

HYDROCARBONS IN COALS FROM MOORARI AND TIRRAWARRA, COOPER BASIN, SOUTH AUSTRALIA

M. Shibaoka

14th February, 1972

P.O. Box 136,
NORTH RYDE. 2113 N.S.W.

In September, 1971 CSIRO was supplied by the Delhi International Oil Corporation with eight coal samples and one oil sample from the Moorari No. 1, Tirrawarra Nos. 1 and 2. The hydrocarbons extracted from the coal samples have been investigated by gas chromatography, and the results are summarized in this Restricted Investigation Report. The results of analysis of the oil sample will shortly be reported separately.

Methods

n-Alkanes and other hydrocarbons, together with more complex compounds were obtained by solvent extraction of the coal samples. The hydrocarbons were isolated by chromatography, separated by molecular sieves into straight-chain paraffins and branched/cyclic hydrocarbons, and analysed by gas chromatography.

Carbon contents of the samples (dry ash-free basis) were estimated from mean maximum reflectance ($\bar{R}_o$) of vitrinite. The estimated carbon contents of the samples will be checked by chemical analysis and the results provided in a supplementary report.

Results

1. All results so far obtained are listed in Table 1. In Fig. 1, carbon contents of coal samples from the Moorari - Tirrawarra area are plotted against present depth of burial. Points representing the coal samples from the Gidgealpa - Tinga Tingana area, including the Moomba samples, and the line of best fit are transferred to this diagram from Fig. 1 of the previous report (Investigation Report 277R). All samples from the Moorari - Tirrawarra area occupy positions indicating much lower carbon content for a given depth than those from the Gidgealpa - Tinga Tingana area. Two possible explanations for this fact may be offered: (1) In both areas, depths of burial of coal seams did not differ as much as now when they were metamorphosed and reached to the present rank of coalification. But after that, the Gidgealpa - Tinga Tingana area was uplifted about 1500 - 2000 ft relative to the Moorari - Tirrawarra area.

(2) The geothermal gradient in the past was different in the two areas*. More detailed investigation should be carried out before a definite conclusion can be drawn. However, fortunately many oil wells have penetrated overlying formations which contain coal seams and coal lenses, for instance the Winton Formation and Walloon Formation. If coal particles are found in oil well cuttings from these formations, it would be possible to estimate the geothermal gradient in the past in each area.

2. According to the Carbon Ratio theory, liquid hydrocarbons are not generally encountered in sediments when the fixed carbon content (dry ash-free) of the coal exceeds about 65% (equivalent to a carbon content of about 85% dry ash-free) and the most promising interval of organic metamorphism for the occurrence of oil lies between 47% and 60% fixed carbon (White, 1920; Fuller, 1919 and Ammosov, 1961). In the Moorari - Tirrawarra area, the carbon content of coals from the oil producing horizon (Gidgealpa Formation) is well above this limit, but in fact a large petroleum reserve has been confirmed. Wassojewitsch et al think that the boundary between "main phase of petroleum formation" and "wet gas and condensate" is where the volatile matter is 26% (dry ash-free) (equivalent to a carbon content of about 89%) though the most promising range is where the volatile matter is 36% to 40% (equivalent to carbon contents of 85% and 81% respectively). More detailed investigation should be carried out in this area before a definite conclusion can be drawn.

3. The distribution patterns of n-alkanes of the Moorari - Tirrawarra coals are similar to those of some Gidgealpa coals which show very broad peaks between C_{13} and C_{25}. The peaks are not so high as those for the Moomba coals which are more advanced in degree of coalification (carbon

---

Footnote * According to the data supplied by the Delhi Australian Petroleum Ltd, the present geothermal gradient seems to become lower towards the north: Strzelecki No. 1 = 40°F/1000 ft?, Moomba Nos. 1 and 2 = 23 and 26°F/1000 ft, Gidgealpa Nos. 1 - 7 = 15 - 18°F/1000 ft, Merrimelia Nos. 1 - 4 = 16 - 17°F/1000 ft and Innamincka No. 1 = 14°F/1000 ft.

content 88.6 and 89.0%). The Tinga Tingana coal of lower rank (carbon content 79.6%) has a peak around C_{23} - C_{25}, which is also different from the Moorari - Tirrawarra coals. O.K.

4. The odd - even carbon number concentration preference (C.P.I.) for the Moorari - Tirrawarra coals is about the same as that for the Moomba coals. All Moorari - Tirrawarra coals show very high pristane/phytane ratios.

References

1. Ammosov, I.I., 1961; Alteration stages of sedimentary rocks and paragenetic relations of mineral fuels. Sov. Geol. 4. Translation by Associated Technical Services, Inc.

2. Fuller, M.L., 1919; Relation of oil to carbon ratios of Pennsylvanian coals in Northern Texas. Econ. Geol. 14, pp. 536-542.

3. Wassojewitsch, N.B., Kortschagina, Ju.I., Lopatin, N.W., Tschernyschew, W.W. and Tschernikov, K.A., 1969; Die Hauptphase der Erdölbildung. Z. angew. Geol. 15, s. 612-621.

4. White, D., 1920; Genetic problems affecting search for new oil regions. Bull. Amer. Mining Met. 65, pp. 176-198.

TABLE 1

Analysis of hydrocarbons extracted from coals

Well	MOORARI NO. 1		TIRRAWARRA NO. 1			TIRRAWARRA NO. 2		
Core	1	3	1	5	5	1	2	4
Lab. No.	31914	31915	31916	31917	31918	31919	31920	31921
Depth (ft)	8900	9622	8448	9026	9049	9045	9181	9725.5
Nature of sample	coal	coal	coal	coal	coal	coal	coal	coal
Percent total extract	~0.8	0.66	0.52	0.64	0.46	1.08	0.90	0.64
Alkanes, mgm/gm	0.69	0.37	0.35	1.1	0.49	2.1	2.3	1.0
Pristane : Phytane	2.6	5.4	7.8	5.9	5.6	4.6	3.0	3.9
Pristane, % rel. to n-alkanes	4.4	7.9	5.1	2.6	4.3	4.8	5.8	3.8
Phytane, % rel. to n-alkanes	1.8	1.6	0.8	0.5	0.8	1.1	2.1	1.1
C.P.I. * (C_{23} - C_{33})	1.07	1.07	1.14	1.00	0.93	1.06	1.03	1.00
n-ALKANES DISTRIBUTION (%)								
n - carbon no.								
11	0.7	0.7	0.9	1.1	0.6	1.3	1.0	2.9
12	3.1	3.5	2.9	3.5	3.9	2.7	2.8	6.4
13	5.1	8.1	5.0	5.5	6.5	4.0	5.7	10.0
14	6.9	9.7	6.5	7.3	8.0	5.6	9.1	11.2
15	8.3	10.4	7.8	7.7	9.4	7.8	10.5	10.8
16	9.3	8.5	7.8	7.3	7.3	7.7	11.3	9.0
17	10.7	8.8	7.7	7.2	8.6	8.7	11.5	10.3
18	10.6	8.4	8.8	9.1	8.6	8.9	10.7	9.7
19	8.6	6.7	7.9	7.3	6.5	7.5	8.3	6.0
20	6.6	5.3	7.0	6.6	5.9	6.9	6.2	5.0
21	5.6	4.4	6.6	6.2	5.4	6.2	4.5	3.7
22	4.3	3.8	5.9	5.5	5.1	5.6	3.5	3.1
23	3.8	3.0	5.7	5.8	4.5	5.5	2.5	2.2
24	2.9	2.5	4.4	5.7	4.8	4.8	1.9	1.9
25	2.0	2.0	3.6	4.2	3.5	3.8	1.1	1.2
26	1.2	1.4	1.8	2.6	2.3	2.4	0.6	0.7
27	1.0	1.2	1.5	1.9	1.7	1.8	0.4	0.5
28	0.8	0.8	1.0	1.0	1.1	1.0	0.2	0.3
29	0.4	0.5	0.4	0.7	0.4	0.7	0.1	0.2
30	0.4	0.3	0.3	0.5	0.5	0.5	0.1	0.1
31	0.2	0.2	0.2	0.2	0.2	0.3	0.06	0.1
32	0.1	0.1	0.1			0.1	0.02	0.1
33	0.6	0.1	0.2					
34	0.6							
Dry ash-free basis, Carbon (%) estimated from reflectance of vitrinite	85	**	85	88	86	86	87	88

* C.P.I. - Carbon Preference Index = $\frac{\%\ (\text{odd-no. n-alkanes } C_{25} - C_{33}) + \%\ (\text{odd no. n-alkanes } C_{23} - C_{31})}{2 \times (\text{even-no. n-alkanes } C_{24} - C_{32})}$

** Insufficient vitrinite

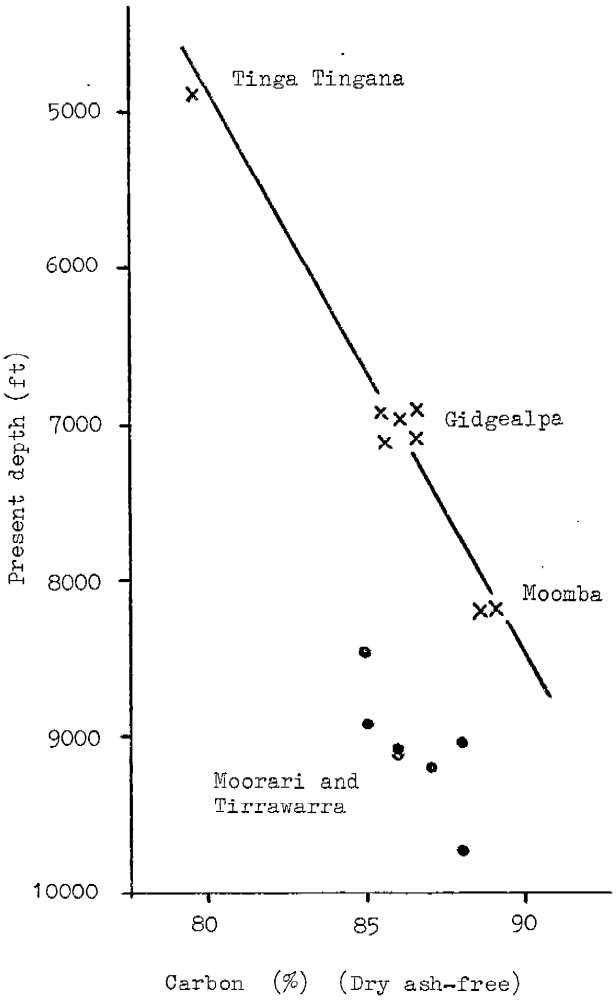

Figure 1. Carbon Contents of Coals at Depths in the Cooper Basin

RESTRICTED
CLASSIFICATION

RESTRICTED INVESTIGATION
REPORT 507R

CSIRO

MINERALS RESEARCH LABORATORIES

DIVISION OF MINERALOGY

GAS CHROMATOGRAPHIC ANALYSIS OF TIRRAWARRA OIL AND CHEMICAL ANALYSIS OF TIRRAWARRA AND MOORARI COALS

K.W. Gould and M. Shibaoka

P.O. Box 136
NORTH RYDE, N.S.W. 2113

OCTOBER 1972

In September 1971, CSIRO was supplied by the Delhi International Oil Corporation with eight coal samples and one oil sample from the Moorari No.1, Tirrawarra No.1 and Tirrawarra No.2 Wells. The hydrocarbons extracted from the coal samples were investigated by gas chromatography and the carbon contents of the coal samples were estimated from their reflectance under the microscope. The results were reported to the Company in Restricted Investigation Report 460R. However, at that time, the chemical analysis of the coal samples and the gas chromatographic analysis of the oil sample were not available. These analyses have recently been carried out and the results are included in this report.

Results

The results of chemical analyses of the coal samples are shown in Table 1. It was expected that the volatile matter of the coal would decrease as the depth of the coal seam becomes greater, whilst the fixed carbon of proximate analyses and the carbon content of ultimate analyses would increase. However, such relationships were not always observed, probably due to the very large amount of mineral matter in several samples.

The difference between the carbon content estimated from the reflectance of vitrinite and the chemically determined value is less than 1.6% excepting for two samples which were very rich in mineral matter (Fig.1). The reflectance measurement seems to be a more reliable method for mineral matter-rich coals than the direct measurement.

The concentration of boron in three Tirrawarra coal samples has been investigated by atomic emission spectrography (Table 2). All samples investigated showed low boron contents, which suggests

that the coal seams were not affected by marine water during coal seam deposition or at an early stage of diagenesis.

Fig.2 is the gas chromatography of Tirrawarra oil; the percentage of n-alkanes is shown in Table 3. The pristane/phytane ratio of this oil sample is very high.

TABLE 1. ANALYSES OF COAL SAMPLES

LAB. NO.	31914	31915	31916	31917	31918	31919	31920	31921
DETAILS BORE	MOORARI 1	MOORARI 1	TIRRAWARRA 1	TIRRAWARRA 1	TIRRAWARRA 1	TIRRAWARRA 2	TIRRAWARRA 2	TIRRAWARRA 2
DEPTH (Ft)	8900	9622	8448	9026	9049	9045	9181	9725'6"
CORE	1	3	1	5	5	1	2	4
Air dried basis								
Moisture	1.6	0.5	1.4	1.6	1.4	1.6	1.2	0.1
Ash	9.5	57.9	36.8	2.5	12.5	3.8	10.6	26.3
Volatile matter	27.6	13.8	21.5	24.6	23.4	28.8	21.8	19.9
Fixed carbon	61.3	27.8	40.3	71.3	62.7	65.8	66.4	53.7
Calorific value(Btu/lb)	13,290	5,890	8,770	14,500	12,770	14,580	13,360	10,940
Carbon	76.4	34.6	50.9	84.2	74.4	82.9	77.6	63.5
Hydrogen	4.6	2.3	3.3	4.5	4.2	4.9	4.2	3.8
Nitrogen	1.6	0.5	1,0	1.8	1.5	1.6	1.4	1.0
Sulphur (total)	0.3	0.2	0.4	0.3	0.2	0.4	0.3	0.4
Oxygen	6.0	4.0	6.2	5.1	5.8	4.8	4.7	4.9
CO_2	0.04	0.00	0.00	0.00	0.11	0.00	0.00	0.00
Swelling No	1½	½	1	1	1	6½	1½	1
Dry ash-free basis								
Volatile matter	31.0	33.2	34.8	25.7	27.2	30.4	24.7	27.0
Fixed carbon	69.0	66.8	65.2	74.3	72.8	69.6	75.3	73.0
Calorific value(Btu/lb)	14,950	14,150	14,210	15,130	14,840	15,410	15,150	14,860
Carbon	85.9	83.0	82.4	87.8	86.5	87.6	88.0	86.3
Hydrogen	5.2	5.5	5.4	4.7	4.9	5.2	4.8	5.2
Nitrogen	1.8	1.2	1.7	1.9	1.8	1.7	1.6	1.4
Sulphur (total)	0.4	0.6	0.6	0.3	0.2	0.5	0.3	0.5
Oxygen	6.7	9.7	9.9	5.3	6.6	5.0	5.3	6.6

TABLE 2. CONCENTRATION OF BORON

(parts per million on air-dried coal basis)

LAB. NO. BORE CORE	31914 MOORARI 1 1	31916 TIRRAWARRA 1 1	31921 TIRRAWARRA 2 4
Boron	5.5	15	5.2

TABLE 3. ALKANE DISTRIBUTION IN TIRRAWARRA OIL

LAB NO.	31793
WELL AND OIL	TIRRAWARRA NO.2 DST NO.8
TOTAL n-ALKANES %	67.40
PRISTANE %	2.17
PHYTANE %	0.29
PRISTANE/PHYTANE RATIO	7.38
n-ALKANE DISTRIBUTION CARBON NUMBER	
10	10.34
11	7.35
12	7.51
13	8.27
14	5.85
15	5.44
16	3.59
17	3.19
18	2.60
19	3.15
20	1.93
21	2.24
22	1.58
23	1.38
24	1.47
25	0.90
26	0.61

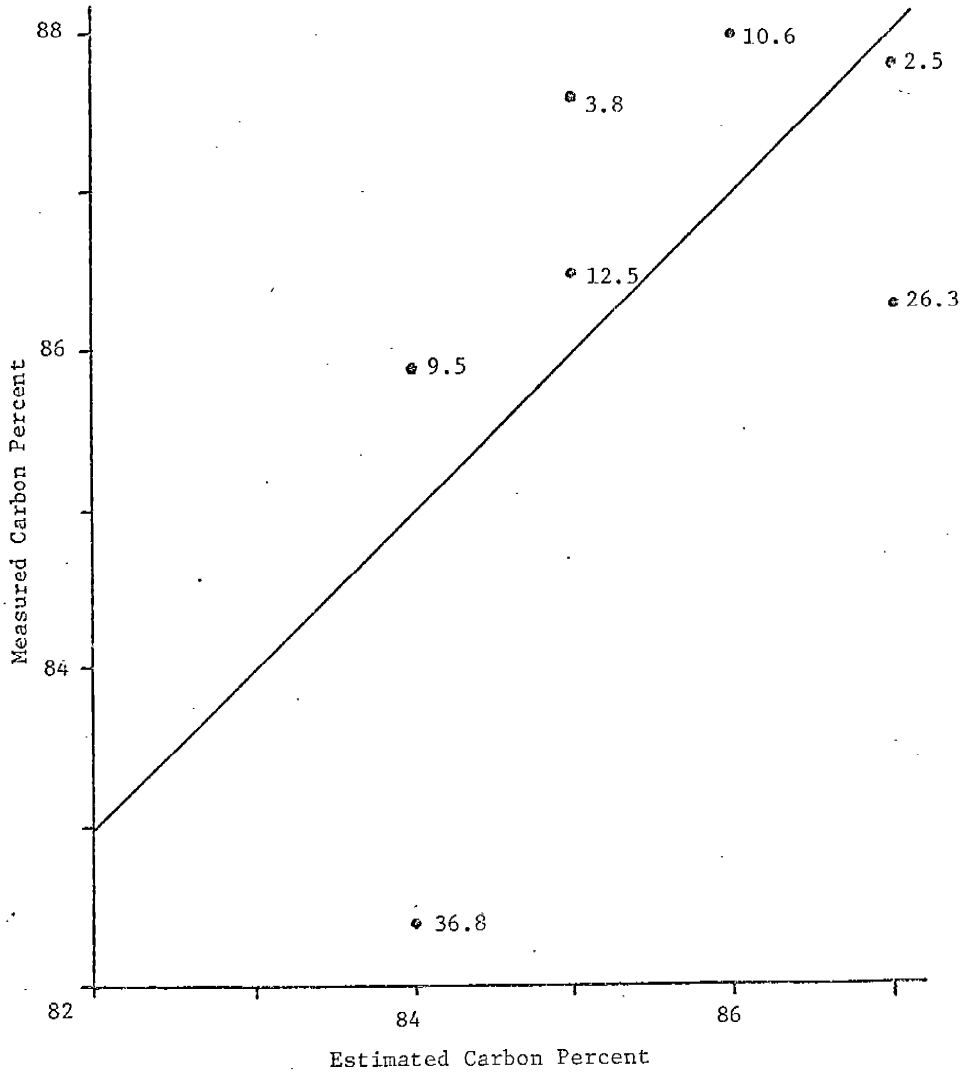

FIG. 1. Comparison of carbon content estimated from reflectance of vitrinite and chemically determined carbon content. Values in the diagram show ash yield of the samples.

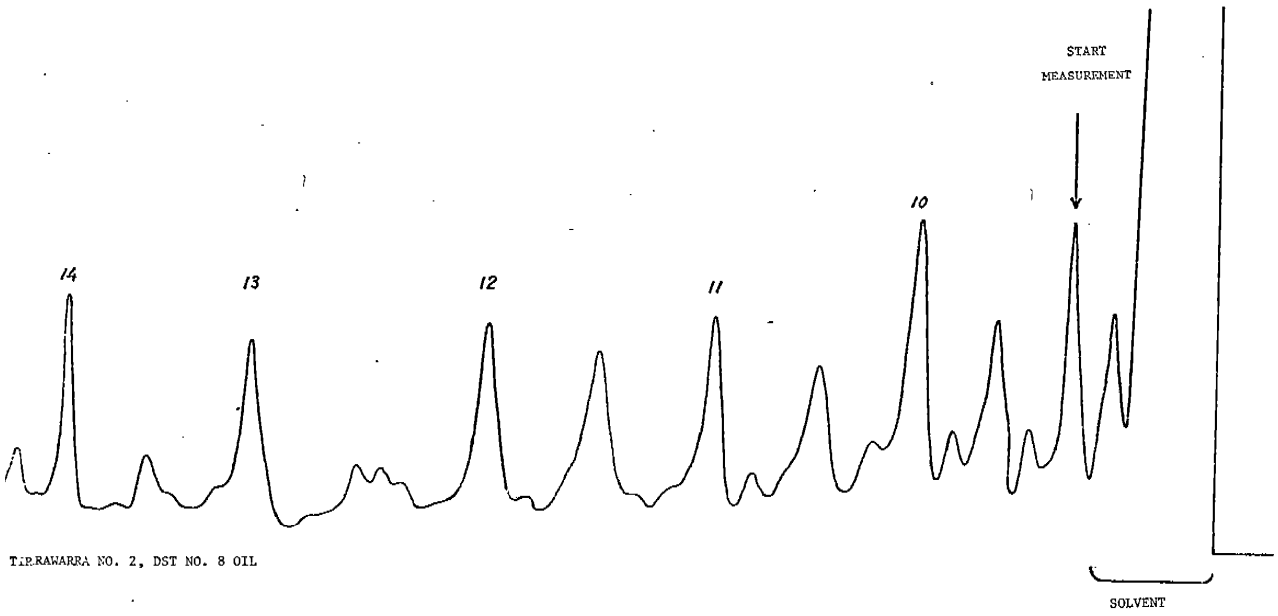

TIRRAWARRA NO. 2, DST NO. 8 OIL

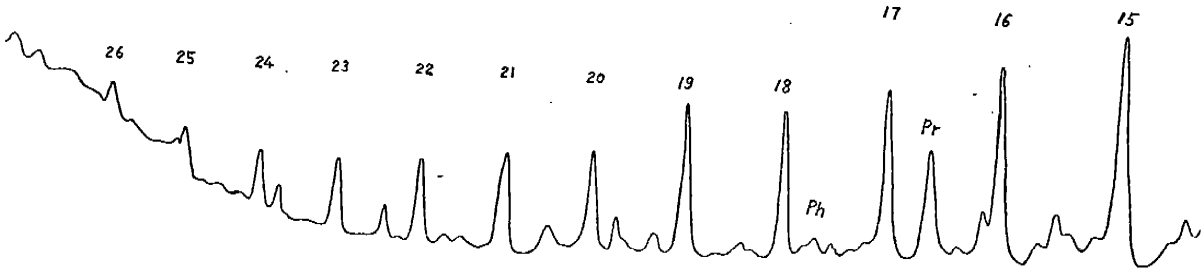

FIG. 2. GAS CHROMATOGRAPHIC ANALYSIS OF

CSIRO DIVISION OF MINERALOGY
P.O. BOX 136
NORTH RYDE N.S.W. 2113
AUSTRALIA

RESTRICTED INVESTIGATION
REPORT 577R

REFLECTANCE OF COALS FROM GIDGEALPA NO.3, AND TINGA TINGANA NO.1 WELLS, COOPER BASIN, SOUTH AUSTRALIA

Fourteen ditch cuttings samples from Gidgealpa No.3 and ten from Tinga Tingana No.1 were supplied by Delhi International Oil Corporation. After a preliminary examination with a stereo-microscope for visual evidence of coal grains, seven of the Gidgealpa and six of the Tinga Tingana samples were prepared for reflectance measurement by crushing to below 1½ mm, floating in some cases at s.g. of 2.34, mounting in cold setting resin, and polishing a cross section of the grains.

Maximum reflectance measurements were made on vitrinite in green light (546 nm) with immersion oil R.I.1.515. Histograms of the results are shown in Figs. 1 and 3. From a study of these histograms and some data on variations in the type of vitrinite measured, mean maximum reflectance values are calculated for typical vitrinite, and these have been plotted against depth as shown in Figs 2 and 4.

Reflectance/Depth gradients for these two wells, 0.006% per 100 ft. at Gidgealpa and 0.005% per 100 ft. at Tinga Tingana are slightly less than that at Innamincka No.1 (0.007% per 100 ft.), which is incidentally similar to the gradient in the Bowen-Surat Basin up to a reflectance of 0.6%.

A.J.R. BENNETT & M. SHIBAOKA
DECEMBER 1973

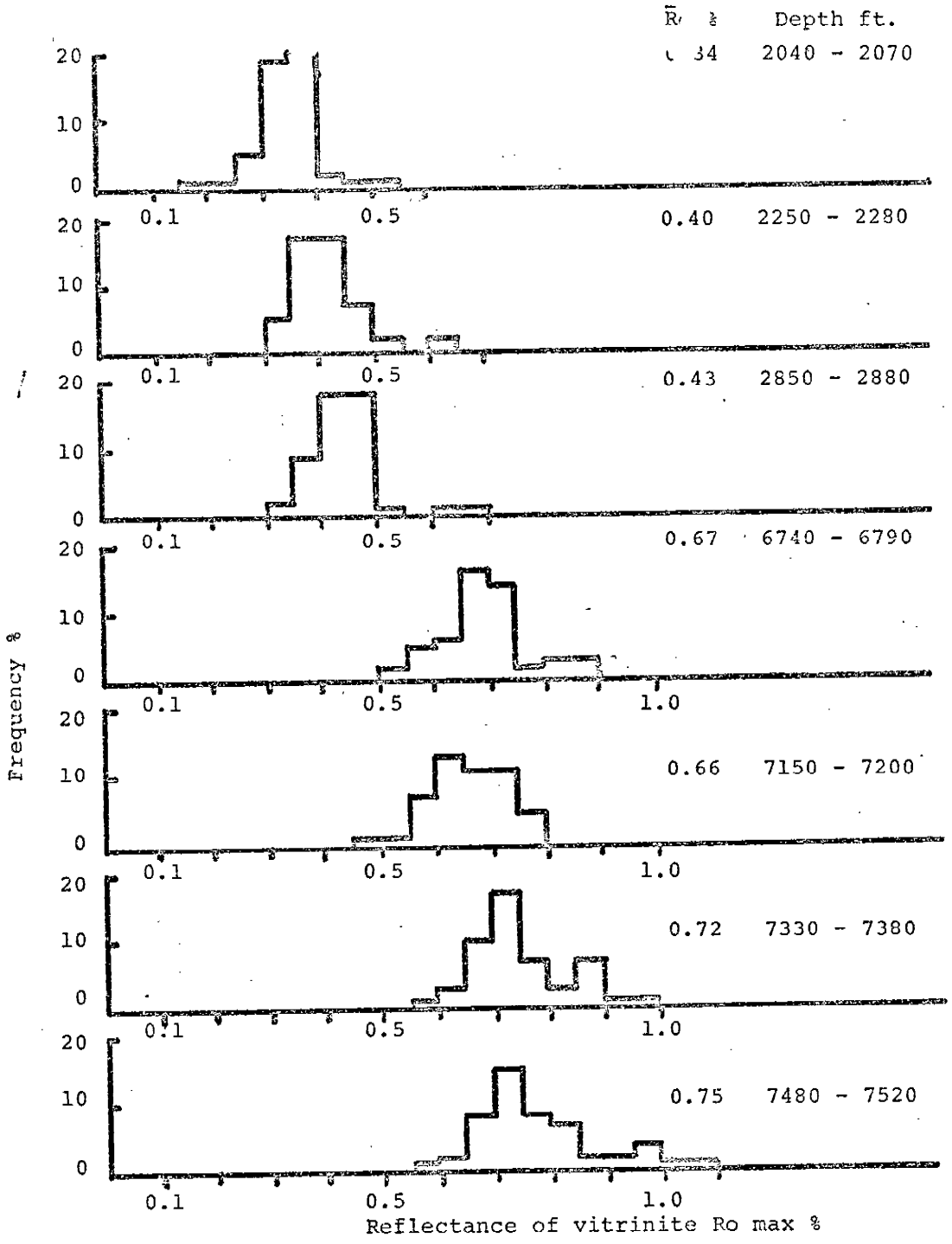

FIG. 1. Reflectance histrograms of Gidgealpa No.3 coals

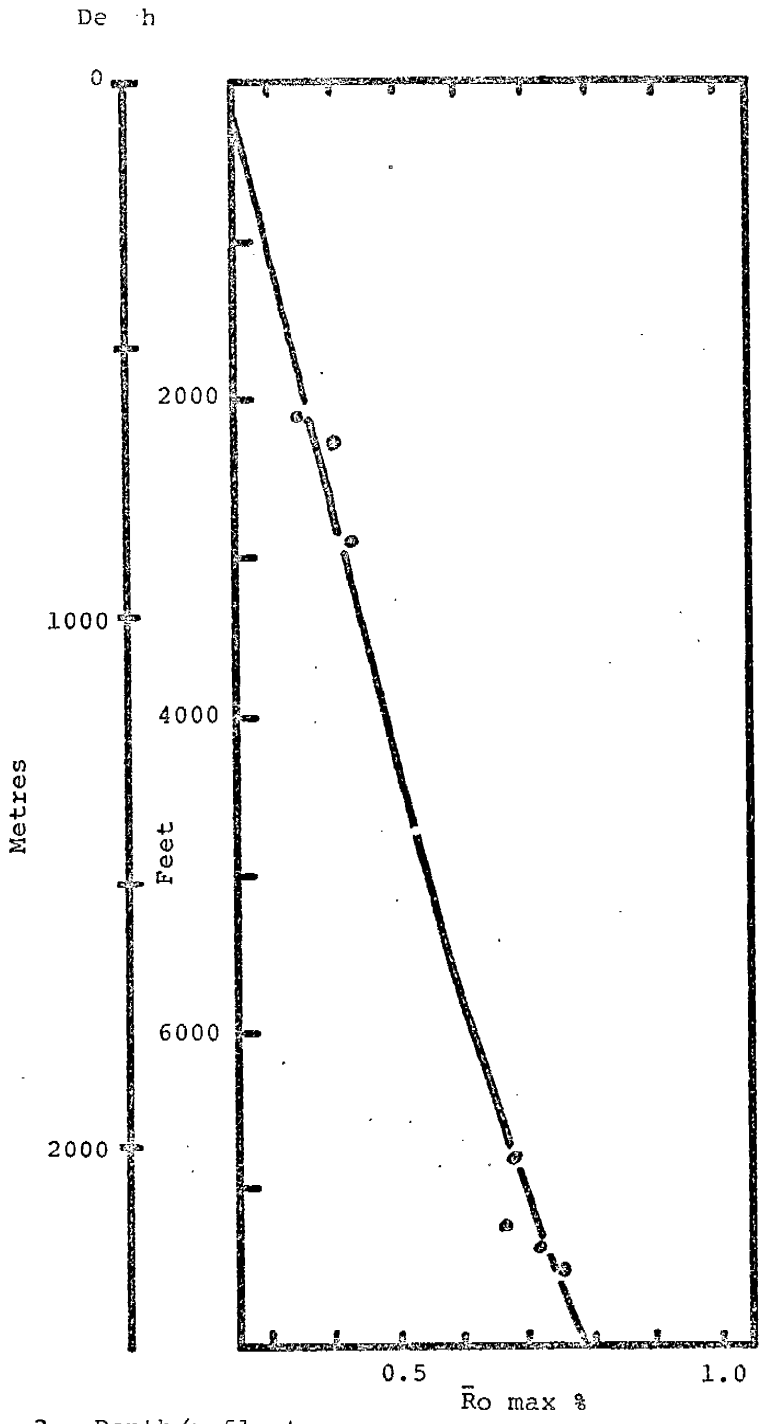

FIG. 2. Depth/reflectance curve for Gidgealpa No.3 Well.

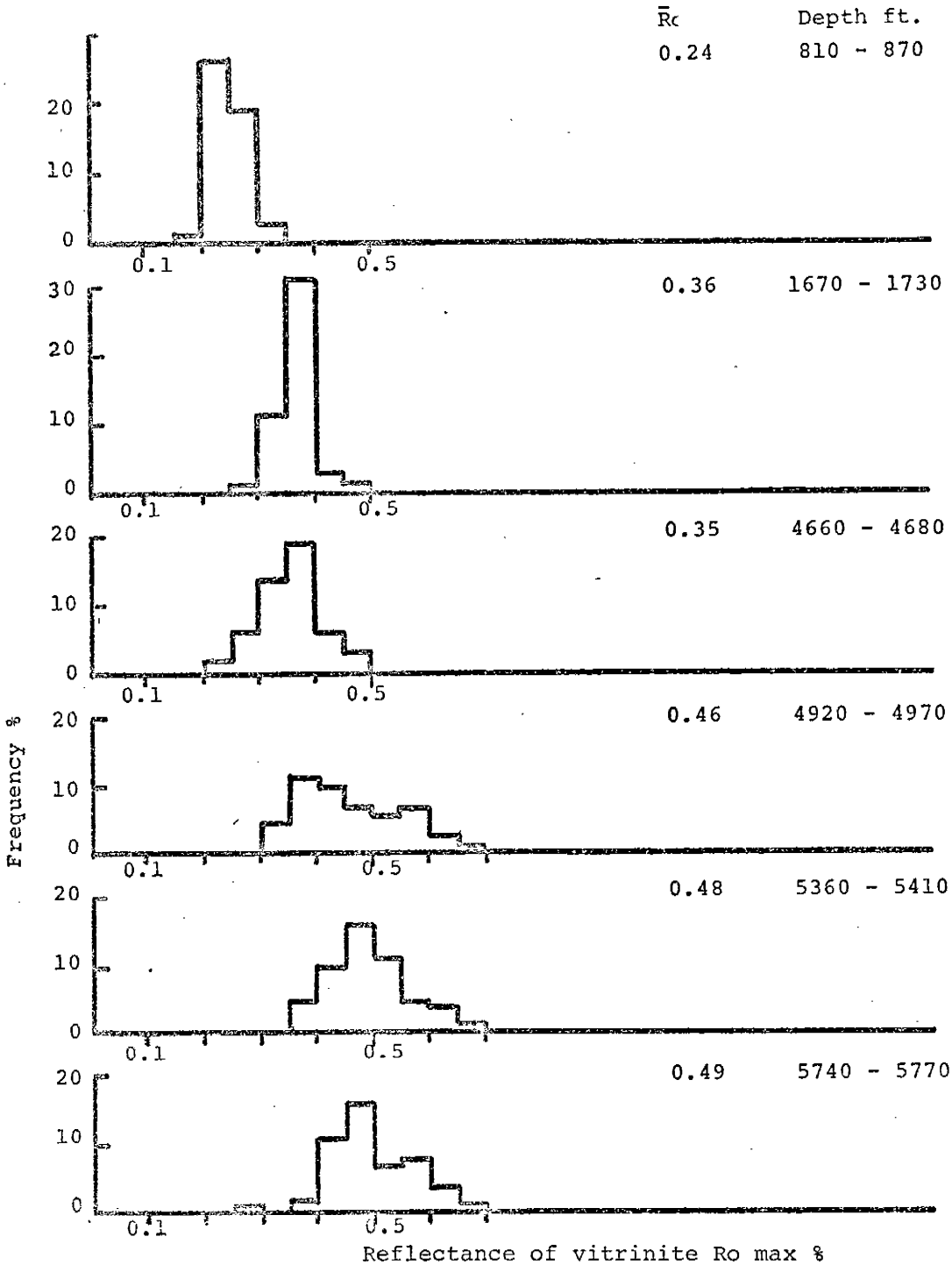

FIG. 3. Reflectance histograms of Tinga Tingana coals.

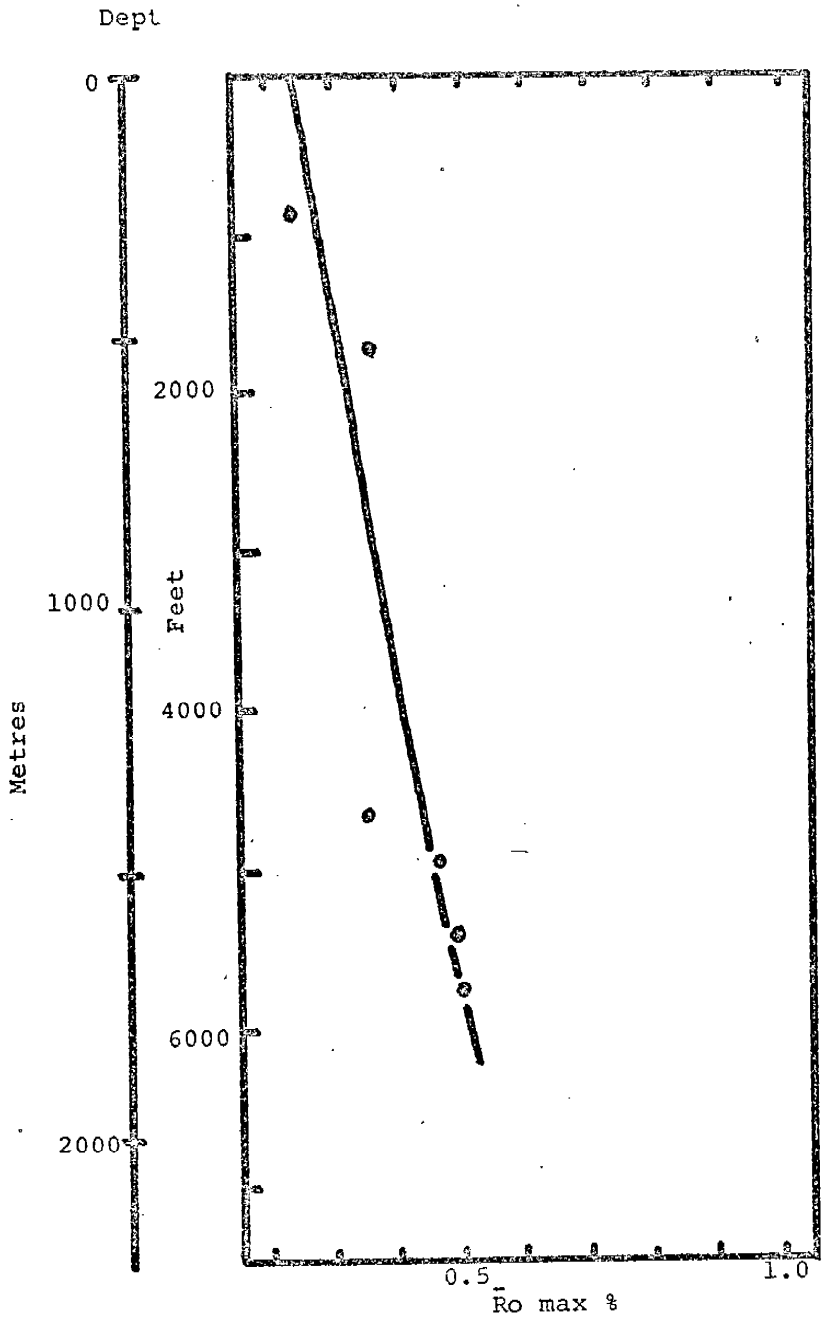

FIG. 4. Depth/reflectance curve for Tinga Tingana No.1 Well.

File 100-2-G

RESTRICTED INVESTIGATION REPORT 620R

CSIRO

MINERALS RESEARCH LABORATORIES

DIVISION OF MINERALOGY

PETROGRAPHIC COMPOSITION OF COALS FROM GIDEALPA NO.3, INNAMINCKA NO.1 AND TINGA TINGANA NO.1 WELLS, COOPER BASIN, SOUTH AUSTRALIA

M. SMYTH

CSIRO Division of Mineralogy
P.O. Box 136
North Ryde N.S.W. 2113
Australia

MAY 1974

CSIRO

MINERALS RESEARCH LABORATORIES

1974 SEP 17 PM 2:19

P.O. BOX 136, NORTH RYDE, N.S.W., AUST. 2113. *SITUATED DELHI ROAD, NORTH RYDE.* TELEPHONE 888 1666. TELEGRAMS *MINRES NORTH RYDE*

TO: Delhi International Oil Corporation

Errors in IR 620R - depths in Table 1 should be:

Gidgealpa No. 3		Tinga Tingana No. 1	
622 - 631	U. Cret.	247 - 265	U. Cret.
686 - 695		509 - 527	
869 - 878		1420 - 1426	Permian
2054 - 2070		1480	
2179 - 2195	Permian	1500 - 1515	
2234 - 2249		1634 - 1649	
2280 - 2292		1750 - 1759	

Innamincka No. 1

85 - 91	U. Cret.
137 - 152	
290 - 311	
521 - 530	
899 - 914	
2097 - 2100	Permain
2176 - 2188	
2256 - 2271	

... probably from about 1530m

M. Smyth

INTRODUCTION

Many ditch cutting samples from Gidgealpa No.3, Innamincka No.1 and Tinga Tingana No.1 wells, covering a wide geological succession (Permian to Cretaceous) were supplied to CSIRO by Delhi International Oil Corporation.

The samples were originally requested for reflectance measurements, the results of which have been reported to the company in IR 524R and IR 577R. These samples have also been used to make the petrographic analyses which form the subject of the present report.

It is not certain whether coal samples obtained from ditch cuttings by gravity separation represent the average composition of the original coal seams. However, all samples were treated similarly and processed by the same preparation technique. Results are therefore expected to give some information about the stratigraphical variation of the petrographic composition of the coal seams. The fact that all these wells show a very similar tendency supports this assumption.

In order to investigate the potential of rocks as hydrocarbon sources, not only the coals, but also the organic material dispersed in interseam sediments should be studied. (This work is in progress).

In this preliminary report, only the results of petrographic analysis of the coals, completed to date, are given. These results could give information about the sedimentary history of this basin.

SAMPLE PREPARATION

See Restricted Investigation Report 577R

RESULTS

To date analyses have been carried out on coals from the Cretaceous to the Permian in three wells: Gidgealpa No.3, Innamincka No.1 and Tinga Tingana No.1. Results of the petrographic analyses are shown in Table 1 and in Fig. 1.

There are distinct differences in the vitrinite content between the Cretaceous coals and the Permo-Triassic coals. Furthermore among the Cretaceous coals a clear upwards increase in vitrinite occurs in all three cases.

The Permain coals show fluctuations in their vitrinite contents. The lower two coals from Innamincka No.1 (2343-2356 m and 2428-2444 m) are supposed to be of Devonian age according to the well log. However, reflectance measurements of the sample from 2428-2444 m indicate that it is a caving. Both of these "Devonian" coals are probably cavings.

DISCUSSION

The vitrinite content of a coal could be regarded as giving an indication of the type of sedimentary environment in which the coal accumulated. Vitrinite-rich coals are thought to have accumulated in rapidly subsiding, unstable conditions, whilst vitrinite-poor coals have accumulated in more slowly subsiding, stable environments. Where coal measures are thick

the coal seams tend to be rich in vitrinite, where coal measures are thin the coal seams tend to be poor in vitrinite. Thus the petrographic composition of coal seams appears to reflect the rate of deposition (or subsidence) as a whole. (Shibaoka and Smyth, 1973).

From Fig. 1 it appears that the Cooper Basin in Permian times was fluctuating between slowly and more rapidly subsiding conditions. From the Triassic or Jurassic onwards, the rate of subsidence of the basin might have increased steadily, as shown by the progressive increase in the quantity of vitrinite in the coals, although there are wide gaps between sampled points in the profile from the Jurassic to the Lower Cretaceous. The changes in coal composition suggest that at any given time until the end of the Upper Cretaceous, the rate of subsidence was similar in Innamincka No.1 and Tinga Tingana No.1 and slower in Gidgealpa No.3, but that the acceleration of the subsidence rate during the Cretaceous was greater in Gidgealpa No.3

CONCLUSIONS

Coals from the Permian in the three wells have variable petrographic compositions, but tend to be vitrinite-poor, whilst coals from the Cretaceous are vitrinite-rich. There is a continuous upward increase in vitrinite content, shown very clearly in the Upper Cretaceous coals.

If vitrinite content may be taken as an indication of the rate of subsidence, the Cooper Basin subsided more and more rapidly from the Permain to the end of the Cretaceous.

REFERENCES

Shibaoka, M. and Smyth, Michelle. 1973. "Coal petrology and formation of coal seams in some Australian sedimentary basins". 45th ANZAAS Congress, Perth. Abstracts Section 3, pp 140-142.

TABLE 1

Maceral analyses of coals from the Cooper Basin (mineral matter free)

AGE	DEPTH, m	VITRINITE	EXINITE	MICRINITE	SEMIFUSINITE	FUSINITE
GIDGEALPA NO. 3						
Upper Cretaceous	669-679	90	2	1	7	-
	738-748	83	7	4	5	1
	935-945	70	4	6	19	1
Middle-Lower Jurassic	2211-2228	27	20	21	31	1
Permian	2346-2362	17	9	48	24	2
	2405-2421	60	11	13	14	2
	2454-2467	30	9	34	27	tr
INNAMINCKA NO.1						
Upper Cretaceous	92-98	98	-	-	2	tr
	148-164	95	2	tr	3	tr
	312-335	88	9	1	2	-
Lower Cretaceous	561-571	83	3	5	8	1
	968-984	77	2	2	18	1
Permian	2257-2261	55	5	15	22	3
Devonian	2343-2356	44	11	28	15	2
	2428-2444*	69	21	4	2	4
TINGA TINGANA NO.1						
Upper Cretaceous	266-285	95	1	-	4	tr
	548-568	85	5	5	5	tr
Permian	1529-1535	63	13	13	10	1
	1594	75	9	8	4	4
	1614-1631	50	3	17	26	4
	1759-1775	28	6	24	39	3
	1883-1893	61	5	15	17	2

* from reflectance measurements this appears to be a caving, probably from about 1650 m.

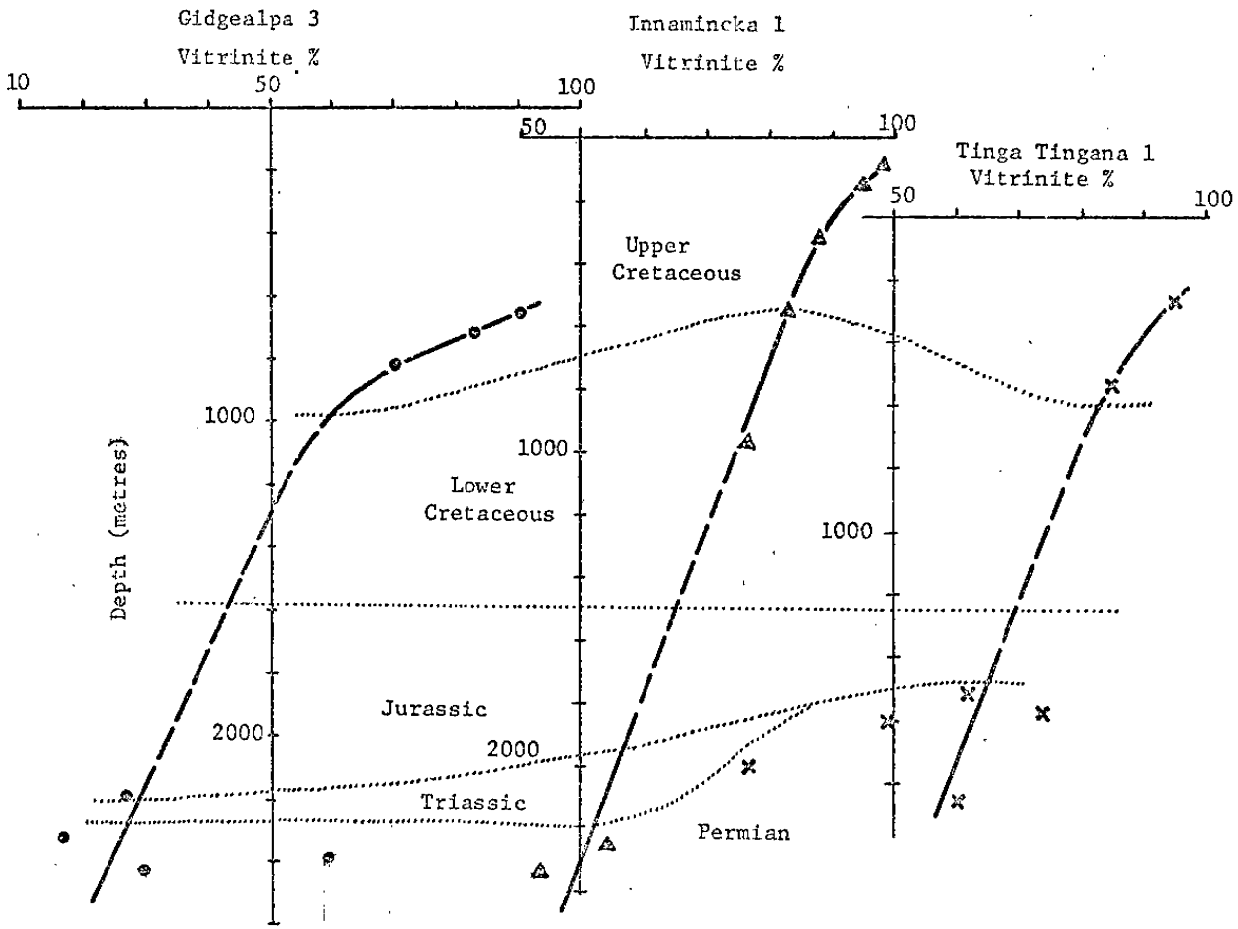

Fig. 1. Stratigraphical variation of vitrinite content in some Cooper Basin coals.

RESTRICTED INVESTIGATION REPORT 1131R

CSIRO

INSTITUTE OF EARTH RESOURCES

CARBON DIOXIDE IN NATURAL GAS FROM THE COOPER BASIN

D. RIGBY AND J.W. SMITH

FUEL GEOSCIENCE UNIT
CSIRO INSTITUTE OF EARTH RESOURCES
PO BOX 136, NORTH RYDE
N.S.W., AUSTRALIA, 2113

MAY 1980

INTRODUCTION

Current views appear to favour the thermal decomposition of humic (coaly) materials as the source of the bulk of the carbon dioxide in natural gas from the Cooper Basin.

Recent isotopic data suggest such an origin to be unlikely and indicate a source associated with the under-lying granite.

DISCUSSION

The occurrence and composition of gaseous and liquid hydrocarbons in the Cooper Basin, South Australia, are of considerable consequence from both economic and fundamental viewpoints. The variability in the "wetness" and the carbon dioxide contents of the gas provide an excellent opportunity to further the understanding of gas genesis and allow an evaluation of stable isotope ratio measurements to be made in this regard. In addition, regional differences in sediment temperatures, and above all the appearance of "hot spots" above the granite basement, permit the influence of localised temperatures on gas and hydrocarbon composition to be determined.

Previous studies have been largely concerned with the establishment of the variable thermal histories of the region and with the determination of paleo- and present temperature. (Shibaoka and Bennett 1977, Kantsler et al. 1978, Middleton 1979).

Although Smyth (1979) has raised the question of whether dispersed organic matter, d.o.m., rather than seam coal should be regarded as the more likely hydrocarbon source, no doubt appears to exist that land-plant materials are the source of both gaseous and liquid hydrocarbons.

Indeed, whatever the precise source of the hydrocarbons, or the thermal histories of the sediments, it is generally agreed that vitrinite reflectance measurements, which here range from 0.6 to 6.6 per cent (Kantsler et al. 1978, Schwebel et al. 1980) permit a realistic estimate of current sediment temperatures to be made.

Accordingly it might be expected, in view of the data of Stahl (1976, 1977) and the uniformity of the humic source material, that the "wetness" of gases in the Cooper Basin might decrease with increase in vitrinite reflectance values above 0.8 per cent. That this is not the case has been explained by Schwebel et al. (1980) by the migration updip of hotter gases. Of greater significance is the suggestion by the same authors that the carbon dioxide content of natural gases may be a guide to thermal histories and sediment temperatures (as indicated by vitrinite reflectance values) because the concentration of carbon dioxide directly reflects the effects of increasing temperatures on the thermal decomposition of humic, non-marine, source materials.

Such a suggestion is contrary to the established understanding of the nature and composition of the gases released during the maturation of land plant residues. From both theory and observance, it is abundantly clear that carbon dioxide and water are the major products of the maturation of brown coals and lignites. With increasing coalification, and a corresponding decrease in the oxygen content of the humic residue, methane becomes an increasingly important component of product gases as the concentration of carbon dioxide in these decreases. For example, in medium volatile coals of vitrinite reflectance near 1.3 per cent, the concentration of carbon dioxide in seam gas rarely exceeds 2 per cent (the remainder is methane) and decreases further as the rank of the coal increases. In Fig. 1, the decrease in the oxygen content of coals with increase in vitrinite reflectance is shown graphically.

Accordingly, on the evidence, if the carbon dioxide content of natural gases is a product of the thermal cracking of parent humic (coaly) materials, sediment temperatures should be indirectly related to the carbon dioxide content of the natural gas when the vitrinite reflectance of humic residues is greater than 0.6 per cent.

It could be argued that the carbon dioxide contents of natural gases represent the total carbon dioxide generated and retained since the earliest stages of gas production. It has been shown (Gould & Smith 1980) that the vast quantities of carbon dioxide generated by the decarboxylation of brown coals have a $\delta^{13}C$ value of $-24‰$. Therefore, it might be expected that, when the carbon dioxide concentration in natural gas is high, the $\delta^{13}C$ value of the carbon dioxide might approximate, or more closely approach this value. That this is not the case is shown in Fig. 2. On the

contrary, although the carbon dioxide contents of the gas range from 0.5 to 51.3 per cent, the δ^{13} value of the carbon dioxide remains relatively consistent at -6.9±2.9‰ PDB. Accordingly, on isotopic evidence, it is difficult to accept this gas as being a product of early maturation which has been long retained in the sediment. Experience in Australian coal mines has shown that high concentrations of carbon dioxide with this isotopic composition cannot be generated within coal seams. Where seam gas of this composition is met, the carbon dioxide always appears to be derived from an external magmatic source (Smith & Gould 1980, Gould & Smith, 1980).

The basement granite in the Cooper Basin appears to represent such a source, particularly in view of the hot spot temperatures due to localized radio-activity (Middleton, 1979). Previous evidence also suggests that carbon dioxide in natural gases may be so derived (Tiratsoo, 1972). However, whatever the source of the carbon dioxide in the granite, whether fluid inclusions or decomposable carbonates or even "organic" materials, etc., higher temperatures will lead to both an increasing loss of carbon dioxide from the granite and to an increase in the vitrinite reflectance of humic sediments above these "hot spots". Therefore, the direct relationship between vitrinite reflectance and the carbon dioxide contents of associated natural gas as observed by Schwebel et al. (1980) is to be expected, although a different interpretation of these data is required.

Similarly, as shown in Fig. 3, the increasing dryness of the natural gas with increasing carbon dioxide content is more realistically explained on the understanding that carbon dioxide contents depend directly on the temperature of the granite and not on the extent of the thermal decomposition of humic materials. Further support for the view that basement granite is the major source of the carbon dioxide in the Cooper Basin was provided by simple tests on a piece of granite core recovered from the Moomba well (ex M. Middleton).

Combustion in oxygen of freshly-cut, clean chips from the interior of the core gave total yields of carbon dioxide of from 7.3 to 8.4 ml/grm, (representing carbon contents of 0.39% and 0.45% respectively) with $\delta^{13}C$ values ranging from -7.9‰ to -8.1‰ PDB. 8.7 per cent of this total carbon dioxide was liberated below 400°C.

In similar experiments, in which granite chips were pyrolysed at reduced pressures in the absence of oxygen, gas yields were always significantly higher at 8.8, 8.9 and 12.3 ml/grm. Variable concentrations of carbon monoxide (2.8% to 8.3%) and hydrogen (4.1% to 23.2%) were observed in collected gas. However, when gas volumes were corrected for their hydrogen contents, the carbon contents of the chips were calculated to be from 0.39% to 0.62%, values very similar to those obtained by combustion.

Under these conditions, the percentage of the total gas released below 420°C varied from 2.1% to 11.1%, the highest value being recorded when the granite chip was finely ground before pyrolysis.

Isotopic analyses on total gases released by pyrolysis gave δ^{13} values of -48.7‰ , -21.5‰ and -7.6‰ respectively for methane, carbon monoxide and carbon dioxide. The concentrations of the components in the total gas were 0.2%, 5.2% and 90.4% respectively.

Reaction of powdered granite with phosphoric acid gave carbon dioxide yields of from 2.95 to 4.69 ml/grm (representing carbonate carbon contents of from 0.15% to 0.25%) with a constant $\delta^{13}C$ value of -9.2‰.

A measure of the organic carbon content was obtained by reacting the powdered granite with 50% hydrochloric acid and combusting the acid insoluble residue in oxygen. Carbon dioxide yields were 0.52 ml/grm (representing an organic carbon content of 0.03%), $\delta^{13}C$ values varied from -25.2‰ to -26.7‰ PDB.

After examination, R.W.T. Wilkins (private communication) reports that fluid inclusions are small, mainly <10 μm in diameter and typical of granites. No liquid carbon dioxide is visible and thus, if present, carbon dioxide must be of low density. He doubts that the fluid inclusions seen could yield appreciable carbon dioxide.

CONCLUSIONS

On this isotopic and chemical evidence, the more acceptable source for the bulk of the carbon dioxide in the Cooper Basin gases appears to be the underlying granite. Whether this is primary carbon dioxide included in the granite or whether this gas results from the thermal decomposition of associated carbonates is not known at this stage. However, both sources

appear capable of yielding carbon dioxide with an isotopic composition which approximates that of the carbon dioxide in the natural gas.

Direct thermal decomposition of coal at higher temperatures appears to be prohibited as the source of the carbon dioxide on account of the $\delta^{13}C$ value and the concentration of this gas.

The exact nature of the products of the reaction of water with coal at high temperatures has not been determined. However, in coal mines where seam gases commonly contain 90% or more of carbon dioxide, no observable evidence of this proposed major reaction between water and coal has been documented. The most recent views on this subject also favour an external magmatic source for high concentrations of carbon dioxide in coal mines.

REFERENCES

Gould, K.W. and Smith, J.W., 1980. Isotopic studies of geochemical factors in outbursting. Proc. Aus. I.M.M. "The Occurrence, Prediction and Control of Outbursts in Coal Mines, Brisbane 1980".

Kantsler, A.J., Cook, A.C. and Smith G.G., 1978a. Lateral and vertical rank variation. Implications for hydrocarbon exploration. APEA Journal 18, 143-156.

Middleton, M.F., 1979. Heat flow in the Moomba, Big Lake and Toolachee gas fields of the Cooper Basin, and implications for hydrocarbon maturation. Aust. Soc. Explor. Geophys. Bull. 10, 149-155.

Shibaoka, M. and Bennett, A.J.R., 1977. Patterns of diagenesis in some Australian sedimentary basins. Aust. Petrol. Explor. Assoc. J. 17, 58-63.

Smith, J.W. and Gould, K.W., 1980. An isotopic study of the role of carbon dioxide in outbursts in coal mines. Geochem. J. In press.

Smyth, M., 1979. Hydrocarbon generation in the Fly Lake-Brolga area of the Cooper Basin. APEA Journal 19, 108-114.

Stahl, W., 1976. Economically important applications of carbon isotope data on natural gases and crude oils. Nuclear Techniques in Geochemistry and Geophysics. Vienna, Nov. 1974. Int. Atom. Energy Agency. Vienna 1976.

Stahl, W., 1977. Carbon and nitrogen isotopes in hydrocarbon research and exploration. Chem. Geol. 20, 121-149.

Schwebel, D.A., Devine, S.B. and Riley, M., 1980. Source, maturity and gas composition relationships in the Southern Cooper Basin. APEA Journal 20, 191-200.

Tiratsoo, E.N. Natural Gas. 2nd Edit. Scientific Press, England 1972.

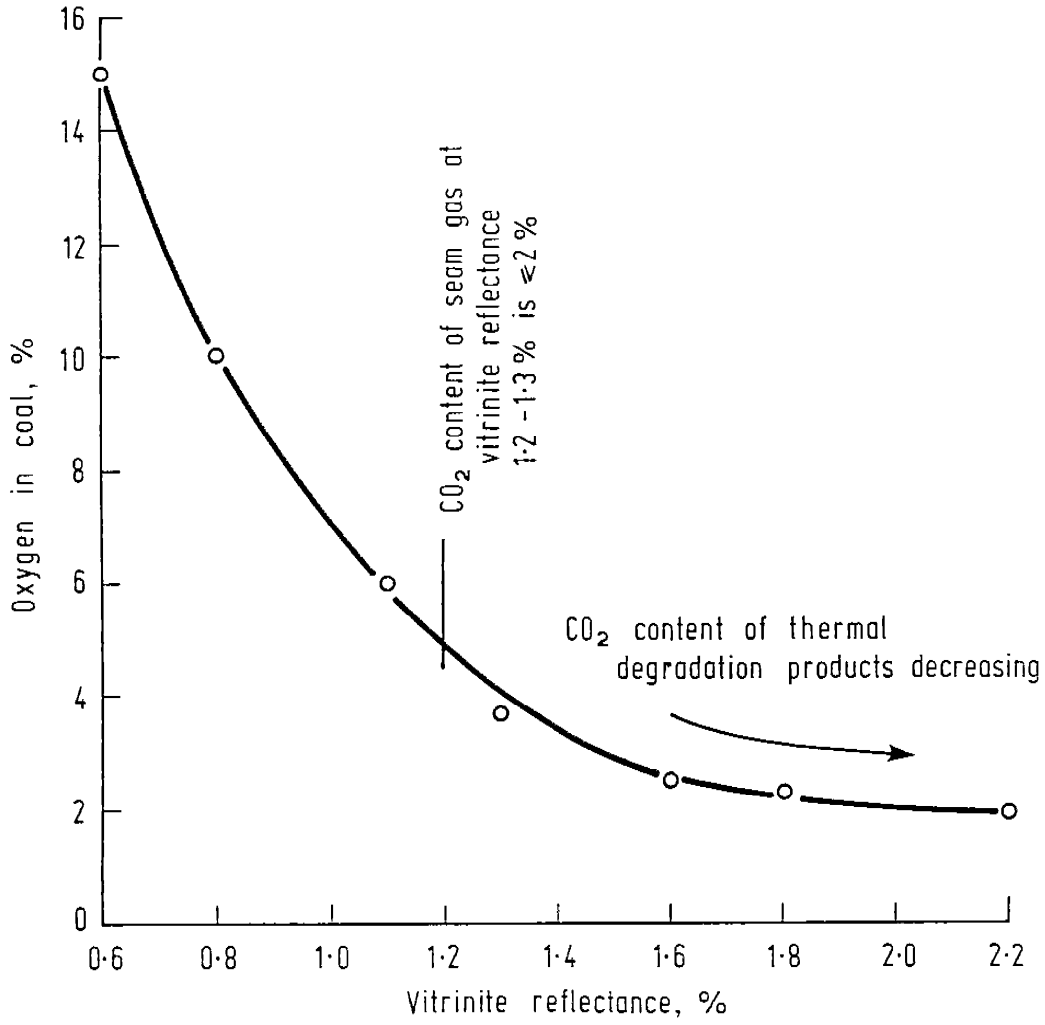

FIG. 1. TO ILLUSTRATE DECREASING OXYGEN CONTENT OF COAL WITH INCREASING COAL MATURITY

Fig. Rees + Jones Smith IR 113.1 R

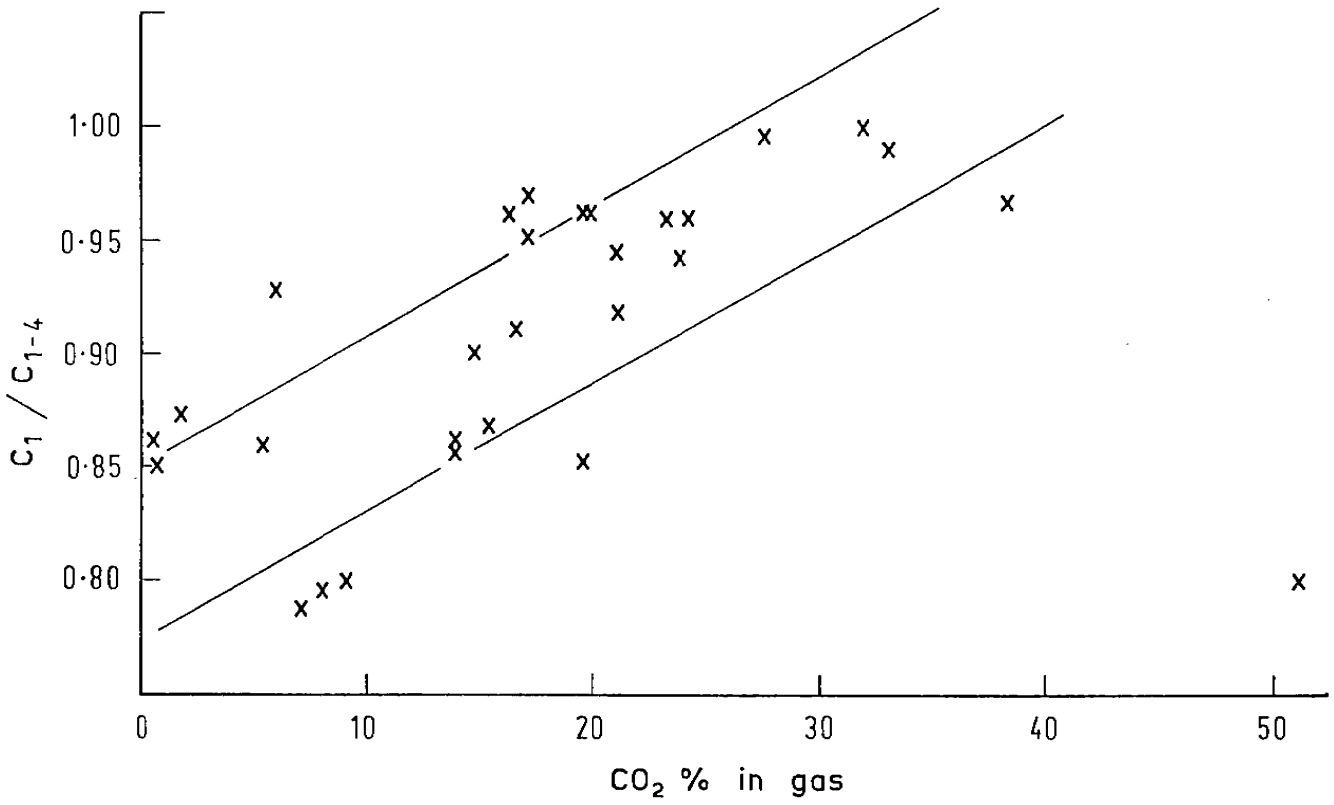

FIG. 3. TO ILLUSTRATE DECREASE IN "WETNESS" OF GAS WITH INCREASING CARBON DIOXIDE CONTENT

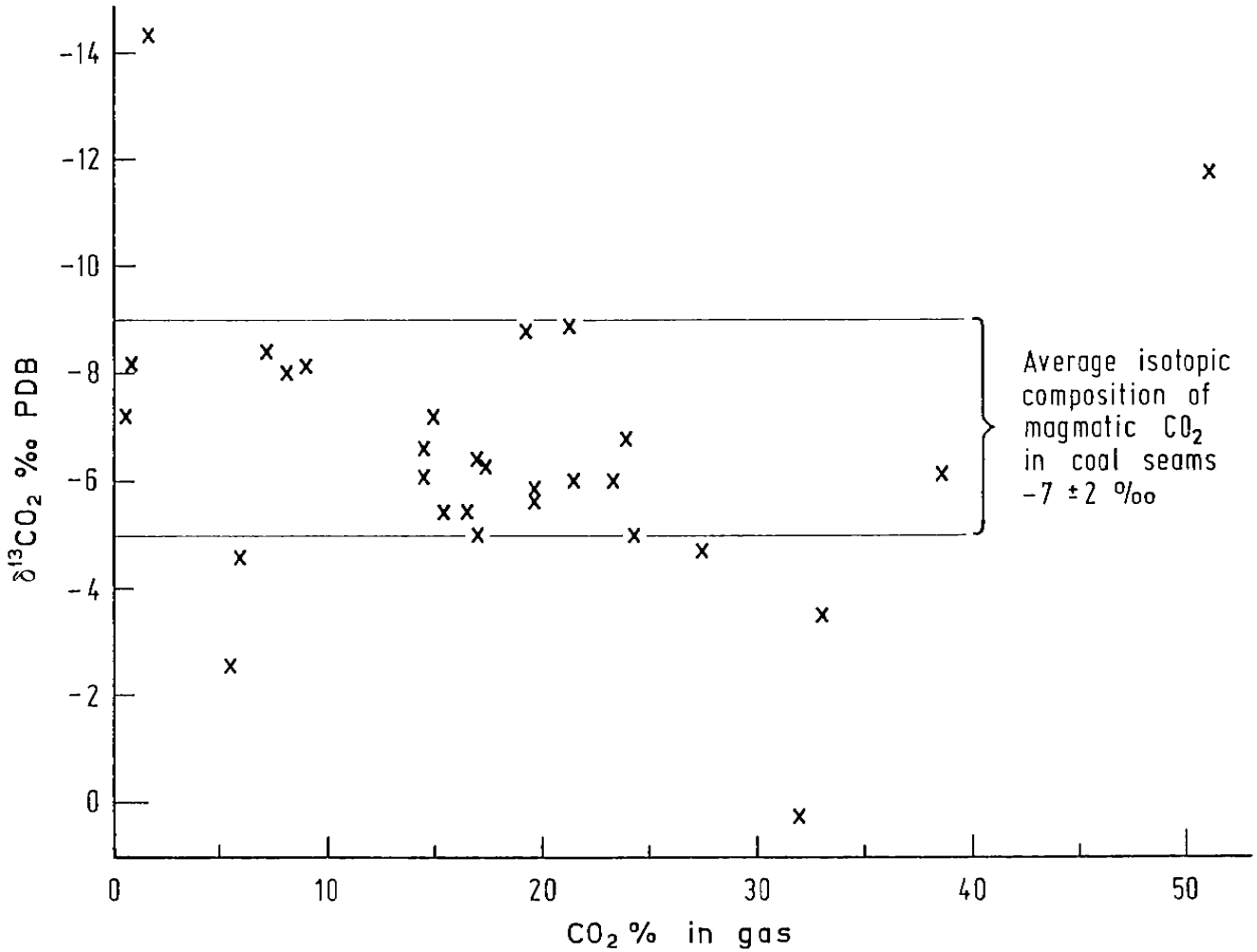

FIG. 2. RELATIONSHIP BETWEEN ^{13}C CONTENT OF CARBON DIOXIDE AND CONCENTRATION IN GAS

RESTRICTED INVESTIGATION REPORT 1377R

OPEN FILE

CSIRO

INSTITUTE OF ENERGY AND EARTH RESOURCES

DIVISION OF FOSSIL FUELS

GEOCHEMICAL PROSPECTING FOR NATURAL GAS IN THE COOPER BASIN, SOUTH AUSTRALIA 1980.

R.P. PHILP AND T. GILBERT

P.O. BOX 136
NORTH RYDE, NSW
AUSTRALIA 2113.

JANUARY 1983.

1. INTRODUCTION

In a previous report (RIR 1215R) a summary was given of the results obtained from a geochemical prospecting survey in the Cooper Basin in 1979. That survey showed that it was possible to determine hydrocarbon concentrations of soil samples in the field by gas chromatography and surface anomalies could be detected.

In the present survey a new sampling technique was used that enabled the gas chromatograph to be located at a central campsite rather than being mobile in a vehicle. It was felt that this would improve analysis and sampling efficiency. This survey was again carried out in collaboration with the South Australian Department of Mines and Energy and we duly acknowledge all the valuable help and assistance given by the department.

2. METHODS AND TECHNIQUES

Equipment

The drilling and analytical equipment were basically the same as in 1979 as described in RIR 1215R. A two man motorized hand-held auger was used for the first half of the survey because the drilling vehicle's engine became unserviceable before the survey began. The gas chromatograph and integrator were the same units as used before but were mounted in the laboratory caravan in the camp. The soil gas sampling prove was replaced by 2 metre lengths of 1/8inch o.d. copper tubing terminated on the tops with swagelok fittings which fitted the traps. The sampling vehicle had the generator and vacuum pump fitted for the 1979 survey.

Surveying and Drilling

The survey used a 1 km x 1 km seismic line grid which had been bulldozed for the Strzelecki development seismic survey (Woolkannie Seismic Survey). Samples were taken at $\frac{1}{2}$ kilometre spacing. The sample points between line intersections and on the ends of lines were measured out using the vehicle's odometer. Where the $\frac{1}{2}$ km grid was completed

with a central point the sampling position was located using an optical square and the vehicle odometer (e.g. 1b, 1c, 1d etc.). The surveyed sample point numbers are shown on Figure 1.

Immediately after drilling the holes to a depth of 1.7 metres, a copper sampling tube was lowered into the hole and the hole was backfilled with cuttings. A trap similar to that described in the first survey was attached to the top of the sampling tube and the free air in the tube and trap was drawn out by pumping the hole for 30 seconds. This was achieved by attaching the trap to the vacuum pump system on the vehicle using a flexible tube and needle valve. The trap was finally capped using a solid male plug and marked with flagging tape for easy relocation. The sampling tubes were then left undisturbed for 48 hours to allow the soil gases time to re-establish equilibrium.

The Sampling Method

A dewar flask containing lqiuid nitrogen was placed under the trap and the trap was cooled for 30 seconds. The solid metal plug was removed and the open end of the trap was attached to a needle valve connected to the vacuum pump by flexible tubing. The valve was opened and 400 mls of soil gas were pumped through the cooled trap. The vacuum line and the tube were removed in turn from the trap and the open ends were sealed with solid metal plugs marked with the number of the sample. The trap was then completely immersed in the liquid nitorgen until analysis.

During sampling there was usually a gradual slowing down of the rate of flow through the trap due to icing up. After analysis this water was removed by passing helium through the traps which were connected in series and kept in the oven of the G.C. overnight at 160°C.

To ascertain the volume of gas pumped through the trap, the volume of the exhaust gas from the vacuum pump was measured by displacement of water.

To test for data reproducibility, 20 sample tubes were left in the ground after the first sampling round and then resampled eighteen days

later. As a further test of the validity of these data, two close-spaced hexagonal patterns were established, using 7 sampling sites, each 10 metres from adjacent sites. These sites were located on two different lines midway between two sample points. One site was on a sand flat, the other on a claypan.

RESULTS

The results of the 1980 survey are plotted on Figures 2 to 5 and are listed in Appendix 1.

A comparison of these results with the 1979 survey carried out over the same area showed few if any meaningful comparisons between the two sets of results. The test to determine reproducibility also showed that this was poor. This lack of reproducibility and in-ability to compare results from previous surveys highlights some of the problems with this type of survey described in a recent review, 1 (Philp and Crisp, 1982).

The detection of the sources of natural gas seepages in the Cooper Basin Region is complicated by the effect of aquifers on the gas flow. In the Strzelecki area the two main Eromanga Basin aquifers are the Namur Sandstone Member and the Hutton Sandstone. In this region their combined thickness is approximately 300 metres. Water velocities in the aquifers in the South Australian part of the Eromanaga Basin have been estimated at 0.2 - 0.4 m per year (Bowering, 1982). From Smith et al. (1971), it is possible to work out a formula for the diffusion rate of gases through an aquifer. Methane has the fastest diffusion rate. The velocity of the vertical diffusion rate V for depth D (m) for methane is:

$$V = \frac{1392}{1400} \text{ cm/1000 yrs} = \text{approx 1 cm/1000 yrs}$$
$$\text{or 1 metre in 100,000 years.}$$

Therefore the minimum time required for the methane gas to vertically traverse a 200 metre thick aquifer is 20,000,000 years. If the slowest-flowing water is moving horizontally at 0.2 metres/year, this means the leaking methane will exit from the aquifer 4,000 kilometres downstream from the entry point. Note that this value is a best case for only one

of the two main Eromanga aquifers. However natural gas seepages for the Strzelecki area could have been sourced from the Coorikiana Sandstone which lies well above the artesian aquifers.

CONCLUSIONS

Overall it cannot be concluded that this survey was an outstanding success. Reasons that can be advanced from this include the fact that the sample holes might have been too shallow, no allowancewas made for changes in soil type (i.e. sand vs clay); gases might have leaked from traps or gas chromatograph during analysis.

In order for the type of survey to be successful a fairly large commitment of finance is necessary. It requires several vehicles, mobile drill rigs, experienced operators and various other types of logistical support. We were attempting the survey on a shoe-string budget and this in many ways could have contributed to the lack of success of these surveys.

On the results of the surveys run to date it would be difficult to completely dismiss the soil-gas field sampling method. Before testing this method further it will be necessary to make the analytical technique operator-proof by replacing plugs in the traps with needle valves. Secondly, the long-term monitoring of a number of sample points of different depths and soil types will be necessary. This may demonstrate with certainty the optimum sampling depth, optimum waiting time between drilling and sampling and also reveal the stability or otherwise of an anomaly over time. Thirdly, for experiments of this type a geologically simpler area should be chosen, preferably with only one hydrocarbon entrapping horizon and no thick aquifers above the accumulation.

ACKNOWLEDGEMENTS

We wish to acknowledge all the help and assistance provided by the Department of Mines and Energy, South Australia, in particular Mr. D. Vinall. Furthermore we wish to acknowledge the fact that Figs. 1 - 5 are reproduced, with permission, from a report written by the Department of Mines and Energy on the same survey.

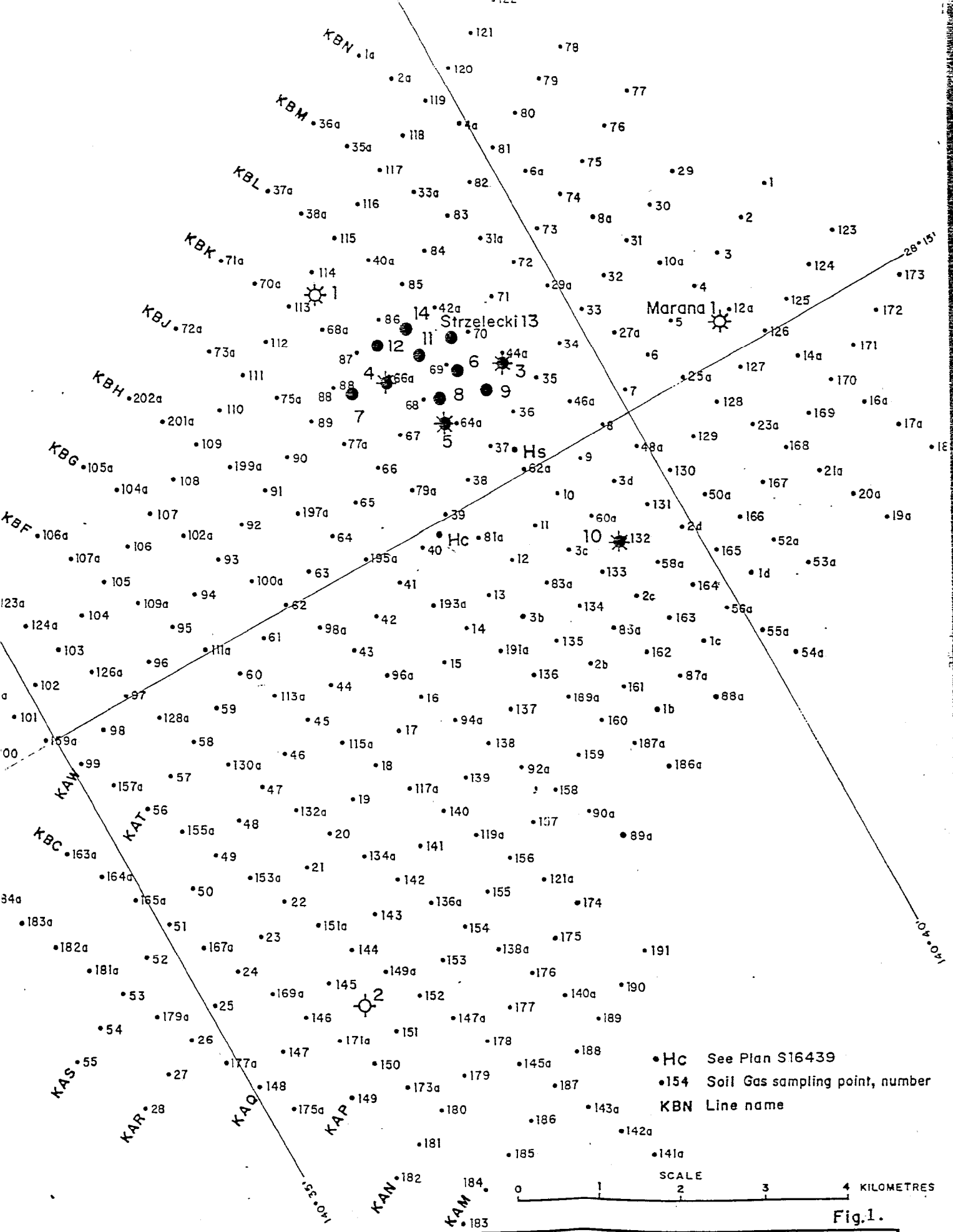

Fig.1.

DEPARTMENT OF MINES AND ENERGY
SOUTH AUSTRALIA

SOIL GAS SURVEY
COOPER BASIN, 1980
SOIL GAS SAMPLE LOCATIONS

COMPILED D.V.	CDO 18·11·82 DATE
DRAWN M. B.	SCALE 1:60 000
DATE Sept. '82	PLAN NUMBER S16415
CHECKED	

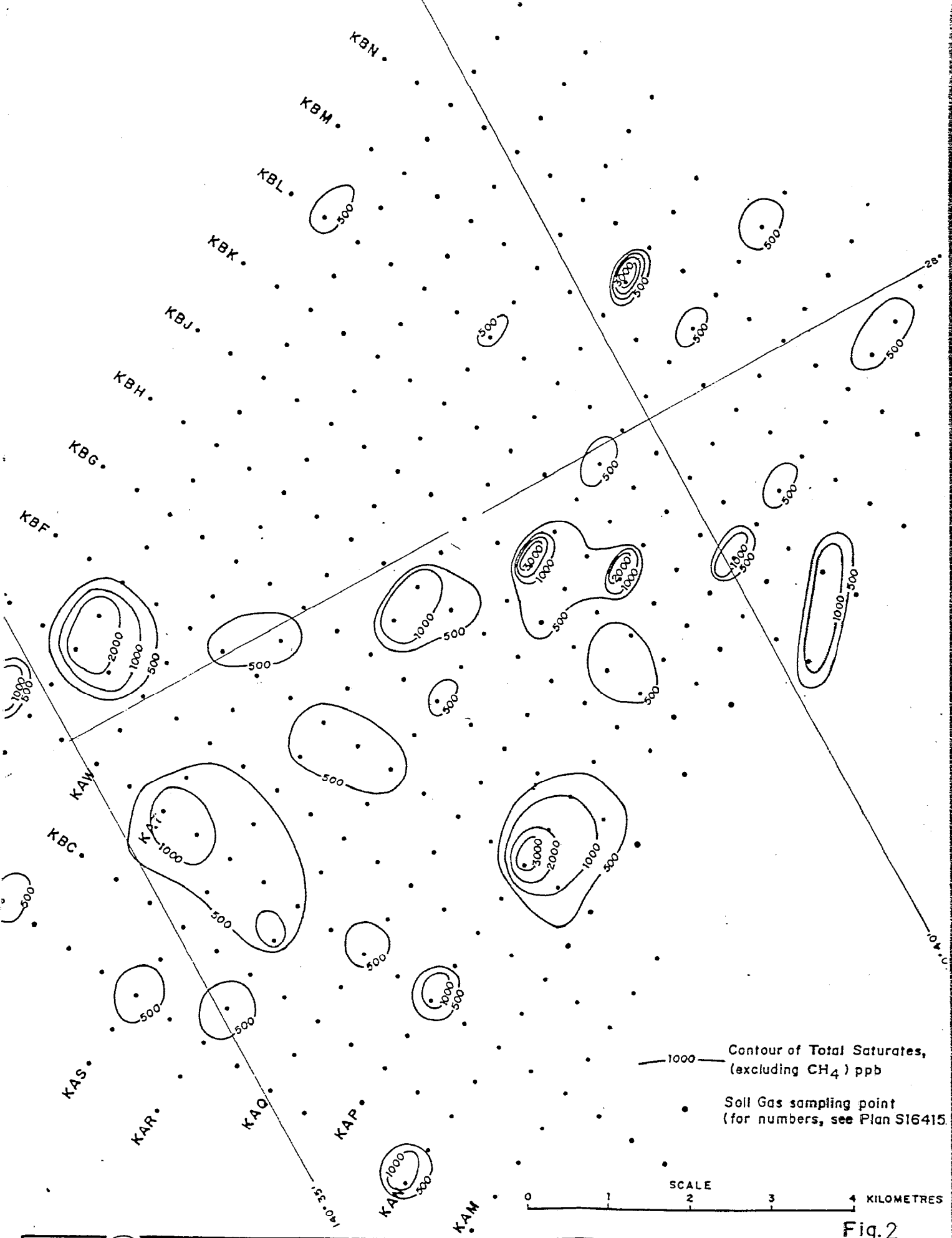

Fig. 2

DEPARTMENT OF MINES AND ENERGY
SOUTH AUSTRALIA

SOIL GAS SURVEY
COOPER BASIN, 1980
TOTAL SATURATES EXCLUDING CH_4

COMPILED D.V.	COO 18-11-82 DATE
DRAWN M.B.	SCALE 1:60 000
DATE Sept. '82	PLAN NUMBER S16424
CHECKED	

2872

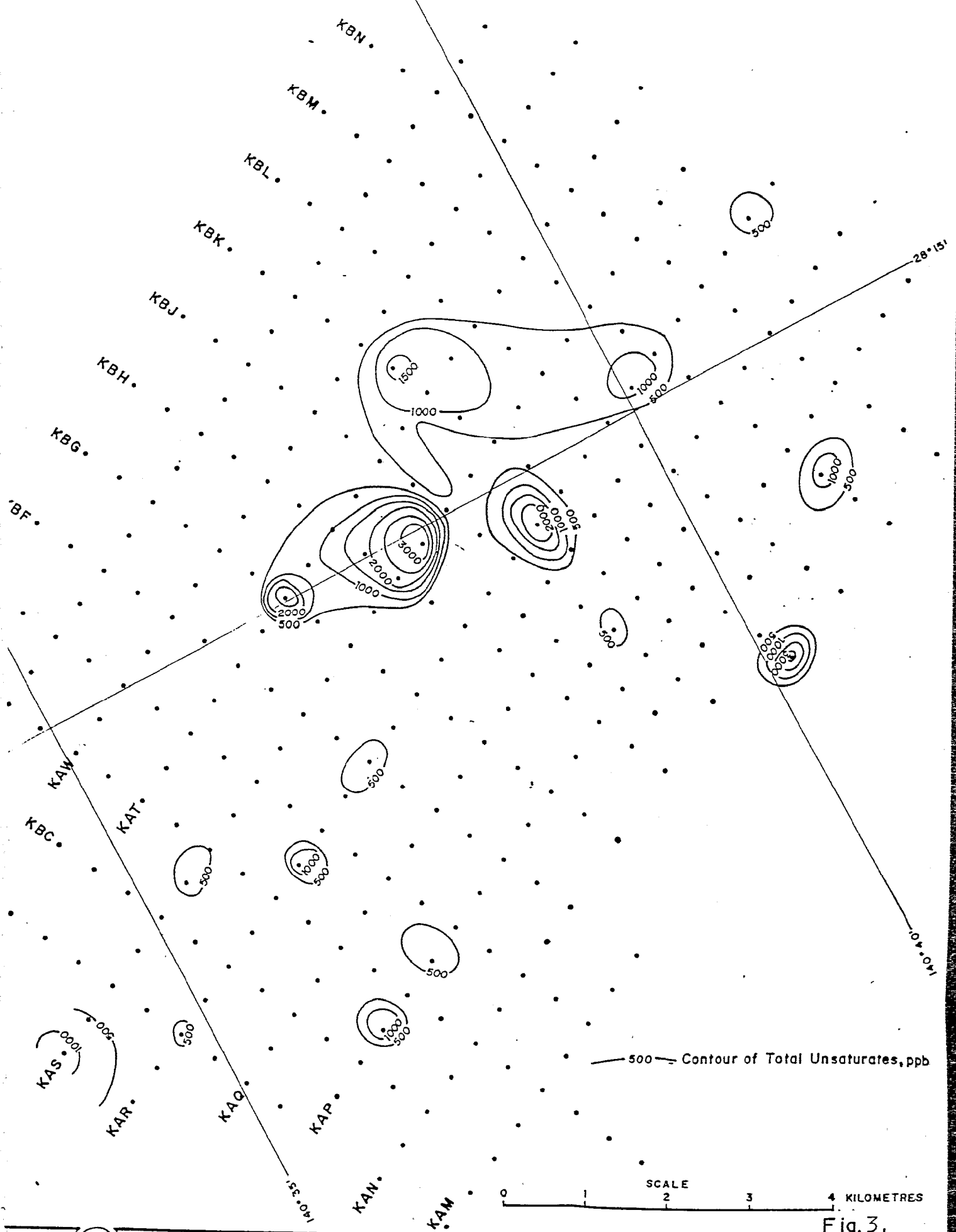

Fig. 3.

DEPARTMENT OF MINES AND ENERGY
SOUTH AUSTRALIA

SOIL GAS SURVEY
COOPER BASIN, 1980
TOTAL UNSATURATES

COMPILED D.V.	CDO 18·11·82 DATE
DRAWN M. B.	SCALE 1 : 60 000
DATE Sept. '82	PLAN NUMBER
CHECKED	S16426

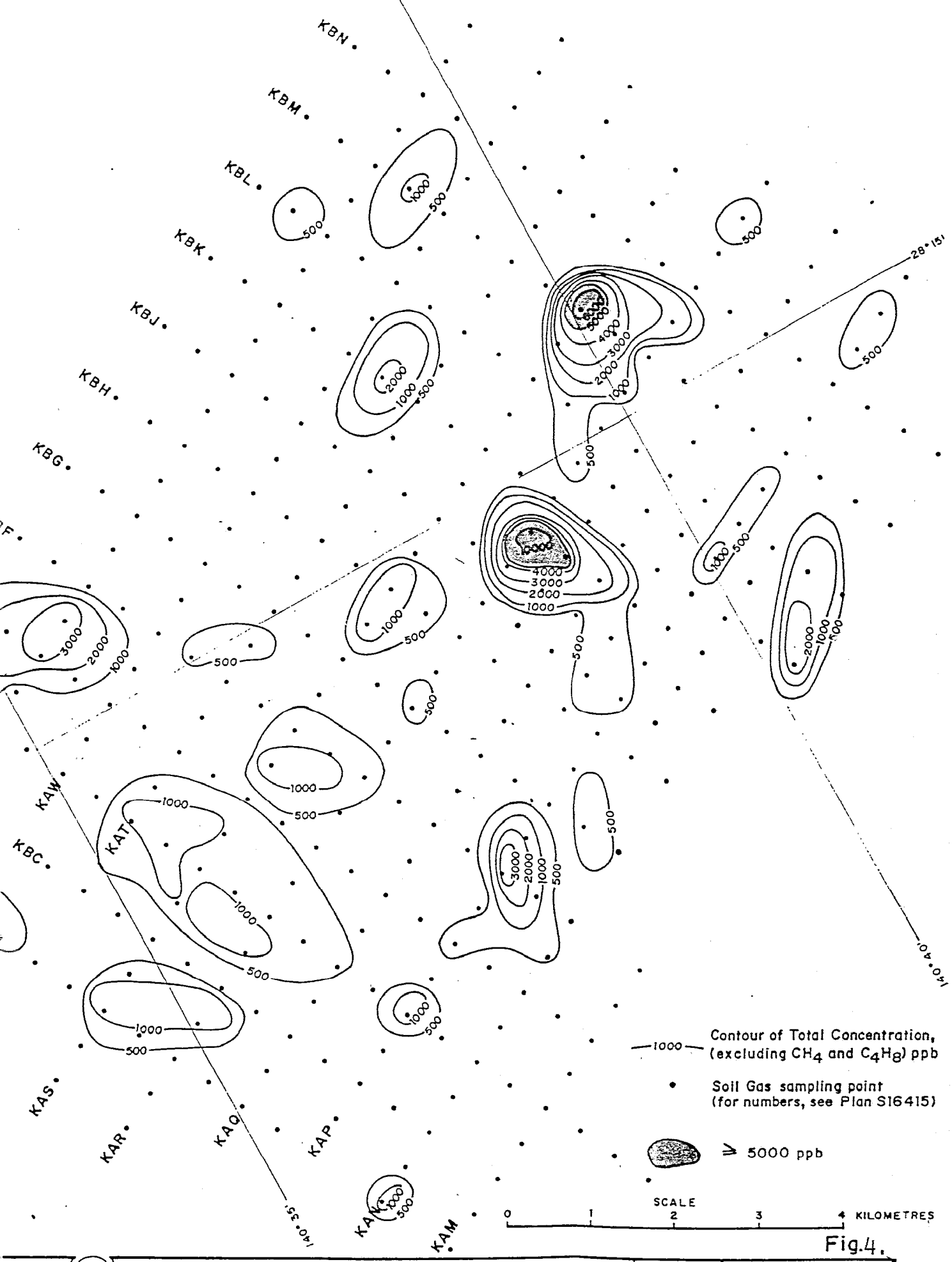

Fig.4.

DEPARTMENT OF MINES AND ENERGY
SOUTH AUSTRALIA

SOIL GAS SURVEY

COOPER BASIN, 1980

TOTAL CONCENTRATION EXCLUDING CH_4 AND C_4H_8

COMPILED D.V.	18·11·82 DATE
DRAWN M.B.	SCALE 1:60 000
DATE Sept. '82	PLAN NUMBER
CHECKED	S16423

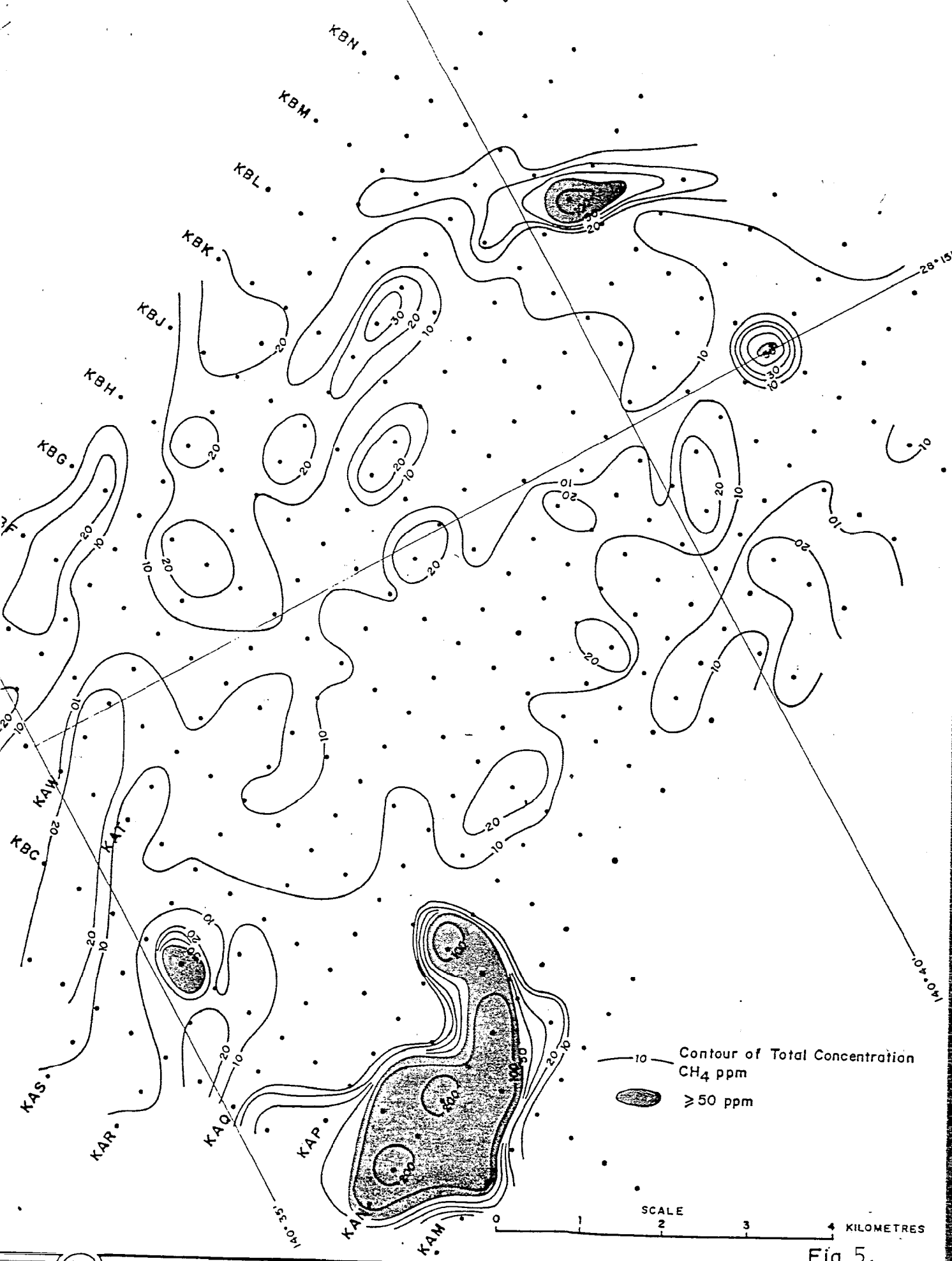

Fig. 5.

DEPARTMENT OF MINES AND ENERGY
SOUTH AUSTRALIA

SOIL GAS SURVEY
COOPER BASIN, 1980
TOTAL CONCENTRATION CH_4

COMPILED D.V.	CDO 18-11-82 DATE
DRAWN M.B.	SCALE 1:60 000
DATE Sept. '82	PLAN NUMBER
CHECKED	S16425

1980 Hydrcarbon Values (PPM)

Line No.	Methane	Saturates Excluding Methane	Unsaturates	Total Excluding Methane & Butene
KAR 1	15.9	0.150	0	0.15
2	8.9	0.500	0.650	0.56
3	0.32	0.113	0.004	0.117
4	17.1	0.120	0.420	0.21
5	24.1	0.770	0.250	1.02
6	16.9	0.160	0.600	0.38
7	10.9	0.460	1.370	0.75
8	3.1	0.130	0	0.13
9	3.8	0.5773	0.0125	0.581
10	18.49	8.880	2.430	11.25
12	15.6	3.000	0.320	3.23
13	13.62	0.074	0	0.074
14	13.84	0.281	0.010	0.2904
15	15.80	0.074	0.006	0.078
16	2.6	0.920	0.330	0.950
17	26.8	0	0.170	0.50
18	16.7	0.540	0.660	0.940
19	-	-	-	-
20	29.0	0.250	0.300	0.29
21	11.9	0.360	1.080	0.63
22	8.17	0.568	0.080	0.593
23	14.78	1.240	0	1.24
24	8.74	0.089	0.017	0.106
25	19.6	1.000	0.250	1.060
26	10.5	0.280	0.510	0.370
27	8.6	0.120	0.150	0.13
28	10.8	0.110	0.340	0.16
KAS 29	24.5	0	0	0
30	6.6	0	0	0
31	15.4	0.100	0.260	0.13

Line No.	Methane	Saturates Excluding Methane	Unsaturates	Total Excluding Methane & Butene
KAS 32	17.7	3.270	3.020	5.030
33	-	-	-	-
34	-	-	-	-
35	-	-	-	-
36	-	-	-	-
37	-	-	-	-
38	5.9	0.140	0.140	0.17
39	20.6	0.090	0.490	0.26
40	31.5	0.070	3.570	0.26
41	9.2?	34.73?	2.210	35.140
42	33.82	1.012	0.080	1.091
43	3.95	0.401	0.010	0.411
44	9.9	0.25	0.260	0.33
45	2.24	0.855	0.062	0.917
46	13.95	0.944	0.119	1.059
47	2.4	0.130	0.360	0.40
48	45.54	0.932	0.019	0.948
49	5.4	0.830	0.490	0.870
50	5.0	0.980	0.600	0.98
51	-	-	-	-
52	2.6	0	0	0
53	8.7	0.979	0.154	1.128
54	12.1	0.160	0.490	0.350
55	9.0	0.290	1.100	1.230
KAT 56	3.3	1.240	0.117	1.321
57	1.24	0.523	0.016	0.534
58	15.13	0.260	0.160	0.360
59	7.46	0.180	0.120	0.24
60	9.0	0.014	0	0.014
61	7.36	0.539	0.006	0.545
62	11.95	0.230	2.740	0.370
63	7.05	0.330	0.890	0.62
64	4.32	0	0	0
65	5.7	0	0	0

Line No.	Methane	Saturates Excluding Methane	Unsaturates	Total Excluding Methane & Butene
KAT 66	24.6	0	0	0
67	23.6	0.130	0.600	0.130
68	9.5	0	0	0
69	8.3	0.02	0	0
70	4.0	0.500	0.500	0.70
71	1.00	0.092	0.011	0.103
72	10.8	0.030	0.020	0.040
73	1.1	0.010	0.020	0.03
74	106.97	0.076	0	0.076
75	-	-	-	-
76	18.49	0.083	0.104	0.132
77	4.7	0.020	0.090	0.04
KAW 78	4.0	0	0	0
79	1.38	0	0	0
80	5.92	0.450	0	0.45
81	26.5	0.024	0.006	0.025
82	31.6	0.020	0.0012	0.021
83	16.7	0.013	0.003	0.013
84	1.89	0	0	0
85	29.14	0.075	0.091	0.162
86	34.9	0.190	0.149	0.269
87	21.03	0.180	0.310	0.196
88	20.16	0.186	0.008	0.188
89	20.91	0.047	0.009	0.055
90	27.88	0.080	0.005	0.083
91	10.20	0.040	0.008	0.0483
92	13.22	0.102	0.085	0.153
93	30.79	0	0.002	0
94	16.31	0.017	0.002	0.019
95	0.11	0	0	0
96	18.05	0.051	0.166	0.053
97	25.85	0.022	0.027	0.049
98	38.7	0.043	0.424	0.445
99	6.96	0.013	0.041	0.014

Line No.	Methane	Saturates Excluding Methane	Unsaturates	Total Excluding Methane & Butene
KAX100	16.3	0.071	0.187	0.212
101	24.3	0.005	0	0.006
102	18.84	0.095	0.100	0.145
103	19.54	2.958	0.051	3.009
104	19.24	2.227	0.032	2.2593
105	-	-	-	-
106	8.94	0.159	0.005	0.159
107	2.84	0	0	0
108	6.31	0.169	0.595	0.757
109	37.1	0.024	0.089	0.091
110	17.68	0.014	0.004	0.014
111	-	-	-	-
112	29.38	0	0.013	0.002
113	25.36	0	0.029	0.016
114	39.44	0.021	0.0003	0.021
115	24.72	0.073	0.049	0.109
116	20.45	0	0	0
117	25.7	0.107	0.216	0.287
118	0.53	0	0	0
119	13.9	0.138	0.019	0.149
120	0.5	0	0	0
121	1	0	0	0
122	150.07	0	0	0
KAQ123	26.6	0.036	0.076	0.112
124	2.26	0	0	0
125	1.76	0	0	0
126	54.85	0.004	0.002	0.011
127	5.97	0.0036	0	0.0036
128	17.46	0.093	0.022	0.115
129	28.9	0	0	0
130	4.57	0.072	0.036	0.101
131	19.08	0	0	0
132	3.28	0.347	0.020	0.367

Line No.	Methane	Saturates Excluding Methane	Unsaturates	Total Excluding Methane & Butene
KAQ133	9.99	2.270	0.0002	2.270
134	17.27	0.191	0.020	0.211
135	17.37	0.160	0.012	0.172
136	-	-	-	-
137	-	-	-	-
138	11.02	0	0	0
139	14.88	0.085	0.010	0.089
140	8.94	0.055	0.014	0.069
141	-	-	-	-
142	1.96	0.078	0.012	0.082
143	1.48	0.021	0.004	0.021
144	2.12	0.601	0.013	0.606
145	2.85	0	0	0
146	2.48	0.142	0.057	0.166
147	-	-	-	-
148	2.68	0.296	0.057	0.32
KAP149	-	-	-	-
150	3.5	0.017	0.007	0.019
151	3.21	0.007	0.007	0.028
152	1.69	1.309	0.014	1.313
153	3.94	0.014	0.828	0.052
154	132.2	0.298	0.250	0.548
155	2.78	0.072	0.036	0.101
156	1.27	3.280	0.035	3.297
157	3.41	1.364	0.050	1.399
158	14.4	0	0.0005	0.0005
159	0.29	0.322	0.006	0.327
160	2.08	0.068	0.006	0.072
161	8.65	0.764	0.015	0.776
162	1.76	0.111	0.027	0.122
163	4.38	0.096	0.004	0.10
164	2.27	0	0.009	0.009

Line No.	Methane	Saturates Excluding Methane	Unsaturates	Total Excluding Methane & Butene
KAP165	0.98	1.595	0.027	1.622
166	3.13	0.489	0.023	0.509
167	2.29	0.934	0.015	0.949
168	3.19	0	0	0
169	6.77	0	0	0
170	1.75	0.152	0.198	0.35
171	2.90	0.571	0.020	0.591
172	14.26	0.953	0.004	0.956
173	-	-	-	-
KAN174	2.90	0.049	0.006	0.055
175	14.26	0.481	0.274	0.699
176	-	-	-	-
177	135.59	0	0	0
178	93.55	0.049	0.032	0.059
179	233.94	0.032	0.038	0.057
180	134.8	0.082	0.022	0.104
181	219.8	0.118	0.073	0.16
182	115.0	1.367	0.124	1.462
KAM183	7.13	0.042	0.029	0.071
184	6.41	0	0	0
185	122.0	0.114	0	0.114
186	-	-	-	-
187	1.76	0	0	0
188	5.95	0.071	0.115	0.11
189	4.88	0.033	0.289	0.054
KBN 1a	-	-	-	-
2a	2.9	0.011	0.045	0.023
4a	4.2	0.055	0.034	0.082
6a	2.9	0	0	0
8a	13.4	0.023	0.003	0.023
10a	-	-	-	-
12a	3.19	0.036	0.005	0.041
14a	3.51	0.006	0.289	0.041

Line No.	Methane	Saturates Excluding Methane	Unsaturates	Total Excluding Methane & Butene
KBN 16a	3.16	0	0	0
17a	11.10	0.036	0.001	0.037
18a	3.73	0	0	0
KBM 19a	0	0.030	0	0.030
20a	-	-	-	-
21a	0	0.027	0.022	0.036
23a	2.81	0	0	0
25a	8.08	0.004	0.003	0.007
27a	2.74	0	0	0
29a	19.9	0.071	0.044	0.095
31a	30.72	0.104	0.047	0.151
33a	27.6	0.205	0.948	1.125
35a	29.51	0.120	0.024	0.144
36a	11.6	0.054	0.003	0.057
KBL 37a	3.79	0	0	0
38a	8.78	0.599	0.017	0.613
40a	0.11	0.119	0.031	0.130
42a	12.1	0.126	0.013	0.130
44a	-	-	-	-
46a	8.6	0	0.800	0.8
48a	16.4	0.034	0.034	0.068
50a	26.85	0.041	0.005	0.046
52a	50.23	0.074	0.044	0.116
53a	21.48	1.685	0.026	1.711
KDK 54a	31.35	0	3.000	2.11
55a	0.807	0	0.010	0.102
56a	13.3	0.006	0.006	0.108
58a	2.02	0.150	0	0.15
60a	21.4	0.185	0.020	0.201
62a	2.97	0	0	0
64a	5.02	0	0	0
66a	0.26	0.610	1.500	2.11
68a	1.24	0.038	0.004	0.041

Line No.	Methane	Saturates Excluding Methane	Unsaturates	Total Excluding Methane & Butene
KDK 70a	16.7	0.001	0.006	0.006
71a	29.4	0.056	0.111	0.137
KBJ 72a	0.83	0	0	0
73a	30.6	0.057	0.007	0.064
75a	18.9	0.071	0.035	0.101
77a	1.52	0.065	0.006	0.070
79a	4.6	0	0	0
81a	7.85	0.060	0.002	0.062
83a	-	-	-	-
85a	48.8	0.404	0.537	0.843
87a	17.4	0.063	0.090	0.149
88a	8.7	0.148	0.074	0.208
KBG 89a	-	-	-	-
90a	6.88	0.845	0.003	0.843
92a	29.1	0.082	0.006	0.087
94a	-	-	-	-
96a	19.7	0.047	0.054	0.084
98a	7.2	0.048	0.021	0.054
100a	7.05	0.293	0.113	0.390
102a	23.96	0.036	0.037	
104a	25.9	0.054	0.005	0.059
105a	4.9	0	0	0
KBF106a	14.79	0.099	0.003	0.101
107a	26.88	0.021	0.004	0.025
109a	3.78	0.083	0.008	0.088
111a	4.31	0.687	0.004	0.688
113a	26.03	0.036	0.005	0.04
115a	-	-	-	-
117a	7.65	0.236	0.011	0.238
119a	15.35	0.115	0.003	0.116
121a	3.13	0	0	0
KBE123a	9.58	0.098	0.086	0.159
124a	19.19	0.014	0.006	0.015
126a	4.35	1.212	0.030	1.242
128a	17.77	0.127	0.083	0.174

Line No.	Methane	Saturates Excluding Methane	Unsaturates	Total Excluding Methane & Butene
KBE130a	37.37	0.013	0.023	0.028
132a	-	-	-	-
134a	-	-	-	-
136a	.5.28	0.047	0.006	0.052
138a	82.78	0.036	0.040	0.076
140a	26.2	0	0.002	0.002
KBD141a	22.6	0.058	0.086	0.137
142a	18.0	0.013	0.002	0.016
143a	27.95	0.033	0.011	0.042
145a	162.96	0.128	0.025	0.138
147a	6.62	0.145	0.012	0.154
149a	8.29	0.046	0.028	0.070
151a	2.10	0.030	0.016	0.039
153a	3.37	0	0	0
155a	13.76	0	0	0
157a	32.03	0.012	0	0.012
159a	1.22	0	0	0
161a	6.3	1.198	0.082	1.259
162a	25.77	0	0	0
KBC163a	25.16	0.039	0.181	0.215
164a	33.26	0.364	0.031	0.381
165a	6.19	0.056	0.016	0.072
167a	57.32	0.020	0.018	0.037
169a	17.3	0.065	0.008	0.069
171a	0.74	0	0	0
173a	112.48	0.024	0.038	0.062
KBB175a	35.28	0.022	0.001	0.022
177a	24.62	0.065	0.013	0.066
179a	-	-	-	-
181a	28.46	0.120	0.002	0.121
18a	28.27	0.135	0.004	0.138
183a	0.75	0	0	0
184a	24.64	0.985	0.078	0.998
KBH186a	5.39	0	0	0

Line No.	Methane	Saturates Excluding Methane	Unsaturates	Total Excluding Methane & Butene
KBH187a	3.02	0	0	0
189a	2.60	0	0	0
191a	-	-	-	-
193a	17.7	0.709	0.021	0.73
195a	-	-	-	-
197a	-	-	-	-
199a	0.06	0	0	0
201a	0.905	0.179	0.007	0.186
202a	4.69	0	0	0
No line names				
1a	2.53	0.089	0.002	0.089
2b	0.611	0.702	0.112	0.706
3b	9.10	0.704	0	0.704
1c	1.83	0.232	0.006	0.239
2c	2.97	0	0	0
3c	2.40	0	0	0
1d	3.26	0.167	0.003	0.170
2d	1.72	0	0	0
3d	10.34	0.103	0.068	0.171

COOPER BASIN

ROCK-EVAL PYROLYSIS DATA SAMPLED FROM CORE HELD AT MINES AND ENERGY RESOURCES OF SOUTH AUSTRALIA BY SANTOS IN 1995/96

TABLE 1

ROCK-EVAL PYROLYSIS DATA (one run)

CUDDAPAN FORMATION Oct-95

SAMPLES	DEPTH (ft)		TMAX	S1	S2	S3	S1+S2	S2/S3	PI	PC	TOC	HI	OI
Beanbush 1	8719.25	c1	457	0.05	0.30	0.13	0.35	2.31	0.14	0.03	0.53	57	25
Beanbush 1	8720.00	c1	459	0.04	0.29	0.10	0.33	2.90	0.12	0.03	0.63	46	16
Beanbush 1	8728.42	c1	458	0.06	0.42	0.07	0.48	6.00	0.13	0.04	1.05	40	7
Beanbush 1	8740.67	c1	439	0.29	4.04	0.15	4.33	26.93	0.07	0.36	2.23	181	7
Beanbush 1	8742.50	c1	437	0.47	6.28	0.19	6.75	33.05	0.07	0.56	3.19	197	6

TMAX = Max. temperature S2
S1 + S2 = Potential yield
PC = Pyrolysable carbon
OI = Oxygen Index

S1 = Volatile hydrocarbons (HC
S3 = Organic carbon dioxide
TOC = Total organic carbon
nd = no data

S2 = HC generating potential
PI = Production index
HI = Hydrogen index

GEOTECHNICAL SERVICES PTY LTD

TABLE 1

ROCK-EVAL PYROLYSIS DATA (one run)

TOOLACHEE FORMATION

Sep-9

SAMPLES	DEPTH (ft)		TMAX	S1	S2	S3	S1+S2	S2/S3	PI	PC	TOC	HI	OI
Tilparee A1	5943.75	c1	434	0.61	12.26	0.45	12.87	27.24	0.05	1.07	8.96	137	5
Tilparee A1	5950.00	c1	439	6.12	89.75	3.54	95.87	25.35	0.06	7.96	70.20	128	5
Tilparee A1	5974.17	c1	439	1.69	44.07	1.38	45.76	31.93	0.04	3.80	26.10	169	5
Tilparee A1	5983.67	c1	436	1.61	34.85	1.29	36.46	27.02	0.04	3.03	22.50	155	6
Tilparee A1	5993.33	c1	441	7.21	114.23	4.13	121.44	27.66	0.06	10.08	89.60	127	5
Tilparee A1	5998.50	c1	443	0.47	4.78	0.41	5.25	11.66	0.09	0.44	7.78	61	5
Marana 1	6324.67	c1	452	14.65	113.44	2.58	128.09	43.97	0.11	10.63	77.20	147	3
Marana 1	6328.00	c1	448	0.78	7.48	0.14	8.26	53.43	0.09	0.69	4.96	151	3
Marana 1	6340.00	c1	452	2.39	24.00	1.01	26.39	23.76	0.09	2.19	15.00	160	7
Marana 1	6347.83	c1	450	3.12	39.60	0.88	42.72	45.00	0.07	3.55	21.70	182	4
Wanara 1	6137.00	c1	443	2.07	13.54	0.45	15.61	30.09	0.13	1.30	9.70	140	5
Wanara 1	6157.75	c1	451	1.13	8.41	0.17	9.54	49.47	0.12	0.79	4.29	196	4
Wanara 1	6163.17	c1	451	0.43	2.56	0.14	2.99	18.29	0.14	0.25	2.45	104	6
Wanara 1	6167.58	c1	448	2.80	20.88	0.54	23.68	38.67	0.12	1.97	12.50	167	4
Wanara 1	6173.50	c2	451	10.29	76.96	1.56	87.25	49.33	0.12	7.24	37.40	206	4
Wanara 1	6180.00	c3	446	1.27	7.97	0.27	9.24	29.52	0.14	0.77	5.27	151	5
Wanara 1	6181.92	c3	452	17.39	104.89	4.27	122.28	24.56	0.14	10.15	75.10	140	6
Wanara 1	6185.00	c3	456	0.54	2.82	0.16	3.36	17.63	0.16	0.28	3.00	94	5
Wanara 1	6192.50	c3	462	0.21	0.87	0.11	1.08	7.91	0.19	0.09	1.34	65	8
Wanara 1	6207.33	c3	448	4.48	32.40	1.20	36.88	27.00	0.12	3.06	17.50	185	7
Mudlalee 1	5871.42	c1	443	0.31	2.01	0.61	2.32	3.30	0.13	0.19	2.88	70	21
Mudlalee 1	5884.25	c1	442	1.38	19.32	0.87	20.70	22.21	0.07	1.72	11.90	162	7
Mudlalee 1	5890.42	c1	442	1.23	13.21	0.63	14.44	20.97	0.09	1.20	11.80	112	5
Mudlalee 1	5895.75	c1	442	1.40	15.13	0.77	16.53	19.65	0.08	1.37	11.80	128	7

TMAX = Max. temperature S2
S1 = Volatile hydrocarbons (HC)
S2 = HC generating potential
S1+S2 = Potential yield
S3 = Organic carbon dioxide
PI = Production index
PC = Pyrolysable carbon
TOC = Total organic carbon
HI = Hydrogen index

TABLE 1

ROCK-EVAL PYROLYSIS DATA (one run)

TOOLACHEE FORMATION

Oct-95

SAMPLES	DEPTH (ft)		TMAX	S1	S2	S3	S1 + S2	S2/S3	PI	PC	TOC	HI	OI
Daralingie 1	6366.00	c1	448	0.20	1.88	0.25	2.08	7.52	0.10	0.17	2.43	77	10
Daralingie 1	6381.50	c1	439	10.49	139.01	6.76	149.50	20.56	0.07	12.41	78.90	176	9
Daralingie 1	6387.00	c1	443	0.28	2.71	0.25	2.99	10.84	0.09	0.25	2.76	98	9
Daralingie 1	6396.75	c1	440	0.53	3.16	0.29	3.69	10.90	0.14	0.31	2.90	109	10
Daralingie 1	6412.00	c1	441	1.33	20.58	0.68	21.91	30.26	0.06	1.82	12.10	170	6
Daralingie 1	6414.33	c1	439	0.30	4.56	0.24	4.86	19.00	0.06	0.40	3.88	118	6
Daralingie 1	6418.50	c1	440	12.04	182.20	5.74	194.24	31.74	0.06	16.12	75.70	241	8
Daralingie 1	6440.00	c2	440	10.17	99.73	5.65	109.90	17.65	0.09	9.12	67.50	148	8
Daralingie 1	6449.67	c2	446	0.57	5.61	0.27	6.18	20.78	0.09	0.51	6.87	82	4
Daralingie 1	6459.50	c2	442	4.00	58.58	2.91	62.58	20.13	0.06	5.19	31.90	184	9
Daralingie 1	6464.00	c2	445	16.99	238.25	4.27	255.24	55.80	0.07	21.18	73.70	323	6
Daralingie 1	6464.67	c2	436	0.23	1.48	0.45	1.71	3.29	0.13	0.14	1.76	84	26

TMAX = Max. temperature S2
S1 + S2 = Potential yield
PC = Pyrolysable carbon
OI = Oxygen Index

S1 = Volatile hydrocarbons (HC)
S3 = Organic carbon dioxide
TOC = Total organic carbon
nd = no data

S2 = HC generating potential
PI = Production index
HI = Hydrogen index

TABLE 1

ROCK-EVAL PYROLYSIS DATA (one run)

TOOLACHEE FORMATION (1) Oct-95

SAMPLES	DEPTH (ft)		TMAX	S1	S2	S3	S1+S2	S2/S3	PI	PC	TOC	HI	OI
Gidgealpa 5	6886.50	c1	441	8.51	78.71	4.25	87.22	18.52	0.10	7.24	77.90	101	5
Gidgealpa 5	6893.50	c1	439	0.31	2.44	0.19	2.75	12.84	0.11	0.23	2.55	96	7
Gidgealpa 5	6909.75	c1	440	2.76	39.02	1.54	41.78	25.34	0.07	3.47	23.70	165	6
Gidgealpa 5	6918.50	c2	438	0.31	2.32	0.21	2.63	11.05	0.12	0.22	2.75	84	8
Gidgealpa 5	6921.00	c2	439	1.18	15.34	1.25	16.52	12.27	0.07	1.37	9.53	161	13
Gidgealpa 5	6923.50	c2	440	12.05	121.30	4.20	133.35	28.88	0.09	11.07	74.20	163	6
Gidgealpa 5	6950.00	c3	437	0.31	3.08	0.16	3.39	19.25	0.09	0.28	2.80	110	6
Gidgealpa 5	6958.00	c3	438	3.27	45.13	2.47	48.40	18.27	0.07	4.02	30.30	149	8
Gidgealpa 5	6962.83	c3	437	7.70	113.39	3.39	121.09	33.45	0.06	10.05	49.50	229	7
Gidgealpa 5	6965.25	c3	439	0.35	3.27	0.27	3.62	12.11	0.10	0.30	3.14	104	9
Gidgealpa 5	6991.67	c5	440	0.68	12.32	0.46	13.00	26.78	0.05	1.08	5.35	230	9
Gidgealpa 5	6999.83	c5	440	1.22	18.38	0.67	19.60	27.43	0.06	1.63	9.46	194	7
Meranji 7	8061.17	c1	439	0.56	6.64	0.26	7.20	25.54	0.08	0.60	4.63	143	6
Meranji 7	8077.50	c1	440	10.78	156.37	3.33	167.15	46.96	0.06	13.87	71.30	219	5
Meranji 7	8079.25	c1	443	0.20	1.44	0.15	1.64	9.60	0.12	0.14	1.55	93	10
Meranji 7	8087.17	c1	440	0.33	2.86	0.37	3.19	7.73	0.10	0.26	2.92	98	13
Coopers Ck 1	8380.00	c1	439	6.44	103.46	4.32	109.90	23.95	0.06	9.12	58.90	176	7
Coopers Ck 1	8382.25	c1	432	0.38	7.02	0.71	7.40	9.89	0.05	0.61	3.95	178	18
Coopers Ck 1	8407.67	c1	440	1.01	27.30	1.32	28.31	20.68	0.04	2.35	15.00	182	9
Coopers Ck 1	8415.00	c1	439	9.10	123.40	5.50	132.50	22.44	0.07	11.00	71.90	172	8

TMAX = Max. temperature S2
S1 = Volatile hydrocarbons (HC
S2 = HC generating potential
S1+S2 = Potential yield
S3 = Organic carbon dioxide
PI = Production index
PC = Pyrolysable carbon
TOC = Total organic carbon
HI = Hydrogen index
OI = Oxygen Index
nd = no data

GEOTECHNICAL SERVICES PTY LTD

TABLE 1

ROCK-EVAL PYROLYSIS DATA (one run)

TOOLACHEE FORMATION (2) Oct-95

SAMPLES	DEPTH (ft)		TMAX	S1	S2	S3	S1+S2	S2/S3	PI	PC	TOC	HI	OI
Fly Lake 1	8446.33	c1	443	7.96	111.01	3.61	118.97	30.75	0.07	9.87	65.40	170	6
Fly Lake 1	8449.50	c1	444	0.96	24.41	0.80	25.37	30.51	0.04	2.11	11.30	216	7
Fly Lake 1	8454.50	c1	445	9.59	149.51	4.55	159.10	32.86	0.06	13.21	73.10	205	6
Fly Lake 1	8456.83	c1	444	1.59	28.98	1.32	30.57	21.95	0.05	2.54	14.40	201	9
Fly Lake 1	8478.50	c1	445	10.75	88.39	4.43	99.14	19.95	0.11	8.23	75.20	118	6
Fly Lake 1	8480.50	c1	448	1.61	13.12	0.45	14.73	29.16	0.11	1.22	6.49	202	7
Moorari 2	9059.00	c1	465	0.11	0.87	0.18	0.98	4.83	0.11	0.08	1.51	58	12
Moorari 2	9066.33	c1	443	9.16	105.09	3.98	114.25	26.40	0.08	9.48	75.40	139	5
Moorari 2	9076.50	c1	445	10.40	166.66	4.54	177.06	36.71	0.06	14.70	74.20	225	6
Moorari 2	9079.00	c1	456	0.28	2.13	0.25	2.41	8.52	0.12	0.20	2.80	76	9
Moorari 2	9085.00	c1	452	0.35	2.29	0.26	2.64	8.81	0.13	0.22	2.85	80	9
Moorari 2	9091.00	c2	457	0.08	0.80	0.08	0.88	10.00	0.09	0.07	1.48	54	5
Moorari 2	9099.08	c2	446	0.45	2.45	0.33	2.90	7.42	0.16	0.24	3.00	82	11
Moorari 2	9099.67	c2	449	10.08	121.68	4.15	131.76	29.32	0.08	10.94	75.80	161	5
Moorari 2	9113.00	c2	449	11.66	149.73	4.21	161.39	35.57	0.07	13.40	80.70	186	5

TMAX = Max. temperature S2
S1 = Volatile hydrocarbons (HC
S2 = HC generating potential
S1+S2 = Potential yield
S3 = Organic carbon dioxide
PI = Production index
PC = Pyrolysable carbon
TOC = Total organic carbon
HI = Hydrogen index
OI = Oxygen Index
nd = no data

GEOTECHNICAL SERVICES PTY LTD

TABLE 1

ROCK-EVAL PYROLYSIS DATA (one run)

EPSILON FORMATION

Sep-95

SAMPLES	DEPTH (ft)		TMAX	S1	S2	S3	S1 + S2	S2/S3	PI	PC	TOC	HI	OI
Munkarie 2	6826.00	c1	458	3.56	30.81	0.73	34.37	42.21	0.10	2.85	18.60	166	4
Munkarie 2	6828.00	c1	461	6.17	35.65	2.02	41.82	17.65	0.15	3.47	29.30	122	7
Munkarie 2	6857.17	c1	451	0.79	6.09	0.16	6.88	38.06	0.11	0.57	4.21	145	4
Munkarie 2	6870.08	c1	448	1.68	12.61	0.25	14.29	50.44	0.12	1.19	8.67	145	3
Munkarie 2	6899.67	c2	451	1.27	10.48	0.21	11.75	49.90	0.11	0.98	6.45	162	3
Munkarie 2	6901.50	c2	452	1.09	9.14	0.21	10.23	43.52	0.11	0.85	5.24	174	4
Munkarie 2	6912.17	c2	446	0.60	3.88	0.31	4.48	12.52	0.13	0.37	4.05	96	8
Munkarie 2	6922.00	c2	450	0.37	1.83	0.32	2.20	5.72	0.17	0.18	2.95	62	11
Munkarie 2	6929.00	c2	453	0.29	0.88	1.10	1.17	0.80	0.25	0.10	1.73	51	64
Toolachee 1	6487.25	c2	452	0.23	0.57	1.64	0.80	0.35	0.29	0.07	1.27	45	129
Toolachee 1	6489.67	c2	445	0.41	2.56	0.21	2.97	12.19	0.14	0.25	2.96	86	7
Munkarie 4	6806.25	c1	446	1.58	14.71	0.24	16.29	61.29	0.10	1.35	7.80	189	3
Munkarie 4	6811.75	c1	448	13.92	155.35	1.87	169.27	83.07	0.08	14.05	62.30	249	3
Munkarie 4	6819.92	c1	446	0.64	3.65	0.72	4.29	5.07	0.15	0.36	3.83	95	19
Munkarie 4	6834.00	c1	452	1.64	22.41	0.58	24.05	38.64	0.07	2.00	10.10	222	6
Munkarie 4	6849.33	c1	443	0.71	2.82	0.91	3.53	3.10	0.20	0.29	3.77	75	24
Toolachee 23	6947.67	c1	446	0.45	2.43	0.25	2.88	9.72	0.16	0.24	3.39	72	7
)olachee 23	6953.00	c1	447	0.24	0.67	0.16	0.91	4.19	0.26	0.08	1.27	53	13
Toolachee 23	6955.00	c1	454	17.28	158.05	2.23	175.33	70.87	0.10	14.55	79.70	198	3
Toolachee 23	6968.42	c1	447	0.57	5.23	0.19	5.80	27.53	0.10	0.48	2.99	175	6
Toolachee 23	6977.08	c2	447	0.26	1.27	0.30	1.53	4.23	0.17	0.13	1.97	64	15
Toolachee 23	6986.17	c2	449	0.22	1.06	0.25	1.28	4.24	0.17	0.11	1.98	54	13
Toolachee 23	6998.92	c2	447	0.55	3.43	0.27	3.98	12.70	0.14	0.33	4.11	83	7
Toolachee 23	7005.33	c2	455	18.72	150.72	3.27	169.44	46.09	0.11	14.06	78.90	191	4

TMAX = Max. temperature S2
S1 = Volatile hydrocarbons (HC)
S2 = HC generating potential
S1 + S2 = Potential yield
S3 = Organic carbon dioxide
PI = Production index
PC = Pyrolysable carbon
TOC = Total organic carbon
HI = Hydrogen index

TABLE 1

ROCK-EVAL PYROLYSIS DATA (one run)

EPSILON FORMATION Oct-95

SAMPLES	DEPTH (ft)		TMAX	S1	S2	S3	S1+S2	S2/S3	PI	PC	TOC	HI	OI
Moorari 1	8901.00	c1	450	0.59	4.30	0.21	4.89	20.48	0.12	0.41	4.29	100	5
Moorari 1	8905.50	c1	448	1.46	21.36	0.46	22.82	46.43	0.06	1.89	12.80	167	4
Moorari 1	8910.50	c1	455	0.25	0.94	0.08	1.19	11.75	0.21	0.10	1.34	70	6
Moorari 1	8913.50	c1	442	0.14	1.25	0.05	1.39	25.00	0.10	0.12	1.33	94	4
:oorari 1	8923.83	c1	447	0.44	4.90	0.12	5.34	40.83	0.08	0.44	2.63	186	5
Moorari 1	8926.25	c1	448	0.34	3.27	0.11	3.61	29.73	0.09	0.30	2.10	156	5
Moorari 1	8931.08	c1	445	15.10	175.60	4.20	190.70	41.81	0.08	15.83	76.10	231	6
Moorari 1	8943.58	c1	446	0.70	5.88	0.20	6.58	29.40	0.11	0.55	3.78	156	5
Moorari 1	8951.00	c1	448	0.99	2.62	0.18	3.61	14.56	0.27	0.30	2.07	127	9
Moorari 1	8957.33	c1	446	0.49	3.26	0.16	3.75	20.38	0.13	0.31	2.28	143	7
Mudrangie 1	9052.00	c2	448	0.92	8.66	0.33	9.58	26.24	0.10	0.80	5.23	166	6
Mudrangie 1	9061.67	c2	444	0.26	1.50	0.44	1.76	3.41	0.15	0.15	2.39	63	18
Mudrangie 1	9064.83	c2	446	11.13	112.88	3.40	124.01	33.20	0.09	10.29	76.40	148	4
Mudrangie 1	9074.00	c2	451	14.32	182.68	4.02	197.00	45.44	0.07	16.35	79.00	231	5
Mudrangie 1	9092.25	c3	452	0.61	5.34	0.22	5.95	24.27	0.10	0.49	4.05	132	5
Mudrangie 1	9106.50	c3	441	0.20	1.18	0.19	1.38	6.21	0.14	0.11	1.52	78	13
Mudrangie 1	9115.58	c3	448	0.17	0.78	0.25	0.95	3.12	0.18	0.08	1.25	62	20
Mudrangie 1	9125.00	c3	447	0.20	1.22	0.18	1.42	6.78	0.14	0.12	1.65	74	11
Mudrangie 1	9131.58	c3	446	0.30	1.85	0.37	2.15	5.00	0.14	0.18	2.78	67	13
›onatie 1	9562.58	c3	451	14.51	158.94	2.98	173.45	53.34	0.08	14.40	76.70	207	4
Coonatie 1	9585.67	c3	449	0.35	3.36	0.23	3.71	14.61	0.09	0.31	2.93	115	8
Coonatie 1	9590.00	c3	452	0.48	3.11	0.35	3.59	8.89	0.13	0.30	2.99	104	12

TMAX = Max. temperature S2
S1 = Volatile hydrocarbons (HC)
S2 = HC generating potential
S1 + S2 = Potential yield
S3 = Organic carbon dioxide
PI = Production index
PC = Pyrolysable carbon
TOC = Total organic carbon
HI = Hydrogen index
OI = Oxygen Index
nd = no data

GEOTECHNICAL SERVICES PTY LTD

TABLE 1

ROCK-EVAL PYROLYSIS DATA (one run)

EPSILON FORMATION

Oct-95

SAMPLES	DEPTH (ft)		TMAX	S1	S2	S3	S1 + S2	S2/S3	PI	PC	TOC	HI	OI
Yapeni 1	6838.58	c1	443	15.04	174.12	3.57	189.16	48.77	0.08	15.70	75.50	231	5
Pando North 1	6113.25	c3	431	0.11	1.19	0.85	1.30	1.40	0.08	0.11	1.78	67	48
Pando North 1	6119	c3	441	7.15	167.94	6.56	175.09	25.60	0.04	14.53	69.40	242	9
Pando North 1	6121.92	c3	436	2.01	50.45	2.35	52.46	21.47	0.04	4.35	26.80	188	9
Pando 2	5806.83	c1	431	0.56	10.76	0.51	11.32	21.10	0.05	0.94	4.71	228	11
Pando 2	5809.25	c1	433	12.26	169.24	8.39	181.50	20.17	0.07	15.06	75.50	224	11
Pando 2	5819	c1	434	0.29	2.96	0.37	3.25	8.00	0.09	0.27	2.61	113	14
Pando 2	5823	c1	435	13.36	135.97	8.04	149.33	16.91	0.09	12.39	70.60	193	11
Lake Hope 1	6681.75	c1	429	0.15	2.43	1.63	2.58	1.49	0.06	0.21	2.70	90	60
Lake Hope 1	6688.75	c1	432	0.13	2.75	0.37	2.88	7.43	0.05	0.24	3.02	91	12
Lake Hope 1	6694	c1	431	5.19	159.03	11.25	164.22	14.14	0.03	13.63	72.90	218	15

TMAX = Max. temperature S2
S1 = Volatile hydrocarbons (HC)
S2 = HC generating potential
S1 + S2 = Potential yield
S3 = Organic carbon dioxide
PI = Production index
PC = Pyrolysable carbon
TOC = Total organic carbon
HI = Hydrogen index
OI = Oxygen Index
nd = no data

TABLE 1

ROCK-EVAL PYROLYSIS DATA (one run)

MURTEREE SHALE Oct-95

SAMPLES	DEPTH (ft)		TMAX	S1	S2	S3	S1 + S2	S2/S3	PI	PC	TOC	HI	OI
Pando 1	5618.00	c3	433	0.28	1.04	0.29	1.32	3.59	0.21	0.11	1.50	69	19
Pando 1	5629.50	c3	438	0.49	2.36	0.26	2.85	9.08	0.17	0.24	2.54	93	10
Pando 1	5632.83	c3	437	0.68	2.72	0.49	3.40	5.55	0.20	0.28	3.26	83	15
Wancoocha 1	5788.75	c1	435	1.54	30.00	2.57	31.54	11.67	0.05	2.62	19.30	155	13
Wancoocha 1	5791.42	c1	437	6.66	148.08	8.98	154.74	16.49	0.04	12.84	75.20	197	12
Wancoocha 1	5795.50	c1	437	4.40	71.00	5.60	75.40	12.68	0.06	6.26	56.30	126	10
Wancoocha 1	5804.50	c1	437	0.23	3.87	0.45	4.10	8.60	0.06	0.34	3.16	122	14
Wancoocha 1	5815.33	c1	433	0.12	1.43	1.22	1.55	1.17	0.08	0.13	1.80	79	68
Wancoocha 1	5827.00	c1	432	0.10	0.84	0.49	0.94	1.71	0.11	0.08	1.34	63	37
Wancoocha 1	5842.00	c1	436	0.13	0.95	0.30	1.08	3.17	0.12	0.09	1.72	55	17

TMAX = Max. temperature S2
S1 = Volatile hydrocarbons (HC)
S2 = HC generating potential
S1 + S2 = Potential yield
S3 = Organic carbon dioxide
PI = Production index
PC = Pyrolysable carbon
TOC = Total organic carbon
HI = Hydrogen index
OI = Oxygen Index
nd = no data

GEOTECHNICAL SERVICES PTY LTD

TABLE 1

ROCK-EVAL PYROLYSIS DATA (one run)

MURTEREE SHALE (1)

Oct-95

SAMPLES	DEPTH (ft)		TMAX	S1	S2	S3	S1+S2	S2/S3	PI	PC	TOC	HI	OI
Gidgealpa 9	7075.0	c1	439	0.40	1.70	2.34	2.10	0.73	0.19	0.17	2.78	61	84
Gidgealpa 9	7081.0	c1	435	0.53	2.79	1.01	3.32	2.76	0.16	0.28	3.61	77	28
Gidgealpa 9	7091.0	c1	436	0.34	2.24	0.35	2.58	6.40	0.13	0.21	2.51	89	14
Gidgealpa 9	7099.0	c1	439	1.17	11.98	0.51	13.15	23.49	0.09	1.09	6.45	186	8
Gidgealpa 9	7107.0	c1	441	0.43	2.92	0.21	3.35	13.90	0.13	0.28	1.80	162	12

TMAX = Max. temperature S2
S1 + S2 = Potential yield
PC = Pyrolysable carbon
OI = Oxygen Index

S1 = Volatile hydrocarbons (HC)
S3 = Organic carbon dioxide
TOC = Total organic carbon
nd = no data

S2 = HC generating potential
PI = Production index
HI = Hydrogen index

GEOTECHNICAL SERVICES PTY LTD

TABLE 1

ROCK-EVAL PYROLYSIS DATA (one run)

MURTEREE SHALE (2) Oct-95

SAMPLES	DEPTH (ft)		TMAX	S1	S2	S3	S1+S2	S2/S3	PI	PC	TOC	HI	OI
Tirrawarra 4	8801.08	c1	442	0.29	1.72	0.36	2.01	4.78	0.14	0.17	2.33	74	15
Tirrawarra 4	8810.50	c1	440	0.30	2.19	0.32	2.49	6.84	0.12	0.21	2.97	74	11
Tirrawarra 4	8811.67	c1	449	0.20	1.04	0.94	1.24	1.11	0.16	0.10	0.67	155	140
Tirrawarra 4	8822.83	c1	442	0.31	1.99	0.36	2.30	5.53	0.13	0.19	3.59	55	10
Tirrawarra 4	8832.17	c1	441	0.31	1.57	0.36	1.88	4.36	0.16	0.16	2.47	64	15
Tirrawarra 4	8843.25	c1	444	0.29	1.61	0.38	1.90	4.24	0.15	0.16	2.16	75	18
Tirrawarra 4	8852.00	c1	443	0.30	1.81	0.29	2.11	6.24	0.14	0.18	1.99	91	15
Tirrawarra 4	8860.58	c1	438	0.44	2.42	0.32	2.86	7.56	0.15	0.24	2.64	92	12
Mudrangie 1	9135.58	c4	454	0.14	0.66	0.82	0.80	0.80	0.18	0.07	1.34	49	61
Mudrangie 1	9144.25	c4	459	0.15	0.64	2.26	0.79	0.28	0.19	0.07	1.61	40	140
Mudrangie 1	9151.58	c4	446	0.36	1.69	0.38	2.05	4.45	0.18	0.17	2.70	63	14
Mudrangie 1	9162.50	c4	454	0.12	0.45	0.30	0.57	1.50	0.21	0.05	1.04	43	29
Mudrangie 1	9166.00	c4	448	0.26	1.52	0.21	1.78	7.24	0.15	0.15	2.49	61	8

TMAX = Max. temperature S2
S1 = Volatile hydrocarbons (HC
S2 = *HC generating potential*
S1+S2 = Potential yield
S3 = Organic carbon dioxide
PI = Production index
PC = Pyrolysable carbon
TOC = Total organic carbon
HI = Hydrogen index
OI = Oxygen Index
nd = no data

GEOTECHNICAL SERVICES PTY LTD

TABLE 1

ROCK-EVAL PYROLYSIS DATA (one run)

PATCHAWARRA FORMATION

Sep-9

SAMPLES	DEPTH (ft)		TMAX	S1	S2	S3	S1+S2	S2/S3	PI	PC	TOC	HI	OI
Sturt 8	6315.67	c1	436	24.30	172.15	3.15	196.45	54.65	0.12	16.31	69.80	247	5
Sturt 8	6332.58	c2	438	2.13	26.49	0.71	28.62	37.31	0.07	2.38	11.40	232	6
Sturt 8	6339.50	c2	438	26.52	153.22	3.47	179.74	44.16	0.15	14.92	73.40	209	5
Sturt 8	6342.00	c2	437	5.52	51.62	1.01	57.14	51.11	0.10	4.74	21.30	242	5
Sturt 8	6347.58	c2	438	18.75	190.35	2.76	209.10	68.97	0.09	17.36	56.30	338	5
Thurakinna 2	7487.50	c1	448	0.70	3.24	1.05	3.94	3.09	0.18	0.33	3.33	97	32
Thurakinna 2	7491.50	c1	449	7.43	64.67	1.01	72.10	64.03	0.10	5.98	28.80	225	4
Thurakinna 2	7502.92	c1	448	0.45	2.80	0.20	3.25	14.00	0.14	0.27	2.53	111	8
Thurakinna 2	7514.00	c1	450	0.68	5.03	0.17	5.71	29.59	0.12	0.47	3.08	163	6
Thurakinna 2	7531.50	c1	446	0.57	3.70	0.15	4.27	24.67	0.13	0.35	2.31	160	6
Thurakinna 2	7535.25	c1	448	3.73	47.93	1.19	51.66	40.28	0.07	4.29	16.50	290	7
Thurakinna 2	7540.25	c1	454	0.42	2.28	0.24	2.70	9.50	0.16	0.22	2.05	111	12
Daralingie 2	7238.25	c1	446	1.20	5.52	0.26	6.72	21.23	0.18	0.56	4.18	132	6
Daralingie 2	7252.33	c1	450	1.59	9.94	0.41	11.53	24.24	0.14	0.96	6.28	158	7
Daralingie 2	7268.00	c1	449	0.59	2.48	0.43	3.07	5.77	0.19	0.25	2.99	83	14
Daralingie 2	7276.25	c1	450	0.69	2.98	0.49	3.67	6.08	0.19	0.30	3.44	87	14
Daralingie 2	7284.00	c1	451	0.62	2.77	0.45	3.39	6.16	0.18	0.28	3.14	88	14
Daralingie 2	7307.00	c2	451	1.02	4.55	0.25	5.57	18.20	0.18	0.46	3.92	116	6
Daralingie 2	7310.33	c2	452	1.47	6.54	0.75	8.01	8.72	0.18	0.66	5.31	123	14
Daralingie 2	7327.50	c2	450	0.59	2.28	0.60	2.87	3.80	0.21	0.24	2.58	88	23
Daralingie 2	7337.50	c2	453	1.21	8.40	0.19	9.61	44.21	0.13	0.80	5.40	156	4
Daralingie 2	7359.00	c3	454	0.37	2.11	0.20	2.48	10.55	0.15	0.21	2.39	88	8
Daralingie 2	7389.50	c4	457	9.82	71.29	1.72	81.11	41.45	0.12	6.73	42.70	167	4
Daralingie 2	7392.75	c4	452	0.39	1.93	0.64	2.32	3.02	0.17	0.19	2.10	92	30
Daralingie 2	7458.00	c6	459	0.69	2.64	3.88	3.33	0.68	0.21	0.28	4.51	59	86
Daralingie 2	7461.50	c6	453	1.34	8.31	0.32	9.65	25.97	0.14	0.80	8.69	96	4
Daralingie 2	7470.00	c6	459	18.91	125.27	2.02	144.18	62.01	0.13	11.97	75.30	166	3
Daralingie 2	7481.00	c6	453	1.59	7.55	0.34	9.14	22.21	0.17	0.76	6.02	125	6
Daralingie 2	7489.67	c7	449	2.14	10.32	0.56	12.46	18.43	0.17	1.03	8.92	116	6
Daralingie 2	7506.00	c7	451	1.90	8.05	0.42	9.95	19.17	0.19	0.83	7.26	111	6
Daralingie 2	7508.00	c7	459	3.88	26.44	0.83	30.32	31.86	0.13	2.52	17.50	151	5
Daralingie 2	7513.25	c7	448	0.62	2.30	0.37	2.92	6.22	0.21	0.24	2.58	89	14
Daralingie 2	7521.17	c7	452	1.66	9.89	0.24	11.55	41.21	0.14	0.96	7.31	135	3
Daralingie 2	7536.50	c7	458	0.24	1.00	0.15	1.24	6.67	0.19	0.10	1.23	81	12
Daralingie 2	7541.25	c7	450	0.26	0.78	0.12	1.04	6.50	0.25	0.09	1.24	63	10

TMAX = Max. temperature S2
S1 = Volatile hydrocarbons (HC)
S2 = HC generating potential
S1+S2 = Potential yield
S3 = Organic carbon dioxide
PI = Production index
PC = Pyrolysable carbon
TOC = Total organic carbon
HI = Hydrogen index

TABLE 1

ROCK-EVAL PYROLYSIS DATA (one run)

PATCHAWARRA FORMATION

Sep-9

SAMPLES	DEPTH (ft)		TMAX	S1	S2	S3	S1 + S2	S2/S3	PI	PC	TOC	HI	OI
Narcoonowie 1	6086.50	c1	442	0.82	6.64	0.18	7.46	36.89	0.11	0.62	3.61	184	5
Narcoonowie 1	6092.17	c1	447	9.16	102.51	2.44	111.67	42.01	0.08	9.27	36.80	279	7
Narcoonowie 1	6092.25	c1	442	1.30	7.56	0.23	8.86	32.87	0.15	0.74	4.07	186	6
Narcoonowie 1	6096.00	c1	440	0.77	2.25	0.27	3.02	8.33	0.25	0.25	2.16	104	13
Narcoonowie 1	6107.50	c1	446	19.41	166.21	4.95	185.62	33.58	0.10	15.41	75.90	219	7
Narcoonowie 1	6109.50	c1	442	0.75	3.87	0.15	4.62	25.80	0.16	0.38	3.25	119	5
Pelketa 1	7074.67	c1	443	2.92	12.88	0.77	15.80	16.73	0.18	1.31	11.90	108	6
Pelketa 1	7076.25	c1	453	4.26	31.29	0.78	35.55	40.12	0.12	2.95	16.40	191	5
Pelketa 1	7084.08	c1	446	1.43	8.86	0.27	10.29	32.81	0.14	0.85	6.24	142	4
Pelketa 1	7087.50	c1	452	11.54	93.75	2.34	105.29	40.06	0.11	8.74	58.20	161	4
Murteree 1	6516.58	c2	435	1.38	12.78	0.77	14.16	16.60	0.10	1.18	7.47	171	10
Murteree 1	6518.58	c2	444	0.99	11.41	0.40	12.40	28.53	0.08	1.03	5.79	197	7
Murteree 1	6539.00	c2	433	1.02	6.76	0.79	7.78	8.56	0.13	0.65	5.73	118	14
Murteree 1	6550.42	c2	438	0.49	4.44	0.32	4.93	13.88	0.10	0.41	2.88	154	11
Murteree 1	6559.50	c2	445	6.83	69.75	1.33	76.58	52.44	0.09	6.36	27.90	250	5
Murteree 1	6566.83	c2	445	1.89	26.00	0.52	27.89	50.00	0.07	2.31	9.43	276	6
Murteree 1	6598.50	c3	446	12.23	137.90	3.35	150.13	41.16	0.08	12.46	54.90	251	6
Murteree 1	6602.00	c3	443	0.45	4.19	0.22	4.64	19.05	0.10	0.39	3.31	127	7
Murteree 1	6619.00	c3	455	0.37	1.97	0.18	2.34	10.94	0.16	0.19	2.58	76	7
Murteree 1	6646.00	c3	445	1.74	18.58	0.51	20.32	36.43	0.09	1.69	8.44	220	6
Pinna 1	6393.00	c1	439	0.71	5.98	0.26	6.69	23.00	0.11	0.56	3.79	158	7
Pinna 1	6400.42	c1	441	0.33	2.67	0.16	3.00	16.69	0.11	0.25	1.92	139	8

TMAX = Max. temperature S2
S1 = Volatile hydrocarbons (HC)
S2 = HC generating potential
S1 + S2 = Potential yield
S3 = Organic carbon dioxide
PI = Production index
PC = *Pyrolysable carbon*
TOC = Total organic carbon
HI = Hydrogen index

TABLE 1

ROCK-EVAL PYROLYSIS DATA (one run)

PATCHAWARRA FORMATION

Oct-95

SAMPLES	DEPTH (ft)		TMAX	S1	S2	S3	S1+S2	S2/S3	PI	PC	TOC	HI	OI
Jack Lake 1	9765.00	c2	465	12.04	98.67	2.04	110.71	48.37	0.11	9.19	65.40	151	3
Jack Lake 1	9766.00	c2	468	2.48	6.94	0.47	9.42	14.77	0.26	0.78	6.88	101	7
Jack Lake 1	9788.00	c2	465	1.09	8.68	0.17	9.77	51.06	0.11	0.81	5.75	151	3
Jack Lake 1	9789.50	c2	464	1.31	9.06	0.19	10.37	47.68	0.13	0.86	5.72	158	3
Jack Lake 1	9793.25	c2	468	11.92	84.51	1.92	96.43	44.02	0.12	8.00	55.40	153	3
Pelican 3	8641.00	c1	472	0.20	0.39	2.86	0.59	0.14	0.34	0.05	0.81	48	353
Pelican 3	8650.50	c1	460	0.57	1.94	0.43	2.51	4.51	0.23	0.21	2.01	97	21
Pelican 3	8653.50	c1	453	18.66	167.67	2.41	186.33	69.57	0.10	15.47	71.70	234	3
Pelican 3	8663.33	c1	458	0.61	2.74	0.15	3.35	18.27	0.18	0.28	2.27	121	7
Pelican 3	8693.75	c1	460	1.30	3.02	0.11	4.32	27.45	0.30	0.36	2.02	150	5
Pelican 3	8700.42	c1	452	2.31	5.20	0.22	7.51	23.64	0.31	0.62	4.04	129	5
Merrimelia 4	7712.00	c1	444	0.26	1.02	0.17	1.28	6.00	0.20	0.11	1.10	93	15
Merrimelia 4	7724.00	c1	448	22.83	215.83	3.66	238.66	58.97	0.10	19.81	79.95	270	5
Merrimelia 4	7726.00	c1	447	0.86	6.80	0.19	7.66	35.79	0.11	0.64	3.56	191	5
Merrimelia 4	7734.25	c1	449	0.36	1.28	0.61	1.64	2.10	0.22	0.14	1.37	93	45
Merrimelia 4	7745.83	c1	442	0.79	5.82	0.22	6.61	26.45	0.12	0.55	2.94	198	7
Merrimelia 3	7868.00	c12	450	0.31	2.13	0.12	2.44	17.75	0.13	0.20	1.71	125	7
Merrimelia 3	7873.67	c12	449	0.25	2.09	0.07	2.34	29.86	0.11	0.19	1.35	155	5
Merrimelia 3	7880.75	c12	448	0.66	4.16	0.16	4.82	26.00	0.14	0.40	2.74	152	6
Merrimelia 3	7886.75	c12	448	0.32	2.10	0.24	2.42	8.75	0.13	0.20	1.43	147	17
Merrimelia 3	7892.17	c12	446	0.85	5.25	0.16	6.10	32.81	0.14	0.51	3.18	165	5
Merrimelia 3	7901.42	c12	451	2.10	21.63	0.30	23.73	72.10	0.09	1.97	10.30	210	3
Merrimelia 3	7903.00	c12	450	8.04	87.11	1.64	95.15	53.12	0.08	7.90	31.10	280	5
Merrimelia 1	8083.00	c7	451	0.66	5.69	0.15	6.35	37.93	0.10	0.53	4.63	123	3
Merrimelia 1	8086.17	c7	451	15.10	178.91	4.23	194.01	42.30	0.08	16.10	83.20	215	5
Merrimelia 1	8092.50	c7	450	6.99	83.78	2.42	90.77	34.62	0.08	7.53	39.40	213	6
Merrimelia 1	8101.50	c7	449	5.70	61.00	2.30	66.70	26.52	0.09	5.54	26.20	233	9
Merrimelia 1	8113.17	c7	449	0.83	7.74	0.28	8.57	27.64	0.10	0.71	4.19	185	7
Merrimelia 1	8120.75	c7	448	4.21	60.94	1.47	65.15	41.46	0.06	5.41	19.30	316	8
Merrimelia 1	8130.50	c7	452	5.20	52.91	1.56	58.11	33.92	0.09	4.82	27.60	192	6
Merrimelia 1	8136.33	c7	451	5.10	35.05	1.01	40.15	34.70	0.13	3.33	19.20	183	5
Merrimelia 1	8141.00	c8	451	0.46	2.20	0.29	2.66	7.59	0.17	0.22	1.97	112	15
Meranji 4	9106.17	c1	454	11.37	142.01	3.06	153.38	46.41	0.07	12.73	83.50	170	4
Meranji 4	9108.00	c1	455	1.92	32.55	0.86	34.47	37.85	0.06	2.86	14.30	228	6
Meranji 4	9113.50	c1	459	0.14	1.08	0.39	1.22	2.77	0.11	0.10	1.92	56	20
Meranji 4	9118.67	c1	468	1.00	15.20	0.26	16.20	58.46	0.06	1.34	14.10	108	2
Meranji 4	9134.67	c1	455	1.28	14.47	0.69	15.75	20.97	0.08	1.31	10.90	133	6
Gidgealpa 5	7228.33	c11	437	0.43	3.00	0.38	3.43	7.89	0.13	0.28	2.28	132	17
Gidgealpa 5	7238.17	c11	442	13.48	159.26	3.57	172.74	44.61	0.08	14.34	64.90	245	6
Gidgealpa 5	7248.67	c11	443	3.79	48.62	1.63	52.41	29.83	0.07	4.35	21.60	225	8
Gidgealpa 5	7253.50	c11	439	0.41	2.46	0.45	2.87	5.47	0.14	0.24	2.12	116	21
Gidgealpa 5	7259.00	c11	442	3.96	49.63	1.30	53.59	38.18	0.07	4.45	15.40	322	8
Gidgealpa 5	7276.00	c12	nd	nd	nd	nd	nd	nd	nd	nd	0.11	nd	nd
Gidgealpa 5	7287.00	c12	nd	nd	nd	nd	nd	nd	nd	nd	0.13	nd	nd
Merrimelia 1	7972.50	c4	440	6.98	93.39	5.00	100.37	18.68	0.07	8.33	80.50	116	6
Merrimelia 1	7992.00	c5	444	1.92	21.71	0.83	23.63	26.16	0.08	1.96	12.70	171	7
Merrimelia 1	7998.25	c5	444	1.42	19.06	0.69	20.48	27.62	0.07	1.70	11.50	166	6
Merrimelia 1	8008.50	c5	447	0.63	6.64	0.15	7.27	44.27	0.09	0.60	3.72	178	4

TABLE 1

ROCK-EVAL PYROLYSIS DATA (one run)

PATCHAWARRA FORMATION

Oct-95

SAMPLES	DEPTH (ft)		TMAX	S1	S2	S3	S1 + S2	S2/S3	PI	PC	TOC	HI	OI
Merrimelia 1	8031.83	c6	442	0.65	4.69	0.25	5.34	18.76	0.12	0.44	3.95	119	6
Merrimelia 1	8034.50	c6	444	0.78	6.60	0.31	7.38	21.29	0.11	0.61	4.95	133	6
Merrimelia 1	8046.50	c6	445	4.27	53.84	2.17	58.11	24.81	0.07	4.82	44.90	120	5
Merrimelia 1	8060.33	c6	450	9.23	98.47	3.33	107.70	29.57	0.09	8.94	60.10	164	6
Merrimelia 1	8063.00	c6	455	5.42	23.14	2.47	28.56	9.37	0.19	2.37	20.40	113	12
Merrimelia 1	8071.25	c6	448	0.76	8.74	0.22	9.50	39.73	0.08	0.79	5.06	173	4
Leleptian 2	9539.75	c2	455	1.53	20.34	0.44	21.87	46.23	0.07	1.82	12.30	165	4
Leleptian 2	9540.25	c1	462	0.28	2.32	0.10	2.60	23.20	0.11	0.22	2.43	95	4
Leleptian 2	9550.83	c1	459	0.39	4.12	0.10	4.51	41.20	0.09	0.37	3.65	113	3
Leleptian 2	9556.58	c1	461	0.32	3.51	0.17	3.83	20.65	0.08	0.32	2.74	128	6
Leleptian 2	9562.25	c1	456	6.45	109.76	1.01	116.21	108.67	0.06	9.65	44.70	246	2
Leleptian 2	9576.33	c1	453	0.62	8.81	0.22	9.43	40.05	0.07	0.78	4.95	178	4
Gidgealpa 5	7068.00	c8	440	1.12	12.70	0.41	13.82	30.98	0.08	1.15	7.75	164	5
Gidgealpa 5	7074.00	c8	450	0.28	1.69	0.16	1.97	10.56	0.14	0.16	2.68	63	6
Gidgealpa 5	7093.00	c8	444	0.45	2.93	0.19	3.38	15.42	0.13	0.28	3.23	91	6
Gidgealpa 5	7103.58	c8	442	7.37	97.66	2.52	105.03	38.75	0.07	8.72	32.90	297	8
Gidgealpa 5	7112.42	c8	441	3.61	25.61	1.03	29.22	24.86	0.12	2.43	21.50	119	5
Gidgealpa 5	7125.17	c8	441	0.80	8.16	0.25	8.96	32.64	0.09	0.74	4.79	170	5
Gidgealpa 5	7127.83	c9	446	6.56	45.04	2.48	51.60	18.16	0.13	4.28	37.10	121	7
Gidgealpa 5	7133.83	c9	444	19.40	189.83	5.25	209.23	36.16	0.09	17.37	75.70	251	7
Gidgealpa 5	7134.50	c9	442	2.91	36.44	0.60	39.35	60.73	0.07	3.27	12.10	301	5
Gidgealpa 5	7161.92	c10	443	0.48	3.05	0.19	3.53	16.05	0.14	0.29	2.92	104	7
Gidgealpa 5	7169.08	c10	446	18.81	160.90	4.63	179.71	34.75	0.10	14.92	80.50	200	6
Gidgealpa 5	7171.00	c10	443	9.43	100.37	2.91	109.80	34.49	0.09	9.11	39.90	252	7
Gidgealpa 5	7172.50	c10	439	0.70	5.66	0.26	6.36	21.77	0.11	0.53	4.24	133	6
Gidgealpa 5	7187.50	c10	448	0.31	1.04	2.49	1.35	0.42	0.23	0.11	1.64	63	152
Gidgealpa 5	7189.50	c10	440	24.77	212.74	4.69	237.51	45.36	0.10	19.71	78.20	272	6
Gidgealpa 5	7194.00	c10	442	0.20	1.06	0.41	1.26	2.59	0.16	0.10	1.04	102	39
Gidgealpa 5	7205.50	c10	440	0.66	5.14	0.26	5.80	19.77	0.11	0.48	3.19	161	8
Gidgealpa 5	7211.00	c10	437	0.65	4.62	0.85	5.27	5.44	0.12	0.44	3.24	143	26
Gidgealpa 5	7211.75	c10	442	21.40	231.77	4.76	253.17	48.69	0.08	21.01	79.40	292	6
Jack Lake 2	8840.17	c1	445	5.00	89.31	1.89	94.31	47.25	0.05	7.83	36.30	246	5
Jack Lake 2	8841.00	c1	446	2.47	36.08	0.92	38.55	39.22	0.06	3.20	18.00	200	5
Jack Lake 2	8844.50	c1	445	0.69	6.31	0.16	7.00	39.44	0.10	0.58	3.49	181	5
Jack Lake 2	8860.58	c1	453	0.18	1.16	0.18	1.34	6.44	0.13	0.11	1.26	92	14
Jack Lake 2	8866.67	c1	451	0.15	0.93	0.07	1.08	13.29	0.14	0.09	1.28	73	5
Jack Lake 2	8876.17	c1	nd	nd	nd	nd	nd	nd	nd	nd	0.49	nd	nd
Kanowana 1	9039.08	c2	450	12.34	128.77	3.77	141.11	34.16	0.09	11.71	80.40	160	5
Kanowana 1	9048.17	c2	448	11.91	102.72	3.33	114.63	30.85	0.10	9.51	77.20	133	4
Kanowana 1	9058.83	c2	446	1.39	15.72	0.32	17.11	49.13	0.08	1.42	8.44	186	4
Kanowana 1	9060.83	c2	450	1.34	17.78	0.36	19.12	49.39	0.07	1.59	10.20	174	4
Kanowana 1	9062.00	c2	452	11.93	144.73	4.19	156.66	34.54	0.08	13.00	78.00	186	5
Kanowana 1	9069.50	c2	450	6.79	102.52	2.91	109.31	35.23	0.06	9.07	44.40	231	7
Kanowana 1	9075.50	c2	452	0.98	15.39	0.45	16.37	34.20	0.06	1.36	8.37	184	5
Kanowana 1	9076.50	c2	454	0.40	3.26	0.11	3.66	29.64	0.11	0.30	3.18	103	3
Kanowana 1	9291.67	c3	461	0.14	0.88	0.09	1.02	9.78	0.14	0.08	1.06	83	8
Kanowana 1	9300.00	c3	459	0.13	1.14	0.06	1.27	19.00	0.10	0.11	1.26	90	5
Kanowana 1	9322.50	c3	453	0.54	3.97	0.39	4.51	10.18	0.12	0.37	4.45	89	9

TABLE 1

ROCK-EVAL PYROLYSIS DATA (one run)

PATCHAWARRA FORMATION

Oct-95

SAMPLES	DEPTH (ft)		TMAX	S1	S2	S3	S1 + S2	S2/S3	PI	PC	TOC	HI	OI
Kanowana 1	9335.92	c3	459	0.16	1.70	0.15	1.86	11.33	0.09	0.15	1.96	87	8
Gidgealpa 5	7034.50	c7	440	0.23	1.17	1.87	1.40	0.63	0.16	0.12	1.72	68	109
Gidgealpa 5	7045.00	c7	441	5.95	89.33	2.31	95.28	38.67	0.06	7.91	32.40	276	7
idgealpa 5	7050.00	c7	442	1.19	15.83	0.70	17.02	22.61	0.07	1.41	9.11	174	8
Gidgealpa 5	7056.50	c7	443	12.26	145.09	5.09	157.35	28.50	0.08	13.06	73.90	196	7
Jack Lake 1	8674.00	c1	442	0.51	7.61	0.17	8.12	44.76	0.06	0.67	3.73	204	5
Jack Lake 1	8675.33	c1	445	13.10	201.74	5.92	214.84	34.08	0.06	17.83	78.90	256	8
Jack Lake 1	8680.58	c1	473	0.10	0.36	0.09	0.46	4.00	0.22	0.04	0.84	43	11
Jack Lake 1	8707.25	c1	444	0.22	1.95	0.11	2.17	17.73	0.10	0.18	2.08	94	5
Jack Lake 1	8709.75	c1	445	0.17	1.40	0.08	1.57	17.50	0.11	0.13	1.61	87	5
Jack Lake 1	8723.58	c1	441	0.73	12.71	0.47	13.44	27.04	0.05	1.12	6.15	207	8
Jack Lake 1	8728.00	c1	462	7.03	85.16	1.75	92.19	48.66	0.08	7.65	44.20	193	4
Gidgealpa 5	7007.42	c6	440	0.12	0.72	0.12	0.84	6.00	0.14	0.07	1.05	69	11
Gidgealpa 5	7019.00	c6	440	1.87	28.98	0.80	30.85	36.23	0.06	2.56	10.70	271	7
Gidgealpa 6	7314.00	c3	440	1.03	13.20	0.49	14.23	26.94	0.07	1.18	6.67	198	7
Gidgealpa 6	7327.00	c3	442	4.05	62.64	1.79	66.69	34.99	0.06	5.54	21.30	294	8
Gidgealpa 6	7336.17	c3	436	0.46	3.90	0.24	4.36	16.25	0.11	0.36	2.92	134	8
Gidgealpa 6	7345.17	c3	440	2.04	21.98	0.87	24.02	25.26	0.08	1.99	10.90	202	8
Gidgealpa 6	7346.33	c3	441	18.33	197.45	5.78	215.78	34.16	0.08	17.91	76.20	259	8
Gidgealpa 6	7362.00	c3	436	0.34	1.76	0.48	2.10	3.67	0.16	0.17	2.20	80	22
Gidgealpa 6	7364.75	c3	437	0.50	4.18	0.41	4.68	10.20	0.11	0.39	3.61	116	11
Gidgealpa 6	7371.00	c4	441	13.86	124.35	7.42	138.21	16.76	0.10	11.47	76.80	162	10
Kanowana 1	8921.00	c1	439	1.73	24.86	1.45	26.59	17.14	0.07	2.21	11.00	226	13
Kanowana 1	8927.67	c1	443	0.31	2.56	0.37	2.87	6.92	0.11	0.24	2.65	97	14
Kanowana 1	8935.42	c1	446	2.44	41.29	1.05	43.73	39.32	0.06	3.63	19.80	209	5
Kanowana 1	8938.50	c1	443	3.63	61.09	3.72	64.72	16.42	0.06	5.37	24.60	248	15
Kanowana 1	8943.17	c1	444	3.62	54.50	2.15	58.12	25.35	0.06	4.82	21.70	251	10

TMAX = Max. temperature S2
S1 + S2 = Potential yield
PC = Pyrolysable carbon
OI = Oxygen Index

S1 = Volatile hydrocarbons (HC)
S3 = Organic carbon dioxide
TOC = Total organic carbon
nd = no data

S2 = HC generating potential
PI = Production index
HI = Hydrogen index

TABLE 1

ROCK-EVAL PYROLYSIS DATA (one run)

PATCHAWARRA FORMATION

Oct-95

SAMPLES	DEPTH (ft)		TMAX	S1	S2	S3	S1+S2	S2/S3	PI	PC	TOC	HI	OI
Fly Lake 3	9374.25	c5	464	0.29	0.68	5.80	0.97	0.12	0.30	0.08	1.41	48	411
Fly Lake 2	9274.25	c5	456	2.74	28.64	0.60	31.38	47.73	0.09	2.60	18.80	152	3
Fly Lake 2	9278.17	c5	453	2.96	44.44	1.40	47.40	31.74	0.06	3.93	20.50	217	7
Fly Lake 2	9287.67	c5	456	2.39	21.77	0.35	24.16	62.20	0.10	2.01	12.80	170	3
Fly Lake 2	9289.42	c5	454	14.11	149.62	2.61	163.73	57.33	0.09	13.59	69:20	216	4
Fly Lake 2	9302.00	c5	454	16.78	157.06	2.84	173.84	55.30	0.10	14.43	80.20	196	4
Fly Lake 2	9306.42	c5	459	0.42	4.03	0.20	4.45	20.15	0.09	0.37	4.54	89	4
Fly Lake 2	9314.33	c5	456	3.55	39.91	1.69	43.46	23.62	0.08	3.61	19.80	202	9
Fly Lake 2	9315.00	c5	453	16.78	163.66	2.84	180.44	57.63	0.09	14.98	80.50	203	4
Fly Lake 2	9324.75	c5	456	0.27	1.07	1.45	1.34	0.74	0.20	0.11	1.50	71	97
Fly Lake 2	9327.83	c5	454	2.84	43.53	0.86	46.37	50.62	0.06	3.85	18.80	232	5
Fly Lake 3	9196.50	c3	nd	nd	nd	nd	nd	nd	nd	nd	0.31	nd	nd
Fly Lake 3	9204.83	c3	456	9.63	69.08	2.56	78.71	26.98	0.12	6.53	54.10	128	5
Fly Lake 3	9216.00	c3	457	0.17	1.03	0.12	1.20	8.58	0.14	0.10	1.11	93	11
Fly Lake 3	9221.67	c3	451	0.09	0.60	0.07	0.69	8.57	0.13	0.06	0.74	81	9
Fly Lake 2	9204.58	c4	454	12.34	109.36	3.42	121.70	31.98	0.10	10.10	78.30	140	4
Fly Lake 2	9212.50	c4	455	0.23	1.03	0.14	1.26	7.36	0.18	0.10	1.73	60	8
Fly Lake 2	9220.17	c4	447	1.73	21.67	0.54	23.40	40.13	0.07	1.94	11.40	190	5
Fly Lake 2	9246.75	c4	452	2.23	26.33	0.39	28.56	67.51	0.08	2.37	15.90	166	2
Fly Lake 2	9250.33	c4	452	5.24	72.17	1.45	77.41	49.77	0.07	6.43	38.80	186	4
Fly Lake 2	9257.50	c4	451	9.31	110.17	3.01	119.48	36.60	0.08	9.92	64.40	171	5
Fly Lake 1	8962.00	c5	452	9.00	91.35	3.96	100.35	23.07	0.09	8.33	79.50	115	5
Fly Lake 1	8974.00	c5	449	7.95	85.57	3.52	93.52	24.31	0.09	7.76	77.50	110	5
Fly Lake 1	8997.50	c5	450	8.43	97.25	3.62	105.68	26.86	0.08	8.77	68.90	141	5
Moorari 5	9249.08	c2	451	3.53	47.93	1.37	51.46	34.99	0.07	4.27	20.20	237	7
Moorari 5	9252.83	c2	452	0.43	2.26	0.12	2.69	18.83	0.16	0.22	1.87	121	6
Moorari 5	9260.25	c2	450	0.77	6.14	0.17	6.91	36.12	0.11	0.57	4.05	152	4
Moorari 5	9273.00	c2	451	1.60	18.14	0.47	19.74	38.60	0.08	1.64	9.80	185	5
Moorari 5	9275.17	c2	453	1.54	14.55	0.41	16.09	35.49	0.10	1.34	8.68	168	5
Moorari 2	9462.17	c3	453	0.44	1.36	0.11	1.80	12.36	0.24	0.15	1.44	94	8
Moorari 2	9467.92	c3	453	0.31	2.84	0.08	3.15	35.50	0.10	0.26	2.48	115	3
Moorari 2	9471.08	c3	452	14.52	125.28	3.39	139.80	36.96	0.10	11.60	75.20	167	5
Moorari 2	9486.25	c3	455	2.76	3.24	0.23	6.00	14.09	0.46	0.50	2.85	114	8
Moorari 2	9491.25	c3	456	1.46	14.70	0.38	16.16	38.68	0.09	1.34	11.20	131	3
Moorari 3	9052.00	c3	456	3.93	49.84	1.57	53.77	31.75	0.07	4.46	26.30	190	6
Moorari 3	9053.67	c3	458	1.11	5.86	0.24	6.97	24.42	0.16	0.58	5.19	113	5
Moorari 3	9062.17	c3	451	1.19	11.87	0.37	13.06	32.08	0.09	1.08	5.90	201	6
Moorari 3	9068.42	c3	465	0.26	1.32	0.13	1.58	10.15	0.16	0.13	1.98	67	7
Moorari 3	9073.75	c3	452	2.28	25.78	0.82	28.06	31.44	0.08	2.33	15.60	165	5
Moorari 3	9075.50	c3	458	0.38	0.76	6.42	1.14	0.12	0.33	0.09	1.14	67	563
Moorari 3	9086.00	c3	454	15.75	111.59	3.53	127.34	31.61	0.12	10.57	81.20	137	4
Fly Lake 2	9018.25	c3	444	1.34	22.52	0.49	23.86	45.96	0.06	1.98	9.39	240	5
Fly Lake 2	9038.50	c3	445	0.72	13.86	0.29	14.58	47.79	0.05	1.21	6.77	205	4
Fly Lake 2	9052.25	c3	447	2.39	27.79	0.77	30.18	36.09	0.08	2.50	18.20	153	4
Fly Lake 2	9059.00	c3	448	0.12	0.51	1.83	0.63	0.28	0.19	0.05	1.06	48	173
Fly Lake 2	9068.75	c3	447	0.14	0.56	1.35	0.70	0.41	0.20	0.06	1.10	51	123

TABLE 1

ROCK-EVAL PYROLYSIS DATA (one run)

PATCHAWARRA FORMATION

Oct-95

SAMPLES	DEPTH (ft)		TMAX	S1	S2	S3	S1+S2	S2/S3	PI	PC	TOC	HI	OI
Fly Lake 1	9313.83	c6	452	1.23	4.75	0.21	5.98	22.62	0.21	0.50	2.65	179	8
Fly Lake 1	9319.67	c6	464	0.45	1.55	0.12	2.00	12.92	0.23	0.17	1.66	93	7
Fly Lake 1	9322.00	c6	455	12.22	94.81	1.85	107.03	51.25	0.11	8.88	47.90	198	4
Fly Lake 1	9326.67	c6	455	17.88	122.71	2.88	140.59	42.61	0.13	11.67	71.00	173	4
Fly Lake 1	9329.00	c6	456	0.48	1.68	0.09	2.16	18.67	0.22	0.18	1.59	106	6
Fly Lake 1	9356.58	c7	449	1.29	12.11	0.33	13.40	36.70	0.10	1.11	5.58	217	6
Fly Lake 3	9536.58	c9	457	1.36	14.31	0.24	15.67	59.63	0.09	1.30	6.80	210	4
Fly Lake 3	9544.67	c9	457	4.81	52.68	1.20	57.49	43.90	0.08	4.77	22.50	234	5
Fly Lake 3	9547.17	c9	463	1.19	8.76	0.24	9.95	36.50	0.12	0.83	6.74	130	4
Fly Lake 3	9568.25	c9	459	0.62	2.89	0.14	3.51	20.64	0.18	0.29	2.09	138	7
Fly Lake 3	9573.17	c9	458	5.17	41.31	1.14	46.48	36.24	0.11	3.86	17.10	242	7
Fly Lake 3	9575.50	c9	463	2.01	3.88	0.14	5.89	27.71	0.34	0.49	2.98	130	5
Fly Lake 3	9579.08	c9	457	1.95	17.11	0.32	19.06	53.47	0.10	1.58	7.24	236	4
Moorari 7	9523.17	c1	454	0.75	6.15	0.16	6.90	38.44	0.11	0.57	3.68	167	4
Moorari 7	9530.50	c1	457	0.30	1.37	0.11	1.67	12.45	0.18	0.14	1.81	76	6
Moorari 7	9535.33	c1	464	1.67	4.69	1.79	6.36	2.62	0.26	0.53	6.62	71	27
Moorari 7	9539.83	c1	452	12.45	132.36	1.90	144.81	69.66	0.09	12.02	56.40	235	3
Moorari 7	9541.50	c1	465	0.57	2.66	0.10	3.23	26.60	0.18	0.27	2.83	94	4
Moorari 7	9547.00	c1	457	0.67	3.77	0.07	4.44	53.86	0.15	0.37	2.52	150	3
Moorari 7	9550.00	c1	459	0.57	2.16	0.07	2.73	30.86	0.21	0.23	1.80	120	4
Fly Lake 3	9428.08	c6	454	18.58	165.28	2.07	183.86	79.85	0.10	15.26	67.30	246	3
Fly Lake 3	9431.67	c6	465	0.70	2.65	0.25	3.35	10.60	0.21	0.28	2.77	96	9
Fly Lake 3	9440.67	c6	458	1.31	5.84	0.15	7.15	38.93	0.18	0.59	3.47	168	4
Fly Lake 3	9447.50	c6	454	1.59	3.78	0.20	5.37	18.90	0.30	0.45	2.75	137	7
Fly Lake 3	9451.75	c6	459	1.72	6.85	1.08	8.57	6.34	0.20	0.71	6.49	106	17
Fly Lake 3	9464.58	c7	454	1.43	18.06	0.47	19.49	38.43	0.07	1.62	7.89	229	6
Fly Lake 3	9473.25	c7	454	14.56	150.51	2.67	165.07	56.37	0.09	13.70	65.80	229	4
Fly Lake 3	9479.50	c8	457	0.86	3.59	0.32	4.45	11.22	0.19	0.37	3.30	109	10
Fly Lake 3	9490.25	c8	455	0.29	1.38	0.09	1.67	15.33	0.17	0.14	1.70	81	5
Fly Lake 3	9505.42	c8	460	0.67	3.02	0.09	3.69	33.56	0.18	0.31	nd	nd	nd
Fly Lake 3	9512.00	c8	453	0.77	5.80	0.15	6.57	38.67	0.12	0.55	nd	nd	nd
Fly Lake 3	9521.08	c8	457	1.21	6.52	0.15	7.73	43.47	0.16	0.64	5.01	130	3
Fly Lake 3	9524.67	c8	459	22.07	132.61	2.43	154.68	54.57	0.14	12.84	80.90	164	3
Fly Lake 3	9534.25	c8	460	0.34	1.87	0.12	2.21	15.58	0.15	0.18	1.67	112	7
Fly Lake 2	9392.83	c6	460	0.42	1.17	0.75	1.59	1.56	0.26	0.13	1.69	69	44
Fly Lake 2	9400.33	c6	462	0.19	0.67	0.18	0.86	3.72	0.22	0.07	1.08	62	17
Fly Lake 3	9309.08	c4	451	12.07	133.16	1.88	145.23	70.83	0.08	12.05	58.20	229	3
Fly Lake 3	9313.83	c4	454	3.84	24.83	1.34	28.67	18.53	0.13	2.38	15.50	160	9
Fly Lake 3	9317.42	c4	453	0.38	1.49	1.89	1.87	0.79	0.20	0.16	2.00	75	95
Fly Lake 3	9318.50	c4	454	1.83	22.16	0.41	23.99	54.05	0.08	1.99	11.00	201	4
Fly Lake 3	9335.00	c4	453	0.78	6.45	0.19	7.23	33.95	0.11	0.60	3.66	176	5
Fly Lake 3	9342.00	c4	451	10.52	119.40	1.86	129.92	64.19	0.08	10.78	47.50	251	4
Fly Lake 3	9347.17	c4	448	7.20	81.20	1.60	88.40	50.75	0.08	7.34	32.40	251	5
Fly Lake 3	9351.33	c4	456	0.26	1.45	0.11	1.71	13.18	0.15	0.14	1.67	87	7
Fly Lake 3	9365.25	c5	452	7.76	108.09	1.73	115.85	62.48	0.07	9.62	42.20	256	4
Fly Lake 3	9368.42	c5	464	0.15	0.38	4.41	0.53	0.09	0.28	0.04	0.76	50	580

TABLE 1

ROCK-EVAL PYROLYSIS DATA (one run)

PATCHAWARRA FORMATION Oct-95

SAMPLES	DEPTH (ft)		TMAX	S1	S2	S3	S1+S2	S2/S3	PI	PC	TOC	HI	OI
Fly Lake 1	8796.00	c2	448	0.32	3.24	0.15	3.56	21.60	0.09	0.30	2.61	124	6
Fly Lake 1	8800.75	c2	445	2.04	28.10	0.73	30.14	38.49	0.07	2.50	16.50	170	4
Fly Lake 1	8802.00	c2	447	9.34	147.19	4.85	156.53	30.35	0.06	12.99	71.90	205	7
Fly Lake 1	8808.83	c2	462	0.27	1.68	0.20	1.95	8.40	0.14	0.16	2.10	80	10
Fly Lake 1	8809.83	c2	445	4.34	76.86	2.52	81.20	30.50	0.05	6.74	28.30	272	9
Fly Lake 1	8818.17	c2	459	0.25	2.00	0.26	2.25	7.69	0.11	0.19	2.25	89	12
Fly Lake 1	8830.00	c2	444	3.30	51.32	1.91	54.62	26.87	0.06	4.53	24.30	211	8
Fly Lake 1	8830.67	c2	450	0.59	7.15	0.29	7.74	24.66	0.08	0.64	7.20	99	4
Fly Lake 1	8851.83	c3	444	10.00	121.47	3.43	131.47	35.41	0.08	10.91	76.20	159	5
Fly Lake 1	8864.17	c3	444	10.97	195.72	3.68	206.69	53.18	0.05	17.16	73.30	267	5
Fly Lake 1	8918.75	c4	450	0.28	2.30	0.33	2.58	6.97	0.11	0.21	2.01	114	16
Fly Lake 1	8935.00	c4	445	1.49	23.65	0.62	25.14	38.15	0.06	2.09	10.80	219	6
Fly Lake 1	8936.83	c4	453	0.32	2.42	0.20	2.74	12.10	0.12	0.23	2.60	93	8
Mudrangie 1	9332.50	c5	451	5.43	66.40	2.03	71.83	32.71	0.08	5.96	37.40	178	5
Mudrangie 1	9334.50	c5	456	0.47	4.22	0.18	4.69	23.44	0.10	0.39	4.02	105	4
Mudrangie 1	9343.17	c5	451	0.76	12.13	0.45	12.89	26.96	0.06	1.07	7.25	167	6
Mudrangie 1	9350.67	c5	452	0.82	8.54	0.28	9.36	30.50	0.09	0.78	5.90	145	5
Mudrangie 1	9362.00	c5	451	0.59	5.74	0.15	6.33	38.27	0.09	0.53	4.00	144	4
Fly Lake 2	8801.33	c1	444	0.57	8.15	0.18	8.72	45.28	0.07	0.72	4.97	164	4
Fly Lake 2	8802.50	c1	444	15.41	172.50	3.16	187.91	54.59	0.08	15.60	78.60	219	4
Fly Lake 2	8809.33	c1	445	0.24	1.79	0.13	2.03	13.77	0.12	0.17	1.72	104	8
Fly Lake 2	8821.33	c1	454	9.26	325.13	2.75	334.39	118.23	0.03	27.75	65.40	497	4
Fly Lake 2	8829.67	c1	441	0.90	9.77	0.27	10.67	36.19	0.08	0.89	5.27	185	5
Fly Lake 2	8845.50	c1	445	15.86	186.72	5.25	202.58	35.57	0.08	16.81	81.40	229	6
Fly Lake 2	8854.17	c1	443	0.95	11.54	0.33	12.49	34.97	0.08	1.04	6.72	172	5
Fly Lake 2	8857.92	c2	446	1.23	15.17	0.56	16.40	27.09	0.08	1.36	7.13	213	8
Fly Lake 2	8860.42	c2	446	17.06	166.60	4.67	183.66	35.67	0.09	15.24	77.50	215	6
Fly Lake 2	8861.67	c2	444	0.57	6.90	0.22	7.47	31.36	0.08	0.62	4.44	155	5
Fly Lake 2	8867.00	c2	444	15.65	156.17	4.52	171.82	34.55	0.09	14.26	80.90	193	6
Fly Lake 2	8873.92	c2	444	2.53	20.89	0.72	23.42	29.01	0.11	1.94	10.60	197	7
Fly Lake 2	8899.00	c2	451	0.26	1.15	0.16	1.41	7.19	0.18	0.12	1.38	83	12
Fly Lake 2	8908.17	c2	451	0.26	1.72	0.13	1.98	13.23	0.13	0.16	1.75	98	7

TMAX = Max. temperature S2
S1 = Volatile hydrocarbons (HC)
S2 = HC generating potential
S1 + S2 = Potential yield
S3 = Organic carbon dioxide
PI = Production index
PC = Pyrolysable carbon
TOC = Total organic carbon
HI = Hydrogen index
OI = Oxygen Index
nd = no data

GEOTECHNICAL SERVICES PTY LTD

TABLE 1

ROCK-EVAL PYROLYSIS DATA (one run)

PATCHAWARRA FORMATION Nov-95

SAMPLES	DEPTH (ft)		TMAX	S1	S2	S3	S1+S2	S2/S3	PI	PC	TOC	HI	OI
Kujani 2	6743.08	c1	437	2.44	45.51	0.51	47.95	89.24	0.05	3.98	11.90	382	4

TMAX = Max. temperature S2
S1 = Volatile hydrocarbons (HC)
S2 = HC generating potential
S1+S2 = Potential yield
S3 = Organic carbon dioxide
PI = Production index
PC = Pyrolysable carbon
TOC = Total organic carbon
HI = Hydrogen index
OI = Oxygen Index
nd = no data

GEOTECHNICAL SERVICES PTY LTD

TABLE 1

ROCK-EVAL PYROLYSIS DATA (one run)

TIRRAWARRA FORMATION

Oct-95

SAMPLES	DEPTH (ft)		TMAX	S1	S2	S3	S1+S2	S2/S3	PI	PC	TOC	HI	OI
Moorari 9	9724.58	c3	460	0.53	1.81	0.05	2.34	36.20	0.23	0.19	1.17	155	4
Moorari 9	9757.17	c4	nd	nd	nd	nd	nd	nd	nd	nd	0.30	nd	nd
Moorari 9	9787.75	c5	462	0.07	0.39	0.05	0.46	7.80	0.15	0.04	0.61	64	8
Moorari 9	9815.83	c5	459	0.37	2.30	0.07	2.67	32.86	0.14	0.22	1.66	139	4

TMAX = Max. temperature S2
S1 + S2 = Potential yield
PC = Pyrolysable carbon
OI = Oxygen Index

S1 = Volatile hydrocarbons (HC)
S3 = Organic carbon dioxide
TOC = Total organic carbon
nd = no data

S2 = HC generating potential
PI = Production index
HI = Hydrogen index

GEOTECHNICAL SERVICES PTY LTD

RETURN TO
EXPLORATION
GROUP
LIBRARY
038440

COOPER BASIN DISCOVERIES

AND

PERMO-TRIASSIC OIL AND GAS CHARACTERISTICS

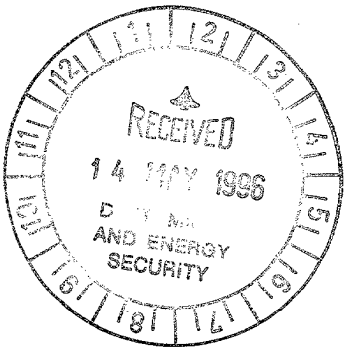

J.W. Hunt,
Regional Studies Group
Delhi Petroleum Pty Ltd
June, 1985
JWH/111/29kli

CONTENTS

INTRODUCTION

OIL DISCOVERIES

GAS DISCOVERIES

OIL CHARACTERISTICS

GAS CHARACTERISTICS

1) CARBON DIOXIDE

2) GAS WETNESS

LOCATION OF OIL DISCOVERIES

LOCATION OF GAS DISCOVERIES

CONCLUSIONS

FIGURES

1. Oil discoveries, Tirrawarra Sandstone, southern Cooper Basin

2. Oil discoveries, Patchawarra Formation, southern Cooper Basin

3. Oil discoveries, Toolachee Formation, southern Cooper Basin

4. Oil discoveries, Nappamerri Formation, southern Cooper Basin

5. Gas discoveries, Tirrawarra Sandstone, southern Cooper Basin

6. Gas discoveries, Patchawarra Formation, southern Cooper Basin

7. Gas discoveries, Patchawarra Formation, northern Cooper Basin

8. Gas discoveries, Epsilon Formation, southern Cooper Basin

9. Gas discoveries, Daralingie beds, southern Cooper Basin

10. Gas discoveries, Toolachee Formation, southern Cooper Basin

11. Oil and Gas discoveries, Toolachee Formation, northern Cooper Basin

12. Gas discoveries, Nappamerri Formation, southern Cooper Basin

13. Pour point and API gravity, Permo-Triassic oils

14. Pour point and API gravity, Permo-Triassic condensates

15. % CO_2, Merrimelia and Tirrawarra Formations, southern Cooper Basin

16. % CO_2, Patchawarra Formation, southern Cooper Basin

17. % CO_2, Epsilon Formation and Daralingie beds, southern Cooper Basin

18. % CO_2, Toolachee and Nappamerri Formations, southern Cooper Basin

19. % Wet Gas, Merrimelia and Tirrawarra Formations, southern Cooper Basin

20. % Wet Gas, Patchawarra Formation, southern Cooper Basin

21. % Wet Gas, Epsilon Formation and Daralingie beds, southern Cooper Basin

22. % Wet Gas, Toolachee and Nappamerri Formations, southern Cooper Basin

ENCLOSURES

1. Oil discoveries, Tirrawarra Sandstone, southern Cooper Basin
2. Oil discoveries, Patchawarra Formation, southern Cooper Basin
3. Oil discoveries, Toolachee Formation, southern Cooper Basin
4. Oil discoveries, Nappamerri Formation, southern Cooper Basin
5. Gas discoveries, Tirrawarra Sandstone, southern Cooper Basin
6. Gas discoveries, Patchawarra Formation, southern Cooper Basin
7. Gas discoveries, Epsilon Formation, southern Cooper Basin
8. Gas discoveries, Daralingie beds, southern Cooper Basin
9. Gas discoveries, Toolachee Formation, southern Cooper Basin
10. Gas discoveries, Nappamerri Formation, southern Cooper Basin
11. % CO_2, Merrimelia and Tirrawarra Formations, southen Cooper Basin
12. % CO_2, Patchawarra Formation, southern Cooper Basin
13. % CO_2, Epsilon Formation and Daralingie beds, southern Cooper Basin
14. % CO_2, Toolachee and Nappamerri Formations, southern Cooper Basin
15. % Wet Gas, Merrimelia and Tirrawarra Formations, southern Cooper Basin
16. % Wet Gas, Patchawarra Formation, southern Cooper Basin
17. % Wet Gas, Epsilon Formation and Daralingie beds, southern Cooper Basin
18. % Wet Gas, Toolachee and Nappamerri Formations, southern Cooper Basin

TABLES

Table 1: Merrimelia Sandstone Hydrocarbon Discoveries and Occurrences

Table 2: Tirrawarra Sandstone Hydrocarbon Discoveries and Occurrences

Table 3: Patchawarra Formation Hydrocarbon Discoveries and Occurrences

Table 4: Epsilon Formation Hydrocarbon Discoveries and Occurrences

Table 5: Daralingie Beds Hydrocarbon Discoveries and Occurrences

Table 6: Toolachee Formation Hydrocarbon Discoveries and Occurrences

Table 7: Nappamerri Formation Hydrocarbon Discoveries and Occurrences

INTRODUCTION

This report summarises basic data relating to hydrocarbon characteristics and discoveries in the Permo-Triassic Cooper Basin. It includes data presented in an earlier report (April, 1985) - "An interim report on the composition of gas in the Gidgealpa Group, Cooper Basin".

Whether a discovery consists of oil or gas or both is not always a simple question. The hydrocarbon contents of a reservoir are defined at the conditions of temperature and pressure in the reservoir, and may differ from the phases present at the surface, and change with production. Thus some gas flows from the Tirrawarra Sandstone in the base of the Cooper Basin sequence are considered to exist as part of the oil phase in the reservoir, and this gas type is referred as "solution gas" or "associated gas". Conversely, liquid hydrocarbons, which are often associated with Permo-Triassic gas flows, exist in the gas phase in the reservoir. This liquid is here referred to as "condensate". Moreover, reference of a hydrocarbon phase at the surface to oil or gas in the reservoir, may not be possible without analytical work, usually pressure - volume - temperature (PVT) modelling. In the absence of such analysis some doubt may and often does remain about the phase classification of a hydrocarbon discovery.

Hydrocarbon discoveries in the Cooper Basin have been made in almost every formation, although oil discoveries are more restricted in both stratigraphic distribution and size, than gas discoveries. The distribution of oil and gas is as follows:

	Oil	Gas
1) Nappameri Formation	X	X
2) Toolachee Formation	X	X
3) Daralingie beds		X
4) Epsilon Formation		X
5) Patchawarra Formation	X	X
6) Tirrawarra Sandstone (and Merrimelia Formation)	X	X

Of these the Toolachee and Patchawarra Formations, which make up the main part of the section, contain the majority of discoveries. Table 1 and the following maps and enclosures, document "discovery wells", best flow rates or recoveries and some oil and gas characteristics.

A discovery well is one which recovered a measurable amount of oil, or flowed gas at a significent rate. More rarely, untested hydrocarbon saturation maybe indicated from log analysis. For the purpose of evaluating the geological controls of hydrocarbon distribution some wells with marginal (20-50%) hydrocarbon saturations, or "tight" accumulations have also been included. Table 1 summarises discoveries according to the discovery well and date, best flow or recovery, and where available some hydrocarbon type parameters. The data are derived mainly form the summary of test results in the Delhi geological data base, or from production data or log evaluation results. Where a test spanned more than one formation it has usually been possible to assign any discovery to only one formation, on the basis of log analysis (sand distribution and hydrocarbon saturation).

OIL DISCOVERIES

Significant oil discoveries are restricted to the Tirrawarra Sandstone and the Patchawarra , Toolachee and Nappamerri Formations. The distribution of discoveries within these formations is shown in summary in Figures 1 to 4* and in detail in Enclosures 1 to 4*. Tirrawarra oil accounts for the majority of Permo-Triassic reserves with minor amounts present in the other three formations. Tirrawarra oil reservoirs are often of marginal porosity and permeability, and reservoir stimulation is usually necessary for production. This and the problem of formation damage makes the assessment of test results for Tirrawarra Sandstone reservoirs difficult. Thus many of the discoveries shown for the Tirrawarra Sandstone are based on log analysis combined with marginal test results, or sometimes only the former.

In Brolga 1 and Fly Lake 1 oil accumulations are found in the base of the Patchawarra Formation and both these wells have intersected a major Tirrawarra Sandstone oil accumulation. The basal Patchawarra reservoir may be the uppermost of a multiple reservoir sequence which crosses the Tirrawarra Sandstone - Patchawarra Formation boundary. Oil listed for the Patchawarra Formation in Tirrawarra 1 is known only form recovery on production.

* Zero edge, structural elements and isopachs are from Castro, C. and Kuang, K.S., 1985.

GAS DISCOVERIES

Significant gas flows on test have been recorded from all sandy Cooper Basin formations. However the Toolachee and Patchawarra Formations contain the majority of reserves (about 90%). The distribution of gas discoveries within the formations is shown in summary in Figures 5 to 12, and in detail in Enclosures 5 to 10.

The data shown in Enclosures 5 to 10 are for the best flow rates obtained, and in some of the larger fields several wells may be shown. The flow data commonly are based on a 3/4" bottom choke - 1/2" top choke test configuration. However a significant number of tests were made with other configurations, the most common being a 5/8" bottom choke - 7/16" top choke, and the data are therefore not strictly comparable in a quantative sense.

In the Cooper Basin a flow rate of >0.5 MMCFD on test is generally economic. Some test results returning flows of <0.5 MMCFD are shown in Enclosures 5 to 10, and these flows (and the complementary interpreted categories) have been subdivided into tight, gas-saturated (<50% Sw) reservoirs ("tight gas"), and porous but marginally saturated, or restricted reservoirs ("minor gas").

In the Tirrawarra Sandstone and Patchawarra Formation, gas in several test flows is interpreted to exist in the liquid phase in the reservoir. These flows are not shown in the Figures or Enclosures but are included in Table 1, identified by the comment "associated gas".

OIL CHARACTERISTICS

Cooper Basin oils are in general similiar to Eromanga Basin oils (Moore, 1985) although they are often more mature reflecting greater depth of burial. Permo-Triassic oils are typically medium to light (30^{o} to 60^{o} API) (Fig. 13) and paraffinic, with variable low to high wax contents. Thus the pour points may range form low to high.

The composition of the oils reflects both source material and maturity. The nC15 to nC25 alkanes which account for the bulk of hydrocarbons in high wax oils were probably produced from a well preserved terrestrial woody-herbaceous source. However, oxidation of the same source material would probably have led to the formation of a light, low wax oil by selective destruction of the high molecular weight hydrocarbon (Tybor, 1985).

A microbial source influence has been interpreted in Cooper-Eromanga Basin crude oils for both these types (Tybor, 1975).

Thermal maturation also may account for the differentiation of oil type. Thus, with the loss of heavier n-alkanes through cracking, oils become lighter and less waxy (Fig. 14) until finally only post-mature condensate and gas remain.

GAS CHARACTERISTICS

Spatial and temporal variation in the characteristics of Cooper Basin gas has previously been reported by Hunt (1985) in "An interim report on the composition of gas in the Gidgealpa Group, Cooper Basin". That report is now included herein.

The gas composition parameters of economic interest are % carbon dioxide, and % wet gas in the Cooper Basin. These parameters, abstracted from the Delhi geological data base were compiled at a scale of 1:250,000, and the median values of the data contoured. The contoured maps, reduced to a scale of 1:500,000, appear in Figures 15 to 22 and Enclosures 11 to 18.

Because of the general sparseness of data, results for adjacent formations have been combined in the following groups.

(a) Merrimelia and Tirrawarra Formations

(b) Patchawarra Formation

(c) Epsilon Formation and Daralingie beds and

(d) Toolachee and Nappamerri Formations.

Most data are available for the Patchawarra Formation, and the pattern of distribution in the Patchawarra Formation has been used as a guide in contouring the distribution in the other intervals. In the enclosures, areas of poor control are indicated by dashing the contours.

1. CARBON DIOXIDE (reported as % molar volume)

The carbon dioxide content of produced gas is important because it dilutes saleable hydrocarbons from which it must be separated. In general the distributions shown in Figures 15 to 18 Enclosures 11 to 14 are based on data from larger rather than smaller flows where possible. Where several values were available for the one well or nearby wells an approximate median value has been taken for the contouring value. Usually where multiple results were available the range of results was small compared with the total variation over the basin.

Vertical variation of % CO_2 in the Permian section is also small compared with the total range of values in the spatial distribution. Thus the spatial patterns shown in overlying intervals are in general similar, and little variation was introduced by combining results from the adjacent intervals.

The distribution of CO_2 in the gas mainly reflects variation in the depth of burial of the Permian sediments rather than thermal maturity. Thus the highest contents are found in the deeper Nappamerri and Patchawarra Troughs and lowest contents are found on the margins and on contemporaneous highs within the basins. The origin of CO_2 in Permian gas of the Cooper Basin has been discussed by Schwebel et al. (1980) and Kantsler et al. (1983).

2. GAS WETNESS

Gas wetness is esentially a measure of the methane content (C_1) of the gas and was calculated by the following formula:

$$\text{Wet Gas} = C_2 + C_3 + C_4 \;/\; C_1 + C_2 + C_3 + C_4 \;\%,$$

following Schwebel et al., (1980). Most gas wetness values fall in the range of 5 - 30%, and values shown in Figures 19 to 22 Enclosures 15 to 18 were calculated from data in the Delhi geological data base. Where data for several samples from the one interval or adjacent bores were available the median value has been used as a contouring value.

The pattern of distribution in the Patchawarra Formation where most data are available, has been used as a guide in contouring the overlying and underlying intervals, and vertical variation in the succession is not large. Control in the northern Cooper Basin is poor because of sparse data.

The pattern of spatial variation of gas wetness is inversely related to thermal maturity. Thus the content of C_2+ hydrocarbons increases from the Nappamerri Trough to contemporaneous highs within the basin and towards the basin margins.

LOCATION OF GAS DISCOVERIES

The Patchawarra and Toolachee Formations contain the majority of gas reserves in the Cooper Basin (~90% based on Middleton,1985). Within the Patchawarra Formation two major economic provinces are proposed: they are reservoirs disposed around the northwestern (GMI Ridge) and southeastern margin (Della - Nappacoongee, Toolachee and Dullingari - Wolgolla trends) of the Nappamerri Trough, and the Tirrawarra and associated trends within the Patchawarra Trough. The GMI trend also contains most discoveries in the Tirrawarra Sandstone, but discoveries in the overlying Epsilon Formation and Daralingie beds are concentrated on the southeastern margin of the Nappamerri Trough.

Other significant discoveries in the Patchawarra Formation are located on the Pepita - Naccowlah - Jackson (PNJ) Ridge and cross cutting Arrabury trend on the northern margin of the Nappamerri Trough.

For the Nappamerri Trough province the combination of early growth, and justapostion and interfingering of troughs and highs is significant in the location of discoveries particularly on the southeastern margin. In the Patchawarra Trough province discoveries have been made on early growth structures and also within the thicker part of the sequence. This may reflect the cooler geothermal regime within the Patchawarra Trough and consequent preservation of porosity in its deeper parts.

The pattern of discoveries in the Toolachee Formation is similar to that in the Patchawarra Formation except that they are concentrated more around the southern and northwestern margin of the Nappamerri Trough, and do not extend as far towards the margins of the basin. This may reflect a lower level of maturation which is expected in the higher interval.

In the northern Cooper Basin the PNJ Ridge, and Aarabury and Durham Downs trends have also flowed gas from the Toolachee Formation. Within the Nappamerri Formation the few gas discoveries are concentrated mainly on the GMI Ridge and Tirrawarra trends.

CONCLUSIONS

Within the better explored South Australian sector of the southern Cooper Basin, there is a clear association between early growth and the juxtaposition of structural elements for hydrocarbon discoveries in the Nappamerri Trough and surrounds. Within the Patchawarra Trough, the thicker parts of the sequence are also prospective probably reflecting a cooler geothermal regime in that area.

By analogy, but without considering variation in maturation, sand development, porosity or seal, the PNJ Trend and southern margin of the Nappamerri Trough, particularly features such as the Orientos trend which projects into the trough, must be considered prospective for Permian gas. Much of the northern Cooper Basin also remains prospective but untested on the basis of this pattern.

REFERENCES

Hunt, J.W., 1985. An interim report on the composition of gas in the Gidgealpa Group, Cooper Basin. Unpubl. report of the Regional Studies Group, Delhi Petroleum Pty Ltd.

Kantsler, A.J., Prudence, T.J.C., Cook, A.C. and Zwigulis, M., 1983. Hydrocarbon habitat of the Cooper/Eromanga Basin, Australia. APEA Jour., 23, 75-92.

Middleton, M.P., 1985. South Australia, PEL 5&6, Exploration summary and five year plan. Unpubl. report of Delhi Petroleum Pty Ltd.

Moore, P.S., 1985. Some basic geochemical facts about Eromanga Basin oils: an update, June 1985. Unpubl. report of the Regional Studies Group, Delhi Petroleum Pty Ltd.

Tybor, P., 1985. Crude oil characterisation correlation study of twenty crude oils from the Cooper - Eromanga Basin, South Australia. An unpubl. report of Analabs to Delhi Petroleum Pty Ltd.

Schwebel, D.A., Devine, S.B. and Riley, M. 1980. Source maturity and gas composition relationships in the southern Cooper Basin. APEA Jour., 20 (1), 191-200.

KEY TO ABBREVIATIONS: - TABLES 1 - 7

HC Type

= hydrocarbon type

Cond. = condensate

* = interpreted from log analysis

Oil Character/ Well or Gas Character/Well

/3 = sample from well No. 3.

Gas Wetness = $\%C_2 + C_3 + C_4/C_1 + C_2 + C_3 + C_4$

Best Flow Rate or Recovery/Well

G = gas	C = cut
C = condensate	T = trace
O = oil	NT = not tested
W = water	rec = recovery
M = mud	V = very
WC = water cushion	S = slightly

Gas flow rate - MMCFD = cubic feet/day x 10^6

Cond. flow rate - BCPD = barrels of condensate/day

Oil flow rate - BOPD = barrels of oil/day

GTS, OTS = gas/oil to surface, rate not recorded

RTSTM = gas to surface, rate to small to be measured

NGTS, NOTS = no gas/oil to surface

eg 202m (or B) VSGCMWTO/2

= 202 metres (or barrels) very slightly gas cut muddy water, trace oil/well No. 2.

Comment

tight = low porosity (<9%) or permeability or both
marginal Sw= approx. 50% water saturation
restricted = limited development of reservoir
variable = variable porosity/permeability in reservoir
minor = mainly water saturated reservoir but with some hydrocarbon saturation 50%

Note: all wells appearing in Tables 1 - 7 are considered to have some hydrocarbon saturation >50%, although the hydrocarbons are not necessarily be recoverable.

TABLE 1: MERRIMELIA SANDSTONE HYDROCARBON DISCOVERIES AND OCCURRENCES

D[redacted]overy Well	Discovery Date	HC Type	Oil Character/Well Gravity (°API)	Oil Character/Well Pour Point (°C)	Gas Character/Well CO_2 (%)	Gas Character/Well Gas Wetness (%)	Best Flow Rate or Recovery/Well	Comment
B[redacted]runa 1	1982	Gas*			-	-	RTSTM/1	marginal Sw
Gidgealpa 3	1963	Gas			-	-	2-3 MMCFD/3	variable

TABLE 2: TIRRAWARRA SANDSTONE HYDROCARBON DISCOVERIES AND OCCURRENCES

covery Well	Discovery Date	HC Type	Oil Character/Well Gravity (°API)	Oil Character/Well Pour Point (°C)	Gas Character/Well CO_2 (%)	Gas Character/Well Gas Wetness (%)	Best Flow Rate or Recovery/Well	Comment
ree 1	1982	Oil	47.1/1	9/1			rec. 9m 0,55m OCM, 27m SOCM 301m WTO, 110m MTO/1	tight
Lake 1	1971	Gas			33.8/35	0.0/35	4.6 MMCFD/35	Variable/tight
Bookabourdie 1	1984	Gas			-	-	8.7 MMCFD/1	
"	"	Cond.	42.5/2	-6/2			223 BCPD/1	
B. lga 2	1972	Gas			26.0/1	44.8/1	0.1 MMCFD/2	tight, associated gas.
"	"	Oil	-	-			rec. 30m 0, 73m O&GCM, 110m GCMW, 55m O&GCM/2	
Coonatie 1	1971	Gas			16.6/1	23.7/1	0.2 MMCFD/2	tight
Lake 1	1971	Gas			-	-	2.5 MMCFD/6	associated gas
"	"	Oil	40.8/1	6/1			450 BOPD/6	
dgealpa 16	1979	Gas			15.1/16	14.0/16	1.1 MMCFD/16	
" 7	1965	Oil	31.0/7	-			rec. 84m 0, 159m MW/7	marginal Sw
k Lake 1	1982	Gas*			-	-	RTSTM/1	high Sw
owana 1	1973	Gas			20.4/1	33.6/1	0.3 MMCFD/1	associated gas
"	"	Oil	-	-			rec. 305m GCMW, 244m VGMWTO/1	formation damage
rieke 1	1971	Oil	-	-			rec. 37m G&SOCM/1	tight
leptian 1	1984	Oil	-	-			29m VO&GCW, 170m VSO&GCW, 209m GCW, 169m VM&GCW/1	marginal Sw
Merrimelia 13	1982	Gas			15.4/13	9.1/13	9.2 MMCFD/14	
"	"	Oil	41.9/13	-5/13			rec. 0.3m 0, 20m W/13	restricted, minor oil
Mitchie 1	1982	Gas			-	-	0.3 MMCFD/1	tight
ari 1	1971	Gas			24.4/1	41.8/1	1.5 MMCFD/6	associated gas
"	"	Oil	39.8/6	2/6			404 BOPD/6	
drangie 2	1972	Gas			21.0/2	40.0/2	0.2 MMCFD/2	tight
"	"	Oil	43.7/2	11/2			rec. 235m G&OCM/2	tight
Packsaddle 1	1970	Oil*	-	-			NT	? tight
ta 1	1984	Oil	-	-			rec. 350m 0, 1067m 0 &GCM, 503m W/1	misrun
Tirrawarra 1	1970	Gas			39.2/1	23.4/1	4.0 MMCFD/2	associated gas
"	"	Oil	49.2/9	3/9			1536 BOPD/2	
Toonman 1	1983	Gas			-	-	0.04 MMCFD/1	tight
kina 1	1982	Gas			17.2/1	41.4/1	0.7 MMCFD/1	associated gas
"	"	Oil	48.8/1	-6/1			rec 10BO, 13BO&C, 79BO&C&M/1	
urra 1	1970	Oil	-	-			rec 18m 0, 198m M &GCWC, 76m GCM/1	tight

TABLE 3: PATCHAWARRA FORMATION HYDROCARBON DISCOVERIES AND OCCURRENCES

[illegible]covery W[illegible]	Discovery Date	HC Type	Oil Character/Well Gravity (°API)	Oil Character/Well Pour Point (°C)	Gas Character/Well CO_2 (%)	Gas Character/Well Gas Wetness (%)	Best Flow Rate or Recovery/Well	Comment
[illegible]ree 1	1982	Gas			27.4/1	22.0/1	3.0 MMCFD/1	
"	"	Cond.	-	-			12 BCPD/1	
[illegible]na 1	1985	Gas			-	-	9.4 MMCFD/1	
"	"	Cond.	43.0/1	-				
[illegible]lera 1	1984	Gas			16.9/1	16.4/1	8.5 MMCFD/1	
"	"	Cond.	39.4/1	12/1			160 BCPD/1	
[illegible]gundi 1	1985	Gas			-	-	8.9 MMCFD/1	
"	"	Oil	41.2/1	-			rec 12m O, 21m SOCW/1	
Baratta 1	1985	Gas			-	-	3.7 MMCFD/1	
[illegible]rolka 1	1976	Gas			-	-	1.6 MMCFD/1	
B[illegible]rolka E. 1	1982	Gas			-	-	0.1 MMCFD/1	tight
[illegible]rvulah 1	1984	Gas			17.9/1	2.1/1	4.3 MMCFD/1	
B[illegible]ibush 1	1980	Gas			4.1/1	13.3/1	1.5 MMCFD/1	mainly tight, restricted
[illegible] Lake 1	1971	Gas			23.9/1	2.8/1	9.6 MMCFD/33	
B[illegible]la 1	1984	Gas			8.5/1	15.0/1	0.2 MMCFD/1	high Sw
[illegible]kabourdie 1	1984	Gas			2.3/2	19.4/2	0.1 MMCFD/1	variable
"	"	Cond.	53/2	3/2				
Brolga 1	1972	Gas			24.5/1	21.8/1	7.8 MMCFD/2	middle Patchawarra
"	"	Cond	50.6/1	-3/1				
"	"	Oil	-	-			70 BOPD/2	basal Patchawarra
[illegible]mby 1	1972	Gas			17.8/1	6.5/1	7.2 MMCFD/2	
B[illegible]e 1	1972	Gas			-	-	8.7 MMCFD/1	
[illegible]rley 1	1971	Gas			-	-	NGTS	tight
[illegible]lum 1	1983	Gas			-	-	9.0 MMCFD/1	
"	"	Cond.	-	-			13 BCPD/1	
[illegible]chilara 1	1978	Gas			19.6/1	9.4/1	0.4 MMCFD/1	marginal Sw, tight
C[illegible]natie 1	1971	Gas			12.0/2	18.9/2	0.5 MMCFD/2	tight
[illegible]ppers Creek 1	1971	Gas			-	-	0.3 MMCFD/1	tight
[illegible] apirrie 1	1980	Gas			18.8/1	18.9/1	4.0 MMCFD/1	tight
"	"	Cond.	41.7/1	10/1				
[illegible]lingie 2	1967	Gas			6.6/11	17.1/11	7.9 MMCFD/9	
"	"	Cond.	49.0/11	-15/11				
[illegible]la 8	1980	Gas			13.1/10	4.6/10	11.7 MMCFD/10	
" 1	1970	Oil	26.0/1	-			rec. 853m GCO emulsified W/1	
[illegible]hee 1	1981	Gas			19.4/1	8.1/1	3.6 MMCFD/1	
Du[illegible]ingari 2	1972	Gas			18.0/2	5.7/2	8.7 MMCFD/2	
[illegible]lingari N.1	1979	Gas			18.5/4	4.9/4	9.6 MMCFD/1	
[illegible]am Downs 2	1984	Gas			-	-	0.2 MMCFD/2	tight
E[illegible]silon 1	1972	Gas			12.5/1	7.6/1	5.8 MMCFD/1	restricted
"	"	Cond.	43.0/1	9/1				

TABLE 3: PATCHAWARRA FORMATION HYDROCARBON DISCOVERIES AND OCCURRENCES (Continued)

Discovery Well	Discovery Date	HC Type	Oil Character/Well Gravity (°API)	Oil Character/Well Pour Point (°C)	Gas Character/Well CO_2 (%)	Gas Character/Well Gas Wetness (%)	Best Flow Rate or Recovery/Well	Comment
F Lake 1	1971	Gas			27.7/1	23.0/1	10.0 MMCFD/6	middle Patchawarra
"	"	Oil	46.9/7	-5/7			OTS/7	basal Patchawarra
G ealpa 3	1964	Gas			10.7/5	34.0/5	6.0 MMCFD/5	
"	"	Cond.	-	-			408 BCPD/17	
J k Lake 1	1982	Gas			22.6/1	25.0/1	9.2 MMCFD/1	
"	"	Cond.	42.3/1	-5/1				
K owana 1	1973	Gas			45.3/1	20.7/1	8.5 MMCFD/1	
"	"	Cond.	36.1/1	-2/1				
Karmona 1	1976	Oil	-	-			rec. 229m O, 57m MWCO/1	
K ona East 1	1982	Gas			10.7/1	19.0/1	3.1 MMCFD/1	
"		Cond.	58.7/1	-5/1			110 BCPD/1	
K lor 1	1984	Gas			17.9/1	15.7/1	10.0 MMCFD/1	
K a 1	1981	Gas			18.7/2A	14.5/2A	7.0 MMCFD/2A	
"	"	Cond.	45.6/1	-5/1				
K an 2	1979	Gas			10.8/3	15.5/3	2.2 MMCFD/3	
"	"	Cond.	50.4/1	-21/1				
K y 1	1978	Gas			28.1/1	0.0/1	2.5 MMCFD/1	tight
Ku ieke 1	1971	Gas			29.1/1	23.8/1	0.3 MMCFD/1	tight
L eptian 1	1984	Gas			38.9/1	22.9/1	6.5 MMCFD/1	
"	"	Cond.	41.9/1	-15/1				
Lowanna 1	1984	Gas			19.4/1	5.2/1	RTSTM/1	tight
M imelia 4	1964	Gas			15.5/1	22.3/1	2.8 MMCFD/4	
Mi..gana 1	1983	Gas*			-	-	RTSTM/1	tight
M lion 1	1984	Gas*			-	-	RTSTM/1	tight
Mc ba 1	1966	Gas			28.2/7	0.0/7	7.3 MMCFD/6	tight
Moomba Nth 1	1984	Gas			-	-	1.5 MMCFD/1	
M ari 1	1971	Gas			-	-	14.9 MMCFD/1	
"	"	Cond.	55.4/1	-				
M ra 1	1981	Gas			3.6/2	3.7/2	9.5 MMCFD/2	
Mu angie 1	1970	Gas			34.8/2	13.8/2	3.9 MMCFD/1	
M kah 1	1983	Gas			-	-	8.5 MMCFD/2	mineral
"	"	Cond.	-	-			132 BCPD/2	
Munkarie 1	1978	Gas			13.9/1	15.6/1	9.9 MMCFD/3	
"	"	Cond.	45.4/1	-5/1			122 BCPD/4	
Packsaddle 1	1970	Gas			2.7/1	3.7/1	2.3 MMCFD/1	generally tight
P ing 1	1980	Gas*			20.7/1	15.6/1	RTSTM/1	generally tight
Pe ita 1	1979	Gas*			-	-	NGTS/1	tight
P drinie 1	1983	Gas*			12.3/1	4.9/1	RTSTM/1	marginal Sw
R ona 1	1982	Gas			36.1/1	25.0/1	6.3 MMCFD/1	
"	"	Cond.	41.9/1	-5/1				
R neath 1	1969	Gas			11.4/1	16.8/1	8.0 MMCFD/1	
"	"	Cond.	-	-			26 BCPD/1	

TABLE 3: PATCHAWARRA FORMATION HYDROCARBON DISCOVERIES AND OCCURRENCES (Continued)

covery l	Discovery Date	HC Type	Oil Character/Well Gravity (°API)	Oil Character/Well Pour Point (°C)	Gas Character/Well CO_2 (%)	Gas Character/Well Gas Wetness (%)	Best Flow Rate or Recovery/Well	Comment
ke Hole 1	1984	Gas*			20.6/1	24.3/1	RTSTM/1	variable Sw, tight
Strzelecki 15	1983	Oil	42/15	-			38m O, 47m G&OCMW 93m SGCW/15	marginal Sw
lalia 1	1970	Gas			-	-	0.3 MMCFD/1	high Sw
Tartulla 1	1981	Gas*			-	-	RTSTM/1	tight
ee Queens 1	1984	Gas*			-	-	NGTS/1	tight
Tindilpie 1	1970	Gas			-	-	1.8 MMCFD/1	
rawarra 1	1970	Gas			34.3/9	21.2/9	10.1 MMCFD/25	
"	"	Cond.	44.6/8	4/8			362 BCPD/45	
"	"	Oil	-	-				rec. on production
rawarra W	1983	Gas			35.7/1	24.8/1	2.3 MMCFD/1	generally tight
Toolachee 1	1969	Gas			12.5/9	13.1/9	11.0 MMCFD/13	
"	"	Cond.	54.4/30	-25/30				
Toonman 1		Gas			-	-	0.2 MMCFD/1	tight
coocha 2	1984	Gas			1.4/2	27.1/2	2.2 MMCFD/2	associated gas
"	"	Oil	45.4/2	21/2			1747 BOPD/2	
ptana 1	1981	Gas*			-	-	NGTS/1	tight
oinnie 1	1979	Gas			13.8/1	11.7/1	1.8 MMCFD/1	
Wimma 1	1981	Gas*			-	-	GTS/1	tight
jolla 1	1973	Gas			10.3/1	21.0/1	1.9 MMCFD/1	
Woo 1	1978	Gas			23.3/1	8.1/1	0.1 MMCFD/1	tight
cumma 1	1980	Gas*			20.0/1	19.3/1	RTSTM/1	tight
ia 1	1984	Gas			15.4/1	14.8/1	9.9 MMCFD/1	
"	"	Cond.	39.0/2	9/2			195 BCPD/1	
eni 1	1981	Gas			-	-	0.1 MMCFD/1	tight

TABLE 4: EPSILON FORMATION HYDROCARBON DISCOVERIES AND OCCURRENCES

Discovery Well	Discovery Date	HC Type	Oil Character/Well Gravity (°API)	Oil Character/Well Pour Point (°C)	Gas Character/Well CO_2 (%)	Gas Character/Well Gas Wetness (%)	Best Flow Rate or Recovery/Well	Comment
Ashby 1	1978	Gas			8.3/1	6.5/1	7.2 MMCFD/1	
Big Lake 6	1971	Gas			18.0/6	9.1/6	7.7 MMCFD/6	
Burley 1	1971	Gas			27.8/2	2.4/2	0.9 MMCFD/1	
Burke 4	1972	Gas			-	-	0.5 MMCFD/2	restricted
Coonchilara 1	1978	Gas			14.9/1	18.8/1	0.2 MMCFD/1	
Coonatie 1	1971	Gas			30.2/1	24.2/1	1.2 MMCFD/1	
Daralingie 1	1967	Gas			-	-	4.0 MMCFD/5	restricted
Dilchee 1	1981	Gas*			17.8/1	13.9/1	RTSTM/1	restricted
Dullingari N 1	1979	Gas			-	-	0.2 MMCFD/1	restricted
Epsilon 2	1972	Gas			11.0/2	10.5/2	1.6 MMCFD/2	
Fly Lake 1	1971	Gas			21.7/1	20.7/1	5.8 MMCFD/1	
Hume 1	1981	Gas*			-	-	NGTS/1	restricted, tight
Innamincka 1	1959	Gas			-	-	0.1 MMCFD/1	restricted
Kerna 1	1981	Gas			13.5/2A	14.1/2A	0.6 MMCFD/1	restricted
Kidman 1	1977	Gas			13.4/1	17.2/1	0.4 MMCFD/1	restricted
Kirby 1	1978	Gas*			-	-	NGTS/1	tight
Kudrieke 1	1971	Gas*			-	-	NGTS/1	tight
Lepena 1	1985	Gas			-	-	6.3 MMCFD/1	
McLeod 1	1983	Gas			31.4/1	0.0/1	0.7 MMCFD/1	tight
Moolion	1984	Gas*			-	-	NT	restricted
Munkarie 1	1983	Gas			11.0/1	15.6/1	7.0 MMCFD/1	variable
"	"	Cond.	47.2/1	-5/1				
Toolachee 1	1969	Gas			8.6/3	25.0/3	9.4 MMCFD/28	
Wills 1	1981	Gas			0.0/1	20.2/1	1.2 MMCFD/1	
Wooloo 1	1978	Gas			17.2/1	27.2/1	0.4 MMCFD/1	restricted
Yalpeni 1	1981	Gas			6.2/1	23.9/1	9.7 MMCFD/1	
"	"	Cond.	49.6/1	-				

TABLE 5: DARALINGIE BEDS HYDROCARBON DISCOVERIES AND OCCURRENCES

Discovery Well	Discovery Date	HC Type	Oil Character/Well		Gas Character/Well		Best Flow Rate or Recovery/Well	Comment
			Gravity (^{o}API)	Pour Point (^{o}C)	CO_2 (%)	Gas Wetness (%)		
Big Lake 2	1972	Gas			14.4/2	6.1/2	7.3 MMCFD/9	
Burke 4	1982	Gas			15.3/1	9.0/1	9.4 MMCFD/4	
Burley 2	1984	Gas*			-	-	NT	tight
Dullingari 2	1972	Gas			13.5/2	13.6/2	7.9 MMCFD/2	
Moomba 1	1966	Gas			15.8/12	9.6/12	9.4 MMCFD/12	

TABLE 6: TOOLACHEE FORMATION HYDROCARBON DISCOVERIES AND OCCURRENCES

Discovery Well	Discovery Date	HC Type	Oil Character/Well Gravity (°API)	Oil Character/Well Pour Point (°C)	Gas Character/Well CO_2 (%)	Gas Character/Well Gas Wetness (%)	Best Flow Rate or Recovery/Well	Comment
A ona 1	1985	Gas			-	-	8.2 MMCFD/1	
rrolka 1	1976	Gas			-	-	1.6 MMCFD/1	
rolka East	1982	Gas			11.0/1	8.5/1	0.2 MMCFD/1	tight
Baryulah 1	1984	Gas			17.0/1	16.4/1	0.4 MMCFD	major gas not tested
Lake 1	1971	Gas			16.1/2	5.9/2	10.4 MMCED/2	
Bu.ke 1	1972	Gas			14.3/1	9.1/1	10.4 MMCFD/1	
rley 1	1971	Gas			28.3/1	0.0/1	0.2 MCFD/1	tight, minor Sh
C llum 2	1983	Gas*			17.1/1	6.6/1	RTSTM/2	restricted
Coonatie 1	1971	Gas			25.4/1	28.0/1	14.4 MMCFD/1	
kwood 1	1981	Gas*			-	-	RTSTM/1	tight, marginal Sw
Della 1	1970	Gas			13.5/6	4.6/6	11.0 MMCFD/1	
"	"	Oil	-	-			rec. 55m MOCM/1	-? minor oil.
D lingari 2	1962	Gas			10.6/2	12.3/2	10.3 MMCFD/17	
"	"	Cond.	41.8/2	-2/2				
ham Downs 1	1973	Gas			10.9/2	17.9/2	10.9 MMCFD/2	
Epsilon 1	1972	Gas			10.6/1	10.5/1	7.4 MMCFD/3	restricted
"	"	Cond.	53.0/3	-25/3			12BCPD/3	variable Sw
Fly Lake 6	1982	Gas*			-	-	NT	restricted
dgealpa 2	1964	Gas			13.8/13	6.1/13	11.2 MMCFD/7	
G gealpa 7	1965	Cond.	35/8	21/8			rec. 10 BCPD/19	
"	"	Oil	33.5/9	21/9			rec. 5 BOPD, 400 BGCWPD/7	minor oil
lamincka 2	1959	Gas			-	-	0.1 MMCFD/2	marginal Sw, ?tight
rmona 1	1976	Oil*	-	-			229m O, 57m MWCO/1	
mona E. 1	1976	Gas			12.4/1	28.7/1	9.7 MMCFD/1	
"	"	Cond.	50.1/1	-5/1			170 BCPD/1	
lman 1	1977	Gas			9.6/1	18.8/1	10.9 MMCFD/1	
"	"	Cond.	46.5/1	-4/1				
by 1	1978	Gas*			23.6/1	3.9/1	RTSTM/1	tight
L ena 1	1985	Gas			-	-	8.4 MMCFD/1	
wanna 1	1984	Gas			12.1/1	18.6/1	0.6 MMCFD/1	tight, marginal Sw
abooka 1	1981	Gas			10.4/2	10.5/2	9.5 MMCFD/2	
Marana 1	1982	Gas			6.0/1	16.7/1	8.3 MMCFD/1	
"	"	Cond.	50.1/1	-5/1				
Mceod 1	1983	Gas			25.2/1	0.0/1	0.3 MMCFD/1	tight
rrimelia	1964	Gas			14.8/5	10.6/5	6.2 MMCFD/14	variable
M lion 1	1984	Gas			-	-	3.8 MMCFD/1	
mba 1	1966	Gas			13.8/10	5.8/10	9.2 MMCFD/10	
rari 1	1971	Gas			20.6/1	20.3/1	13.0 MMCFD/1	
"	"	Cond.	58.0/1	-			240 BCPD/1	
era 1	1981	Gas			-	-	11.0 MMCFD/3	
M rangie 1	1970	Gas			0.9/1	22.2/1	6.1 MMCFD/1	

TABLE 6: TOOLACHEE FORMATION HYDROCARBON DISCOVERIES AND OCCURRENCES (Continued)

Discovery Well	Discovery Date	HC Type	Oil Character/Well Gravity (°API)	Oil Character/Well Pour Point (°C)	Gas Character/Well CO_2 (%)	Gas Character/Well Gas Wetness (%)	Best Flow Rate or Recovery/Well	Comment
M rangie 2	1970	Oil	-	-			rec. 55m OCM,101m GCM, 37m SWCM/2	
kah 1	1983	Gas			-	-	10.3 MMCFD/1	
M karie 4	1978	Gas			6.5/4	19.5/4	8.5 MMCFD/4	
"	"	Cond	-	-			245 BCPD/4	
N cowlah S. 1	1983	Gas			12.0/1	8.1/1	8.4 MMCFD/1	
Nappacoongie 1	1965	Gas			14.4/3	3.9/3	0.4 MMCFD/3	high Sw
drinie 1	1983	Gas			20.8/2	3.5/2	1.5 MMCFD/2	
Strzelecki 1	1971	Gas			6.5/1	13.0/1	5.0 MMCFD/1	
"	"	Cond.	47.5/3	-5/3				
"	"	Oil	38.6/10	25/10			OTS/10	200 BOPD after cleanup
tulla 1	1981	Gas			-	-	7.6 MMCFD/1	
"	1981	Cond.	49.9/1	-5/1				
"	"	Oil	48.0/1	-5/1			rec. 3m O, 40m G&OCWM, 98m G&OCM/1	
dilpie 1	1970	Gas*			-	-	NGTS/1	mainly high Sw
rrawarra 1	1970	Gas			-	-	6.0 MCFD/14	
ara 1	1981	Gas			7.0/1	13.6/1	5.3 MMCFD/1	
"	"	Cond.	48.1/1	-5/1				
tana 1	1981	Gas			-	-	0.5 MMCFD/1	tight
eena 1	1980	Gas			3.5/1	8.8/1	11.4 MMCFD/1	
ma 1	1981	Gas			-	-	1.0 MMCFD/1	
lkina 1	1982	Gas			22.5/1	50.0/1	4.1 MMCFD/1	
"	"	Cond.	55.4/1	-5/1				

TABLE 7: NAPPAMERRI FORMATION HYDROCARBON DISCOVERIES AND OCCURRENCES

Discovery Well	Discovery Date	HC Type	Oil Character/Well		Gas Character/Well		Best Flow Rate or Recovery/Well	Comment
			Gravity (°API)	Pour Point (°C)	CO_2 (%)	Gas Wetness (%)		
Bulah 1	1984	Oil	-	-			Rec 259m GCMTO/1	restricted, high Sw
Bookabourdie 1	1984	Gas			12.2/2	22.1/2	6.9 MMCFD/1	
Da a 4	1971	Gas			-	-	0.1 MMCFD/4	restricted, marginal Sw
Epsilon 3	1985	Gas			7.4/3	14.9/3	7.1 MMCFD/3	
"	"	Cond	46.0/3	-25/3			230 BCPD/3	
Kirby 1	1978	Gas			10.9/1	9.7/1	0.6 MMCFD/1	restricted, tight
Merimelia 2	1965	Gas			11.3/6	11.0/6	10.0 MMCFD/5	
"	"	Oil	33.4/7	25/7	-	-	2850 BOPD/7	
Mackie 1	1984	Gas			-	-	0.1 MMCFD/1	
"	"	Oil	32.1/1	40/1	-	-	rec. 30m 0,894m SGCW/1	high Sw
Moorari 3	1981	Gas			-	-	3.4 MMCFD/3	
Mount Howitt 1	1966	Gas*			-	-	RTSTM/1	restricted
Packsaddle 4	1984	Gas			-	-	6.0 MMCFD/4	
Perrinie 1	1983	Oil	-	-			rec. 91m 0,1981m O&GCW/3	high Sw
Woolkina 1	1982	Oil	53.5/1	-5/1	-	-	rec. 14.2 BGCO, 13 BW, 32.4 BGCM/1	marginal Sw

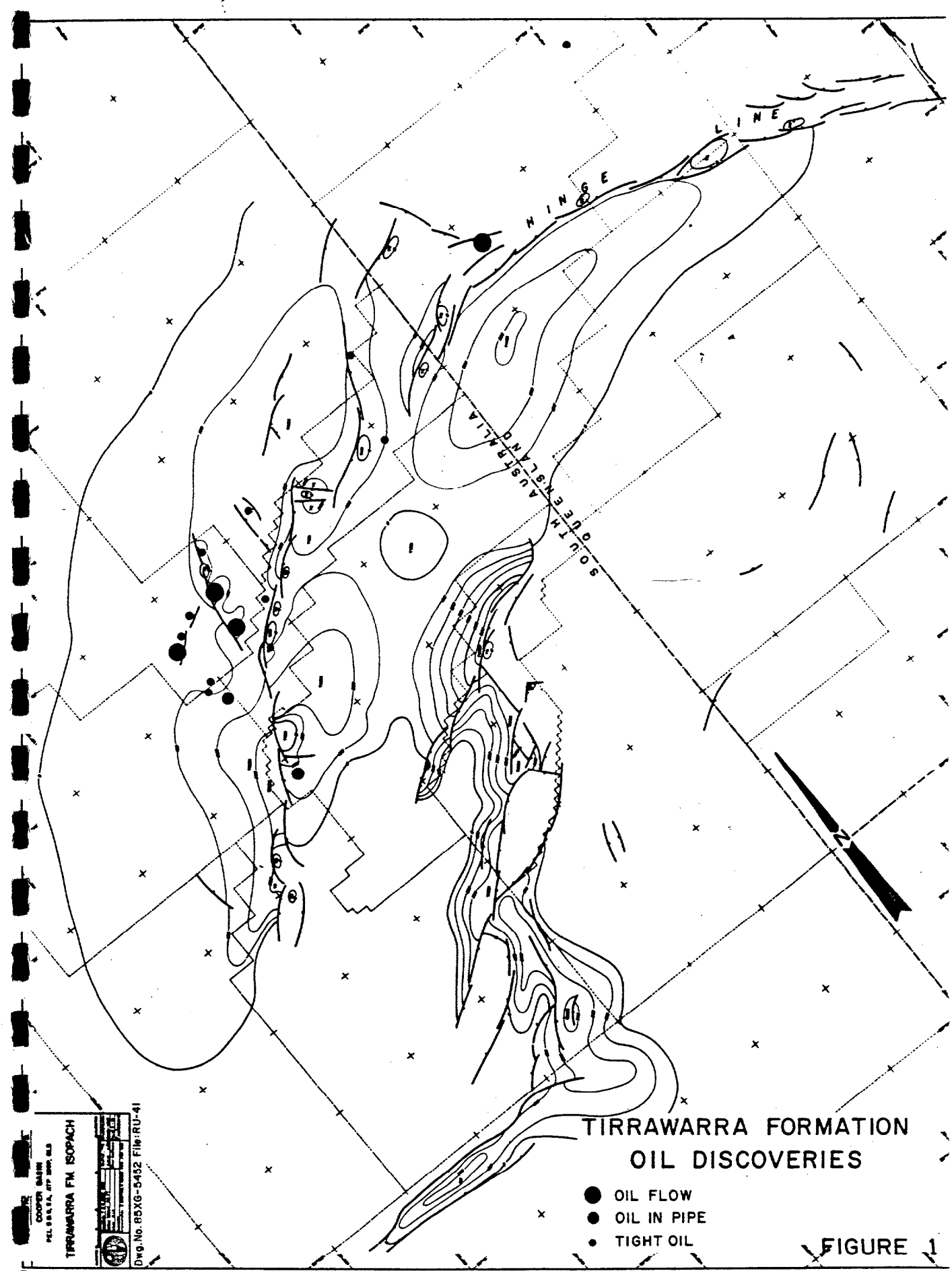
HINGE LINE
SOUTH AUSTRALIA
QUEENSLAND
TIRRAWARRA FORMATION
OIL DISCOVERIES
OIL FLOW
OIL IN PIPE
TIGHT OIL
TIRRAWARRA FM. ISOPACH
Dwg.No.85X6-5452 File:RU-41

FIGURE 1

HINGE LINE
SOUTH GIDGEALPA HIGH
PATCHAWARRA FM.
OIL DISCOVERIES
OIL FLOW
OIL IN PIPE
TIGHT OIL
N
COOPER BASIN
PATCHAWARRA FM ISOPACH
Dwg No. 85XG-5453 File: RU-41

FIGURE 2

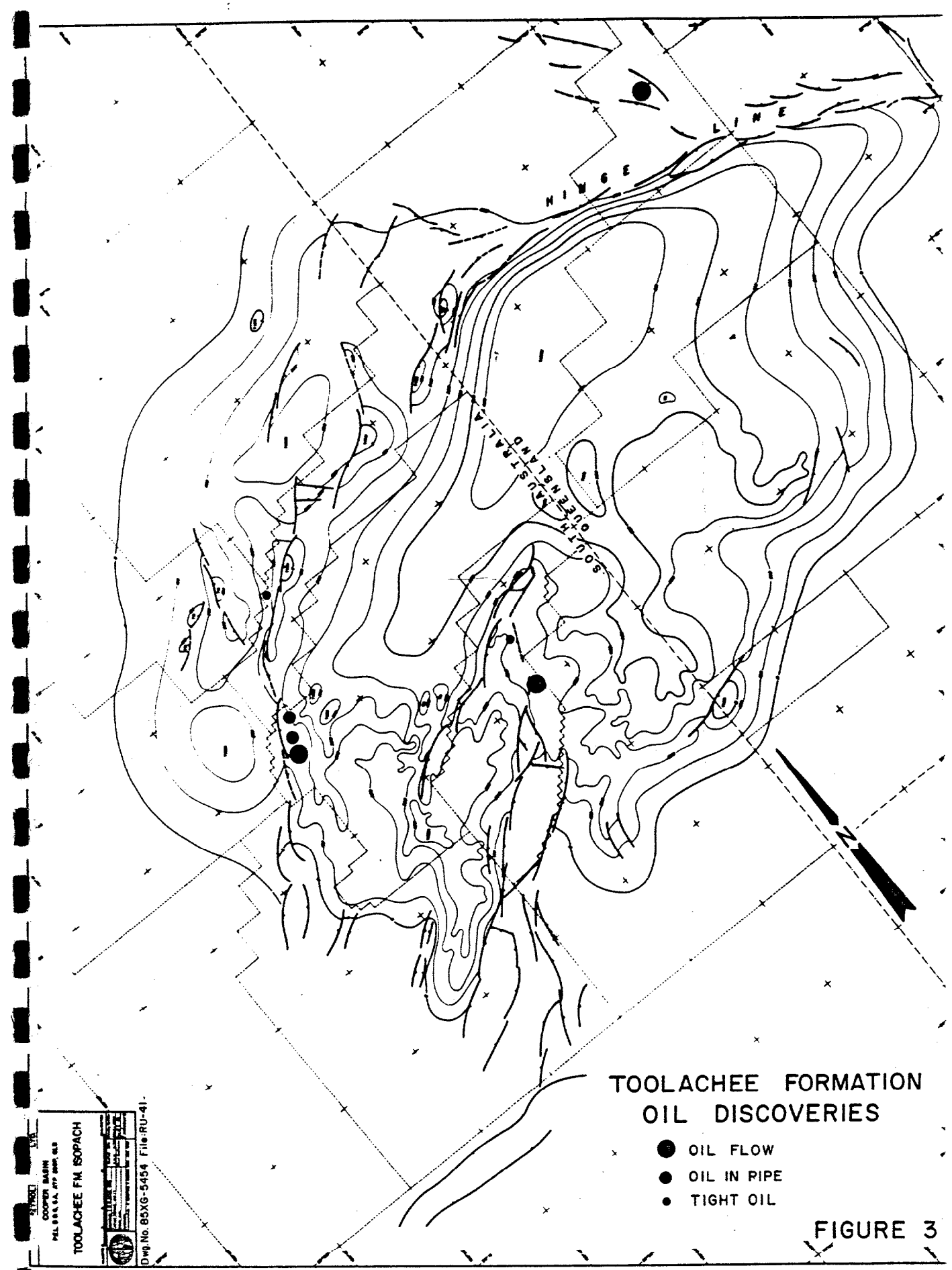
HINGE LINE
SOUTH TAUNQUE ISLAND
N
TOOLACHEE FORMATION
OIL DISCOVERIES
OIL FLOW
OIL IN PIPE
TIGHT OIL
TOOLACHEE FM. ISOPACH
COOPER BASIN
Dwg.No. 85XG-5454 File:RU-41-

FIGURE 3

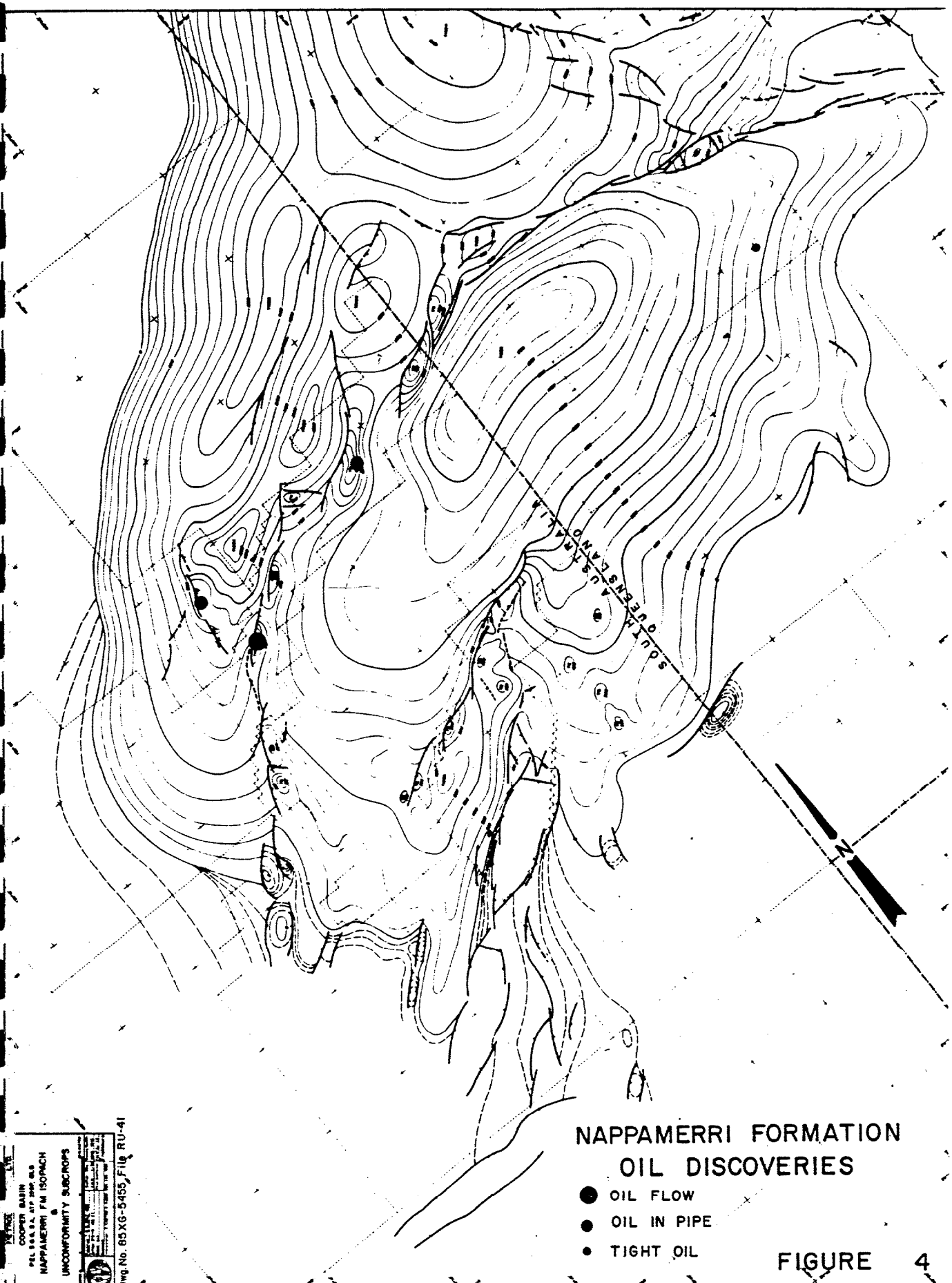

NAPPAMERRI FORMATION
OIL DISCOVERIES

- OIL FLOW
- OIL IN PIPE
- TIGHT OIL

FIGURE 4

COOPER BASIN
NAPPAMERRI FM ISOPACH
&
UNCONFORMITY SUBCROPS

Dwg No. 85XG-5455, File RU-41

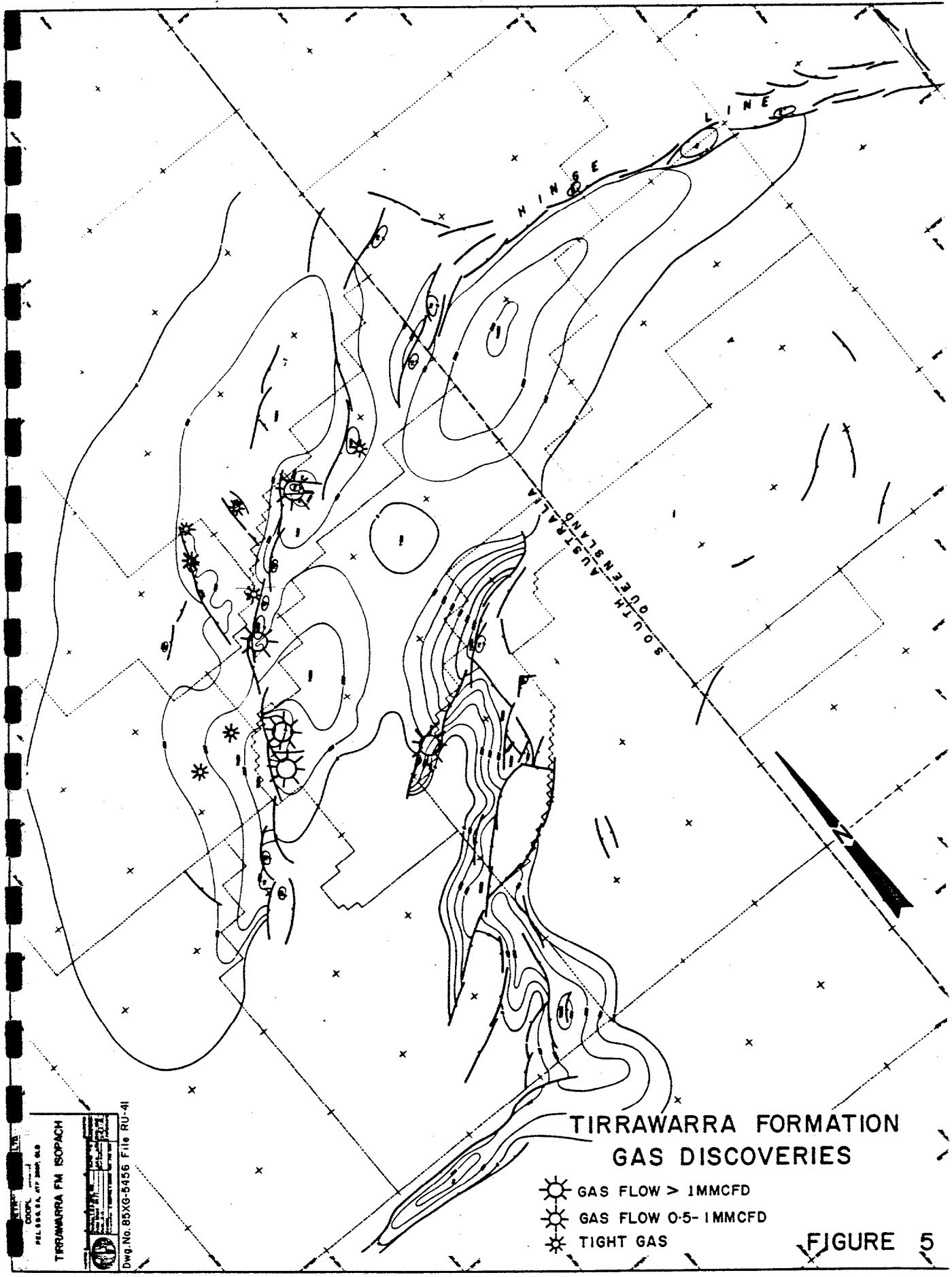
HINGE LINE
SOUTH AUSTRALIA
QUEENSLAND
N
TIRRAWARRA FORMATION
GAS DISCOVERIES
GAS FLOW > 1MMCFD
GAS FLOW 0·5-1MMCFD
TIGHT GAS
TIRRAWARRA FM ISOPACH
Dwg.No. 85XG-5456 File RU-41

FIGURE 5

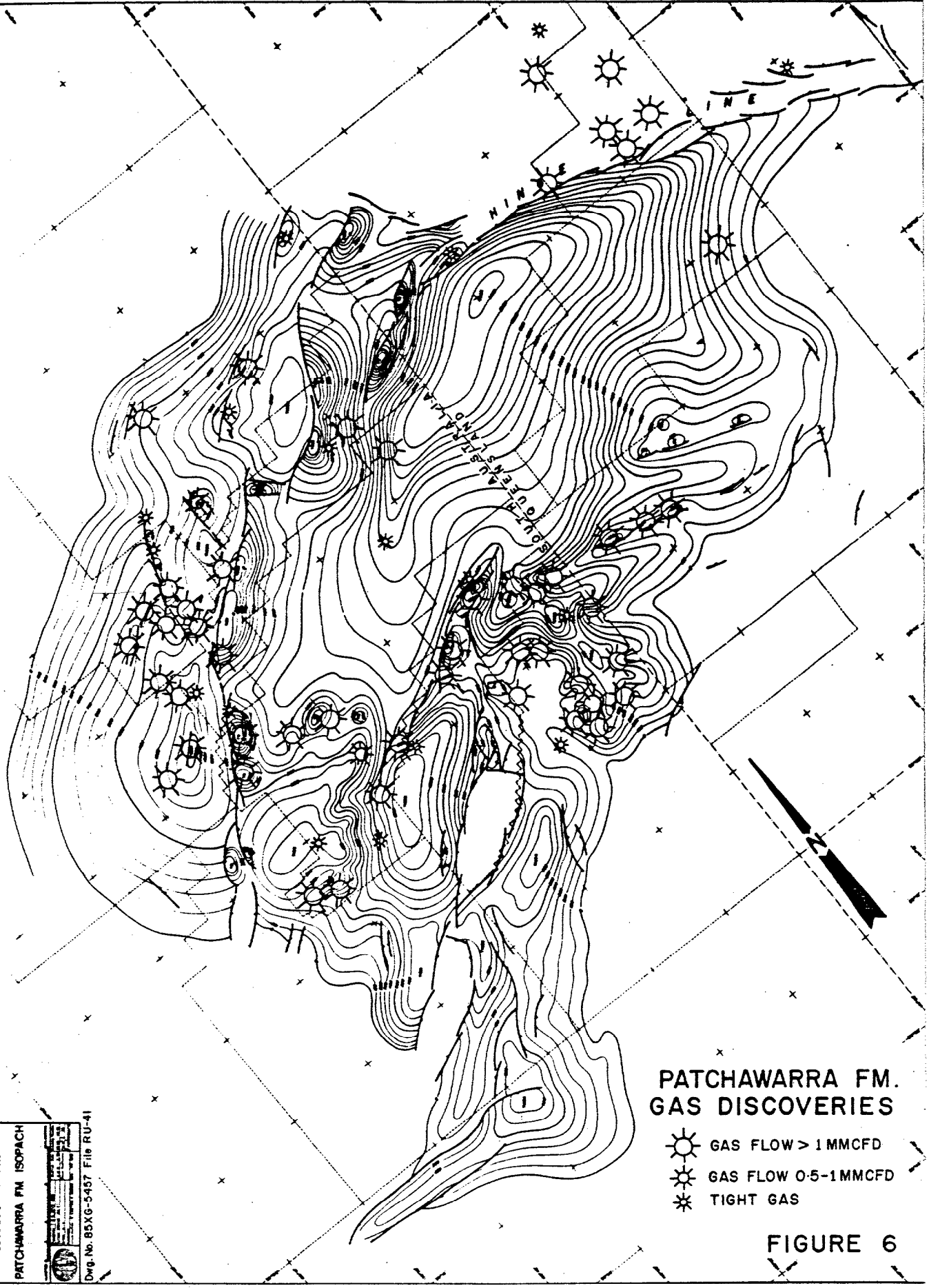
HINGE
HINGE
BLOUDEWATER ESTUARY
PATCHAWARRA FM. GAS DISCOVERIES
GAS FLOW > 1 MMCFD
GAS FLOW 0·5-1 MMCFD
TIGHT GAS
PATCHAWARRA FM ISOPACH
Dwg. No. 85XG-5457 File RU-41

FIGURE 6

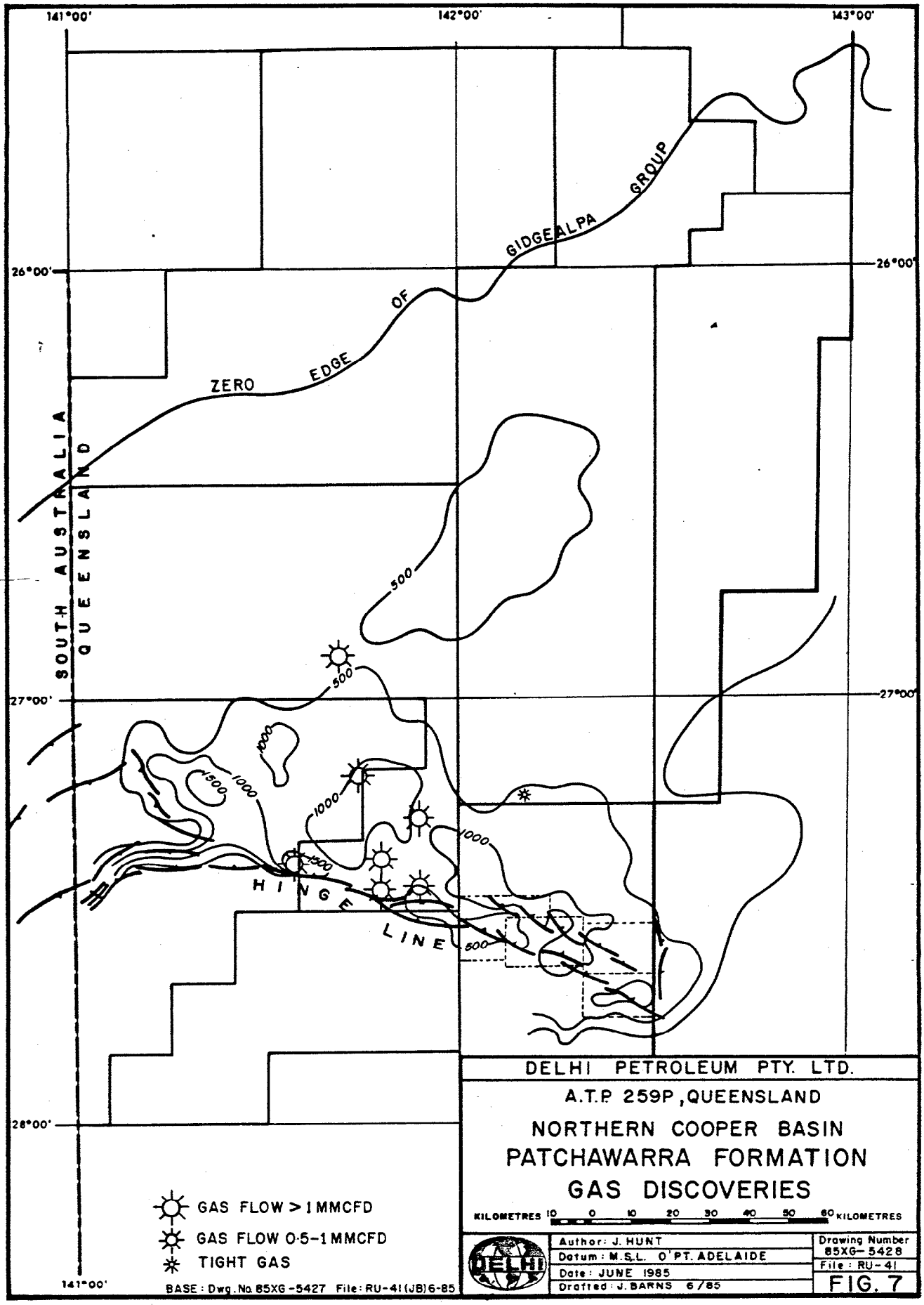
141°00'
142°00'
143°00'
26°00'
27°00'
28°00'
GIDGEALPA GROUP
ZERO EDGE OF
SOUTH AUSTRALIA
QUEENSLAND
500
1000
1500
HINGE LINE
GAS FLOW > 1 MMCFD
GAS FLOW 0·5–1 MMCFD
TIGHT GAS
BASE : Dwg. No. 85XG-5427 File: RU-41(JB)6-85
DELHI PETROLEUM PTY. LTD.
A.T.P. 259P, QUEENSLAND
NORTHERN COOPER BASIN
PATCHAWARRA FORMATION
GAS DISCOVERIES
KILOMETRES 10 0 10 20 30 40 50 60 KILOMETRES
Author: J. HUNT
Datum: M.S.L. O'PT. ADELAIDE
Date: JUNE 1985
Drafted: J. BARNS 6/85
Drawing Number 85XG-5428
File: RU-41
FIG. 7

EPSILON FORMATION
GAS DISCOVERIES

- GAS FLOW > 1MMCFD
- GAS FLOW 0·5-1MMCFD
- TIGHT GAS

FIGURE 8

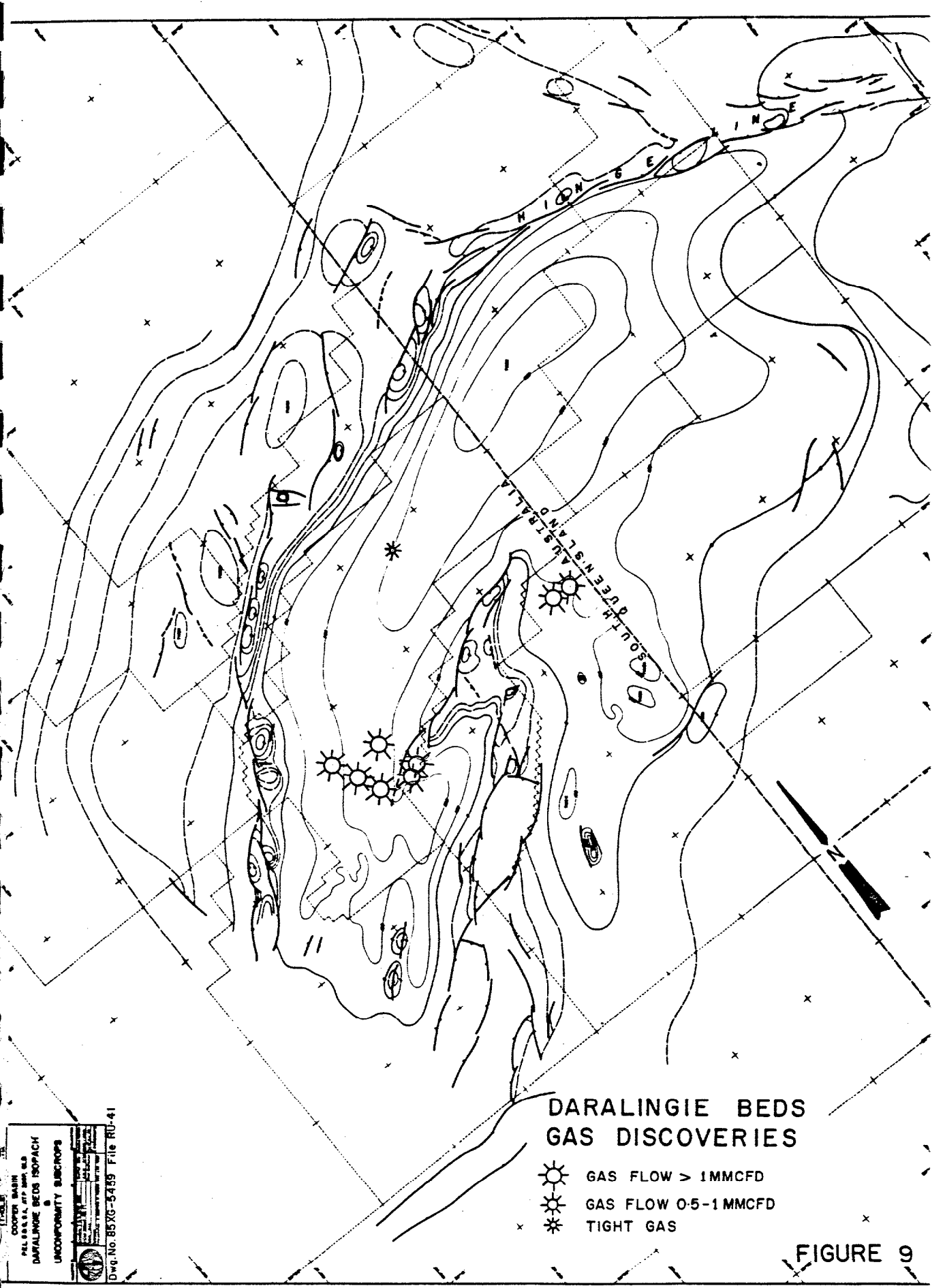
HIDDEN LINE
SOUTH AUSTRALIA
QUEENSLAND
N
DARALINGIE BEDS
GAS DISCOVERIES
GAS FLOW > 1 MMCFD
GAS FLOW 0·5-1 MMCFD
TIGHT GAS
FIGURE 9
COOPER BASIN
DARALINGIE BEDS ISOPACH
&
UNCONFORMITY SUBCROPS
Dwg.No. 85XG-5439 File RU-41

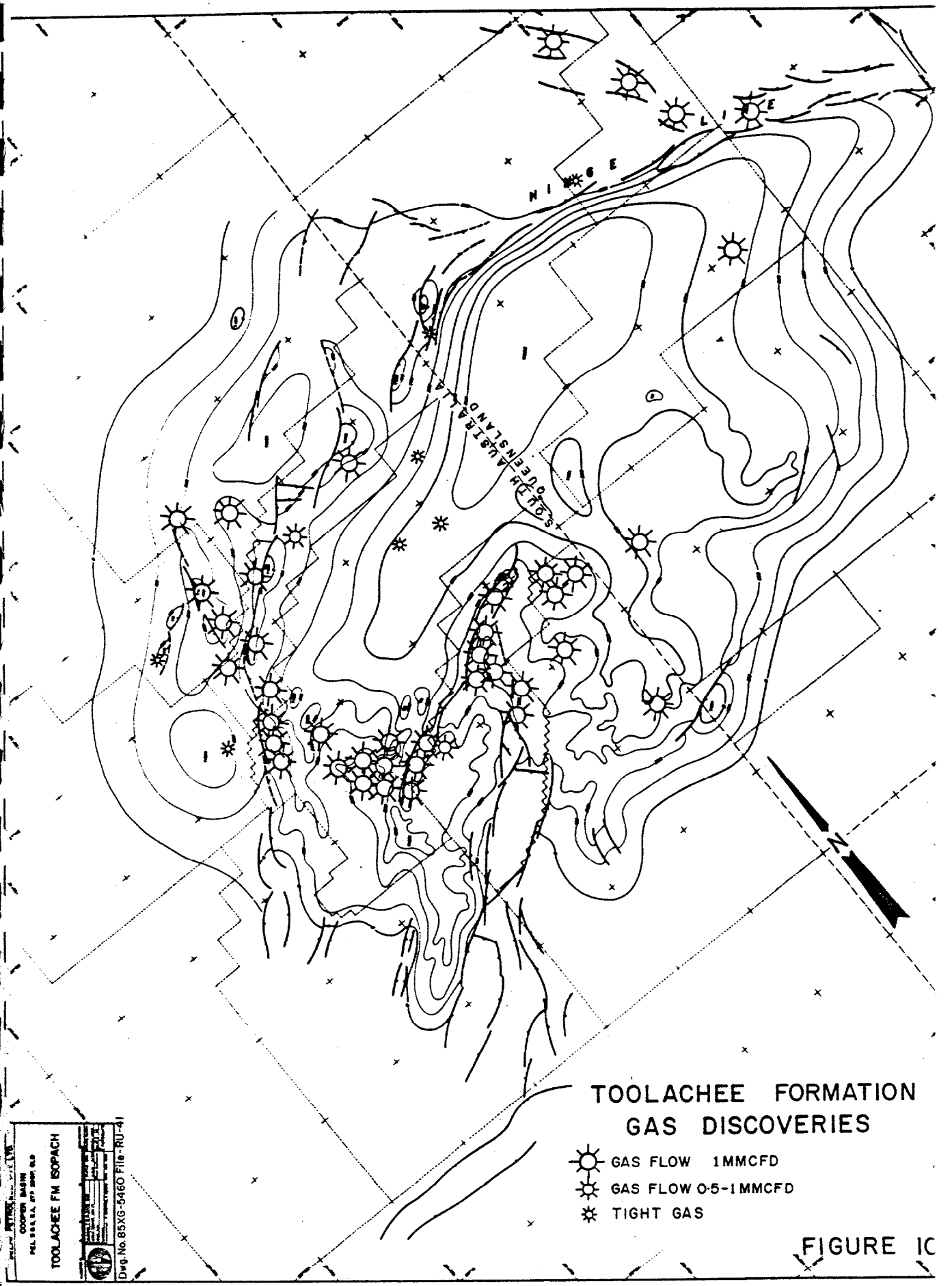
RIDGE
SOUTH QUEENSLAND
N
TOOLACHEE FORMATION
GAS DISCOVERIES
GAS FLOW 1MMCFD
GAS FLOW 0·5-1MMCFD
TIGHT GAS
TOOLACHEE FM ISOPACH
Dwg.No.85XG-5460 File-RU-41

FIGURE 10

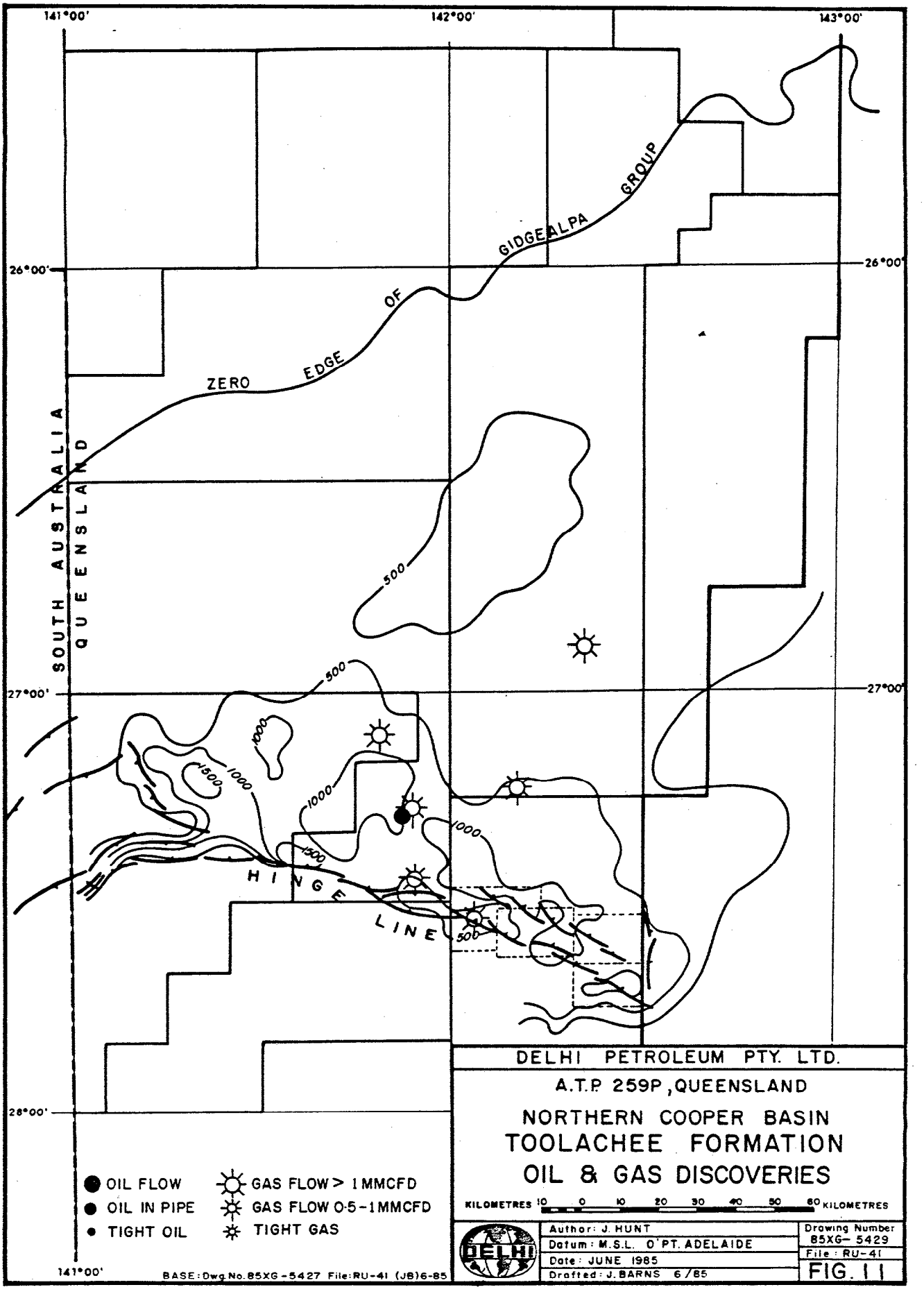
141°00'
142°00'
143°00'
26°00'
27°00'
28°00'
GIDGEALPA GROUP
EDGE OF ZERO
SOUTH AUSTRALIA
QUEENSLAND
500
1000
1500
HINGE LINE
OIL FLOW
OIL IN PIPE
TIGHT OIL
GAS FLOW > 1 MMCFD
GAS FLOW 0·5 - 1 MMCFD
TIGHT GAS
BASE: Dwg. No. 85XG-5427 File: RU-41 (JB)6-85
DELHI PETROLEUM PTY. LTD.
A.T.P. 259P, QUEENSLAND
NORTHERN COOPER BASIN
TOOLACHEE FORMATION
OIL & GAS DISCOVERIES
KILOMETRES 10 0 10 20 30 40 50 60 KILOMETRES
DELHI
Author: J. HUNT
Datum: M.S.L. O'PT. ADELAIDE
Date: JUNE 1985
Drafted: J. BARNS 6/85
Drawing Number 85XG-5429
File: RU-41
FIG. 11

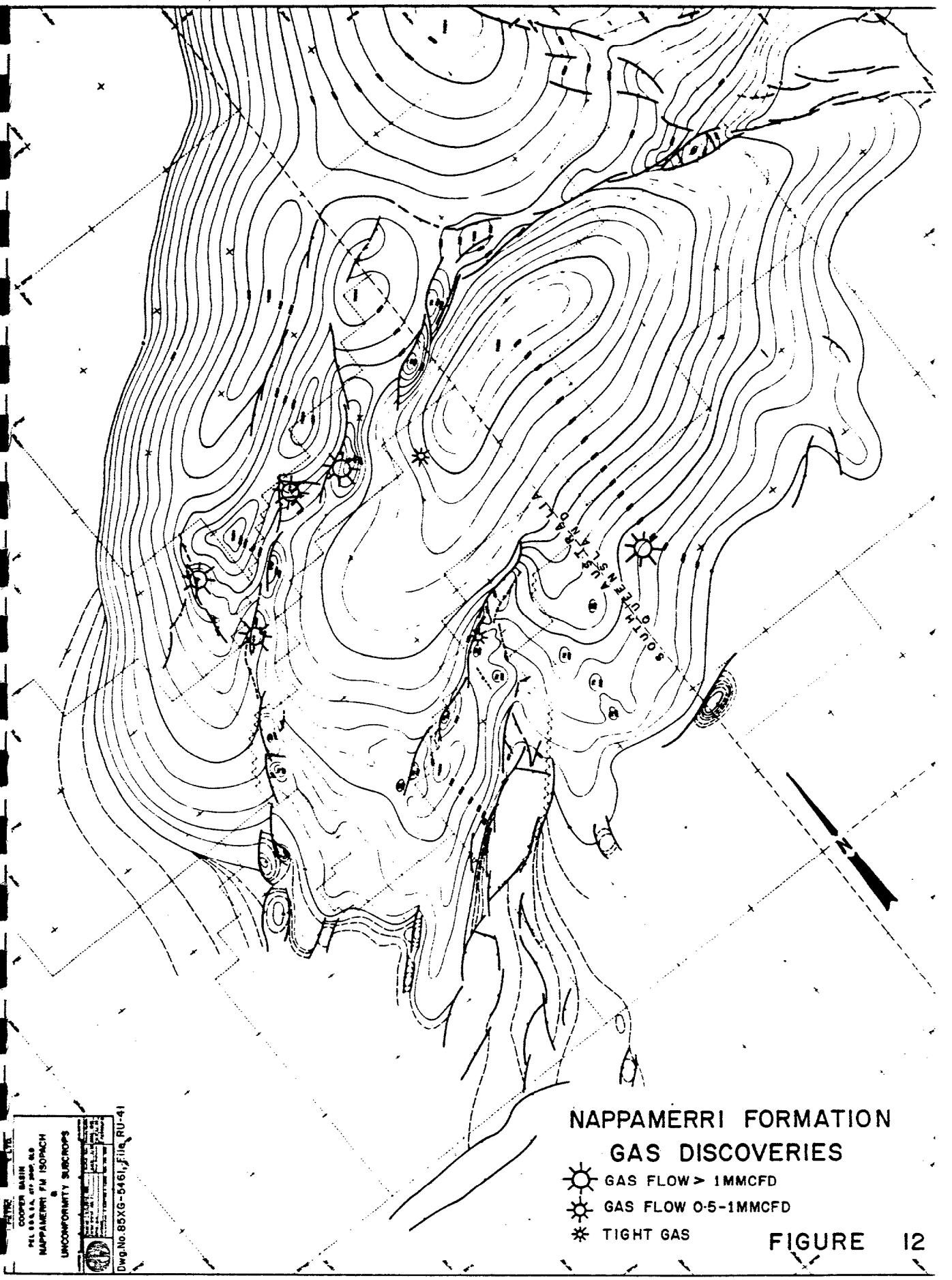
SOUTHERN SHELF
NAPPAMERRI FORMATION
GAS DISCOVERIES
GAS FLOW > 1MMCFD
GAS FLOW 0·5-1MMCFD
TIGHT GAS
FIGURE 12
COOPER BASIN
NAPPAMERRI FM ISOPACH
&
UNCONFORMITY SUBCROPS
Dwg No. 85XG-5461, File RU-41

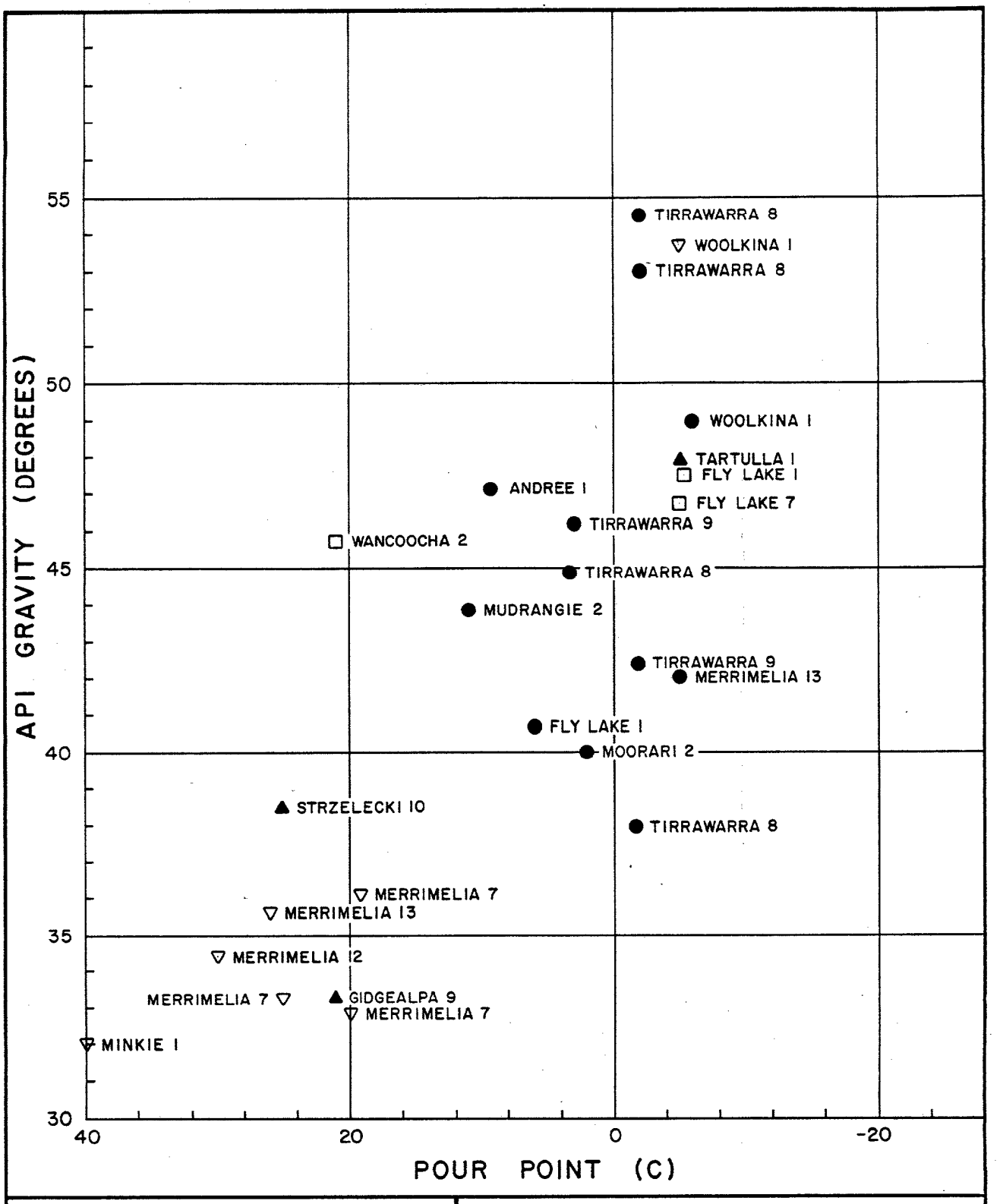

LEGEND

- ▽ - NAPPAMERRI FM.
- ▲ - TOOLACHEE FM.
- ■ - EPSILON FM.
- □ - PATCHAWARRA FM.
- ● - TIRRAWARRA SST.

DELHI PETROLEUM PTY. LTD.

API GRAVITY AND POUR POINT
PERMO-TRIASSIC
OIL

DELHI	Author. J. HUNT	Date. JUNE 1985
	Drafted. W. ASPINALL	Fig. 13
	Dwg. No. 85XG-5479 File. RD-45	

Base Dwg. No. 85XG-5478, File RD-45

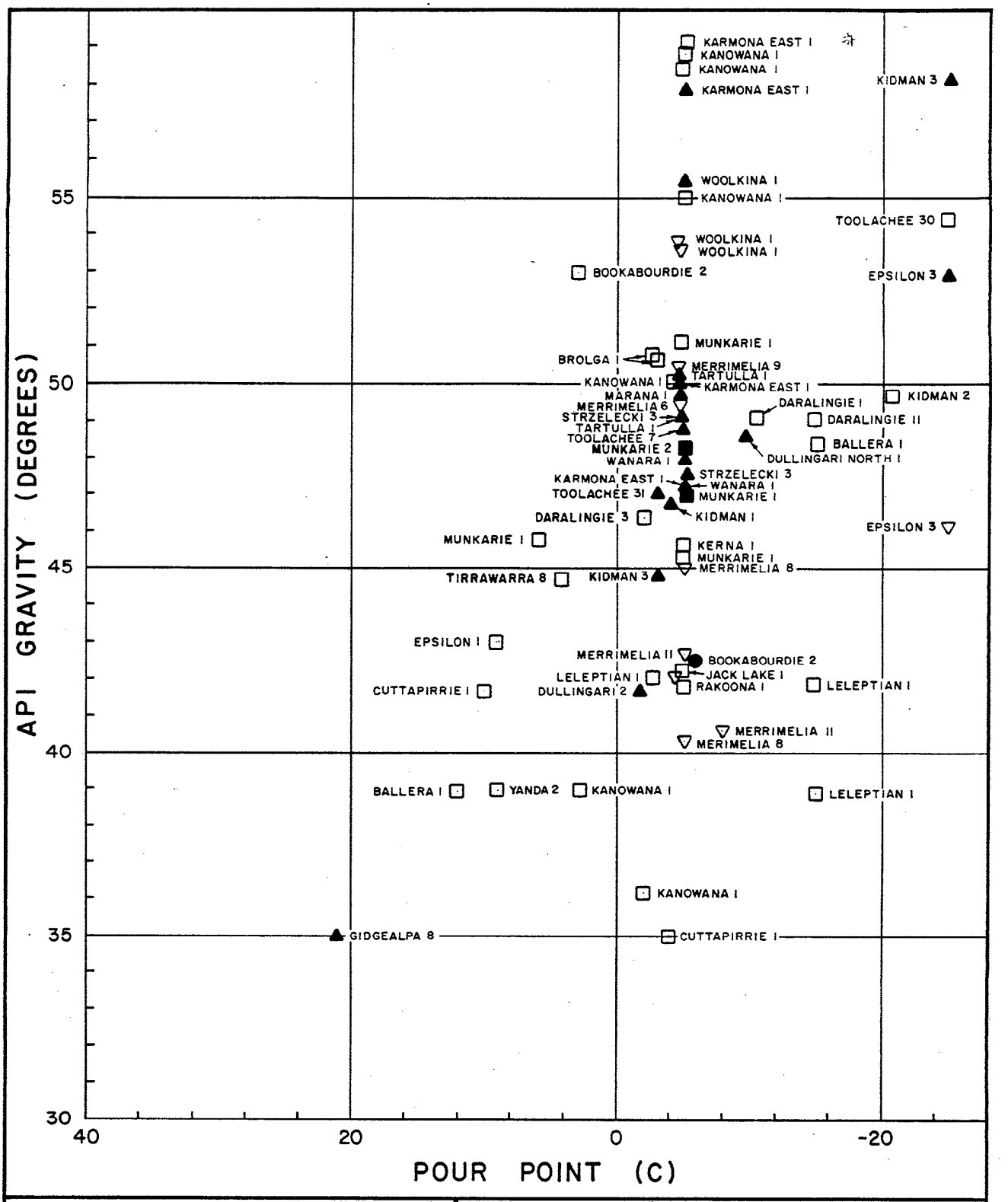

LEGEND

- ▽ - NAPPAMERRI FM.
- ▲ - TOOLACHEE FM.
- ■ - EPSILON FM.
- □ - PATCHAWARRA FM.
- ● - TIRRAWARRA SST.

DELHI PETROLEUM PTY. LTD.

API GRAVITY AND POUR POINT
PERMO-TRIASSIC CONDENSATE

DELHI	Author. J. HUNT	Date. JUNE 1985
	Drafted. W. ASPINALL	Fig. 14
	Dwg. No. 85XG-5480 File. RD-45	

Base Dwg. No. 85XG-5478, File RD-45

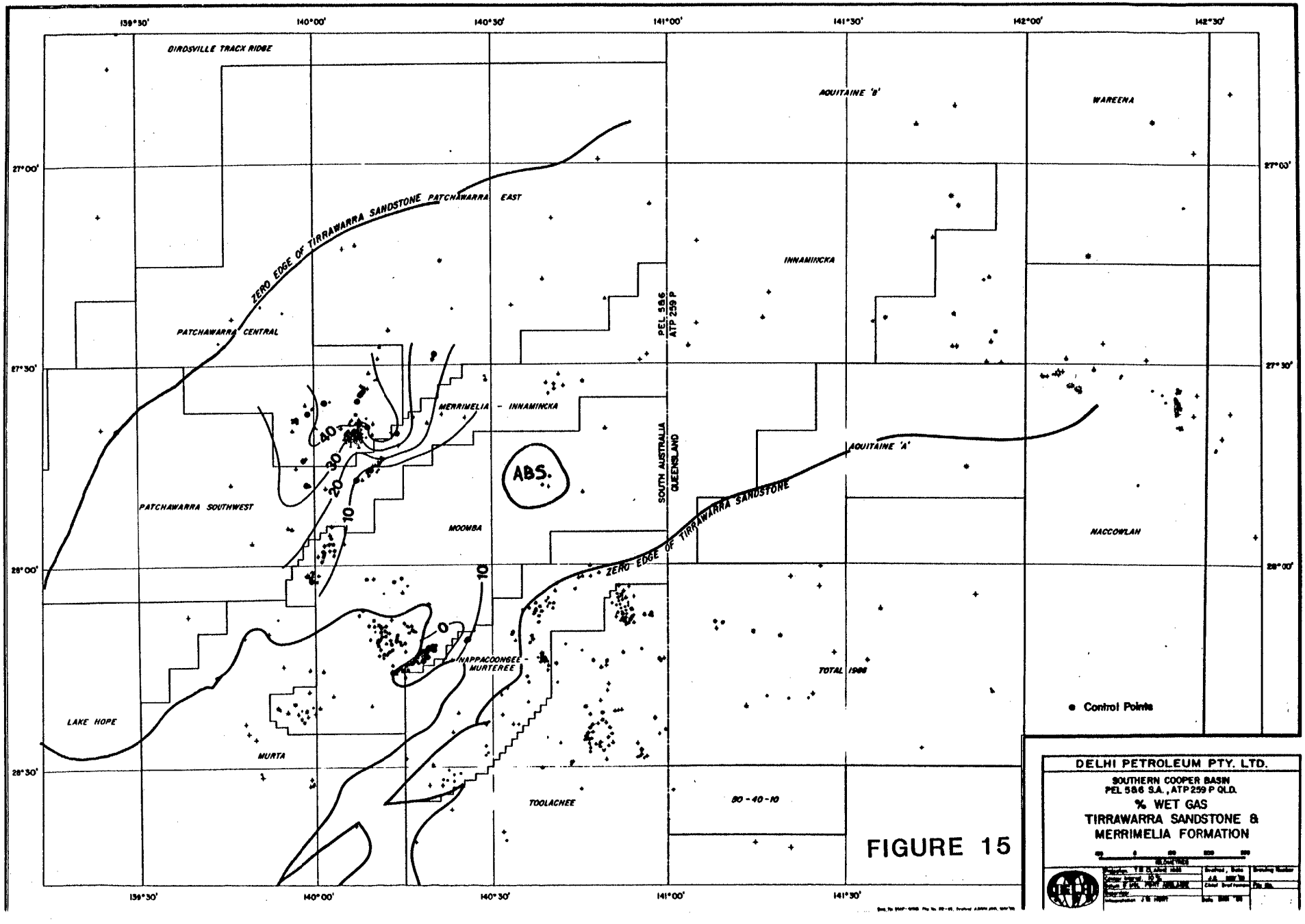
139°30'
140°00'
140°30'
141°00'
141°30'
142°00'
142°30'
27°00'
27°30'
28°00'
28°30'
BIRDSVILLE TRACK RIDGE
AQUITAINE 'B'
WAREENA
ZERO EDGE OF TIRRAWARRA SANDSTONE
PATCHAWARRA EAST
INNAMINCKA
PATCHAWARRA CENTRAL
PEL 586
ATP 259 P
MERRIMELIA - INNAMINCKA
40
30
20
10
ABS.
SOUTH AUSTRALIA
QUEENSLAND
AQUITAINE 'A'
PATCHAWARRA SOUTHWEST
MOOMBA
NACCOWLAH
ZERO EDGE OF TIRRAWARRA SANDSTONE
10
0
NAPPACOONGEE - MURTEREE
TOTAL 1968
Control Points
LAKE HOPE
MURTA
TOOLACHEE
80 - 40 - 10
DELHI PETROLEUM PTY. LTD.
SOUTHERN COOPER BASIN
PEL 586 S.A., ATP 259 P QLD.
% WET GAS
TIRRAWARRA SANDSTONE &
MERRIMELIA FORMATION
FIGURE 15

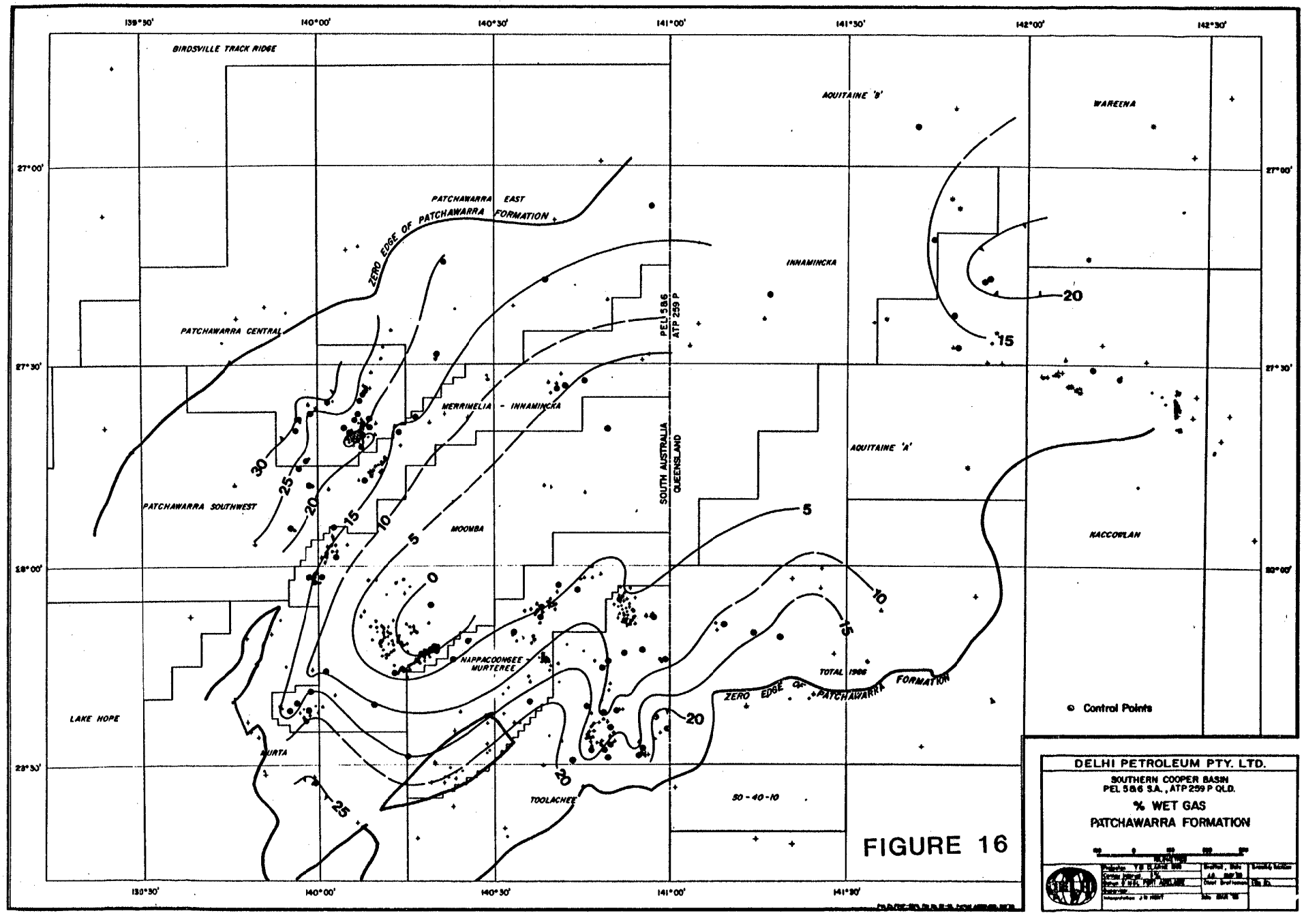
139°30'
140°00'
140°30'
141°00'
141°30'
142°00'
142°30'
27°00'
27°30'
28°00'
28°30'
BIRDSVILLE TRACK RIDGE
AQUITAINE 'B'
WAREENA
PATCHAWARRA EAST
ZERO EDGE OF PATCHAWARRA FORMATION
INNAMINCKA
PATCHAWARRA CENTRAL
PEL 586
ATP 259 P
MERRINELIA - INNAMINCKA
SOUTH AUSTRALIA
QUEENSLAND
AQUITAINE 'A'
PATCHAWARRA SOUTHWEST
MOOMBA
NACCOWLAH
NAPPACOONSEE
MURTEREE
TOTAL 1986
ZERO EDGE OF PATCHAWARRA FORMATION
LAKE HOPE
MURTA
TOOLACHEE
50 - 40 - 10
0
5
10
15
20
25
30
Control Points
DELHI PETROLEUM PTY. LTD.
SOUTHERN COOPER BASIN
PEL 586 S.A., ATP 259 P QLD.
% WET GAS
PATCHAWARRA FORMATION
FIGURE 16

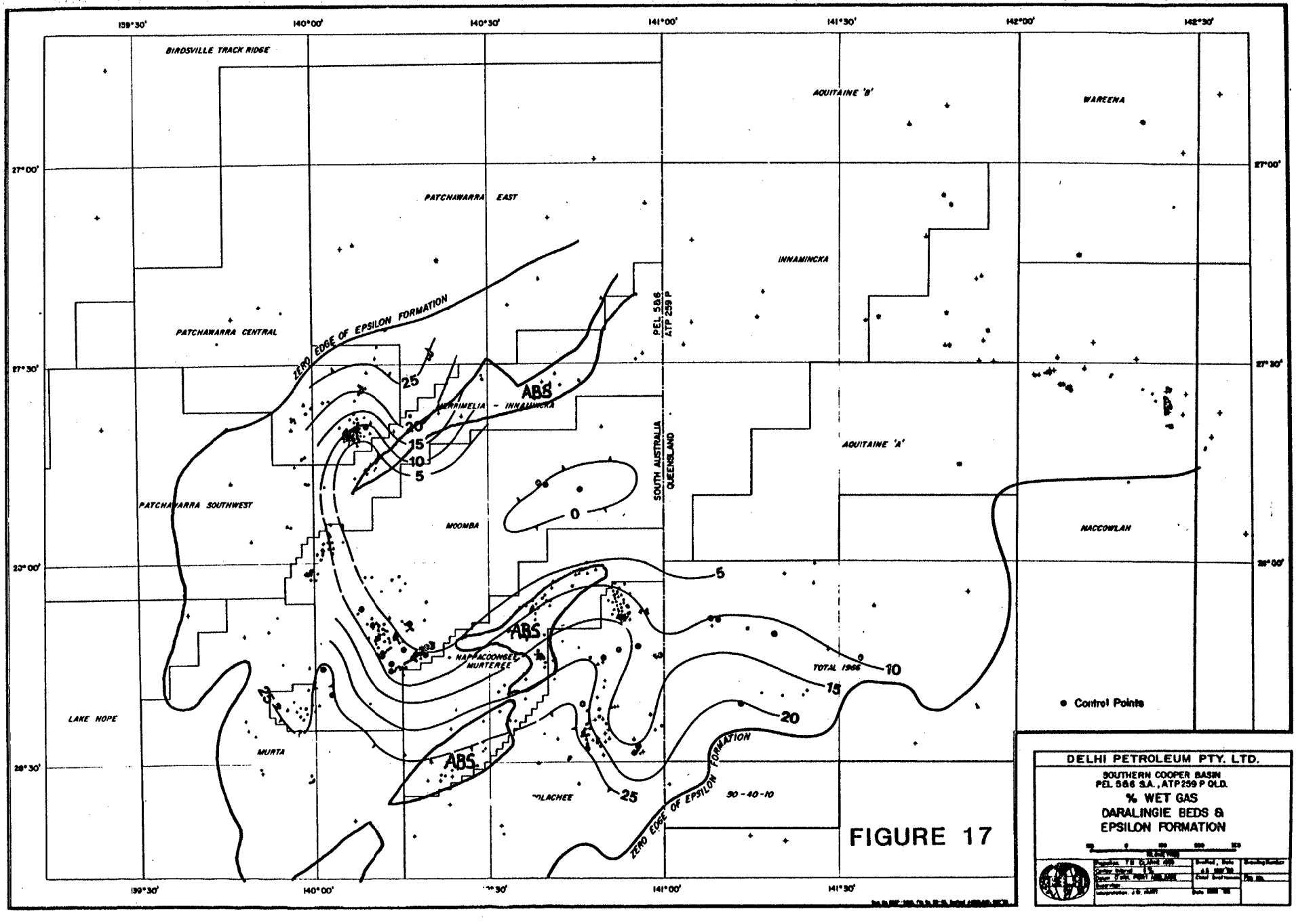
139°30'
140°00'
140°30'
141°00'
141°30'
142°00'
142°30'
27°00'
27°30'
28°00'
28°30'
BIRDSVILLE TRACK RIDGE
AQUITAINE 'B'
WAREENA
PATCHAWARRA EAST
INNAMINCKA
PATCHAWARRA CENTRAL
PEL 586
ATP 259 P
ZERO EDGE OF EPSILON FORMATION
25
20
15
10
5
ABS
MERRIMELIA - INNAMINCKA
SOUTH AUSTRALIA
QUEENSLAND
AQUITAINE 'A'
PATCHAWARRA SOUTHWEST
MOOMBA
0
NACCOWLAH
5
ABS
NAPPACOONGEE - MURTEREE
TOTAL 1966
10
15
20
LAKE HOPE
MURTA
ABS
25
ZERO EDGE OF EPSILON FORMATION
90 - 40 - 10
Control Points
FIGURE 17
DELHI PETROLEUM PTY. LTD.
SOUTHERN COOPER BASIN
PEL 586 S.A., ATP 259 P QLD.
% WET GAS
DARALINGIE BEDS &
EPSILON FORMATION

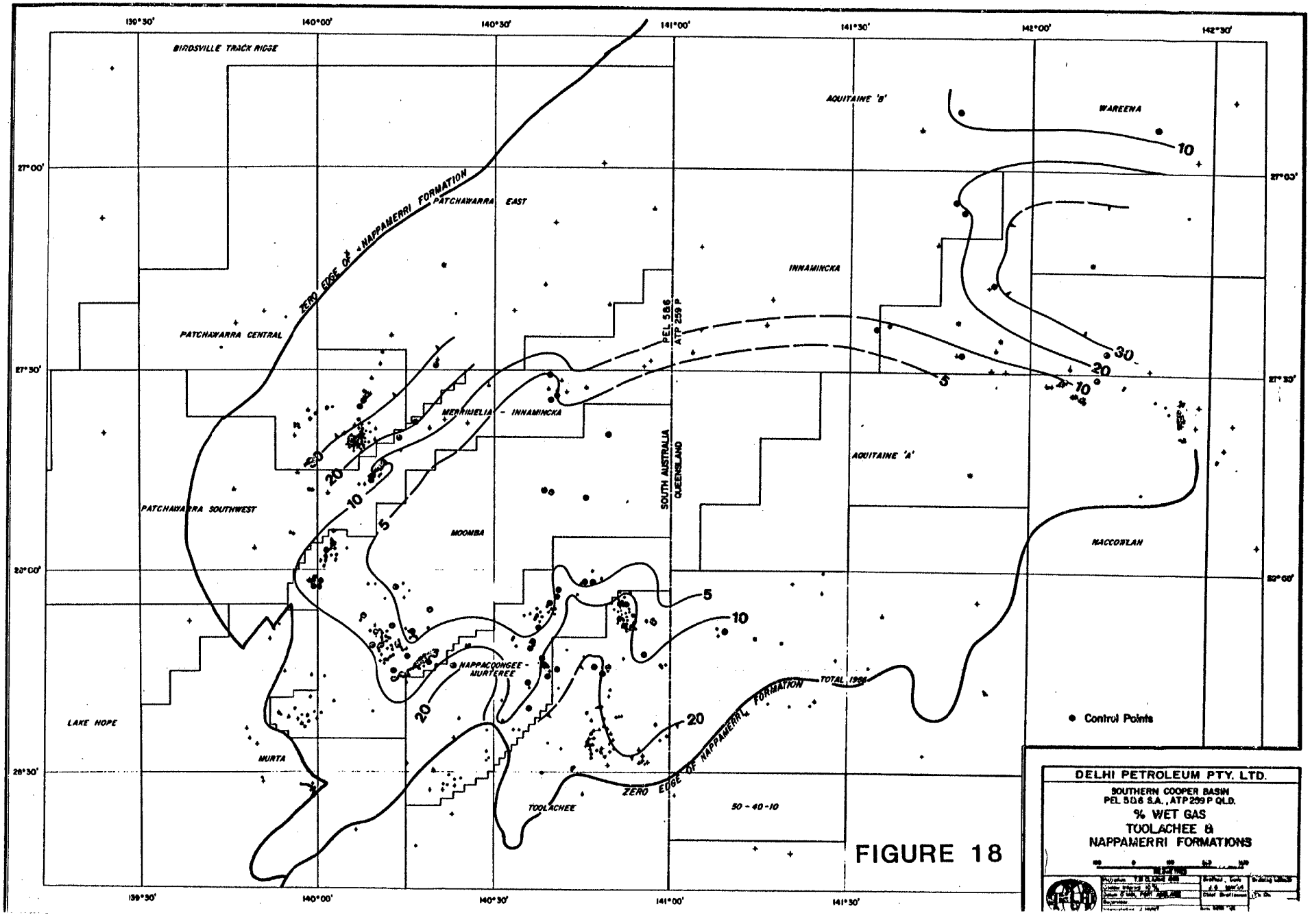
139°30'
140°00'
140°30'
141°00'
141°30'
142°00'
142°30'
27°00'
27°30'
28°00'
28°30'
BIRDSVILLE TRACK RIDGE
AQUITAINE 'B'
WAREENA
PATCHAWARRA EAST
ZERO EDGE OF NAPPAMERRI FORMATION
INNAMINCKA
PATCHAWARRA CENTRAL
PEL 586
ATP 259 P
MERRIMELIA - INNAMINCKA
SOUTH AUSTRALIA
QUEENSLAND
AQUITAINE 'A'
PATCHAWARRA SOUTHWEST
MOOMBA
NACCOWLAH
NAPPACOONGEE - MURTEREE
TOTAL 1966
LAKE HOPE
MURTA
TOOLACHEE
ZERO EDGE OF NAPPAMERRI FORMATION
50 - 40 - 10
5
10
20
30
Control Points
DELHI PETROLEUM PTY. LTD.
SOUTHERN COOPER BASIN
PEL 5&6 S.A., ATP 259 P QLD.
% WET GAS
TOOLACHEE & NAPPAMERRI FORMATIONS

FIGURE 18

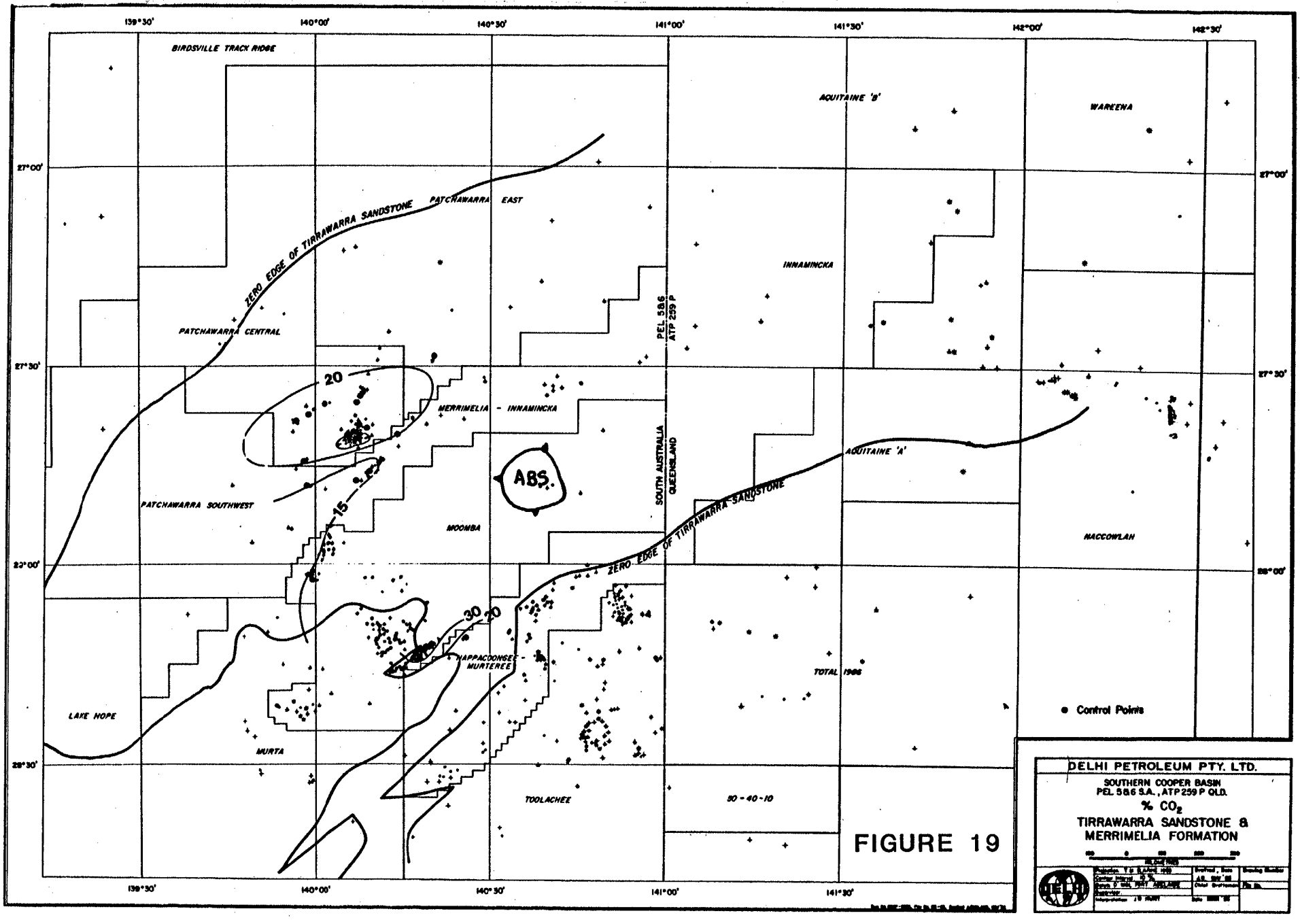
139°30'
140°00'
140°30'
141°00'
141°30'
142°00'
142°30'
27°00'
27°30'
28°00'
28°30'
BIRDSVILLE TRACK RIDGE
AQUITAINE 'B'
WAREENA
ZERO EDGE OF TIRRAWARRA SANDSTONE
PATCHAWARRA EAST
INNAMINCKA
PATCHAWARRA CENTRAL
PEL 5&6
ATP 259 P
20
MERRIMELIA - INNAMINCKA
ABS.
SOUTH AUSTRALIA
QUEENSLAND
AQUITAINE 'A'
15
PATCHAWARRA SOUTHWEST
MOOMBA
MACCOWLAH
ZERO EDGE OF TIRRAWARRA SANDSTONE
30
20
HAPPACOONGEE - MURTEREE
TOTAL 1966
LAKE HOPE
Control Points
MURTA
TOOLACHEE
50 - 40 - 10
FIGURE 19
DELHI PETROLEUM PTY. LTD.
SOUTHERN COOPER BASIN
PEL 5&6 S.A., ATP 259 P QLD.
% CO_2
TIRRAWARRA SANDSTONE &
MERRIMELIA FORMATION

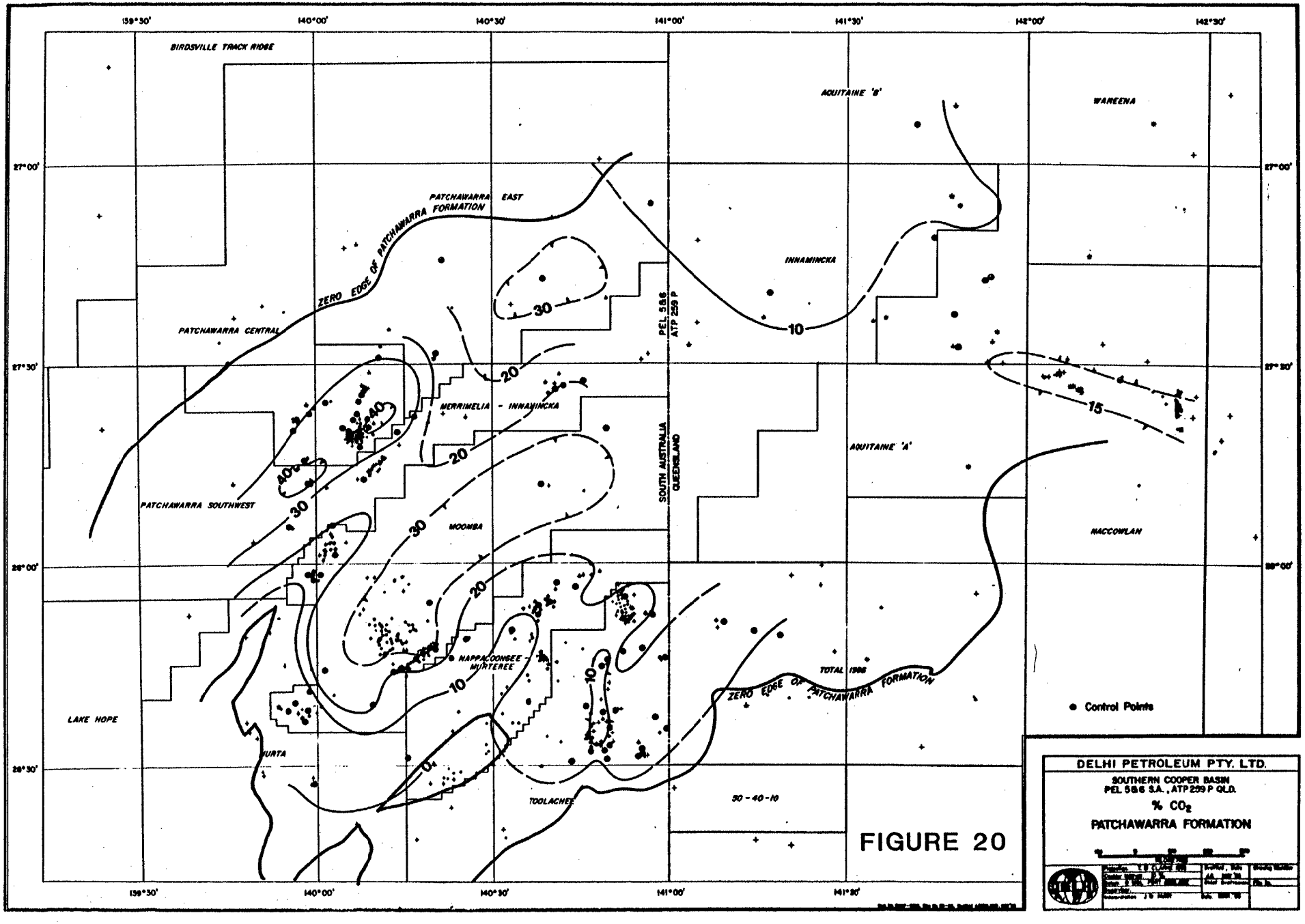

DELHI PETROLEUM PTY. LTD.

SOUTHERN COOPER BASIN
PEL 5&6 S.A., ATP 259 P QLD.

% CO_2

PATCHAWARRA FORMATION

FIGURE 20

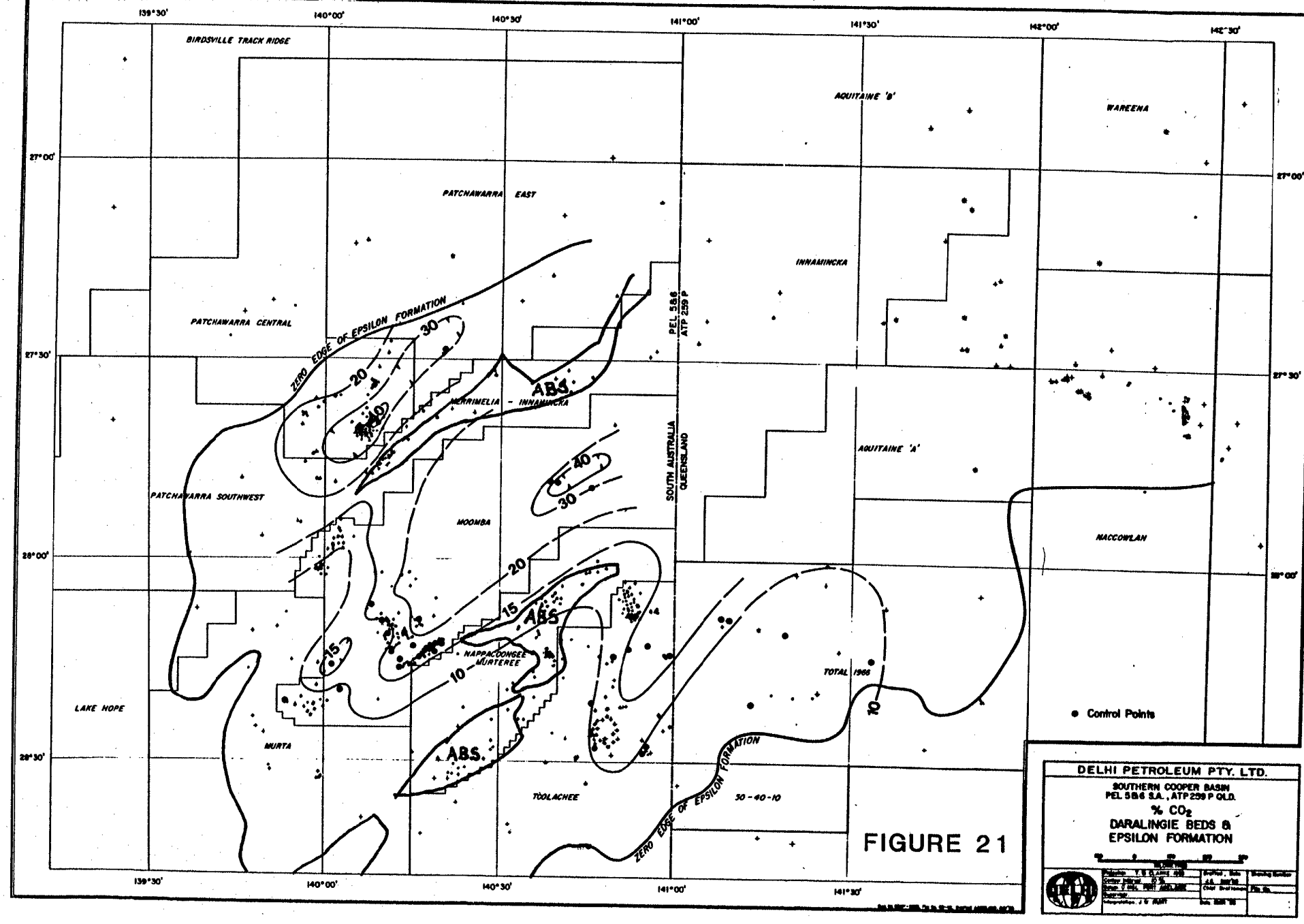

DELHI PETROLEUM PTY. LTD.

SOUTHERN COOPER BASIN
PEL 5&6 S.A., ATP 259 P QLD.

% CO_2

DARALINGIE BEDS & EPSILON FORMATION

FIGURE 21

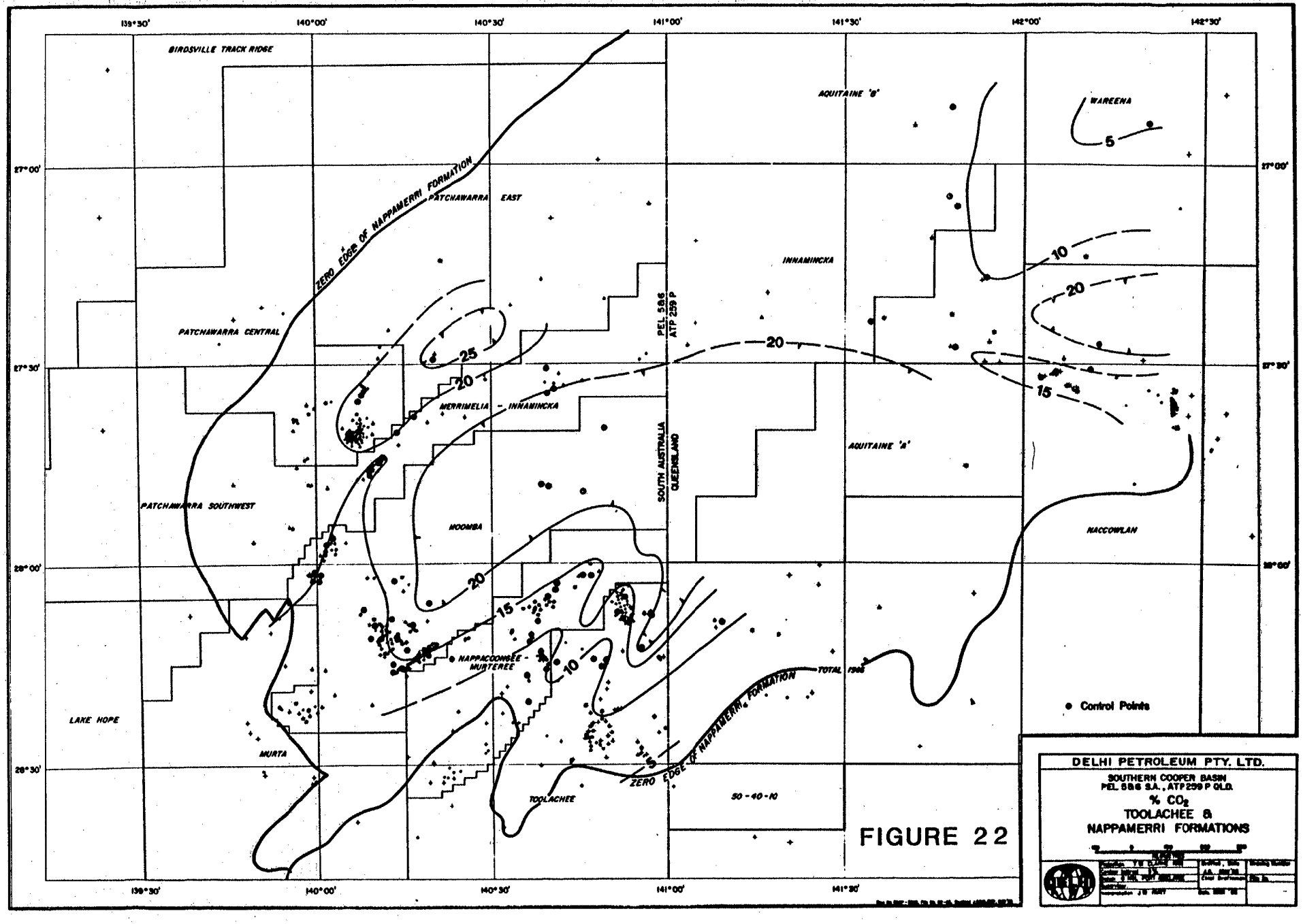
139°30'
140°00'
140°30'
141°00'
141°30'
142°00'
142°30'
27°00'
27°30'
28°00'
28°30'
BIRDSVILLE TRACK RIDGE
ZERO EDGE OF NAPPAMERRI FORMATION
PATCHAWARRA EAST
PATCHAWARRA CENTRAL
PATCHAWARRA SOUTHWEST
MERRIMELIA - INNAMINCKA
MOOMBA
NAPPACOOMEE - MURTEREE
LAKE HOPE
MURTA
TOOLACHEE
ZERO EDGE OF NAPPAMERRI FORMATION
TOTAL 1948
50 - 40 - 10
PEL 586
ATP 259 P
SOUTH AUSTRALIA
QUEENSLAND
AQUITAINE 'B'
INNAMINCKA
AQUITAINE 'A'
WAREENA
NACCOWLAH
5
10
15
20
25
20
20
15
10
5
Control Points
DELHI PETROLEUM PTY. LTD.
SOUTHERN COOPER BASIN
PEL 586 S.A., ATP 259 P QLD.
% CO_2
TOOLACHEE &
NAPPAMERRI FORMATIONS

FIGURE 22

139°30' 140°00' 140°30' 141°00' 141°30' 142°00' 142°30'

27°00' 27°30' 28°00' 28°30'

BIRDSVILLE TRACK RIDGE

PATCHAWARRA EAST

PATCHAWARRA CENTRAL

PATCHAWARRA SOUTHWEST

Tirrawarra Sandstone Zero Edge

?

YANPURRA
18m O, 198m M & GCWC/1

KUDRIEKE
37m GB SOCM/1

BROLGA
30m O, 73m O & GCM,
110m GCMW, 55m O & GCM/2

MOORARI
404 BOPD/6
40/6, 2/6

WOOLKINA
10 BO, 13 BO & C,
79 BO & C & M/1
49/1 - 6/1

FLY LAKE
450 BOPD/6
41/1, 6/1

MUDRANGIE
235m G & O CM/2
44/2, 11/2

TIRRAWARRA
1536 BOPD/2
45/7, 3/8

ANDREE
9m O, 82m OCM
301m WTO, 110m MTO/1
47/1, 9/1

LELEPTIAN
199m O & GCW,
378m M & GCW

MERRIMELIA
0.3m O, 20m W/13
42/13, - 5/13

KANOWANA
305m GCMW
244m VGCMWTO/1
FORMATION DAMAGE

GIDGEALPA
84m O,
159m MW/7
31/7 -

0
ABSENT

MERRIMELIA - INNAMINCKA

MOOMBA

NAPPACOONGEE - MURTEREE

Tirrawarra Sandstone Zero Edge

LAKE HOPE

MURTA

TOOLACHEE

PEL 586
ATP 259 P

SOUTH AUSTRALIA
QUEENSLAND

AQUITAINE 'B'

INNAMINCKA

PEPITA
350m O, 803m W,
1067m O & VGCM/1

PACKSADDLE
INTERPRETED/1

AQUITAINE 'A'

WAREENA

NACCOWLAH

TOTAL 1966

50 - 40 - 10

WELL NAME
FLOW OR RECOVERY / WELL N°
API GRAVITY / WELL N°, POUR POINT / WELL N°.

TEST RESULTS

- OIL FLOW, BOPD
- OIL IN PIPE
- TRACE OIL
- TIGHT OIL
- TRACE TIGHT OIL

Dwg No 85XG-5260, File No. RD-42, Drafted J.GOWLAND, MAY 85

DELHI PETROLEUM PTY. LTD.

SOUTHERN COOPER BASIN
PEL 586 S.A., ATP 259 P QLD.

OIL DISCOVERIES
TIRRAWARRA SST./ MERRIMELIA FM.

SCALE 1 : 500 000
100 0 100 200 300
KILOMETRES

Projection TM CLARKE 1858	Drafted, Date	Drawing Number
Contour Interval -	J.G JUNE '85	85XG-5409
Datum O' MSL PORT ADELAIDE	Chief Draftsman	File No. R1-42
Supervisor		Enclosure 1
Interpretation J.W HUNT	Date MAY '85	

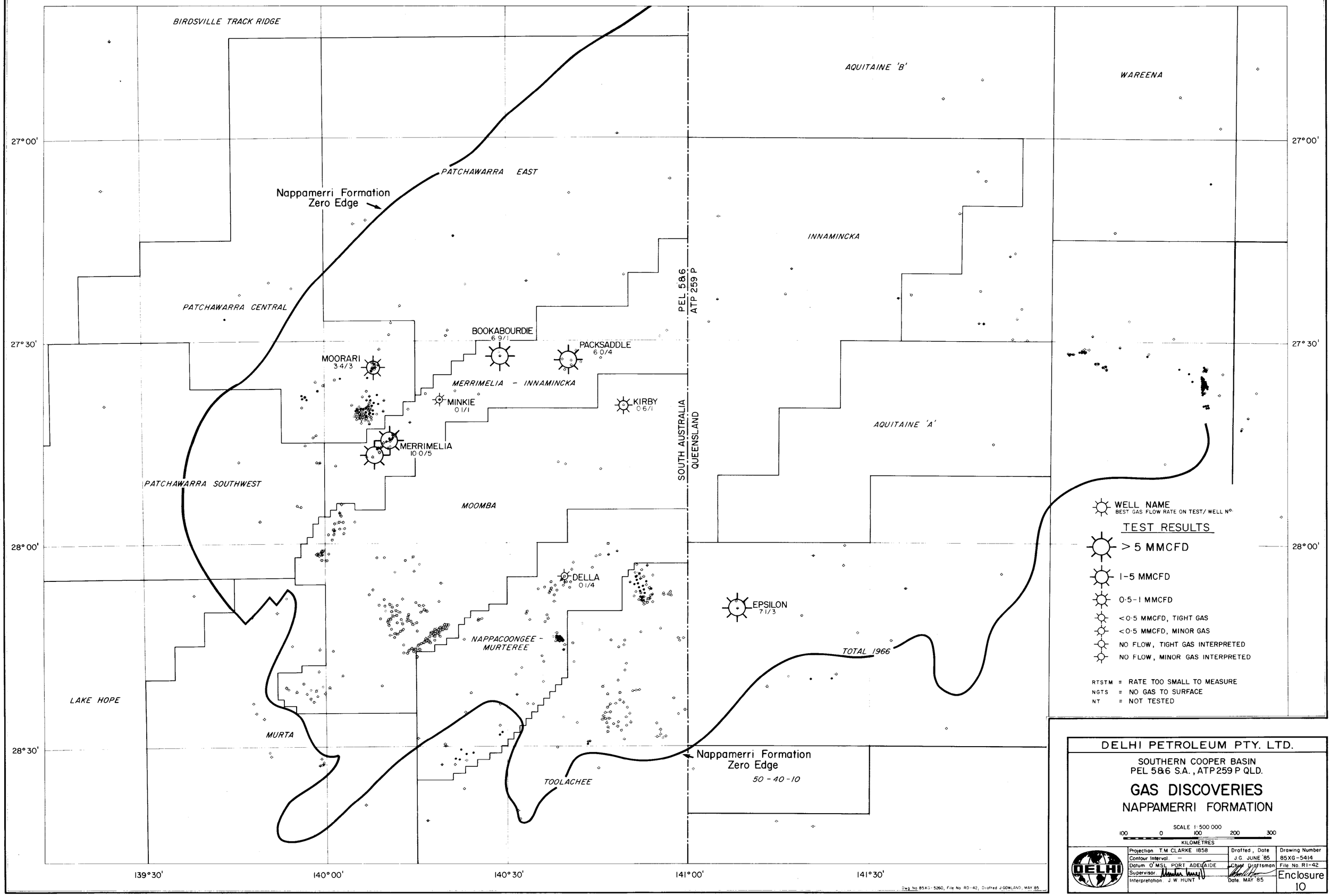

Dwg No 85XG-5260, File No RD-42, Drafted J.GOWLAND, MAY 85

DELHI PETROLEUM PTY. LTD.

SOUTHERN COOPER BASIN
PEL 5&6 S.A., ATP259 P QLD.

GAS DISCOVERIES
NAPPAMERRI FORMATION

SCALE 1:500 000
100 0 100 200 300
KILOMETRES

Projection T.M CLARKE 1858	Drafted, Date J.G. JUNE '85	Drawing Number 85XG-5414
Contour Interval —		
Datum 0' MSL PORT ADELAIDE	Chief Draftsman	File No. R1-42
Supervisor		Enclosure 10
Interpretation J.W. HUNT	Date. MAY '85	

139°30' 140°00' 140°30' 141°00' 141°30' 142°00' 142°30'

27°00' 27°30' 28°00' 28°30'

BIRDSVILLE TRACK RIDGE

AQUITAINE 'B'

WAREENA

ZERO EDGE OF TIRRAWARRA SANDSTONE

PATCHAWARRA EAST

INNAMINCKA

PATCHAWARRA CENTRAL

PEL 586
ATP 259 P

SOUTH AUSTRALIA
QUEENSLAND

20

MERRIMELIA - INNAMINCKA

AQUITAINE 'A'

ZERO EDGE OF TIRRAWARRA SANDSTONE

PATCHAWARRA SOUTHWEST

15

MOOMBA

NACCOWLAH

30 20

NAPPACOONGEE - MURTEREE

TOTAL 1966

● Control Points

LAKE HOPE

MURTA

TOOLACHEE

50 - 40 - 10

Dwg No 85XP-5260, File No. RD-42, Drafted J.GOWLAND, MAY '85

DELHI PETROLEUM PTY. LTD.

SOUTHERN COOPER BASIN
PEL 586 S.A., ATP259 P QLD.

% CO_2

TIRRAWARRA SANDSTONE & MERRIMELIA FORMATION

SCALE 1:500 000

100 0 100 200 300

KILOMETRES

Projection. T.M. CLARKE 1858	Drafted, Date J.G. MAY '85	Drawing Number 85XG-5145
Contour Interval. 10 %		
Datum. 0' MSL PORT ADELAIDE	Chief Draftsman	File No. AA-14
Supervisor.		
Interpretation. J.W. HUNT	Date. MAR. '85	Encl. 11

139°30' 140°00' 140°30' 141°00' 141°30' 142°00' 142°30'

27°00' 27°30' 28°00' 28°30'

BIRDSVILLE TRACK RIDGE

PATCHAWARRA EAST

PATCHAWARRA CENTRAL

PATCHAWARRA SOUTHWEST

MOOMBA

LAKE HOPE

MURTA

TOOLACHEE

NAPPACOONGEE - MURTEREE

MERRIMELIA - INNAMINCKA

INNAMINCKA

AQUITAINE 'B'

WAREENA

AQUITAINE 'A'

NACCOWLAH

PEL 5&6
ATP 259 P

SOUTH AUSTRALIA
QUEENSLAND

ZERO EDGE OF EPSILON FORMATION

Daralingie Beds
Zero Edge

TOTAL 1966

50 - 40 - 10

10 15 20 30 40

Control Points

Dwg. No. 85XP-5260, File No. RD-42, Drafted J.GOWLAND, MAY'85

DELHI PETROLEUM PTY. LTD.

SOUTHERN COOPER BASIN
PEL 5&6 S.A., ATP259 P QLD.

% CO_2
DARALINGIE BEDS &
EPSILON FORMATION

SCALE 1:500 000
100 0 100 200 300
KILOMETRES

Projection. T. M. CLARKE 1858	Drafted, Date J.G. MAY'85	Drawing Number 85XG-5143
Contour Interval. 10 %		
Datum. O' MSL, PORT ADELAIDE	Chief Draftsman	File No. AA-14
Supervisor.		
Interpretation. J.W. HUNT	Date. MAR.'85	Encl.12

139°30' 140°00' 140°30' 141°00' 141°30' 142°00' 142°30'

27°00' 27°30' 28°00' 28°30'

BIRDSVILLE TRACK RIDGE

AQUITAINE 'B'

WAREENA

PATCHAWARRA EAST

ZERO EDGE OF PATCHAWARRA FORMATION

INNAMINCKA

PATCHAWARRA CENTRAL

PEL 586
ATP 259 P

SOUTH AUSTRALIA
QUEENSLAND

MERRIMELIA - INNAMINCKA

AQUITAINE 'A'

PATCHAWARRA SOUTHWEST

MOOMBA

NACCOWLAH

NAPPACOONGEE - MURTEREE

TOTAL 1966

ZERO EDGE OF PATCHAWARRA FORMATION

LAKE HOPE

Patchawarra Formation
Zero Edge

MURTA

TOOLACHEE

50 - 40 - 10

● Control Points

Dwg. No. 85XP-5260, File No. RD-42, Drafted J.GOWLAND, MAY'85

DELHI PETROLEUM PTY. LTD.

SOUTHERN COOPER BASIN
PEL 586 S.A., ATP 259 P QLD.

% CO_2

PATCHAWARRA FORMATION

SCALE 1:500 000

100 0 100 200 300

KILOMETRES

Projection. T. M. CLARKE 1858	Drafted, Date J.G. MAY '85	Drawing Number 85XG - 5144
Contour Interval. 10 %		
Datum. 0' MSL, PORT ADELAIDE	Chief Draftsman	File No. AA - 14
Supervisor.		
Interpretation. J. W. HUNT	Date. MAR. '85	Encl. 13

139°30' 140°00' 140°30' 141°00' 141°30' 142°00' 142°30'

27°00' 27°30' 28°00' 28°30'

BIRDSVILLE TRACK RIDGE

ZERO EDGE OF NAPPAMERRI FORMATION

PATCHAWARRA EAST

PATCHAWARRA CENTRAL

PATCHAWARRA SOUTHWEST

MERRIMELIA – INNAMINCKA

MOOMBA

NAPPACOONGEE - MURTEREE

LAKE HOPE

MURTA

TOOLACHEE

PEL 5&6
ATP 259 P

SOUTH AUSTRALIA
QUEENSLAND

AQUITAINE 'B'

INNAMINCKA

AQUITAINE 'A'

50 - 40 - 10

WAREENA

NACCOWLAH

25 20 15 10 5

TOTAL 1966

ZERO EDGE OF NAPPAMERRI FORMATION

● Control Points

Dwg. No. 85XP-5260, File No. RD-42, Drafted J.GOWLAND, MAY'85

DELHI PETROLEUM PTY. LTD.

SOUTHERN COOPER BASIN
PEL 5&6 S.A., ATP 259 P QLD.

% CO_2
TOOLACHEE & NAPPAMERRI FORMATIONS

SCALE 1:500 000

100 0 100 200 300

KILOMETRES

Projection. T.M. CLARKE 1858	Drafted, Date J.G. MAY'85	Drawing Number 85XG-5142
Contour Interval. 5%		
Datum. O'MSL/PORT ADELAIDE	Chief Draftsman	File No. AA-14
Supervisor.		
Interpretation. J.W. HUNT	Date. MAR. '85	Encl. 14

139°30' 140°00' 140°30' 141°00' 141°30' 142°00' 142°30'

27°00'

27°30'

28°00'

28°30'

BIRDSVILLE TRACK RIDGE

AQUITAINE 'B'

WAREENA

ZERO EDGE OF TIRRAWARRA SANDSTONE

PATCHAWARRA EAST

PATCHAWARRA CENTRAL

INNAMINCKA

PEL. 5&6
ATP 259 P

MERRIMELIA - INNAMINCKA

40

30

20

10

SOUTH AUSTRALIA
QUEENSLAND

AQUITAINE 'A'

ZERO EDGE OF TIRRAWARRA SANDSTONE

PATCHAWARRA SOUTHWEST

MOOMBA

NACCOWLAH

10

0

NAPPACOONGEE - MURTEREE

TOTAL 1966

● Control Points

LAKE HOPE

MURTA

TOOLACHEE

50 - 40 - 10

Dwg No. 85XP-5260, File No. RD-42, Drafted J.GOWLAND, MAY '85

DELHI PETROLEUM PTY. LTD.

SOUTHERN COOPER BASIN
PEL 5&6 S.A., ATP259 P QLD.

% WET GAS
TIRRAWARRA SANDSTONE & MERRIMELIA FORMATION

SCALE 1:500 000

100 0 100 200 300

KILOMETRES

Projection. T.M. CLARKE 1858	Drafted, Date J.G. MAY'85	Drawing Number 85XG-5146
Contour Interval. 10 %	Chief Draftsman	File No. AA-14
Datum. O' MSL. PORT ADELAIDE	Date. MAR. '85	Encl. 15
Supervisor.		
Interpretation. J.W. HUNT		

139°30' 140°00' 140°30' 141°00' 141°30' 142°00' 142°30'

27°00' 27°30' 28°00' 28°30'

BIRDSVILLE TRACK RIDGE

PATCHAWARRA EAST

ZERO EDGE OF PATCHAWARRA FORMATION

PATCHAWARRA CENTRAL

PATCHAWARRA SOUTHWEST

MERRIMELIA - INNAMINCKA

MOOMBA

NAPPACOONGEE - MURTEREE

LAKE HOPE

MURTA

TOOLACHEE

INNAMINCKA

AQUITAINE 'B'

WAREENA

AQUITAINE 'A'

NACCOWLAH

50 - 40 - 10

TOTAL 1966

ZERO EDGE OF PATCHAWARRA FORMATION

PEL 5&6
ATP 259 P

SOUTH AUSTRALIA
QUEENSLAND

30 25 20 15 10 5 0 5 10 15 20 20 25

Patchawarra Formation
Zero Edge

● Control Points

DELHI PETROLEUM PTY. LTD.

SOUTHERN COOPER BASIN
PEL 5&6 S.A., ATP 259 P QLD.

% WET GAS
PATCHAWARRA FORMATION

SCALE 1:500 000
100 0 100 200 300
KILOMETRES

Projection. T.M. CLARKE 1858	Drafted, Date J.G. MAY'85	Drawing Number 85XG-5148
Contour Interval. 5%		
Datum. O'MSL PORT ADELAIDE	Chief Draftsman	File No. AA-14
Supervisor.		Encl. 16
Interpretation. J.W. HUNT	Date. MAR.'85	

Dwg No 85XP-5260, File No. RD-42, Drafted J.GOWLAND, MAY'85

139°30' 140°00' 140°30' 141°00' 141°30' 142°00' 142°30'

27°00' 27°30' 28°00' 28°30'

BIRDSVILLE TRACK RIDGE

AQUITAINE 'B'

WAREENA

PATCHAWARRA EAST

INNAMINCKA

PATCHAWARRA CENTRAL

PEL 586
ATP 259 P

ZERO EDGE OF EPSILON FORMATION

Daralingie Beds
Zero Edge

25

MERRIMELIA - INNAMINCKA

20

15

10

5

SOUTH AUSTRALIA
QUEENSLAND

AQUITAINE 'A'

PATCHAWARRA SOUTHWEST

0

MOOMBA

NACCOWLAH

5

Daralingie Beds
Zero Edge

NAPPACOONGEE - MURTEREE

TOTAL 1966

10

15

20

25

LAKE HOPE

MURTA

TOOLACHEE

25

50 - 40 - 10

ZERO EDGE OF EPSILON FORMATION

● Control Points

Dwg No 85XP-5260, File No. RD-42, Drafted J.GOWLAND, MAY'85

DELHI PETROLEUM PTY. LTD.

SOUTHERN COOPER BASIN
PEL 586 S.A., ATP 259 P QLD.

% WET GAS
DARALINGIE BEDS & EPSILON FORMATION

SCALE 1:500 000

100 0 100 200 300

KILOMETRES

Projection. T.M. CLARKE 1858	Drafted, Date J.G. MAY'85	Drawing Number 85XG-5147
Contour Interval. 5%		
Datum. 0 MSL. PORT ADELAIDE	Chief Draftsman	File No. AA-14
Supervisor.		
Interpretation. J.W. HUNT	Date. MAR '85	Encl. 17

139°30' 140°00' 140°30' 141°00' 141°30' 142°00' 142°30'

27°00'

27°30'

28°00'

28°30'

BIRDSVILLE TRACK RIDGE

PATCHAWARRA EAST

ZERO EDGE OF NAPPAMERRI FORMATION

PATCHAWARRA CENTRAL

PATCHAWARRA SOUTHWEST

LAKE HOPE

MURTA

MERRIMELIA - INNAMINCKA

MOOMBA

NAPPACOONGEE - MURTEREE

TOOLACHEE

ZERO EDGE OF NAPPAMERRI FORMATION

TOTAL 1966

50 - 40 - 10

AQUITAINE 'B'

INNAMINCKA

AQUITAINE 'A'

WAREENA

NACCOWLAH

PEL 5&6
ATP 259 P

SOUTH AUSTRALIA
QUEENSLAND

30
20
10
5
10
5
20
10
5
20

● Control Points

Dwg. No. 85XP-5260, File No. RD-42, Drafted J.GOWLAND, MAY'85

DELHI PETROLEUM PTY. LTD.

SOUTHERN COOPER BASIN
PEL 5&6 S.A., ATP 259 P QLD.

% WET GAS
TOOLACHEE & NAPPAMERRI FORMATIONS

SCALE 1:500 000

100 0 100 200 300

KILOMETRES

Projection. T.M. CLARKE 1858	Drafted, Date J. G. MAY'85	Drawing Number 85XG-5149
Contour Interval. 10 %		
Datum. 0' MSL PORT ADELAIDE	Chief Draftsman	File No. AA-14
Supervisor.		
Interpretation. J. HUNT	Date. MAR. '85	Encl. 18

DELHI

139°30' 140°00' 140°30' 141°00' 141°30' 142°00' 142°30'

27°00'

27°30'

28°00'

28°30'

BIRDSVILLE TRACK RIDGE

PATCHAWARRA EAST

Patchawarra Formation
Zero Edge

PATCHAWARRA CENTRAL

PATCHAWARRA SOUTHWEST

BROLGA
70 BOPD/2

FLY LAKE
OTS/7
47/7, 5/7

MERRIMELIA - INNAMINCKA

MOOMBA

DELLA
853m GCO
emulsified W/I
26/1

STRZELECKI
38m O,93m SGCW
47m G & OCMW/15
42/15

BAGUNDI
12m O,21m SOCW/I
41/1

LAKE HOPE

MURTA

WANCOOCHA
1747 BOPD/2
45/2, 21/2

TOOLACHEE

Patchawarra Formation
Zero Edge

PEL 586
ATP 259 P

SOUTH AUSTRALIA
QUEENSLAND

AQUITAINE 'B'

WAREENA

INNAMINCKA

KARMONA
229m O, 57m MWCO/I

AQUITAINE 'A'

TOTAL 1966

NACCOWLAH

50 - 40 - 10

WELL NAME
FLOW OR RECOVERY / WELL N°.
API GRAVITY / WELL N°, POUR POINT / WELL N°.

TEST RESULTS

- OIL FLOW, BOPD
- OIL IN PIPE
- TRACE OIL
- TIGHT OIL
- TRACE TIGHT OIL

Dwg No 85XG-5260, File No RD-42, Drafted J.GOWLAND, MAY 85

DELHI PETROLEUM PTY. LTD.

SOUTHERN COOPER BASIN
PEL 586 S.A., ATP 259 P QLD.

OIL DISCOVERIES
PATCHAWARRA FORMATION

SCALE 1:500 000
100 0 100 200 300
KILOMETRES

Projection TM CLARKE 1858	Drafted, Date J.G. JUNE '85	Drawing Number 85XG-5408
Contour Interval –		
Datum O'MSL PORT ADELAIDE	Chief Draftsman	File No RI-42
Supervisor		Enclosure 2
Interpretation J.W. HUNT	Date MAY '85	

139°30' 140°00' 140°30' 141°00' 141°30' 142°00' 142°30'

27°00' 27°30' 28°00' 28°30'

BIRDSVILLE TRACK RIDGE

PATCHAWARRA EAST

PATCHAWARRA CENTRAL

PATCHAWARRA SOUTHWEST

MERRIMELIA - INNAMINCKA

MOOMBA

NAPPACOONGEE - MURTEREE

LAKE HOPE

MURTA

TOOLACHEE

AQUITAINE 'B'

WAREENA

INNAMINCKA

AQUITAINE 'A'

NACCOWLAH

TOTAL 1966

50 - 40 - 10

Toolachee Formation Zero Edge

Toolachee Formation Zero Edge

PEL 5&6
ATP 259 P

SOUTH AUSTRALIA
QUEENSLAND

MUDRANGIE
55m OCM
101m GCM,
37m SWCM

GIDGEALPA
5 BOPD, 400 B GCWPD
34/9, 21/9

DELLA
55m OCM/1

STRZELECKI
OTS/10
39/10, 25/10

KARMONA
229m 0,57m MWCO/1

TARTULLA
3m O, 48m G & OCWM,
98m G & OCM/1
48/1, -5/1

WELL NAME
FLOW OR RECOVERY / WELL N°
API GRAVITY / WELL N°, POUR POINT / WELL N°

TEST RESULTS

- OIL FLOW, BOPD
- OIL IN PIPE
- TRACE OIL
- TIGHT OIL
- TRACE TIGHT OIL

Dwg No 85XG-5260, File No RD-42, Drafted J GOWLAND, MAY 85

DELHI PETROLEUM PTY. LTD.

SOUTHERN COOPER BASIN
PEL 5&6 S.A., ATP 259 P QLD.

OIL DISCOVERIES
TOOLACHEE FORMATION

SCALE 1:500 000

100 0 100 200 300

KILOMETRES

Projection T.M. CLARKE 1858	Drafted, Date	Drawing Number
Contour Interval –	J.G. JUNE '85	85XG-5407
Datum 0 MSL, PORT ADELAIDE	Chief Draftsman	File No. RI-42
Supervisor		Enclosure 3
Interpretation J.W. HUNT	Date MAY '85	

139°30' 140°00' 140°30' 141°00' 141°30' 142°00' 142°30'

27°00' 27°30' 28°00' 28°30'

BIRDSVILLE TRACK RIDGE

PATCHAWARRA EAST

Nappamerri Formation
Zero Edge

PATCHAWARRA CENTRAL

PATCHAWARRA SOUTHWEST

MOOMBA

NAPPACOONGEE - MURTEREE

LAKE HOPE

MURTA

TOOLACHEE

MERRIMELIA - INNAMINCKA

AQUITAINE 'B'

WAREENA

INNAMINCKA

AQUITAINE 'A'

NACCOWLAH

TOTAL 1966

Nappamerri Formation
Zero Edge
50 - 40 - 10

PEL 586
ATP 259 P

SOUTH AUSTRALIA
QUEENSLAND

WOOLKINA
14 BGCO, 13 BW,
32 8 GCM/1,
54/1, - 5/1

PONDRINIE
91m O,
1981 m 0 8 GCW/3

MINKIE
30 m O,
894m SGCW/1
32/1 —

MERRIMELIA
2850 BOPD/7
33/7, 25/7

BARYULAH
55m GCM, TO/1

WELL NAME
FLOW OR RECOVERY / WELL N°.
API GRAVITY / WELL N°., POUR POINT / WELL N°.

TEST RESULTS

- OIL FLOW, BOPD
- OIL IN PIPE
- TRACE OIL
- TIGHT OIL
- TRACE TIGHT OIL

Dwg No 85X-5260, File No RD-42, Drafted J GOWLAND MAY 85

DELHI PETROLEUM PTY. LTD.

SOUTHERN COOPER BASIN
PEL 586 S.A., ATP 259 P QLD.

OIL DISCOVERIES
NAPPAMERRI FORMATION

SCALE 1:500 000
100 0 100 200 300
KILOMETRES

Projection T M CLARKE 1858	Drafted, Date J.G. JUNE '85	Drawing Number 85XG-5406
Contour Interval —		
Datum O'MSL PORT ADELAIDE	Chief Draftsman	File No. R1-42
Supervisor		Enclosure 4
Interpretation J.W. HUNT	Date MAY '85	

139°30' 140°00' 140°30' 141°00' 141°30' 142°00' 142°30'

27°00' 27°30' 28°00' 28°30'

BIRDSVILLE TRACK RIDGE

PATCHAWARRA EAST

PATCHAWARRA CENTRAL

PATCHAWARRA SOUTHWEST

AQUITAINE 'B'

WAREENA

INNAMINCKA

MOOMBA

NAPPACOONGEE - MURTEREE

MERRIMELIA - INNAMINCKA

LAKE HOPE

MURTA

TOOLACHEE

TOTAL 1966

50 - 40 - 10

AQUITAINE 'A'

Tirrawarra Sandstone Zero Edge

Tirrawarra Sandstone Zero Edge

PEL 5&6
ATP 259 P

SOUTH AUSTRALIA
QUEENSLAND

MITCHIE 0·3/1

COONATIE 0·2/2

BOOKABOURDIE 8·7/1

MUDRANGIE 0·2/2

MERRIMELIA 9·2/14

0
ABSENT

JACK LAKE RTSTM/1

GIDGEALPA 2·3/3

GIDGEALPA 1·1/16

BIG LAKE 4·6/35

BURUNNA RTSTM/1

WELL NAME
BEST GAS FLOW RATE ON TEST/WELL N°

TEST RESULTS

- > 5 MMCFD
- 1-5 MMCFD
- 0·5-1 MMCFD
- <0·5 MMCFD, TIGHT GAS
- <0·5 MMCFD, MINOR GAS
- NO FLOW, TIGHT GAS INTERPRETED
- NO FLOW, MINOR GAS INTERPRETED

RTSTM = RATE TOO SMALL TO MEASURE
NGTS = NO GAS TO SURFACE
NT = NOT TESTED

Dwg No. 85XG-5260, File No. RD-42, Drafted J.GOWLAND, MAY'85

DELHI PETROLEUM PTY. LTD.

SOUTHERN COOPER BASIN
PEL 5&6 S.A., ATP 259 P QLD.

GAS DISCOVERIES
TIRRAWARRA SST./MERRIMELIA FM.

SCALE 1:500 000
100 0 100 200 300
KILOMETRES

Projection T.M CLARKE 1858	Drafted, Date J.G. JUNE '85	Drawing Number 85XG-5410
Contour Interval	Chief Draftsman	File No. R1-42
Datum O' MSL PORT ADELAIDE	Supervisor	Enclosure 5
Interpretation J.W HUNT	Date MAY '85	

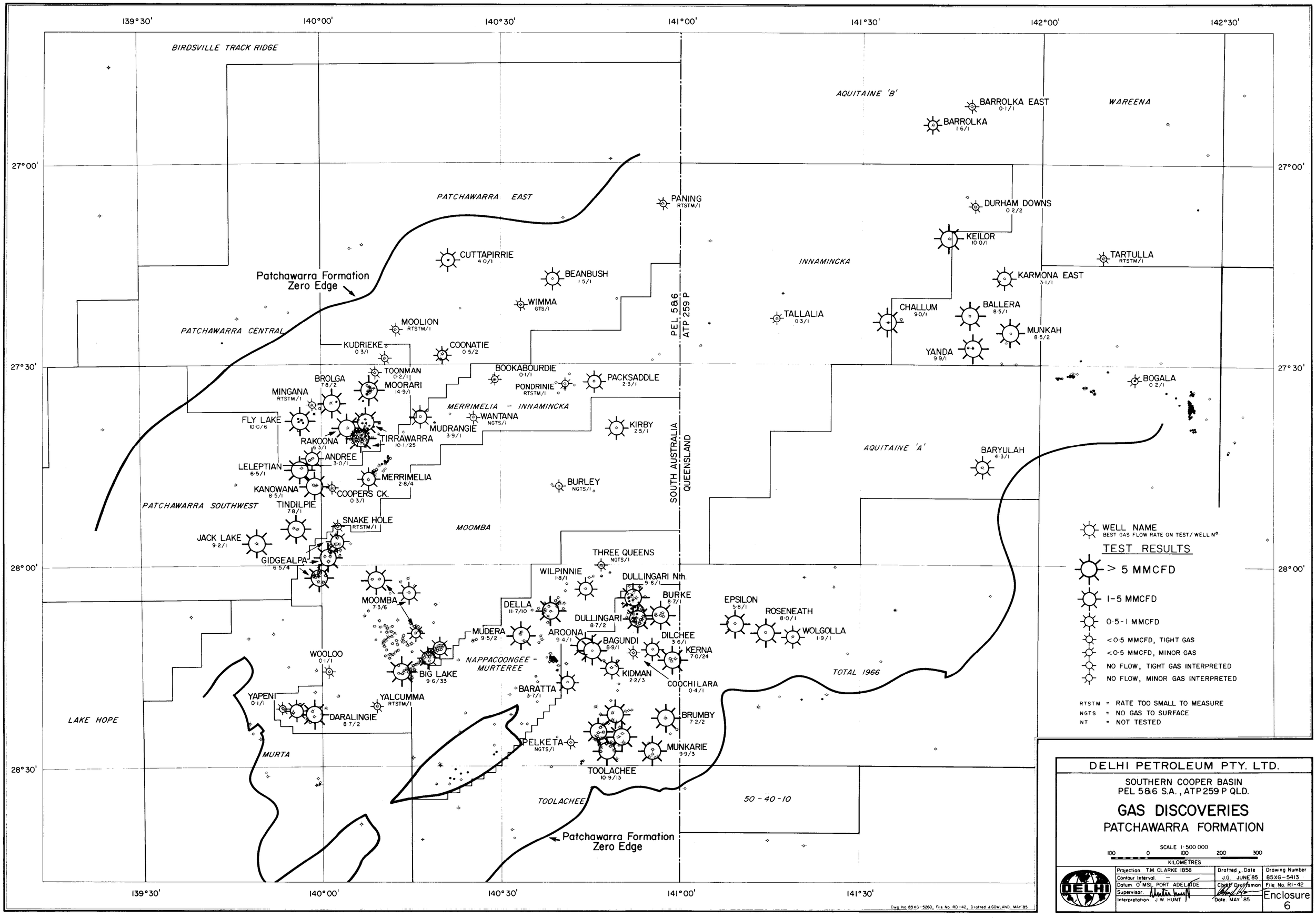

DELHI PETROLEUM PTY. LTD.

SOUTHERN COOPER BASIN
PEL 5&6 S.A., ATP 259 P QLD.

GAS DISCOVERIES
PATCHAWARRA FORMATION

SCALE 1:500 000
100 0 100 200 300
KILOMETRES

Projection. TM CLARKE 1858		Drafted. Date	Drawing Number
Contour Interval. —		J.G. JUNE '85	85XG-5413
Datum. O' MSL PORT ADELAIDE		Chief Draftsman	File No. R1-42
Supervisor.			Enclosure 6
Interpretation. J.W. HUNT		Date. MAY '85	

Dwg. No 85XG-5260, File No. RD-42, Drafted J.GOWLAND, MAY '85

139°30' 140°00' 140°30' 141°00' 141°30' 142°00' 142°30'

27°00' 27°30' 28°00' 28°30'

BIRDSVILLE TRACK RIDGE

PATCHAWARRA EAST

PATCHAWARRA CENTRAL

PATCHAWARRA SOUTHWEST

LAKE HOPE

MURTA

MOOMBA

TOOLACHEE

NAPPACOONGEE - MURTEREE

MERRIMELIA - INNAMINCKA

AQUITAINE 'B'

WAREENA

INNAMINCKA

AQUITAINE 'A'

50 - 40 - 10

TOTAL 1966

PEL 586
ATP 259 P

SOUTH AUSTRALIA
QUEENSLAND

Epsilon Formation
Zero Edge

MOOLION
NT/1

KUDRIEKE
NGTS/1

COONATIE
12/1

INNAMINCKA
0.1/1

FLY LAKE
5.8/1

KIRBY
NGTS/1

BURLEY
0.9/1

McLEOD
0.7/1

DULLINGARI Nth.
0.2/1

BURKE
0.5/2

LEPENA
6.3/1

EPSILON
1.6/2

HUME
NGTS/1

COOCHILARA
0.2/1

DILCHEE
RTSTM/1

KERNA
0.6/1

KIDMAN
0.4/1

ASHBY
7.2/1

WOOLOO
0.4/1

BIG LAKE
7.7/6

YAPENI
9.7/1

DARALINGIE
4.0/5

WILLS
1.2/1

TOOLACHEE
9.4/28

MUNKARIE
7.0/1

Epsilon Formation
Zero Edge

WELL NAME
BEST GAS FLOW RATE ON TEST/ WELL N°

TEST RESULTS

- > 5 MMCFD
- 1-5 MMCFD
- 0.5-1 MMCFD
- <0.5 MMCFD, TIGHT GAS
- <0.5 MMCFD, MINOR GAS
- NO FLOW, TIGHT GAS INTERPRETED
- NO FLOW, MINOR GAS INTERPRETED

RTSTM = RATE TOO SMALL TO MEASURE
NGTS = NO GAS TO SURFACE
NT = NOT TESTED

Dwg No 85XG-5260, File No RD-42, Drafted J GOWLAND, MAY 85

DELHI PETROLEUM PTY. LTD.

SOUTHERN COOPER BASIN
PEL 586 S.A., ATP 259 P QLD.

GAS DISCOVERIES
EPSILON FORMATION

SCALE 1:500 000
100 0 100 200 300
KILOMETRES

Projection T.M. CLARKE 1858	Drafted, Date J.G. JUNE '85	Drawing Number 85XG-5412
Contour Interval –		
Datum O'MSL PORT ADELAIDE	Chief Draftsman	File No. RI-42
Supervisor		Enclosure 7
Interpretation J.W. HUNT	Date MAY '85	

139°30' 140°00' 140°30' 141°00' 141°30' 142°00' 142°30'

27°00'

27°30'

28°00'

28°30'

BIRDSVILLE TRACK RIDGE

AQUITAINE 'B'

WAREENA

PATCHAWARRA EAST

PATCHAWARRA CENTRAL

INNAMINCKA

PEL 586
ATP 259 P

Daralingie Beds
Zero Edge

MERRIMELIA - INNAMINCKA

SOUTH AUSTRALIA
QUEENSLAND

AQUITAINE 'A'

BURLEY
NT/2

PATCHAWARRA SOUTHWEST

MOOMBA

MOOMBA
9 4/12

BIG LAKE
7 3/2

NAPPACOONGEE - MURTEREE

DULLINGARI
7 9/2

BURKE
9 4/4

TOTAL 1966

LAKE HOPE

MURTA

TOOLACHEE

50 - 40 - 10

Daralingie Beds
Zero Edge

WELL NAME
BEST GAS FLOW RATE ON TEST/ WELL N°

TEST RESULTS

- > 5 MMCFD
- 1-5 MMCFD
- 0·5-1 MMCFD
- <0·5 MMCFD, TIGHT GAS
- <0·5 MMCFD, MINOR GAS
- NO FLOW, TIGHT GAS INTERPRETED
- NO FLOW, MINOR GAS INTERPRETED

RTSTM = RATE TOO SMALL TO MEASURE
NGTS = NO GAS TO SURFACE
NT = NOT TESTED

Dwg No 85XG-5260, File No RD-42, Drafted J GOWLAND, MAY 85

DELHI PETROLEUM PTY. LTD.

SOUTHERN COOPER BASIN
PEL 586 S.A., ATP259 P QLD.

GAS DISCOVERIES
DARALINGIE BEDS

SCALE 1:500 000
100 0 100 200 300
KILOMETRES

Projection T.M. CLARKE 1858	Drafted, Date J.G. JUNE '85	Drawing Number 85XG-5411
Contour Interval —		
Datum O' MSL PORT ADELAIDE	Chief Draftsman	File No. RI-42
Supervisor		Enclosure 8
Interpretation J.W. HUNT	Date. MAY '85	

139°30' 140°00' 140°30' 141°00' 141°30' 142°00' 142°30'

27°00' 27°30' 28°00' 28°30'

BIRDSVILLE TRACK RIDGE

PATCHAWARRA EAST

PATCHAWARRA CENTRAL

PATCHAWARRA SOUTHWEST

LAKE HOPE

MURTA

MOOMBA

INNAMINCKA

MERRIMELIA - INNAMINCKA

AQUITAINE 'B'

AQUITAINE 'A'

WAREENA

TOOLACHEE

TOTAL 1966

50 - 40 - 10

Toolachee Formation Zero Edge

Toolachee Formation Zero Edge

PEL 586
ATP 259 P

SOUTH AUSTRALIA
QUEENSLAND

WIMMA 1·0/1

MOOLION 3·8/1

COONATIE 14·1/1

MOORARI / WOOLKINA 13·0/1 4·1/1

MUDRANGIE 6·1/1

PONDRINIE 1·5/2

FLY LAKE NT/6

WANTANA 0·5/1

KIRBY RTSTM/1

TIRRAWARRA 6·0/14

MERRIMELIA 6·2/14

INNAMINCKA 0·1/2

BARROLKA EAST 0·2/1

WAREENA 11·4/1

DURHAM DOWNS 10·9/2

TARTULLA 7·6/1

KARMONA EAST 9·7/1

CHALLUM RTSTM/2

MUNKAH 10·3/1

NACCOWLAH Sth. 8·4/1

BARYULAH 0·4/1

BURLEY 0·2/1

McLEOD 0·3/1

TINDILPIE NGTS/1

GIDGEALPA 11·2/7

NAPPACOONGEE 0·4/3

CORKWOOD RTSTM/1

DELLA 11·0/1

DULLINGARI 10·3/17

BURKE 10·4/1

EPSILON 7·4/1

MUDERA 11·0/3

MARABOOKA 9·5/2

LEPENA 8·4/1

AROONA 8·2/1

MOOMBA 9·2/10

LOWANNA 0·6/1

STRZELECKI 5·0/1

KIDMAN 10·9/1

BIG LAKE 10·4/2

WANARA 5·3/1

MARANA 8·3/1

MUNKARIE 8·5/4

WELL NAME
BEST GAS FLOW RATE ON TEST/ WELL N°

TEST RESULTS

- > 5 MMCFD
- 1-5 MMCFD
- 0·5-1 MMCFD
- <0·5 MMCFD, TIGHT GAS
- <0·5 MMCFD, MINOR GAS
- NO FLOW, TIGHT GAS INTERPRETED
- NO FLOW, MINOR GAS INTERPRETED

RTSTM = RATE TOO SMALL TO MEASURE
NGTS = NO GAS TO SURFACE
NT = NOT TESTED
✳ = MAJOR GAS NOT TESTED

Dwg No 85XG-5260, File No RD-42, Drafted J GOWLAND, MAY 85

DELHI PETROLEUM PTY. LTD.

SOUTHERN COOPER BASIN
PEL 5&6 S.A., ATP 259 P QLD.

GAS DISCOVERIES
TOOLACHEE FORMATION

SCALE 1:500 000
100 0 100 200 300
KILOMETRES

Projection T.M. CLARKE 1858		Drafted, Date	Drawing Number
Contour Interval		J.G. JUNE '85	85XG-5415
Datum O'MSL PORT ADELAIDE		Chief Draftsman	File No. RI-42
Supervisor			Enclosure 9
Interpretation J.W. HUNT	Date. MAY '85		

8426 R 14

INDEXED

The Australian
Mineral Development
Laboratories

Flemington Street, Frewville,
South Australia 5063
Phone Adelaide 79 1662
Telex AA 82520

Please address all
correspondence to
P.O. Box 114 Eastwood
SA 5063
In reply quote:

Your Ref:

amdel

17 September 1979

GS 1/1/231 (B3923/79)

11.06.368

Director-General,
Department of Mines & Energy,
PO Box 151,
EASTWOOD, SA 5063.

Attention: Dr D.M. McKirdy

SOURCE-ROCK STUDIES -

S.A. SEDIMENTARY BASINS

PROGRESS REPORT NO.22

OPEN FILE
(To be passed by hand)

Investigation and Report by: H. Sears

Manager, Geological Services Division: Dr Keith J. Henley

Keith Henley

for Norton Jackson
Managing Director

jd

Pilot Plant: Osman Place
Thebarton S.A.
Telephone 43 8053
Branch Laboratory: Perth

PIRSA
R2001/00430
0221481

OIL ANALYSIS

AMDEL
JOB NO. 3923/79

SAMPLE NO:	A1192/79
WELL:	Gidgealpa 7
TEST:	Drill Stem test 6.
INTERVAL:	7225 - 7240'
FORMATION:	Tirrawarra
TYPE OF SAMPLE:	Oil + 210°C fraction

Results of Analysis

API Gravity (whole sample) 36.8

Saturates	71.2 %	by wt.
Aromatics	21.3 %	
Polar compounds	4.0 %	
Asphaltenes	1.0 %	
Loss	2.5 %	

n-Alkane distribution of saturates: C.E.P.

n-Alkane	C_{12}	C_{13}	C_{14}	C_{15}	C_{16}	C_{17}	C_{18}	C_{19}	C_{20}	C_{21}	C_{22}
Rel. abundance	-	1.6	3.4	5.2	6.7	7.2	7.8	8.2	8.4	8.5	8.3
n-Alkane	C_{23}	C_{24}	C_{25}	C_{26}	C_{27}	C_{28}	C_{29}	C_{30}	C_{31}	C_{32}	C_{33}
Rel. abundance	8.0	7.5	7.0	4.8	3.5	2.0	1.3	0.6	-	-	-

Isoprenoids distribution in saturates:

IP14	IP15	IP16	IP18	Pristane	Phytane
-	0.16	0.94	1.15	2.34	0.49

$\frac{IP15}{IP16}$	$\frac{IP16}{IP18}$	$\frac{IP18}{Pr}$	$\frac{Pr}{Ph}$	$\frac{IP15}{nC_{14}}$	$\frac{IP16}{nC_{15}}$	$\frac{IP18}{nC_{16}}$	$\frac{Pr}{nC_{17}}$	$\frac{Ph}{nC_{18}}$
0.17	0.82	0.49	4.75	0.048	0.18	0.17	0.33	0.065

OIL ANALYSIS

ANDEL
JOB NO. 3923/79

SAMPLE NO:	A1193/79
WELL:	Gidgealpa 7
TEST:	Extended flow test
INTERVAL:	7230 - 7294'
FORMATION:	Tirrawarra
TYPE OF SAMPLE:	Oil + 210°C fraction

Results of Analysis

API Gravity (whole sample) 38.4

Saturates	69.3	% by wt.
Aromatics	23.2	%
Polar compounds	3.8	%
Asphaltenes	0.4	%
Loss	3.3	%

n-Alkane distribution of saturates: O.E.P:

n-Alkane	C_{12}	C_{13}	C_{14}	C_{15}	C_{16}	C_{17}	C_{18}	C_{19}	C_{20}	C_{21}	C_{22}
Rel. abundance	-	2.3	4.2	6.1	7.7	8.2	8.7	8.9	8.6	8.2	7.6
n-Alkane	C_{23}	C_{24}	C_{25}	C_{26}	C_{27}	C_{28}	C_{29}	C_{30}	C_{31}	C_{32}	C_{33}
Rel. abundance	7.1	6.3	5.8	3.9	2.9	1.5	1.0	0.5	0.3	0.2	-

Isoprenoids distribution in saturates:

IP14	IP15	IP16	IP18	Pristane	Phytane
-	0.27	1.19	1.38	2.76	0.61

$\frac{IP15}{IP16}$	$\frac{IP16}{IP18}$	$\frac{IP18}{Pr}$	$\frac{Pr}{Ph}$	$\frac{IP15}{nC_{14}}$	$\frac{IP16}{nC_{15}}$	$\frac{IP18}{nC_{16}}$	$\frac{Pr}{nC_{17}}$	$\frac{Ph}{nC_{18}}$
0.22	0.86	0.50	4.5	0.065	0.20	0.18	0.34	0.07

OIL ANALYSIS

AMDEL
JOB NO. 3923/79

SAMPLE NO:	A1194/79
WELL:	Gidgealpa 15
TEST:	Production test
INTERVAL:	6720 - 6792'
FORMATION:	Toolachee
TYPE OF SAMPLE:	Condensate + 210°C fraction

Results of Analysis

API Gravity (whole sample) 46.8

Saturates	64.1 %	by wt.
Aromatics	21.7 %	
Polar compounds	0.9 %	
Asphaltenes	- %	
Loss	13.3 %	

n-Alkane distribution of saturates: O.E.P.

n-Alkane	C_{12}	C_{13}	C_{14}	C_{15}	C_{16}	C_{17}	C_{18}	C_{19}	C_{20}	C_{21}	C_{22}
Rel. abundance	15.8	17.7	15.8	13.0	10.1	7.2	5.3	4.0	2.9	2.3	1.8
n-Alkane	C_{23}	C_{24}	C_{25}	C_{26}	C_{27}	C_{28}	C_{29}	C_{30}	C_{31}	C_{32}	C_{33}
Rel. abundance	1.5	1.1	0.8	0.4	0.3	-	-	-	-	-	-

Isoprenoids distribution in saturates:

IP14	IP15	IP16	IP18	Pristane	Phytane
2.15	1.21	3.18	1.31	2.06	0.28

$\frac{IP15}{IP16}$	$\frac{IP16}{IP18}$	$\frac{IP18}{Pr}$	$\frac{Pr}{Ph}$	$\frac{IP15}{nC_{14}}$	$\frac{IP16}{nC_{15}}$	$\frac{IP18}{nC_{16}}$	$\frac{Pr}{nC_{17}}$	$\frac{Ph}{nC_{18}}$
0.38	2.4	0.65	7.3	0.075	0.25	0.13	0.29	0.055

OIL ANALYSIS

ANDEE
JOB NO. 3923/79

SAMPLE NO:	A1195/79
WELL:	Gidgealpa 16
TEST:	Drill Stem test 2
INTERVAL:	6936 - 6967'
FORMATION:	Toolachee
TYPE OF SAMPLE:	Oil, + 210°C fraction.

Results of Analysis

API Gravity (whole sample) 29.5

Saturates	72.0	% by wt.
Aromatics	21.1	%
Polar compounds	4.4	%
Asphaltenes	1.2	%
Loss	1.3	%

n-Alkane distribution of saturates: O.E.P.

n-Alkane	C_{12}	C_{13}	C_{14}	C_{15}	C_{16}	C_{17}	C_{18}	C_{19}	C_{20}	C_{21}	C_{22}
Rel. abundance	-	0.4	0.8	1.3	1.9	2.5	3.3	4.1	5.2	6.7	8.3
n-Alkane	C_{23}	C_{24}	C_{25}	C_{26}	C_{27}	C_{28}	C_{29}	C_{30}	C_{31}	C_{32}	C_{33}
Rel. abundance	10.1	10.9	12.1	9.3	8.0	4.8	4.2	2.6	1.8	1.1	0.8

Isoprenoids distribution in saturates:

IP14	IP15	IP16	IP18	Pristane	Phytane
-	-	0.19	0.38	0.75	0.22

$\frac{IP15}{IP16}$	$\frac{IP16}{IP18}$	$\frac{IP18}{Pr}$	$\frac{Pr}{Ph}$	$\frac{IP15}{nC_{14}}$	$\frac{IP16}{nC_{15}}$	$\frac{IP18}{nC_{16}}$	$\frac{Pr}{nC_{17}}$	$\frac{Ph}{nC_{18}}$
-	0.5	0.5	3.4	-	0.15	0.20	0.30	0.060

OIL ANALYSIS

AMDEL
JOB NO. 3923/79

SAMPLE NO:	A1196/79
WELL:	Tirrawarra 2
TEST:	Production test
INTERVAL:	9784 - 9846'
FORMATION:	Tirrawarra
TYPE OF SAMPLE:	Oil, + 210°C fraction

Results of Analysis

API Gravity (whole sample) 46.1

Saturates	68.7	% by wt.
Aromatics	21.7	%
Polar compounds	2.2	%
Asphaltenes	0.9	%
Loss	6.5	%

n-Alkane distribution of saturates: O.E.P.

n-Alkane	C_{12}	C_{13}	C_{14}	C_{15}	C_{16}	C_{17}	C_{18}	C_{19}	C_{20}	C_{21}	C_{22}
Rel. abundance	3.5	6.6	8.6	9.6	9.6	8.3	7.8	7.2	6.5	6.0	5.5
n-Alkane	C_{23}	C_{24}	C_{25}	C_{26}	C_{27}	C_{28}	C_{29}	C_{30}	C_{31}	C_{32}	C_{33}
Rel. abundance	5.1	4.4	4.0	2.7	2.1	1.1	0.8	0.4	0.3	-	-

Isoprenoids distribution in saturates:

IP14	IP15	IP16	IP18	Pristane	Phytane
0.96	0.99	2.94	2.13	5.12	0.81

$\frac{IP15}{IP16}$	$\frac{IP16}{IP18}$	$\frac{IP18}{Pr}$	$\frac{Pr}{Ph}$	$\frac{IP15}{nC_{14}}$	$\frac{IP16}{nC_{15}}$	$\frac{IP18}{nC_{16}}$	$\frac{Pr}{nC_{17}}$	$\frac{Ph}{nC_{18}}$
0.34	1.38	0.42	6.3	0.115	0.105	0.30	0.62	0.125

OIL ANALYSIS

ANDEL
JOB NO. 3923/79

SAMPLE NO:	A1197/79
WELL:	Tirrawarra 3
TEST:	Production test
INTERVAL:	9132 - 9150'
FORMATION:	Tirrawarra
TYPE OF SAMPLE:	Condensate, + 210°C fraction

Results of Analysis

API Gravity (whole sample) 51.1

Saturates	69.3	% by wt.
Aromatics	18.1	%
Polar compounds	1.2	%
Asphaltenes	-	%
Loss	11.3	%

n-Alkane distribution of saturates: O.E.P.

n-Alkane	C_{12}	C_{13}	C_{14}	C_{15}	C_{16}	C_{17}	C_{18}	C_{19}	C_{20}	C_{21}	C_{22}
Rel. abundance	8.7	11.1	11.8	11.4	10.2	8.3	7.0	5.9	5.0	4.4	3.8
n-Alkane	C_{23}	C_{24}	C_{25}	C_{26}	C_{27}	C_{28}	C_{29}	C_{30}	C_{31}	C_{32}	C_{33}
Rel. abundance	3.3	2.7	2.3	1.6	1.2	0.6	0.3	0.2	-	-	-

Isoprenoids distribution in saturates:

IP14	IP15	IP16	IP18	Pristane	Phytane
1.13	0.90	2.86	1.81	3.24	0.68

$\frac{IP15}{IP16}$	$\frac{IP16}{IP18}$	$\frac{IP18}{Pr}$	$\frac{Pr}{Ph}$	$\frac{IP15}{nC_{14}}$	$\frac{IP16}{nC_{15}}$	$\frac{IP18}{nC_{16}}$	$\frac{Pr}{nC_{17}}$	$\frac{Ph}{nC_{18}}$
0.31	1.58	0.56	4.8	0.075	0.25	0.19	0.39	0.10

OIL ANALYSIS

AMDEL
JOB NO. 3923/79

SAMPLE NO:	A1198/79
WELL:	Tirrawarra 6
TEST:	Drill Stem test 2
INTERVAL:	9637 - 9774'
FORMATION:	Tirrawarra
TYPE OF SAMPLE:	Oil, + 210°C fraction

Results of Analysis

API Gravity (whole sample) 40.7

Saturates	62.1 %	by wt.
Aromatics	22.3 %	
Polar compounds	3.5 %	
Asphaltenes	1.3 %	
Loss	10.8 %	

n-Alkane distribution of saturates: O.E.P.

n-Alkane	C_{12}	C_{13}	C_{14}	C_{15}	C_{16}	C_{17}	C_{18}	C_{19}	C_{20}	C_{21}	C_{22}
Rel. abundance	2.1	5.1	9.1	12.4	13.2	11.3	9.9	8.3	6.8	5.5	4.4
n-Alkane	C_{23}	C_{24}	C_{25}	C_{26}	C_{27}	C_{28}	C_{29}	C_{30}	C_{31}	C_{32}	C_{33}
Rel. abundance	3.4	2.7	2.1	1.5	1.1	0.5	0.3	0.2	-	-	-

Isoprenoids distribution in saturates:

IP14	IP15	IP16	IP18	Pristane	Phytane
0.60	1.12	3.61	3.35	5.92	2.06

$\frac{IP15}{IP16}$	$\frac{IP16}{IP18}$	$\frac{IP18}{Pr}$	$\frac{Pr}{Ph}$	$\frac{IP15}{nC_{14}}$	$\frac{IP16}{nC_{15}}$	$\frac{IP18}{nC_{16}}$	$\frac{Pr}{nC_{17}}$	$\frac{Ph}{nC_{18}}$
0.31	1.08	0.57	2.9	0.125	0.29	0.255	0.52	0.21

OIL ANALYSIS

AMDEL
JOB NO. 3923/79

SAMPLE NO:	A1199/79
WELL:	Tirrawarra 8
TEST:	Drill Stem Test 7
INTERVAL:	9535 - 9675'
FORMATION:	Tirrawarra
TYPE OF SAMPLE:	Oil, +210°C fraction

Results of Analysis

API Gravity (whole sample) 50.1

Saturates	66.3	% by wt.
Aromatics	24.5	%
Polar compounds	2.1	%
Asphaltenes	0.1	%
Loss	7.0	%

n-Alkane distribution of saturates: O.E.P.

n-Alkane	C_{12}	C_{13}	C_{14}	C_{15}	C_{16}	C_{17}	C_{18}	C_{19}	C_{20}	C_{21}	C_{22}
Rel. abundance	3.4	6.1	8.2	9.1	9.4	8.3	7.9	7.4	6.7	6.3	5.7
n-Alkane	C_{23}	C_{24}	C_{25}	C_{26}	C_{27}	C_{28}	C_{29}	C_{30}	C_{31}	C_{32}	C_{33}
Rel. abundance	5.3	4.5	4.1	2.8	2.2	1.2	0.8	0.4	0.2		

Isoprenoids distribution in saturates:

IP14	IP15	IP16	IP18	Pristane	Phytane
0.90	0.90	2.71	2.00	4.87	0.77

$\frac{IP15}{IP16}$	$\frac{IP16}{IP18}$	$\frac{IP18}{Pr}$	$\frac{Pr}{Ph}$	$\frac{IP15}{nC_{14}}$	$\frac{IP16}{nC_{15}}$	$\frac{IP18}{nC_{16}}$	$\frac{Pr}{nC_{17}}$	$\frac{Ph}{nC_{18}}$
0.33	1.35	0.41	6.3	0.11	0.30	0.21	0.59	0.10

OIL ANALYSIS

AMDEL
JOB NO. 3923/79

SAMPLE NO:	A1200/79
WELL:	Tirrawarra 9
TEST:	Drill Stem test 4
INTERVAL:	9601 - 9742'
FORMATION:	Tirrawarra
TYPE OF SAMPLE:	Oil, + 210°C fraction

Results of Analysis

API Gravity (whole sample) 40.4

Saturates	67.2	% by wt.
Aromatics	20.5	%
Polar compounds	1.5	%
Asphaltenes	0.1	%
Loss	10.7	%

n-Alkane distribution of saturates: O.E.P.

n-Alkane	C_{12}	C_{13}	C_{14}	C_{15}	C_{16}	C_{17}	C_{18}	C_{19}	C_{20}	C_{21}	C_{22}
Rel. abundance	5.7	9.5	11.3	11.5	10.8	8.9	8.0	6.5	5.5	4.8	4.2
n-Alkane	C_{23}	C_{24}	C_{25}	C_{26}	C_{27}	C_{28}	C_{29}	C_{30}	C_{31}	C_{32}	C_{33}
Rel. abundance	3.8	3.1	2.7	1.7	1.2	0.5	0.3	0.2			

Isoprenoids distribution in saturates:

IP14	IP15	IP16	IP18	Pristane	Phytane
0.95	0.89	2.59	1.64	3.00	0.61

$\frac{IP15}{IP16}$	$\frac{IP16}{IP18}$	$\frac{IP18}{Pr}$	$\frac{Pr}{Ph}$	$\frac{IP15}{nC_{14}}$	$\frac{IP16}{nC_{15}}$	$\frac{IP18}{nC_{16}}$	$\frac{Pr}{nC_{17}}$	$\frac{Ph}{nC_{18}}$
0.34	1.58	0.55	4.9	0.080	0.225	0.15	0.34	0.08

OIL ANALYSIS

AMDEL JOB NO. 3923/79

SAMPLE NO:	A1201/79
WELL:	Fly Lake 1
TEST:	Isochronal test
INTERVAL:	8591 - 9170'
FORMATION:	Patchawarra
TYPE OF SAMPLE:	Condensate, + 210°C fraction

Results of Analysis

API Gravity (whole sample) 51.7

Saturates	69.9	%	by wt.
Aromatics	16.8	%	
Polar compounds	1.5	%	
Asphaltenes	--	%	
Loss	11.8	%	

n-Alkane distribution of saturates: O.E.P.

n-Alkane	C_{12}	C_{13}	C_{14}	C_{15}	C_{16}	C_{17}	C_{18}	C_{19}	C_{20}	C_{21}	C_{22}
Rel. abundance	11.3	12.5	12.0	10.9	9.5	7.5	6.4	5.4	4.7	4.1	3.5
n-Alkane	C_{23}	C_{24}	C_{25}	C_{26}	C_{27}	C_{28}	C_{29}	C_{30}	C_{31}	C_{32}	C_{33}
Rel. abundance	3.2	2.8	2.4	1.6	1.1	0.6	0.4	0.1	--	--	--

Isoprenoids distribution in saturates:

IP14	IP15	IP16	IP18	Pristane	Phytane
2.19	1.41	3.24	1.62	3.39	0.63

$\frac{IP15}{IP16}$	$\frac{IP16}{IP18}$	$\frac{IP18}{Pr}$	$\frac{Pr}{Ph}$	$\frac{IP15}{nC_{14}}$	$\frac{IP16}{nC_{15}}$	$\frac{IP18}{nC_{16}}$	$\frac{Pr}{nC_{17}}$	$\frac{Ph}{nC_{18}}$
0.43	2.00	0.48	5.3	0.12	0.30	0.17	0.45	0.10

OIL ANALYSIS

AMDEL JOB NO. 3923/79

SAMPLE NO:	A1202/79
WELL:	Fly Lake 1
TEST:	Production test
INTERVAL:	9297 - 9383 '
FORMATION:	Tirrawarra
TYPE OF SAMPLE:	Oil, + 210°C fraction

Results of Analysis

API Gravity (whole sample) 52.0

Saturates	56.0	% by wt.
Aromatics	30.2	%
Polar compounds	3.3	%
Asphaltenes	0.6	%
Loss	9.9	%

n-Alkane distribution of saturates: O.E.P.

n-Alkane	C_{12}	C_{13}	C_{14}	C_{15}	C_{16}	C_{17}	C_{18}	C_{19}	C_{20}	C_{21}	C_{22}
Rel. abundance	4.4	8.2	10.2	10.9	10.4	8.7	7.6	6.8	5.8	5.2	4.6
n-Alkane	C_{23}	C_{24}	C_{25}	C_{26}	C_{27}	C_{28}	C_{29}	C_{30}	C_{31}	C_{32}	C_{33}
Rel. abundance	4.2	3.7	3.3	2.3	1.7	1.0	0.6	0.3	0.2	--	--

Isoprenoids distribution in saturates:

IP14	IP15	IP16	IP18	Pristane	Phytane
1.05	0.90	2.70	1.75	3.75	0.60

$\frac{IP15}{IP16}$	$\frac{IP16}{IP18}$	$\frac{IP18}{Pr}$	$\frac{Pr}{Ph}$	$\frac{IP15}{nC_{14}}$	$\frac{IP16}{nC_{15}}$	$\frac{IP18}{nC_{16}}$	$\frac{Pr}{nC_{17}}$	$\frac{Ph}{nC_{18}}$
0.33	1.55	0.46	6.40	0.09	0.25	0.17	0.43	0.08

OIL ANALYSIS

ANDEL 3923/79
JOB NO.

SAMPLE NO:	A1203/79
WELL:	Fly Lake 2
TEST:	Production test
INTERVAL:	9549 - 9555'
FORMATION:	Tirrawarra
TYPE OF SAMPLE:	Oil, + 210°C fraction

Results of Analysis

API Gravity (whole sample) 49.6

Saturates	61.7 %	by wt.
Aromatics	25.6 %	
Polar compounds	2.9 %	
Asphaltenes	0.4 %	
Loss	9.4 %	

n-Alkane distribution of saturates: O.E.P.

n-Alkane	C_{12}	C_{13}	C_{14}	C_{15}	C_{16}	C_{17}	C_{18}	C_{19}	C_{20}	C_{21}	C_{22}
Rel. abundance	1.6	4.4	7.3	9.1	9.7	8.6	8.2	7.7	6.9	6.4	5.8
n-Alkane	C_{23}	C_{24}	C_{25}	C_{26}	C_{27}	C_{28}	C_{29}	C_{30}	C_{31}	C_{32}	C_{33}
Rel. abundance	5.5	4.9	4.5	3.5	2.8	1.5	1.0	0.5	0.3	0.2	--

Isoprenoids distribution in saturates:

IP14	IP15	IP16	IP18	Pristane	Phytane
0.75	1.00	3.15	2.40	6.60	0.90

$\frac{IP15}{IP16}$	$\frac{IP16}{IP18}$	$\frac{IP18}{Pr}$	$\frac{Pr}{Ph}$	$\frac{IP15}{nC_{14}}$	$\frac{IP16}{nC_{15}}$	$\frac{IP18}{nC_{16}}$	$\frac{Pr}{nC_{17}}$	$\frac{Ph}{nC_{18}}$
0.31	1.32	0.36	7.2	0.135	0.345	0.25	0.77	0.115

OIL ANALYSIS

AMDEL 3923/79
JOB NO.

SAMPLE NO:	A1204/79
WELL:	Moorari I
TEST:	Drill stem test 6
INTERVAL:	9562 - 9640'
FORMATION:	Tirrawarra
TYPE OF SAMPLE:	Oil, + 210°C fraction

Results of Analysis

API Gravity (whole sample) 45.8

Saturates	55.6 %	by wt.
Aromatics	20.3 %	
Polar compounds	3.3 %	
Asphaltenes	0.3 %	
Loss	20.5 %	

n-Alkane distribution of saturates: O.E.P.

n-Alkane	C_{12}	C_{13}	C_{14}	C_{15}	C_{16}	C_{17}	C_{18}	C_{19}	C_{20}	C_{21}	C_{22}
Rel. abundance	1.1	4.5	8.1.	10.2	10.7	9.4	8.6	7.8	6.7	6.1	5.4
n-Alkane	C_{23}	C_{24}	C_{25}	C_{26}	C_{27}	C_{28}	C_{29}	C_{30}	C_{31}	C_{32}	C_{33}
Rel. abundance	5.0	4.4	4.1	3.0	2.3	1.2	0.8	0.4	0.3	--	--

Isoprenoids distribution in saturates:

IP14	IP15	IP16	IP18	Pristane	Phytane
0.55	0.90	3.0	2.5	5.8	0.90

$\frac{IP15}{IP16}$	$\frac{IP16}{IP18}$	$\frac{IP18}{Pr}$	$\frac{Pr}{Ph}$	$\frac{IP15}{nC_{14}}$	$\frac{IP16}{nC_{15}}$	$\frac{IP18}{nC_{16}}$	$\frac{Pr}{nC_{17}}$	$\frac{Ph}{nC_{18}}$
0.29	1.21	0.43	6.55	0.11	0.295	0.23	0.62	0.105

OIL ANALYSIS

ANDEL 3923/79
JOB NO.

SAMPLE NO:	A1205/79
WELL:	Mudrangie 2
TEST:	Drill stem test 4
INTERVAL:	10205 - 10282'
FORMATION:	Tirrawarra
TYPE OF SAMPLE:	Oil, + 210°C fraction

Results of Analysis

API Gravity (whole sample)	39.2
Saturates	67.6 % by wt.
Aromatics	17.4 %
Polar compounds	2.0 %
Asphaltenes	0.1 %
Loss	12.9 %

n-Alkane distribution of saturates:

O.E.P.

n-Alkane	C_{12}	C_{13}	C_{14}	C_{15}	C_{16}	C_{17}	C_{18}	C_{19}	C_{20}	C_{21}	C_{22}
Rel. abundance	2.8	5.9	8.4	9.6	9.8	8.6	7.8	7.2	6.6	6.0	5.5
n-Alkane	C_{23}	C_{24}	C_{25}	C_{26}	C_{27}	C_{28}	C_{29}	C_{30}	C_{31}	C_{32}	C_{33}
Rel. abundance	5.3	4.6	4.2	2.9	2.3	1.1	0.8	0.4	0.2	--	--

Isoprenoids distribution in saturates:

IP14	IP15	IP16	IP18	Pristane	Phytane
0.85	0.85	2.6	1.65	4.10	0.7

$\frac{IP15}{IP16}$	$\frac{IP16}{IP18}$	$\frac{IP18}{Pr}$	$\frac{Pr}{Ph}$	$\frac{IP15}{nC_{14}}$	$\frac{IP16}{nC_{15}}$	$\frac{IP18}{nC_{16}}$	$\frac{Pr}{nC_{17}}$	$\frac{Ph}{nC_{18}}$
0.32	1.55	0.41	6.00	0.10	0.27	0.17	0.47	0.085

OIL ANALYSIS

AMOCO 3923/79
JOB NO.

SAMPLE NO: A1206/79

WELL: Strzelecki 3

TEST: Drill stem test 1

INTERVAL: 4015 - 4105' ?

FORMATION:

TYPE OF SAMPLE: Oil, + 210°C fraction

Results of Analysis

API Gravity (whole sample) 49.2

Saturates	83.8 %	by wt.
Aromatics	10.3 %	
Polar compounds	1.6 %	
Asphaltenes	0.3 %	
Loss	4.0 %	

n-Alkane distribution of saturates: O.E.P.

n-Alkane	C_{12}	C_{13}	C_{14}	C_{15}	C_{16}	C_{17}	C_{18}	C_{19}	C_{20}	C_{21}	C_{22}
Rel. abundance	--	1.0	2.3	3.8	5.5	6.7	7.4	7.4	7.2	7.8	8.3
n-Alkane	C_{23}	C_{24}	C_{25}	C_{26}	C_{27}	C_{28}	C_{29}	C_{30}	C_{31}	C_{32}	C_{33}
Rel. abundance	9.5	9.2	8.8	5.8	4.3	2.4	1.5	0.7	0.3	--	--

Isoprenoids distribution in saturates:

IP14	IP15	IP16	IP18	Pristane	Phytane
--	--	0.65	0.80	1.95	0.55

$\frac{IP15}{IP16}$	$\frac{IP16}{IP18}$	$\frac{IP18}{Pr}$	$\frac{Pr}{Ph}$	$\frac{IP15}{nC_{14}}$	$\frac{IP16}{nC_{15}}$	$\frac{IP18}{nC_{16}}$	$\frac{Pr}{nC_{17}}$	$\frac{Ph}{nC_{18}}$
--	0.86	0.40	3.5	--	0.175	0.14	0.29	0.075

OIL ANALYSIS

AMDEL JOB NO. 3923/79

SAMPLE NO: A1207/79

WELL: Stzelecki 3

TEST: Drill stem test 2

INTERVAL: 5420 - 5503'

FORMATION: Birkhead

TYPE OF SAMPLE: Oil, + 210°C fraction

Results of Analysis

API Gravity (whole sample) 43.7

Saturates	87.0	% by wt.
Aromatics	8.6	%
Polar compounds	2.9	%
Asphaltenes	0.3	%
Loss	1.2	%

n-Alkane distribution of saturates:

O.E.P.

n-Alkane	C_{12}	C_{13}	C_{14}	C_{15}	C_{16}	C_{17}	C_{18}	C_{19}	C_{20}	C_{21}	C_{22}
Rel. abundance	--	0.8	2.3	4.6	7.1	9.0	10.6	11.2	10.8	10.8	9.8
n-Alkane	C_{23}	C_{24}	C_{25}	C_{26}	C_{27}	C_{28}	C_{29}	C_{30}	C_{31}	C_{32}	C_{33}
Rel. abundance	9.1	6.1	4.3	1.8	1.1	0.4	0.2	--	--	--	--

Isoprenoids distribution in saturates:

IP14	IP15	IP16	IP18	Pristane	Phytane
--	--	0.70	1.08	2.85	0.80

$\frac{IP15}{IP16}$	$\frac{IP16}{IP18}$	$\frac{IP18}{Pr}$	$\frac{Pr}{Ph}$	$\frac{IP15}{nC_{14}}$	$\frac{IP16}{nC_{15}}$	$\frac{IP18}{nC_{16}}$	$\frac{Pr}{nC_{17}}$	$\frac{Ph}{nC_{18}}$
--	0.65	0.38	3.5	--	0.155	0.15	0.31	0.08

OIL ANALYSIS

ANDEL
JOB NO. 3923/79

SAMPLE NO: A1208/79

WELL: Strzelecki 3

TEST: Drill stem test 3

INTERVAL: 5515 - 5539'

FORMATION: Birkhead Fm

TYPE OF SAMPLE: Oil, +210°C fraction

Results of Analysis

API Gravity (whole sample) 44.2

Saturates	86.5 %	by wt.
Aromatics	7.0 %	
Polar compounds	2.2 %	
Asphaltenes	0.4 %	
Loss	3.9 %	

n-Alkane distribution of saturates: O.E.P.

n-Alkane	C_{12}	C_{13}	C_{14}	C_{15}	C_{16}	C_{17}	C_{18}	C_{19}	C_{20}	C_{21}	C_{22}
Rel. abundance	1.4	3.2	4.8	6.4	7.6	8.6	9.5	9.7	9.2	9.2	8.3
n-Alkane	C_{23}	C_{24}	C_{25}	C_{26}	C_{27}	C_{28}	C_{29}	C_{30}	C_{31}	C_{32}	C_{33}
Rel. abundance	8.1	5.7	4.2	2.0	1.2	0.5	0.2	--	--	--	--

Isoprenoids distribution in saturates:

IP14	IP15	IP16	IP18	Pristane	Phytane
—	0.25	1.15	1.05	2.70	0.70

$\frac{IP15}{IP16}$	$\frac{IP16}{IP18}$	$\frac{IP18}{Pr}$	$\frac{Pr}{Ph}$	$\frac{IP15}{nC_{14}}$	$\frac{IP16}{nC_{15}}$	$\frac{IP18}{nC_{16}}$	$\frac{Pr}{nC_{17}}$	$\frac{Ph}{nC_{18}}$
0.22	1.10	0.38	3.9	0.05	0.18	0.135	0.32	0.075

OIL ANALYSIS

ANDEL
JOB NO. 3923/79

SAMPLE NO:	A1209/79
WELL:	Strzelecki 3
TEST:	Drill stem test 4
INTERVAL:	6025 - 6115 '
FORMATION:	Tolachee
TYPE OF SAMPLE:	Condensate, + 210°C fraction

Results of Analysis

API Gravity (whole sample)	46.3
Saturates	91.5 % by wt.
Aromatics	7.8 %
Polar compounds	0.2 %
Asphaltenes	-- %
Loss	0.5 %

n-Alkane distribution of saturates: O.E.P.

n-Alkane	C_{12}	C_{13}	C_{14}	C_{15}	C_{16}	C_{17}	C_{18}	C_{19}	C_{20}	C_{21}	C_{22}
Rel. abundance	3.2	6.3	8.8	10.4	11.1	10.7	9.8	8.5	7.0	6.1	5.0
n-Alkane	C_{23}	C_{24}	C_{25}	C_{26}	C_{27}	C_{28}	C_{29}	C_{30}	C_{31}	C_{32}	C_{33}
Rel. abundance	4.5	3.3	2.5	1.4	0.8	0.5	0.2	--	--	--	--

Isoprenoids distribution in saturates:

IP14	IP15	IP16	IP18	Pristane	Phytane
--	0.50	1.70	1.35	2.55	0.70

$\frac{IP15}{IP16}$	$\frac{IP16}{IP18}$	$\frac{IP18}{Pr}$	$\frac{Pr}{Ph}$	$\frac{IP15}{nC_{14}}$	$\frac{IP16}{nC_{15}}$	$\frac{IP18}{nC_{16}}$	$\frac{Pr}{nC_{17}}$	$\frac{Ph}{nC_{18}}$
0.27	1.27	0.53	3.75	0.055	0.165	0.12	0.24	0.07

OIL ANALYSIS

AMDEL
JOB NO. 3923/79

SAMPLE NO: A1210/79

WELL: Strzelecki 3

TEST: Drill stem test 5

INTERVAL: 6146 - 6215 '

FORMATION: Toolachee

TYPE OF SAMPLE: Condensate, + 210°C fraction

Results of Analysis

API Gravity (whole sample) 46.0

Saturates	93.6	%	by wt.
Aromatics	4.8	%	
Polar compounds	0.8	%	
Asphaltenes	--	%	
Loss	0.8	%	

n-Alkane distribution of saturates: O.E.P.

n-Alkane	C_{12}	C_{13}	C_{14}	C_{15}	C_{16}	C_{17}	C_{18}	C_{19}	C_{20}	C_{21}	C_{22}
Rel. abundance	5.7	9.1	11.5	12.3	11.9	10.6	9.0	7.3	5.7	4.7	3.7
n-Alkane	C_{23}	C_{24}	C_{25}	C_{26}	C_{27}	C_{28}	C_{29}	C_{30}	C_{31}	C_{32}	C_{33}
Rel. abundance	3.1	2.1	1.4	0.9	0.6	0.3	0.1	--	--	--	--

Isoprenoids distribution in saturates:

IP14	IP15	IP16	IP18	Pristane	Phytane
0.65	0.65	2.0	1.45	2.45	0.60

$\frac{IP15}{IP16}$	$\frac{IP16}{IP18}$	$\frac{IP18}{Pr}$	$\frac{Pr}{Ph}$	$\frac{IP15}{nC_{14}}$	$\frac{IP16}{nC_{15}}$	$\frac{IP18}{nC_{16}}$	$\frac{Pr}{nC_{17}}$	$\frac{Ph}{nC_{18}}$
0.32	1.40	0.59	4.25	0.055	0.165	0.12	0.23	0.065

OIL ANALYSIS

AMDEL 3923/79
JOB NO.

SAMPLE NO:	A1211/79
WELL:	Della 4
TEST:	Isochronal test
INTERVAL:	6506 - 6605'
FORMATION:	Toolachee
TYPE OF SAMPLE:	Condensate, + 210°C fraction

Results of Analysis

API Gravity (whole sample) 42.3

Saturates	80.2	%	by wt.
Aromatics	13.3	%	
Polar compounds	0.9	%	
Asphaltenes	--	%	
Loss	5.6	%	

n-Alkane distribution of saturates: O.E.P.

n-Alkane	C_{12}	C_{13}	C_{14}	C_{15}	C_{16}	C_{17}	C_{18}	C_{19}	C_{20}	C_{21}	C_{22}
Rel. abundance	5.4	9.3	11.3	11.5	10.6	9.0	7.8	6.4	5.2	4.7	4.3
n-Alkane	C_{23}	C_{24}	C_{25}	C_{26}	C_{27}	C_{28}	C_{29}	C_{30}	C_{31}	C_{32}	C_{33}
Rel. abundance	4.2	3.4	2.8	1.7	1.3	0.7	0.4	--	--	--	--

Isoprenoids distribution in saturates:

IP14	IP15	IP16	IP18	Pristane	Phytane
0.80	0.80	2.20	1.45	1.95	0.65

$\frac{IP15}{IP16}$	$\frac{IP16}{IP18}$	$\frac{IP18}{Pr}$	$\frac{Pr}{Ph}$	$\frac{IP15}{nC_{14}}$	$\frac{IP16}{nC_{15}}$	$\frac{IP18}{nC_{16}}$	$\frac{Pr}{nC_{17}}$	$\frac{Ph}{nC_{18}}$
0.36	1.50	0.75	2.90	0.07	0.19	0.14	0.22	0.085

OIL ANALYSIS

AMDEL JOB NO. 3923/79

SAMPLE NO:	A1212/79
WELL:	Della 5A
TEST:	Isochronal test
INTERVAL:	6263 - 6401'
FORMATION:	Toolachee
TYPE OF SAMPLE:	Condensate, + 210°C fraction

Results of Analysis

API Gravity (whole sample) 42.5

Saturates	79.9	% by wt.
Aromatics	12.0	%
Polar compounds	1.3	%
Asphaltenes	--	%
Loss	6.8	%

n-Alkane distribution of saturates: O.E.P.

n-Alkane	C_{12}	C_{13}	C_{14}	C_{15}	C_{16}	C_{17}	C_{18}	C_{19}	C_{20}	C_{21}	C_{22}
Rel. abundance	6.4	10.4	12.3	12.4	11.3	9.0	7.4	6.0	5.0	4.2	3.7
n-Alkane	C_{23}	C_{24}	C_{25}	C_{26}	C_{27}	C_{28}	C_{29}	C_{30}	C_{31}	C_{32}	C_{33}
Rel. abundance	3.4	3.0	2.4	1.4	1.0	0.5	0.2	--	--	--	--

Isoprenoids distribution in saturates;

IP14	IP15	IP16	IP18	Pristane	Phytane
0.74	0.80	2.00	1.27	1.68	0.54

$\frac{IP15}{IP16}$	$\frac{IP16}{IP18}$	$\frac{IP18}{Pr}$	$\frac{Pr}{Ph}$	$\frac{IP15}{nC_{14}}$	$\frac{IP16}{nC_{15}}$	$\frac{IP18}{nC_{16}}$	$\frac{Pr}{nC_{17}}$	$\frac{Ph}{nC_{18}}$
0.40	1.58	0.76	3.15	0.075	0.19	0.13	0.215	0.085

OIL ANALYSIS

AMDEL JOB NO. 3923/79

SAMPLE NO:	A1213/79
WELL:	Della 6
TEST:	Isochronal test
INTERVAL:	6540 - 6618'
FORMATION:	Toolachee
TYPE OF SAMPLE:	Condensate, + 210^{0}C fraction

Results of Analysis

API Gravity (whole sample) 43.3

Saturates	83.5 %	by wt.
Aromatics	13.1 %	
Polar compounds	1.1 %	
Asphaltenes	-- %	
Loss	2.3 %	

n-Alkane distribution of saturates: O.E.P.

n-Alkane	C_{12}	C_{13}	C_{14}	C_{15}	C_{16}	C_{17}	C_{18}	C_{19}	C_{20}	C_{21}	C_{22}
Rel. abundance	6.9	10.9	12.5	12.1	11.0	9.1	7.7	6.1	4.8	4.3	3.7
n-Alkane	C_{23}	C_{24}	C_{25}	C_{26}	C_{27}	C_{28}	C_{29}	C_{30}	C_{31}	C_{32}	C_{33}
Rel. abundance	3.5	2.7	2.2	1.2	0.8	0.3	0.2	--	--	--	--

Isoprenoids distribution in saturates:

IP14	IP15	IP16	IP18	Pristane	Phytane
1.00	0.85	2.35	1.50	1.95	0.65

$\frac{IP15}{IP16}$	$\frac{IP16}{IP18}$	$\frac{IP18}{Pr}$	$\frac{Pr}{Ph}$	$\frac{IP15}{nC_{14}}$	$\frac{IP16}{nC_{15}}$	$\frac{IP18}{nC_{16}}$	$\frac{Pr}{nC_{17}}$	$\frac{Ph}{nC_{18}}$
0.37	1.58	0.76	3.10	0.07	0.20	0.14	0.22	0.085

OIL ANALYSIS

AMDEL
JOB NO. 3823.79

SAMPLE NO:	A1214/79
WELL:	Daralingie 1
TEST:	Isochronal test
INTERVAL:	6959 - 7192'
FORMATION:	Patchawarra
TYPE OF SAMPLE:	Condensate, + 210°C fraction

Results of Analysis

API Gravity (whole sample) 54.0

Saturates	81.2	% by wt.
Aromatics	7.9	%
Polar compounds	0.7	%
Asphaltenes	--	%
Loss	10.2	%

n-Alkane distribution of saturates: O.E.P.

n-Alkane	C_{12}	C_{13}	C_{14}	C_{15}	C_{16}	C_{17}	C_{18}	C_{19}	C_{20}	C_{21}	C_{22}
Rel. abundance	6.2	9.2	10.9	11.2	10.8	9.5	8.4	7.0	5.8	5.2	4.4
n-Alkane	C_{23}	C_{24}	C_{25}	C_{26}	C_{27}	C_{28}	C_{29}	C_{30}	C_{31}	C_{32}	C_{33}
Rel. abundance	4.0	2.9	2.2	1.2	0.8	0.3	0.1	--	--	--	--

Isoprenoids distribution in saturates:

IP14	IP15	IP16	IP18	Pristane	Phytane
0.90	0.85	2.50	1.60	3.35	0.70

$\frac{IP15}{IP16}$	$\frac{IP16}{IP18}$	$\frac{IP18}{Pr}$	$\frac{Pr}{Ph}$	$\frac{IP15}{nC_{14}}$	$\frac{IP16}{nC_{15}}$	$\frac{IP18}{nC_{16}}$	$\frac{Pr}{nC_{17}}$	$\frac{Ph}{nC_{18}}$
0.33	1.56	0.48	4.7	0.075	0.225	0.15	0.35	0.085

OIL ANALYSIS

ANDEL
JOB NO. 3923/79

SAMPLE NO:	A1215/79
WELL:	Brolga 1
TEST:	Drill stem test 3
INTERVAL:	9085 - 9180 '
FORMATION:	Patchawarra
TYPE OF SAMPLE:	Condensate, + 210°C fraction

Results of Analysis

API Gravity (whole sample) 48.9

Saturates	78.1	%	by wt.
Aromatics	13.8	%	
Polar compounds	1.6	%	
Asphaltenes	--	%	
Loss	6.5	%	

n-Alkane distribution of saturates: O.E.P.

n-Alkane	C_{12}	C_{13}	C_{14}	C_{15}	C_{16}	C_{17}	C_{18}	C_{19}	C_{20}	C_{21}	C_{22}
Rel. abundance	8.6	11.0	12.2	11.6	10.4	8.7	7.3	6.0	4.7	4.2	3.6
n-Alkane	C_{23}	C_{24}	C_{25}	C_{26}	C_{27}	C_{28}	C_{29}	C_{30}	C_{31}	C_{32}	C_{33}
Rel. abundance	3.2	2.6	2.1	1.3	1.1	0.8	0.4	0.2	--	--	--

Isoprenoids distribution in saturates:

IP14	IP15	IP16	IP18	Pristane	Phytane
1.20	0.95	2.80	1.75	3.35	0.65

$\frac{IP15}{IP16}$	$\frac{IP16}{IP18}$	$\frac{IP18}{Pr}$	$\frac{Pr}{Ph}$	$\frac{IP15}{nC_{14}}$	$\frac{IP16}{nC_{15}}$	$\frac{IP18}{nC_{16}}$	$\frac{Pr}{nC_{17}}$	$\frac{Ph}{nC_{18}}$
0.34	1.63	0.52	5.2	0.08	0.24	0.165	0.38	0.090

OIL ANALYSIS

AMDEL
JOB NO. 3923/79

SAMPLE NO:	A 1216/79
WELL:	Brolga 1
TEST:	Drill stem test 4
INTERVAL:	9239 - 9362 '
FORMATION:	Patchawarra
TYPE OF SAMPLE:	Condensate, + 210°C fraction

Results of Analysis

API Gravity (whole sample) 48.0

Saturates	74.0 %	by wt.
Aromatics	17.7 %	
Polar compounds	1.6 %	
Asphaltenes	-- %	
Loss	6.7 %	

n-Alkane distribution of saturates: O.E.P.

n-Alkane	C_{12}	C_{13}	C_{14}	C_{15}	C_{16}	C_{17}	C_{18}	C_{19}	C_{20}	C_{21}	C_{22}
Rel. abundance	8.3	11.4	12.4	11.9	10.6	9.0	7.4	6.0	4.8	4.2	3.6
n-Alkane	C_{23}	C_{24}	C_{25}	C_{26}	C_{27}	C_{28}	C_{29}	C_{30}	C_{31}	C_{32}	C_{33}
Rel. abundance	3.2	2.4	2.0	1.1	1.0	0.5	0.2	--	--	--	--

Isoprenoids distribution in saturates:

IP14	IP15	IP16	IP18	Pristane	Phytane
1.20	0.90	2.65	1.75	2.85	0.60

$\frac{IP15}{IP16}$	$\frac{IP16}{IP18}$	$\frac{IP18}{Pr}$	$\frac{Pr}{Ph}$	$\frac{IP15}{nC_{14}}$	$\frac{IP16}{nC_{15}}$	$\frac{IP18}{nC_{16}}$	$\frac{Pr}{nC_{17}}$	$\frac{Ph}{nC_{18}}$
0.34	1.52	0.60	4.80	0.07	0.22	0.165	0.32	0.080

OIL ANALYSIS

AMDEL JOB NO. 3923/79

SAMPLE NO:	A1217/79
WELL:	Burke 1
TEST:	Production test
INTERVAL:	7849 - 8029'
FORMATION:	Patchawarra
TYPE OF SAMPLE:	Condensate, + 210°C fraction

Results of Analysis

API Gravity (whole sample) 42.6

Saturates	73.7	% by wt.
Aromatics	14.7	%
Polar compounds	0.7	%
Asphaltenes	--	%
Loss	10.9	%

n-Alkane distribution of saturates: O.E.P.

n-Alkane	C_{12}	C_{13}	C_{14}	C_{15}	C_{16}	C_{17}	C_{18}	C_{19}	C_{20}	C_{21}	C_{22}
Rel. abundance	5.5	8.3	9.6	9.8	9.5	8.6	7.7	6.7	5.9	5.4	5.2
n-Alkane	C_{23}	C_{24}	C_{25}	C_{26}	C_{27}	C_{28}	C_{29}	C_{30}	C_{31}	C_{32}	C_{33}
Rel. abundance	5.3	4.3	3.6	2.0	1.5	0.8	0.3	--	--	--	--

Isoprenoids distribution in saturates:

IP14	IP15	IP16	IP18	Pristane	Phytane
--	0.50	1.35	1.05	1.24	0.45

$\frac{IP15}{IP16}$	$\frac{IP16}{IP18}$	$\frac{IP18}{Pr}$	$\frac{Pr}{Ph}$	$\frac{IP15}{nC_{14}}$	$\frac{IP16}{nC_{15}}$	$\frac{IP18}{nC_{16}}$	$\frac{Pr}{nC_{17}}$	$\frac{Ph}{nC_{18}}$
0.35	1.28	0.86	2.63	0.05	0.14	0.11	0.14	0.060

OIL ANALYSIS

AMDEL
JOB NO. 3923/79

SAMPLE NO:	A1218/79
WELL:	Burke 1
TEST:	Production test
INTERVAL:	7115 - 7215 '
FORMATION:	Toolachee
TYPE OF SAMPLE:	Condensate + 210°C fraction

Results of Analysis

API Gravity (whole sample) 47.4

Saturates	70.0	%	by wt.
Aromatics	12.6	%	
Polar compounds	0.9	%	
Asphaltenes	--	%	
Loss	16.5	%	

n-Alkane distribution of saturates: O.E.P:

n-Alkane	C_{12}	C_{13}	C_{14}	C_{15}	C_{16}	C_{17}	C_{18}	C_{19}	C_{20}	C_{21}	C_{22}
Rel. abundance	5.7	9.7	11.4	11.5	10.7	9.3	8.0	6.6	5.4	4.8	4.3
n-Alkane	C_{23}	C_{24}	C_{25}	C_{26}	C_{27}	C_{28}	C_{29}	C_{30}	C_{31}	C_{32}	C_{33}
Rel. abundance	4.0	3.0	2.4	1.4	1.0	0.5	0.2	6.1	--	--	--

Isoprenoids distribution in saturates:

IP14	IP15	IP16	IP18	Pristane	Phytane
0.70	0.70	1.95	1.30	1.70	0.45

$\frac{IP15}{IP16}$	$\frac{IP16}{IP18}$	$\frac{IP18}{Pr}$	$\frac{Pr}{Ph}$	$\frac{IP15}{nC_{14}}$	$\frac{IP16}{nC_{15}}$	$\frac{IP18}{nC_{16}}$	$\frac{Pr}{nC_{17}}$	$\frac{Ph}{nC_{18}}$
0.34	1.53	0.76	3.8	0.09	0.17	0.12	0.18	0.055

OIL ANALYSIS

ANDEL
JOB NO. 3923/79

SAMPLE NO:	A 1219/79
WELL:	Kanowana 1
TEST:	Production test
INTERVAL:	9300 - 9351 '
FORMATION:	Patchawarra
TYPE OF SAMPLE:	Condensate, +210°C fraction

Results of Analysis

API Gravity (whole sample) 39.6

Saturates	71.5 %	by wt.
Aromatics	15.5 %	
Polar compounds	1.4 %	
Asphaltenes	-- %	
Loss	11.6 %	

n-Alkane distribution of saturates: O.E.P.

n-Alkane	C_{12}	C_{13}	C_{14}	C_{15}	C_{16}	C_{17}	C_{18}	C_{19}	C_{20}	C_{21}	C_{22}
Rel. abundance	3.6	8.2	10.9	11.4	10.9	9.5	8.3	7.1	5.9	5.3	4.9
n-Alkane	C_{23}	C_{24}	C_{25}	C_{26}	C_{27}	C_{28}	C_{29}	C_{30}	C_{31}	C_{32}	C_{33}
Rel. abundance	4.6	3.4	2.6	1.5	1.1	0.6	0.2	--	--	--	--

Isoprenoids distribution in saturates:

IP14	IP15	IP16	IP18	Pristane	Phytane
1.35	1.15	3.30	1.75	3.50	0.80

$\frac{IP15}{IP16}$	$\frac{IP16}{IP18}$	$\frac{IP18}{Pr}$	$\frac{Pr}{Ph}$	$\frac{IP15}{nC_{14}}$	$\frac{IP16}{nC_{15}}$	$\frac{IP18}{nC_{16}}$	$\frac{Pr}{nC_{17}}$	$\frac{Ph}{nC_{18}}$
0.35	1.88	0.50	4.50	0.10	0.29	0.16	0.37	0.095

OIL ANALYSIS

AMDEL JOB NO. 3923/79

SAMPLE NO:	A1220/79
WELL:	Dullingari 2
TEST:	Isochronal test
INTERVAL:	8047 - 8493'
FORMATION:	Patchawarra
TYPE OF SAMPLE:	Condensate, + 210°C fraction

Results of Analysis

API Gravity (whole sample) 32.9

Saturates	41.2	% by wt.
Aromatics	35.5	%
Polar compounds	2.3	%
Asphaltenes	--	%
Loss	21.0	%

n-Alkane distribution of saturates: O.E.P.

n-Alkane	C_{12}	C_{13}	C_{14}	C_{15}	C_{16}	C_{17}	C_{18}	C_{19}	C_{20}	C_{21}	C_{22}
Rel. abundance	4.2	10.4	13.2	13.4	12.2	10.1	8.3	6.3	4.9	4.5	3.4
n-Alkane	C_{23}	C_{24}	C_{25}	C_{26}	C_{27}	C_{28}	C_{29}	C_{30}	C_{31}	C_{32}	C_{33}
Rel. abundance	3.0	2.2	1.6	1.0	0.8	0.4	0.1	--	--	--	--

Isoprenoids distribution in saturates:

IP14	IP15	IP16	IP18	Pristane	Phytane
--	0.85	2.25	1.55	1.65	0.60

$\frac{IP15}{IP16}$	$\frac{IP16}{IP18}$	$\frac{IP18}{Pr}$	$\frac{Pr}{Ph}$	$\frac{IP15}{nC_{14}}$	$\frac{IP16}{nC_{15}}$	$\frac{IP18}{nC_{16}}$	$\frac{Pr}{nC_{17}}$	$\frac{Ph}{nC_{18}}$
0.38	1.42	0.96	2.78	0.065	0.165	0.13	0.16	0.070

OIL ANALYSIS

AMDEL
JOB NO. 3923/79

SAMPLE NO:	A 1221/79
WELL:	Dullingari 2
TEST:	Isochronal test
INTERVAL:	6950 - 7264'
FORMATION:	Toolachee
TYPE OF SAMPLE:	Condensate, + 210°C fraction

Results of Analysis

API Gravity (whole sample) 52.7

Saturates	74.0	% by wt.
Aromatics	7.3	%
Polar compounds	0.7	%
Asphaltenes	--	%
Loss	18.0	%

n-Alkane distribution of saturates: O.E.P.

n-Alkane	C_{12}	C_{13}	C_{14}	C_{15}	C_{16}	C_{17}	C_{18}	C_{19}	C_{20}	C_{21}	C_{22}
Rel. abundance	6.2	10.8	12.8	13.1	11.9	10.1	8.2	6.5	4.9	4.0	3.3
n-Alkane	C_{23}	C_{24}	C_{25}	C_{26}	C_{27}	C_{28}	C_{29}	C_{30}	C_{31}	C_{32}	C_{33}
Rel. abundance	2.7	2.1	1.5	0.8	0.6	0.3	0.2	--	--	--	--

Isoprenoids distribution in saturates:

IP14	IP15	IP16	IP18	Pristane	Phytane
1.50	1.25	3.45	1.95	3.60	0.75

$\frac{IP15}{IP16}$	$\frac{IP16}{IP18}$	$\frac{IP18}{Pr}$	$\frac{Pr}{Ph}$	$\frac{IP15}{nC_{14}}$	$\frac{IP16}{nC_{15}}$	$\frac{IP18}{nC_{16}}$	$\frac{Pr}{nC_{17}}$	$\frac{Ph}{nC_{18}}$
0.37	1.76	0.54	4.85	0.10	0.265	0.16	0.37	0.09

OIL ANALYSIS

AMDEL
JOB NO.3923/79

SAMPLE NO: A1223/79

WELL: Dullingari 2

TEST: Isochronal test

INTERVAL:

FORMATION:

TYPE OF SAMPLE: Condensate, + 210°C fraction

Results of Analysis

API Gravity (whole sample) 34.7

Saturates	49.2	% by wt.
Aromatics	41.0	%
Polar compounds	1.9	%
Asphaltenes	--	%
Loss	7.9	%

n-Alkane distribution of saturates:

O.E.P.

n-Alkane	C_{12}	C_{13}	C_{14}	C_{15}	C_{16}	C_{17}	C_{18}	C_{19}	C_{20}	C_{21}	C_{22}
Rel. abundance	7.8	11.7	13.0	12.8	11.5	9.5	7.8	6.0	4.6	3.8	3.1
n-Alkane	C_{23}	C_{24}	C_{25}	C_{26}	C_{27}	C_{28}	C_{29}	C_{30}	C_{31}	C_{32}	C_{33}
Rel. abundance	2.7	2.1	1.5	0.9	0.7	0.4	0.1	--	--	--	--

Isoprenoids distribution in saturates:

IP14	IP15	IP16	IP18	Pristane	Phytane
0.74	0.92	2.15	1.53	1.48	0.55

$\frac{IP15}{IP16}$	$\frac{IP16}{IP18}$	$\frac{IP18}{Pr}$	$\frac{Pr}{Ph}$	$\frac{IP15}{nC_{14}}$	$\frac{IP16}{nC_{15}}$	$\frac{IP18}{nC_{16}}$	$\frac{Pr}{nC_{17}}$	$\frac{Ph}{nC_{18}}$
0.43	1.40	1.05	2.65	0.07	0.17	0.13	0.15	0.07

OIL ANALYSIS

AMDEL JOB NO. 3923/79

SAMPLE NO: A1224/79

WELL: Kidman 1

TEST: Drill stem test 1

INTERVAL: 6578 - 6622'

FORMATION: Toolachee

TYPE OF SAMPLE: Condensate, + 210°C fraction

Results of Analysis

API Gravity (whole sample) 50.9

Saturates	86.0 %	by wt.
Aromatics	8.9 %	
Polar compounds	1.0 %	
Asphaltenes	%	
Loss	4.1 %	

n-Alkane distribution of saturates: O.E.P.

n-Alkane	C_{12}	C_{13}	C_{14}	C_{15}	C_{16}	C_{17}	C_{18}	C_{19}	C_{20}	C_{21}	C_{22}
Rel. abundance	8.9	12.9	14.4	13.9	12.1	10.0	7.8	5.9	4.2	3.2	2.3
n-Alkane	C_{23}	C_{24}	C_{25}	C_{26}	C_{27}	C_{28}	C_{29}	C_{30}	C_{31}	C_{32}	C_{33}
Rel. abundance	1.7	1.1	0.8	0.3	0.3	0.2	--	--	--	--	--

Isoprenoids distribution in saturates:

IP14	IP15	IP16	IP18	Pristane	Phytane
1.43	0.98	2.94	1.66	2.56	0.60

$\frac{IP15}{IP16}$	$\frac{IP16}{IP18}$	$\frac{IP18}{Pr}$	$\frac{Pr}{Ph}$	$\frac{IP15}{nC_{14}}$	$\frac{IP16}{nC_{15}}$	$\frac{IP18}{nC_{16}}$	$\frac{Pr}{nC_{17}}$	$\frac{Ph}{nC_{18}}$
0.33	1.77	0.65	4.25	0.070	0.21	0.135	0.26	0.080

OIL ANALYSIS

AMDEL
JOB NO.

SAMPLE NO:	A1225/79
WELL:	Kirby 1
TEST:	Drill stem test 1
INTERVAL:	8399 - 8464 '
FORMATION:	Nappamerri
TYPE OF SAMPLE:	Condensate, + 210°C fraction

Results of Analysis

API Gravity (whole sample) 47.7

Saturates	94.3 %	by wt.
Aromatics	2.0 %	
Polar compounds	1.2 %	
Asphaltenes	%	
Loss	2.5 %	

n-Alkane distribution of saturates: O.E.P.

n-Alkane	C_{12}	C_{13}	C_{14}	C_{15}	C_{16}	C_{17}	C_{18}	C_{19}	C_{20}	C_{21}	C_{22}
Rel. abundance	3.8	7.1	10.3	12.7	13.7	12.8	11.1	8.8	6.3	4.8	3.4
n-Alkane	C_{23}	C_{24}	C_{25}	C_{26}	C_{27}	C_{28}	C_{29}	C_{30}	C_{31}	C_{32}	C_{33}
Rel. abundance	2.4	1.3	0.8	0.3	0.3	0.1	--	--	--	--	--

Isoprenoids distribution in saturates:

IP14	IP15	IP16	IP18	Pristane	Phytane
0.62	0.62	2.69	2.21	3.38	0.86

$\frac{IP15}{IP16}$	$\frac{IP16}{IP18}$	$\frac{IP18}{Pr}$	$\frac{Pr}{Ph}$	$\frac{IP15}{nC_{14}}$	$\frac{IP16}{nC_{15}}$	$\frac{IP18}{nC_{16}}$	$\frac{Pr}{nC_{17}}$	$\frac{Ph}{nC_{18}}$
0.23	1.22	0.65	3.9	0.06	0.21	0.16	0.26	0.08

OIL ANALYSIS

AMDEL JOB NO. 3923/79

SAMPLE NO:	A1226/79
WELL:	Ashby 1
TEST:	Drill stem test 3
INTERVAL:	6412 - 6506'
FORMATION:	
TYPE OF SAMPLE:	Condensate, + 210°C fraction

Results of Analysis

API Gravity (whole sample) 45.7

Saturates	75.3 %	by wt.
Aromatics	6.4 %	
Polar compounds	0.5 %	
Asphaltenes	-- %	
Loss	17.8 %	

n-Alkane distribution of saturates: O.E.P.

n-Alkane	C_{12}	C_{13}	C_{14}	C_{15}	C_{16}	C_{17}	C_{18}	C_{19}	C_{20}	C_{21}	C_{22}
Rel. abundance	5.0	12.5	16.5	16.1	13.1	9.6	7.0	5.0	3.7	3.0	2.4
n-Alkane	C_{23}	C_{24}	C_{25}	C_{26}	C_{27}	C_{28}	C_{29}	C_{30}	C_{31}	C_{32}	C_{33}
Rel. abundance	2.3	1.5	1.2	0.5	0.4	0.2	--	--	--	--	--

Isoprenoids distribution in saturates:

IP14	IP15	IP16	IP18	Pristane	Phytane
2.36	1.96	5.0	1.96	4.25	0.75

$\frac{IP15}{IP16}$	$\frac{IP16}{IP18}$	$\frac{IP18}{Pr}$	$\frac{Pr}{Ph}$	$\frac{IP15}{nC_{14}}$	$\frac{IP16}{nC_{15}}$	$\frac{IP18}{nC_{16}}$	$\frac{Pr}{nC_{17}}$	$\frac{Ph}{nC_{18}}$
0.39	2.55	0.46	5.7	0.12	0.31	0.15	0.44	0.105

OIL ANALYSIS

AMDEL JOB NO. 3923/79

SAMPLE NO:	A1227/79
WELL:	Munkarie 1
TEST:	Drill stem test 1
INTERVAL:	6798-6928'
FORMATION:	Epsilon
TYPE OF SAMPLE:	Condensate, + 210°C fraction

Results of Analysis

API Gravity (whole sample)	46.6
Saturates	82.3 % by wt.
Aromatics	15.4 %
Polar compounds	0.5 %
Asphaltenes	-- %
Loss	1.8 %

n-Alkane distribution of saturates: O.E.P.

n-Alkane	C_{12}	C_{13}	C_{14}	C_{15}	C_{16}	C_{17}	C_{18}	C_{19}	C_{20}	C_{21}	C_{22}
Rel. abundance	8.3	11.6	1.29	13.0	12.2	10.0	8.6	7.1	5.6	4.2	2.9
n-Alkane	C_{23}	C_{24}	C_{25}	C_{26}	C_{27}	C_{28}	C_{29}	C_{30}	C_{31}	C_{32}	C_{33}
Rel. abundance	1.9	1.0	0.5	0.2	--	--	--	--	--	--	--

Isoprenoids distribution in saturates:

IP14	IP15	IP16	IP18	Pristane	Phytane
1.18	0.95	2.65	1.55	3.01	0.59

$\frac{IP15}{IP16}$	$\frac{IP16}{IP18}$	$\frac{IP18}{Pr}$	$\frac{Pr}{Ph}$	$\frac{IP15}{nC_{14}}$	$\frac{IP16}{nC_{15}}$	$\frac{IP18}{nC_{16}}$	$\frac{Pr}{nC_{17}}$	$\frac{Ph}{nC_{18}}$
0.36	1.73	0.51	5.1	0.075	0.205	0.125	0.30	0.07

OIL ANALYSIS

AMDEL JOB NO. 3923/79

SAMPLE NO: A1228/79

WELL: Munkarie 1

TEST: Drill stem test 3

INTERVAL: 7176 - 7249'

FORMATION: Patchawarra

TYPE OF SAMPLE: Condensate, + 210°C fraction

Results of Analysis

API Gravity (whole sample) 49.9

Saturates	82.4	% by wt.
Aromatics	4.4	%
Polar compounds	0.5	%
Asphaltenes		%
Loss	12.7	%

n-Alkane distribution of saturates: O.E.P.

n-Alkane	C_{12}	C_{13}	C_{14}	C_{15}	C_{16}	C_{17}	C_{18}	C_{19}	C_{20}	C_{21}	C_{22}
Rel. abundance	18.7	21.8	17.2	10.9	8.3	6.1	4.3	3.6	2.7	2.1	1.5
n-Alkane	C_{23}	C_{24}	C_{25}	C_{26}	C_{27}	C_{28}	C_{29}	C_{30}	C_{31}	C_{32}	C_{33}
Rel. abundance	1.1	0.7	0.5	--	--	--	--	--	--	--	--

Isoprenoids distribution in saturates:

IP14	IP15	IP16	IP18	Pristane	Phytane
2.64	1.55	2.46	0.91	1.64	0.27

$\frac{IP15}{IP16}$	$\frac{IP16}{IP18}$	$\frac{IP18}{Pr}$	$\frac{Pr}{Ph}$	$\frac{IP15}{nC_{14}}$	$\frac{IP16}{nC_{15}}$	$\frac{IP18}{nC_{16}}$	$\frac{Pr}{nC_{17}}$	$\frac{Ph}{nC_{18}}$
0.63	2.70	0.57	6.00	0.09	0.225	0.11	0.27	0.060

OIL ANALYSIS

AMDEL
JOB NO. 3923/79

SAMPLE NO:	A 1229/79
WELL:	Durham Downs 1
TEST:	Production test
INTERVAL:	8335 - 8350'
FORMATION:	Toolachee
TYPE OF SAMPLE:	Condensate, >210°C fraction

Results of Analysis

API Gravity (whole sample) 48.3

Saturates	77.6	% by wt.
Aromatics	16.3	%
Polar compounds	1.7	%
Asphaltenes		%
Loss	4.4	%

n-Alkane distribution of saturates:

O.E.P.

n-Alkane	C_{12}	C_{13}	C_{14}	C_{15}	C_{16}	C_{17}	C_{18}	C_{19}	C_{20}	C_{21}	C_{22}
Rel. abundance	6.5	11.2	13.7	14.0	12.7	9.7	7.8	5.9	4.6	3.6	2.8
n-Alkane	C_{23}	C_{24}	C_{25}	C_{26}	C_{27}	C_{28}	C_{29}	C_{30}	C_{31}	C_{32}	C_{33}
Rel. abundance	2.2	1.8	1.5	0.9	0.6	0.4	0.2	--	--	--	--

Isoprenoids distribution in saturates:

IP14	IP15	IP16	IP18	Pristane	Phytane
2.00	1.64	3.91	2.09	3.64	0.86

$\frac{IP15}{IP16}$	$\frac{IP16}{IP18}$	$\frac{IP18}{Pr}$	$\frac{Pr}{Ph}$	$\frac{IP15}{nC_{14}}$	$\frac{IP16}{nC_{15}}$	$\frac{IP18}{nC_{16}}$	$\frac{Pr}{nC_{17}}$	$\frac{Ph}{nC_{18}}$
0.42	1.85	0.58	4.2	0.12	0.28	0.165	0.37	0.145

OIL ANALYSIS

AMDEL JOB NO. 3923/79

SAMPLE NO:	A1230/79
WELL:	Epsilon 1
TEST:	(re sample)
INTERVAL:	6358 - 6380'
FORMATION:	Toolachee
TYPE OF SAMPLE:	Condensate, >210°C fraction

Results of Analysis

API Gravity (whole sample) 37.0

Saturates	57.3 % by wt.
Aromatics	28.3 %
Polar compounds	2.0 %
Asphaltenes	-- %
Loss	12.4 %

n-Alkane distribution of saturates: O.E.P.

n-Alkane	C_{12}	C_{13}	C_{14}	C_{15}	C_{16}	C_{17}	C_{18}	C_{19}	C_{20}	C_{21}	C_{22}
Rel. abundance	6.1	10.2	12.3	12.9	12.3	10.1	8.2	6.4	5.2	4.2	3.4
n-Alkane	C_{23}	C_{24}	C_{25}	C_{26}	C_{27}	C_{28}	C_{29}	C_{30}	C_{31}	C_{32}	C_{33}
Rel. abundance	2.7	2.1	1.8	1.0	0.6	0.3	0.2	--	--	--	--

Isoprenoids distribution in saturates:

IP14	IP15	IP16	IP18	Pristane	Phytane
0.88	0.79	2.47	1.68	1.95	0.62

$\frac{IP15}{IP16}$	$\frac{IP16}{IP18}$	$\frac{IP18}{Pr}$	$\frac{Pr}{Ph}$	$\frac{IP15}{nC_{14}}$	$\frac{IP16}{nC_{15}}$	$\frac{IP18}{nC_{16}}$	$\frac{Pr}{nC_{17}}$	$\frac{Ph}{nC_{18}}$
0.32	1.47	0.86	3.15	0.065	0.20	0.135	0.19	0.095

OIL ANALYSIS

AMDEL
JOB NO. 3923/79

SAMPLE NO:	A1231/79
WELL:	Big Lake 2
TEST:	Isochronal test
INTERVAL:	7461 - 7683'
FORMATION:	Toolachee
TYPE OF SAMPLE:	Condensate, >210°C fraction

Results of Analysis

API Gravity (whole sample)	45.4

Saturates	57.3 %	by wt.
Aromatics	21.6 %	
Polar compounds	1.2 %	
Asphaltenes	-- %	
Loss	19.9 %	

n-Alkane distribution of saturates: O.E.P.

n-Alkane	C_{12}	C_{13}	C_{14}	C_{15}	C_{16}	C_{17}	C_{18}	C_{19}	C_{20}	C_{21}	C_{22}
Rel. abundance	8.0	11.0	12.1	11.8	11.0	9.6	7.8	6.5	5.5	4.6	3.8
n-Alkane	C_{23}	C_{24}	C_{25}	C_{26}	C_{27}	C_{28}	C_{29}	C_{30}	C_{31}	C_{32}	C_{33}
Rel. abundance	3.1	2.4	1.7	1.0	0.5	0.2	--	--	--	--	--

Isoprenoids distribution in saturates:

IP14	IP15	IP16	IP18	Pristane	Phytane
0.80	0.73	2.27	1.47	1.80	0.67

$\frac{IP15}{IP16}$	$\frac{IP16}{IP18}$	$\frac{IP18}{Pr}$	$\frac{Pr}{Ph}$	$\frac{IP15}{nC_{14}}$	$\frac{IP16}{nC_{15}}$	$\frac{IP18}{nC_{16}}$	$\frac{Pr}{nC_{17}}$	$\frac{Ph}{nC_{18}}$
0.32	1.55	0.81	2.7	0.06	0.19	0.135	0.20	0.085

OIL ANALYSIS

AMDEL
JOB NO. 3923/79

SAMPLE NO:	A1232/79
WELL:	Big Lake 3
TEST:	Isochronal test
INTERVAL:	7685 - 7761'
FORMATION:	Toolachee
TYPE OF SAMPLE:	Condensate, + 210°C fraction

Results of Analysis

API Gravity (whole sample) 42.4

Saturates	52.8 %	by wt.
Aromatics	28.2 %	
Polar compounds	0.6 %	
Asphaltenes	-- %	
Loss	18.4 %	

n-Alkane distribution of saturates: O.E.P.

n-Alkane	C_{12}	C_{13}	C_{14}	C_{15}	C_{16}	C_{17}	C_{18}	C_{19}	C_{20}	C_{21}	C_{22}
Rel. abundance	12.1	14.9	14.7	13.1	11.2	8.3	6.6	5.1	3.9	3.0	2.3
n-Alkane	C_{23}	C_{24}	C_{25}	C_{26}	C_{27}	C_{28}	C_{29}	C_{30}	C_{31}	C_{32}	C_{33}
Rel. abundance	1.8	1.3	0.9	0.5	0.3	--	--	--	--	--	--

Isoprenoids distribution in saturates:

IP14	IP15	IP16	IP18	Pristane	Phytane
1.4	1.1	2.5	1.3	1.5	0.55

$\frac{IP15}{IP16}$	$\frac{IP16}{IP18}$	$\frac{IP18}{Pr}$	$\frac{Pr}{Ph}$	$\frac{IP15}{nC_{14}}$	$\frac{IP16}{nC_{15}}$	$\frac{IP18}{nC_{16}}$	$\frac{Pr}{nC_{17}}$	$\frac{Ph}{nC_{18}}$
0.43	1.91	0.86	2.8	0.075	0.19	0.115	0.18	0.08

OIL ANALYSIS

AMDEL
JOB NO. 3923/79

SAMPLE NO:	A1233/79
WELL:	Big Lake 4
TEST:	Isochronal test
INTERVAL:	7586- 7914'
FORMATION:	Toolachee-Daralingie
TYPE OF SAMPLE:	Condensate, + 210°C fraction

Results of Analysis

API Gravity (whole sample)	40.0
Saturates	47.9 % by wt.
Aromatics	35.4 %
Polar compounds	1.2 %
Asphaltenes	-- %
Loss	15.5 %

n-Alkane distribution of saturates: O.E.P.

n-Alkane	C_{12}	C_{13}	C_{14}	C_{15}	C_{16}	C_{17}	C_{18}	C_{19}	C_{20}	C_{21}	C_{22}
Rel. abundance	9.0	11.9	12.3	11.6	10.4	8.3	6.9	5.8	4.9	4.3	3.7
n-Alkane	C_{23}	C_{24}	C_{25}	C_{26}	C_{27}	C_{28}	C_{29}	C_{30}	C_{31}	C_{32}	C_{33}
Rel. abundance	3.2	2.6	2.2	1.4	0.9	0.4	0.2	--	--	--	--

Isoprenoids distribution in saturates:

IP14	IP15	IP16	IP18	Pristane	Phytane
0.65	0.65	2.20	1.42	1.75	0.50

$\frac{IP15}{IP16}$	$\frac{IP16}{IP18}$	$\frac{IP18}{Pr}$	$\frac{Pr}{Ph}$	$\frac{IP15}{nC_{14}}$	$\frac{IP16}{nC_{15}}$	$\frac{IP18}{nC_{16}}$	$\frac{Pr}{nC_{17}}$	$\frac{Ph}{nC_{18}}$
0.29	1.55	0.81	3.6	0.05	0.19/0.135		0.21	0.07

OIL ANALYSIS

AMDEL
JOB NO. 3923/79

SAMPLE NO:	A1234/79
WELL:	Big Lake 7
TEST:	Isochronal test
INTERVAL:	7529 - 8207'
FORMATION:	Toolachee – Epsilon
TYPE OF SAMPLE:	Condensate, + 210°C fraction

Results of Analysis

API Gravity (whole sample)	40.6
Saturates	70.1 % by wt.
Aromatics	19.6 %
Polar compounds	1.4 %
Asphaltenes	-- %
Loss	8.9 %

n-Alkane distribution of saturates: O.E.P.

n-Alkane	C_{12}	C_{13}	C_{14}	C_{15}	C_{16}	C_{17}	C_{18}	C_{19}	C_{20}	C_{21}	C_{22}
Rel. abundance	5.0	7.7	9.2	9.9	9.6	8.4	7.8	7.2	6.6	6.1	5.6
n-Alkane	C_{23}	C_{24}	C_{25}	C_{26}	C_{27}	C_{28}	C_{29}	C_{30}	C_{31}	C_{32}	C_{33}
Rel. abundance	5.2	4.3	3.6	2.0	1.1	0.5	0.2	--	--	--	--

Isoprenoids distribution in saturates:

IP14	IP15	IP16	IP18	Pristane	Phytane
0.50	0.55	1.75	1.35	1.70	0.70

$\frac{IP15}{IP16}$	$\frac{IP16}{IP18}$	$\frac{IP18}{Pr}$	$\frac{Pr}{Ph}$	$\frac{IP15}{nC_{14}}$	$\frac{IP16}{nC_{15}}$	$\frac{IP18}{nC_{16}}$	$\frac{Pr}{nC_{17}}$	$\frac{Ph}{nC_{18}}$
0.31	1.29	0.81	2.40	0.06	0.175	0.14	0.20	0.09

OIL ANALYSIS

AMDEL JOB NO. 3923/79

SAMPLE NO: A1235/79

WELL: Big Lake 8

TEST: Isochronal test

INTERVAL: 7469 - 7746'

FORMATION:

TYPE OF SAMPLE: Condensate, + 210°C fraction

Results of Analysis

API Gravity (whole sample) 38.6

Saturates	67.4	% by wt.
Aromatics	23.0	%
Polar compounds	1.1	%
Asphaltenes	--	%
Loss	8.5	%

n-Alkane distribution of saturates: O.E.P.

n-Alkane	C_{12}	C_{13}	C_{14}	C_{15}	C_{16}	C_{17}	C_{18}	C_{19}	C_{20}	C_{21}	C_{22}
Rel. abundance	8.0	11.7	12.5	12.0	10.7	8.5	7.3	6.2	5.3	4.5	3.8
n-Alkane	C_{23}	C_{24}	C_{25}	C_{26}	C_{27}	C_{28}	C_{29}	C_{30}	C_{31}	C_{32}	C_{33}
Rel. abundance	3.0	2.4	1.9	1.1	0.7	0.3	0.1	--	--	--	--

Isoprenoids distribution in saturates:

IP14	IP15	IP16	IP18	Pristane	Phytane
0.95	0.88	2.32	1.36	1.80	0.56

$\frac{IP15}{IP16}$	$\frac{IP16}{IP18}$	$\frac{IP18}{Pr}$	$\frac{Pr}{Ph}$	$\frac{IP15}{nC_{14}}$	$\frac{IP16}{nC_{15}}$	$\frac{IP18}{nC_{16}}$	$\frac{Pr}{nC_{17}}$	$\frac{Ph}{nC_{18}}$
0.38	1.70	0.75	3.2	0.07	0.20	0.12	0.21	0.075

OIL ANALYSIS

ANDEL 3923/79
JOB NO.

SAMPLE NO:	A1236/79
WELL:	Big Lake 9
TEST:	Isochronal test
INTERVAL:	7545 - 7856'
FORMATION:	Toolachee - Daralingie
TYPE OF SAMPLE:	Condensate, + 210°C fraction

Results of Analysis

API Gravity (whole sample) 39.8

Saturates	65.5 %	by wt.
Aromatics	19.7 %	
Polar compounds	1.1 %	
Asphaltenes	-- %	
Loss	13.7 %	

n-Alkane distribution of saturates: O.E.P.

n-Alkane	C_{12}	C_{13}	C_{14}	C_{15}	C_{16}	C_{17}	C_{18}	C_{19}	C_{20}	C_{21}	C_{22}
Rel. abundance	7.5	11.0	12.4	12.7	11.9	9.8	8.4	6.8	5.4	4.3	3.3
n-Alkane	C_{23}	C_{24}	C_{25}	C_{26}	C_{27}	C_{28}	C_{29}	C_{30}	C_{31}	C_{32}	C_{33}
Rel. abundance	2.6	1.9	1.2	0.5	0.3	--	--	--	--	--	--

Isoprenoids distribution in saturates:

IP14	IP15	IP16	IP18	Pristane	Phytane
0.60	0.70	2.35	1.55	1.80	0.80

$\frac{IP15}{IP16}$	$\frac{IP16}{IP18}$	$\frac{IP18}{Pr}$	$\frac{Pr}{Ph}$	$\frac{IP15}{nC_{14}}$	$\frac{IP16}{nC_{15}}$	$\frac{IP18}{nC_{16}}$	$\frac{Pr}{nC_{17}}$	$\frac{Ph}{nC_{18}}$
0.30	1.5	0.88	2.3	0.055	0.19	0.13	0.18	0.096

OIL ANALYSIS

ANDEL
JOB NO. 3923/79

SAMPLE NO:	A1237/79
WELL:	Big Lake 9
TEST:	Isochronal test
INTERVAL:	8081 - 8105'
FORMATION:	
TYPE OF SAMPLE:	Condensate, + 210°C fraction

Results of Analysis

API Gravity (whole sample) 41.5

Saturates	70.5	% by wt.
Aromatics	20.3	%
Polar compounds	0.6	%
Asphaltenes	--	%
Loss	8.6	%

n-Alkane distribution of saturates: O.E.P.

n-Alkane	C_{12}	C_{13}	C_{14}	C_{15}	C_{16}	C_{17}	C_{18}	C_{19}	C_{20}	C_{21}	C_{22}
Rel. abundance	7.0	10.5	12.0	12.4	12.0	10.0	8.6	7.0	5.6	4.5	3.5
n-Alkane	C_{23}	C_{24}	C_{25}	C_{26}	C_{27}	C_{28}	C_{29}	C_{30}	C_{31}	C_{32}	C_{33}
Rel. abundance	2.7	1.9	1.3	0.6	0.3	0.1	--	--	--	--	--

Isoprenoids distribution in saturates:

IP14	IP15	IP16	IP18	Pristane	Phytane
—	0.70	2.3	1.7	1.85	0.85

$\frac{IP15}{IP16}$	$\frac{IP16}{IP18}$	$\frac{IP18}{Pr}$	$\frac{Pr}{Ph}$	$\frac{IP15}{nC_{14}}$	$\frac{IP16}{nC_{15}}$	$\frac{IP18}{nC_{16}}$	$\frac{Pr}{nC_{17}}$	$\frac{Ph}{nC_{18}}$
0.30	1.36	0.92	2.2	0.055	0.185	0.14	0.18	0.095

OIL ANALYSIS

AMDEL JOB NO. 3923/79

SAMPLE NO:	A1238/79
WELL:	Big Lake 10
TEST:	Isochronal test
INTERVAL:	7620 - 8493 '
FORMATION:	Toolachee/Daralingie/Epsilon
TYPE OF SAMPLE:	Condensate, + 210°C fraction

Results of Analysis

API Gravity (whole sample) 40.3

Saturates	58.6	%	by wt.
Aromatics	26.1	%	
Polar compounds	1.3	%	
Asphaltenes	--	%	
Loss	14.0	%	

n-Alkane distribution of saturates: O.E.P.

n-Alkane	C_{12}	C_{13}	C_{14}	C_{15}	C_{16}	C_{17}	C_{18}	C_{19}	C_{20}	C_{21}	C_{22}
Rel. abundance	8.0	11.4	12.5	12.2	11.2	9.0	7.7	6.2	5.2	4.3	3.6
n-Alkane	C_{23}	C_{24}	C_{25}	C_{26}	C_{27}	C_{28}	C_{29}	C_{30}	C_{31}	C_{32}	C_{33}
Rel. abundance	3.0	2.3	1.8	0.4	0.5	0.2	--	--	--	---	--

Isoprenoids distribution in saturates:

IP14	IP15	IP16	IP18	Pristane	Phytane
0.95	0.95	2.35	1.45	1.80	0.65

$\frac{IP15}{IP16}$	$\frac{IP16}{IP18}$	$\frac{IP18}{Pr}$	$\frac{Pr}{Ph}$	$\frac{IP15}{nC_{14}}$	$\frac{IP16}{nC_{15}}$	$\frac{IP18}{nC_{16}}$	$\frac{Pr}{nC_{17}}$	$\frac{Ph}{nC_{18}}$
0.40	1.60	0.82	2.8	0.075	0.20	0.13	0.20	0.085

OIL ANALYSIS

AMDEL JOB NO. 3923/79

SAMPLE NO: A1239/79

WELL: Big Lake 11

TEST: Isochronal test

INTERVAL: 7549 - 8223 '

FORMATION:

TYPE OF SAMPLE: Condensate, + 210°C fraction

Results of Analysis

API Gravity (whole sample) 40.3

Saturates	66.2	% by wt.
Aromatics	23.2	%
Polar compounds	0.9	%
Asphaltenes	--	%
Loss	9.7	%

n-Alkane distribution of saturates: O.E.P.

n-Alkane	C_{12}	C_{13}	C_{14}	C_{15}	C_{16}	C_{17}	C_{18}	C_{19}	C_{20}	C_{21}	C_{22}
Rel. abundance	7.9	11.9	13.3	13.5	12.4	9.8	8.1	6.4	4.9	3.8	2.8
n-Alkane	C_{23}	C_{24}	C_{25}	C_{26}	C_{27}	C_{28}	C_{29}	C_{30}	C_{31}	C_{32}	C_{33}
Rel. abundance	2.0	1.4	0.9	0.5	0.3	0.1	--	--	--	--	--

Isoprenoids distribution in saturates:

IP14	IP15	IP16	IP18	Pristane	Phytane
0.90	0.90	2.60	1.60	1.90	0.65

$\frac{IP15}{IP16}$	$\frac{IP16}{IP18}$	$\frac{IP18}{Pr}$	$\frac{Pr}{Ph}$	$\frac{IP15}{nC_{14}}$	$\frac{IP16}{nC_{15}}$	$\frac{IP18}{nC_{16}}$	$\frac{Pr}{nC_{17}}$	$\frac{Ph}{nC_{18}}$
0.34	1.65	0.83	3.0	0.065	0.19	0.13	0.19	0.080

OIL ANALYSIS

ANDEL JOB NO. 3923/79

SAMPLE NO: A1240/79

WELL: Big Lake 12

TEST: Isochronal test

INTERVAL: 7552 - 8091ft

FORMATION:

TYPE OF SAMPLE: condensate, + 210°C fraction

Results of Analysis

API Gravity (whole sample) 38.0

Saturates	65.5	% by wt.
Aromatics	24.8	%
Polar compounds	1.1	%
Asphaltenes	--	%
Loss	8.6	%

n-Alkane distribution of saturates: O.E.P.

n-Alkane	C_{12}	C_{13}	C_{14}	C_{15}	C_{16}	C_{17}	C_{18}	C_{19}	C_{20}	C_{21}	C_{22}
Rel. abundance	4.5	7.9	9.4	9.8	9.6	8.3	7.5	6.5	5.8	5.4	5.0
n-Alkane	C_{23}	C_{24}	C_{25}	C_{26}	C_{27}	C_{28}	C_{29}	C_{30}	C_{31}	C_{32}	C_{33}
Rel. abundance	4.9	4.6	4.2	2.8	2.1	1.1	0.5	0.1	--	--	--

Isoprenoids distribution in saturates:

IP14	IP15	IP16	IP18	Pristane	Phytane
0.50	0.55	1.8	1.25	1.5	0.6

$\frac{IP15}{IP16}$	$\frac{IP16}{IP18}$	$\frac{IP18}{Pr}$	$\frac{Pr}{Ph}$	$\frac{IP15}{nC_{14}}$	$\frac{IP16}{nC_{15}}$	$\frac{IP18}{nC_{16}}$	$\frac{Pr}{nC_{17}}$	$\frac{Ph}{nC_{18}}$
0.31	1.45	0.81	2.45	0.060	0.185	0.13	0.18	0.085

OIL ANALYSIS

AMDEL
JOB NO. 3923/79

SAMPLE NO:	A1241/79
WELL:	Big Lake 13
TEST:	Isochronal test
INTERVAL:	7654 - 7824 '
FORMATION:	
TYPE OF SAMPLE:	Condensate , + 210° fraction

Results of Analysis

API Gravity (whole sample) 38.2

Saturates	53.9	%	by wt.
Aromatics	30.0	%	
Polar compounds	1.6	%	
Asphaltenes	--	%	
Loss	14.5	%	

n-Alkane distribution of saturates: O.E.P.

n-Alkane	C_{12}	C_{13}	C_{14}	C_{15}	C_{16}	C_{17}	C_{18}	C_{19}	C_{20}	C_{21}	C_{22}
Rel. abundance	8.5	12.7	13.8	13.2	11.9	9.3	7.6	5.9	4.6	3.6	2.8
n-Alkane	C_{23}	C_{24}	C_{25}	C_{26}	C_{27}	C_{28}	C_{29}	C_{30}	C_{31}	C_{32}	C_{33}
Rel. abundance	2.1	1.6	1.1	0.7	0.4	0.2	--	--	--	--	--

Isoprenoids distribution in saturates:

IP14	IP15	IP16	IP18	Pristane	Phytane
1.15	1.20	2.60	1.50	1.85	0.60

$\frac{IP15}{IP16}$	$\frac{IP16}{IP18}$	$\frac{IP18}{Pr}$	$\frac{Pr}{Ph}$	$\frac{IP15}{nC_{14}}$	$\frac{IP16}{nC_{15}}$	$\frac{IP18}{nC_{16}}$	$\frac{Pr}{nC_{17}}$	$\frac{Ph}{nC_{18}}$
0.47	1.76	0.80	3.05	0.09	0.20	0.125	0.20	0.08

OIL ANALYSIS

ANDEL
JOB NO. 3923/79

SAMPLE NO: A1242/79

WELL: Big Lake 14

TEST: Isochronal test

INTERVAL: 7576 - 8134'

FORMATION:

TYPE OF SAMPLE: Condensate, + 210°C fraction

Results of Analysis

API Gravity (whole sample) 39.3

Saturates	59.3	%	by wt.
Aromatics	25.7	%	
Polar compounds	1.5	%	
Asphaltenes	--	%	
Loss	13.5	%	

n-Alkane distribution of saturates: O.E.P.

n-Alkane	C_{12}	C_{13}	C_{14}	C_{15}	C_{16}	C_{17}	C_{18}	C_{19}	C_{20}	C_{21}	C_{22}
Rel. abundance	4.3	8.8	11.3	11.9	11.6	9.7	8.3	6.9	5.8	4.9	4.2
n-Alkane	C_{23}	C_{24}	C_{25}	C_{26}	C_{27}	C_{28}	C_{29}	C_{30}	C_{31}	C_{32}	C_{33}
Rel. abundance	3.7	2.7	1.5	0.8	0.4	--	--	--	--	--	--

Isoprenoids distribution in saturates:

IP14	IP15	IP16	IP18	Pristane	Phytane
0.55	0.75	2.05	1.40	1.85	0.65

$\frac{IP15}{IP16}$	$\frac{IP16}{IP18}$	$\frac{IP18}{Pr}$	$\frac{Pr}{Ph}$	$\frac{IP15}{nC_{14}}$	$\frac{IP16}{nC_{15}}$	$\frac{IP18}{nC_{16}}$	$\frac{Pr}{nC_{17}}$	$\frac{Ph}{nC_{18}}$
0.36	1.47	0.75	2.85	0.065	0.17	0.12	0.19	0.080

OIL ANALYSIS

AMDEL
JOB NO. 3923/79

SAMPLE NO:	A1243/79
WELL:	Big Lake 16
TEST:	
INTERVAL:	7495 - 8162'
FORMATION:	
TYPE OF SAMPLE:	Condensate, +210°C fraction

Results of Analysis

API Gravity (whole sample) 37.9

Saturates	60.5	%	by wt.
Aromatics	27.4	%	
Polar compounds	1.3	%	
Asphaltenes	--	%	
Loss	10.8	%	

n-Alkane distribution of saturates: O.E.P.

n-Alkane	C_{12}	C_{13}	C_{14}	C_{15}	C_{16}	C_{17}	C_{18}	C_{19}	C_{20}	C_{21}	C_{22}
Rel. abundance	9.5	14.1	14.9	13.7	11.8	9.4	7.1	5.4	4.2	3.1	2.3
n-Alkane	C_{23}	C_{24}	C_{25}	C_{26}	C_{27}	C_{28}	C_{29}	C_{30}	C_{31}	C_{32}	C_{33}
Rel. abundance	1.7	1.2	0.8	0.4	0.3	0.1	--	--	--	--	--

Isoprenoids distribution in saturates:

IP14	IP15	IP16	IP18	Pristane	Phytane
1.25	1.25	2.85	1.5	1.7	0.6

$\frac{IP15}{IP16}$	$\frac{IP16}{IP18}$	$\frac{IP18}{Pr}$	$\frac{Pr}{Ph}$	$\frac{IP15}{nC_{14}}$	$\frac{IP16}{nC_{15}}$	$\frac{IP18}{nC_{16}}$	$\frac{Pr}{nC_{17}}$	$\frac{Ph}{nC_{18}}$
0.45	1.9	0.77	3.25	0.085	0.205	0.125	0.20	0.095

8426 R 15

The Australian
Mineral Development
Laboratories

Flemington Street, Frewville,
South Australia 5063
Phone Adelaide 79 1662
Telex AA 82520

Please address all
correspondence to
P.O. Box 114 Eastwood
SA 5063
In reply quote: GS 1/1/238 (B3923/79)

Your Ref: 11.06.323

amdel

15 October 1979

Director-General,
Department of Mines & Energy,
PO Box 151,
EASTWOOD, SA 5063.

Attention: Dr D.M. McKirdy

SOURCE-ROCK ANALYSIS -

COOPER BASIN

PROGRESS REPORT NO. 24

OPEN FILE

(to be passed by hand)

Investigation and Report by: Harold Sears

Manager, Geological Services Division: Dr Keith J. Henley

Keith Henley

for Norton Jackson
Managing Director

PIRSA
R2001/00431

jd

Pilot Plant: Osman Place
Thebarton S.A.
Telephone 43 8053
Branch Laboratory: Perth

OIL ANALYSIS

SAMPLE NO: A 1244/79

WELL: Big Lake #17

TEST: Isochronal

INTERVAL: 7592 - 8246 ft

FORMATION:

TYPE OF SAMPLE: Condensate (+210^{o} fraction)

Results of Analysis

API Gravity (whole sample) 44.2

Saturates	86.2	% by wt.
Aromatics	6.2	%
Polar compounds	0.8	%
Asphaltenes	-	%
Loss	6.8	%

n-Alkane distribution of saturates: O.E.P.

n-Alkane	C_{12}	C_{13}	C_{14}	C_{15}	C_{16}	C_{17}	C_{18}	C_{19}	C_{20}	C_{21}	C_{22}
Rel. abundance	3.4	5.3	6.2	6.8	7.2	7.0	7.1	7.2	7.4	7.8	7.5
n-Alkane	C_{23}	C_{24}	C_{25}	C_{26}	C_{27}	C_{28}	C_{29}	C_{30}	C_{31}	C_{32}	C_{33}
Rel. abundance	7.5	6.8	5.9	3.4	2.2	0.9	0.4	-	-	-	-

Isoprenoids distribution in saturates:

IP14	IP15	IP16	IP18	Pristane	Phytane
-	0.28	1.13	1.00	1.27	0.61

$\frac{IP15}{IP16}$	$\frac{IP16}{IP18}$	$\frac{IP18}{Pr}$	$\frac{Pr}{Ph}$	$\frac{IP15}{nC_{14}}$	$\frac{IP16}{nC_{15}}$	$\frac{IP18}{nC_{16}}$	$\frac{Pr}{nC_{17}}$	$\frac{Ph}{nC_{18}}$
0.25	1.14	0.78	2.08	0.045	0.165	0.135	0.18	0.085

OIL ANALYSIS

AMDEL
JOB NO.

SAMPLE NO: A 1245/79

WELL: Big Lake #21

TEST: Isochronal

INTERVAL: 7594 - 8229 ft

FORMATION:

TYPE OF SAMPLE: Condensate (+210° fraction)

Results of Analysis

API Gravity (whole sample) 38.7

Saturates	57.1	%	by wt.
Aromatics	26.4	%	
Polar compounds	1.0	%	
Asphaltenes	-	%	
Loss	15.5	%	

n-Alkane distribution of saturates:

O.E.P.

n-Alkane	C_{12}	C_{13}	C_{14}	C_{15}	C_{16}	C_{17}	C_{18}	C_{19}	C_{20}	C_{21}	C_{22}
Rel. abundance	12.0	15.7	15.1	12.9	10.7	8.2	6.5	5.1	3.9	3.0	2.2
n-Alkane	C_{23}	C_{24}	C_{25}	C_{26}	C_{27}	C_{28}	C_{29}	C_{30}	C_{31}	C_{32}	C_{33}
Rel. abundance	1.7	1.2	0.9	0.5	0.3	0.1	-	-	-	-	-

Isoprenoids distribution in saturates:

IP14	IP15	IP16	IP18	Pristane	Phytane
1.39	1.31	2.63	1.24	1.59	0.54

$\frac{IP15}{IP16}$	$\frac{IP16}{IP18}$	$\frac{IP18}{Pr}$	$\frac{Pr}{Ph}$	$\frac{IP15}{nC_{14}}$	$\frac{IP16}{nC_{15}}$	$\frac{IP18}{nC_{16}}$	$\frac{Pr}{nC_{17}}$	$\frac{Ph}{nC_{18}}$
0.50	2.13	0.78	2.93	0.085	0.205	0.115	0.195	0.085

OIL ANALYSIS

ANDEL
JOB NO.

SAMPLE NO: A 1246/79

WELL: Big Lake #22

TEST: Isochronal

INTERVAL: 7560 - 8430 ft

FORMATION:

TYPE OF SAMPLE: Condensate (+210° fraction)

Results of Analysis

API Gravity (whole sample) 44.1

Saturates	77.0	%	by wt.
Aromatics	13.6	%	
Polar compounds	0.8	%	
Asphaltenes	-	%	
Loss	8.6	%	

n-Alkane distribution of saturates: O.E.P.

n-Alkane	C_{12}	C_{13}	C_{14}	C_{15}	C_{16}	C_{17}	C_{18}	C_{19}	C_{20}	C_{21}	C_{22}
Rel. abundance	4.4	6.9	8.3	9.1	9.4	8.9	8.6	8.1	7.5	6.9	6.1
n-Alkane	C_{23}	C_{24}	C_{25}	C_{26}	C_{27}	C_{28}	C_{29}	C_{30}	C_{31}	C_{32}	C_{33}
Rel. abundance	5.3	4.2	3.2	1.6	1.0	0.4	0.1	-	-	-	-

Isoprenoids distribution in saturates:

IP14	IP15	IP16	IP18	Pristane	Phytane
-	0.50	1.65	1.37	2.50	0.87

$\frac{IP15}{IP16}$	$\frac{IP16}{IP18}$	$\frac{IP18}{Pr}$	$\frac{Pr}{Ph}$	$\frac{IP15}{nC_{14}}$	$\frac{IP16}{nC_{15}}$	$\frac{IP18}{nC_{16}}$	$\frac{Pr}{nC_{17}}$	$\frac{Ph}{nC_{18}}$
0.30	1.20	0.55	2.85	0.060	0.18	0.145	0.28	0.10

OIL ANALYSIS

AMDEL
JOB NO.

SAMPLE NO: A 1247/79

WELL: Big Lake #23

TEST: Isochronal

INTERVAL: 7595 - 8483 ft

FORMATION:

TYPE OF SAMPLE: Condensate (+210° fraction)

Results of Analysis

API Gravity (whole sample) 44.5

Saturates	65.7	%	by wt.
Aromatics	22.3	%	
Polar compounds	1.3	%	
Asphaltenes	-	%	
Loss	10.7	%	

n-Alkane distribution of saturates: O.E.P.

n-Alkane	C_{12}	C_{13}	C_{14}	C_{15}	C_{16}	C_{17}	C_{18}	C_{19}	C_{20}	C_{21}	C_{22}
Rel. abundance	6.5	9.0	9.9	10.1	9.8	8.6	7.8	6.9	6.1	5.5	5.1
n-Alkane	C_{23}	C_{24}	C_{25}	C_{26}	C_{27}	C_{28}	C_{29}	C_{30}	C_{31}	C_{32}	C_{33}
Rel. abundance	4.6	3.9	3.1	1.7	0.9	0.4	0.1	-	-	-	-

Isoprenoids distribution in saturates:

IP14	IP15	IP16	IP18	Pristane	Phytane
-	0.54	1.76	1.28	1.79	0.64

$\frac{IP15}{IP16}$	$\frac{IP16}{IP18}$	$\frac{IP18}{Pr}$	$\frac{Pr}{Ph}$	$\frac{IP15}{nC_{14}}$	$\frac{IP16}{nC_{15}}$	$\frac{IP18}{nC_{16}}$	$\frac{Pr}{nC_{17}}$	$\frac{Ph}{nC_{18}}$
0.31	1.37	0.72	2.80	0.055	0.175	0.13	0.21	0.08

OIL ANALYSIS

AMDEL
JOB NO.

SAMPLE NO: A 1248/79

WELL: Big Lake #24

TEST: Isochronal

INTERVAL: 7636 - 8293 ft

FORMATION:

TYPE OF SAMPLE: Condensate (+210^{o} fraction)

Results of Analysis

API Gravity (whole sample) 41.4

Saturates	56.6	%	by wt.
Aromatics	24.4	%	
Polar compounds	1.2	%	
Asphaltenes	-	%	
Loss	17.8	%	

n-Alkane distribution of saturates: O.E.P.

n-Alkane	C_{12}	C_{13}	C_{14}	C_{15}	C_{16}	C_{17}	C_{18}	C_{19}	C_{20}	C_{21}	C_{22}
Rel. abundance	4.7	8.5	10.2	10.6	10.5	9.1	8.2	7.1	6.3	5.6	5.0
n-Alkane	C_{23}	C_{24}	C_{25}	C_{26}	C_{27}	C_{28}	C_{29}	C_{30}	C_{31}	C_{32}	C_{33}
Rel. abundance	4.6	3.8	3.0	1.6	0.9	0.3	-	-	-	-	-

Isoprenoids distribution in saturates:

IP14	IP15	IP16	IP18	Pristane	Phytane
-	0.54	1.90	1.43	1.90	0.75

$\frac{IP15}{IP16}$	$\frac{IP16}{IP18}$	$\frac{IP18}{Pr}$	$\frac{Pr}{Ph}$	$\frac{IP15}{nC_{14}}$	$\frac{IP16}{nC_{15}}$	$\frac{IP18}{nC_{16}}$	$\frac{Pr}{nC_{17}}$	$\frac{Ph}{nC_{18}}$
0.29	1.33	0.75	2.55	0.055	0.18	0.135	0.21	0.09

OIL ANALYSIS

AMDEL
JOB NO.

SAMPLE NO: A 1249/79

WELL: Big Lake #25

TEST: Isochronal

INTERVAL: 7584 - 8288 ft

FORMATION:

TYPE OF SAMPLE: Condensate (+210°C fraction)

Results of Analysis

API Gravity (whole sample) 41.2

Saturates	60.6	%	by wt.
Aromatics	29.2	%	
Polar compounds	1.7	%	
Asphaltenes	-	%	
Loss	8.5	%	

n-Alkane distribution of saturates: O.E.P.

n-Alkane	C_{12}	C_{13}	C_{14}	C_{15}	C_{16}	C_{17}	C_{18}	C_{19}	C_{20}	C_{21}	C_{22}
Rel. abundance	6.7	9.5	10.5	11.1	11.0	9.5	8.4	7.1	6.0	5.2	4.4
n-Alkane	C_{23}	C_{24}	C_{25}	C_{26}	C_{27}	C_{28}	C_{29}	C_{30}	C_{31}	C_{32}	C_{33}
Rel. abundance	3.7	2.8	2.2	1.1	0.6	0.2	-	-	-	-	-

Isoprenoids distribution in saturates:

IP14	IP15	IP16	IP18	Pristane	Phytane
-	0.63	1.95	1.48	1.95	0.70

$\frac{IP15}{IP16}$	$\frac{IP16}{IP18}$	$\frac{IP18}{Pr}$	$\frac{Pr}{Ph}$	$\frac{IP15}{nC_{14}}$	$\frac{IP16}{nC_{15}}$	$\frac{IP18}{nC_{16}}$	$\frac{Pr}{nC_{17}}$	$\frac{Ph}{nC_{18}}$
0.32	1.32	0.76	2.80	0.06	0.175	0.135	0.20	0.085

OIL ANALYSIS

SAMPLE NO: A 1250/79

WELL: Moomba #9

TEST: Isochronal

INTERVAL: 8074 - 8097 ft

FORMATION: Daralingie

TYPE OF SAMPLE: Condensate (+210°C fraction)

Results of Analysis

API Gravity (whole sample) 40.2

Saturates	46.4	%	by wt.
Aromatics	33.5	%	
Polar compounds	2.8	%	
Asphaltenes	-	%	
Loss	17.3	%	

n-Alkane distribution of saturates: O.E.P.

n-Alkane	C_{12}	C_{13}	C_{14}	C_{15}	C_{16}	C_{17}	C_{18}	C_{19}	C_{20}	C_{21}	C_{22}
Rel. abundance	11.1	15.5	15.6	13.2	10.5	8.0	6.2	4.8	3.7	3.2	2.7
n-Alkane	C_{23}	C_{24}	C_{25}	C_{26}	C_{27}	C_{28}	C_{29}	C_{30}	C_{31}	C_{32}	C_{33}
Rel. abundance	2.3	1.6	0.9	0.4	0.3	-	-	-	-	-	-

Isoprenoids distribution in saturates:

IP14	IP15	IP16	IP18	Pristane	Phytane
1.33	0.51	2.45	1.74	1.54	0.51

$\frac{IP15}{IP16}$	$\frac{IP16}{IP18}$	$\frac{IP18}{Pr}$	$\frac{Pr}{Ph}$	$\frac{IP15}{nC_{14}}$	$\frac{IP16}{nC_{15}}$	$\frac{IP18}{nC_{16}}$	$\frac{Pr}{nC_{17}}$	$\frac{Ph}{nC_{18}}$
0.21	1.41	1.13	3.0	0.033	0.185	0.165	0.19	0.08

OIL ANALYSIS

SAMPLE NO: A 1251/79

WELL: Moomba #10

TEST: Isochronal

INTERVAL: 7589 - 8037 ft

FORMATION: Toolachee - Daralingie

TYPE OF SAMPLE: Condensate (+210°C fraction)

Results of Analysis

API Gravity (whole sample) 41.6

Saturates	49.1	%	by wt.
Aromatics	35.5	%	
Polar compounds	2.4	%	
Asphaltenes	-	%	
Loss	13.0	%	

n-Alkane distribution of saturates: O.E.P.

n-Alkane	C_{12}	C_{13}	C_{14}	C_{15}	C_{16}	C_{17}	C_{18}	C_{19}	C_{20}	C_{21}	C_{22}
Rel. abundance	9.0	14.6	15.3	13.6	10.9	8.1	6.4	5.1	4.2	3.4	2.9
n-Alkane	C_{23}	C_{24}	C_{25}	C_{26}	C_{27}	C_{28}	C_{29}	C_{30}	C_{31}	C_{32}	C_{33}
Rel. abundance	2.2	1.8	1.3	0.7	0.4	0.1	-	-	-	-	-

Isoprenoids distribution in saturates:

IP14	IP15	IP16	IP18	Pristane	Phytane
-	0.65	2.60	1.49	3.2	0.47

$\frac{IP15}{IP16}$	$\frac{IP16}{IP18}$	$\frac{IP18}{Pr}$	$\frac{Pr}{Ph}$	$\frac{IP15}{nC_{14}}$	$\frac{IP16}{nC_{15}}$	$\frac{IP18}{nC_{16}}$	$\frac{Pr}{nC_{17}}$	$\frac{Ph}{nC_{18}}$
0.25	1.75	1.00	3.2	0.043	0.19	0.135	0.185	0.07

AMDEL
JOB NO.

OIL ANALYSIS

SAMPLE NO: A 1252/79

WELL: Moomba #11

TEST: Isochronal

INTERVAL: 7926 - 8245 ft

FORMATION: Toolachee - Daralingie

TYPE OF SAMPLE: Condensate (+210°C fraction)

Results of Analysis

API Gravity (whole sample) 50.2

Saturates	63.2	%	by wt.
Aromatics	23.5	%	
Polar compounds	1.2	%	
Asphaltenes	-	%	
Loss	12.1	%	

n-Alkane distribution of saturates: O.E.P.

n-Alkane	C_{12}	C_{13}	C_{14}	C_{15}	C_{16}	C_{17}	C_{18}	C_{19}	C_{20}	C_{21}	C_{22}
Rel. abundance	14.0	18.6	18.2	14.9	11.2	7.5	5.2	3.4	2.4	1.6	1.1
n-Alkane	C_{23}	C_{24}	C_{25}	C_{26}	C_{27}	C_{28}	C_{29}	C_{30}	C_{31}	C_{32}	C_{33}
Rel. abundance	0.7	0.6	0.4	0.2	-	-	-	-	-	-	-

Isoprenoids distribution in saturates:

IP14	IP15	IP16	IP18	Pristane	Phytane
0.82	0.82	2.38	1.07	0.98	0.30

$\frac{IP15}{IP16}$	$\frac{IP16}{IP18}$	$\frac{IP18}{Pr}$	$\frac{Pr}{Ph}$	$\frac{IP15}{nC_{14}}$	$\frac{IP16}{nC_{15}}$	$\frac{IP18}{nC_{16}}$	$\frac{Pr}{nC_{17}}$	$\frac{Ph}{nC_{18}}$
0.34	2.23	1.08	3.00	0.045	0.16	0.095	0.13	0.065

OIL ANALYSIS

AMDEL
JOB NO.

SAMPLE NO: A 1253/79

WELL: Moomba #12

TEST: Isochronal

INTERVAL: 7718 - 8014 ft

FORMATION: Toolachee - Daralingie

TYPE OF SAMPLE: Condensate (+210°C fraction)

Results of Analysis

API Gravity (whole sample) 38.8

Saturates	63.3	%	by wt.
Aromatics	29.3	%	
Polar compounds	1.9	%	
Asphaltenes	-	%	
Loss	5.5	%	

n-Alkane distribution of saturates: O.E.P.

n-Alkane	C_{12}	C_{13}	C_{14}	C_{15}	C_{16}	C_{17}	C_{18}	C_{19}	C_{20}	C_{21}	C_{22}
Rel. abundance	12.3	15.9	15.5	13.4	11.0	8.2	6.2	4.6	3.4	2.6	2.0
n-Alkane	C_{23}	C_{24}	C_{25}	C_{26}	C_{27}	C_{28}	C_{29}	C_{30}	C_{31}	C_{32}	C_{33}
Rel. abundance	1.5	1.2	0.9	0.5	0.3	0.2	-	-	-	-	-

Isoprenoids distribution in saturates:

IP14	IP15	IP16	IP18	Pristane	Phytane
1.64	1.10	2.67	1.23	1.65	0.48

$\frac{IP15}{IP16}$	$\frac{IP16}{IP18}$	$\frac{IP18}{Pr}$	$\frac{Pr}{Ph}$	$\frac{IP15}{nC_{14}}$	$\frac{IP16}{nC_{15}}$	$\frac{IP18}{nC_{16}}$	$\frac{Pr}{nC_{17}}$	$\frac{Ph}{nC_{18}}$
0.41	2.17	0.75	3.45	0.070	0.20	0.11	0.20	0.075

OIL ANALYSIS

AMDEL
JOB NO.

SAMPLE NO: A 1254/79

WELL: Moomba #14

TEST: Isochronal

INTERVAL: 7522 - 7850 ft

FORMATION: Toolachee-Daralingie

TYPE OF SAMPLE: Condensate (+210°C fraction)

Results of Analysis

API Gravity (whole sample) 36.4

Saturates	64.4	%	by wt.
Aromatics	29.0	%	
Polar compounds	2.0	%	
Asphaltenes	-	%	
Loss	4.6	%	

n-Alkane distribution of saturates: O.E.P.

n-Alkane	C_{12}	C_{13}	C_{14}	C_{15}	C_{16}	C_{17}	C_{18}	C_{19}	C_{20}	C_{21}	C_{22}
Rel. abundance	10.7	14.5	14.6	12.7	10.5	7.9	6.3	5.0	4.0	3.3	2.7
n-Alkane	C_{23}	C_{24}	C_{25}	C_{26}	C_{27}	C_{28}	C_{29}	C_{30}	C_{31}	C_{32}	C_{33}
Rel. abundance	2.2	1.8	1.6	1.0	0.7	0.3	0.2	-	-	-	-

Isoprenoids distribution in saturates:

IP14	IP15	IP16	IP18	Pristane	Phytane
1.58	1.33	2.83	1.25	1.91	0.58

$\frac{IP15}{IP16}$	$\frac{IP16}{IP18}$	$\frac{IP18}{Pr}$	$\frac{Pr}{Ph}$	$\frac{IP15}{nC_{14}}$	$\frac{IP16}{nC_{15}}$	$\frac{IP18}{nC_{16}}$	$\frac{Pr}{nC_{17}}$	$\frac{Ph}{nC_{18}}$
0.47	2.27	0.65	3.30	0.09	0.22	0.12	0.24	0.09

OIL ANALYSIS

AMDEL
JOB NO.

SAMPLE NO: A 1258/79

WELL: Moomba #20

TEST: Isochronal

INTERVAL: 7610 - 7972 ft

FORMATION: Toolachee - Daralingie

TYPE OF SAMPLE: Condensate (+210°C fraction)

Results of Analysis

API Gravity (whole sample) 39.8

Saturates	59.8	%	by wt.
Aromatics	27.1	%	
Polar compounds	1.2	%	
Asphaltenes	-	%	
Loss	11.9	%	

n-Alkane distribution of saturates: O.E.P.

n-Alkane	C_{12}	C_{13}	C_{14}	C_{15}	C_{16}	C_{17}	C_{18}	C_{19}	C_{20}	C_{21}	C_{22}
Rel. abundance	7.4	12.7	15.3	14.8	12.6	9.5	7.2	5.4	4.0	3.0	2.4
n-Alkane	C_{23}	C_{24}	C_{25}	C_{26}	C_{27}	C_{28}	C_{29}	C_{30}	C_{31}	C_{32}	C_{33}
Rel. abundance	1.8	1.4	1.0	0.8	0.4	0.3	-	-	-	-	-

Isoprenoids distribution in saturates:

IP14	IP15	IP16	IP18	Pristane	Phytane
1.18	1.35	3.05	1.60	2.02	0.67

$\frac{IP15}{IP16}$	$\frac{IP16}{IP18}$	$\frac{IP18}{Pr}$	$\frac{Pr}{Ph}$	$\frac{IP15}{nC_{14}}$	$\frac{IP16}{nC_{15}}$	$\frac{IP18}{nC_{16}}$	$\frac{Pr}{nC_{17}}$	$\frac{Ph}{nC_{18}}$
0.44	1.90	0.80	3.0	0.09	0.21	0.125	0.21	0.095

OIL ANALYSIS

AMDEL
JOB NO.

SAMPLE NO: A 1259/79

WELL: Moomba #21

TEST: Isochronal

INTERVAL: 7792 - 7972 ft

FORMATION:

TYPE OF SAMPLE: Condensate (+210°C fraction)

Results of Analysis

API Gravity (whole sample) 39.9

Saturates	54.3	% by wt.
Aromatics	38.4	%
Polar compounds	2.0	%
Asphaltenes	-	%
Loss	5.3	%

n-Alkane distribution of saturates: O.E.P.

n-Alkane	C_{12}	C_{13}	C_{14}	C_{15}	C_{16}	C_{17}	C_{18}	C_{19}	C_{20}	C_{21}	C_{22}
Rel. abundance	8.4	13.9	16.8	15.5	13.1	9.5	7.0	4.8	3.4	2.4	1.7
n-Alkane	C_{23}	C_{24}	C_{25}	C_{26}	C_{27}	C_{28}	C_{29}	C_{30}	C_{31}	C_{32}	C_{33}
Rel. abundance	1.2	0.9	0.6	0.4	0.3	0.1	-	-	-	-	,-

Isoprenoids distribution in saturates:

IP14	IP15	IP16	IP18	Pristane	Phytane
1.02	1.16	2.98	1.53	1.75	0.55

$\frac{IP15}{IP16}$	$\frac{IP16}{IP18}$	$\frac{IP18}{Pr}$	$\frac{Pr}{Ph}$	$\frac{IP15}{nC_{14}}$	$\frac{IP16}{nC_{15}}$	$\frac{IP18}{nC_{16}}$	$\frac{Pr}{nC_{17}}$	$\frac{Ph}{nC_{18}}$
0.39	1.95	0.88	3.00	0.07	0.19	0.115	0.185	0.085

OIL ANALYSIS

AMDEL
JOB NO.

SAMPLE NO: A 1260/79

WELL: Moomba #24

TEST: Isochronal

INTERVAL: 7746 - 7884 ft

FORMATION:

TYPE OF SAMPLE: Condensate (+210°C fraction)

Results of Analysis

API Gravity (whole sample) 41.1

Saturates	61.9	%	by wt.
Aromatics	32.9	%	
Polar compounds	1.1	%	
Asphaltenes	-	%	
Loss	4.1	%	

n-Alkane distribution of saturates:

O.E.P.

n-Alkane	C_{12}	C_{13}	C_{14}	C_{15}	C_{16}	C_{17}	C_{18}	C_{19}	C_{20}	C_{21}	C_{22}
Rel. abundance	7.5	12.9	14.8	14.3	12.5	9.6	7.6	5.6	4.2	3.2	2.4
n-Alkane	C_{23}	C_{24}	C_{25}	C_{26}	C_{27}	C_{28}	C_{29}	C_{30}	C_{31}	C_{32}	C_{33}
Rel. abundance	1.8	1.4	1.0	0.6	0.4	0.2	-	-	-	-	-

Isoprenoids distribution in saturates:

IP14	IP15	IP16	IP18	Pristane	Phytane
1.29	1.29	3.02	1.51	2.23	0.72

$\frac{IP15}{IP16}$	$\frac{IP16}{IP18}$	$\frac{IP18}{Pr}$	$\frac{Pr}{Ph}$	$\frac{IP15}{nC_{14}}$	$\frac{IP16}{nC_{15}}$	$\frac{IP18}{nC_{16}}$	$\frac{Pr}{nC_{17}}$	$\frac{Ph}{nC_{18}}$
0.43	2.0	0.68	3.1	0.085	0.21	0.12	0.23	0.095

AMDEL
JOB NO.

OIL ANALYSIS

SAMPLE NO: A 1261/79

WELL: Moomba #29

TEST: Isochronal

INTERVAL: 7767 - 7855 ft

FORMATION:

TYPE OF SAMPLE: Condensate (+210°C fraction)

Results of Analysis

API Gravity (whole sample) 38.8

Saturates	56.5	% by wt.
Aromatics	33.4	%
Polar compounds	1.9	%
Asphaltenes	-	%
Loss	8.2	%

n-Alkane distribution of saturates: O.E.P.

n-Alkane	C_{12}	C_{13}	C_{14}	C_{15}	C_{16}	C_{17}	C_{18}	C_{19}	C_{20}	C_{21}	C_{22}
Rel. abundance	11.0	14.5	14.8	13.5	11.2	8.5	6.5	4.9	3.8	2.9	2.3
n-Alkane	C_{23}	C_{24}	C_{25}	C_{26}	C_{27}	C_{28}	C_{29}	C_{30}	C_{31}	C_{32}	C_{33}
Rel. abundance	1.8	1.4	1.1	0.7	0.6	0.3	0.2	-	-	-	-

Isoprenoids distribution in saturates:

IP14	IP15	IP16	IP18	Pristane.	Phytane
1.11	1.04	2.57	1.32	1.60	0.56

$\frac{IP15}{IP16}$	$\frac{IP16}{IP18}$	$\frac{IP18}{Pr}$	$\frac{Pr}{Ph}$	$\frac{IP15}{nC_{14}}$	$\frac{IP16}{nC_{15}}$	$\frac{IP18}{nC_{16}}$	$\frac{Pr}{nC_{17}}$	$\frac{Ph}{nC_{18}}$
0.40	1.95	0.83	2.90	0.07	0.19	0.12	0.19	0.085

OIL ANALYSIS

SAMPLE NO: A 1262/79

WELL: Moomba #32

TEST: Isochronal

INTERVAL: 7769 - 7951 ft

FORMATION:

TYPE OF SAMPLE: Condensate (+210°C fraction)

Results of Analysis

API Gravity (whole sample) 40.7

Saturates	56.1	%	by wt.
Aromatics	31.3	%	
Polar compounds	1.3	%	
Asphaltenes	-	%	
Loss	11.3	%	

n-Alkane distribution of saturates:

O.E.P.

n-Alkane	C_{12}	C_{13}	C_{14}	C_{15}	C_{16}	C_{17}	C_{18}	C_{19}	C_{20}	C_{21}	C_{22}
Rel. abundance	7.7	12.0	13.2	12.7	11.3	9.2	7.5	6.0	4.9	4.0	3.3
n-Alkane	C_{23}	C_{24}	C_{25}	C_{26}	C_{27}	C_{28}	C_{29}	C_{30}	C_{31}	C_{32}	C_{33}
Rel. abundance	2.8	2.2	1.6	0.8	0.6	0.2	-	-	-	-	-

Isoprenoids distribution in saturates:

IP14	IP15	IP16	IP18	Pristane	Phytane
0.80	0.80	2.47	1.44	1.83	0.64

$\frac{IP15}{IP16}$	$\frac{IP16}{IP18}$	$\frac{IP18}{Pr}$	$\frac{Pr}{Ph}$	$\frac{IP15}{nC_{14}}$	$\frac{IP16}{nC_{15}}$	$\frac{IP18}{nC_{16}}$	$\frac{Pr}{nC_{17}}$	$\frac{Ph}{nC_{18}}$
0.32	1.72	0.78	2.90	0.06	0.195	0.125	0.20	0.085

OIL ANALYSIS

SAMPLE NO: A 1263/79

WELL; Moomba #34

TEST: Isochronal

INTERVAL: 7756 - 7895 ft

FORMATION:

TYPE OF SAMPLE: Condensate (+210°C fraction)

Results of Analysis

API Gravity (whole sample) 39.6

Saturates	57.3	%	by wt.
Aromatics	30.9	%	
Polar compounds	1.6	%	
Asphaltenes	-	%	
Loss	10.2	%	

n-Alkane distribution of saturates: O.E.P.

n-Alkane	C_{12}	C_{13}	C_{14}	C_{15}	C_{16}	C_{17}	C_{18}	C_{19}	C_{20}	C_{21}	C_{22}
Rel. abundance	8.1	11.9	12.7	11.9	10.3	8.0	6.7	5.7	4.8	4.2	3.7
n-Alkane	C_{23}	C_{24}	C_{25}	C_{26}	C_{27}	C_{28}	C_{29}	C_{30}	C_{31}	C_{32}	C_{33}
Rel. abundance	3.4	2.9	2.4	1.5	1.0	0.6	0.2	-	-	-	-

Isoprenoids distribution in saturates:

IP14	IP15	IP16	IP18	Pristane	Phytane
0.97	0.97	2.31	1.19	1.60	0.60

$\frac{IP15}{IP16}$	$\frac{IP16}{IP18}$	$\frac{IP18}{Pr}$	$\frac{Pr}{Ph}$	$\frac{IP15}{nC_{14}}$	$\frac{IP16}{nC_{15}}$	$\frac{IP18}{nC_{16}}$	$\frac{Pr}{nC_{17}}$	$\frac{Ph}{nC_{18}}$
0.42	1.94	0.75	2.7	0.075	0.195	0.115	0.20	0.09

OIL ANALYSIS

SAMPLE NO: A 1264/79

WELL: Moomba #35

TEST: Isochronal

INTERVAL: 7748 - 7955 ft

FORMATION:

TYPE OF SAMPLE: Condensate (+210°C fraction)

Results of Analysis

API Gravity (whole sample) 41.3

Saturates	48.0	%	by wt.
Aromatics	34.7	%	
Polar compounds	1.4	%	
Asphaltenes	-	%	
Loss	15.9	%	

n-Alkane distribution of saturates:

n-Alkane	C_{12}	C_{13}	C_{14}	C_{15}	C_{16}	C_{17}	C_{18}	C_{19}	C_{20}	C_{21}	C_{22}
Rel. abundance	11.9	15.9	16.0	14.0	11.4	8.3	6.1	4.5	3.3	2.5	2.0
n-Alkane	C_{23}	C_{24}	C_{25}	C_{26}	C_{27}	C_{28}	C_{29}	C_{30}	C_{31}	C_{32}	C_{33}
Rel. abundance	1.4	1.1	0.8	0.5	0.3	-	-	-	-	-	-

Isoprenoids distribution in saturates:

IP14	IP15	IP16	IP18	Pristane	Phytane
1.44	1.27	2.97	1.36	1.69	0.59

$\frac{IP15}{IP16}$	$\frac{IP16}{IP18}$	$\frac{IP18}{Pr}$	$\frac{Pr}{Ph}$	$\frac{IP15}{nC_{14}}$	$\frac{IP16}{nC_{15}}$	$\frac{IP18}{nC_{16}}$	$\frac{Pr}{nC_{17}}$	$\frac{Ph}{nC_{18}}$
0.43	2.20	0.80	2.85	0.08	0.21	0.12	0.20	0.10

OIL ANALYSIS

SAMPLE NO: A 1265/79

WELL; Moomba #39

TEST: Isochronal

INTERVAL: 7551 - 7890 ft

FORMATION:

TYPE OF SAMPLE: Condensate (+210°C fraction)

Results of Analysis

API Gravity (whole sample) 55.0

Saturates	64.4	% by wt.
Aromatics	21.7	%
Polar compounds	1.3	%
Asphaltenes	-	%
Loss	12.8	%

n-Alkane distribution of saturates: O.E.P.

n-Alkane	C_{12}	C_{13}	C_{14}	C_{15}	C_{16}	C_{17}	C_{18}	C_{19}	C_{20}	C_{21}	C_{22}
Rel. abundance	5.8	11.8	15.9	16.8	14.9	11.1	8.2	5.6	3.8	2.4	1.6
n-Alkane	C_{23}	C_{24}	C_{25}	C_{26}	C_{27}	C_{28}	C_{29}	C_{30}	C_{31}	C_{32}	C_{33}
Rel. abundance	0.9	0.7	0.4	0.01	-	-	-	-	-	-	-

Isoprenoids distribution in saturates:

IP14	IP15	IP16	IP18	Pristane.	Phytane
1.03	1.21	3.55	1.87	2.30	0.75

$\frac{IP15}{IP16}$	$\frac{IP16}{IP18}$	$\frac{IP18}{Pr}$	$\frac{Pr}{Ph}$	$\frac{IP15}{nC_{14}}$	$\frac{IP16}{nC_{15}}$	$\frac{IP18}{nC_{16}}$	$\frac{Pr}{nC_{17}}$	$\frac{Ph}{nC_{18}}$
0.34	1.90	0.82	3.05	0.075	0.21	0.125	0.205	0.09

OIL ANALYSIS

AMDEL
JOB NO.

SAMPLE NO: A 1266/79

WELL: Moomba #40

TEST: Isochronal

INTERVAL: 7782 - 7967 ft

FORMATION:

TYPE OF SAMPLE: Condensate (+210°C fraction)

Results of Analysis

API Gravity (whole sample) 45.1

Saturates	65.9	%	by wt.
Aromatics	23.5	%	
Polar compounds	0.7	%	
Asphaltenes	-	%	
Loss	9.9	%	

n-Alkane distribution of saturates:

O.E.P.

n-Alkane	C_{12}	C_{13}	C_{14}	C_{15}	C_{16}	C_{17}	C_{18}	C_{19}	C_{20}	C_{21}	C_{22}
Rel. abundance	3.5	9.4	13.4	14.8	14.3	11.7	9.4	6.9	5.1	3.7	2.7
n-Alkane	C_{23}	C_{24}	C_{25}	C_{26}	C_{27}	C_{28}	C_{29}	C_{30}	C_{31}	C_{32}	C_{33}
Rel. abundance	1.9	1.5	0.9	0.5	0.2	0.1	-	-	-	-	-

Isoprenoids distribution in saturates:

IP14	IP15	IP16	IP18	Pristane	Phytane
0.77	0.94	3.08	1.88	2.83	0.86

$\frac{IP15}{IP16}$	$\frac{IP16}{IP18}$	$\frac{IP18}{Pr}$	$\frac{Pr}{Ph}$	$\frac{IP15}{nC_{14}}$	$\frac{IP16}{nC_{15}}$	$\frac{IP18}{nC_{16}}$	$\frac{Pr}{nC_{17}}$	$\frac{Ph}{nC_{18}}$
0.30	1.65	0.65	3.3	0.07	0.21	0.13	0.24	0.09

OIL ANALYSIS

AMDEL
JOB NO.

SAMPLE NO: A 1267/79

WELL; Moomba #41

TEST: Isochronal

INTERVAL: 7730 - 7882 ft

FORMATION:

TYPE OF SAMPLE: Condensate (+210°C fraction)

Results of Analysis

API Gravity (whole sample) 37.0

Saturates	49.3	%	by wt.
Aromatics	33.3	%	
Polar compounds	0.6	%	
Asphaltenes	-	%	
Loss	16.8	%	

n-Alkane distribution of saturates:

O.E.P.

n-Alkane	C_{12}	C_{13}	C_{14}	C_{15}	C_{16}	C_{17}	C_{18}	C_{19}	C_{20}	C_{21}	C_{22}
Rel. abundance	7.5	14.3	17.1	16.4	13.8	10.2	7.3	5.0	3.1	2.0	1.4
n-Alkane	C_{23}	C_{24}	C_{25}	C_{26}	C_{27}	C_{28}	C_{29}	C_{30}	C_{31}	C_{32}	C_{33}
Rel. abundance	0.9	0.5	0.3	0.2	-	-	-	-	-	-	-

Isoprenoids distribution in saturates:

IP14	IP15	IP16	IP18	Pristane	Phytane
1.20	1.54	3.60	1.71	2.22	0.68

$\frac{IP15}{IP16}$	$\frac{IP16}{IP18}$	$\frac{IP18}{Pr}$	$\frac{Pr}{Ph}$	$\frac{IP15}{nC_{14}}$	$\frac{IP16}{nC_{15}}$	$\frac{IP18}{nC_{16}}$	$\frac{Pr}{nC_{17}}$	$\frac{Ph}{nC_{18}}$
0.43	2.10	0.77	3.25	0.09	0.22	0.125	0.22	0.095

AMDEL
JOB NO.

OIL ANALYSIS

SAMPLE NO: A 1268/79

WELL: Toolachee #1

TEST: Isochronal

INTERVAL: 6852 - 6964 ft

FORMATION: Patchawarra

TYPE OF SAMPLE: Condensate (+210°C fraction)

Results of Analysis

API Gravity (whole sample) 54.8

Saturates	77.3	%	by wt.
Aromatics	8.2	%	
Polar compounds	0.5	%	
Asphaltenes	-	%	
Loss	14.0	%	

n-Alkane distribution of saturates: O.E.P.

n-Alkane	C_{12}	C_{13}	C_{14}	C_{15}	C_{16}	C_{17}	C_{18}	C_{19}	C_{20}	C_{21}	C_{22}
Rel. abundance	7.7	11.1	12.2	12.2	11.4	9.6	8.2	6.8	5.4	4.3	3.5
n-Alkane	C_{23}	C_{24}	C_{25}	C_{26}	C_{27}	C_{28}	C_{29}	C_{30}	C_{31}	C_{32}	C_{33}
Rel. abundance	2.8	2.0	1.5	0.6	0.5	0.2	-	-	-	-	-

Isoprenoids distribution in saturates:

IP14	IP15	IP16	IP18	Pristane	Phytane
1.29	1.03	2.70	1.48	2.95	0.65

$\frac{IP15}{IP16}$	$\frac{IP16}{IP18}$	$\frac{IP18}{Pr}$	$\frac{Pr}{Ph}$	$\frac{IP15}{nC_{14}}$	$\frac{IP16}{nC_{15}}$	$\frac{IP18}{nC_{16}}$	$\frac{Pr}{nC_{17}}$	$\frac{Ph}{nC_{18}}$
0.38	1.83	0.50	4.6	0.085	0.22	0.13	0.31	0.08

OIL ANALYSIS

AMDEL
JOB NO.

SAMPLE NO: A 1269/79

WELL: Toolachee #3

TEST: Isochronal

INTERVAL: 7210 - 7353 ft

FORMATION: Patchawarra

TYPE OF SAMPLE: Condensate (+210°C fraction)

Results of Analysis

API Gravity (whole sample) 53.1

Saturates	80.5	%	by wt.
Aromatics	8.2	%	
Polar compounds	0.4	%	
Asphaltenes	-	%	
Loss	10.9	%	

n-Alkane distribution of saturates:

O.E.P.

n-Alkane	C_{12}	C_{13}	C_{14}	C_{15}	C_{16}	C_{17}	C_{18}	C_{19}	C_{20}	C_{21}	C_{22}
Rel. abundance	7.0	10.4	12.1	12.4	11.7	9.4	8.1	6.6	5.5	4.5	3.7
n-Alkane	C_{23}	C_{24}	C_{25}	C_{26}	C_{27}	C_{28}	C_{29}	C_{30}	C_{31}	C_{32}	C_{33}
Rel. abundance	3.0	2.2	1.7	0.8	0.6	0.3	-	-	-	-	-

Isoprenoids distribution in saturates:

IP14	IP15	IP16	IP18	Pristane	Phytane
1.17	0.92	2.85	1.59	3.15	0.63

$\frac{IP15}{IP16}$	$\frac{IP16}{IP18}$	$\frac{IP18}{Pr}$	$\frac{Pr}{Ph}$	$\frac{IP15}{nC_{14}}$	$\frac{IP16}{nC_{15}}$	$\frac{IP18}{nC_{16}}$	$\frac{Pr}{nC_{17}}$	$\frac{Ph}{nC_{18}}$
0.32	1.80	0.50	5.0	0.075	0.245	0.17	0.39	0.095

ANDEL
JOB NO.

OIL ANALYSIS

SAMPLE NO: : A 1270/79

WELL: Toolachee #4

TEST: Isochronal

INTERVAL: 7165 - 7284 ft

FORMATION: Patchawarra

TYPE OF SAMPLE: Condensate (+210°C fraction)

Results of Analysis

API Gravity (whole sample) 52.0

Saturates	72.1	%	by wt.
Aromatics	8.9	%	
Polar compounds	0.2	%	
Asphaltenes	-	%	
Loss	18.8	%	

n-Alkane distribution of saturates:

O.E.P.

n-Alkane	C_{12}	C_{13}	C_{14}	C_{15}	C_{16}	C_{17}	C_{18}	C_{19}	C_{20}	C_{21}	C_{22}
Rel. abundance	8.2	11.0	12.3	12.4	11.7	9.5	7.9	6.4	5.1	4.1	3.3
n-Alkane	C_{23}	C_{24}	C_{25}	C_{26}	C_{27}	C_{28}	C_{29}	C_{30}	C_{31}	C_{32}	C_{33}
Rel. abundance	2.7	2.1	1.6	0.8	0.6	0.2	0.1	-	-	-	-

Isoprenoids distribution in saturates:

IP14	IP15	IP16	IP18	Pristane	Phytane
0.89	0.72	2.22	1.28	2.11	0.50

$\frac{IP15}{IP16}$	$\frac{IP16}{IP18}$	$\frac{IP18}{Pr}$	$\frac{Pr}{Ph}$	$\frac{IP15}{nC_{14}}$	$\frac{IP16}{nC_{15}}$	$\frac{IP18}{nC_{16}}$	$\frac{Pr}{nC_{17}}$	$\frac{Ph}{nC_{18}}$
0.33	1.75	0.60	4.2	0.06	0.18	0.11	0.22	0.065

OIL ANALYSIS

SAMPLE NO: : A 1271/79

WELL: Toolachee #6

TEST: Isochronal

INTERVAL: 7471 - 7619 ft

FORMATION: Patchawarra

TYPE OF SAMPLE: Condensate (+210°C fraction)

Results of Analysis

API Gravity (whole sample) 47.8

Saturates	67.4	%	by wt.
Aromatics	18.6	%	
Polar compounds	0.4	%	
Asphaltenes	-	%	
Loss	13.6	%	

n-Alkane distribution of saturates: O.E.P.

n-Alkane	C_{12}	C_{13}	C_{14}	C_{15}	C_{16}	C_{17}	C_{18}	C_{19}	C_{20}	C_{21}	C_{22}
Rel. abundance	10.9	14.0	14.4	13.2	11.4	8.7	6.8	5.2	4.0	3.0	2.4
n-Alkane	C_{23}	C_{24}	C_{25}	C_{26}	C_{27}	C_{28}	C_{29}	C_{30}	C_{31}	C_{32}	C_{33}
Rel. abundance	1.9	1.5	1.2	0.7	0.5	0.2	-	-	-	-	-

Isoprenoids distribution in saturates:

IP14	IP15	IP16	IP18	Pristane	Phytane
1.94	1.38	3.20	1.66	2.29	0.60

$\frac{IP15}{IP16}$	$\frac{IP16}{IP18}$	$\frac{IP18}{Pr}$	$\frac{Pr}{Ph}$	$\frac{IP15}{nC_{14}}$	$\frac{IP16}{nC_{15}}$	$\frac{IP18}{nC_{16}}$	$\frac{Pr}{nC_{17}}$	$\frac{Ph}{nC_{18}}$
0.43	1.92	0.73	3.65	0.095	0.24	0.145	0.26	0.09

OIL ANALYSIS

AMDEL
JOB NO.

SAMPLE NO: A 1272/79

WELL; Toolachee #7

TEST: Isochronal

INTERVAL: 7315 - 7365 ft

FORMATION: Parchawarra

TYPE OF SAMPLE: Condensate (+210°C fraction)

Results of Analysis

API Gravity (whole sample) 56.3

Saturates	80.6	%	by wt.
Aromatics	7.8	%	
Polar compounds	0.2	%	
Asphaltenes	-	%	
Loss	11.4	%	

n-Alkane distribution of saturates:

O.E.P.

n-Alkane	C_{12}	C_{13}	C_{14}	C_{15}	C_{16}	C_{17}	C_{18}	C_{19}	C_{20}	C_{21}	C_{22}
Rel. abundance	8.3	12.5	13.8	13.4	11.5	9.1	7.6	6.1	4.8	3.9	3.1
n-Alkane	C_{23}	C_{24}	C_{25}	C_{26}	C_{27}	C_{28}	C_{29}	C_{30}	C_{31}	C_{32}	C_{33}
Rel. abundance	2.4	1.5	1.1	0.5	0.3	0.1	-	-	-	-	-

Isoprenoids distribution in saturates:

IP14	IP15	IP16	IP18	Pristane	Phytane
1.57	1.18	3.07	1.57	3.20	0.52

$\frac{IP15}{IP16}$	$\frac{IP16}{IP18}$	$\frac{IP18}{Pr}$	$\frac{Pr}{Ph}$	$\frac{IP15}{nC_{14}}$	$\frac{IP16}{nC_{15}}$	$\frac{IP18}{nC_{16}}$	$\frac{Pr}{nC_{17}}$	$\frac{Ph}{nC_{18}}$
0.38	1.95	0.49	6.1	0.085	0.23	0.135	0.35	0.07

OIL ANALYSIS

AMDEL
JOB NO.

SAMPLE NO: A 1273/79

WELL: Poolowanna #1

TEST: Drill Stem Test 2

INTERVAL: 8216 - 8328 ft

FORMATION: Poolowanna

TYPE OF SAMPLE: Oil (+210°C fraction)

Results of Analysis

API Gravity (whole sample) 35.4

Saturates	77.1	%	by wt.
Aromatics	13.6	%	
Polar compounds	4.2	%	
Asphaltenes	-	%	
Loss	5.1	%	

n-Alkane distribution of saturates: O.E.P.

n-Alkane	C_{12}	C_{13}	C_{14}	C_{15}	C_{16}	C_{17}	C_{18}	C_{19}	C_{20}	C_{21}	C_{22}
Rel. abundance	0.3	1.0	2.0	3.1	4.1	4.6	5.0	5.5	5.8	6.1	6.3
n-Alkane	C_{23}	C_{24}	C_{25}	C_{26}	C_{27}	C_{28}	C_{29}	C_{30}	C_{31}	C_{32}	C_{33}
Rel. abundance	6.7	6.1	7.1	6.4	6.2	4.9	4.5	4.0	3.7	2.6	2.8

Isoprenoids distribution in saturates:

IP14	IP15	IP16	IP18	Pristane	Phytane
-	-	0.49	0.57	1.05	0.19

$\frac{IP15}{IP16}$	$\frac{IP16}{IP18}$	$\frac{IP18}{Pr}$	$\frac{Pr}{Ph}$	$\frac{IP15}{nC_{14}}$	$\frac{IP16}{nC_{15}}$	$\frac{IP18}{nC_{16}}$	$\frac{Pr}{nC_{17}}$	$\frac{Ph}{nC_{18}}$
-	0.75	0.52	5.65	-	0.13	0.13	0.23	0.035

OIL ANALYSIS

AMDEL
JOB NO.

SAMPLE NO: A 1274/79

WELL: Poolowanna #1

TEST: Drill Stem Test 3

INTERVAL: 8585 - 8642 ft

FORMATION: Peera Peera

TYPE OF SAMPLE: Oil Extrated from Mud. (Contains some benzene plus methyl alcohol +210°C fraction)

Results of Analysis

API Gravity (whole sample) -

Saturates	67.6	% by wt.
Aromatics	17.2	%
Polar compounds	4.4	%
Asphaltenes	1.0	%
Loss	9.8	%

n-Alkane distribution of saturates:

O.E.P.

n-Alkane	C_{12}	C_{13}	C_{14}	C_{15}	C_{16}	C_{17}	C_{18}	C_{19}	C_{20}	C_{21}	C_{22}
Rel. abundance	1.4	3.5	6.1	8.0	10.2	9.2	8.6	7.7	6.7	5.8	4.9
n-Alkane	C_{23}	C_{24}	C_{25}	C_{26}	C_{27}	C_{28}	C_{29}	C_{30}	C_{31}	C_{32}	C_{33}
Rel. abundance	4.6	4.1	4.4	3.9	4.0	2.6	1.8	1.1	0.7	0.4	0.3

Isoprenoids distribution in saturates:

IP14	IP15	IP16	IP18	Pristane	Phytane
0.27	0.35	1.5	1.86	3.63	0.53

$\frac{IP15}{IP16}$	$\frac{IP16}{IP18}$	$\frac{IP18}{Pr}$	$\frac{Pr}{Ph}$	$\frac{IP15}{nC_{14}}$	$\frac{IP16}{nC_{15}}$	$\frac{IP18}{nC_{16}}$	$\frac{Pr}{nC_{17}}$	$\frac{Ph}{nC_{18}}$
0.23	0.80	0.51	6.8	0.06	0.19	0.18	0.39	0.06

OIL ANALYSIS

ANDEL
JOB NO.

SAMPLE NO: A 1275/79

WELL: Corrimal Colliery N.S.W.

TEST: Oil Seep

INTERVAL:

FORMATION:

TYPE OF SAMPLE: Oil (+210°C fraction)

Results of Analysis

API Gravity (whole sample) 37.8

Saturates	72.7	%	by wt.
Aromatics	11.3	%	
Polar compounds	3.2	%	
Asphaltenes	0.4	%	
Loss	12.4	%	

n-Alkane distribution of saturates: O.E.P.

n-Alkane	C_{12}	C_{13}	C_{14}	C_{15}	C_{16}	C_{17}	C_{18}	C_{19}	C_{20}	C_{21}	C_{22}
Rel. abundance	2.5	5.5	7.8	9.1	9.6	9.2	8.8	8.1	7.1	6.5	5.5
n-Alkane	C_{23}	C_{24}	C_{25}	C_{26}	C_{27}	C_{28}	C_{29}	C_{30}	C_{31}	C_{32}	C_{33}
Rel. abundance	4.7	3.6	3.0	2.2	1.8	1.6	1.4	1.0	0.7	0.3	-

Isoprenoids distribution in saturates:

IP14	IP15	IP16	IP18	Pristane	Phytane
1.13	1.02	2.82	1.54	3.64	0.92

$\frac{IP15}{IP16}$	$\frac{IP16}{IP18}$	$\frac{IP18}{Pr}$	$\frac{Pr}{Ph}$	$\frac{IP15}{nC_{14}}$	$\frac{IP16}{nC_{15}}$	$\frac{IP18}{nC_{16}}$	$\frac{Pr}{nC_{17}}$	$\frac{Ph}{nC_{18}}$
0.36	1.85	0.42	3.95	0.13	0.31	0.16	0.39	0.105

OIL ANALYSIS

AMDEL
JOB NO.

SAMPLE NO: A 1276/79

WELL; Etosha 5 - 1A. S.W. Africa

TEST: Oil Seep

INTERVAL:

FORMATION:

TYPE OF SAMPLE: Oil (+210°C fraction)

Results of Analysis

API Gravity (whole sample) 29.9

Saturates	71.4	%	by wt.
Aromatics	17.0	%	
Polar compounds	3.9	%	
Asphaltenes	0.3	%	
Loss	7.4	%	

n-Alkane distribution of saturates: O.E.P.

n-Alkane	C_{12}	C_{13}	C_{14}	C_{15}	C_{16}	C_{17}	C_{18}	C_{19}	C_{20}	C_{21}	C_{22}
Rel. abundance	SATURATES PREDOMINANTLY NAPHTHENIC										
n-Alkane	C_{23}	C_{24}	C_{25}	C_{26}	C_{27}	C_{28}	C_{29}	C_{30}	C_{31}	C_{32}	C_{33}
Rel. abundance	n. alkanes too low to measure.										

Isoprenoids distribution in saturates:

IP14	IP15	IP16	IP18	Pristane	Phytane

$\frac{IP15}{IP16}$	$\frac{IP16}{IP18}$	$\frac{IP18}{Pr}$	$\frac{Pr}{Ph}$	$\frac{IP15}{nC_{14}}$	$\frac{IP16}{nC_{15}}$	$\frac{IP18}{nC_{16}}$	$\frac{Pr}{nC_{17}}$	$\frac{Ph}{nC_{18}}$

OIL ANALYSIS

AMDEL
JOB NO.

SAMPLE NO: A 1278/79

WELL; Gidgealpa 13

TEST: Production test

INTERVAL: 6884 - 7042 ft

FORMATION: Toolachee

TYPE OF SAMPLE: Oil recovered from sludge with benzene plus methyl alcohol

Results of Analysis (+210°C fraction)

API Gravity (whole sample) 28.2

Saturates	59.5	%	by wt.
Aromatics	21.9	%	
Polar compounds	4.3	%	
Asphaltenes	0.7	%	
Loss	13.6	%	

n-Alkane distribution of saturates: O.E.P.

n-Alkane	C_{12}	C_{13}	C_{14}	C_{15}	C_{16}	C_{17}	C_{18}	C_{19}	C_{20}	C_{21}	C_{22}	
Rel. abundance	2.5	6.5	10.0	9.8	8.6	6.6	5.6	4.8	4.4	4.2	4.2	
n-Alkane	C_{23}	C_{24}	C_{25}	C_{26}	C_{27}	C_{28}	C_{29}	C_{30}	C_{31}	C_{32}	C_{33}	C_{34}
Rel. abundance	4.3	4.4	4.7	3.8	3.6	2.7	2.4	1.9	1.6	1.0	1.4	1.0

Isoprenoids distribution in saturates:

IP14	IP15	IP16	IP18	Pristane.	Phytane
0.65	0.90	2.50	1.25	2.15	0.45

$\frac{IP15}{IP16}$	$\frac{IP16}{IP18}$	$\frac{IP18}{Pr}$	$\frac{Pr}{Ph}$	$\frac{IP15}{nC_{14}}$	$\frac{IP16}{nC_{15}}$	$\frac{IP18}{nC_{16}}$	$\frac{Pr}{nC_{17}}$	$\frac{Ph}{nC_{18}}$
0.30	2.0	0.58	4.8	0.09	0.25	0.145	0.32	0.08

OIL ANALYSIS

ANDEL
JOB NO.

SAMPLE NO: A 1279/79

WELL: Gidgealpa #14

TEST: Isochronal

INTERVAL:

FORMATION: 6723 - 6752 ft

TYPE OF SAMPLE: Condensate (+210°C fraction)

Results of Analysis

API Gravity (whole sample) 46.7

Saturates	62.2	%	by wt.
Aromatics	23.4	%	
Polar compounds	1.1	%	
Asphaltenes	-	%	
Loss	13.3	%	

n-Alkane distribution of saturates: O.E.P.

n-Alkane	C_{12}	C_{13}	C_{14}	C_{15}	C_{16}	C_{17}	C_{18}	C_{19}	C_{20}	C_{21}	C_{22}
Rel. abundance	14.1	17.8	17.2	14.7	11.3	7.7	5.5	3.8	2.6	1.9	1.3
n-Alkane	C_{23}	C_{24}	C_{25}	C_{26}	C_{27}	C_{28}	C_{29}	C_{30}	C_{31}	C_{32}	C_{33}
Rel. abundance	0.8	0.6	0.4	0.3	-	-	-	-	-	-	-

Isoprenoids distribution in saturates:

IP14	IP15	IP16	IP18	Pristane	Phytane
2.30	1.55	3.75	1.50	2.40	0.41

$\frac{IP15}{IP16}$	$\frac{IP16}{IP18}$	$\frac{IP18}{Pr}$	$\frac{Pr}{Ph}$	$\frac{IP15}{nC_{14}}$	$\frac{IP16}{nC_{15}}$	$\frac{IP18}{nC_{16}}$	$\frac{Pr}{nC_{17}}$	$\frac{Ph}{nC_{18}}$
0.42	2.60	0.61	5.75	0.09	0.255	0.13	0.31	0.075

OIL ANALYSIS

AMDEL
JOB NO.

SAMPLE NO: A 1280/79

WELL: Moomba #30

TEST: Isochronal

INTERVAL: 7786 - 7920 ft

FORMATION:

TYPE OF SAMPLE: Condensate (+210°C fraction)

Results of Analysis

API Gravity (whole sample) 39.0

Saturates	56.0	%	by wt.
Aromatics	38.7	%	
Polar compounds	0.8	%	
Asphaltenes	-	%	
Loss	5.5	%	

n-Alkane distribution of saturates:

O.E.P.

n-Alkane	C_{12}	C_{13}	C_{14}	C_{15}	C_{16}	C_{17}	C_{18}	C_{19}	C_{20}	C_{21}	C_{22}
Rel. abundance	12.5	16.7	16.4	14.0	11.0	8.6	6.1	4.3	2.9	2.1	1.6
n-Alkane	C_{23}	C_{24}	C_{25}	C_{26}	C_{27}	C_{28}	C_{29}	C_{30}	C_{31}	C_{32}	C_{33}
Rel. abundance	1.3	0.8	0.6	0.5	0.4	0.2	-	-	-	-	-

Isoprenoids distribution in saturates:

IP14	IP15	IP16	IP18	Pristane	Phytane
1.71	1.35	3.00	-	1.82	0.87

$\frac{IP15}{IP16}$	$\frac{IP16}{IP18}$	$\frac{IP18}{Pr}$	$\frac{Pr}{Ph}$	$\frac{IP15}{nC_{14}}$	$\frac{IP16}{nC_{15}}$	$\frac{IP18}{nC_{16}}$	$\frac{Pr}{nC_{17}}$	$\frac{Ph}{nC_{18}}$
0.45	-	-	3.2	0.08	0.215	-	0.21	0.095

OIL ANALYSIS

AMDEL
JOB NO.

SAMPLE NO: A 1281/79

WELL; Moomba #36

TEST: Isochronal

INTERVAL: 7561 - 7949 ft

FORMATION:

TYPE OF SAMPLE: Condensate (+210°C fraction)

Results of Analysis

API Gravity (whole sample) 37.0

Saturates	41.1	% by wt.
Aromatics	40.2	%
Polar compounds	1.2	%
Asphaltenes	-	%
Loss	17.5	%

n-Alkane distribution of saturates:

O.E.P.

n-Alkane	C_{12}	C_{13}	C_{14}	C_{15}	C_{16}	C_{17}	C_{18}	C_{19}	C_{20}	C_{21}	C_{22}
Rel. abundance	7.6	15.1	17.1	15.2	12.4	9.4	6.9	5.0	3.5	2.5	1.9
n-Alkane	C_{23}	C_{24}	C_{25}	C_{26}	C_{27}	C_{28}	C_{29}	C_{30}	C_{31}	C_{32}	C_{33}
Rel. abundance	1.3	0.9	0.6	0.5	0.1	-	-	-	-	-	-

Isoprenoids distribution in saturates:

IP14	IP15	IP16	IP18	Pristane	Phytane
-	0.90	2.60	-	1.17	0.36

$\frac{IP15}{IP16}$	$\frac{IP16}{IP18}$	$\frac{IP18}{Pr}$	$\frac{Pr}{Ph}$	$\frac{IP15}{nC_{14}}$	$\frac{IP16}{nC_{15}}$	$\frac{IP18}{nC_{16}}$	$\frac{Pr}{nC_{17}}$	$\frac{Ph}{nC_{18}}$
0.321	-	-	3.0	0.055	0.17	-	0.125	0.05

OIL ANALYSIS

SAMPLE NO: A 1282/79

WELL: Moomba #37

TEST: Isochronal

INTERVAL: 7762 - 7890 ft

FORMATION:

TYPE OF SAMPLE: Condensate (+210°C fraction)

Results of Analysis

API Gravity (whole sample) 36.4

Saturates	39.4	% by wt.
Aromatics	43.5	%
Polar compounds	0.9	%
Asphaltenes	-	%
Loss	17,2	%

n-Alkane distribution of saturates:

O.E.P.

n-Alkane	C_{12}	C_{13}	C_{14}	C_{15}	C_{16}	C_{17}	C_{18}	C_{19}	C_{20}	C_{21}	C_{22}
Rel. abundance	6.7	13.9	16.5	15.2	12.6	9.5	7.1	5.2	3.7	2.8	2.1
n-Alkane	C_{23}	C_{24}	C_{25}	C_{26}	C_{27}	C_{28}	C_{29}	C_{30}	C_{31}	C_{32}	C_{33}
Rel. abundance	1.6	1.0	0.7	0.5	0.4	0.5	-	-	-	-	-

Isoprenoids distribution in saturates:

IP14	IP15	IP16	IP18	Pristane	Phytane
0.97	1.12	3.06	-	1.79	0.60

$\frac{IP15}{IP16}$	$\frac{IP16}{IP18}$	$\frac{IP18}{Pr}$	$\frac{Pr}{Ph}$	$\frac{IP15}{nC_{14}}$	$\frac{IP16}{nC_{15}}$	$\frac{IP18}{nC_{16}}$	$\frac{Pr}{nC_{17}}$	$\frac{Ph}{nC_{18}}$
0.37	-	-	3.0	0.07	0.20	-	0.19	0.085

OIL ANALYSIS

SAMPLE NO: A 1283/79

WELL: Merrimelia #5

TEST: Isochronal

INTERVAL: 7308 - 7659 ft

FORMATION: Nappermerri/Toolachee

TYPE OF SAMPLE: Condensate (+210°C fraction)

Results of Analysis

API Gravity (whole sample) 52.6

Saturates	60.8	%	by wt.
Aromatics	19.3	%	
Polar compounds	0.9	%	
Asphaltenes	-	%	
Loss	19.0	%	

n-Alkane distribution of saturates: O.E.P.

n-Alkane	C_{12}	C_{13}	C_{14}	C_{15}	C_{16}	C_{17}	C_{18}	C_{19}	C_{20}	C_{21}	C_{22}
Rel. abundance	6.7	11.5	13.3	13.0	11.5	9.6	7.7	6.2	5.0	4.1	3.3
n-Alkane	C_{23}	C_{24}	C_{25}	C_{26}	C_{27}	C_{28}	C_{29}	C_{30}	C_{31}	C_{32}	C_{33}
Rel. abundance	2.8	2.0	1.5	1.0	0.6	0.2	-	-	-	-	-

Isoprenoids distribution in saturates:

IP14	IP15	IP16	IP18	Pristane	Phytane
1.11	1.04	3.07	1.47	3.13	0.55

$\frac{IP15}{IP16}$	$\frac{IP16}{IP18}$	$\frac{IP18}{Pr}$	$\frac{Pr}{Ph}$	$\frac{IP15}{nC_{14}}$	$\frac{IP16}{nC_{15}}$	$\frac{IP18}{nC_{16}}$	$\frac{Pr}{nC_{17}}$	$\frac{Ph}{nC_{18}}$
0.34	2.08	0.47	5.65	0.08	0.24	0.13	0.33	0.07

8426 R 16

The Australian
Mineral Development
Laboratories

Flemington Street, Frewville,
South Australia 5063
Phone Adelaide 79 1662
Telex AA 82520

Please address all
correspondence to
P.O. Box 114 Eastwood
SA 5063
In reply quote: GS 1/1/238 (B960/80, part)

Your Ref: 11.06.323

amdel

3 December 1979

Director-General,
Department of Mines & Energy,
PO Box 151,
EASTWOOD, SA 5063.

Attention: Dr D.M. McKirdy

SOURCE-ROCK ANALYSIS -

COOPER BASIN

PROGRESS REPORT NO. 29

OPEN FILE
(To be passed by hand)

Investigation and Report by: Harold Sears

Manager, Geological Services Division: Dr Keith J. Henley

Keith Henley

for Norton Jackson
Managing Director

RECEIVED
13 DEC 1979
DEPT. OF MINES
AND ENERGY
SECURITY

PIRSA
R2001/00432
02214819

Pilot Plant: Osman Place
Thebarton S.A.
Telephone 43 8053
Branch Laboratory: Perth

OIL ANALYSIS

SAMPLE NO: A3067/79

WELL: Gidgealpa 2

TEST: ~~Drill Stem~~ Cased hole Test 6

INTERVAL: 6773' - 6778'

FORMATION: Toolachee

TYPE OF SAMPLE: Condensate +210°C Fraction

Results of Analysis

API Gravity (whole sample) 44.7

Saturates	68.4	% by wt.
Aromatics	17.9	%
Polar compounds	3.7	%
Asphaltenes	—	%
Loss	10.0	%

n-Alkane distribution of saturates: O.E.P.

n-Alkane	C_{12}	C_{13}	C_{14}	C_{15}	C_{16}	C_{17}	C_{18}	C_{19}	C_{20}	C_{21}	C_{22}
Rel. abundance	1.4	4.5	8.1	10.0	10.6	10.0	9.6	8.3	7.1	6.6	6.0
n-Alkane	C_{23}	C_{24}	C_{25}	C_{26}	C_{27}	C_{28}	C_{29}	C_{30}	C_{31}	C_{32}	C_{33}
Rel. abundance	5.8	4.3	3.7	2.0	1.3	0.5	0.2	--	--	--	--

Isoprenoids distribution in saturates:

IP14	IP15	IP16	IP18	Pristane	Phytane
0.32	0.50	2.04	1.40	2.40	0.52

$\frac{IP15}{IP16}$	$\frac{IP16}{IP18}$	$\frac{IP18}{Pr}$	$\frac{Pr}{Ph}$	$\frac{IP15}{nC_{14}}$	$\frac{IP16}{nC_{15}}$	$\frac{IP18}{nC_{16}}$	$\frac{Pr}{nC_{17}}$	$\frac{Ph}{nC_{18}}$
0.24	1.45	0.58	4.60	0.062	0.205	0.145	0.28	0.07

OIL ANALYSIS

SAMPLE NO: A 3068/80

WELL: Gidgealpa 2

TEST: ~~Drill Stem~~ Cased hole Test 8

INTERVAL: ---

FORMATION: Toolachee

TYPE OF SAMPLE: Condensate + 210°C

Results of Analysis

API Gravity (whole sample) 47.2

Saturates	67.5	%	by wt.
Aromatics	16.7	%	
Polar compounds	6.2	%	
Asphaltenes	--	%	
Loss	9.6	%	

n-Alkane distribution of saturates: O.E.P.

n-Alkane	C_{12}	C_{13}	C_{14}	C_{15}	C_{16}	C_{17}	C_{18}	C_{19}	C_{20}	C_{21}	C_{22}
Rel. abundance	8.5	11.9	13.8	14.6	16.3	14.3	10.0	5.6	2.4	1.0	0.5
n-Alkane	C_{23}	C_{24}	C_{25}	C_{26}	C_{27}	C_{28}	C_{29}	C_{30}	C_{31}	C_{32}	C_{33}
Rel. abundance	0.5	0.4	0.2	--	--	--	--	--	--	--	--

Isoprenoids distribution in saturates:

IP14	IP15	IP16	IP18	Pristane	Phytane
1.10	0.87	3.01	1.98	4.03	0.71

$\frac{IP15}{IP16}$	$\frac{IP16}{IP18}$	$\frac{IP18}{Pr}$	$\frac{Pr}{Ph}$	$\frac{IP15}{nC_{14}}$	$\frac{IP16}{nC_{15}}$	$\frac{IP18}{nC_{16}}$	$\frac{Pr}{nC_{17}}$	$\frac{Ph}{nC_{18}}$
0.29	1.52	0.49	5.67	0.063	0.205	0.12	0.28	0.07

OIL ANALYSIS

SAMPLE NO: A 3069/80

WELL: Gidgealpa 2

TEST: ~~Drill Stem~~ Cased hole Test 9

INTERVAL: 6837' - 6842'

FORMATION: Toolachee

TYPE OF SAMPLE: Condensate, +210°C Fraction

Results of Analysis

API Gravity (whole sample) 36.4

Saturates	75.4	%	by wt.
Aromatics	13.5	%	
Polar compounds	5.5	%	
Asphaltenes	--	%	
Loss	5.6	%	

n-Alkane distribution of saturates: O.E.P.

n-Alkane	C_{12}	C_{13}	C_{14}	C_{15}	C_{16}	C_{17}	C_{18}	C_{19}	C_{20}	C_{21}	C_{22}
Rel. abundance	3.5	7.0	9.5	10.6	11.0	10.2	9.4	7.9	6.6	6.4	5.3
n-Alkane	C_{23}	C_{24}	C_{25}	C_{26}	C_{27}	C_{28}	C_{29}	C_{30}	C_{31}	C_{32}	C_{33}
Rel. abundance	4.8	3.3	2.5	1.2	0.6	0.2	--	--	--	--	--

Isoprenoids distribution in saturates:

IP14	IP15	IP16	IP18	Pristane	Phytane
0.65	0.65	2,29	1.82	3.00	0.73

$\frac{IP15}{IP16}$	$\frac{IP16}{IP18}$	$\frac{IP18}{Pr}$	$\frac{Pr}{Ph}$	$\frac{IP15}{nC_{14}}$	$\frac{IP16}{nC_{15}}$	$\frac{IP18}{nC_{16}}$	$\frac{Pr}{nC_{17}}$	$\frac{Ph}{nC_{18}}$
0.28	1.26	0.61	4.08	0.068	0.215	0.165	0.30	0.08

OIL ANALYSIS

SAMPLE NO: A3070/79

WELL: Gidgealpa 2

TEST: ~~Drill Stem~~ Cased hole Test 10

INTERVAL: 6858' - 6867'

FORMATION: Toolachee

TYPE OF SAMPLE: Condensate, +210°C Fraction

Results of Analysis

API Gravity (whole sample) 36.4

Saturates	72.8	%	by wt.
Aromatics	16.3	%	
Polar compounds	7.7	%	
Asphaltenes	--	%	
Loss	3.2	%	

n-Alkane distribution of saturates:

O.E.P.

n-Alkane	C_{12}	C_{13}	C_{14}	C_{15}	C_{16}	C_{17}	C_{18}	C_{19}	C_{20}	C_{21}	C_{22}
Rel. abundance	0.9	2.9	4.9	6.6	8.8	10.2	10.9	10.0	8.5	8.0	7.3
n-Alkane	C_{23}	C_{24}	C_{25}	C_{26}	C_{27}	C_{28}	C_{29}	C_{30}	C_{31}	C_{32}	C_{33}
Rel. abundance	7.0	5.2	4.2	2.3	1.4	0.7	0.2	--	--	--	--

Isoprenoids distribution in saturates:

IP14	IP15	IP16	IP18	Pristane	Phytane
--	0.23	1.20	1.37	2.63	0.69

$\frac{IP15}{IP16}$	$\frac{IP16}{IP18}$	$\frac{IP18}{Pr}$	$\frac{Pr}{Ph}$	$\frac{IP15}{nC_{14}}$	$\frac{IP16}{nC_{15}}$	$\frac{IP18}{nC_{16}}$	$\frac{Pr}{nC_{17}}$	$\frac{Ph}{nC_{18}}$
0.19	0.88	0.52	3.85	0.12	0.31	0.16	0.41	0.065

OIL ANALYSIS

SAMPLE NO: A3071/79

WELL: Gidgealpa 16

TEST: Drill Stem Test 4

INTERVAL: 7209-7237 ft

FORMATION: Patchawarra

TYPE OF SAMPLE: Condensate +210°C fraction

Results of Analysis

API Gravity (whole sample) 49.9

Saturates	56.4	%	by wt.
Aromatics	19.4	%	
Polar compounds	13.5	%	
Asphaltenes	--	%	
Loss	10.7	%	

n-Alkane distribution of saturates: O.E.P.

n-Alkane	C_{12}	C_{13}	C_{14}	C_{15}	C_{16}	C_{17}	C_{18}	C_{19}	C_{20}	C_{21}	C_{22}
Rel. abundance	17.9	18.2	16.0	12.4	9.4	7.3	5.8	4.2	3.0	2.3	1.6
n-Alkane	C_{23}	C_{24}	C_{25}	C_{26}	C_{27}	C_{28}	C_{29}	C_{30}	C_{31}	C_{32}	C_{33}
Rel. abundance	1.2	0.5	0.2	--	--	--	--	--	--	--	--

Isoprenoids distribution in saturates:

IP14	IP15	IP16	IP18	Pristane	Phytane
2.82	1.88	3.86	1.51	3.01	0.38

$\frac{IP15}{IP16}$	$\frac{IP16}{IP18}$	$\frac{IP18}{Pr}$	$\frac{Pr}{Ph}$	$\frac{IP15}{nC_{14}}$	$\frac{IP16}{nC_{15}}$	$\frac{IP18}{nC_{16}}$	$\frac{Pr}{nC_{17}}$	$\frac{Ph}{nC_{18}}$
0.49	2.56	0.50	8.0	0.12	0.31	0.16	0.41	0.065

OIL ANALYSIS

SAMPLE NO: A3072/79

WELL: Gidgealpa 16

TEST: ~~Drill Stem~~ Cased hole Test 5

INTERVAL: 7224' - 7258'

FORMATION: Tirrawarra

TYPE OF SAMPLE: Condensate, +210°C Fraction

Results of Analysis

API Gravity (whole sample) 49.5

Saturates	73.5	% by wt.
Aromatics	14.9	%
Polar compounds	4.2	%
Asphaltenes	—	%
Loss	7.4	%

n-Alkane distribution of saturates: O.E.P.

n-Alkane	C_{12}	C_{13}	C_{14}	C_{15}	C_{16}	C_{17}	C_{18}	C_{19}	C_{20}	C_{21}	C_{22}
Rel. abundance	12.8	16.7	16.8	14.3	1.20	8.8	6.6	4.4	2.8	1.9	1.5
n-Alkane	C_{23}	C_{24}	C_{25}	C_{26}	C_{27}	C_{28}	C_{29}	C_{30}	C_{31}	C_{32}	C_{33}
Rel. abundance	0.8	0.4	0.2	--	--	--	--	--	--	--	--

Isoprenoids distribution in saturates:

IP14	IP15	IP16	IP18	Pristane	Phytane
1.94	1.21	3.48	1.62	2.91	0.32

$\frac{IP15}{IP16}$	$\frac{IP16}{IP18}$	$\frac{IP18}{Pr}$	$\frac{Pr}{Ph}$	$\frac{IP15}{nC_{14}}$	$\frac{IP16}{nC_{15}}$	$\frac{IP18}{nC_{16}}$	$\frac{Pr}{nC_{17}}$	$\frac{Ph}{nC_{18}}$
0.35	2.15	0.56	9.0	0.07	0.245	0.135	0.33	0.05

OIL ANALYSIS

SAMPLE NO: 3073/79

WELL: Kidman 2

TEST: Drill Stem Test 1

INTERVAL: 6480 to 6547 ft

FORMATION: Toolachee

TYPE OF SAMPLE: Condensate, +210°C Fraction

Results of Analysis

API Gravity (whole sample) 46.5

Saturates	84.5	%	by wt.
Aromatics	8.0	%	
Polar compounds	2.5	%	
Asphaltenes	--	%	
Loss	5.0	%	

n-Alkane distribution of saturates: O.E.P.

n-Alkane	C_{12}	C_{13}	C_{14}	C_{15}	C_{16}	C_{17}	C_{18}	C_{19}	C_{20}	C_{21}	C_{22}
Rel. abundance	8.0	11.3	12.6	12.5	12.0	10.1	9.1	7.2	5.3	4.2	3.3
n-Alkane	C_{23}	C_{24}	C_{25}	C_{26}	C_{27}	C_{28}	C_{29}	C_{30}	C_{31}	C_{32}	C_{33}
Rel. abundance	2.3	1.3	0.8	--	--	--	--	--	--	--	--

Isoprenoids distribution in saturates:

IP14	IP15	IP16	IP18	Pristane	Phytane
	0.77	2.42	1.32	2.42	0.49

$\frac{IP15}{IP16}$	$\frac{IP16}{IP18}$	$\frac{IP18}{Pr}$	$\frac{Pr}{Ph}$	$\frac{IP15}{nC_{14}}$	$\frac{IP16}{nC_{15}}$	$\frac{IP18}{nC_{16}}$	$\frac{Pr}{nC_{17}}$	$\frac{Ph}{nC_{18}}$
0.77	1.83	0.55	4.9	0.06	0.195	0.11	0.24	0.055

OIL ANALYSIS

SAMPLE NO: 3074/79

WELL: Kidman 2

TEST: Drill Stem Test 2

INTERVAL: 6566 - 6622 ft

FORMATION: Toolachee

TYPE OF SAMPLE: Condensate +210°C Fraction

Results of Analysis

API Gravity (whole sample) 46.9

Saturates	82.2	%	by wt.
Aromatics	8.8	%	
Polar compounds	2.3	%	
Asphaltenes	--	%	
Loss	6.7	%	

n-Alkane distribution of saturates: O.E.P.

n-Alkane	C_{12}	C_{13}	C_{14}	C_{15}	C_{16}	C_{17}	C_{18}	C_{19}	C_{20}	C_{21}	C_{22}
Rel. abundance	12.5	15.9	16.7	15.3	13.3	10.4	7.6	4.1	2.0	1.3	0.7
n-Alkane	C_{23}	C_{24}	C_{25}	C_{26}	C_{27}	C_{28}	C_{29}	C_{30}	C_{31}	C_{32}	C_{33}
Rel. abundance	0.2	--	--	--	--	--	--	--	--	--	--

Isoprenoids distribution in saturates:

IP14	IP15	IP16	IP18	Pristane	Phytane
2.71	1.77	4.76	2.05	3.82	0.61

$\frac{IP15}{IP16}$	$\frac{IP16}{IP18}$	$\frac{IP18}{Pr}$	$\frac{Pr}{Ph}$	$\frac{IP15}{nC_{14}}$	$\frac{IP16}{nC_{15}}$	$\frac{IP18}{nC_{16}}$	$\frac{Pr}{nC_{17}}$	$\frac{Ph}{nC_{18}}$
0.37	2.32	0.54	6.3	0.105	0.31	0.155	0.37	0.08

OIL ANALYSIS

SAMPLE NO: 3075/79

WELL: Wackett 1

TEST: Drill Stem Test 3

INTERVAL: 5558 - ?

FORMATION:

TYPE OF SAMPLE: Condensate, +180°C Fraction

Results of Analysis

API Gravity (whole sample) 48.1

Saturates	61.3	% by wt.
Aromatics	8.3	%
Polar compounds	8.7	%
Asphaltenes		%
Loss	21.7	%

n-Alkane distribution of saturates: O.E.P.

n-Alkane	C_{10}	C_{11}	C_{12}	C_{13}	C_{14}	C_{15}	C_{16}	C_{17}	C_{18}	C_{19}	C_{20}
Rel. abundance	12.5	38.3	32.7	12.9	3.0	0.6					
n-Alkane	C_{23}	C_{24}	C_{25}	C_{26}	C_{27}	C_{28}	C_{29}	C_{30}	C_{31}	C_{32}	C_{33}
Rel. abundance											

Isoprenoids distribution in saturates:

IP14	IP15	IP16	IP18	Pristane	Phytane
—	—	—	—	—	—

$\frac{IP15}{IP16}$	$\frac{IP16}{IP18}$	$\frac{IP18}{Pr}$	$\frac{Pr}{Ph}$	$\frac{IP15}{nC_{14}}$	$\frac{IP16}{nC_{15}}$	$\frac{IP18}{nC_{16}}$	$\frac{Pr}{nC_{17}}$	$\frac{Ph}{nC_{18}}$

OIL ANALYSIS

SAMPLE NO: 3076/79

WELL: Wooloo 1

TEST: Drill Stem Test 1

INTERVAL: 7176 - 7294 ft

FORMATION: Epsilon

TYPE OF SAMPLE: Condensate, +180°C Fraction

Results of Analysis

API Gravity (whole sample) 53.7

Saturates	68.5	%	by wt.
Aromatics	6.4	%	
Polar compounds	2.6	%	
Asphaltenes	--	%	
Loss	22.5	%	

n-Alkane distribution of saturates: O.E.P.

n-Alkane	C_{12}	C_{13}	C_{14}	C_{15}	C_{16}	C_{17}	C_{18}	C_{19}	C_{20}	C_{21}	C_{22}
Rel. abundance	13.3	13.2	12.0	10.2	9.4	7.9	7.1	5.9	4.7	4.1	3.6
n-Alkane	C_{23}	C_{24}	C_{25}	C_{26}	C_{27}	C_{28}	C_{29}	C_{30}	C_{31}	C_{32}	C_{33}
Rel. abundance	3.2	2.4	1.6	0.7	0.5	0.2	--	--	--	--	--

Isoprenoids distribution in saturates:

IP14	IP15	IP16	IP18	Pristane	Phytane
1.28	0.68	1.88	0.98	1.73	0.3

$\frac{IP15}{IP16}$	$\frac{IP16}{IP18}$	$\frac{IP18}{Pr}$	$\frac{Pr}{Ph}$	$\frac{IP15}{nC_{14}}$	$\frac{IP16}{nC_{15}}$	$\frac{IP18}{nC_{16}}$	$\frac{Pr}{nC_{17}}$	$\frac{Ph}{nC_{18}}$
0.36	1.92	0.57	5.75	0.055	0.185	0.105	0.22	0.04

OIL ANALYSIS

SAMPLE NO: 3077/79

WELL: Toolachee 9

TEST: Drill Stem Test 2

INTERVAL: 7265-7341 ft

FORMATION: Patchawarra

TYPE OF SAMPLE: Condensate, +210°C Fraction

Results of Analysis

API Gravity (whole sample) 47.2

Saturates	81.4	% by wt.
Aromatics	8.5	%
Polar compounds	1.8	%
Asphaltenes	--	%
Loss	8.3	%

n-Alkane distribution of saturates: O.E.P.

n-Alkane	C_{12}	C_{13}	C_{14}	C_{15}	C_{16}	C_{17}	C_{18}	C_{19}	C_{20}	C_{21}	C_{22}
Rel. abundance	16.0	20.6	14.7	7.5	5.7	5.5	5.4	4.8	4.4	4.4	4.1
n-Alkane	C_{23}	C_{24}	C_{25}	C_{26}	C_{27}	C_{28}	C_{29}	C_{30}	C_{31}	C_{32}	C_{33}
Rel. abundance	3.7	1.9	1.0	0.3	--	--	--	--	--	--	--

Isoprenoids distribution in saturates:

IP14	IP15	IP16	IP18	Pristane	Phytane
				0.82	0.2

$\frac{IP15}{IP16}$	$\frac{IP16}{IP18}$	$\frac{IP18}{Pr}$	$\frac{Pr}{Ph}$	$\frac{IP15}{nC_{14}}$	$\frac{IP16}{nC_{15}}$	$\frac{IP18}{nC_{16}}$	$\frac{Pr}{nC_{17}}$	$\frac{Ph}{nC_{18}}$
			4.1				0.18	0.045

GEOTRACK

SCANNED

THERMAL HISTORY RECONSTRUCTION IN COOPER-EROMANGA BASIN WELLS USING APATITE and ZIRCON FISSION TRACK ANALYSIS and VITRINITE REFLECTANCE

with results from

BEANBUSH-1, BURLEY-1, BURLEY-2, DULLINGARI-1, McLEOD-1, TIRRAWARRA-1 and TOOLACHEE-1

GEOTRACK REPORT #668

A report prepared for the PIRSA, Adelaide

Report prepared by: I. R. Duddy
AFTA determinations by: M.E. Moore

February 1999

GEOTRACK INTERNATIONAL PTY LTD ACN 006 821 209
37 Melville Road, Brunswick West, Victoria 3055 Australia telephone +61 3 9380 1077 facsimile +61 3 9380 1477

Geotrack International Pty Ltd and its officers and employees assume no responsibility and make no representation as to the productivity or profitability of any mineralisation, oil, gas or other material in connection with which this report may be used.

AFTA® and Geotrack® are registered trademarks owned and maintained by Geotrack International Pty Ltd.

THERMAL HISTORY RECONSTRUCTION IN COOPER-EROMANGA BASIN WELLS USING APATITE FISSION TRACK ANALYSIS AND VITRINITE REFLECTANCE
with results from
BEANBUSH-1, BURLEY-1, BURLEY-2, DULLINGARI-1, McLEOD-1, TIRRAWARRA-1 and TOOLACHEE-1

CONTENTS

	Page
Executive Summary	i-v
Paleotemperature analysis summary from Burley-2 well - Table i	vi
Paleotemperature analysis summary from Toolachee-1 well - Table ii	vii
Paleotemperature analysis summary from Beanbush-1 well - Table iii	viii
Paleotemperature analysis summary from Tirrawarra-1 well - Table iv	ix
Summary of paleogeothermal gradient estimates from AFTA and VR data for Cooper-Eromanga Basin wells - Table v	x
Summary of removed section estimates from AFTA and VR data for Cooper-Eromanga Basin wells - Table vi	xi
Schematic thermal history illustration for four Cooper-Eramanga wells - Figure i	xii
Paleogeothermal gradients determined for four Cooper-Eramanga wells - Figure ii	xiii

1. Introduction

1.1	Background and objectives	1
1.2	Report structure	2
1.3	Data quality	3
1.4	Apatite compositions	3
1.5	Thermal history reconstruction and use of thermal gradients vs heat flow	4
1.6	Outline of our approach to interpretation of AFTA and VR data	5
1.7	Paleogeothermal gradients	7
1.8	Eroded section	8

2. Thermal history reconstruction in the Burley-2 well

2.1	Background	10
2.2	Thermal history interpretation of AFTA and ZFTA data and fluid inclusion homogenisation temperatures	10
2.3	Thermal history interpretation of VR data	12
2.4	Thermal history interpretation of ZFTA data	13
2.5	Thermal history synthesis	14
2.6	Paleogeothermal gradients and mechanisms of heating and cooling	15
2.7	Implication fror source rock maturation at Burley-2 well	17

CONTENTS cont'd

		Page
2.8	Estimating section removed by erosion: Burial history reconstruction	17
3.	**Thermal history reconstruction in the Toolachee-1 well**	
3.1	Interpretive format	39
3.2	Thermal history conclusions from the AFTA and VR data	39
4.	**Thermal history reconstruction in the Beanbush-1 well**	
4.1	Interpretive format	60
4.2	Thermal history conclusions from the AFTA and VR data	60
5.	**Thermal history reconstruction in the Tirrawarra-1 well**	
5.1	Interpretive format	78
5.2	Thermal history conclusions from the AFTA and VR data	78
6.	**Concluding remarks: geological history of the Cooper-Eromanga Basin**	
6.1	Comments on recent heating - hot fluid flow	99
6.2	Comments on elevated heat flow in the Mid-Cretaceous	99
6.3	Comments on Mid-Cretaceous uplift and erosion	100
7.	**Further work which would significantly improve knowledge of the geological history of the region**	
7.1	Time of maturation of Mesozoic and Paleozoic source rocks	101
References		102

Appendix A - Sample Details and Geological Data

A.1	Sample details and geological data	A.1
A.2	Stratigraphic details	A.1
A.3	Present temperatures	A.1
A.4	Apatite yields and data quality	A.2
A.5	Zircon yields and data quality	A.2
A.6	Apatite grain morphologies	A.3
A.7	Apatite compositions	A.3
References		A.4

CONTENTS cont'd

Page

Appendix B - Sample Preparation, Analytical Details and Data Presentation

B.1 Sample preparation B.1
B.2 Analytical details B.1
B.3 Data presentation B.4
B.4 A note on terminology B.8

References B.9

Appendix C - Principles of Interpretation of AFTA and ZFTA Data in Sedimentary Basins

C.1 Introduction C.1
C.2 Basic principles of Apatite Fission Track Analysis C.1
C.3 Quantitative understanding of fission track annealing in apatite C.4
C.4 Evidence for elevated paleotemperatures from AFTA C.7
C.5 Quantitative determination of the magnitude of maximum paleotemperature and the timing of cooling using AFTA C.8
C.6 Qualitative assessment of AFTA parameters C.10
C.7 Allowing for tracks inherited from source areas C.10
C.8 Plots of fission track age and mean track length vs depth and temperature C.12
C.9 Determining paleogeothermal gradients and amount of section removed on unconformities C.13
C.10 Thermal history interpretation of Zircon Fission Track Age data C.15

References C.17

Appendix D - Vitrinite Reflectance Measurements

D.1 New vitrinite reflectance determinations D.1
D.2 Integration of vitrinite reflectance data with AFTA D.1
D.3 Open file vitrinite reflectance D.4

References D.2

TABLES

Page

Table i - Paleotemperature analysis summary from Burley-2 well vi

Table ii - Paleotemperature analysis summary from Toolachee-1 wellvii

Table iii - Paleotemperature analysis summary from Beanbush-1 wellviii

Table iv - Paleotemperature analysis summary from Tirrawarra-1 well ix

Table v - Summary of paleogeothermal gradient estimates from AFTA and VR data for Cooper-Eromanga Basin wells x

Table vi - Summary of removed section estimates from AFTA and VR data for Cooper-Eromanga Basin wells xi

Table 2.1 - Summary of AFTA data - samples from the **Burley-2 well** 20

Table 2.2 - Summary of thermal history interpretation of AFTA data in samples from the **Burley-2 well** 21-22

Table 2.3 - Estimates of timing and magnitude of elevated paleotemperatures from AFTA data in samples from the **Burley-2 well** 23-25

Table 3.1 - Summary of AFTA data - samples from the **Toolachee-1 well** 43

Table 3.2 - Summary of thermal history interpretation of AFTA data in samples from the **Toolachee-1 well** 44-46

Table 3.3 - Estimates of timing and magnitude of elevated paleotemperatures from AFTA data in samples from the **Toolachee-1 well** 47-48

Table 4.1 - Summary of AFTA data - samples from the **Beanbush-1 well** 63

Table 4.2 - Summary of thermal history interpretation of AFTA data in samples from the **Beanbush-1 well** 64

Table 4.3 - Estimates of timing and magnitude of elevated paleotemperatures from AFTA data in samples from the **Beanbush-1 well** 65-66

Table 5.1 - Summary of AFTA data - samples from the **Tirrawarra-1 well** 82

Table 5.2 - Summary of thermal history interpretation of AFTA data in samples from the **Tirrawarra-1 well** 83-84

Table 5.3 - Estimates of timing and magnitude of elevated paleotemperatures from AFTA data in samples from the **Tirrawarra-1 well** 85-87

TABLES cont'd

		Page
Table A.1 -	Details of AFTA samples and apatite yields	A.5-A.6
Table A.2 -	Details of ZFTA samples and zircon yields	A.7
Table A.3 -	Summary of Stratigraphy	A.8-11
Table A.4 -	Summary of present temperature measurements	A.12
Table A.5 -	Lower limits of detection for Apatite Analyses	A.13
Table A.6 -	Per cent errors in chlorine content	A.13
Table B.1 -	Apatite fission track analytical results	B.10
Table B.2 -	Length distribution summary data	B.11
Table B.3 -	ZFTA analytical results	B.11a
Data Sheets Glossary		B.28
Analytical data		B.29-B.47
Table D.1 -	Paleotemperatures - vitrinite reflectance nomogram based on Equation 2 of Burnham and Sweeney (1989)	D.3
Table D.2 -	Vitrinite reflectance sample details and results from open file data	D.4-D.8

FIGURES

		Page
Figure i -	Schematic thermal history illustration for four Cooper-Eramanga wells	xii
Figure ii -	Paleogeothermal gradients determined for four Cooper-Eramanga wells	xiii
Figure 2.1 -	AFTA and ZFTA parameters plotted against sample depth and present temperature for samples from the **Burley-2** well	26
Figure 2.2 -	Measured VR data plotted against depth in samples from the **Burley-2** well	27
Figure 2.3 -	Default burial history for the **Burley-2** well	28
Figure 2.4 -	Plot of paleotemperatures derived from AFTA and VR data in the **Burley-2** well	29
Figure 2.5 -	Variation of ZFTA and VR data with respect to depth in three Cooper-Eromanga Basin wells	30
Figure 2.6 -	Maximum likelihood profile of linear paleogeothermal gradient fitted to paleotemperature estimates from AFTA results in the **Burley-2** well	31
Figure 2.7 -	Maximum likelihood profile of linear paleogeothermal gradient fitted to paleotemperature estimates from AFTA and VR results in the **Burley-2** well	32
Figure 2.8 -	Reconstructed thermal history for **Burley-2** well derived from AFTA and VR results	33
Figure 2.9 -	Measured VR data in the **Burley-2** well and the VR profile with depth predicted from the reconstructed thermal history	34
Figure 2.10 -	Predicted development of maturity with time in the **Burley-2** well, controlled by the AFTA results	35
Figure 2.11 -	Maximum likelihood profile of estimated total section removed by uplift and erosion in the **Burley-2** well	36
Figure 2.12 -	Crossplot of total removed section with respect to the level of unconformity in the **Burley-2** well	37
Figure 2.13 -	Possible burial history consistent with the thermal history reconstruction in the **Burley-2** well	38
Figure 3.1 -	AFTA parameters plotted against sample depth and present temperature for samples from the **Toolachee-1** well	49
Figure 3.2 -	Measured VR data plotted against depth in samples from the **Toolachee-1** well	50
Figure 3.3 -	Default burial history for the **Toolachee-1** well	51

FIGURES cont'd

Page

Figure 3.4 - Plot of paleotemperatures derived from AFTA and VR data in the **Toolachee-1** well 52

Figure 3.5 - Maximum likelihood profile of linear paleogeothermal gradient fitted to paleotemperature estimates from AFTA and VR results in the **Toolachee-1** well 53

Figure 3.6 - Reconstructed thermal history for **Toolachee-1** well derived from AFTA and VR results 54

Figure 3.7 - Maximum likelihood profile of estimated total section removed by uplift and erosion in the **Toolachee-1** well 55

Figure 3.8 - Crossplot of total removed section with respect to the level of unconformity in the **Toolachee-1** well 56

Figure 3.9 - Possible burial history consistent with the thermal history reconstruction in the **Toolachee-1** well 57

Figure 3.10- Measured VR data in the **Toolachee-1** well and the VR profile with depth predicted from the reconstructed thermal history 58

Figure 3.11- Predicted development of maturity with time in the **Toolachee-1** well, controlled by the AFTA results 59

Figure 4.1 - AFTA parameters plotted against sample depth and present temperature for samples from the **Beanbush-1** well 67

Figure 4.2 - Measured VR data plotted against depth in samples from the **Beanbush-1** well 68

Figure 4.3 - Default burial history for the **Beanbush-1** well 69

Figure 4.4 - Plot of paleotemperatures derived from AFTA and VR data in the **Beanbush-1** well 70

Figure 4.5 - Maximum likelihood profile of linear paleogeothermal gradient fitted to paleotemperature estimates from AFTA and VR results in the **Beanbush-1** well 71

Figure 4.6 - Reconstructed thermal history for **Beanbush-1** well derived from AFTA and VR results 72

Figure 4.7 - Maximum likelihood profile of estimated total section removed by uplift and erosion in the **Beanbush-1** well 73

Figure 4.8 - Crossplot of total removed section with respect to the level of unconformity in the **Beanbush-1** well 74

Figure 4.9 - Possible burial history consistent with the thermal history reconstruction in the **Beanbush-1** well 75

FIGURES cont'd

Page

Figure 4.10 - Measured VR data in the **Beanbush-1** well and the VR profile with depth predicted from the reconstructed thermal history 76

Figure 4.11 - Predicted development of maturity with time in the **Beanbush-1** well, controlled by the AFTA results 77

Figure 5.1 - AFTA parameters plotted against sample depth and present temperature for samples from the **Tirrawarra-1** well 88

Figure 5.2 - Measured VR data plotted against depth in samples from the **Tirrawarra-1** well 89

Figure 5.3 - Default burial history for the **Tirrawarra-1** well 90

Figure 5.4 - Plot of paleotemperatures derived from AFTA and VR data in the **Tirrawarra-1** well 91

Figure 5.5 - Maximum likelihood profile of linear paleogeothermal gradient fitted to paleotemperature estimates from AFTA and VR results in the **Tirrawarra-1** well 92

Figure 5.6 - Reconstructed thermal history for **Tirrawarra-1** well derived from AFTA and VR results 93

Figure 5.7 - Maximum likelihood profile of estimated total section removed by uplift and erosion in the **Tirrawarra-1** well 94

Figure 5.8 - Crossplot of total removed section with respect to the level of unconformity in the **Tirrawarra-1** well 95

Figure 5.9 - Possible burial history consistent with the thermal history reconstruction in the **Tirrawarra-1** well 96

Figure 5.10 - Measured VR data in the **Tirrawarra-1** well and the VR profile with depth predicted from the reconstructed thermal history 97

Figure 5.11 - Predicted development of maturity with time in the **Tirrawarra-1** well, controlled by the AFTA results 98

Figure A.1a - Present temperature profile calculated for well **Beanbush-1** well A.14

Figure A.1b Present temperature profile calculated for well **Tirrawarra-1** well A.14

Figure A.2a - Distribution of chlorine content in samples from **Burley-2** well A.15

Figure A.2b - Distribution of chlorine content in samples from **Toolachee-1** well A.16

Figure A.2c - Distribution of chlorine content in samples from **Beanbush-1** well A.17

FIGURES cond

		Page
Figure A.2d -	Distribution of chlorine content in samples from **Tirrawarra-1** well	A.18
Figure B.1 -	Construction of a radial plot	B.12
Figure B.2 -	Simplified structure of radial plots	B.13
Figure B.3a-	Single grain age figures for samples from **Burley-2** well	B.14-15
Figure B.3b-	Single grain age figures for samples from **Toolachee-1** well	B.16
Figure B.3c-	Single grain age figures for samples from **Beanbush-1** well	B.17
Figure B.3d-	Single grain age figures for samples from **Tirrawarra-1** well	B.18-19
Figure B.4a-	Distribution of confined track lengths in samples from **Burley-2** well	B.20
Figure B.4b-	Distribution of confined track lengths in samples from **Toolachee-1** well	B.21
Figure B.4c-	Distribution of confined track lengths in samples from **Beanbush-1** well	B.22
Figure B.4d-	Distribution of confined track lengths in samples from **Tirrawarra-1** well	B.23
Figure B.5a-	Single grain age figures for samples from Cooper/Eromanga Basin wels	B.23a-23b
Figure B.6a-	Plots of single grain age against weight percent chlorine for samples from **Burley-2** well	B.24
Figure B.6b-	Plots of single grain age against weight percent chlorine for samples from **Toolachee-1** well	B.25
Figure B.6c-	Plots of single grain age against weight percent chlorine for samples from **Beanbush-1** well	B.26
Figure B.6d-	Plots of single grain age against weight percent chlorine for samples from **Tirrawarra-1** well	B.27
Figure C.1a -	Comparison of mean length in Otway Basin reference wells with predictions of Laslett et al. (1987) model	C.18
Figure C.1b -	Comparison of mean length in apatites of the same Cl content as Durango from Otway Group samples with predictions of Laslett et al. (1987) model	C.18

FIGURES cont'd

Page

Figure C.2 - Comparison of mean length in apatites of differing chlorine compositions C.19

Figure C.3 - Comparison of mean length in Otway Basin reference wells with predictions of new multi-compositional annealing model C.19

Figure C.4 - Histogram of Cl contents in typical samples C.20

Figure C.5 - Comparison of mean length in Otway Basin reference wells with predictions of Crowley et al. (1991) model or F-apatite C.21

Figure C.6 - Comparison of mean length in Otway Basin reference wells with predictions of Crowley et al. (1991) model for Durango apatite C.21

Figure C.7 - Changes in radial plots of post-depositional annealing C.22

Figure C.8 - Typical AFTA parameters
a Maximum temperatures now
b Hotter in the past C.23

Figure C.9 - Constraint of paleogeothermal gradient C.24

Figure C.10 - Estimation of section removed C.25

THERMAL HISTORY RECONSTRUCTION IN THE BEANBUSH-1, BURLEY-1, BURLEY-2, DULLINGARI-1, McLEOD-1, TIRRAWARRA-1 and TOOLACHEE-1 wells, COOPER-EROMANGA BASIN

USING APATITE and ZIRCON FISSION TRACK ANALYSIS and VITRINITE REFLECTANCE

EXECUTIVE SUMMARY

Aims and objectives

This report presents the results of a THR™ thermal history reconstruction study using a combination AFTA® (Apatite Fission Track Analysis), ZFTA™ (Zircon Fission Track Analysis), and vitrinite reflectance data from seven wells in the **Cooper-Eromanga Basin, South Australia.** The study was carried out by **Geotrack International Pty Ltd** in association with the **Department of Mines and Energy Resources, South Australia.**

The primary aim of this study is to provide a thermal history framework for understanding the post-Paleozoic thermal evolution of parts of the Cooper-Eromanga Basin, South Australia, based on result from the **Beanbush-1, Burley-1, Burley-2, Dullingari-1, McLeod-1, Tirrawarra-1 and Toolachee-1 wells**, within which the structural, burial and hydrocarbon histories can be constrained.

Specifically, AFTA and ZFTA are used to identify any episodes of elevated paleotemperatures which have affected each of the wells studied, to estimate the timing and magnitude of maximum paleotemperatures and to place constraints on any subsequent episodes of heating and cooling. Vitrinite reflectance (VR) data are also used to provide estimates of maximum paleotemperatures, the timing of which are interpreted on the basis of information provided by AFTA and/or ZFTA from associated samples. The resulting thermal history constraints are integrated into a coherent thermal history synthesis to provide a solid framework for evaluation of the burial/erosional and source rock maturation histories of the wells studied.

In detail, estimates of maximum paleotemperature from AFTA, ZFTA and VR over a range of depths are used to constrain paleogeothermal gradients, which are used to infer the mechanisms responsible for the various episodes of heating and cooling (Section 1.3). Where possible, estimates of section removed by uplift and erosion are obtained from the paleotemperature constraints, allowing reconstruction of the burial history. Burial history

reconstruction depends on a number of assumptions, in respect of the thermal structure of the eroded section, which is not directly known (Section 1.4). Therefore, the erosion estimates are best regarded as indicative of the general magnitude of removed section, and careful integration with estimates by other techniques (e.g., sonic velocity compaction studies, seismic reconstruction, etc.) is always desirable. Comparison of data from all wells within the geological setting allows a regional framework to be established, within which the implications of the regional variation of thermal history concerning patterns of hydrocarbon generation can be understood.

Sample details

A total of 15 samples from the **Cooper-Eromanga Basin wells Burley-2, Toolachee-1, Beanbush-1 and Tirrawarra-1,** originally provided by Mines and Energy Resources, South Australia, as a part of a NERDDC study (1988) are re-processed here using Geotrack's proprietary multi-compositional Apatite Fission Track Analysis (AFTA®) technology. ZFTA™ Zircon Fission Track Analysis results from five samples from the **Burley-1, McLeod-1 and Dullingari-1** are also included in the study as a part of an investigation of the timing of the high organic maturation levels observed in some of the deeper parts of the Cooper Basin sequence.

Details of all AFTA samples, including depths (TVD), stratigraphic ages and estimates of present temperature for each sample, are provided in Table A.1. ZFTA sample details are provided in Table A.2.

No new vitrinite reflectance samples were processed in the current study, but VR data was provided by PIRSA from each AFTA well, along with additional data from the Tirrawarra-2, 16 and 17 wells and these are reproduced in Table D.2 (Appendix D).

Report Structure

Thermal history results from each well are summarised in Tables i to vi with a schematic illustrations of the main features of the thermal history reconstruction presented in Figure i and ii.

Key conclusions

Thermal History

1. The AFTA thermal history results from the **Burley-2, Toolachee-1, Beanbush-1 and Tirrawarra-1** wells investigated in this report indicate either that the present-day temperatures estimated from corrected BHT values are too high, or they have increased to present-day levels in the geologically recent past. Given that results from all four wells give consistent results, we conclude that the present-day temperatures have been estimated accurately, and that they therefore must have increased to present levels recently. Modelling of the multi-compositional AFTA kinetics indicates that this temperature increase certainly occurred within the last 5 Ma in the four wells studied, and probably within the last 2 Ma. The results also provide estimates of the maximum possible "steady state" geothermal gradient that could have been operating immediately prior to temperature increasing in the last 2 Ma (see Tables i to Table iv).

2. When allowance is made for the recent increase in temperatures, integration of AFTA and VR results further indicate that the Early Cretaceous and older sections were subjected to an earlier period of heating and cooling in which maximum paleotemperature were experienced. The best independent estimates of the time of cooling from maximum paleotemperatures are based on the AFTA results from the Toolachee-1 and Beanbush-1 wells, which indicate that cooling began at some time between 125 and 75 Ma. AFTA results from the other wells constrain cooling to some time prior to 50 Ma, with constraints implicit in the stratigraphic age of the samples analysed providing an effective upper limit for cooling of ~97 Ma in Burley-2. Integration of all of these lines of evidence indicates that regional cooling from maximum paleotemperatures began at some time between ~97 and 75 Ma.

3. Paleogeothermal gradients defined by the AFTA and VR maximum paleotemperatures are significantly higher than either the "steady state" or recently increased present-day geothermal gradients in all wells. Maximum likelihood estimates with ± 95% confidence limits are summarised in Table v. This indicates a period of significantly elevated basal heat flow at each well site. Assuming that the decline in heat-flow (measured by the decline in paleogeothermal gradient) observed in these four wells is a regionally synchronous phenomenon, then a reasonable geological timing consistent with all constraints would be between the end of Winton Formation deposition at ~97 Ma and 75 Ma (indicated by AFTA).

4. Conservative interpretation of zircon fission track results (ZFTA) from Permian and older rocks in the deepest parts of **Burley-2 and Mcleod-1 wells** where VR values are ≥ 5%, suggest heating at temperatures of ≥300°C on an elevated geothermal gradient occurred at some time within the last ~150 Ma. More tenuous limited single grain ZFTA results suggest a tighter timing between ~90 and 50 Ma. Either timing is totally compatible with the AFTA results shallower in the section, giving additional confidence that the high gradient paleotemperature profiles defined by the AFTA and VR results represent the same thermal event ~97 Ma and 75 Ma.

Burial History

5. Extrapolation of the paleogeothermal gradient results from each well allows estimation of the magnitude of erosion that may have been associated with cooling from elevated paleotemperatures. Magnitudes of erosion allowed by extrapolation of the thermal history results as represented by the maximum likelihood estimates and ±95% confidence limits as summarised for each well in Table vi. In general, less than 300 m of uplift and erosion is indicated at the top Winton Formation unconformity.

Geological implications

6. The thermal history analysis shows that Cretaceous-Tertiary cooling in the Cooper-Eromanga Basin is dominated by decline in paleogeothermal gradient with little (maximum likelihood values between 0 and 500 m - Table vi) or no associated post-Winton Formation erosion.

Maturation History

7. The integrated AFTA thermal history reconstruction for the Burley-2, Toolachee-1, Beanbush-1 and Tirrawarra-1 wells implies that most of the Cretaceous and *all* of the older section reached maximum maturity at some time between 97 and 75 Ma. That is, all potential source rocks of Cretaceous to at least Permian in age attained their currently measured maturity at this time.

8. There is no evidence for any significant hydrocarbon generation (i.e no active source rock maturation) at the present-day, or within the last 2 Ma. The most active maturation phase occurred during deposition of the Cretaceous section during a period of significantly elevated basal heat flow.

9. Cessation of maturation resulted from rapid decline in basal heat flow with only a minor amount of cooling attributable to uplift and erosion on the top Winton unconformity.

Recommendations

10. Additional zircon fission track analysis in wells where measured VR levels are ~5% or greater may enable better information of the time of cessation of maturation in the deeper section.

Table i: Paleotemperature analysis summary - AFTA and VR samples from the Burley-2 well, Cooper-Eromanga Basin, South Australia (Geotrack Report #668).

Sample number	Average depth (TVD)	Present temperature*1	Stratigraphic age	From AFTA and VR — Early Episode: Maximum paleotemperature	Early Episode: Onset of cooling	Late Episode*3: Heating from paleotemperature	Late Episode*3: Time interval
GC	(m)	(°C)	(Ma)	(°C)	(Ma)	(°C)	(Ma)
VR1	341	40	97-90	42	-	NA	-
VR2	498	50	97-90	52	-	NA	-
668-168	553	53	97-90	<110	prior to 50	<47 to present	"2 to 0"
VR3	681	61	97-90	67	-	NA	-
668-169	754	66	97-90	<120	post-depn	<57 to present	"2 to 0"
VR4	773	67	97-90	74	-	NA	-
VR5	828	70	97-90	90	-	NA	-
VR6	892	74	100-97	88	-	NA	-
VR7	974	79	100-97	94	-	NA	-
VR8	1038	83	103-100	94	-	NA	-
668-170	1056	84	103-100	<130	prior to 50	<72 to present	"2 to 0"
VR9	1102	87	103-100	98	-	NA	-
VR10	1253	96	106-103	107	-	NA	-
668-171	1266	97	117.5-106	<110	prior to 7	<83 to present	7 to 0
VR11	1376	104	117.5-106	105	-	NA	-
VR12	1673	122	135-117.5	124	-	NA	-
668-172	1748	126	141.5-135	>140	prior to 15	<107 to present	"2 to 0"
VR13	1760	127	141.5-135	125	-	NA	-
VR14	1876	134	148-147	165	-	NA	-
VR15	1949	138	148-147	166	-	NA	-
668-174	1977	140	148-147	>115	post-depn	<119 to present	"2 to 0"
VR16	2004	142	148-147	175	-	NA	-
VR17	2083	147	157-150	185	-	NA	-
VR18	2105	148	157-150	186	-	NA	-
VR19	2256	157	188-157	181	-	NA	-
VR20	2269	158	188-157	191	-	NA	-
VR21	2673	183	255-249	248	-	NA	-
VR22	2699	184	255-249	249	-	NA	-
VR23	2737	187	255-249	249	-	NA	-
VR24	2760	188	255-249	248	-	NA	-
VR25	2800	190	255-249	252	-	NA	-
VR26	2821	192	255-249	260	-	NA	-
VR27	2867	194	267-262	264	-	NA	-
VR28	2918	198	267-262	262	-	NA	-
VR29	3028	204	273-270	279	-	NA	-
VR30	3092	208	273-270	284	-	NA	-
VR31	3269	219	295-275	~350	-	NA	-
VR32	3336	223	295-275	>350	-	NA	-
VR33	3357	224	295-275	>350	-	NA	-
VR34	3443	230	295-275	>350	-	NA	-
VR35	3491	233	295-275	>350	-	NA	-
VR36	3543	236	295-275	>350	-	NA	-
VR37	3638	241	298-296.5	>350	-	NA	-
VR38	3659	243	298-296.5	>350	-	NA	-
AFTA Timing overlap Burley-2					**97 to 50 Ma*2**		**"2 to 0"*3**

NA: Not applicable

*1 Present temperatures based on geothermal gradient of 61°C/km and a surface temperature of 20°C - Appendix A.

*2 Timing from overlap of AFTA and stratigraphic constraints in Burley-2.

*3 Timing represents a consistent timing from all wells studied for increase in geothermal gradients to the present-day levels. Temperatures are maximum possible temperature allowed by AFTA over the last 2 Ma - see text for details.

Table ii: Paleotemperature analysis summary - AFTA and VR samples from the Toolachee-1 well, Cooper-Eromanga Basin, South Australia (Geotrack Report #668).

Sample number	Average depth (TVD)	Present temp-erature*1	Strati-graphic age	From AFTA and VR: Early Episode		Late Episode*3	
				Maximum paleotemperature	Onset of cooling	Heating from paleotemperature	Time interval
GC	(m)	(°C)	(Ma)	(°C)	(Ma)	(°C)	(Ma)
VR39*4	663	53	97-90	56	-	NA	-
VR40*4	1300	86	135-118	93	-	NA	-
668-223	1646	104	157-147	>110	prior to 75	<86 to present	20 to 0
VR41*4	1666	105	157-147	122	-	NA	-
VR42*4	1700	106	237-186	127	-	NA	-
668-224	1705	107	237-186	>120	130 to 60	<88 to present	2 to 0
VR43	1849	114	255-249	136	-	NA	-
VR44*4	1870	115	255-249	150	-	NA	-
VR45*4	1900	117	255-249	148	-	NA	-
VR46*4	1913	117	267-262	152	-	NA	-
VR47*4	1983	121	273-270	157	-	NA	-
VR48*4	2035	123	275-273	162	-	NA	-
VR49*4	2100	127	295-275	162	-	NA	-
VR50	2106.7	127	295-275	156	-	NA	-
VR51	2109.7	127	295-275	159	-	NA	-
VR52*4	2123	128	295-275	164	-	NA	-
VR53*4	2265	135	304-300	172	-	NA	-
VR54*4	2303	137	304-300	174	-	NA	-
VR55*4	2315	138	304-300	175	-	NA	-
AFTA Timing overlap Toolachee-1				**130 to 75 Ma*2**			**"2 to 0"*3**

NA: Not applicable

*1 Present temperatures based on geothermal gradient of 51°C/km and a surface temperature of 20°C - Appendix A.

*2 Timing from overlap of integrated AFTA, VR and stratigraphic constraints in Toolachee-1.

*3 Timing represents a consistent timing from all wells studied for increase in geothermal gradients to the present-day levels. Temperatures are maximum possible temperature allowed by AFTA over the last 2 Ma - see text for details.

*4 Additional VR results from the Toolachee-9

Table iii: Paleotemperature analysis summary - AFTA and VR samples from the Beanbush-1 well, Cooper-Eromanga Basin, South Australia (Geotrack Report #668).

Sample number	Average depth (TVD)	Present temp-erature*1	Strati-graphic age	From AFTA and VR: Early Episode		Late Episode*3	
				Maximum paleotemperature	Onset of cooling	Heating from paleotemperature	Time interval
GC	(m)	(°C)	(Ma)	(°C)	(Ma)	(°C)	(Ma)
VR56	457.2	38	97-90	<40	-	NA	-
VR57	914.4	55	97-90	75	-	NA	-
VR58	1216.2	67	100-97	77	-	NA	-
VR59	1371.6	73	103-100	79	-	NA	-
VR60	1527.1	79	117.5-106	75	-	NA	-
VR61	1828.8	90	117.5-106	100	-	NA	-
VR62	1947.7	95	135-117.5	94	-	NA	-
VR63	2020.2	98	135-117.5	119	-	NA	-
668-238	2051	99	141.5-135	<125	125 to 70	<90 to present	2 to 0
VR64	2231.1	106	148-147	105	-	NA	-
VR65	2307.3	109	150-148	117	-	NA	-
668-240	2356	110	157-150	<140	"100 to 45"	<100 to present	2 to 0
VR66	2383.5	112	150-148	111	-	NA	-
VR67	2441.5	114	188-157	109	-	NA	-
VR68	2606.0	120	188-157	130	-	NA	-
VR69	2664.7	122	188-157	124	-	NA	-
VR70	2758.4	126	249-236.5	128	-	NA	-
VR71	2987.0	135	249-236.5	119	-	NA	-
VR72	3203.5	143	255-249	160	-	NA	-
VR73	3267.5	145	273-262	166	-	NA	-
VR74	3301.0	147	295-275	166	-	NA	-
VR75	3310.8	147	295-275	166	-	NA	-
VR76	3365.0	149	295-275	175	-	NA	-
VR77	3422.9	151	295-275	188	-	NA	-
VR78	3514.3	155	295-275	181	-	NA	-
VR79	3548.6	156	295-275	188	-	NA	-
VR80	3605.8	158	298-296.5	173	-	NA	-
VR81	3608.1	159	298-296.5	184	-	NA	-
AFTA Timing overlap			**Beanbush-1**		**125 to 70 Ma*2**		**"2 to 0"*3**

NA: Not applicable

*1 Present temperatures based on geothermal gradient of 38.5°C/km and a surface temperature of 20°C - Appendix A.

*2 Timing from overlap of integrated AFTA, VR and stratigraphic constraints.

*3 Timing represents a consistent timing from all wells studied for increase in geothermal gradients to the present-day levels. Temperatures are maximum possible temperature allowed by AFTA over the last 2 Ma - see text for details.

Table iv: Paleotemperature analysis summary for Tirrawarra-1 - AFTA and VR samples from the Cooper-Eromanga Basin, South Australia (Geotrack Report #668).

Sample number	Average depth (TVD)	Present temp-erature*1	Strati-graphic age	From AFTA and VR: Early Episode		Late Episode*3	
				Maximum paleotemperature	Onset of cooling	Heating from paleotemperature	Time interval
GC	(m)	(°C)	(Ma)	(°C)	(Ma)	(°C)	(Ma)
668-152	407	37	97-90	<105	post-deposition	<34 to present	2 to 0
668-156	1586	86	103-100	<105	post-deposition	<75 to present	2 to 0
668-157	1669	89	135-117.5	<110	post-deposition	<78 to present	2 to 0
668-158	1827	96	147-141.5	<115	post-deposition	<84 to present	2 to 0
668-160	2010	103	157-150	<125	post-deposition	<90 to present	2 to 0
VR82	2012	103	157-150	109	-	NA	-
VR83	2575	127	255-249	154	-	NA	-
VR84	2756	134	295-275	170	-	NA	-
Tirrawarra-16							
VR85	2939	142	?296.5-295	153	-	NA	-
Tirrawarra-2							
VR86	2965	143	?298-296.5	190	-	NA	-
Tirrawarra-17							
VR87	2970	143	?298-296.5	158	-	NA	-
AFTA Timing overlap Tirrawaara-1					**97 to 75 Ma*2**		**"2 to 0"*3**

NA: Not applicable

*1 Present temperatures based on geothermal gradient of 41.5°C/km and a surface temperature of 20°C - Appendix A.

*2 Timing from overlap of integrated AFTA, VR and stratigraphic constraints from all wells studied as no direct timing evidence is available fom the Tirrawarra-1 AFTA samples.

*3 Timing represents a consistent timing from all wells studied for increase in geothermal gradients to the present-day levels. Temperatures are maximum possible temperature allowed by AFTA over the last 2 Ma - see text for details.

Table v: Summary of paleogeothermal gradient estimates from AFTA and VR data for Cooper-Eromanga Basin wells (Geotrack Report #668)

Well	Present day*1 geothermal gradient (°C/km)	Paleogeothermal gradients (°C/km)*2 mid- to Late Cretaceous*6 (~97 to 75 Ma)
Burley-2	61 (50)	82.5*3 (76 - 91) 89*4 (84.5 - 94)
Toolachee-1	51 (40)	75.5*4 (69 - 82)
Beanbush-1	38.5 (30)	46*4 (40.5 - 51.5)
Tirrawarra-1	41.5 (35)	60.5*5 (44.5 - 70.5)

*1 Based on corrected BHT data. AFTA results indicate that the present-day gradients in these wells have *increased* to present levels relatively recently, certainly within the last 5 Ma, probably within the last 2 Ma. The value in brackets is the *maximum* value of present-day gradients allowed by AFTA prior to the recent increase. Lower values are possible prior to the recent increase but these cannot be independently estimated - see text for details.

*2 Maximum likelihood value with ±95% confidence interval range in brackets. Gradients estimated to the top of the Winton Formation.

*3 Estimated from paleotemperatures derived from the AFTA results alone from the whole pre-Tertiary section.

*4 Estimated from paleotemperatures derived from the AFTA and VR results from the whole pre-Tertiary section.

*5 Estimated from paleotemperatures derived from AFTA and VR results only in Tirrawarra-1.

*7 The best independent timing constraints on the time of decline in elevated paleogeothermal gradient are 130 to 75 Ma and 125 to 70 Ma based on AFTA data from Toolachee-1 and Beanbush-1, respectively. AFTA data from other wells generally indicate any time prior to 75 Ma is viable with stratigraphic constraints providing an upper limit of ~97 Ma (Burley-2). Assuming decline in heat flow to be a synchronous regional phenomenon, then a geological reasonable timing consistent with constraints would be at the end of Winton Formation deposition at ~90 Ma (within the 97 to 75 Ma range).

Table vi: Summary of removed section estimates from AFTA and VR data for Cooper-Eromanga Basin wells (Geotrack Report #668)

Well	Total removed section estimates (m)*1,2 Mid to Late Cretaceous*3 (97 to 75 Ma)
Burley-2	0*4 (0 - 100)
Toolachee-1	150*4 (0 - 300)
Beanbush-1	500*4 (150 - 850)
Tirrawarra-1	100*4 (0 - 850)

*1 Maximum likelihood value with ±95% confidence interval range in brackets. Paleo-surface temperature of 0°C assumed.
*2 Total removed section with respect to the unconformity at the top of the Winton Formation.
*3 Timing of the heating and cooled episode constrained by a combination of AFTA and stratigraphic data.
*4 Derived from the AFTA and VR results from the whole pre-Tertiary section in each well.

Notes: Details of maximum likelihood estimation of paleogeothermal gradient and section removed are provided in Section 1 and Appendix C (Section C.9). The allowed ranges of values of paleogeothermal gradient and section removed (within ±95% confidence limits) are highly correlated.

Estimation of section removed depends on the assumption that the paleogeothermal gradient is linear and can be extrapolated through the removed section to the paleo-surface temperature. If this assumption is not valid (e.g., if the paleo-thermal effects were due to fluid flow, with a higher paleogeothermal gradient in the shallower [removed] section), the estimated section removed will not be accurate.

The paleotemperature constraints (Tables i to iv) and the estimated paleogeothermal gradient through the preserved section (Table v) are not affected by any of the assumptions required in order to estimate the amount of section removed, and can be regarded as reliable.

The amount of section removed has been estimated for an assumed paleo-surface temperature of 0°C. The resulting estimate can be adjusted to refer to other values of paleo-surface temperature simply by adding or subtracting the depth interval corresponding to the difference between the preferred value and 0°C, as appropriate, for the maximum likelihood value of paleogeothermal gradient.

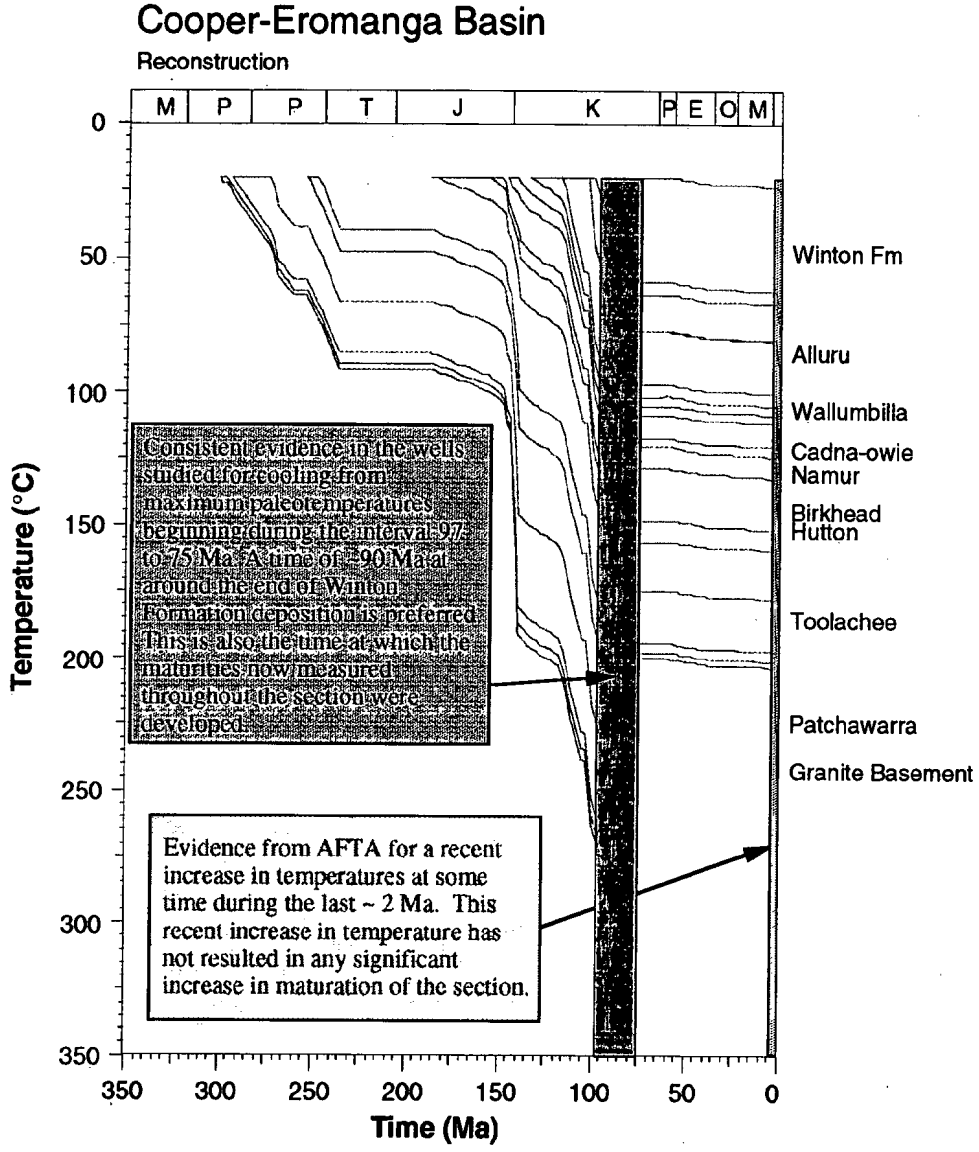

Figure i: Schematic illustration of the main features of the thermal history derived from AFTA, ZFTA and VR paleotemperature results, **Burley-2, Toolachee-1, Beanbush-1 and Tirrawarra-1 wells, Cooper-Eromanga Basin.** Values given in Tables i to iv.

Rapid cooling in the mid-Cretaceous - early Tertiary results from decline in paleogeothermal gradient without any significant uplift and erosion on the top-Winton Formation unconformity.

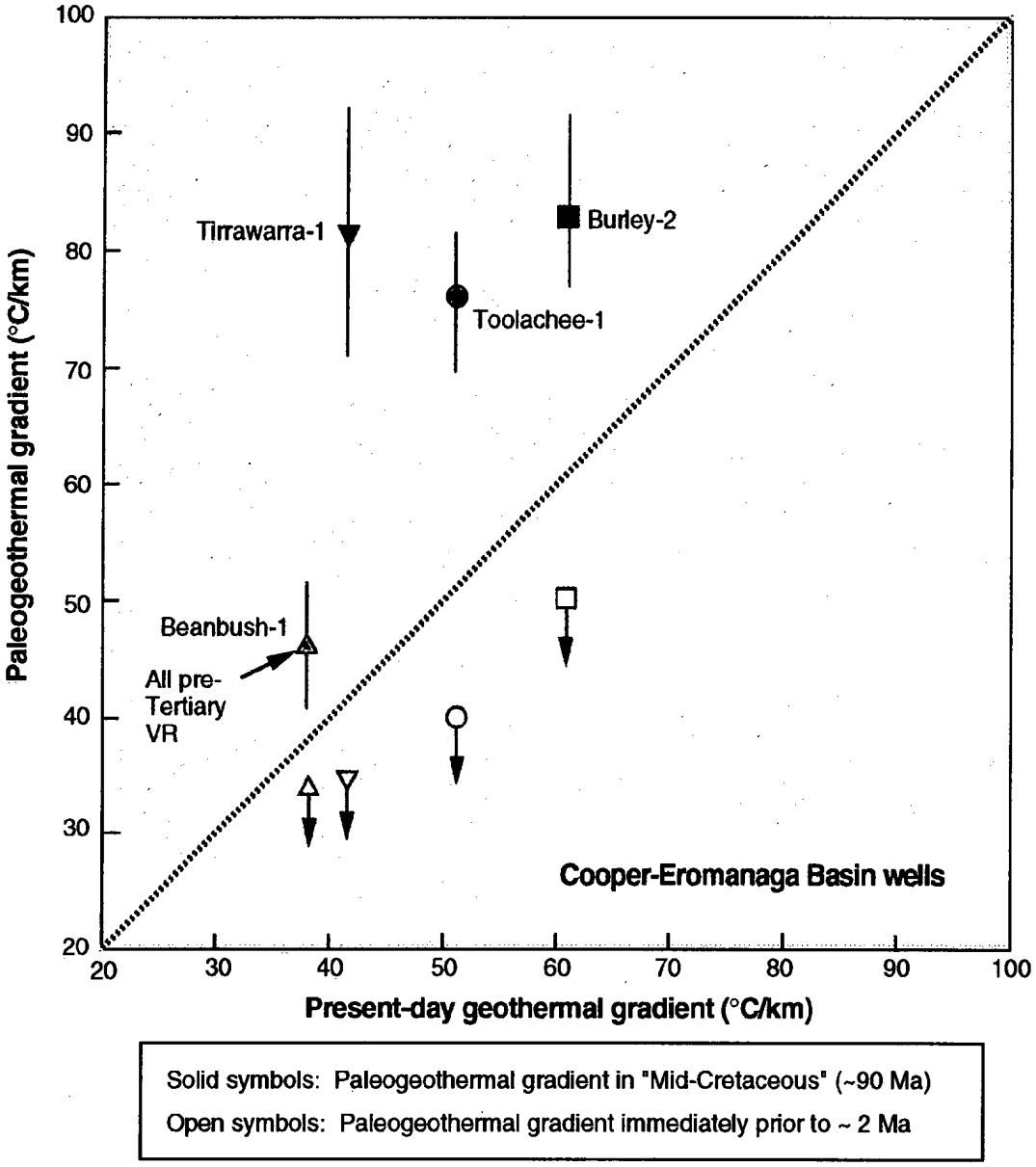

Figure ii: Paleogeothermal gradients determined from AFTA and VR paleotemperature results versus present-day gradient for four **Eromanga Basin wells.** Values given in Table v.

1. Introduction

1.1 Background and objectives of this study

This report presents the results of a THR™ thermal history reconstruction study using a combination AFTA® (Apatite Fission Track Analysis), ZFTA™ (Zircon Fission Track Analysis), and vitrinite reflectance data from seven wells in the **Cooper-Eromanga Basin, South Australia.** The study was carried out by **Geotrack International Pty Ltd** in association with the **Department of Mines and Energy Resources, South Australia**.

The primary aim of this study is to provide a thermal history framework for understanding the post-Paleozoic thermal evolution of parts of the Cooper-Eromanga Basin, South Australia, based on result from the **Beanbush-1, Burley-1, Burley-2, Dullingari-1, McLeod-1, Tirrawarra-1 and Toolachee-1 wells**, within which the structural, burial and hydrocarbon histories can be constrained.

A total of 15 samples from the **Cooper-Eromanga Basin wells Burley-2, Toolachee-1, Beanbush-1 and Tirrawarra-1,** originally provided by Mines and Energy Resources, South Australia, as a part of a NERDDC study (1988) are re-processed here using Geotrack's proprietary multi-compositional Apatite Fission Track Analysis (AFTA®) technology. ZFTA™ Zircon Fission Track Analysis results from five samples from the **Burley-1, McLeod-1 and Dullingari-1** are also included in the study as a part of an investigation of the timing of the high organic maturation levels observed in some of the deeper parts of the Cooper Basin sequence.

Details of all AFTA samples, including depths (TVD), stratigraphic ages and estimates of present temperature for each sample, are provided in Table A.1. ZFTA sample details are provided in Table A.2

AFTA is used to identify any episodes of elevated paleotemperatures which have affected the region, to estimate the timing and magnitude of maximum paleotemperatures and to place constraints on any subsequent episodes of heating and cooling. VR data are also used to provide estimates of maximum paleotemperatures, the timing of which is interpreted on the basis of information provided by AFTA. Paleotemperature constraints from AFTA and VR are then integrated into a coherent thermal history synthesis. Estimates of maximum paleotemperature from AFTA and VR over a range of depths are used to constrain paleogeothermal gradients, which are used to infer the origins of the various episodes of heating and cooling (Section 1.7).

Where possible, estimates of section removed by uplift and erosion are obtained from the paleotemperature constraints, allowing reconstruction of the burial history. Burial history reconstruction depends on a number of assumptions, with respect to the thermal structure of the eroded section, which are not directly known (Section 1.8). Therefore, the results should be regarded as indicative of the general magnitude and corroboration of the removed section estimates by other techniques (e.g., sonic velocity compaction studies, seismic reconstruction on structures, etc.) is always desirable. Comparison of data from all wells with the geological setting then allows a regional framework to be established, within which the implications of the regional variation of thermal history concerning patterns of hydrocarbon generation can be understood.

1.2 Report structure

The main conclusions of this report are summarised in the Executive Summary. The thermal history interpretations of AFTA, ZFTA and VR data for the **Burley-2, Toolachee-1, Beanbush-1 and Tirrawarra-1** wells are summarised in Tables i to iv, in terms of quantitative constraints on maximum paleotemperatures and timing of major thermal episodes. Estimates of paleogeothermal gradient and the magnitude of removed section in each well are summarised in Tables v and vi, respectively. Figure i provides a generalised illustration of the main features of the constrained thermal history derived from AFTA and VR data for consistent results from all wells. Figure ii compares present-day and paleogeothermal gradients determined in each well.

In Section 1, introductory aspects of the report are discussed, including comments on data quality. The approach to thermal history reconstruction employed in this report is also described in Section 1.and Sections 2 to 5 summarise the thermal history interpretation of the AFTA, ZFTA and VR data for **Burley-2, Toolachee-1, Beanbush-1 and Tirrawarra-1**, respectively. Each of these sections also include evaluation of the paleogeothermal gradients, section removed and burial reconstructions at each well site. A thermal history synthesis, including comments on similarities and differences between wells is given in Section 6. In the concluding section, Section 7, recommendations are made for additional work which may resolve some outstanding uncertainties.

Supporting information is provided in four Appendices. Details of all AFTA samples including depths, stratigraphic details and present temperatures in each well, are presented in Appendix A, together with the yields of detrital apatite obtained after mineral separation, apatite grain morphologies and apatite compositions (Cl contents).

Sample preparation and analytical details are described in Appendix B, followed by the presentation of all AFTA data, including raw track counts and fission track ages for individual grains. Details of the presentation of data in the form of Tables and Figures throughout the report are also discussed in detail in Appendix B. Appendix C outlines the principles employed in interpreting the AFTA data in terms of thermal history. In Appendix D, VR results supplied for the study are listed. Appendix D also discusses the principles involved in integrating AFTA and VR data to provide coherent thermal history interpretations.

1.3 Data quality

AFTA data

The new AFTA data generated for this report are generally of excellent quality (see Table A.1 (Appendix A).

ZFTA data

ZFTA data included and generated for this report are generally of excellent quality.

VR data

The quality of the MESA supplied VR results is difficult to assess without access to the full maceral descriptions but in general, the results appear to provide a consistent data set.

1.4 Apatite compositions

The annealing kinetics of fission tracks in apatite are affected by chemical composition, specifically the Cl content, as explained in more detail in Appendix C. Thus, an assessment of the chlorine content in apatite is essential in interpreting AFTA data, providing greater accuracy in establishing the time and magnitude of thermal events.

For this study, chlorine compositions were determined for all individual apatite grains in which fission track ages were determined and lengths measured for all samples which provided apatite from the six wells studied.

The measured range of chlorine contents of dated grains and grains in which lengths were measured is shown in histogram format in Figure A.2. A plot of single grain age versus weight % chlorine is shown in Figure B.5. Chlorine contents, which are

presented in numerical format for age grains, appear in the fission track age summary sheets in Appendix B.

1.5 Thermal history reconstruction and use of thermal gradients vs heat flow

Most approaches to thermal history reconstruction in sedimentary basins are based on consideration of the variation of heat flow through time, using models often based solely on theoretical grounds. However, this approach is beset by problems, particularly in sections which have been hotter in the past. Use of a heat flow-based approach depends critically on knowledge of thermal conductivities through the section. When considerable section has been removed, no information is available on lithologies (and hence thermal conductivities) in the removed section. In addition, large variation in thermal conductivities within similar lithological units (e.g., Corrigan, 1991) introduces considerable uncertainty into the relationship between heat flow and thermal gradient, even in relatively simple cases. For further illustration of these problems, see Waples et al. (1992). The influence of factors such as porosity, compaction and diagenesis is difficult to assess quantitatively, and the effects of greater depth of burial are unpredictable in a sequence affected by uplift and erosion, particularly when the magnitude of burial is unknown before the analysis. A heat flow-based approach to determining amounts of removed section is subject to considerable uncertainty because of problems such as these. This point has been discussed in greater detail by Duddy et al. (1991).

It is also important to realise the validity of theoretical heat-flow models is largely untested. High heat flow associated with rifting and early subsidence leaves no measurable effect if subsidence later in the basin's history has caused higher temperatures than those attained during the assumed high heat-flow episode. In many sedimentary basins, deep burial late in the subsidence history has caused maximum temperatures, and no record of earlier heat-flow variation is preserved either in the level of measured source rock maturity or in the AFTA parameters, as these data are dominated by the effects of maximum paleotemperature. Elevated heat-flow episodes associated with rifting are known to leave a measurable signature only where cooling has occurred shortly after the initial rifting phase, and where temperatures have subsequently remained low through to the present day (Duddy et al., 1991).

We have adopted an alternative approach, based on measurement of thermal gradients (present and past), using an integrated AFTA and VR methodology, because of these problems with a heat flow-based approach to thermal history reconstruction.

This approach yields direct measurement of the time at which cooling from maximum paleotemperatures began (from AFTA), and the paleogeothermal gradient at that time (from AFTA and VR). The style of cooling from maximum paleotemperatures to present temperatures can also be constrained (from AFTA). This approach allows definition of all the major facets of the thermal history of a sedimentary section through time, and is based on *directly measurable parameters*, rather than on *assumed* values of highly unpredictable factors. The information provided can still ultimately be interpreted in terms of paleo-heat flow if desired.

It should also be appreciated that the thermal history prior to the time at which cooling from maximum paleotemperatures begins, cannot be constrained from any of the available in-situ paleotemperature indicators based on thermally activated reactions. This arises because of the dominance of temperature over time in the kinetics of the systems employed in this way (i.e., fission track annealing, vitrinite reflectance, etc.). For this reason, these data can only constrain the thermal history from the onset of cooling from maximum paleotemperatures to the present day. Information on the earlier history can only be obtained indirectly, e.g., from geological information, perhaps by reconstructing patterns of burial based on section preserved in neighbouring regions, from theoretical heat-flow models (given the above caveats), or possibly by more subtle means, such as the presence of residual hydrocarbon products generated during earlier heating to lower peak paleotemperatures.

1.6 Outline of our approach to interpretation of AFTA and VR data

Interpretation of AFTA and VR data in this report begins by assessing whether the AFTA and/or VR data in each sample could have been produced if the sample has never been hotter than its present temperature at any time since deposition. The burial history derived from the stratigraphy of the preserved sedimentary section and the present geothermal gradient are used to predict a "Default Thermal History" for each sample, which forms the basis of interpretation.

If the data show a greater degree of fission track annealing and/or a higher VR value than expected on the basis of this history, the sample must have been hotter at some time in the past. In this case, the AFTA data are analysed to provide estimates of the magnitude of the maximum paleotemperature in that sample, and the timing of cooling from the thermal maximum. VR data provide an independent estimate of maximum paleotemperature. Paleotemperature estimates from both AFTA and VR are then used

to reconstruct a paleogeothermal gradient and, where appropriate, to estimate the amount of section removed by uplift and erosion.

The heating rate assumed in calculating paleotemperatures affects the magnitude of paleotemperature required to produce a given set of data. As AFTA and VR data do not independently constrain the heating rate, paleotemperatures are estimated by assuming simple linear heating between a point on the Default Thermal History and the maximum paleotemperature. This will not give the actual paleotemperature in general, but this procedure at least allows AFTA and VR data to be analysed within a common thermal history framework in the absence of any other constraint on heating rate. If any evidence of the real time-scale of heating is available, this can easily be incorporated into the analysis. Note AFTA data provide some constraint on cooling rates, as explained in more detail in Appendix C.

Estimates of maximum paleotemperature from AFTA are often quoted in terms of a range of paleotemperatures, as the data can often be explained by a variety of scenarios. Paleotemperature estimates from VR are usually quoted to the nearest degree Celsius as the value which predicts the measured reflectance. This is not meant to imply VR data can be used to estimate paleotemperatures to this degree of precision. VR data from individual samples typically show a scatter equivalent to a range of between ±5 and ±10°C. Estimates from a series of samples are normally used to define a paleotemperature profile in samples from a well or a regional trend in paleotemperatures from outcrop samples.

If the data show a lower degree of fission track annealing and/or a lower VR value than expected on the basis of the Default Thermal History, this suggests either present temperatures may be overestimated or temperatures have increased very recently. In such cases, the data may allow an estimate of the true thermal gradient, or some estimate of the time over which temperatures have increased.

Further discussion of the methodology employed in interpreting AFTA and VR data are given in Appendices C and D.

AFTA data are interpreted using a new multi-compositional kinetic model for fission track annealing in apatite developed by Geotrack, details of which are provided in Appendix C. Vitrinite reflectance data are interpreted using the distributed activation energy model describing the evolution of VR, with temperature and time developed by Burnham and Sweeney (1989) (see also Sweeney and Burnham, 1990), as implemented in the BasinMod™ software package of Platte River Associates (using version 3.15).

1.7 Paleogeothermal gradients

Basic principles

A series of paleotemperature estimates from AFTA and/or VR over a range of depths can be used to reconstruct a paleotemperature profile through the preserved section. The slope of this profile defines the paleogeothermal gradient. As explained by Bray et al. (1992), the shape of the paleotemperature profile and the magnitude of the paleogeothermal gradient provides unique insights into the origin and nature of the heating and cooling episodes expressed in the observed paleotemperatures.

Linear paleotemperature profiles with paleogeothermal gradients close to the present-day geothermal gradient provide strong evidence that heating was caused by greater depth of burial with no significant increase in basal heat-flow, implying in turn that cooling was due to uplift and erosion. Paleogeothermal gradients significantly higher than the present-day geothermal gradient suggest that heating was due, at least in part, to increased basal heat flow, while a component of deeper burial may also be important as discussed in the next section. Paleogeothermal gradients significantly lower than the present-day geothermal gradient suggest that a simple conductive model is inappropriate, and more complex mechanisms must be sought for the observed heating. One common cause of low paleogeothermal gradients is transport of hot fluids shallow in the section. However, the presence of large thicknesses of sediment with uniform lithology dominated by high thermal conductivities can produce similar paleotemperature profiles, and each case has to be considered individually.

A paleotemperature profile can only be characterised by a single value of paleogeothermal gradient when the profile is linear. Departures from linearity may occur where strong contrasts in thermal conductivities occur within the section, or where hot fluid movement or intrusive bodies have produced localised heating effects. In such cases, a single value of paleogeothermal gradient cannot be calculated. However, it is important to recognise that the validity of the paleotemperatures determined from AFTA and/or VR are independent of these considerations, and can still be used to control possible thermal history models.

Estimation of paleogeothermal gradients in this report

Paleogeothermal gradients have been estimated, using methods outlined in Appendix C, for each well analysed for this report in which paleotemperature estimates are available over a range of depths. These methods provide a best estimate of the gradient ("maximum likelihood value") and upper and lower 95% confidence limits on this estimate (analogous to ±2s limits). The "goodness of fit" is displayed in the form

of a log-likelihood profile, which is expected to show good quadratic behaviour for a dataset which agrees with a linear profile. This analysis depends on the assumption that the paleogeothermal gradient through the preserved section is linear. Visual inspection is usually sufficient to confirm or deny this assumption.

1.8 Eroded section

Basic principles

Subject to a number of important assumptions, extrapolation of a linear paleotemperature profile to a paleo-surface temperature allows estimation of the amount of eroded section represented by an unconformity, as explained in more detail in Section C.9 (Appendix C).

Specifically, this analysis assumes:

- The paleotemperature profile through the preserved section is linear;
- The paleogeothermal gradient through the preserved section can be extrapolated linearly through the missing section;
- The paleo-surface temperature is known; and,
- The heating rate used to estimate the paleotemperatures defining the paleogeothermal gradient is correct.

It is important to realise that any method of determining the amount of eroded section based on thermal methods is subject to these and/or additional assumptions. For example, methods based on heat-flow modelling must assume values of thermal conductivities in the eroded section, which can never be known with confidence. Such models also require some initial assumption of the amount of eroded section to allow for the effect of compaction on thermal conductivity. Methods based on geothermal gradients, as used in this study, are unaffected by this consideration, and can therefore provide independent estimates of the amount of eroded section. However, these estimates are always subject to the assumptions set out above and should be considered with this in mind.

Estimation of eroded section in this report

The analysis used to estimate paleogeothermal gradients is easily extended to provide maximum likelihood values of eroded section for an assumed paleo-surface temperature, together with ±95% confidence limits. These parameters are quoted for each well in which the paleotemperature profile suggests that heating may have been due, at least in part, to deeper burial.

However, it is emphasised that such interpretations are not unique and alternative interpretations are always possible. For instance, the paleogeothermal gradient through the missing section may have been much higher than in the preserved section where the eroded section was dominated by units with high thermal conductivities, and extrapolation of a linear gradient will lead to overestimation of the eroded section.

For the well analysed in this report, the estimates of eroded section are conditional on:

- Heating rates of 10°C/Ma and cooling rates of 1°C/Ma in each episode, and
- A paleo-surface temperature equal to the present value of 20°C,

as well as the other assumptions outlined above. The effects of higher paleo-surface temperatures can be simply allowed for by subtracting the depth increment corresponding to the increase in temperature, for the appropriate value of paleogeothermal gradient. For instance, if the paleogeothermal gradient was 45°C/km and the paleo-surface temperature was 10°C higher than the value assumed in this report, the estimated eroded section should be reduced by 222 metres. Different heating rates can be allowed for in similar fashion, with an order of magnitude change in heating rate equivalent to a 10°C change in paleotemperature (paleotemperatures increase for higher heating rates, and decrease for lower heating rates). For typical values, the assumed value of heating rate will not affect the shape or slope of the paleotemperature profile significantly.

2. Thermal history reconstruction in the Burley-2 well

2.1 Background

The samples processed for AFTA in **Burley-2** are listed in Table A.1 (Appendix A) and open file VR results are listed in Table D.2 (Appendix D). The stratigraphy of the section drilled is summarised in Table A.3 and shown in Figure 2.1. The present-day geothermal gradient is calculated from corrected BHT data at 61°C/km for a surface temperature of 20°C (Appendix A). Note however, that the AFTA results indicate that the present-day geothermal gradient has increased to this level only in the recent geological past as discussed in Section 2.2.

2.2 Thermal history interpretation of AFTA and ZFTA data and fluid inclusion homogenisation temperatures

Evidence for elevated paleotemperatures from AFTA

Fission track parameters for each sample are summarised in Table 2.1 and plotted against depth and present temperature in Figure 2.1. Also presented in Table 2.1 are values of fission track age and mean track length predicted on the basis of the Default Thermal History for each sample (See Section 1.6 and Appendix C). These default values take into account the range of chlorine contents measured in each sample (Figure A.2a, Appendix A). The Default Thermal History, as defined in section 1.6, is a thermal history of each sample based on the burial history as derived from the preserved stratigraphy in **Burley-2** (Figure 2.1) using constant values of paleogeothermal gradient and paleo-surface temperature adopted from present-day values.

Evidence for elevated paleotemperatures in each AFTA sample from **Burley-2** is summarised in Table 2.2.

Constraints on the duration of present-day temperatures from AFTA

Kinetic modelling of the AFTA results in two of the deeper samples, GC668-171 and 172, indicate that the present-day temperatures based on a geothermal gradient of 61°C/km (for a 20°C surface temperature) determined from corrected BHT measurements have increased to present levels only very recently. AFTA shows that sample GC668-171 cannot have resided at the present temperature of 97°C for more than ~7 Ma, with a maximum possible temperature of ~88°C for any heating longer

duration. Note that temperatures may have been lower than 88°C, but it is not possible to estimate this independently. Similarly, the present temperature of 126°C in sample GC668-172 is too high, with a "steady-state" temperature no higher than 120°C during the Tertiary allowed by the AFTA results. Heating from 120°C to 126°C at 1 Ma is allowed also, while heating from 110°C to 126°C is considered most likely. AFTA results from the remaining AFTA samples would allow lower present temperatures, but do not require them.

Using these maximum possible "steady-state" present temperature estimates from AFTA gives a *maximum* possible "steady-state" present-day geothermal gradient of ~56.3°C/km as shown in Figure 2.4. No minimum estimate of the "steady-state" present-day geothermal gradient is possible from AFTA in the case of recent heating.

Fluid inclusion homogenisation temperatures

Fluid inclusion homogenisation temperatures (Russell and Bone, 1989) from diagenetic quartz are also available from Burley-2 and these are plotted in Figure 2.4. These results define a geothermal gradient of ~50°C/km, consistent with the AFTA-revised *maximum* "steady-state" present-day gradient of ~56.3°C/km. Thus, it is possible that the fluid inclusion temperatures may reflect the precipitation of quartz in the "normal" thermal regime prior to the recent increase in temperatures revealed by the AFTA results. Revised present-day temperature estimates for each sample derived from a revised present-day gradient of 50°C/km are listed in Table i and plotted in Figure 2.4.

Timing and magnitude of paleotemperatures from AFTA

Interpretations of the magnitude and timing of paleotemperatures which are required (or allowed) by AFTA in each AFTA sample are discussed in Table 2.3. These estimates have been obtained by modelling the fission track age and length parameters for each sample through likely thermal history scenarios to determine the range of conditions giving predictions consistent with the measured data.

In summary, AFTA results in samples from the shallower section in **Burley-2** constrain the measured maximum paleotemperatures to occurring at some time prior to 50 Ma and from the stratigraphic ages of the affected AFTA samples (GC668-168, -169, -170,) we can infer an upper limit of post-Winton Formation Late Albian age of sample GC668-168 , ~97 Ma) for the time of cooling. AFTA results from deeper samples (GC668-172, -174) allow post-depositional paleotemperatures higher than present-temperatures, but do not require, them as discussed in Table 2.3. However, integration of the VR results (Section 2.3) at the level of these deeper AFTA samples

provides further information on the timing of maximum paleotemperatures indicated by the VR. For example, VR results at around the sample depth as AFTA sample GC668-172, are interpreted to be ~150 to 160°C, and such a temperature is allowed by the AFTA results only at ~90 Ma (Figure 2.4).

Further refinement of the timing is available from integration with the ZFTA results as discussed below and in the Thermal History Synthesis (Section 2.6).

AFTA thermal history results for **Burley-2** are summarised in Table i (Executive Summary).

2.3 Thermal history interpretation of VR data

Evidence for elevated paleotemperatures from VR data

Open file vitrinite reflectance data from **Burley-2,** ranging in value from ~0.29 % to 7.0 %, are listed in Table D.2 and plotted against depth in Figure 2.2. Also shown in Figure 2.2 is the VR profile (Profile 1) predicted from the Default Thermal History, i.e. the thermal history of the well if the section has never been hotter than present temperatures based on a *measured* present-day geothermal gradient of 61°C/km. Also shown is a second predicted profile (Profile 2) based on the *AFTA-revised* (steady-state) present-day geothermal gradient of 56.3°C/km (see above). The burial history derived from the preserved stratigraphy used in calculating these profiles is shown in Figure 2.3.

Measured VR data in Burley-2 plot close to, or marginally below, both of the predicted Default History profiles in the section down to ~1750 m depth but plot above the predicted profiles in section deeper than ~1750 m (Figure 2.2).

At face value, this suggests that the shallower section (<1750 m) is likely to be close to maximum paleotemperatures at the present-day, with many of the VR results slightly underestimating the true maximum paleotemperatures. On the other hand, the section deeper than ~1750 m must have cooled from maximum paleotemperatures higher than present temperatures at some time after deposition.

Magnitude of maximum paleotemperatures from VR data

Maximum paleotemperatures have been determined in each VR sample using the heating and cooling rate interpretation framework outlined in Sections 1.6 to 1.8, and the kinetic description of Burnham and Sweeney (1989). Estimates of maximum

paleotemperature range from 42°C to >350°C as summarised in Table i and plotted against depth in Figure 2.4.

2.4 Thermal history interpretation of ZFTA data

Evidence for elevated paleotemperatures from ZFTA in several Cooper-Eromanga Basin wells

Samples from the deeper levels of three Cooper-Eromanga Basin wells (**Burley-2, McLeod-1 and Dullingari-1** - the ZFTA data come from Burley-1 rather than Burley-2, due to limited sample availability) have been analysed using ZFTA in a previous research study, and the results are summarised here.

Figure 2.5 shows central zircon fission track ages in samples from each well plotted against depth, together with VR values in these wells. The variation of stratigraphic age with depth in each well is also shown.

It is clear that the deepest ZFTA sample analysed from Burley-1 (8642-25; 3109 m 199°C) and both samples from Mcleod-1 (8642-26 and 27; 3584 m and 3746 m, 221 and 230°C, respectively) show significant age reduction compared to the depositional age of these samples. Sample 8642-25 from Burley-1 comes from a VR level around 4% and shows a moderate but significant degree of age reduction. Sample 8624-26 from Mcleod-1 shows a similar degree of age reduction at a VR level of just over 5%. In sample 8642-27 from Mcleod-1, appreciable age reduction below the stratigraphic age has occurred. This sample comes from granitic basement in this well, so no VR data are available at the same depth, but extrapolating VR data from shallower depths suggests a value between 6 and 7% at this depth. The radial plots of single grain age data in these samples (Figure 2.5) shows that individual grains within each sample have undergone variable degrees of age reduction (assuming a uniform original source), suggesting some form of compositional control on annealing rates. At the depth of sample 8624-53, from Dullingari-1 (2948 m, 171°C), the VR level is rather lower, at ~2.5%, and the ZFTA data from this sample show no detectable age reduction (Figure 2.5).

Timing and magnitude of paleotemperatures from ZFTA

Results from studies in other regions of the world have shown that fission tracks in zircons show no measurable signs of annealing at VR levels less than ~5% $R_O max$, equating to paleotemperatures of approximately 300°C. This is in good agreement with the basic observations discussed above, with the ZFTA results thus suggesting

the deeper sections in Burley-1 and 2 and McLeod-1 have been exposed to maximum paleotemperatures >~300°C at some time after deposition.

The timing of the paleotemperatures which produced the ZFTA age reduction is uncertain. Present-day thermal gradients are quite high in these wells, at between 50 and 60°C/km (see Appendix A), and the present-day temperatures of the analysed ZFTA samples are between 171 and 220°C (Table A.2). However, AFTA and VR data from these and other wells in the suggest these high gradients are a relatively recent feature (having increased in the last 2 Ma or so), so it is unlikely that present-day temperatures are responsible for the observed ZFTA results.

The rapid decrease in zircon fission track age with depth towards TD in Mcleod-1 (Figure 2.5) suggests that the time of total annealing would be younger than the measured central age of 159.8±16.2 Ma in sample 8642-27. The youngest individual grain age in sample 8642-27 is 71.3 ±9.6 Ma (Appendix B; 1 sigma error) which at face value suggests that cooling from maximum paleotemperatures began between ~50 and 90 Ma, *or younger* (i.e. allowing ± 2 sigma errors).

A similar interpretation is made for sample 8642-25 from Burley-2, where the youngest individual zircon grain age is 140 ± 11 Ma (Appendix B), suggests that cooling began between ~120 and 160 Ma, *or younger* (i.e. allowing ± 2 sigma errors).

Constraints on the time of maximum heating from ZFTA, AFTA, VR and the preserved stratigraphy are synthesised in Section 2.5.

2.5 Thermal history synthesis

Recent heating

The Burley-2 AFTA results show that present temperatures, based on a corrected present-day geothermal gradient of 61°C/km cannot have been in existence for more than ~7 Ma. Results from other wells in the basin show similar recent increases in temperature, perhaps as recent at 1 or 2 million years before present. The AFTA results allow an estimate of 56.3°C/km from the maximum possible geothermal gradient operating immediately prior to 7 Ma in Burley-2. This is consistent with a paleogeothermal gradient of ~50°C/km defined by a small number of fluid inclusion homogenisation temperatures (Figure 2.4), suggesting that the diagenetic quartz

overgrowths hosting the fluid inclusions were precipitated prior to the recent increase in geothermal gradient.

Timing of maximum paleotemperatures

Based on stratigraphic grounds, the VR results indicate that maximum paleotemperatures occurred at some time since the Late Jurassic as this is the youngest section in Burley-2 where the VR results unequivocally demonstrate paleotemperatures higher than present temperatures after deposition (see Figure 2.4).

The AFTA results in the shallower section constrain the measured maximum paleotemperatures to have operated at some time prior to 50 Ma and the stratigraphic ages of the affected AFTA samples (GC668-168) provide a refined upper limit of post-Wallumbilla Formation (L. Albian , ~97 Ma;) for the time of cooling.

Finally, conservative interpretation of zircon fission track results (ZFTA) from the deepest parts of Burley-2 and Mcleod-1 where VR values are ≥ 5%, suggest heating at temperatures of ≥300°C occurred since ~150 Ma. Less conservative interpretation of the limited single grain ZFTA results to suggest a time between ~90 and 50 Ma (representing ±2 sigma errors on the youngest single grain age).

All of this information together consistently indicates that cooling from the elevated heat flow regime began at some time between 97 and 50 Ma, and probably between 90 and 50 Ma, with ~90 Ma favoured on broad regional geological/tectonic grounds.

Thermal History parameters for Burley-2 derived from AFTA, ZFTA and VR results and summarised in Table i.

2.6 Paleogeothermal gradients and the mechanism of heating and cooling

Introduction

Paleogeothermal gradients for the Cretaceous - Tertiary (~97 to 50 Ma) period of maximum paleotemperatures are determined from the paleotemperature results using the quantitative approach explained in Section 1.6 and Appendix C.

Cretaceous - Tertiary (~97 to 50 Ma) heating

Considering the AFTA maximum paleotemperature estimates alone as listed in Table i and plotted against depth in Figure 2.4, the results define a best-fit linear

paleogeothermal gradient of 82.5°C/km (76 to 91°C/km at ±95% confidence limits), as illustrated in Figure 2.6)

The AFTA and the VR paleotemperature results throughout the well also define a reasonably linear paleogeothermal gradient, with a best-fit value of 89°C/km (84.5 to 94°C/km at ±95% confidence limits (Figure 2.7).

Thus, even though there is not a great deal of overlap between the AFTA results in the upper 2 km of the section and the deeper VR values (see Figure 2.4), both data sets define similar high paleogeothermal gradients at the time of maximum paleotemperatures at some time between 97 and 50 Ma (Section 2.5).

A slightly better fit to the paleotemperature results are obtained by fitting a dog-leg paleogeothermal gradient with the change in gradient at about the level of the Murta Fm, the deeper VR results defining an even higher paleogeothermal gradient. However, given likely VR suppression in some parts of the well (e.g. at about the level of AFTA sample GC668-172 comparison of AFTA and VR shows that the VR results are too low - see Figure 2.4), apparent breaks in the VR paleotemperature trend are probably largely an illusion. Therefore, gradients have not been formally determined for a dog-leg interpretation.

In summary, regardless of the emphasis placed on different paleotemperatures data sets, the paleotemperature results consistently indicate that the paleogeothermal gradient at the time of maximum paleotemperatures (at some time between 97 and 50 Ma) was significantly higher than the present-day geothermal gradient (and even higher than the geothermal gradient that operated immediately prior to the Recent as discussed above). Paleogeothermal gradient estimates are listed in Table v.

These results indicate that cooling from Cretaceous-Tertiary maximum paleotemperatures was dominated by decline from a highly elevated heat flow episode.

The simplest reconstructed thermal history for **Burley-2** consistent with the data is illustrated in Figure 2.8, and is based on a constant surface temperature of 20°C and a paleogeothermal gradient of 89°C/km up until cooling began at 90 Ma (within the possible range from 97 to 50 Ma), at which point it declined to 50°C/km (from AFTA and fluid inclusion results), rising again to 61°C/km at 2 Ma (within the last 7 Ma allowed by AFTA).

2.7 Implications for source rock maturation at Burley-2

The maturity-depth profile in **Burley-2** derived from the reconstructed thermal history shown in Figure 2.8, together with the measured VR data and AFTA-equivalent VR levels, is provided in Figure 2.9. Predicted maturity levels (using the maturation algorithm of Burnham and Sweeney, 1989) throughout the section agree very well with the measured results. Slight mismatch in the Jurassic section around 1750 m is attributed to slight geochemical suppression (see Section 2.3). Note also that measured VR values > ~ 5% in the deeper part of the well cannot be predicted by the maturation algorithm of Burnham and Sweeney, (1989).

Figure 2.10 shows the variation of maturity with time for the **Burley-2** well (using the maturation algorithm of Burnham and Sweeney, 1989) derived from the reconstructed thermal history shown in Figure 2.8. This reconstruction illustrates that maximum maturity in most (Alluru Fm and deeper) of the drilled section was reached at 90 Ma (97 to 50 Ma allowed), immediately prior to decline in paleogeothermal gradient that commenced at this time. The reconstructed history predicts a minor increase in maturity in the upper part of the section (Macunda Fm and shallower) over the last 90 Ma, but only at maturities less than that required for significant oil generation. No significant maturation can be attributed to the recent increase in geothermal gradient over the last ~2 Ma.

This plot shows that maturities generally suitable for generation of oil from typical source rocks (~0.5 to 1.3% Romax) were reached by the section between the Alluru and Namur Formations, at around 100 to 90 Ma. Sections deeper than the Namur reached gas maturities, or greater, at this time.

2.8 Estimating section removed by erosion: Burial history reconstruction

Introduction

The results presented in the previous sections provide good constraints on the thermal and maturation histories for the **Burley-2 well** as illustrated in Figures 2.8 to 2.10, but reconstruction of the burial history is more speculative as it depends not only on the various assumptions described in Section 1.7, but also on the mechanism of heating. The principal difficulty lies with definition of the paleogeothermal gradient *through the removed section* which must be assumed, as with all methods used in basin analysis and modelling. Adopting the simplest approach, the paleogeothermal

gradient through the removed section is assumed to be equivalent to those measured in the preserved section as listed in Table vi. This assumption may be invalid if the elevated paleotemperatures are caused by processes involving lateral or local introduction of heat, such as through a confined aquifer or igneous intrusions (for example), but we note there is no indications of such effects in Burley-2. Also, in order to estimate the total amount of additional section necessary to achieve the observed paleotemperatures it is necessary to identify the unconformity representing the time interval within which the burial and erosional episodes occurred, so that the analysis outlined in Section 1.7 can be carried out in terms of depth below that unconformity.

Removed section estimates determined by these methods for the Cretaceous - Tertiary heating episode identified in the **Burley-2 well** are summarised in Table vi (Executive Summary).

97 to 50 Ma - Cretaceous - Tertiary episode

The AFTA and VR results provide a good constraint on the time of cooling from maximum paleotemperatures beginning between **97 and 50 Ma** in the **Burely-2 well.** This timing overlaps the time range represented by the unconformity at ~108.5 m bKB between the Cretaceous Winton Formation and the Tertiary Eyre Formation (~90 to 60 Ma). Therefore the analysis of removed section in this cooling episode has been carried out in terms of depth with respect to this unconformity.

Note that in Section 2.6 estimates of paleogeothermal gradient were made on the AFTA results alone and on the integrated AFTA and VR results. In both approaches paleogeothermal gradient estimates were similar. Therefore, in determining the magnitude of removed section, only the integrated results are used.

Following the procedures outlined in Section 1.7, extrapolating the allowed range of paleogeothermal gradients determined from the AFTA and VR data shown in Figure 2.7 to an assumed paleo-surface temperature of 0°C results in a range of allowed values for the amount of removed section from 0 to 100 m, with a maximum likelihood value of 0 m (Figure 2.11). Note that a paleo-surface temperature of 0°C was used because higher values results in negative values of uplift and erosion. Figure 2.12 illustrates the correlation between values of the Cretaceous - Tertiary paleo-gradient and section removed allowed by the AFTA and VR data, within ±95% confidence limits. That is, any set of paired values inside the contoured region are compatible with the data at 95% confidence limits. In effect, the results indicate that erosion on the top Winton unconformity is insignificant, and further emphasises that

the high paleotemperatures identified in Burley-2 are best explained by elevated heat flow without any significant additional burial.

Burial history reconstruction

The reconstructed thermal history for Burley-2 strongly suggests that the major controls on the maturation history has been variation in heat flow without significant contribution from additional burial and recognised unconformities. Thus, the reconstructed burial history is best represented by the preserved stratigraphy in the well. This is illustrated in Figure 2.13.

Table 2.1: Summary of AFTA data in samples from the Burley-2 well, Cooper-Eromanga Basin, South Australia (Geotrack Report #668)

Sample number	Average depth*1	Present temperature*2	Stratigraphic Age	Measured Mean track length	Default mean track length *3	Measured apatite fission track age *4	Default fission track age*3
GC	(m)	(°C)	(Ma)	(µm)	(µm)	(Ma)	(Ma)
668-168*5	553	53	97-90	13.27±0.19	13.6	*115.5±12.1*	87
668-169*5	754	66	97-90	13.15±0.23	13.1	*117.5±12.4*	85
668-170*5	1056	84	103-101	12.04±0.38	11.9	*108.5±12.4*	82
668-171*5	1266	97	117.5-106	12.49±0.78	11.3	106.9±10.5	62
668-172*5	1748	126	141.5-135	11.40±0.73	9.1	*42.0±8.4*	3.3
668-174*5	1977	140	148-147	11.29±1.28	0	*2.1±1.3*	0

*1 All depths quoted are true vertical depth (TVD) with respect to KB.

*2 See Appendix A for a discussion of present temperature estimation.

*3 AFTA values predicted from the "Default Thermal History" (Section 1.6); i.e., assuming that each sample is now at its maximum temperature since deposition. The values refer only to tracks formed after deposition. Samples may also contain tracks inherited from sediment provenance areas. Calculation of the Default values refer to actual measured compositions of apatites analysed within a particular sample, which is discussed in Appendix A.

*4 Central fission track age quoted (in italics) where P(chi sq) < 5%

*5 Sample data reprocessed specifically for this report and discussed in deatil in Tables 2.2 and 2.3.

Table 2.2: Summary of thermal history interpretation of AFTA data in samples from the Burley-2 well, Eromanga Basin, South Australia (Geotrack Report #668)

Sample number	Do AFTA data require any revision of present temperature?	Evidence of higher temperatures in the past from length data?	Evidence of higher temperatures in the past from fission track age data?	Conclusion
668-168 553 m	No But would allow a lower present temperature as required by deeper samples	No [Mean track length is similar to that predicted from Default History.]	No [Central fission track age and all single grain ages are significantly older than, or similar to, those predicted on the basis of the Default Thermal History]	No direct evidence to suggest that the sample was subjected to paleotemperatures higher than present temperatures at any time after deposition. Note, however, that the AFTA results from deeper samples indicates a very recent increase in present temperatures which may mask evidence of higher paleotemperatures.
668-169 754 m	No But would allow a lower present temperature as required by deeper samples	No [Mean track length is similar to that predicted from Default History.]	No [Central fission track age and all single grain ages are significantly older than, or similar to, those predicted on the basis of the Default Thermal History]	No direct evidence to suggest that the sample was subjected to paleotemperatures higher than present temperatures at any time after deposition. Note, however, that the AFTA results from deeper samples indicates a very recent increase in present temperatures which may mask evidence of higher paleotemperatures.
668-170 1056 m	No But would allow a lower present temperature as required by deeper samples	No [Mean track length is similar to that predicted from Default History.]	No [Pooled fission track age is significantly older than that predicted on the basis of the Default Thermal History]	No direct evidence to suggest that the sample was subjected to paleotemperatures higher than present temperatures at any time after deposition. Note, however, that the AFTA results from deeper samples indicates a very recent increase in present temperatures which may mask evidence of higher paleotemperatures.

Note: Interpretation of AFTA data is based on comparison of measured AFTA parameters with values predicted from "Default Thermal History" (Section 1.6); i.e., assuming that each sample is now at its maximum temperature since deposition. The predicted values for each sample are summarised in Table 2.1, and refer only to tracks formed after deposition. Samples may also contain tracks inherited from sediment provenance areas, which must be allowed for in interpreting the data. Calculations refer to apatites with the compositional range appropriate to each sample, as explained in Appendix A.

Table 2.2 (cont.): Burley-2

Sample number	Do AFTA data require any revision of present temperature?	Evidence of higher temperatures in the past from length data?	Evidence of higher temperatures in the past from fission track age data?	Conclusion
668-171 1266 m	Yes Modelling of the AFTA length parameters suggest either the present temperature of 97°C has been acting for only a short time, or is incorrect.	No [Mean track length is similar to that predicted from Default History.]	No [Central fission track age and all single grain ages are significantly older than, or similar to, those predicted on the basis of the Default Thermal History]	Modelling of the AFTA parameters for the range of apatite chlorine contents in the sample indicates that this sample cannot have resided at the present temperature for more than a few thousand years, suggesting either that the present temperature is transient, or incorrect.
668-172 1748 m	Yes Modelling of the AFTA age and length parameters suggest either the present temperature of 126°C has been acting for only a short time, or is incorrect.	No [Mean track length is similar to that predicted from Default History.]	No [Central fission track age and all single grain ages are significantly older than or similar to that predicted on the basis of the Default Thermal History]	Modelling of the AFTA parameters for the range of apatite chlorine contents in the sample indicates that this sample cannot have resided at the present temperature for more than a few thousand years, suggesting either that the present temperature is transient, or incorrect.
668-174 1748 m	No, equivocal Fission tracks are effectively totally annealed at the present temperature >~140°C.	No [Mean track length is based on only two measurements and considerably longer than predicted from Default History].	No [Central fission track age and all single grain ages are totally, or near totally annealed, similar to that predicted on the basis of the Default Thermal History]	Modelling of the AFTA parameters for the range of apatite chlorine contents in the sample indicates that this sample cannot have resided at the present temperature for more than a few thousand years, suggesting either that the present temperature is transient, or incorrect.

Note: Interpretation of AFTA data is based on comparison of measured AFTA parameters with values predicted from "Default Thermal History" (Section 1.6); i.e., assuming that each sample is now at its maximum temperature since deposition. The predicted values for each sample are summarised in Table 2.1, and refer only to tracks formed after deposition. Samples may also contain tracks inherited from sediment provenance areas, which must be allowed for in interpreting the data. Calculations refer to apatites with the compositional range appropriate to each sample, as explained in Appendix A.

Table 2.3: Estimates of timing and magnitude of elevated paleotemperatures from AFTA data in samples from the Burley-2 well, Cooper-Eromanga Basin, South Australia (Geotrack Report #668)

Sample number	Stratigraphic Age	Present temperature	Early episode		Late episode		Comments
			Maximum paleo-temperature	Onset of cooling	Peak paleo-temperature	Duration of heating	
GC	(Ma)	(°C)	(°C)	(Ma)	(°C)	(Ma)	
668-168 553 m	97-90 Early Cretaceous	53	*(70 to 110*	*prior to 50)*	No constraint		The AFTA data show no definite requirement for post-depositional paleotemperatures any higher than the present temperature of 54°C, but would allow higher paleotemperatures within the specified limits. The data show no evidence for the present temperature increasing to the present level recently as required by AFTA in samples GC668-171 & 172, but would allow this. The AFTA results predict a *maximum* possible VR level of ~0.63% based on the allowed paleotemperature of 110°C prior to 50 Ma. This is consistent with a measured VR level at around this depth of 0.36%.
668-169 754 m	97-90 Early Cretaceous	66	*(<120*	*post-deposition)*	No constraint		The AFTA data show no definite requirement for post-depositional paleotemperatures any higher than the present temperature of 66°C, but would allow higher paleotemperatures within the specified limits. The data show no evidence for the present temperature increasing to the present level recently as required by AFTA in samples GC668-171 & 172, but would allow this. The AFTA results predict a *maximum* possible VR level of ~0.67% based on a paleotemperature of 110°C allowed after deposition. This is consistent with a measured VR level at around this depth of 0.39%.

Note: **Brackets** surrounding italicised time/temperature constraints indicate that the AFTA results allow, but *do not* require a discrete event at this time.

*1 Based on measured present-day geothermal gradient of 61°C/km and a surface temperature of 20°C. As discussed in this table AFTA indicates that this is a recent developed transient thermal regime, and that lower temperatures must have persisted until this recent increase.

Table 2.3 (cont.): Burley-2 (Geotrack Report #668)

Sample number GC	Stratigraphic Age (Ma)	Present*1 temperature (°C)	Early episode Maximum paleo-temperature (°C)	Early episode Onset of cooling (Ma)	Late episode Peak paleo-temperature (°C)	Late episode Duration of Heating (Ma)	Comments
668-170 1056 m	103-101 Early Cretaceous	84	*(<130 including (90-100*	*prior to 50) including prior to 60)*	No constraint		The AFTA data have no definite requirement for post-depositional paleotemperatures any higher than the present temperature of 84°C, but would allow higher paleotemperatures within the specified limits. The data show no evidence for the present temperature increasing to the present level recently as required by AFTA in samples GC668-171 & 172, but would allow this. The AFTA results predict a *maximum* possible VR level of less than 0.74% based on a paleotemperature of 130°C allowed prior to 50 Ma, consistent with measured VR levels at around this depth of 0.51 to 0.53%. Note that when combined with AFTA, these measured VR levels are constrained to being developed prior to 60 Ma (and after 103 Ma based on the stratigraphic age of the sample.
668-171 1266 m	117.5-106 Early Cretaceous	97	<110	prior to 7	<88°C	7	A key sample. Evidence mainly from the AFTA length data clearly indicate that this sample cannot have resided near the present temperature of 97°C for more than ~7 Ma, compared to at least 30 Ma inferred from the preserved stratigraphy. Further, AFTA allows a maximum possible temperature of ~88°C for any longer heating duration, implying that the temperature has increased to its present value only recently. Note that the pre-increase temperature may have been lower than 88°C, but this cannot be estimated from the AFTA data alone. Allowing for this transient recent temperature increase, the AFTA results further indicate that the maximum *sustained* post-depositional temperatures must have been less than ~110°C, and predict a VR level less than 0.65 %. This is consistent with a measured VR level at around this depth of 0.58%.

Note: **Brackets** surrounding italicised time/temperature constraints indicate that the AFTA results allow, but *do not* require a discrete event at this time.
*1 Based on measured present-day geothermal gradient of 61°C/km and a surface temperature of 20°C. As discussed in this table AFTA indicates that this is a recent developed transient thermal regime, and that lower temperatures must have persisted until this recent increase.

Table 2.3 (cont.): Burley-2 (Geotrack Report #668)

Sample number GC	Stratigraphic Age (Ma)	Present*1 temperature (°C)	Early episode Maximum paleo-temperature (°C)	Early episode Onset of cooling (Ma)	Late episode Peak paleo-temperature (°C)	Late episode Duration of Heating (Ma)	Comments
668-172 1748 m	141.5-135 Early Cretaceous	126	>120 including >145	prior to 15 including if at 90	<120 <115	2 5	A key sample. Evidence from the fission track age and length data clearly indicate that this sample cannot have resided at the present temperature of 126°C for more than ~2 Ma. It is not possible to estimate both the pre-increase temperature and time of this temperature increase from the AFTA data alone. For example, heating from <120°C to 126°C during that last 1 Ma is allowed, as is heating from <115°C to 126°C during that last 5 Ma. If the pre-increase temperature can be independently estimate then AFTA can be used to determine the heating duration at the higher measured present temperature. Allowing for a transient recent temperature increase, the AFTA results further indicate that the maximum *sustained* post-depositional temperatures must have been greater than ~120°C prior to 15 Ma, and greater than ~145°C for heating prior to 90 Ma. AFTA predicts a minimum VR level ~0.75% (for 120°C) at this depth. Measured VR results around this AFTA sample range from ~ 0.68 to 1.15 %, with only the highest values thought to reflect the true thermal history of the section.
668-174 1977 m	148-147 Late Jurassic	140	>100	post-deposition	No constraint		Modelling of the AFTA parameters for a present temperature of 140°C is consistent with the observed total of near total annealing for the range of chlorine contents up to ~0.4 wt% in the apatite grains analysed. However, the measured results would be compatible with any sustained present temperature greater than ~115°C, and thus would also be consistent with a recent increase in present-day temperatures require by AFTA in shallower samples GC668-171 and 172. The AFTA results predict minimum VR levels ~0.68% at this depth.

Note: **Brackets** surrounding italicised time/temperature constraints indicate that the AFTA results allow, but *do not* require a discrete event at this time.

*1 Based on measured present-day geothermal gradient of 61°C/km and a surface temperature of 20°C. As discussed in this table AFTA indicates that this is a recent developed transient thermal regime, and that lower temperatures must have persisted until this recent increase.

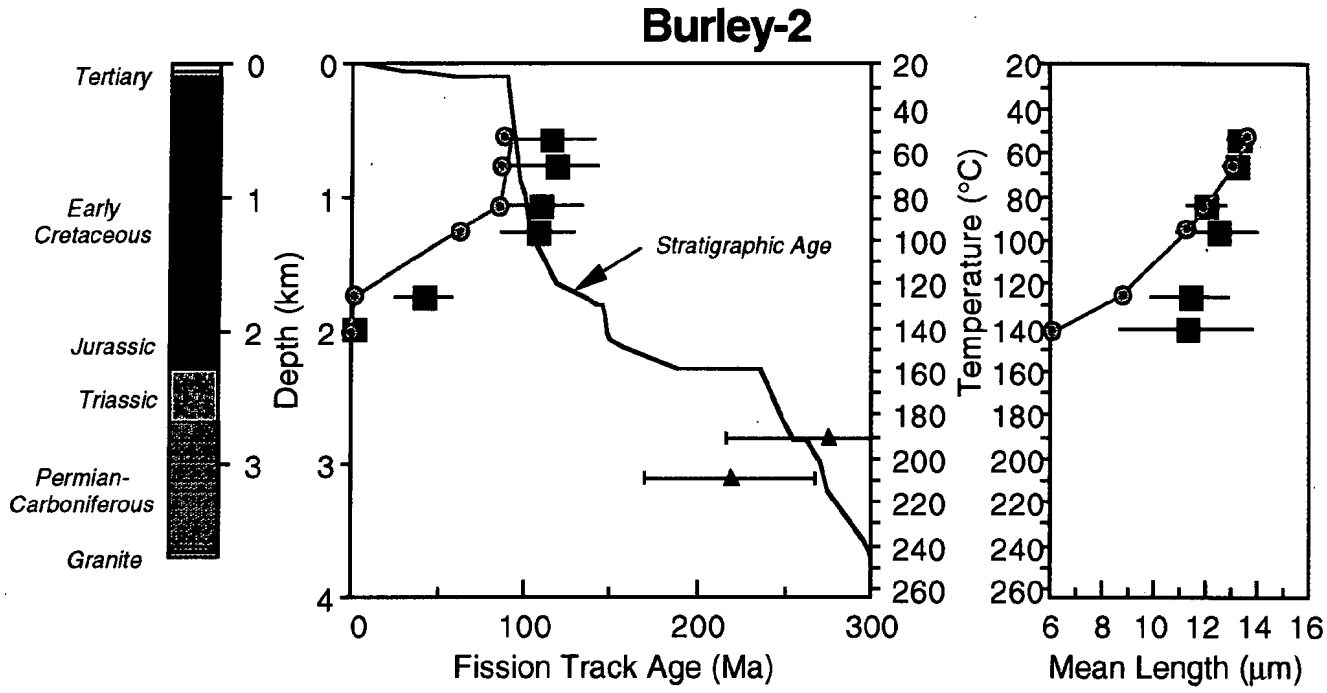

Figure 2.1: Measured AFTA (square) and ZFTA (triangle) parameters plotted against sample depth and present temperature for samples from the **Burley-2 well, Cooper-Eromanga Basin** (note ZFTA samples from Burley-1). Round symbols are AFTA parameters predicted from the Default History. Comparison of the Default History parameters with the measured data suggest that the section has increased to the present temperatures in the recent geological past. The variation of stratigraphic age with depth is also shown, as the solid line in the central panel.

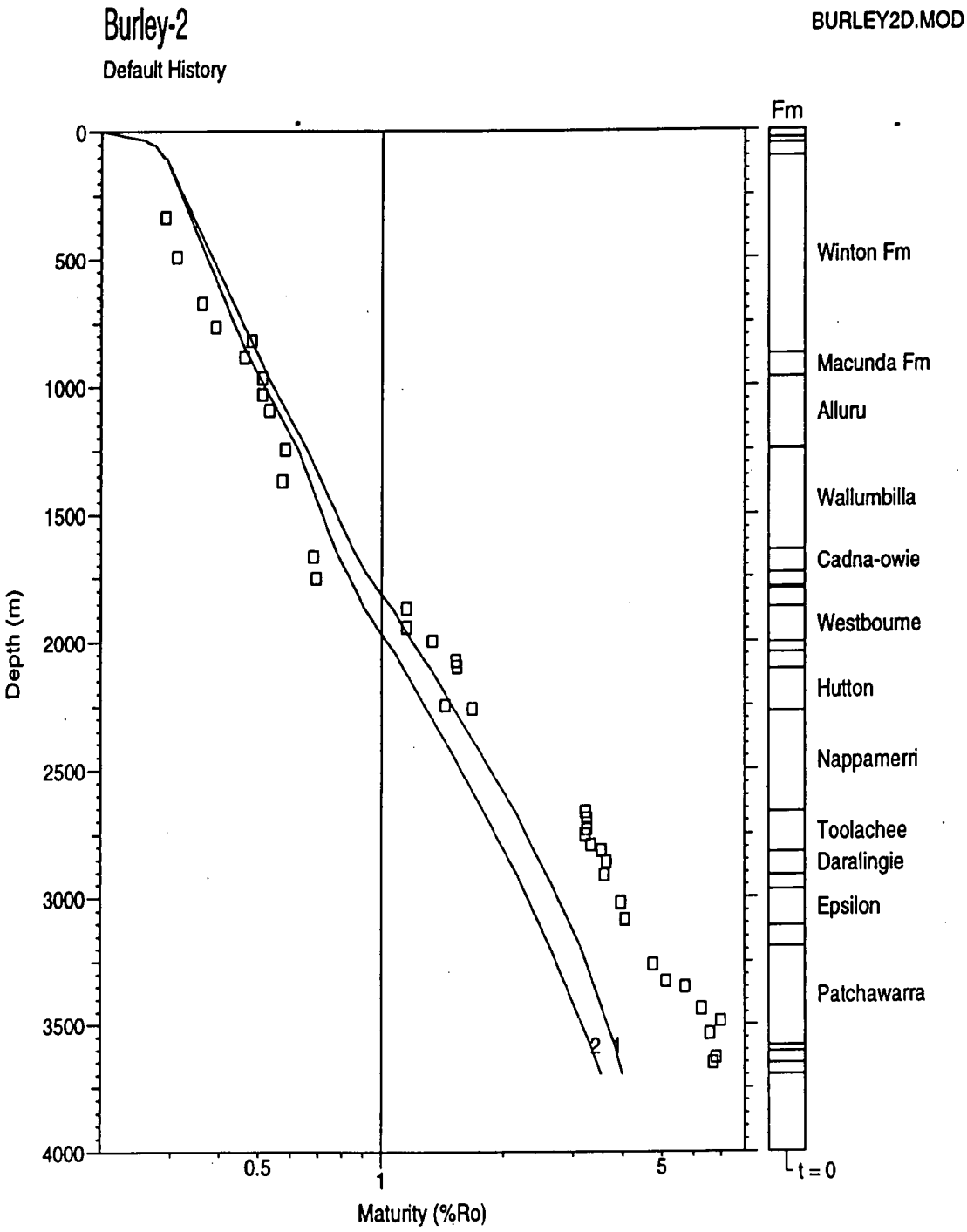

Figure 2.2: Measured vitrinite reflectance data in samples from the **Burley-2 well, Cooper-Eromanga Basin** plotted against depth (with respect to KB). A VR profile (Profile 1) predicted from the "Default History" (Section 1.6) is also shown, i.e., the profile expected if samples throughout the section are currently at their maximum temperature since deposition (based on a *measured* present-day geothermal gradient of 61°C/km, and a constant surface temperature of 20°C - Appendix A). Also shown is a second predicted profile (Profile 2) based on the *AFTA-revised* (steady-state) present-day geothermal gradient of 56.3°C/km (see text). Down to ~1750 m the measured VR results tend to fall below the predicted profile suggesting either that they are incorrect or that the estimated present temperatures are too high. Deeper than ~1750 m the VR results begin to progressively diverge above the predicted profile, suggesting that this part of the section was subjected to maximum paleotemperature higher than present temperatures since deposition. See text for details.

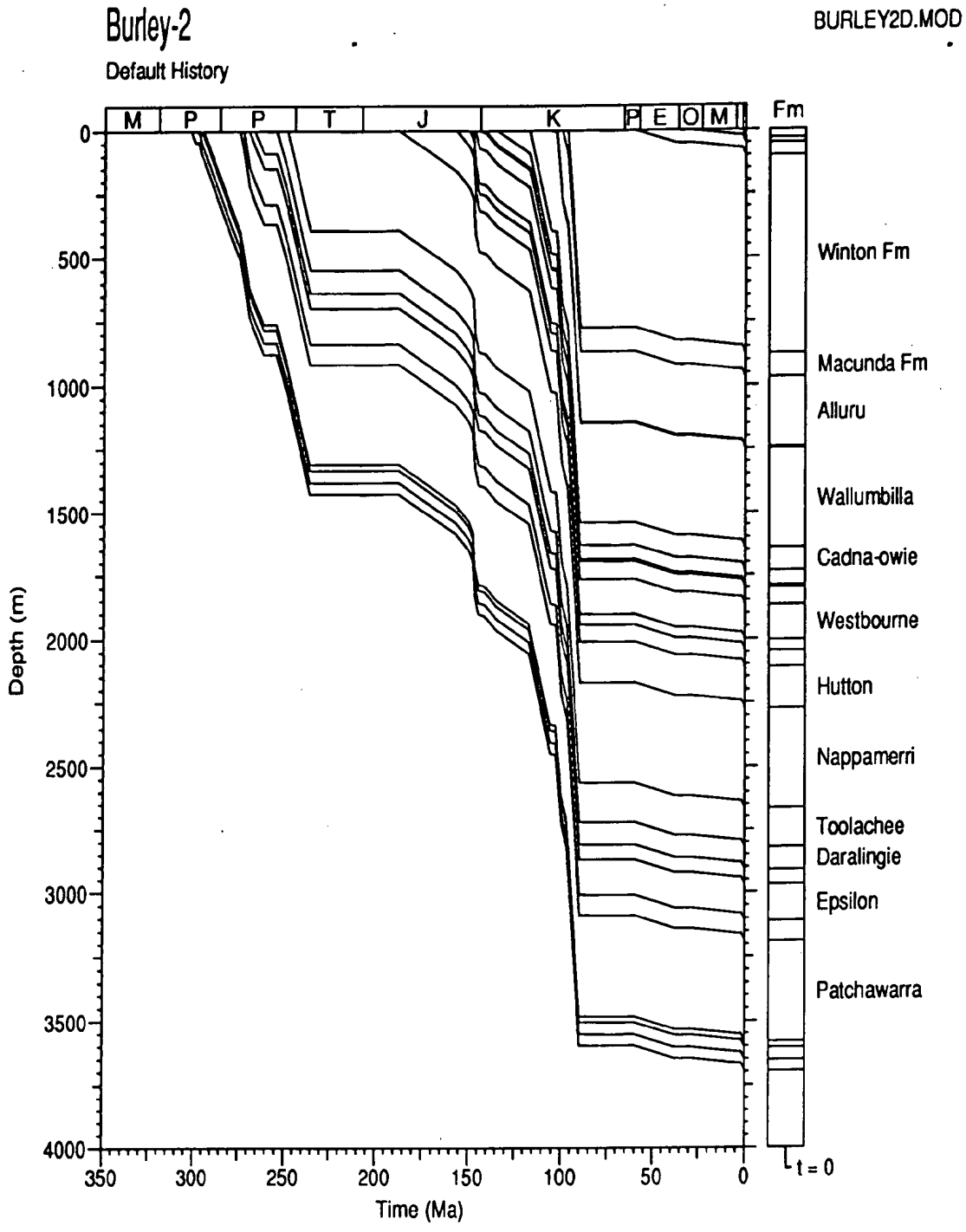

Figure 2.3: Default Burial History for the **Burley-2 well, Cooper-Eromanga Basin**, derived from the preserved section which, combined with the present-day thermal conditions, is used in predicting the VR profiles shown in Figure 2.2.

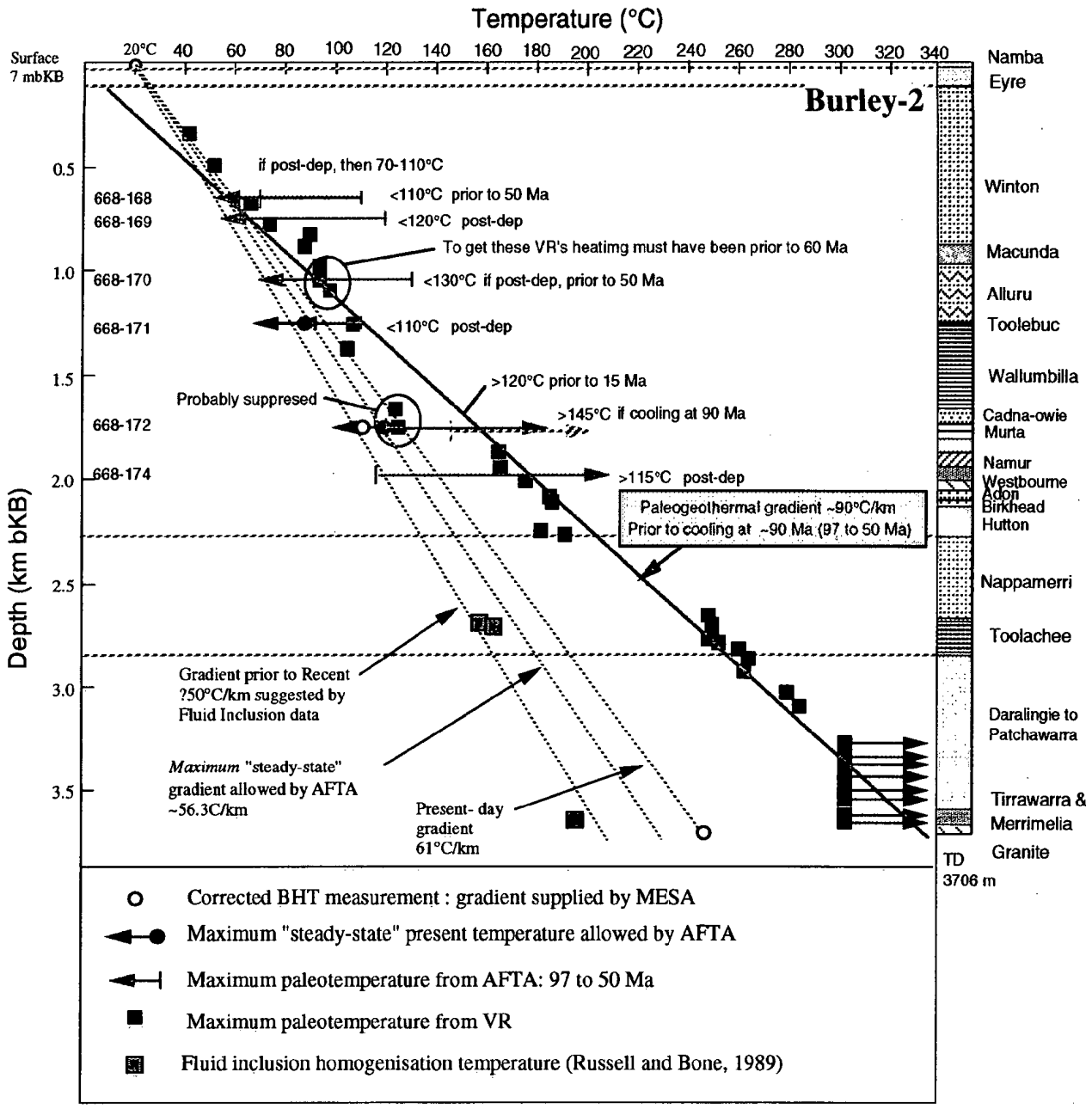

Figure 2 .4: Plot of paleotemperatures derived from AFTA and VR data in the **Burley-2 well, Eromanga Basin**, against sample depth and the estimated present temperature profile for this well (see Appendix A). - see text.

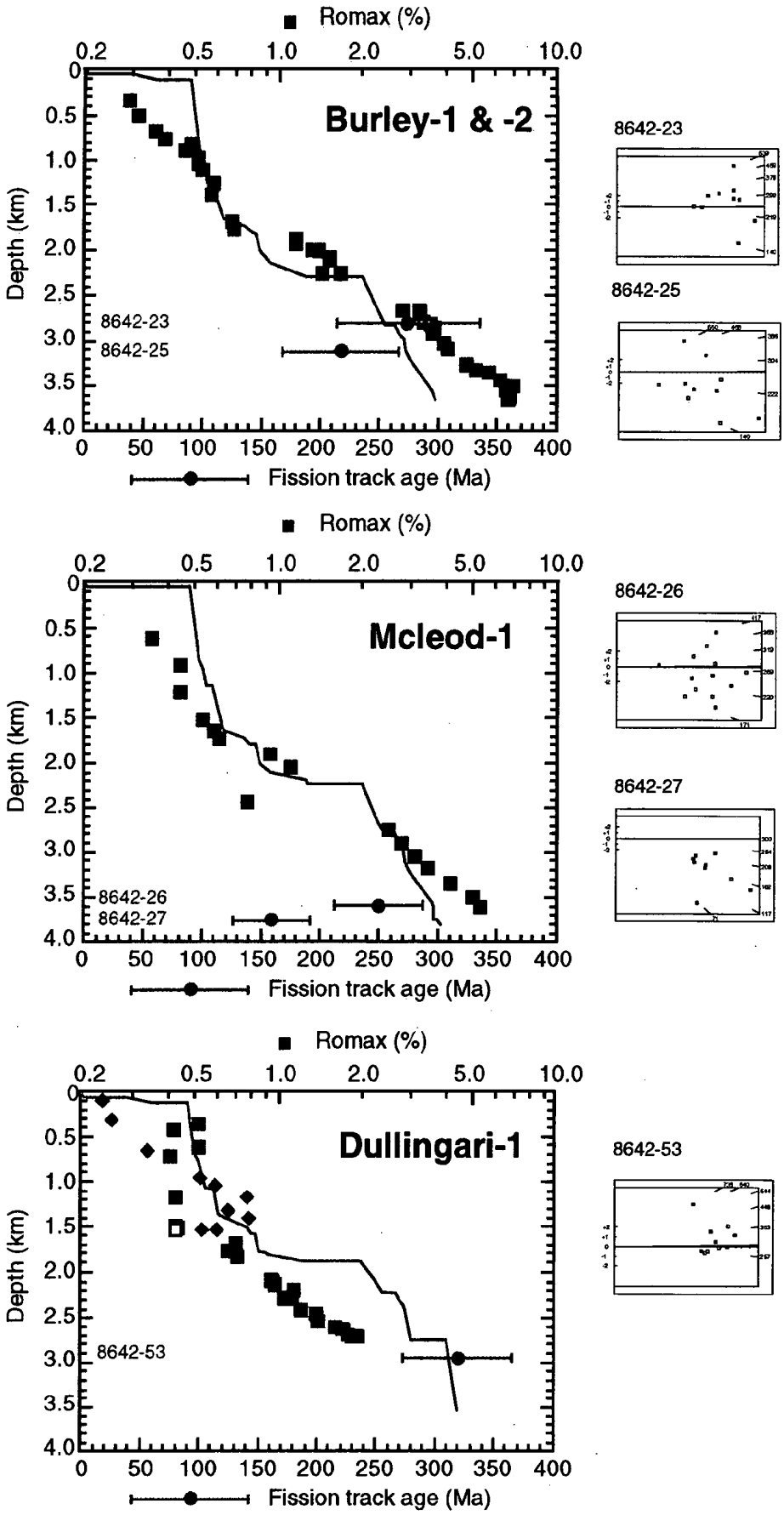

Figure 2.5: Variation of zircon fission track age and vitrinite reflectance with depth in three Cooper-Eromanga Basin wells. Fission track ages less than the appropriate stratigraphic age in samples from Burley-1 and -2 (8642-25) and Mcleod-1 (8642-26 & 27), corresponding to VR levels >~5%, indicate heating at maximum paleotemperatures significantly higher than present temperatures. See text

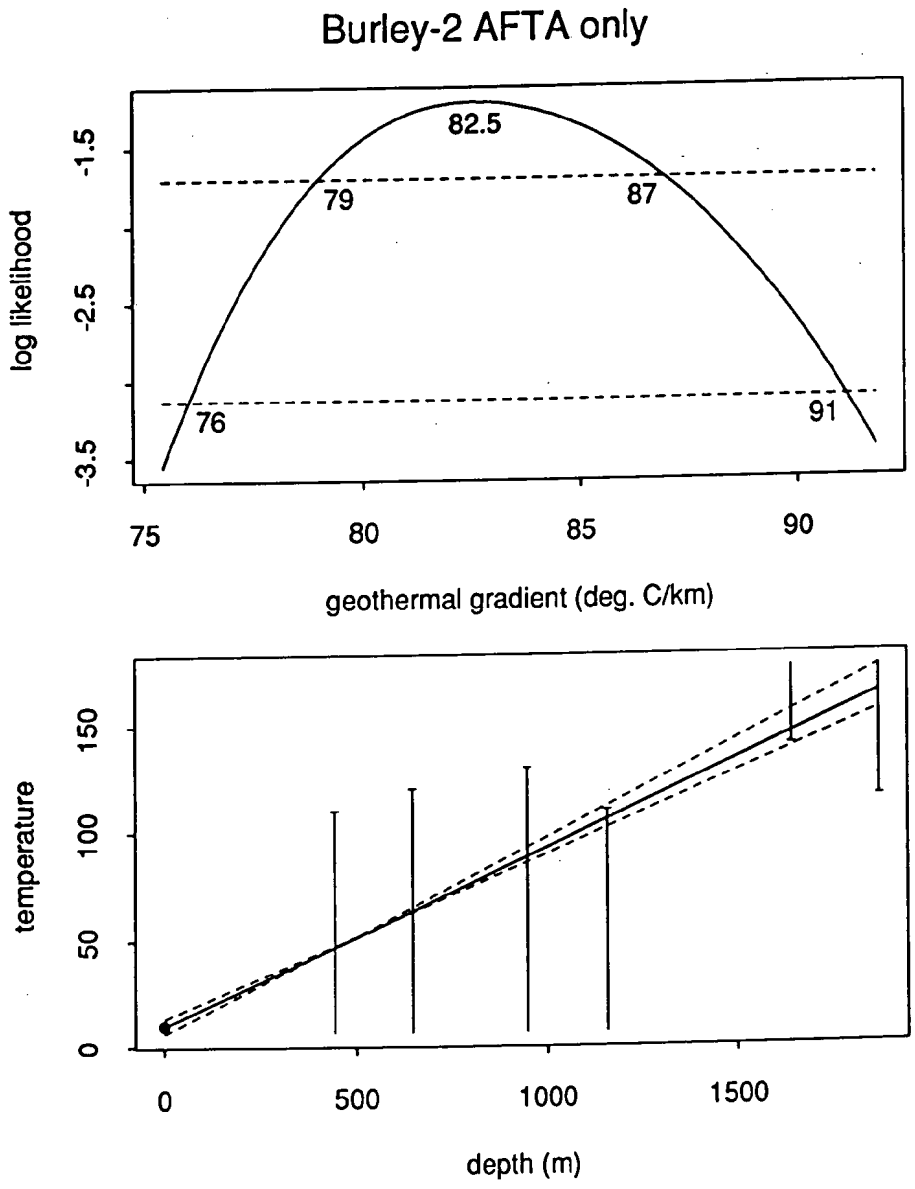

Figure 2.6: Upper: Maximum likelihood profile of linear paleogeothermal gradient fitted to the Cretaceous - Tertiary (~97 to 50 Ma) paleotemperature estimates from the AFTA results alone in the **Burley-2 well**. The profile shows good quadratic behaviour suggesting a well constrained value, with upper and lower 95% confidence limits of 91 and 76°C/km, respectively, and a best-fit value of 82.5°C/km. The methodology employed in deriving this profile is outlined in Appendix C.

Lower: Maximum paleotemperature estimates from AFTA in the **Burley-2 well**, with fitted profile (solid line) and lines (dashed) representing upper and lower 95% confidence limits.

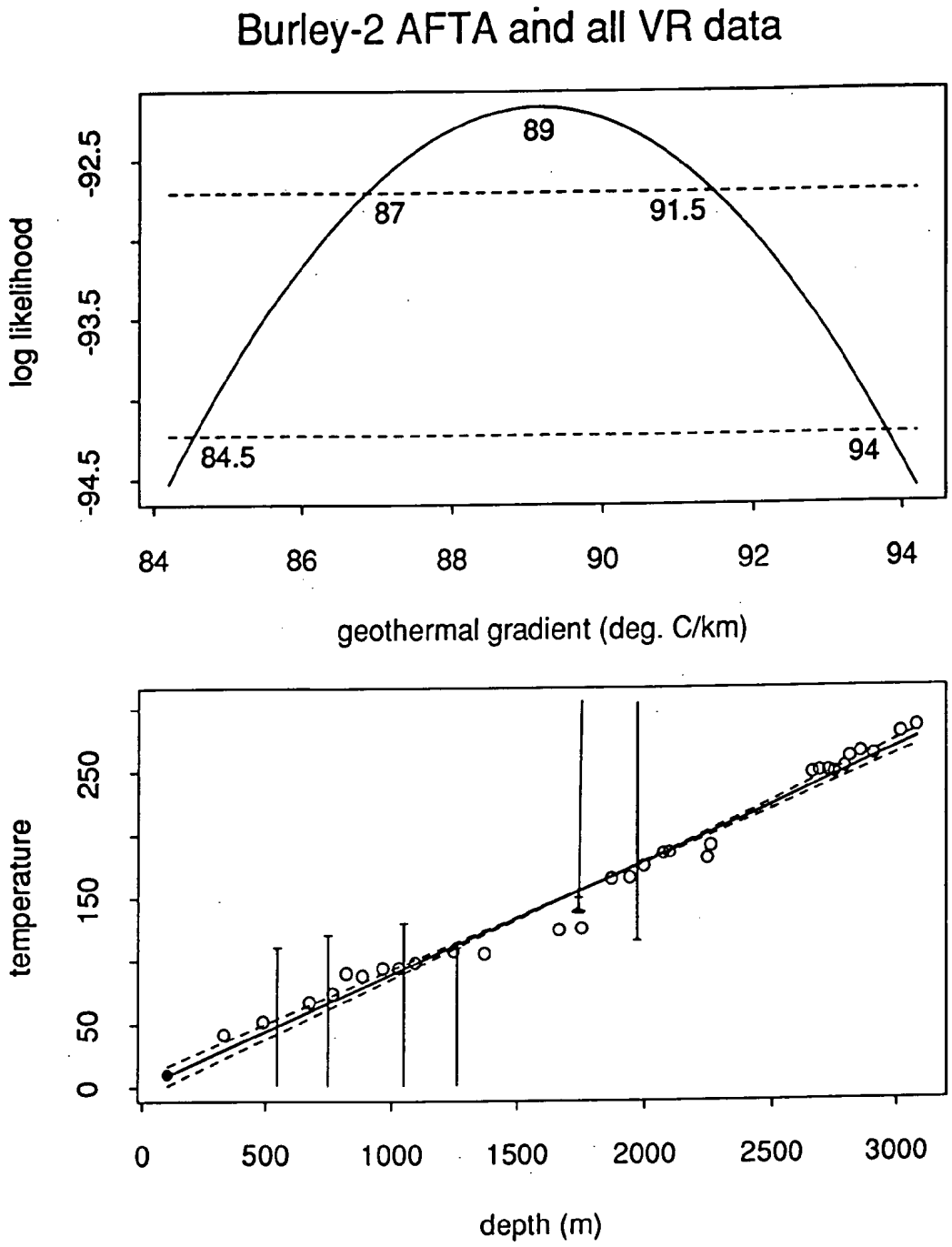

Figure 2.7: Upper: Maximum likelihood profile of linear paleogeothermal gradient fitted to the Cretaceous - Tertiary (~97 to 50 Ma) paleotemperature estimates from AFTA and VR results in the **Burley-2 well**. The profile shows good quadratic behaviour suggesting a well constrained value, with upper and lower 95% confidence limits of 94 and 84.5°C/km, respectively, and a best-fit value of 89°C/km. The methodology employed in deriving this profile is outlined in Appendix C.

Lower: Maximum paleotemperature estimates from AFTA and VR in the **Burley-2 well**, with fitted profile (solid line) and lines (dashed) representing upper and lower 95% confidence limits.

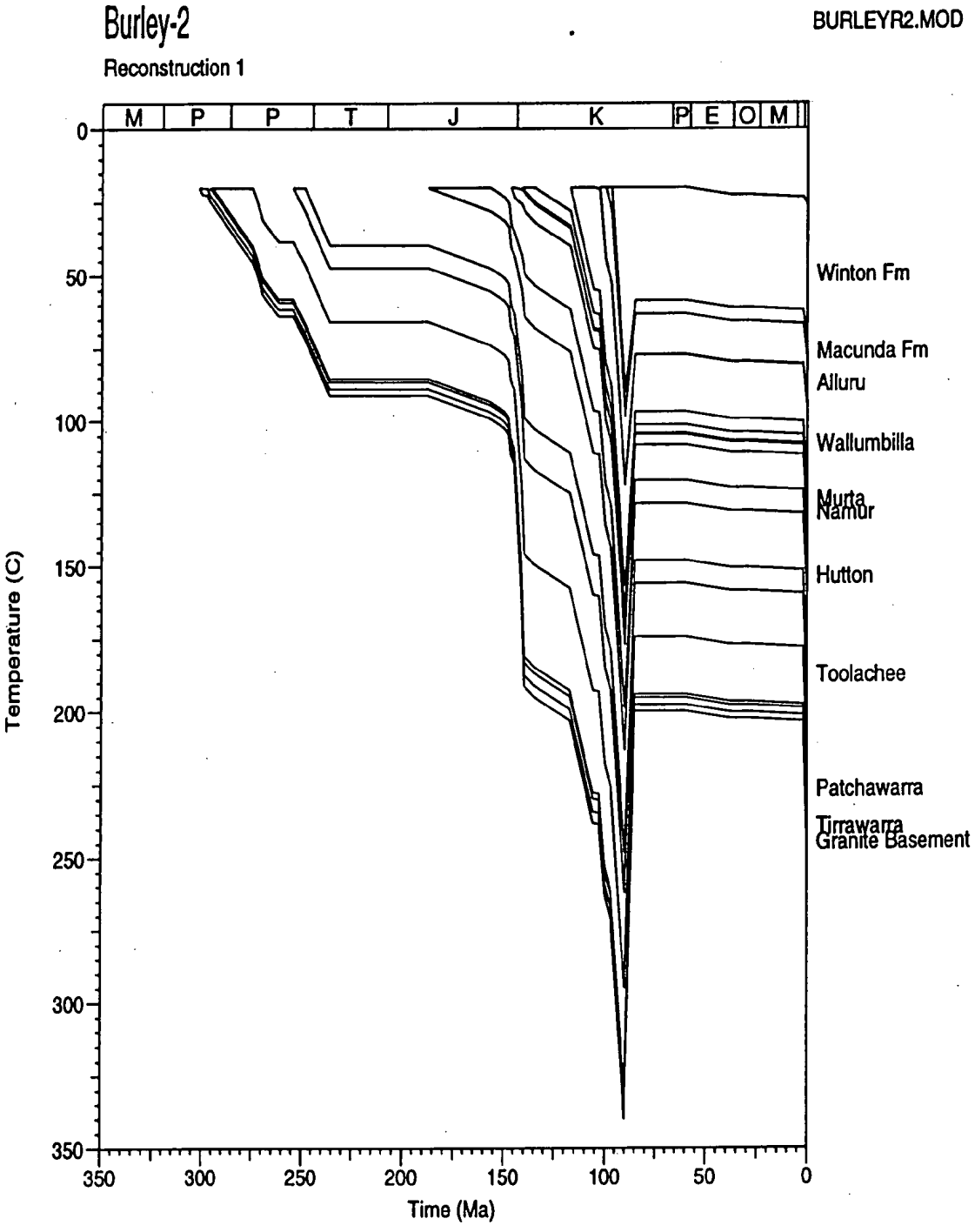

Figure 2.8: Reconstructed thermal history for **Burley-2** derived from the AFTA and VR results. Based on and a paleogeothermal gradient of 89°C/km up until cooling began at 90 Ma (within the possible range from 97 to 50 Ma), at which point it declined to 50°C/km (from AFTA and fluid inclusion results), rising again to 61°C/km at 2 Ma (within the last 7 Ma allowed by AFTA). The paleo-surface temperature is 0°C at 90 Ma and 20°C otherwise.

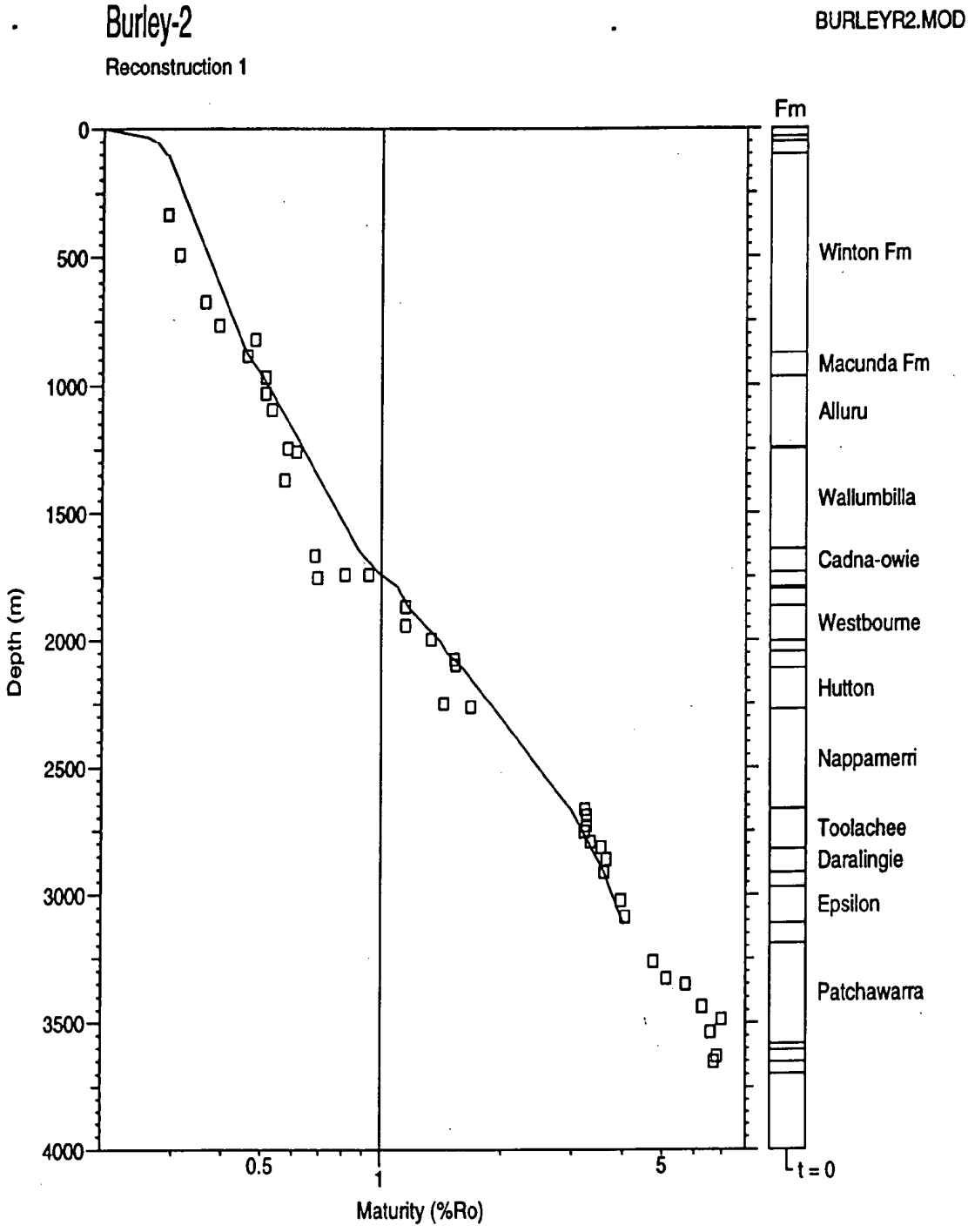

Figure 2.9: Measured vitrinite reflectance data in the **Burley-2 well,** and the VR profile with depth predicted from the reconstructed thermal history. The measured vitrinite values shows a very good match to the predicted profile throughout most of the section, with slightly low measured values at around 1750 m attributed to minor geochemical suppression. The thermal history results show that these maturity values measured at the present-day reached these levels in the Cretaceous - Tertiary as illustrated in Figure 2.8. Note that the Burnham and Sweeney relationship only predicts VR up to ~4.7%. See text for further details.

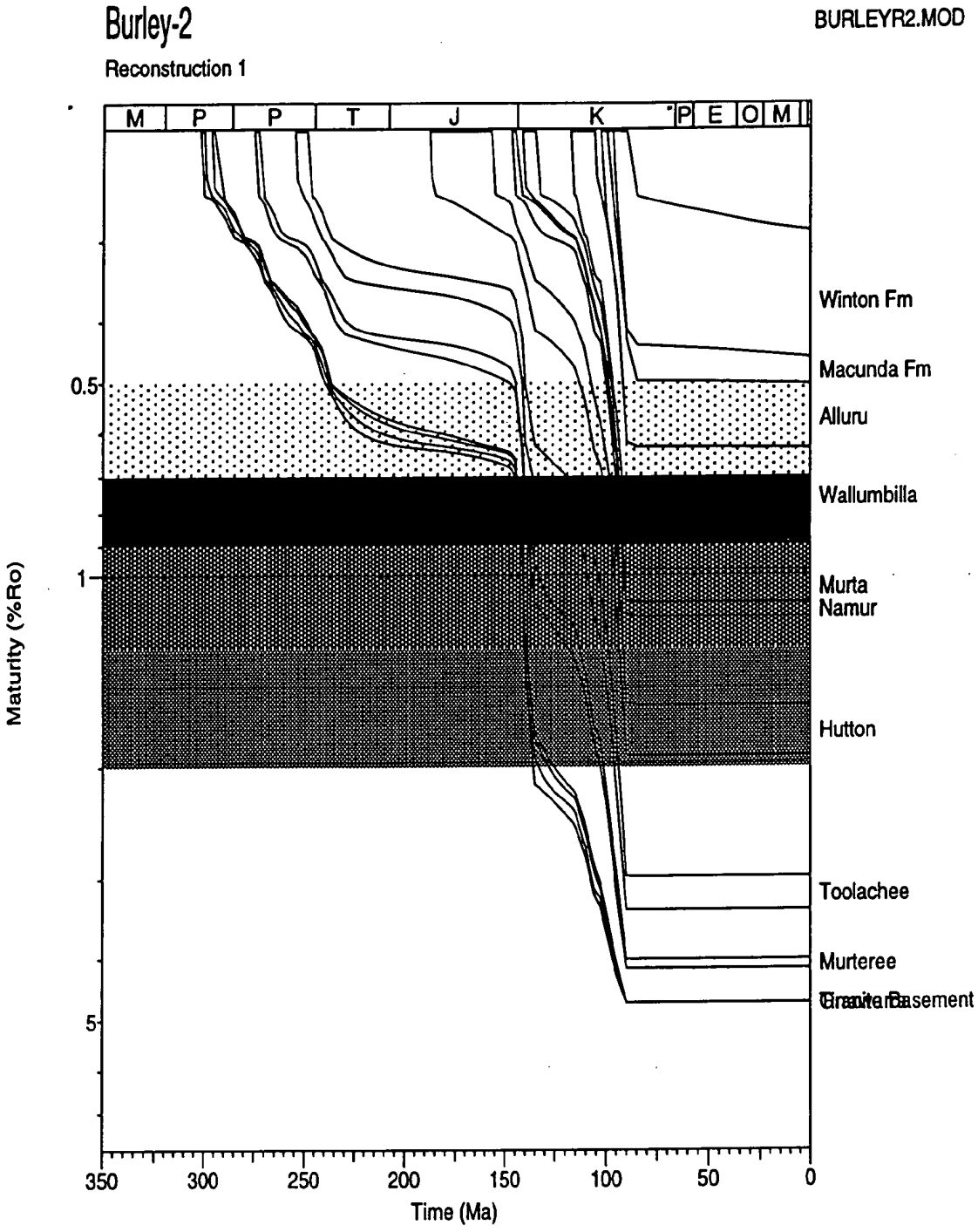

Figure 2.10: Predicted development of maturity with time (using Burnham and Sweeney, 1989) in the **Burley-2 well,** controlled by the AFTA results. Maximum maturity is shown as being reached at the 90 Ma (97 to 50 Ma allowed by the results), after progressive heating resulting from burial through the Early Cretaceous. This reconstruction illustrates that maximum maturity in most of the drilled section (Alluru Fm and deeper) was reached at 90 Ma (97 to 50 Ma allowed), immediately prior to decline in paleogeothermal gradient that commenced at this time. The reconstructed history predicts a minor increase in maturity in the upper part of the section (Macunda Fm and shallower) over the last 90 Ma, but only at maturities less than that required for significant oil generation. No significant maturation can be attributed to the recent increase in geothermal gradient over the last ~2 Ma

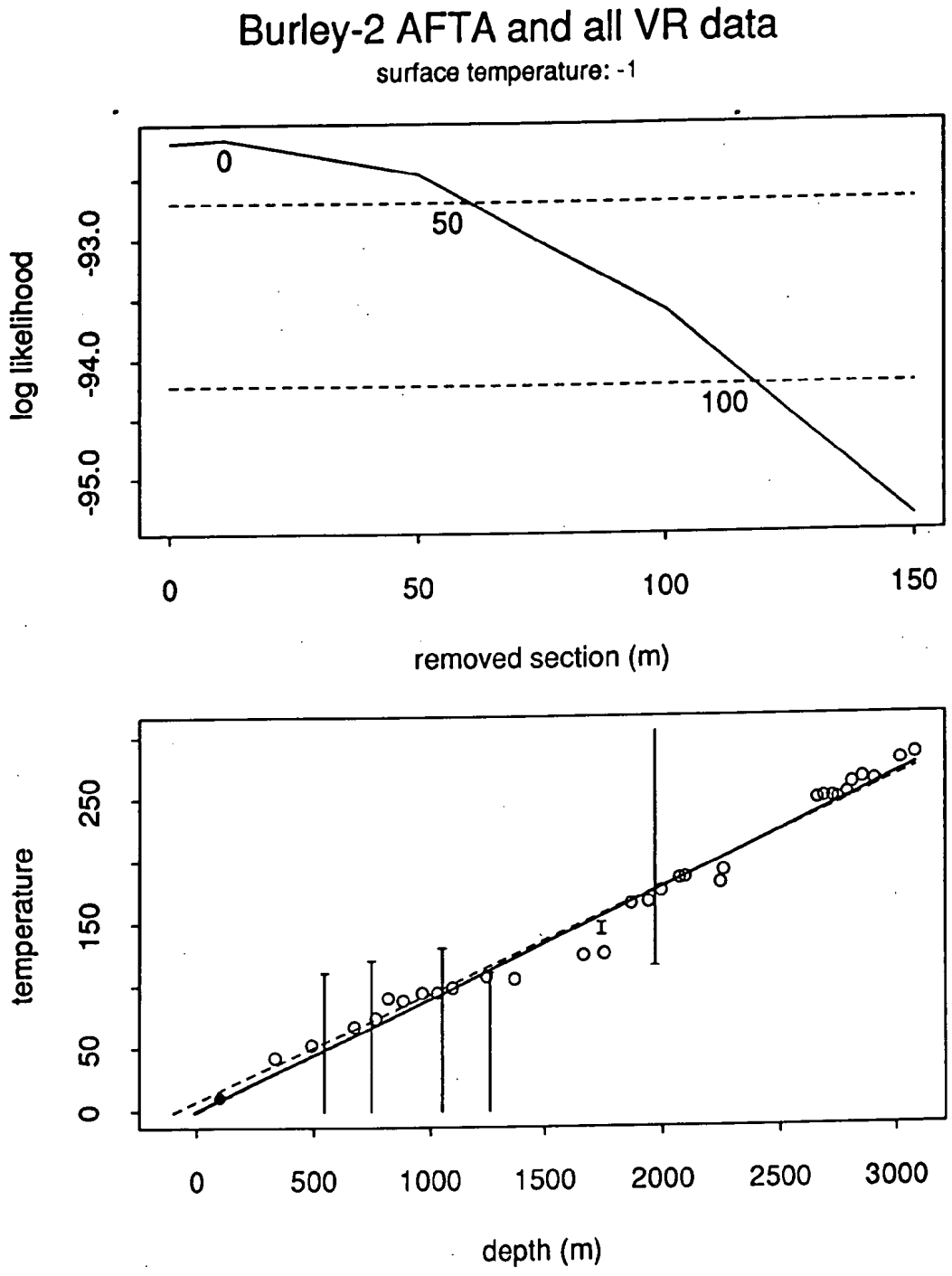

Figure 2.11: Upper: Maximum likelihood profile of estimated *total* section removed by uplift and erosion at the level of the unconformity at the top Winton Formation (~108.5 mTVD bKB) since the Cretaceous-Tertiary heating episode (~97 to 50 Ma) in the **Burley-2 well**, derived from the AFTA and VR constrained paleogeothermal gradient shown in Figure 2.7, assuming a paleo-surface temperature of 0°C. The profile gives an upper 95% confidence limit of 100 metres, and a well defined best-fit value of 0 metres. No lower intercept is defined as the best fit estimate is at the unconformity surface. The methodology employed in deriving this profile is outlined in Appendix C.

Lower: Maximum paleotemperature estimates from AFTA and VR data in the **Burley-2 well**, with fitted profile (solid line) and lines (dashed) representing upper and lower 95% confidence limits, extrapolated to the assumed paleo-surface temperature of 0°C.

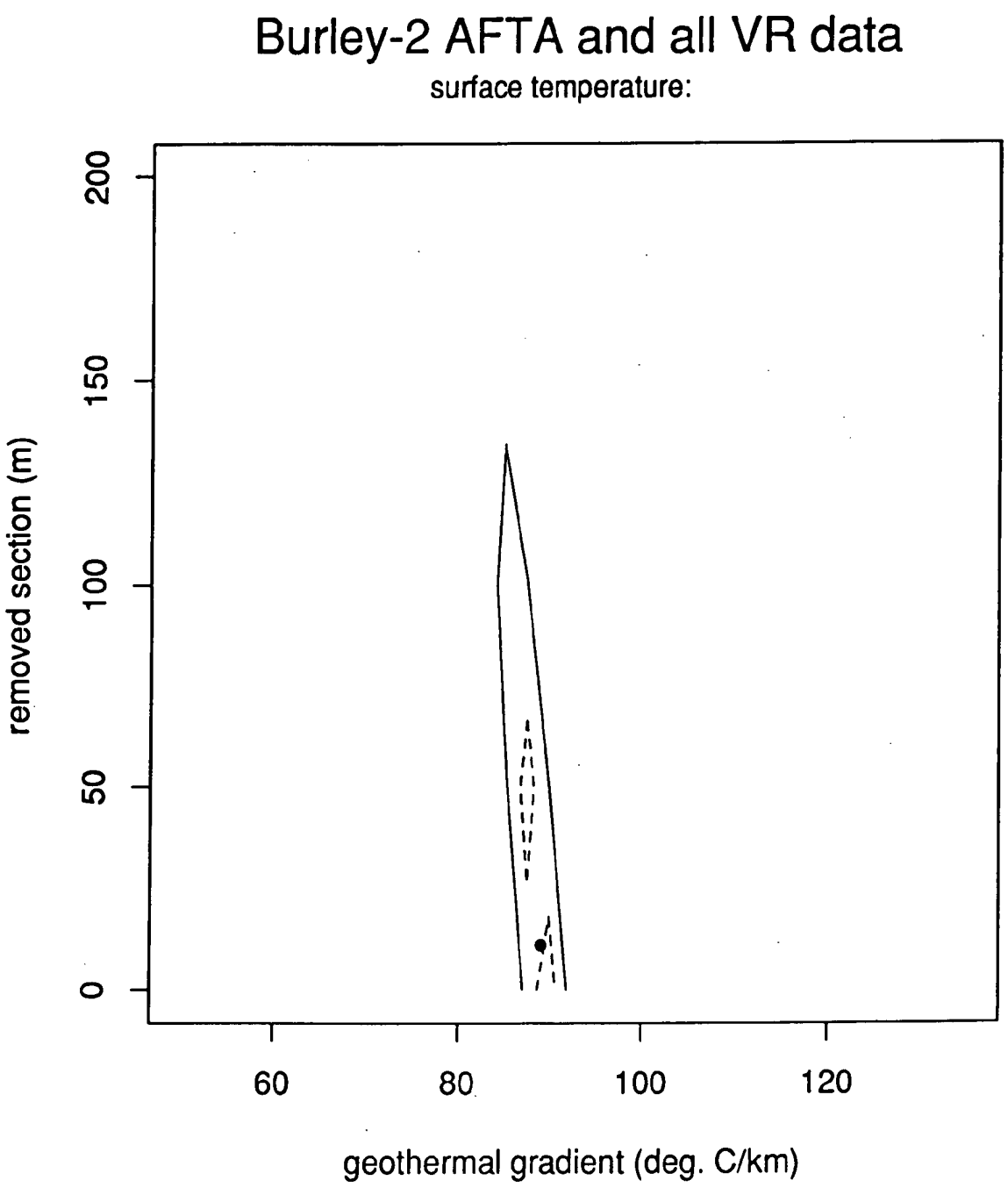

Figure 2.12: Crossplot of total removed section with respect to the level of the unconformity at the top Winton Formation (~108.5 mTVD bKB) since the Cretaceous-Tertiary heating episode (~97 to 50 Ma) in the **Burley-2 well**, showing the range of values (within the contoured region) compatible with the maximum paleotemperatures derived from AFTA data at the 95% confidence level. In effect, the thermal history reconstruction requires insignificant erosion on the top Winton Fm unconformity, with the identified cooling almost entirely attributable to decline in paleogeothermal gradient.

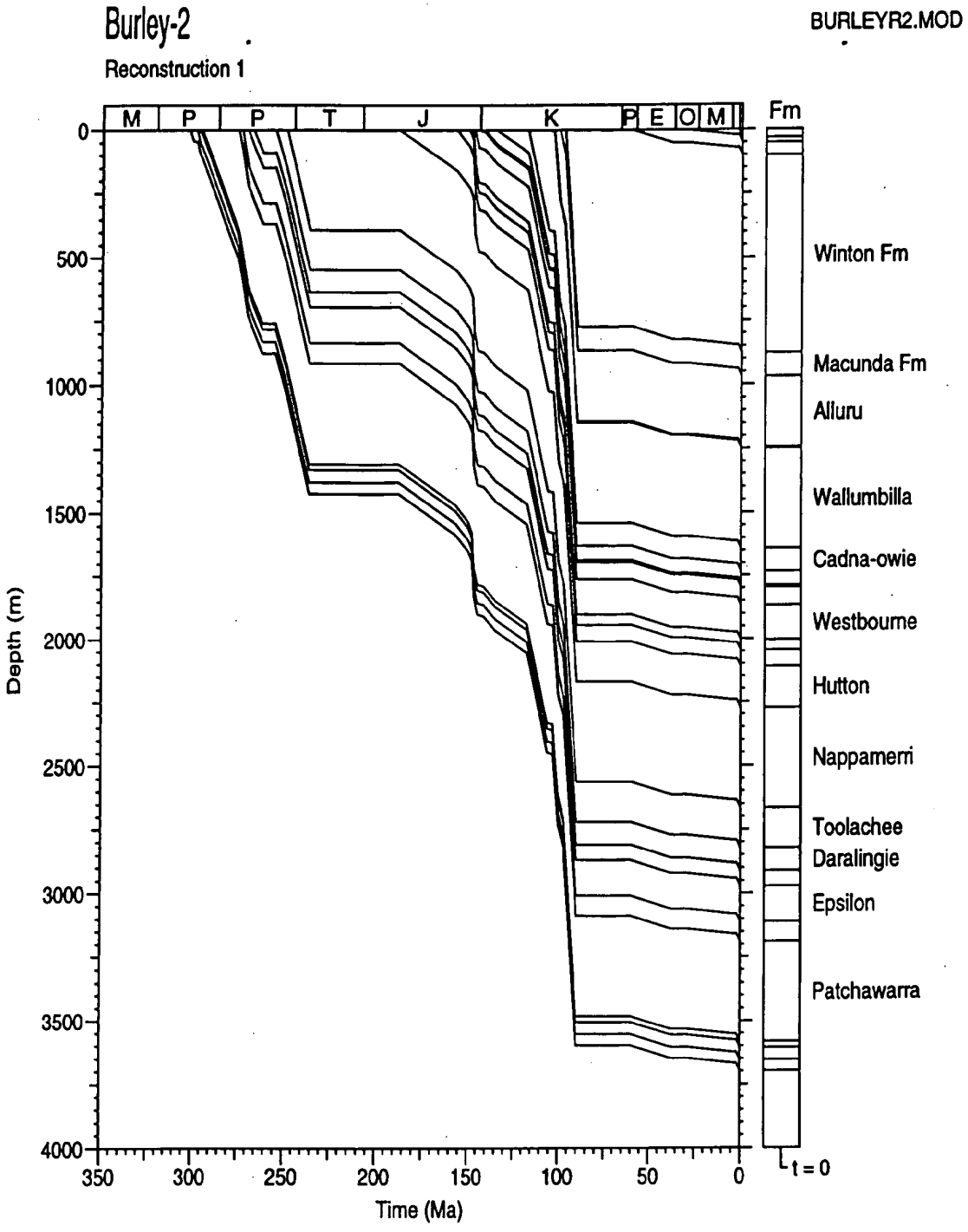

Figure 2.13: Possible burial history consistent with the thermal history reconstruction in the **Burley-2 well**. The history involves cooling from maximum paleotemperatures at 90 Ma (97 to 50 Ma allowed by the integrated thermal history results) but without significant uplift and erosion at any point in the history. Up to ~100 m of erosion is allowed on the top Winton Formation unconformity associated with a large in decline in paleogeothermal gradient commencing at some time between 97 and 50 Ma. See text for details.

3. Thermal history reconstruction in the Toolachee-1 well

3.1 Interpretive format

Interpretation of the AFTA and VR thermal history data in the Toolachee-1 well follows the format established for Burley-2 provided in full in Section 2.

- The samples processed for AFTA are listed in Table A.1 (Appendix A).
- Stratigraphy of the section drilled is summarised in Table A.3 and shown in Figure 3.1.
- The present-day geothermal gradient calculated from corrected BHT data = 51°C/km for a surface temperature of 20°C (Appendix A).

3.2 Thermal history conclusions from the AFTA and VR data

Introduction - Basic data

- Measured fission track parameters and Default History parameters for each sample are summarised in Table 3.1 and plotted against depth and present temperature in Figure 3.1.
- Evidence for elevated paleotemperatures in each AFTA sample from **Toolachee-1** is summarised in Table 3.2.
- Interpretations of the magnitude and timing of paleotemperatures which are required (or allowed) by AFTA in each sample are discussed in Table 3.3.
- Open file vitrinite reflectance data from **Toolachee-1,** ranging in value from ~0.32 % to 1.32%, are listed in Table D.2 and plotted against depth in Figure 3.2 together with a predicted profile based on the Default Thermal History (see Section 1.6). The Default Burial History is given in Figure 3.3.

Duration of present-day thermal conditions

- The AFTA results (Figure 3.1) indicate that the present-day geothermal gradient has increased to the measured level of ~51°C/km from ~40°C/km, or less, at some time within the last 2 Ma (Table 3.3).

Maximum paleotemperatures from AFTA and VR

- Maximum paleotemperature estimates from VR range from 56 to 175°C (Table ii) and are higher than present temperatures throughout most of the section, with

the difference increasing with depth (Figure 3.4). AFTA paleotemperature estimates are generally minimum estimates of maximum paleotemperature as discussed in Table 3.3.

Time of cooling from maximum paleotemperatures from AFTA and VR

- Integration of the AFTA and VR results in sample GC668-223, indicates that a maximum paleotemperature of ~122°C indicated by the VR results can only have occurred prior to ~75 Ma. Similarly, a maximum paleotemperature of ~127°C indicated by the VR results in sample GC668-224 is constrained by the AFTA results to have occurred between ~130 and 60 Ma, with a best-fit timing of 99 Ma. Overlapping results for these samples suggests a common event between ~130 and 75 Ma. Paleotemperature estimates from all AFTA and VR samples are summarised in Table ii and plotted against depth in Figure 3.4.

Paleogeothermal gradient at time of maximum paleotemperatures - thermal history reconstruction

- The paleogeothermal gradient at the time of Cretaceous-Tertiary **maximum paleotemperatures (130 to 75 Ma)** determined from the AFTA and VR results is 75.5°C/km (maximum likelihood estimate), with 69 to 82°C/km allowed at the 95% confidence limits (Figure 3.5). The allowed range is significantly higher than the present-day gradient, indicating a period of significantly elevated heat flow at some time between 130 to 75 Ma, corresponding to the time of maximum paleotemperatures. Paleogeothermal gradient estimates in the **Toolachee-1 well** are summarised in Table v (Executive Summary).

- The simplest reconstructed thermal history for **Toolachee-1** consistent with the data is illustrated in Figure 3.6, and is based on a paleogeothermal gradient of 75.5°C/km up until cooling began at 90 Ma (within the possible range from 130 to 75 Ma), at which point it declined to 40°C/km (from AFTA), rising again to 51°C/km at 2 Ma (from AFTA). The surface temperature at 90 Ma is interpreted to have been 0°C (the results are not sensitive to the paleo-surface temperature but reconstruction of the burial history was based on this assumption in order to get a positive intercept at the top of the Winton Fm unconformity. The paleo-surface temperature is assumed to have risen to 20°C in the late Tertiary.

Removed section estimates - burial history reconstruction

- Extrapolation of the allowed range of Cretaceous-Tertiary (130 to 75 Ma) paleogeothermal gradients determined from the AFTA and VR data shown in Figure 3.5 to an assumed paleo-surface temperature of 0°C results in a range of allowed values for the amount of removed section from ~0 to 300 m, with a maximum likelihood value of 150 m (Figure 3.7). Correlation between the paleogeothermal gradient and the magnitude of removed section required to explain the paleotemperature results is illustrated in Figure 3.8.

- Removed section estimates determined by these methods for the Cretaceous - Tertiary heating episode identified in the **Toolachee-1 well** are summarised in Table vi (Executive Summary).

- The reconstructed thermal history for **Toolachee-1** strongly suggests that the major controls on the maturation history has been variation in heat flow with only a minor contribution from additional burial at recognised unconformities. The reconstructed burial history is best represented by the preserved stratigraphy in the well plus the best-fit estimate of 150 m of section eroded at the top Winton Formation unconformity as illustrated in Figure 3.9.

Maturation History

- The maturity-depth profile in **Toolachee-1** derived from the reconstructed thermal history shown in Figure 3.6, together with the measured VR data (from a number of Toolachee Field wells) and AFTA-equivalent VR levels, is provided in Figure 3.10. Predicted maturity levels (using the maturation algorithm of Burnham and Sweeney, 1989) agree very well with the measured results throughout the section, for a linear Cretaceous-Tertiary paleogeothermal gradient of 75.5°C/km.

- Figure 3.11 shows the variation of maturity with time for the **Toolachee-1** well (using the maturation algorithm of Burnham and Sweeney, 1989) derived from the reconstructed thermal history shown in Figure 3.6. This reconstruction illustrates that maximum maturity in most of the drilled section (Macunda Fm and deeper) was reached at 90 Ma (130 to 75 Ma allowed), immediately prior to decline in paleogeothermal gradient that commenced at this time. The reconstructed history predicts a minor increase in maturity in the upper part of the section (Winton Fm and shallower) over the last 90 Ma, but only at

maturities less than that required for significant oil generation. No significant maturation can be attributed to the recent increase in geothermal gradient over the last ~2 Ma.

Table 3.1: Summary of AFTA data in samples from the Toolachee-1 well, Cooper-Eromanga Basin, South Australia (Geotrack Report #668)

Sample number	Average depth*1	Present temperature*2	Stratigraphic Age	Measured Mean track length	Default mean track length *3	Measured apatite fission track age *4	Default fission track age*3
GC	(m)	(°C)	(Ma)	(µm)	(µm)	(Ma)	(Ma)
668-61	303	35	97-90	15.14±0.09	14.4	98.4±7.6	90
668-64	776	59	100-97	14.66±0.14	13.4	*165.2±27.5*	92
668-67	1242	83	100-97	13.90±0.10	12.0	*123.3±12.9*	96
668-68	1388	90	141.5-135	13.92±0.14	11.5	146.8±12.1	109
668-69	1507	96	147-145	13.97±0.14	11.1	*157.7±18.5*	109
668-223*5	1646	104	157-147	12.34±0.75	10.2	94.9±14.8	75
668-224*5	1705	107	237-186	12.90±0.54	10.0	96.1±14.2	108
668-70	1852	114	255-249	8.21±1.71	9.0	*94.5±17.3*	71

*1 All depths quoted are true vertical depth (TVD) with respect to KB.

*2 See Appendix A for a discussion of present temperature estimation.

*3 AFTA values predicted from the "Default Thermal History" (Section 1.6); i.e., assuming that each sample is now at its maximum temperature since deposition. The values refer only to tracks formed after deposition. Samples may also contain tracks inherited from sediment provenance areas. Calculation of the Default values refer to actual measured compositions of apatites analysed within a particular sample, which is discussed in Appendix A.

*4 Central fission track age quoted (in italics) where P(chi sq) < 5%

*5 Sample data reprocessed specifically for this report and discussed in deatil in Tables 3.2 and 3.3.

Table 3.2: Summary of thermal history interpretation of AFTA data in samples from the Toolachee-1 well, Eromanga Basin, South Australia (Geotrack Report #668)

Sample number	Do AFTA data require any revision of present temperature?	Evidence of higher temperatures in the past from length data?	Evidence of higher temperatures in the past from fission track age data?	Conclusion
668-61 303 m	Yes Modelling of the AFTA length parameters suggests the present temperature of 35°C has been acting for only a short time or is incorrect.	No [Mean track length is ~1 µm longer than that predicted from the Default Thermal History, suggesting a very recent increase in present temperatures has occurred.	No [Pooled fission track age is similar to that predicted on the basis of the Default Thermal History]	No direct evidence to suggest that the sample was subjected to paleotemperatures higher than present temperatures at any time after deposition. Note, however, that the AFTA track length data suggests a very recent increase in present temperatures which may mask evidence of higher paleotemperatures.
668-64 776 m	Yes Modelling of the AFTA length parameters suggests the present temperature of 59°C has been acting for only a short time or is incorrect.	No [Mean track length is ~1 µm longer than that predicted from the Default Thermal History, suggesting a very recent increase in present temperatures has occurred.	No [Central fission track age and all single grain ages are significantly older than, or similar to, those predicted on the basis of the Default Thermal History]	No direct evidence to suggest that the sample was subjected to paleotemperatures higher than present temperatures at any time after deposition. Note, however, that the AFTA track length data suggests a very recent increase in present temperatures which may mask evidence of higher paleotemperatures.
668-67 1242 m	Yes Modelling of the AFTA length parameters suggests the present temperature of 83°C has been acting for only a short time or is incorrect.	No [Mean track length is ~2 µm longer than that predicted from the Default Thermal History, suggesting a very recent increase in present temperatures has occurred.	No [Central fission track age and all single grain ages are significantly older than, or similar to, those predicted on the basis of the Default Thermal History]	No direct evidence to suggest that the sample was subjected to paleotemperatures higher than present temperatures at any time after deposition. Note, however, that the AFTA track length data suggests a very recent increase in present temperatures which may mask evidence of higher paleotemperatures.

Note: Interpretation of AFTA data is based on comparison of measured AFTA parameters with values predicted from "Default Thermal History" (Section 1.6); i.e., assuming that each sample is now at its maximum temperature since deposition. The predicted values for each sample are summarised in Table 3.1, and refer only to tracks formed after deposition. Samples may also contain tracks inherited from sediment provenance areas, which must be allowed for in interpreting the data. Calculations refer to apatites with the compositional range appropriate to each sample, as explained in Appendix A.

Table 3.2: (cont.):

Sample number	Do AFTA data require any revision of present temperature?	Evidence of higher temperatures in the past from length data?	Evidence of higher temperatures in the past from fission track age data?	Conclusion
668-68 1388 m	Yes Modelling of the AFTA length parameters suggests the present temperature of 90°C has been acting for only a short time or is incorrect.	No [Mean track length is ~2 μm longer than that predicted from the Default Thermal History, suggesting a very recent increase in present temperatures has occurred.	No [Pooled fission track age is older than that predicted on the basis of the Default Thermal History]	No direct evidence to suggest that the sample was subjected to paleotemperatures higher than present temperatures at any time after deposition. Note, however, that the AFTA track length data suggests a very recent increase in present temperatures which may mask evidence of higher paleotemperatures.
668-69 1507 m	Yes Modelling of the AFTA parameters suggests the present temperature of 96°C has been acting for only a short time or is incorrect.	No [Mean track length is ~2 μm longer than that predicted from the Default Thermal History, suggesting a very recent increase in present temperatures has occurred.	No [Central fission track age and all single grain ages are significantly older than or similar to that predicted on the basis of the Default Thermal History]	No direct evidence to suggest that the sample was subjected to paleotemperatures higher than present temperatures at any time after deposition. Note, however, that the AFTA track length data suggests a very recent increase in present temperatures which may mask evidence of higher paleotemperatures.

Note: Interpretation of AFTA data is based on comparison of measured AFTA parameters with values predicted from "Default Thermal History" (Section 1.6); i.e., assuming that each sample is now at its maximum temperature since deposition. The predicted values for each sample are summarised in Table 3.1, and refer only to tracks formed after deposition. Samples may also contain tracks inherited from sediment provenance areas, which must be allowed for in interpreting the data. Calculations refer to apatites with the compositional range appropriate to each sample, as explained in Appendix A.

Table 3.2: (cont.):

Sample number	Do AFTA data require any revision of present temperature?	Evidence of higher temperatures in the past from length data?	Evidence of higher temperatures in the past from fission track age data?	Conclusion
668-223 1646 m	Yes Modelling of the AFTA parameters suggests the present temperature of 104°C has been acting for only a short time or is incorrect.	No [Mean track length is ~2 μm longer than that predicted from the Default Thermal History, suggesting a very recent increase in present temperatures has occurred.	No [Pooled fission track age is similar to that predicted on the basis of the Default Thermal History]	No direct evidence to suggest that the sample was subjected to paleotemperatures higher than present temperatures at any time after deposition. Note, however, that the AFTA track length data suggests a very recent increase in present temperatures which may mask evidence of higher paleotemperatures.
668-224 1705 m	Yes Modelling of the AFTA parameters suggests the present temperature of 107°C has been acting for only a short time or is incorrect.	No [Mean track length is ~3 μm longer than that predicted from the Default Thermal History, suggesting a very recent increase in present temperatures has occurred.	No [Pooled fission track age is similar to that predicted on the basis of the Default Thermal History]	No direct evidence to suggest that the sample was subjected to paleotemperatures higher than present temperatures at any time after deposition. Note, however, that the AFTA track length data suggests a very recent increase in present temperatures which may mask evidence of higher paleotemperatures.
668-70 1852 m	Yes Modelling of the AFTA parameters suggests the present temperature of 114°C has been acting for only a short time or is incorrect.	No [Mean track length is similar to that predicted from the Default Thermal History, but it has a large uncertainty due to the paucity of measurements)	No [Central fission track age and all single grain ages are significantly older than or similar to that predicted on the basis of the Default Thermal History]	No direct evidence to suggest that the sample was subjected to paleotemperatures higher than present temperatures at any time after deposition. The AFTA track length data would allow a very recent increase in present temperatures as observed in all other samples, but does not require it.

Note: Interpretation of AFTA data is based on comparison of measured AFTA parameters with values predicted from "Default Thermal History" (Section 1.6); i.e., assuming that each sample is now at its maximum temperature since deposition. The predicted values for each sample are summarised in Table 3.1, and refer only to tracks formed after deposition. Samples may also contain tracks inherited from sediment provenance areas, which must be allowed for in interpreting the data. Calculations refer to apatites with the compositional range appropriate to each sample, as explained in Appendix A.

Table 3.3: Estimates of timing and magnitude of elevated paleotemperatures from AFTA data in samples from the Toolachee-1 well, Cooper-Eromanga Basin, South Australia (Geotrack Report #668)

Sample number GC	Stratigraphic Age (Ma)	Present temperature (°C)	Early episode: Maximum paleo-temperature (°C)	Early episode: Onset of cooling (Ma)	Late episode: Peak paleo-temperature (°C)	Late episode: Onset of heating (Ma)	Comments
668-223 1646 m	157-147 Late Jurassic	104	>110	prior to 75	<86	20 to 0	A key sample. Evidence mainly from the AFTA length data clearly indicate that this sample cannot have resided near the present temperature of 104°C for more than ~20 Ma, compared to ~90 Ma inferred from the preserved stratigraphy. Further, AFTA allows a maximum possible paleotemperature of ~86°C for any longer heating duration, implying that the temperature has increased to its present value only recently. Note that the pre-increase temperature may have been lower than 86°C, but this cannot be estimated from the AFTA data alone. Also, it is not possible to estimate both the pre-increase temperature and the time of this temperature increase from the AFTA data alone, however, a measured VR value of 0.67% at around this depth indicates that the maximum *sustained* post-depositional temperatures were ~122°C. Integration of this maximum paleotemperature with the AFTA data indicate that sustained paleotemperatures >110°C could only have been reached in the interval between Late Jurassic deposition and ~75 Ma. Thus, while the recent increase in temperature demonstrable in this sample significantly complicates the determination of the paleo-thermal history, integration of the AFTA results with independent estimates of paleotemperature allows important constraints to be placed on the time of both maximum paleotemperatures and the duration of the recently developed high temperatures.

Note: **Brackets** surrounding italicised time/temperature constraints indicate that the AFTA results allow, but *do not* require a discrete event at this time.

*1 Based on measured present-day geothermal gradient of 51°C/km and a surface temperature of 20°C. As discussed in this table AFTA indicates that this is a recent developed transient thermal regime, and that lower temperatures must have persisted until this recent increase.

Table 3.3 (cont.): Toolachee-1 (Geotrack Report #668)

Sample number	Stratigraphic Age	Present*1 temperature	Early episode Maximum paleo-temperature	Early episode Onset of cooling	Late episode Peak paleo-temperature	Late episode Onset of Heating	Comments
GC	(Ma)	(°C)	(°C)	(Ma)	(°C)	(Ma)	
668-224 1705 m	237-186 Late Triassic	107	>120	130 to 60	<88	2 to 0	A key sample. Evidence mainly from the AFTA length data clearly indicate that this sample cannot have resided near the present temperature of 107°C for more than ~2 Ma, compared to ~90 Ma inferred from the preserved stratigraphy. Further, AFTA allows a maximum possible temperature of ~88°C for any longer heating duration, implying that the temperature has increased to its present value only recently. Note that the pre-increase temperature may have been lower than 88°C, but this cannot be estimated from the AFTA data alone. Also, it is not possible to estimate both the pre-increase temperature and time of this temperature increase from the AFTA data alone, however, a measured VR value of 0.70% at around this depth indicate that the maximum *sustained* post-depositional temperatures were ~127°C. Integration of this maximum paleotemperature with the AFTA data indicate that sustained paleotemperatures >120°C could only have been reached in the interval between ~130 and 60 Ma. Thus, while the recent increase in temperature demonstrable in this sample significantly complicates the determination of the paleo-thermal history, integration of the AFTA results with independent estimates of paleotemperature allows important constraints to be placed on the time of both maximum paleotemperatures and the duration of the recently developed high temperatures.

Note: **Brackets** surrounding italicised time/temperature constraints indicate that the AFTA results allow, but *do not* require a discrete event at this time.

*1 Based on measured present-day geothermal gradient of 51°C/km and a surface temperature of 20°C. As discussed in this table AFTA indicates that this is a recent developed transient thermal regime, and that lower temperatures must have persisted until this recent increase.

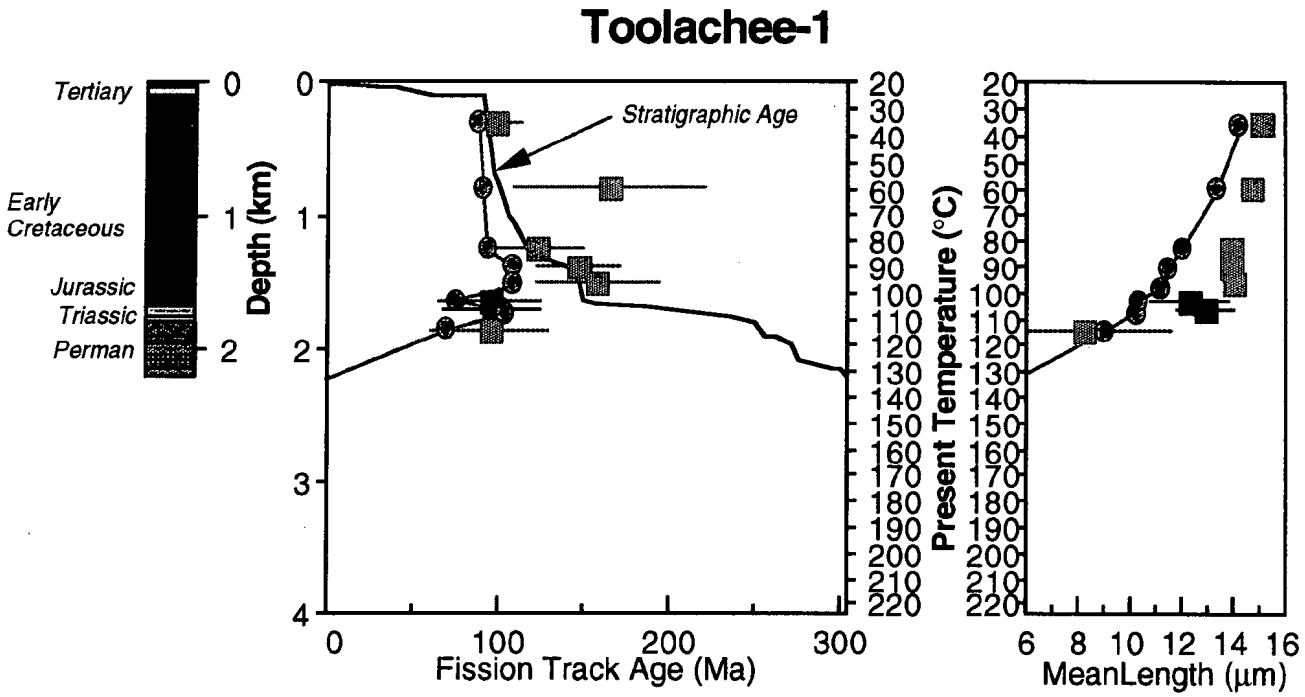

Figure 3.1: AFTA parameters plotted against sample depth and present temperature for samples from the **Toolachee-1 well, Cooper-Eromanga Basin.** Reprocessed data in solid blue; un-reprocessed data in grey (all data in Table 3.1). Round symbols are AFTA parameters predicted from the Default History. Comparison of the Default History parameters with the measured data suggest that the section has increased to the present temperatures in the recent geological past. The variation of stratigraphic age with depth is also shown, as the solid line in the central panel.

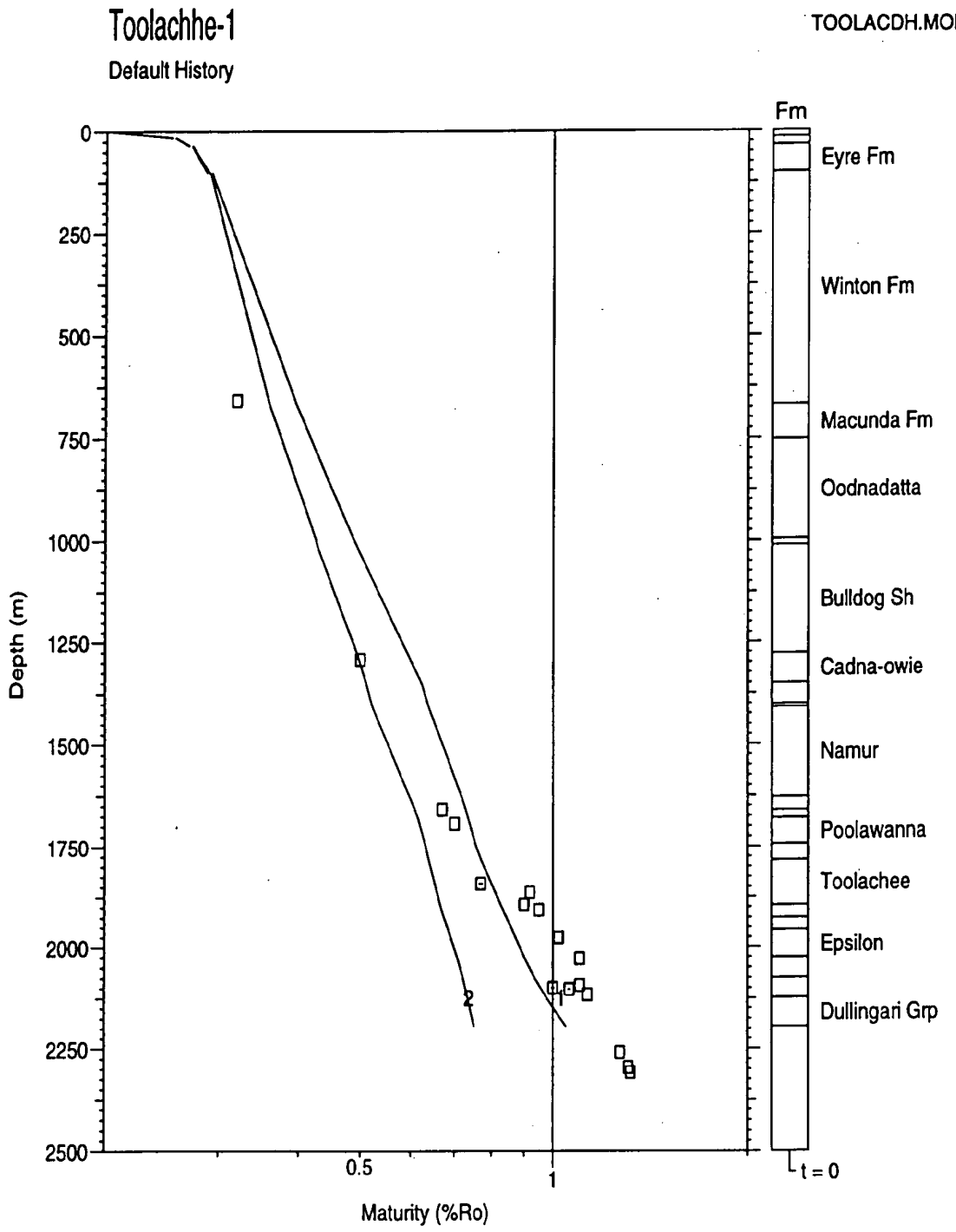

Figure 3.2: Measured vitrinite reflectance data in samples from the **Toolachee-1 well, Cooper-Eromanga Basin** plotted against depth (with respect to KB). A VR profile (Profile 1) predicted from the "Default History" (Section 1.6) is also shown, i.e., the profile expected if samples throughout the section are currently at their maximum temperature since deposition (based on a *measured* present-day geothermal gradient of 51°C/km, and a constant surface temperature of 20°C - Appendix A). Also shown is a second predicted profile (Profile 2) based on the *AFTA-revised* (steady-state) present-day geothermal gradient of 40°C/km (see text). The majority of the measured VR results fall above the predicted profile, more so deeper in the section, suggesting that this part of the section was subjected to maximum paleotemperature significantly higher than present temperatures after deposition. See text for details.

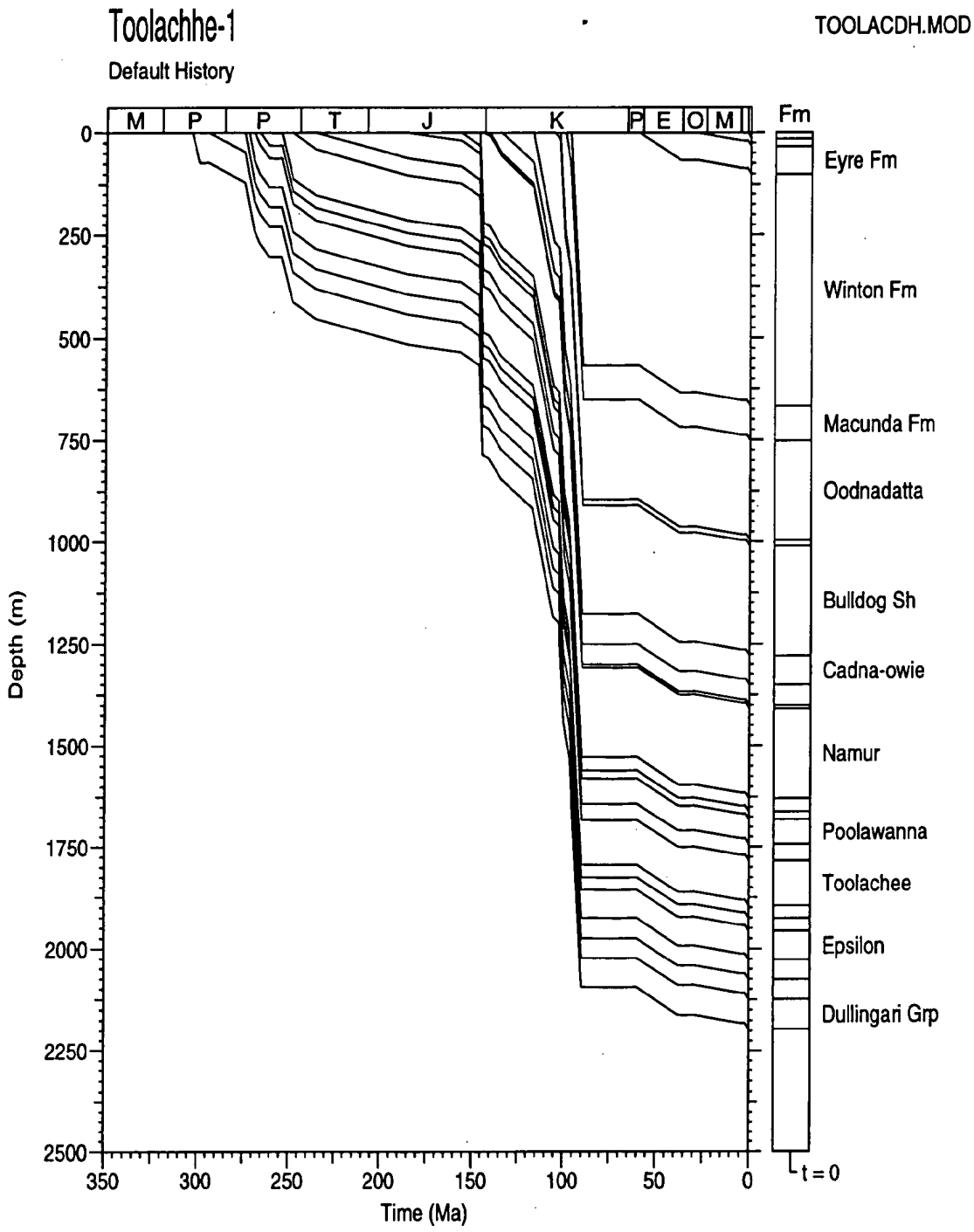

Figure 3.3: Default Burial History for the **Toolachee-1 well, Cooper-Eromanga Basin**, derived from the preserved section which, combined with the present-day thermal conditions, is used in predicting the VR profiles shown in Figure 3.2.

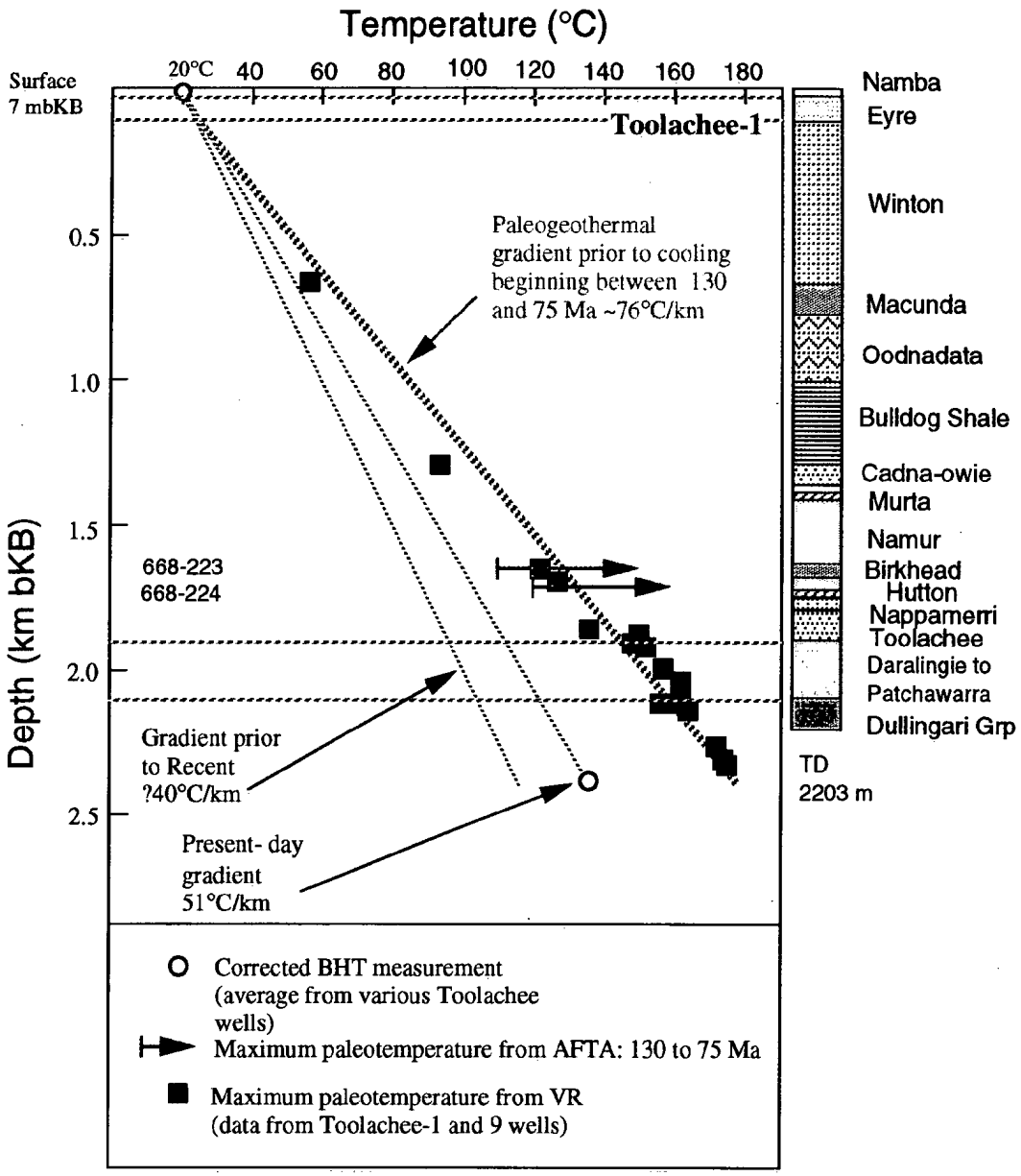

Figure 3 .4: Plot of paleotemperatures derived from AFTA and VR data in the **Toolachee-1 well, Eromanga Basin**, against sample depth and the estimated present temperature profile for this well (see Appendix A).

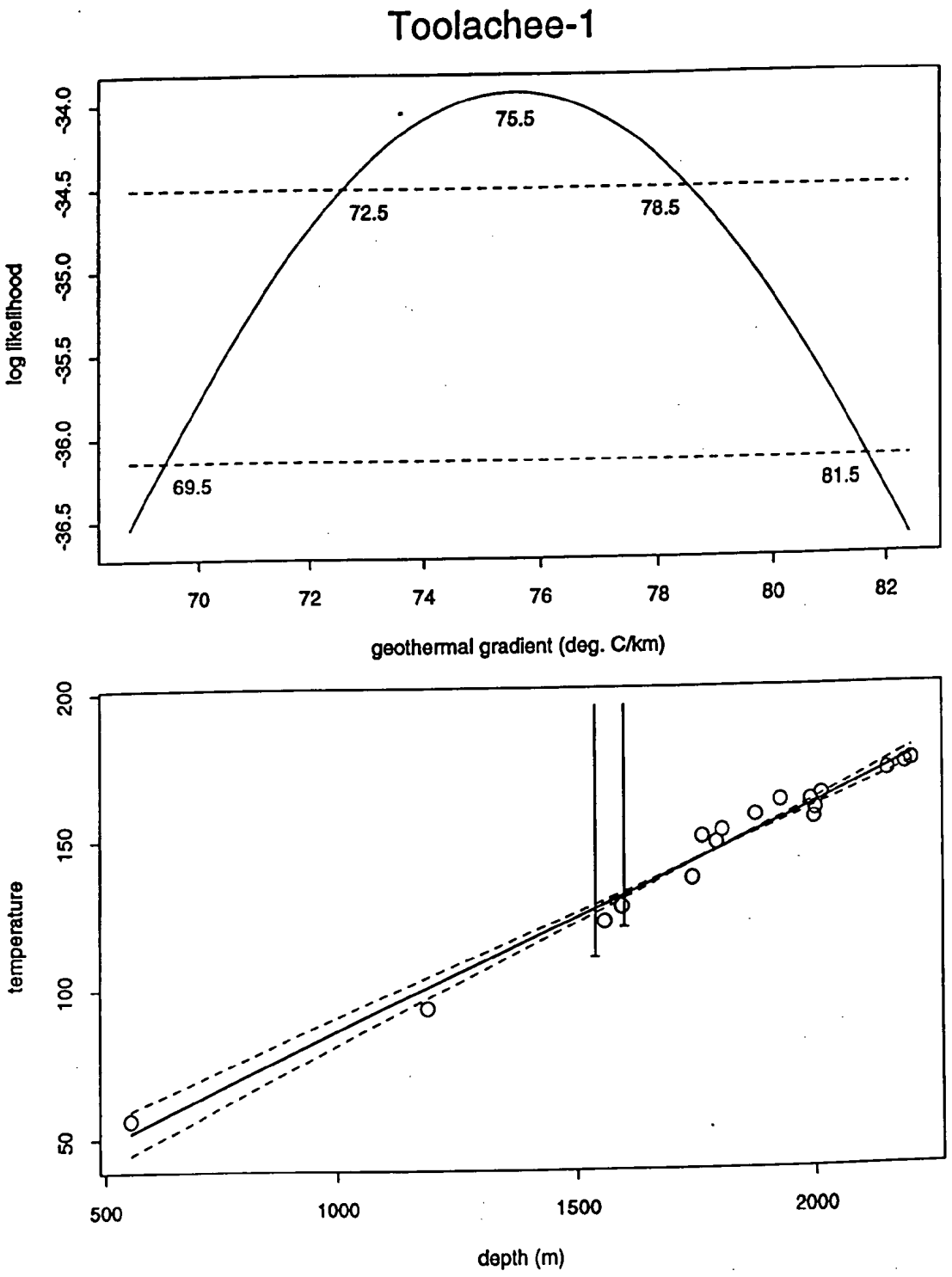

Figure 3.5: Upper: Maximum likelihood profile of linear paleogeothermal gradient fitted to the Cretaceous - Tertiary (~130 to 60 Ma) paleotemperature estimates from the AFTA and VR results in the **Toolachee-1 well**. The profile shows good quadratic behaviour suggesting a well constrained value, with upper and lower 95% confidence limits of 82 and 69°C/km, respectively, and a best-fit value of 75.5°C/km. The methodology employed in deriving this profile is outlined in Appendix C.

Lower: Maximum paleotemperature estimates from AFTA and VR in the **Toolachee-1 well**, with fitted profile (solid line) and lines (dashed) representing upper and lower 95% confidence limits.

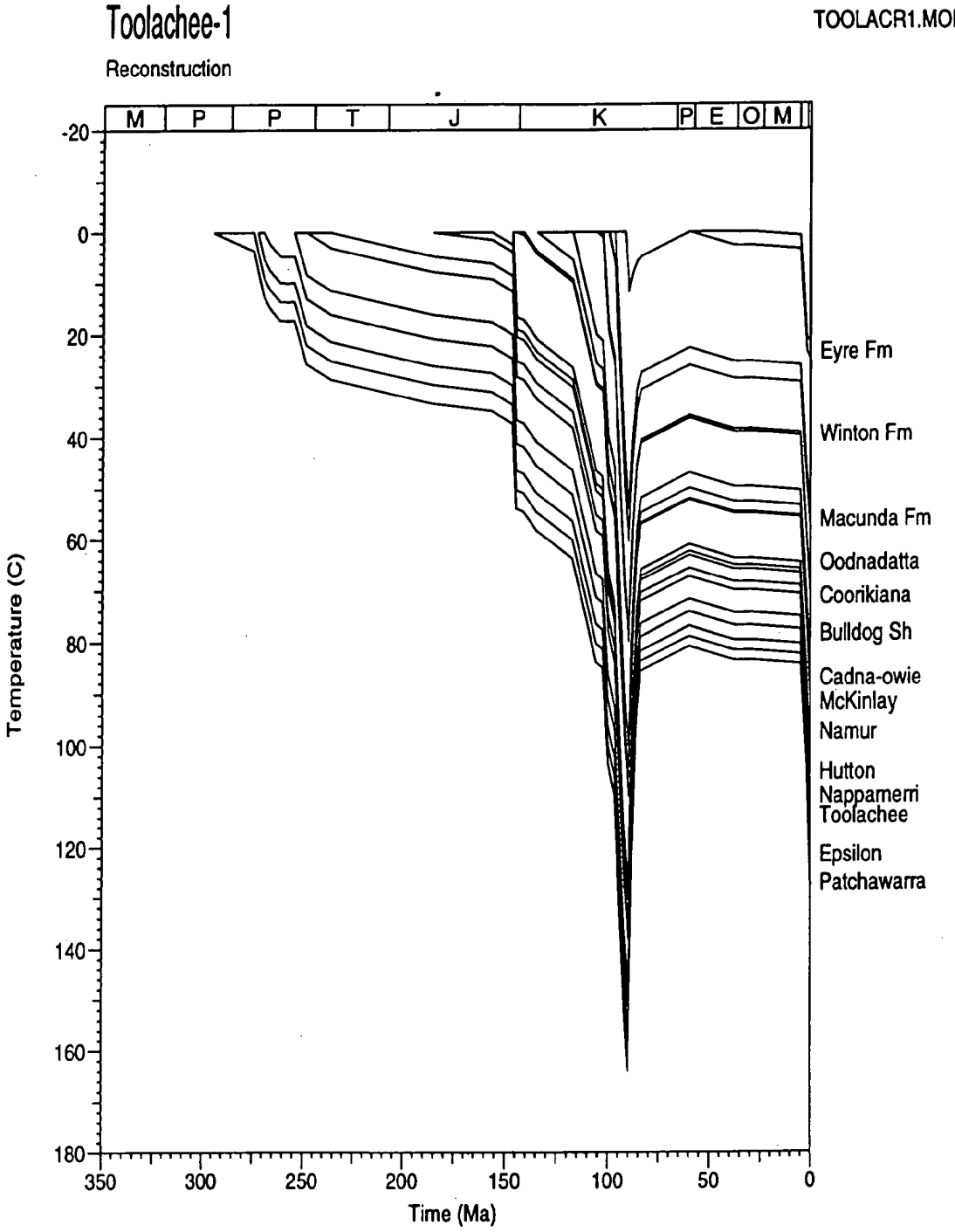

Figure 3.6: Reconstructed thermal history for **Toolachee-1** derived from the AFTA and VR results. Based on a paleogeothermal gradient of 75.5°C/km up until cooling began at 90 Ma (within the possible range from 130 to 60 Ma), at which point it declined to 40°C/km (from AFTA), rising again to 51°C/km at 2 Ma (from AFTA). The surface temperature at 90 Ma is interpreted to have been 0°C (the results are not sensitive to the paleo-surface temperature but reconstruction of the burial history was based on this assumption in order to get a positive intercept at the top of the Winton Fm unconformity. The paleo-surface temperature is assumed to have risen to 20°C in the late Tertiary.

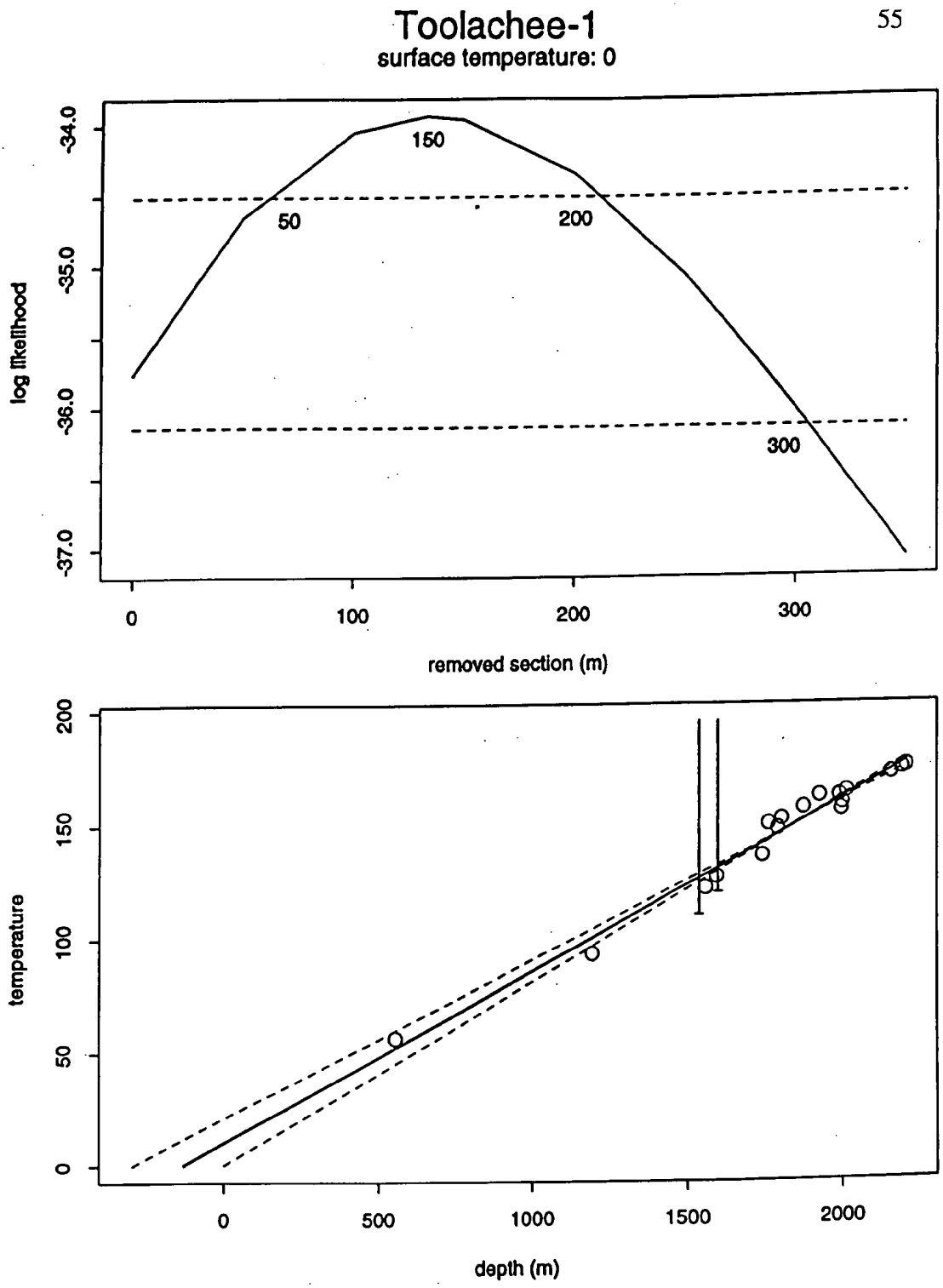

Figure 3.7: Upper: Maximum likelihood profile of estimated *total* section removed by uplift and erosion at the level of the unconformity at the top Winton Formation (~108.2 mTVD bKB) since the Cretaceous-Tertiary heating episode (~130 to 60 Ma) in the **Toolachee-1 well**, derived from the AFTA and VR constrained paleogeothermal gradient shown in Figure 3.5, assuming a paleo-surface temperature of 0°C. The profile gives lower and upper 95% confidence limits of 0 and 300 metres, respectively, and a well defined best-fit value of 150 metres. The methodology employed in deriving this profile is outlined in Appendix C.

Lower: Maximum paleotemperature estimates from AFTA and VR data in the **Toolachee-1 well**, with fitted profile (solid line) and lines (dashed) representing upper and lower 95% confidence limits, extrapolated to the assumed paleo-surface temperature of 0°C.

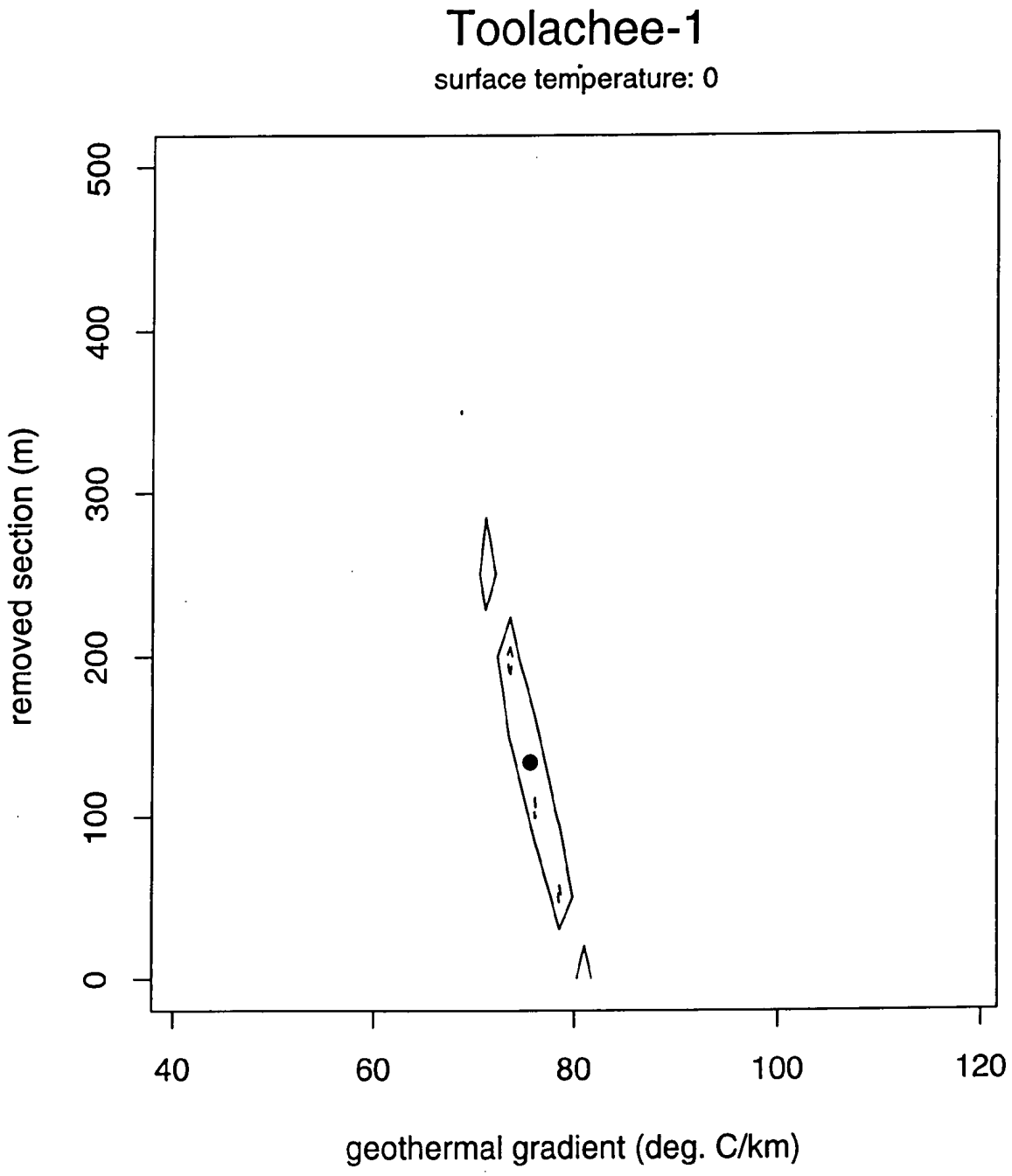

Figure 3.8: Crossplot of total removed section with respect to the level of the unconformity at the top Winton Formation (~108.2 mTVD bKB) since the Cretaceous-Tertiary heating episode (~130 to 60 Ma) in the **Toolachee-1 well**, showing the range of values (within the contoured region) compatible with the maximum paleotemperatures derived from the AFTA and VR data at the 95% confidence level. In effect, the thermal history reconstruction requires only very minor erosion on the top Winton Fm unconformity, with the identified cooling almost entirely attributable to decline in paleogeothermal gradient.

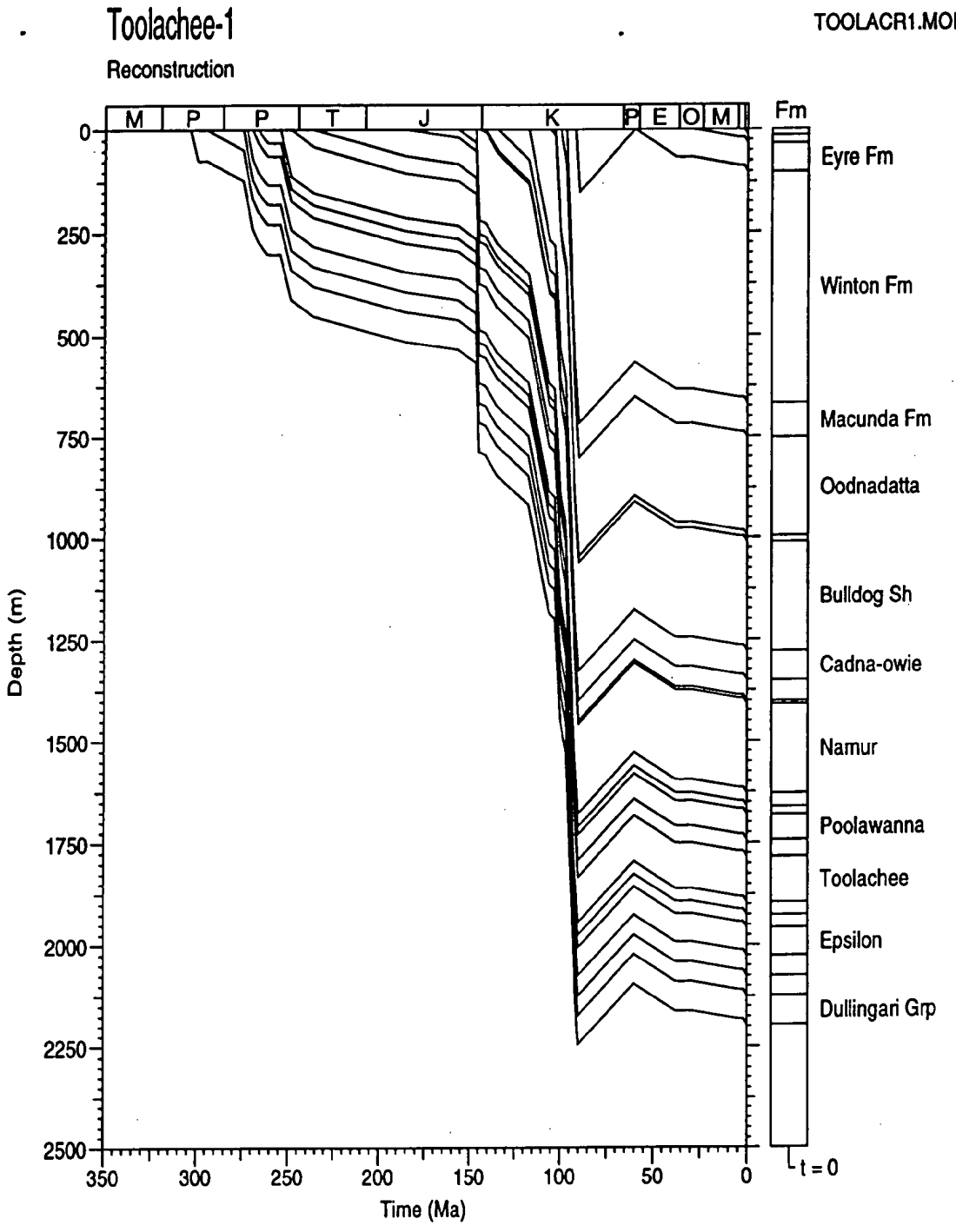

Figure 3.9: Possible burial history consistent with the thermal history reconstruction in the **Toolachee-1 well**. The history involves cooling from maximum paleotemperatures at 90 Ma (130 to 60 Ma allowed by the integrated thermal history results) with 150 m of uplift and erosion beginning at 90 Ma. See text for details.

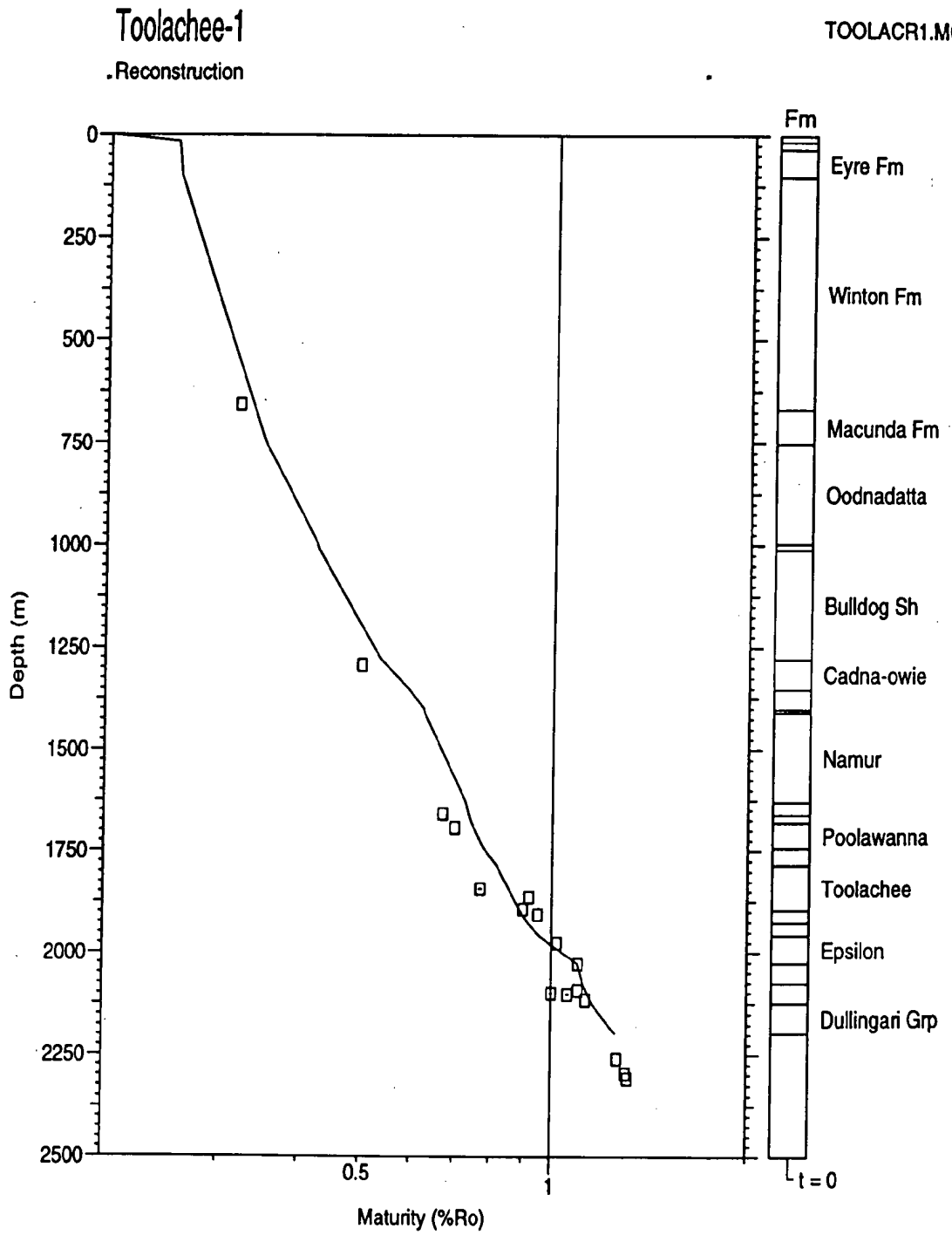

Figure 3.10: Measured vitrinite reflectance data in the **Toolachee-1 well,** and the VR profile with depth predicted from the reconstructed thermal history. The measured vitrinite values shows a very good match to the predicted profile throughout most of the section. The thermal history results show that the maturity values measured at the present-day reached these levels in the Cretaceous - Tertiary as illustrated in Figure 3.6. See text for further details.

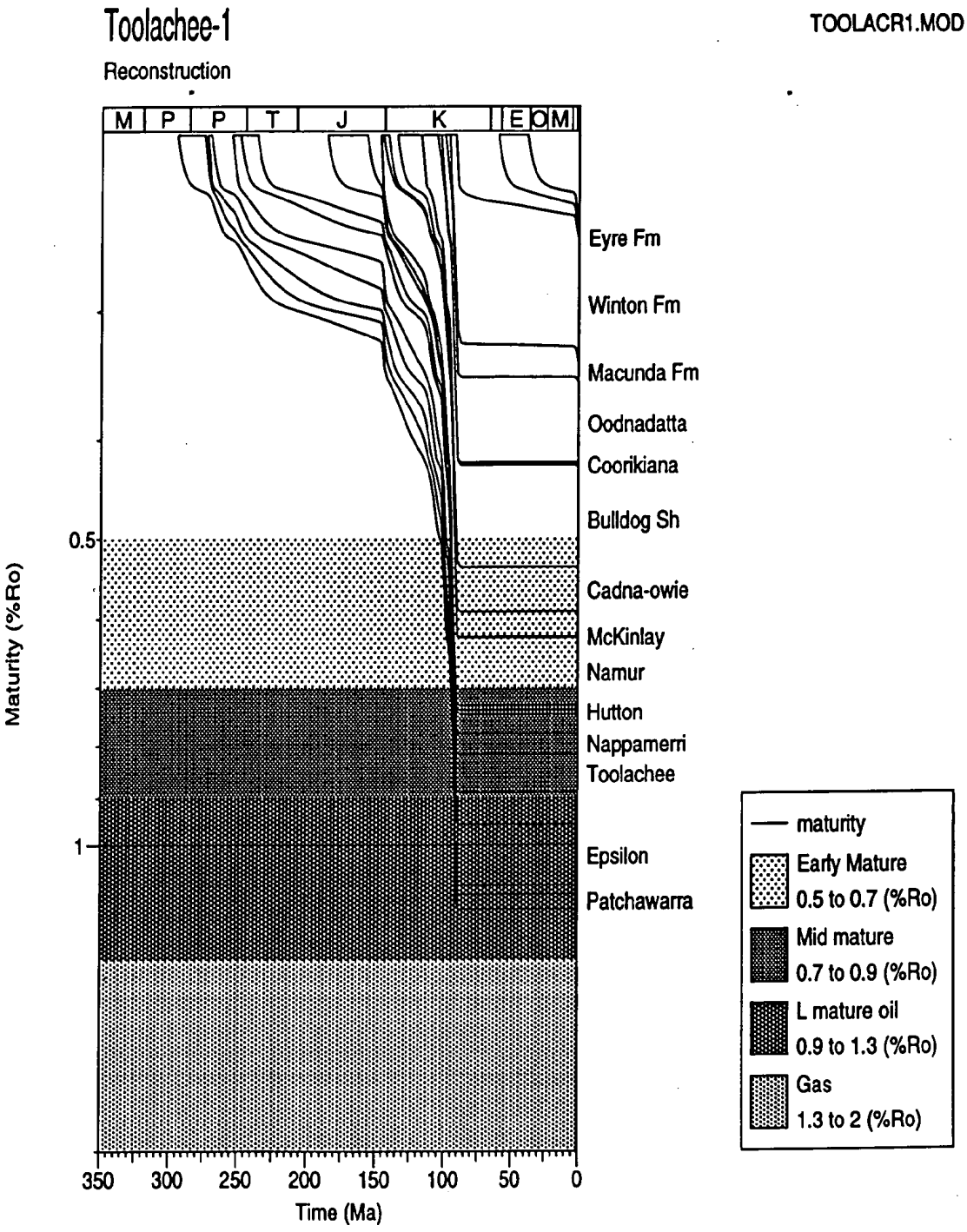

Figure 3.11: Predicted development of maturity with time (using Burnham and Sweeney, 1989) in the **Toolachee-1 well,** controlled by the AFTA results. Maximum maturity is shown as being reached at the 90 Ma (130 to 60 Ma allowed by the results), after progressive heating resulting from burial through the Early Cretaceous. This reconstruction illustrates that maximum maturity in most of the drilled section was reached at 90 Ma (130 to 60 Ma allowed), immediately prior to decline in paleogeothermal gradient and minor uplift and erosion (150 m) that commenced at this time. The reconstructed history predicts a minor increase in maturity in the upper part of the section over the last 90 Ma, but only at maturities less than that required for significant oil generation. No significant maturation can be attributed to the recent increase in geothermal gradient over the last ~2 Ma

4. Thermal history reconstruction in the Beanbush-1 well

4.1 Interpretive format

Interpretation of the AFTA and VR thermal history data in the **Beanbush-1** well follows the format established for Burley-2 provided in full in Section 2.

- The samples processed for AFTA are listed in Table A.1 (Appendix A).
- Stratigraphy of the section drilled is summarised in Table A.3 and shown in Figure 4.1.
- The present-day geothermal gradient calculated from corrected BHT data = 38.5°C/km for a surface temperature of 20°C (Appendix A).

4.2 Thermal history conclusions from the AFTA and VR data

Introduction - Basic data

- Measured fission track parameters and Default History parameters for each sample are summarised in Table 4.1 and plotted against depth and present temperature in Figure 4.1
- Evidence for elevated paleotemperatures in each **Beanbush-1** AFTA sample is summarised in Table 4.2.
- Interpretations of the magnitude and timing of paleotemperatures which are required (or allowed) by AFTA in each sample are discussed in Table 4.3.
- Open file vitrinite reflectance data from **Beanbush-1,** ranging in value from ~0.24 % to 1.5%, are listed in Table D.2 and plotted against depth in Figure 4.2 together with a predicted profile based on the Default Thermal History (see Section 1.6). The Default Burial History is given in Figure 4.3.

Duration of present-day thermal conditions

- The AFTA results (Figure 4.1) indicate that the present-day geothermal gradient has increased to the measured level of ~38.5°C/km from ~30°C/km, or less, at some time within the last 2 Ma (Table 4.3). Published fluid inclusion homogenisation temperatures (Russel and Bone, 1989 - see Figure 4.4) fall on a paleogeothermal gradient of ~34°C/km, lower than the present-day gradient, and may have developed prior to the recent increase in geothermal gradient (see also discussion for the Burley-2 well.

Maximum paleotemperatures from AFTA and VR

- Maximum paleotemperature estimates from VR range from <40 to 188°C (Table iii) and are higher than present temperatures throughout most of the section, with the difference increasing with depth (Figure 4.4). AFTA paleotemperature estimates are presented as *maximum* estimates of maximum paleotemperature after integration with the VR results as discussed in Table 4.3 and plotted in Figure 4.4.

Time of cooling from maximum paleotemperatures from AFTA and VR

- Integration of the AFTA and VR results in samples GC668-238 and 240 from Beanbush-1 indicates that maximum paleotemperatures indicated by the VR results can only have occurred during the interval **125 to 70 Ma.** Paleotemperature estimates from all AFTA and VR samples are summarised in Table iii and plotted against depth in Figure 4.4.

Paleogeothermal gradient at time of maximum paleotemperatures - thermal history reconstruction

- The paleogeothermal gradient at the time of Cretaceous-Tertiary maximum paleotemperatures (125 to 70 Ma) determined from the AFTA and VR results is 46°C/km (maximum likelihood estimate), with 40.5 to 51.5°C/km allowed at the 95% confidence limits (Figure 4.5). The allowed range is significantly higher than the present-day gradient (and even higher than the proposed steady-state gradient operating prior to 2 Ma), indicating a period of significantly elevated heat flow at some time between 125 and 70 Ma, corresponding to the time of maximum paleotemperatures. Paleogeothermal gradient estimates in the **Beanbush-1 well** are summarised in Table v (Executive Summary).

- The simplest reconstructed thermal history for **Beanbush-1** consistent with the data is illustrated in Figure 4.6, and is based on a paleogeothermal gradient of 46°C/km up until cooling began at 90 Ma (within the possible range from 125 to 70 Ma), at which point it declined to 30°C/km (from AFTA), rising to 38.5°C/km at 2 Ma (from AFTA). The surface temperature at 90 Ma is interpreted to have been 0°C (the results are not sensitive to the paleo-surface temperature but reconstruction of the burial history was based on this assumption in order to get a positive intercept at the top of the Winton Fm unconformity. The paleo-surface temperature is assumed to have risen to 20°C in the late Tertiary.

Removed section estimates - burial history reconstruction

- Extrapolation of the allowed range of Cretaceous-Tertiary (125 to 70 Ma) paleogeothermal gradients determined from the AFTA and VR data shown in Figure 4.5 to an assumed paleo-surface temperature of 0°C results in a range of allowed values for the amount of removed section from 150 to 850 m, with a maximum likelihood value of 500 m (Figure 4.7). Correlation between the paleogeothermal gradient and the magnitude of removed section required to explain the paleotemperature results is illustrated in Figure 4.8.

- Removed section estimates determined by these methods for the Cretaceous - Tertiary heating episode identified in the **Beanbush-1 well** are summarised in Table vi (Executive Summary).

- The reconstructed thermal history for **Beanbush-1** strongly suggests that the major controls on the maturation history has been variation in heat flow with a minor contribution from additional burial at the top Winton Formation unconformity. The reconstructed burial history is represented by the preserved stratigraphy in the well plus the best-fit estimate of 500 m of section eroded at the top Winton Formation unconformity as illustrated in Figure 4.9.

Maturation History

- The maturity-depth profile in **Beanbush-1** derived from the reconstructed thermal history shown in Figure 4.6, together with the measured VR data and AFTA-equivalent VR levels, is provided in Figure 4.10. Predicted maturity levels (using the maturation algorithm of Burnham and Sweeney, 1989) agree very well with the measured results throughout the section, for a linear Cretaceous-Tertiary paleogeothermal gradient of 46°C/km.

- Figure 4.11 shows the variation of maturity with time for the **Beanbush-1** well (using the maturation algorithm of Burnham and Sweeney, 1989) derived from the reconstructed thermal history shown in Figure 4.6. This reconstruction illustrates that maximum maturity in most of the drilled section was reached at 90 Ma (125 to 70 Ma allowed), immediately prior to decline in paleogeothermal gradient and minor uplift and erosion that commenced at this time. No significant maturation can be attributed to the recent increase in geothermal gradient over the last ~2 Ma.

Table 4.1: Summary of AFTA data in samples from the Beanbush-1 well, Cooper-Eromanga Basin, South Australia (Geotrack Report #668)

Sample number	Average depth*1	Present temperature*2	Stratigraphic Age	Measured Mean track length	Default mean track length *3	Measured apatite fission track age *4	Default fission track age*3
GC	(m)	(°C)	(Ma)	(µm)	(µm)	(Ma)	(Ma)
668-229	398	35	97-90	14.82±0.17	14.4	***134.0±15***	90
668-233	1189	66	100-97	14.15±0.13	13.1	122.0±7.9	87
668-236	1797	89	117.5-106	12.45±0.45	11.6	***143.0±30***	89
668-238*5	2051	99	145-135	9.51±0.57	10.7	***38.0±5.1***	25
668-240*5	2356	110	157-150	11.28±0.33	9.8	***81.4±13.1***	57

*1 All depths quoted are true vertical depth (TVD) with respect to KB.

*2 See Appendix A for a discussion of present temperature estimation.

*3 AFTA values predicted from the "Default Thermal History" (Section 1.6); i.e., assuming that each sample is now at its maximum temperature since deposition. The values refer only to tracks formed after deposition. Samples may also contain tracks inherited from sediment provenance areas. Calculation of the Default values refer to actual measured compositions of apatites analysed within a particular sample, which is discussed in Appendix A.

*4 Central fission track age quoted (in italics) where P(chi sq) < 5%

*5 Sample data reprocessed specifically for this report and discussed in deatil in Tables 4.2 and 4.3.

Table 4.2: Summary of thermal history interpretation of AFTA data in samples from the Beanbush-1 well, Eromanga Basin, South Australia (Geotrack Report #668)

Sample number	Do AFTA data require any revision of present temperature?	Evidence of higher temperatures in the past from length data?	Evidence of higher temperatures in the past from fission track age data?	Conclusion
668-238 2051 m	Yes Modelling of the AFTA age parameters suggests the present temperature of 99°C has been acting for only a short time or is incorrect.	No [Mean track length is ~1 μm longer than that predicted from the Default Thermal History, suggesting a very recent increase in present temperatures has occurred.	No [Central fission track age and all single grain ages are significantly older than, or similar to, those predicted on the basis of the Default Thermal History]	No direct evidence to suggest that the sample was subjected to paleotemperatures higher than present temperatures at any time after deposition. Note, however, that the AFTA track length data suggests a very recent increase in present temperatures which may mask evidence of higher paleotemperatures.
668-240 2356 m	Yes Modelling of the AFTA length and age parameters suggests the present temperature of 110°C has been acting for only a short time or is incorrect.	No [Mean track length is ~1.5 μm longer than that predicted from the Default Thermal History, suggesting a very recent increase in present temperatures has occurred.	No [Central fission track age and all single grain ages are significantly older than, or similar to, those predicted on the basis of the Default Thermal History]	No direct evidence to suggest that the sample was subjected to paleotemperatures higher than present temperatures at any time after deposition. Note, however, that the AFTA track length data suggests a very recent increase in present temperatures which may mask evidence of higher paleotemperatures.

Note: Interpretation of AFTA data is based on comparison of measured AFTA parameters with values predicted from "Default Thermal History" (Section 1.6); i.e., assuming that each sample is now at its maximum temperature since deposition. The predicted values for each sample are summarised in Table 4.1, and refer only to tracks formed after deposition. Samples may also contain tracks inherited from sediment provenance areas, which must be allowed for in interpreting the data. Calculations refer to apatites with the compositional range appropriate to each sample, as explained in Appendix A.

Table 4.3: Estimates of timing and magnitude of elevated paleotemperatures from AFTA data in samples from the Beanbush-1 well, Cooper-Eromanga Basin, South Australia (Geotrack Report #668)

Sample number GC	Stratigraphic Age (Ma)	Present temperature (°C)	Early episode: Maximum paleo-temperature (°C)	Early episode: Onset of cooling (Ma)	Late episode: Peak paleo-temperature (°C)	Late episode: Duration of heating (Ma)	Comments
668-238 2051 m	145-135 Early Cretaceous	99	120 from VR	125 to 70	99 (present)	<10	Evidence from the AFTA data suggest that this sample cannot have resided near the present temperature of 99°C for more than ~10 Ma, compared to ~90 Ma inferred from the preserved stratigraphy. It is not possible to estimate both the pre-increase paleotemperature and the duration of this temperature increase from the AFTA data alone. If the duration of recent heating is assumed to be 4 Ma (a time derived from AFTA results in deeper samples GC668-240), then maximum paleotemperature during this interval must have been less than ~110°C. A second approach is to integrate other information that might constrain the steady-state geothermal gradient. Fluid inclusion homogenisation temperatures (Russell and Bone, 1989) lie on paleogeothermal gradient of ~34°C/km compared to the present day gradient of 38.4°C/km. From this lower gradient the steady-state temperature of this sample prior to the recent increase may have been ~89°C, consistent with a recent increase in gradient. A measured VR value of 0.65% at around this depth indicates that the maximum *sustained* post-depositional temperature was ~120°C. Using this as an independent estimate of maximum paleotemperature, the AFTA results will only allow such a temperature prior to cooling beginning at some time in the interval between ~125 and 70 Ma. Thus, while the recent increase in temperature demonstrable in this sample significantly complicates the determination of the paleo-thermal history, integration of the AFTA results with independent estimates of paleotemperature allows important constraints to be placed on the time of both maximum paleotemperatures and the duration of the recently developed high temperatures.
					<110	if 4	

Note: **Brackets** surrounding italicised time/temperature constraints indicate that the AFTA results allow, but *do not* require a discrete event at this time.

*1 Based on measured present-day geothermal gradient of 38.5°C/km and a surface temperature of 20°C. As discussed in this table AFTA indicates that this is a recent developed transient thermal regime, and that lower temperatures must have persisted until this recent increase.

Table 4.3 (cont.): Beanbush-1 (Geotrack Report #668)

Sample number GC	Stratigraphic Age (Ma)	Present*1 temperature (°C)	Early episode Maximum paleo-temperature (°C)	Early episode Onset of cooling (Ma)	Late episode Peak paleo-temperature (°C)	Late episode Duration of Heating (Ma)	Comments
668-240 2356 m	157-150 Late Jurassic	110	(<140	(90 assumed)	100 (present)	<4	Evidence from the AFTA length data clearly indicate that this sample cannot have resided near the present temperature of 110°C for more than ~4 Ma, compared to ~90 Ma inferred from the preserved stratigraphy. It is not possible to estimate both the pre-increase paleotemperature and the duration of this temperature increase from the AFTA data alone. One approach is to integrate other information that might constrain the steady-state geothermal gradient. Fluid inclusion homogenisation temperatures (Russell and Bone, 1989) lie on paleogeothermal gradient of ~34°C/km compared to the present day gradient of 38.4°C/km. From this lower gradient the steady-state temperature of this sample prior to the recent increase may have been ~100°C, consistent with a recent increase in gradient. A measured VR value of 0.65% at around this depth indicates that the maximum *sustained* post-depositional temperature was ~120°C. Using this as an independent estimate of maximum paleotemperature, the AFTA results will only allow such a temperature prior to cooling beginning at some time in the interval between ~100 and 45 Ma. One complicating factor is that this VR value may be a little low compared with the trend defined by deeper and shallower data. However, if cooling is assumed to have begun at 90 Ma (a time consistent with AFTA results from this and other wells, as well as regional geological considerations), then the maximum paleotemperature allowed by AFTA is ~140°C. Thus, while the recent increase in temperature demonstrable in this sample significantly complicates the determination of the paleo-thermal history, integration of the AFTA results with independent estimates of paleotemperature, allows important constraints to be placed on the time of both maximum paleotemperatures and the duration of the recently developed high temperatures.
			120 from VR	100 to 45			

Note: **Brackets** surrounding italicised time/temperature constraints indicate that the AFTA results allow, but *do not* require a discrete event at this time.

*1 Based on measured present-day geothermal gradient of 38.5°C/km and a surface temperature of 20°C. As discussed in this table AFTA indicates that this is a recent developed transient thermal regime, and that lower temperatures must have persisted until this recent increase.

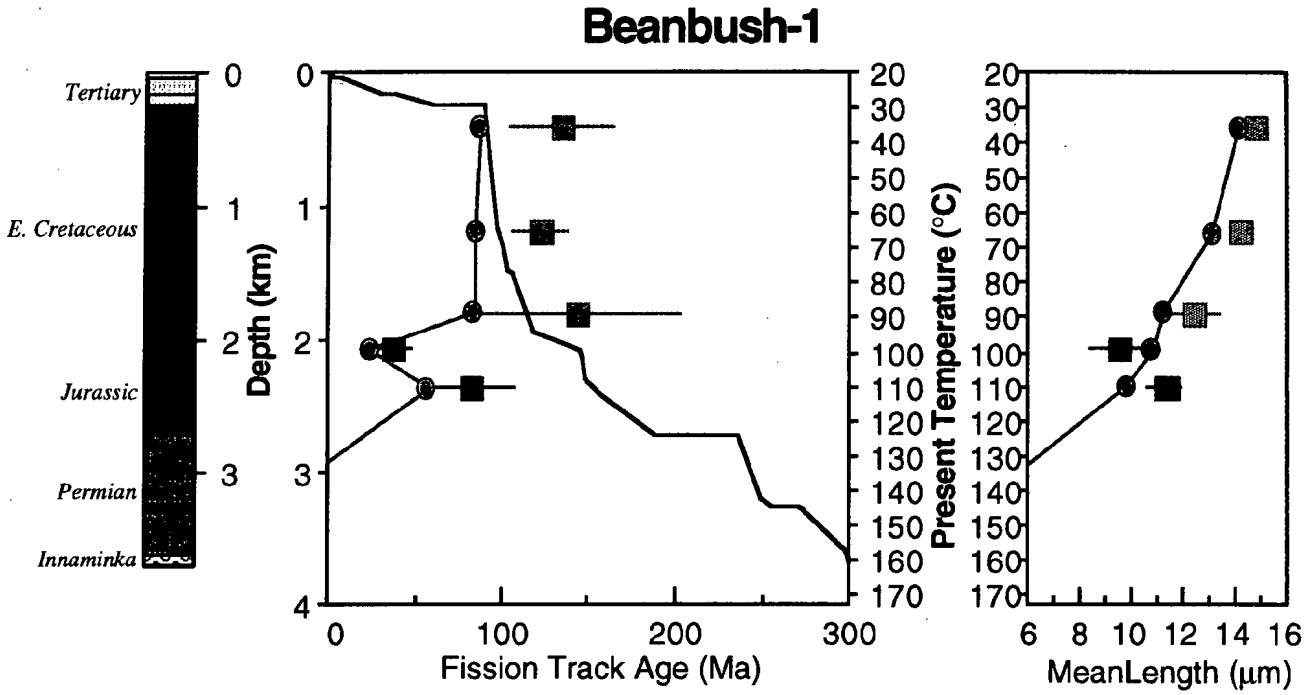

Figure 4.1: AFTA parameters plotted against sample depth and present temperature for samples from the **Beanbush-1 well, Cooper-Eromanga Basin.** Reprocessed data in solid blue; un-reprocessed data in grey (all data in Table 4.1). Round symbols are AFTA parameters predicted from the Default History. Comparison of the Default History parameters with the measured data suggest that the section has increased to the present temperatures in the recent geological past. The variation of stratigraphic age with depth is also shown, as the solid line in the central panel.

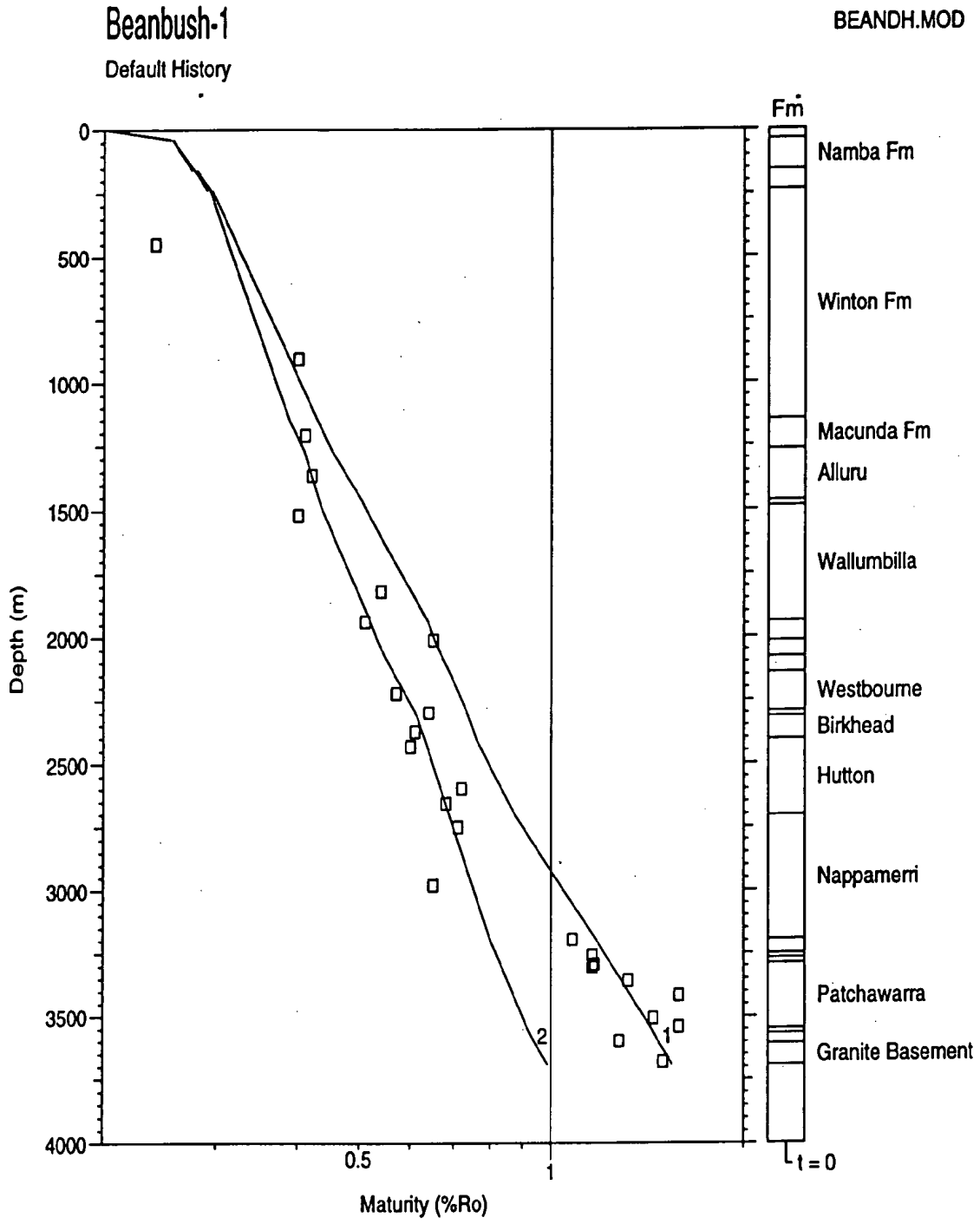

Figure 4.2: Measured vitrinite reflectance data in samples from the **Beanbush-1 well, Cooper-Eromanga Basin** plotted against depth (with respect to KB). A VR profile (Profile 1) predicted from the "Default History" (Section 1.6) is also shown, i.e., the profile expected if samples throughout the section are currently at their maximum temperature since deposition (based on a *measured* present-day geothermal gradient of 51°C/km, and a constant surface temperature of 20°C - Appendix A). Also shown is a second predicted profile (Profile 2) based on the *AFTA-revised* (steady-state) present-day geothermal gradient of 40°C/km (see text). The majority of the measured VR results fall above the predicted profile, more so deeper in the section, suggesting that this part of the section was subjected to maximum paleotemperature significantly higher than present temperatures after deposition. See text for details.

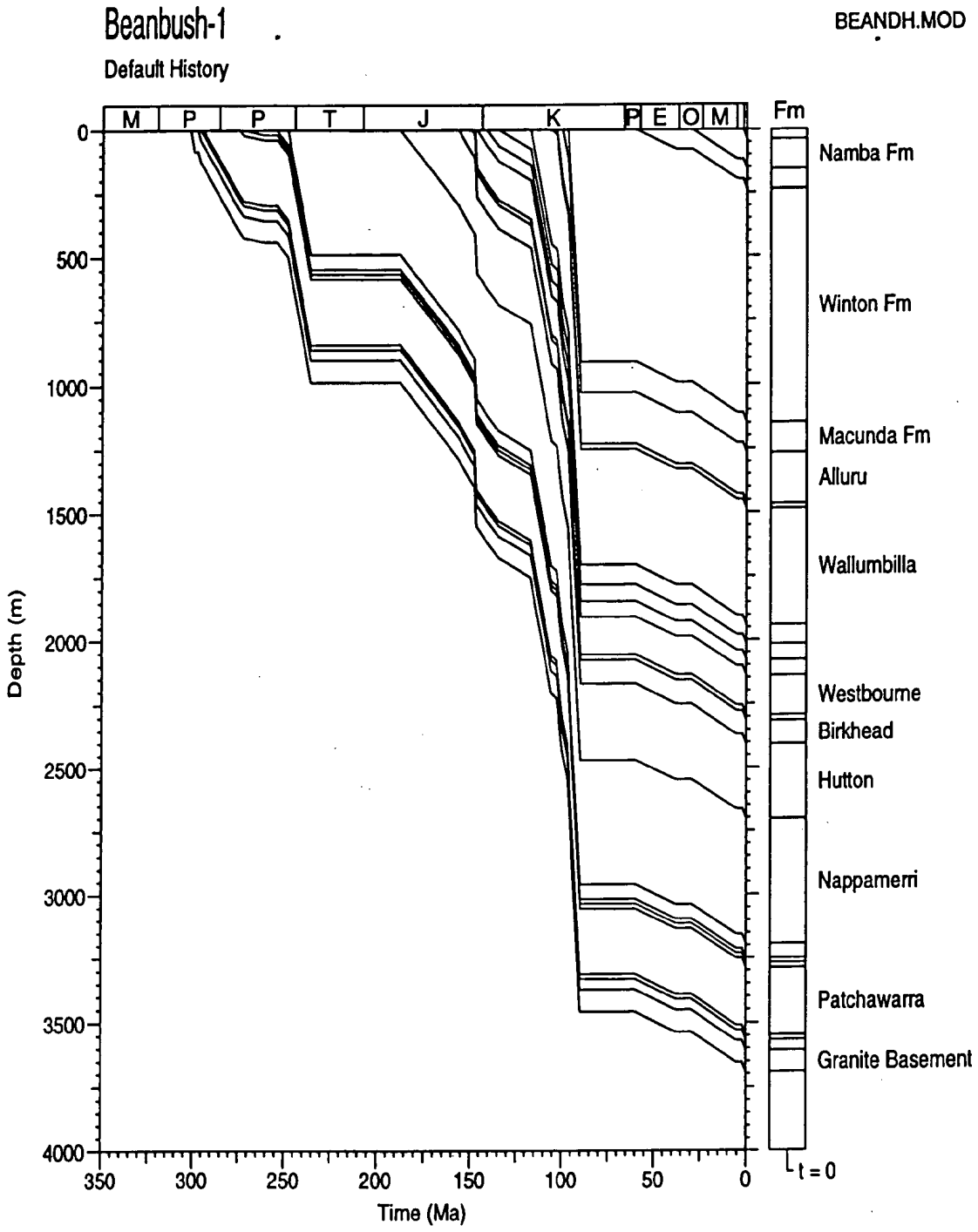

Figure 4.3: Default Burial History for the **Beanbush-1 well, Cooper-Eromanga Basin**, derived from the preserved section which, combined with the present-day thermal conditions, is used in predicting the VR profiles shown in Figure 4.2.

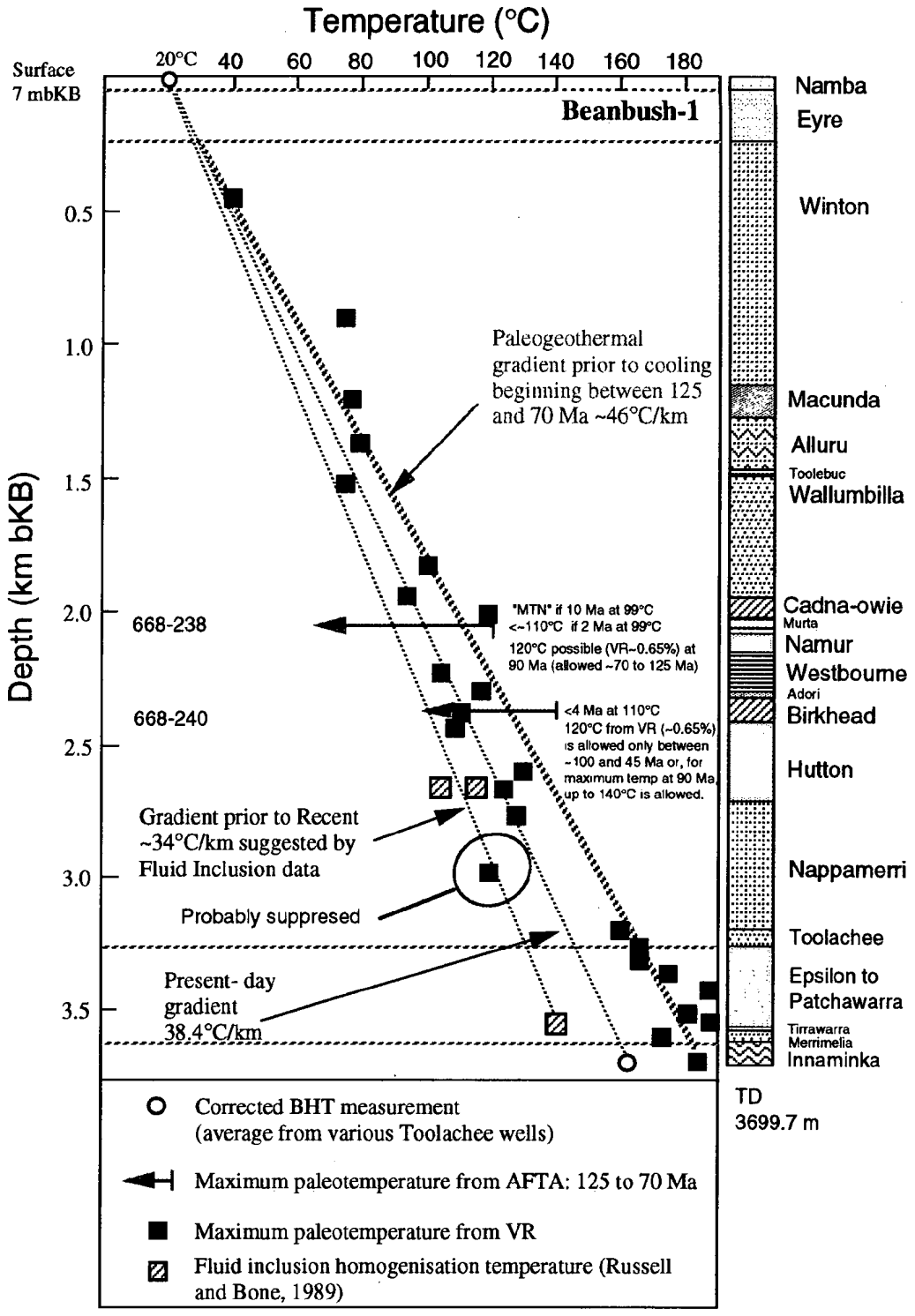

Figure 4.4: Plot of paleotemperatures derived from AFTA and VR data in the **Beanbush-1 well, Eromanga Basin**, against sample depth and the estimated present temperature profile for this well (see Appendix A).

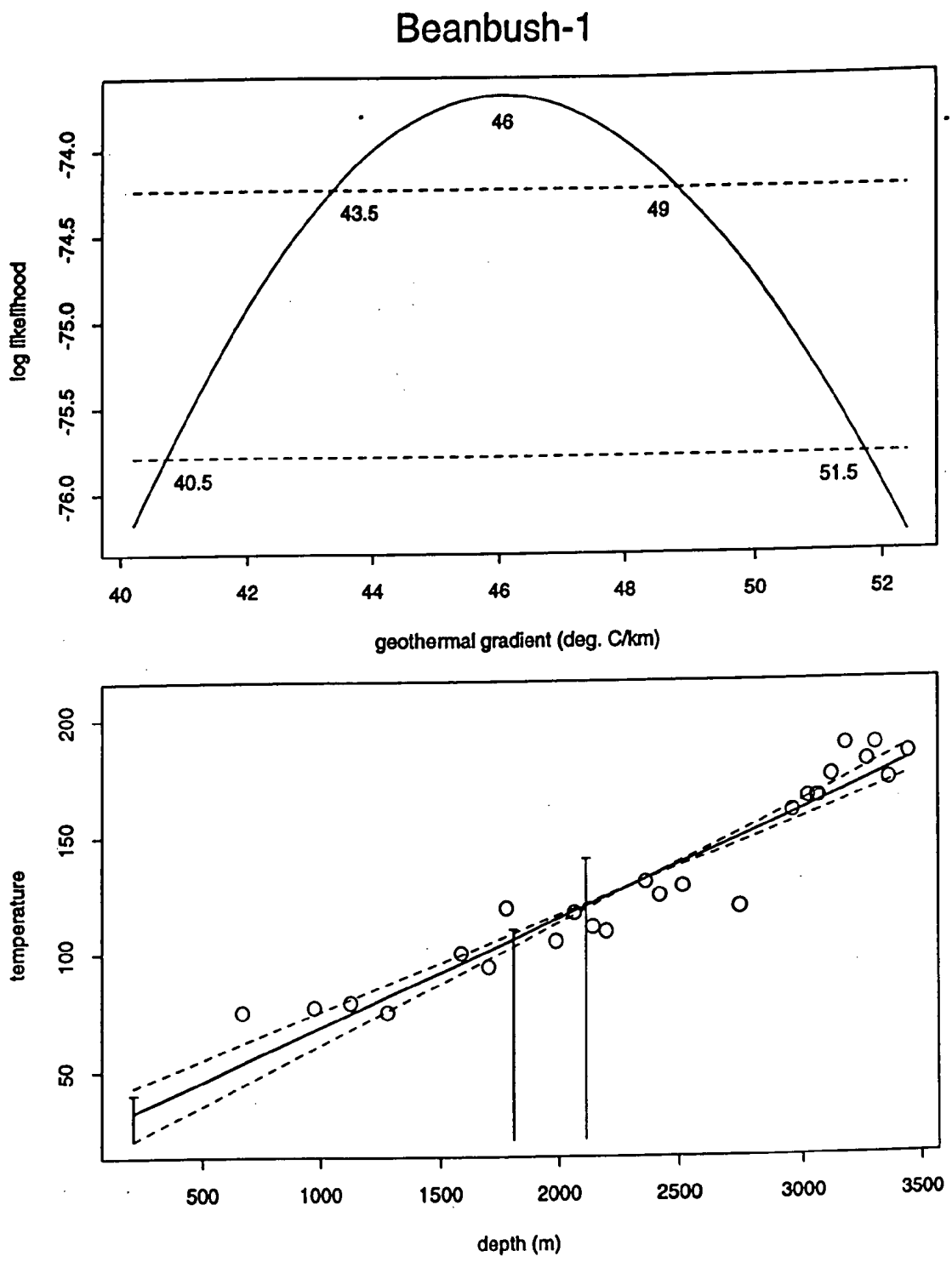

Figure 4.5: Upper: Maximum likelihood profile of linear paleogeothermal gradient fitted to the Cretaceous - Tertiary (~130 to 60 Ma) paleotemperature estimates from the AFTA and VR results in the **Beanbush-1 well**. The profile shows good quadratic behaviour suggesting a well constrained value, with upper and lower 95% confidence limits of 82 and 69°C/km, respectively, and a best-fit value of 75.5°C/km. The methodology employed in deriving this profile is outlined in Appendix C.

Lower: Maximum paleotemperature estimates from AFTA and VR in the **Beanbush-1 well**, with fitted profile (solid line) and lines (dashed) representing upper and lower 95% confidence limits.

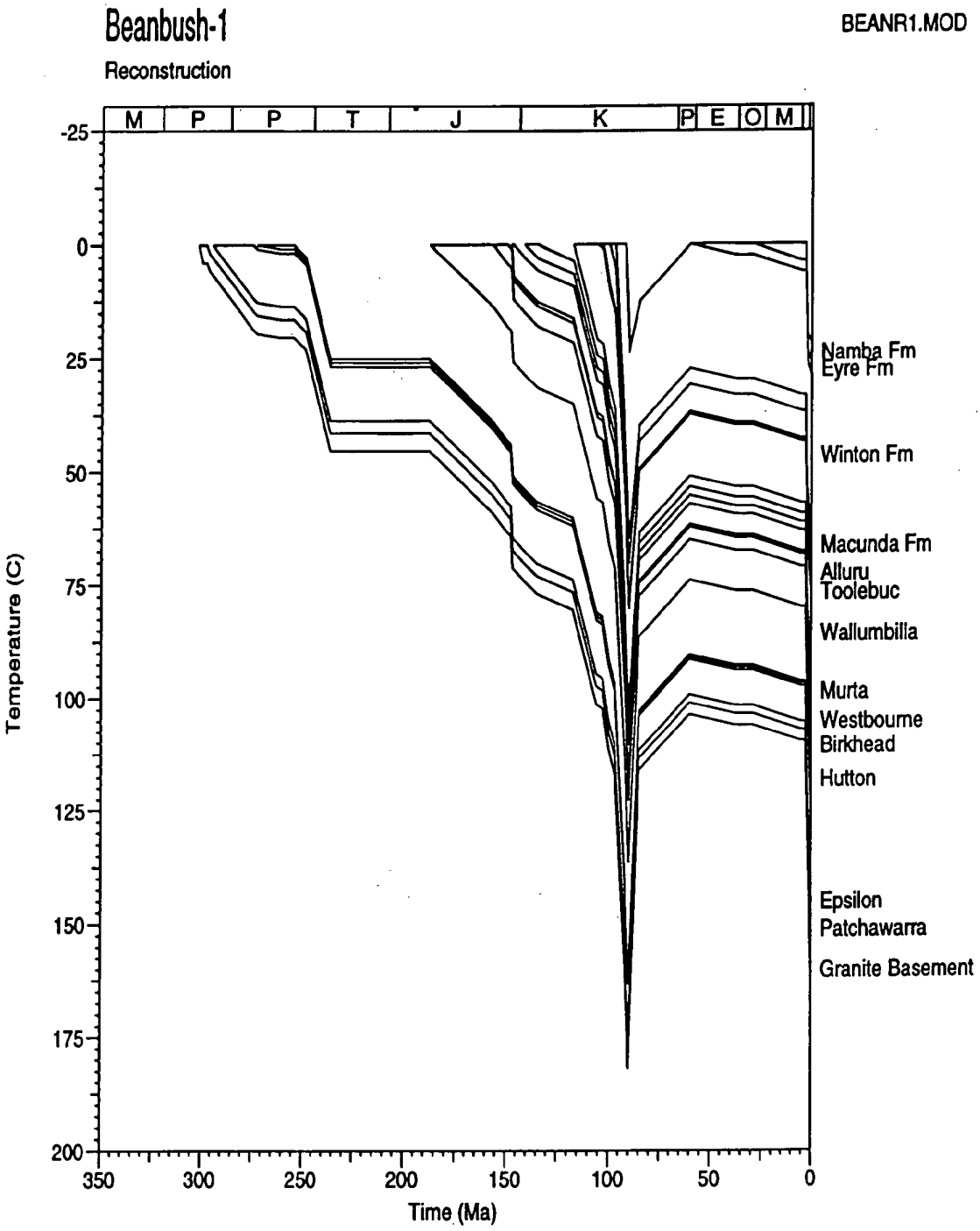

Figure 4.6: Reconstructed thermal history for **Beanbush-1** derived from the AFTA and VR results. Based on a paleogeothermal gradient of 75.5°C/km up until cooling began at 90 Ma (within the possible range from 130 to 60 Ma), at which point it declined to 40°C/km (from AFTA), rising again to 51°C/km at 2 Ma (from AFTA). The surface temperature at 90 Ma is interpreted to have been 0°C (the results are not sensitive to the paleo-surface temperature but reconstruction of the burial history was based on this assumption in order to get a positive intercept at the top of the Winton Fm unconformity. The paleo-surface temperature is assumed to have risen to 20°C in the late Tertiary.

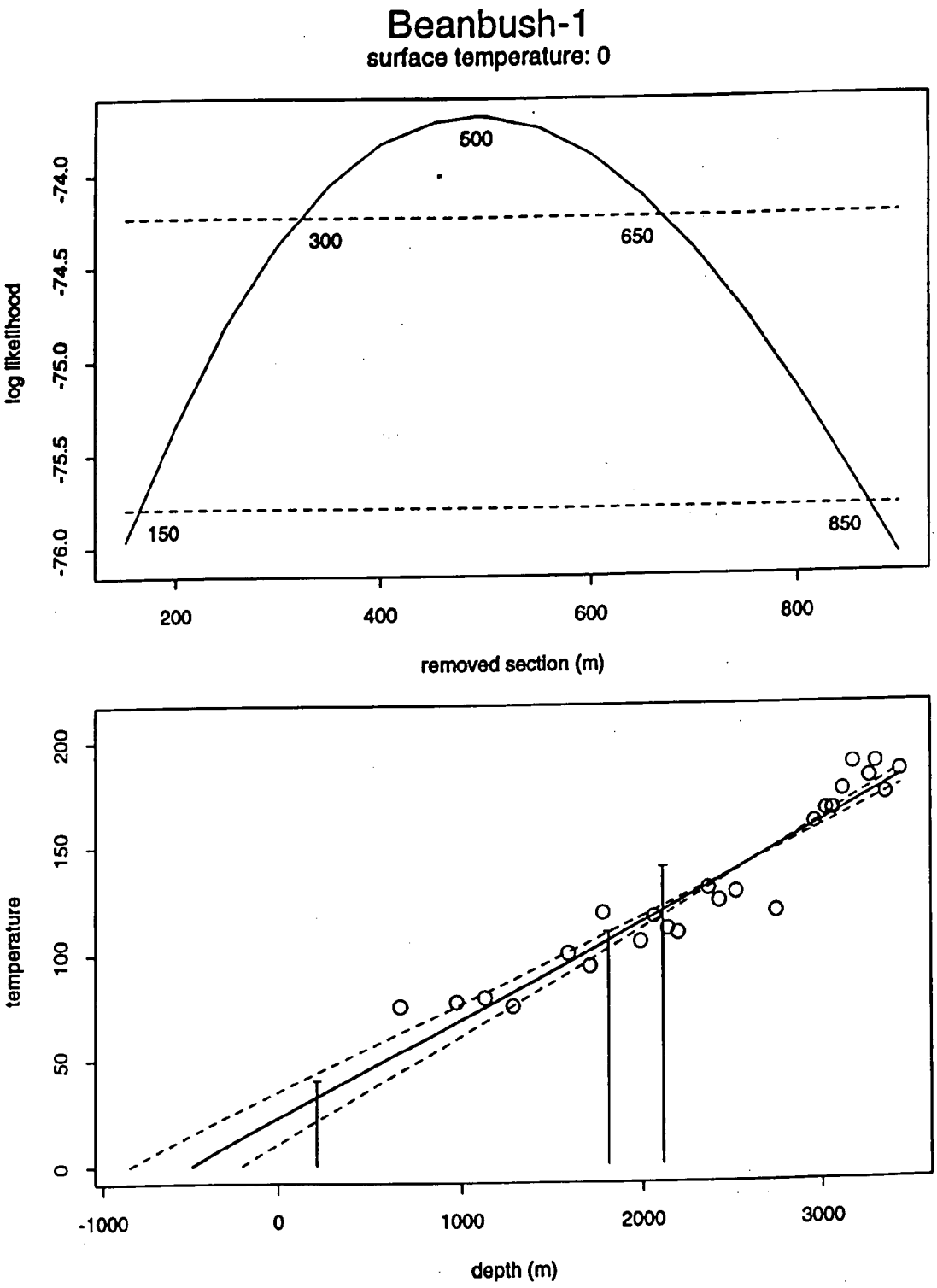

Figure 4.7: Upper: Maximum likelihood profile of estimated *total* section removed by uplift and erosion at the level of the unconformity at the top Winton Formation (~108.2 mTVD bKB) since the Cretaceous-Tertiary heating episode (~130 to 60 Ma) in the **Beanbush-1 well**, derived from the AFTA and VR constrained paleogeothermal gradient shown in Figure 4.5, assuming a paleo-surface temperature of 0°C. The profile gives lower and upper 95% confidence limits of 0 and 300 metres, respectively, and a well defined best-fit value of 150 metres. The methodology employed in deriving this profile is outlined in Appendix C.

Lower: Maximum paleotemperature estimates from AFTA and VR data in the **Beanbush-1 well**, with fitted profile (solid line) and lines (dashed) representing upper and lower 95% confidence limits, extrapolated to the assumed paleo-surface temperature of 0°C.

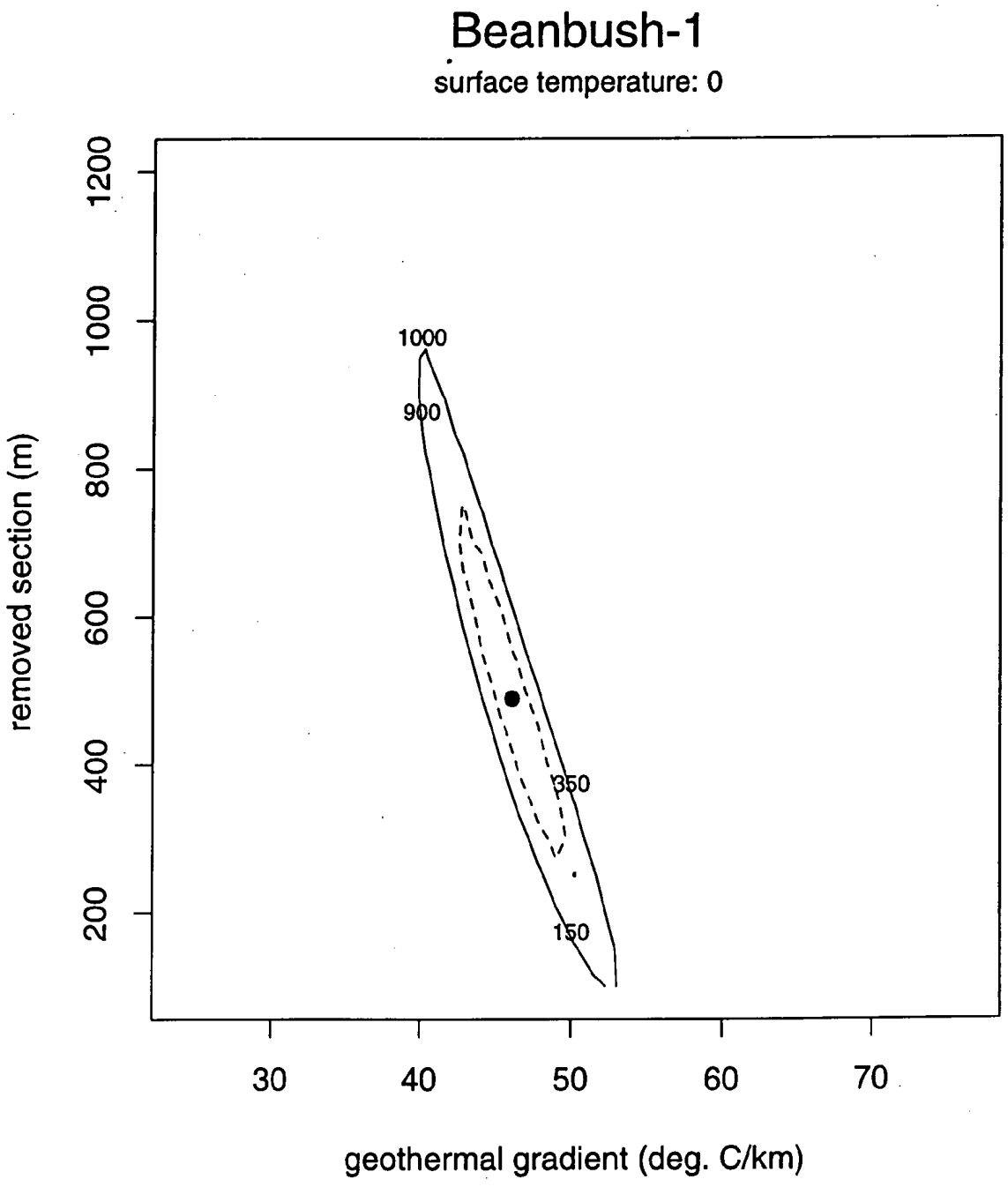

Figure 4.8: Crossplot of total removed section with respect to the level of the unconformity at the top Winton Formation (~108.2 mTVD bKB) since the Cretaceous-Tertiary heating episode (~130 to 60 Ma) in the **Beanbush-1 well**, showing the range of values (within the contoured region) compatible with the maximum paleotemperatures derived from the AFTA and VR data at the 95% confidence level. In effect, the thermal history reconstruction requires only very minor erosion on the top Winton Fm unconformity, with the identified cooling almost entirely attributable to decline in paleogeothermal gradient.

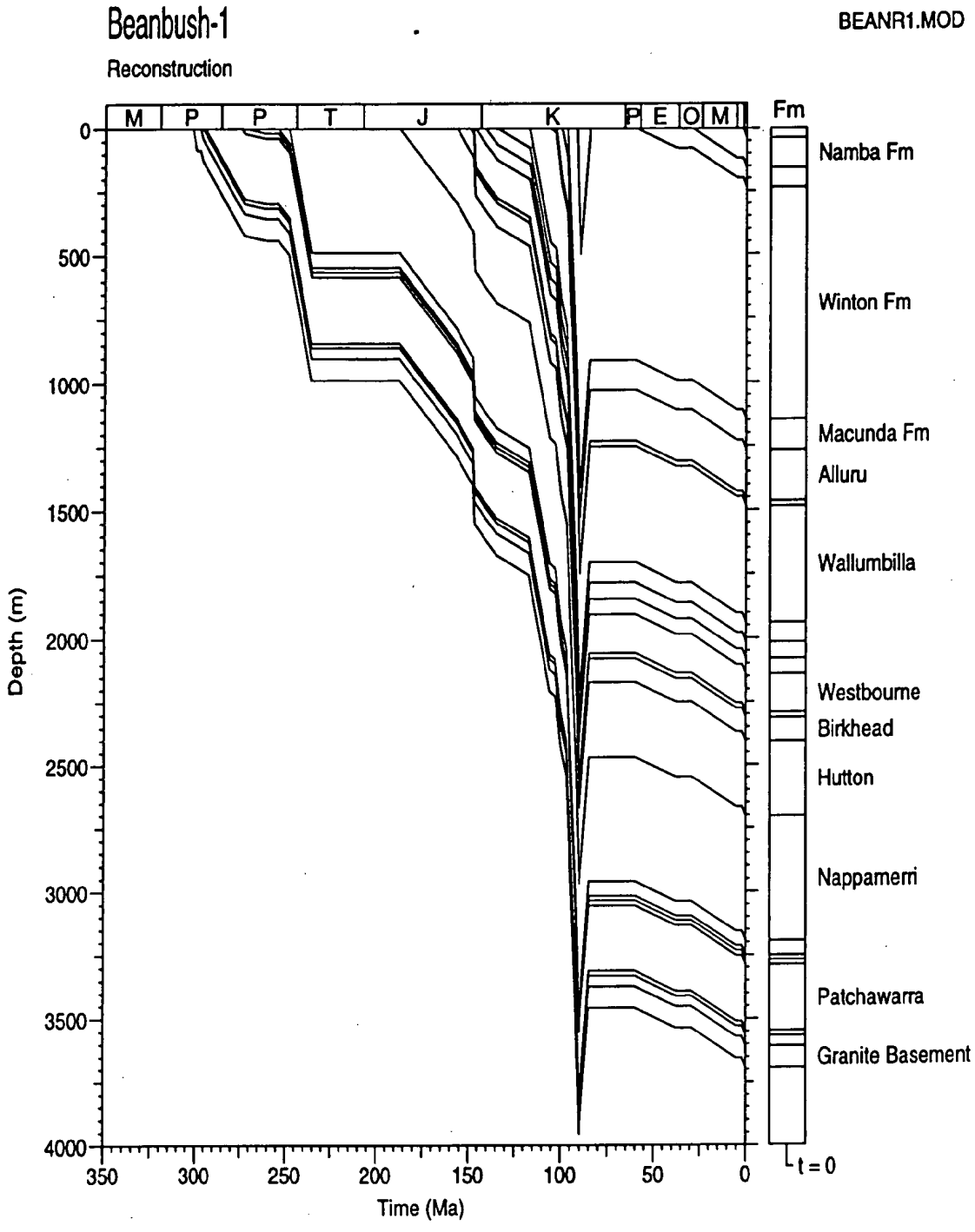

Figure 4.9: Possible burial history consistent with the thermal history reconstruction in the **Beanbush-1 well**. The history involves cooling from maximum paleotemperatures at 90 Ma (130 to 60 Ma allowed by the integrated thermal history results) with 150 m of uplift and erosion beginning at 90 Ma. See text for details.

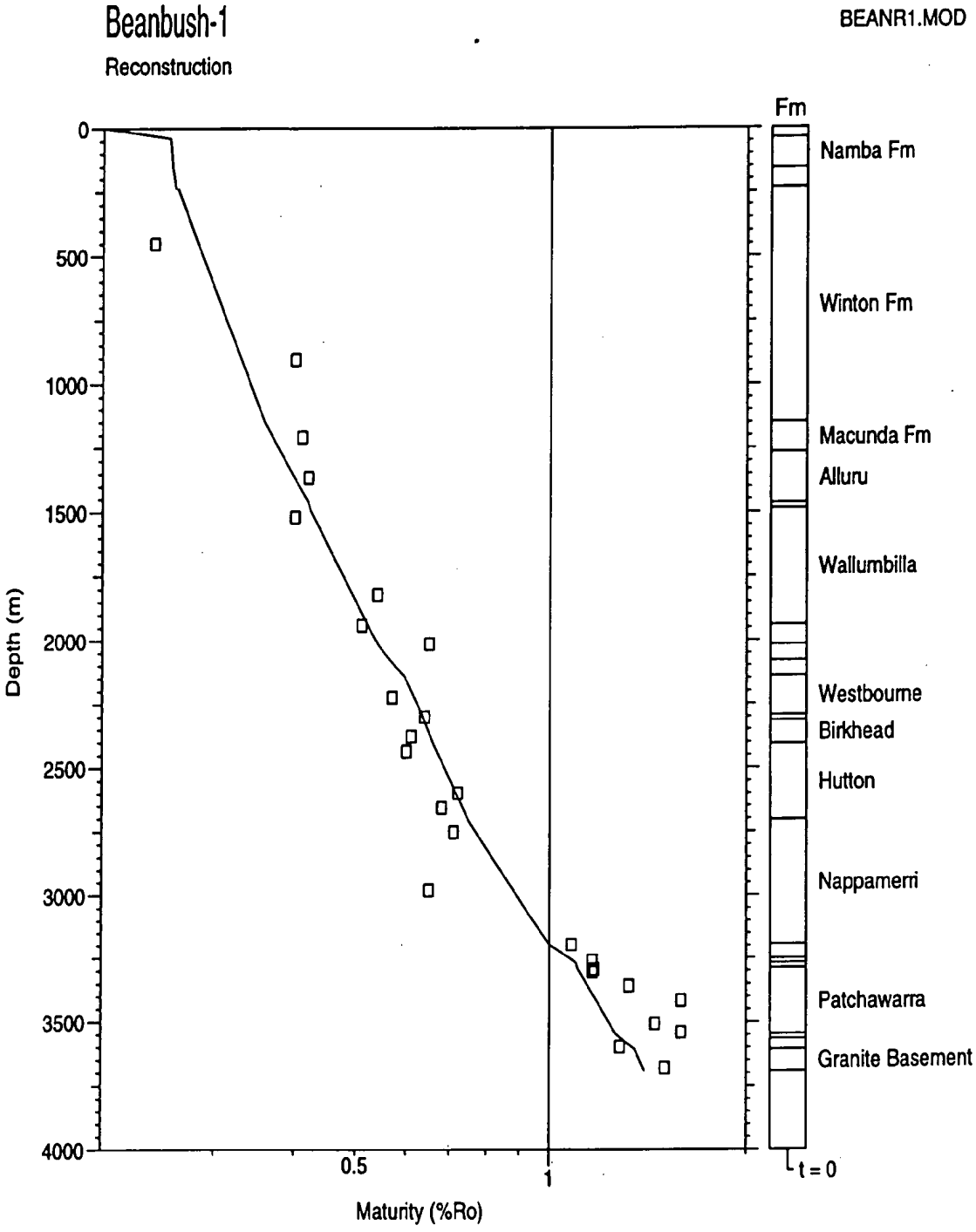

Figure 4.10: Measured vitrinite reflectance data in the **Beanbush-1 well,** and the VR profile with depth predicted from the reconstructed thermal history. The measured vitrinite values shows a very good match to the predicted profile throughout most of the section. The thermal history results show that the maturity values measured at the present-day reached these levels in the Cretaceous - Tertiary as illustrated in Figure 4.6. See text for further details.

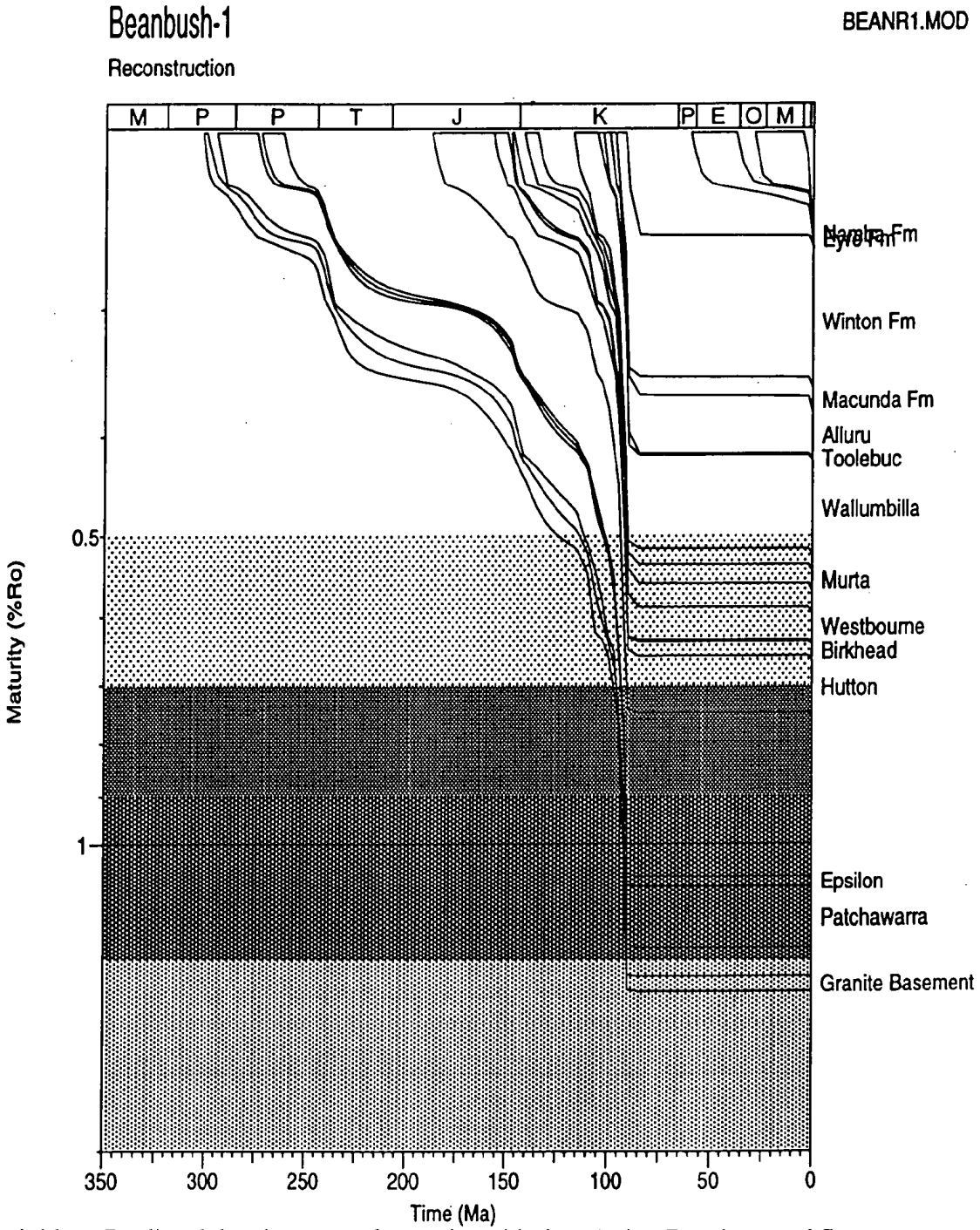

Figure 4.11: Predicted development of maturity with time (using Burnham and Sweeney, 1989) in the **Beanbush-1 well,** controlled by the AFTA results. Maximum maturity is shown as being reached at the 90 Ma (130 to 60 Ma allowed by the results), after progressive heating resulting from burial through the Early Cretaceous. This reconstruction illustrates that maximum maturity in most of the drilled section was reached at 90 Ma (130 to 60 Ma allowed), immediately prior to decline in paleogeothermal gradient and minor uplift and erosion (150 m) that commenced at this time. The reconstructed history predicts a minor increase in maturity in the upper part of the section over the last 90 Ma, but only at maturities less than that required for significant oil generation. No significant maturation can be attributed to the recent increase in geothermal gradient over the last ~2 Ma

5. Thermal history reconstruction in the Tirrawarra-1 well

5.1 Interpretive format

Interpretation of the AFTA and VR thermal history data in the **Tirrawarra-1** well follows the format established for Burley-2 provided in full in Section 2.

- The samples processed for AFTA are listed in Table A.1 (Appendix A).
- Stratigraphy of the section drilled is summarised in Table A.3 and shown in Figure 5.1.
- The present-day geothermal gradient calculated from corrected BHT data = 41.5°C/km for a surface temperature of 20°C (Appendix A).

5.2 Thermal history conclusions from the AFTA and VR data

Introduction - Basic data

- Measured fission track parameters and Default History parameters for each sample are summarised in Table 5.1 and plotted against depth and present temperature in Figure 5.1.
- Evidence for elevated paleotemperatures in each **Tirrawarra-1** AFTA sample is summarised in Table 5.2.
- Interpretations of the magnitude and timing of paleotemperatures which are required (or allowed) by AFTA in each sample are discussed in Table 5.3.
- Open file vitrinite reflectance data from **Tirrawarra-1, -2, -16 & -17,** ranging in value from ~0.6 % to 1.62%, are listed in Table D.2 and plotted against depth in Figure 5.2, together with a predicted profile based on the Default Thermal History (see Section 1.6). The Default Burial History is given in Figure 5.3.

Duration of present-day thermal conditions

- The AFTA results (Figure 5.1) suggest that the present-day geothermal gradient has increased to the measured level of 41.5°C/km from ~35°C/km, or less, at some time within the last 2 Ma (Table 5.3). This is supported by published fluid inclusion homogenisation temperatures (Russel and Bone, 1989 - see Figure 5.4) which fall on a paleogeothermal gradient of ~37°C/km, lower than the present-day gradient, suggesting they may have developed prior to the recent

increase in geothermal gradient (see also discussion for the Burley-2 and Beanbush-1 wells).

Maximum paleotemperatures from AFTA and VR

- Maximum paleotemperature estimates from VR range from ~109 to 190°C (Table iv) and are higher than present temperatures throughout the section, with the difference increasing with depth (Figure 5.4). AFTA paleotemperature estimates are presented as *maximum* estimates of maximum paleotemperature after integration with the VR results as discussed in Table 5.3 and plotted in Figure 5.4.

Time of cooling from maximum paleotemperatures from AFTA and VR

- AFTA results in samples from **Tirrawarra-1** provide no clear evidence for the time of maximum paleotemperatures indicated by the VR results. Stratigraphic distribution of affected samples indicate a maximum probable time of ~112 Ma (Albian age of Alluru Fm). Based on results from other wells we assume that the period of elevated paleogeothermal gradient in this well occurred during the interval **97 to 75 Ma** as defined by the overlapping constraints from **Burely-2 (97 to 50 Ma), Toolachee-1 (130 to 75 Ma) and Beanbush-1 (125 to 70 Ma).** Paleotemperature estimates from all AFTA and VR samples are summarised in Table iii and plotted against depth in Figure 5.4.

Paleogeothermal gradient at time of maximum paleotemperatures - thermal history reconstruction

- The paleogeothermal gradient at the time of Cretaceous-Tertiary maximum paleotemperatures (97 to 75 Ma) determined from the AFTA and VR results is 60.5°C/km (maximum likelihood estimate), with 44.5 to 70.5°C/km allowed at the 95% confidence limits (Figure 5.5). The allowed range is significantly higher than the present-day gradient (and even higher than the proposed steady-state gradient operating prior to 2 Ma), indicating a period of significantly elevated heat flow at some time between 97 and 75 Ma, corresponding to the time of maximum paleotemperatures. Paleogeothermal gradient estimates in the **Tirrawarra-1 well** are summarised in Table v (Executive Summary).

- The simplest reconstructed thermal history for **Tirrawarra-1** consistent with the data is illustrated in Figure 5.6, and is based on a paleogeothermal gradient of 60.5°C/km up until cooling began at 90 Ma (within the possible range from 97 to 75 Ma), at which point it declined to 35°C/km (from AFTA), rising to

41.5°C/km at 2 Ma (from AFTA). The surface temperature at 90 Ma is interpreted to have been 0°C (the results are not sensitive to the paleo-surface temperature but reconstruction of the burial history was based on this assumption in order to get a positive intercept at the top of the Winton Fm unconformity. The paleo-surface temperature is assumed to have risen to 20°C in the late Tertiary.

Removed section estimates - burial history reconstruction

- Extrapolation of the allowed range of Cretaceous-Tertiary (97 to 75 Ma) paleogeothermal gradients determined from the VR data shown in Figure 5.5 to an assumed paleo-surface temperature of 0°C results in a range of allowed values for the amount of removed section from 0 to 850 m, with a maximum likelihood value of 100 m (Figure 5.7). Correlation between the paleogeothermal gradient and the magnitude of removed section required to explain the paleotemperature results is illustrated in Figure 5.8.

- Removed section estimates determined by these methods for the Cretaceous - Tertiary heating episode identified in the **Tirrawarra-1 well** are summarised in Table vi (Executive Summary).

- The reconstructed thermal history for **Tirrawarra-1** strongly suggests that the major controls on the maturation history has been variation in heat flow with a minor contribution from additional burial at the top Winton Formation unconformity. The reconstructed burial history is represented by the preserved stratigraphy in the well plus the best-fit estimate of 100 m of section eroded at the top Winton Formation unconformity as illustrated in Figure 5.9.

Maturation History

- The maturity-depth profile in **Tirrawarra-1** derived from the reconstructed thermal history shown in Figure 5.6, together with the measured VR data and AFTA-equivalent VR levels, is provided in Figure 5.10. Predicted maturity levels (using the maturation algorithm of Burnham and Sweeney, 1989) agree very well with the measured results throughout the section, for a linear Cretaceous-Tertiary paleogeothermal gradient of 60.5°C/km.

- Figure 5.11 shows the variation of maturity with time for the **Tirrawarra-1** well (using the maturation algorithm of Burnham and Sweeney, 1989) derived from the reconstructed thermal history shown in Figure 5.6. This reconstruction

illustrates that maximum maturity in most of the drilled section was reached at 90 Ma (97 to 75 Ma allowed), immediately prior to decline in paleogeothermal gradient and minor uplift and erosion that commenced at this time. No significant maturation can be attributed to the recent increase in geothermal gradient over the last ~2 Ma.

Table 5.1: Summary of AFTA data in samples from the Tirrawarra-1 well, Cooper-Eromanga Basin, South Australia (Geotrack Report #668)

Sample number	Average depth*1	Present temperature*2	Stratigraphic Age	Measured Mean track length	Default mean track length *3	Measured apatite fission track age *4	Default fission track age*3
GC	(m)	(°C)	(Ma)	(μm)	(μm)	(Ma)	(Ma)
668-152*5	407	37	97-90	12.99±0.50	14.4	132.4±12.5	90
668-156*5	1586	86	117.5-100	12.96±0.26	11.8	121.3±11.6	90
668-157*5	1669	89	135-117.5	12.89±0.62	11.6	135.3±18.4	94
668-158*5	1827	96	148-145	11.65±0.74	11.1	*136.7±17.0*	104
668-160*5	2010	103	157-150	9.22±0.56	10.6	*96.1±13.5*	92

*1 All depths quoted are true vertical depth (TVD) with respect to KB.

*2 See Appendix A for a discussion of present temperature estimation.

*3 AFTA values predicted from the "Default Thermal History" (Section 1.6); i.e., assuming that each sample is now at its maximum temperature since deposition. The values refer only to tracks formed after deposition. Samples may also contain tracks inherited from sediment provenance areas. Calculation of the Default values refer to actual measured compositions of apatites analysed within a particular sample, which is discussed in Appendix A.

*4 Central fission track age quoted (in italics) where P(chi sq) < 5%

*5 All sample data reprocessed specifically for this report and discussed in deatil in Tables 3.2 and 3.3.

Table 5.2: Summary of thermal history interpretation of AFTA data in samples from the Tirrawarra-1 well, Eromanga Basin, South Australia (Geotrack Report #668)

Sample number	Do AFTA data require any revision of present temperature?	Evidence of higher temperatures in the past from length data?	Evidence of higher temperatures in the past from fission track age data?	Conclusion
668-152 407 m	No 37°C	Yes, equivocal [Mean track length is ~1 µm shorter than that predicted from the Default Thermal History. Modelling suggests that the shorter tracks may be either inherited from the sediment source terrain or results from paleotemperatures higher than present temperatures after deposition.	No [Pooled fission track age is significantly older than that predicted on the basis of the Default Thermal History]	No direct evidence to suggest that the sample was subjected to paleotemperatures higher than present temperatures at any time after deposition, although the data would allow higher paleotemperatures within specified limits.
668-156 1586 m	Yes Modelling of the AFTA age parameters suggests the present temperature of 86°C has been acting for only a short time or is incorrect.	No [Mean track length is ~1 µm longer than that predicted from the Default Thermal History, suggesting a very recent increase in present temperatures has occurred.	No [Pooled fission track age is significantly older than that predicted on the basis of the Default Thermal History]	No direct evidence to suggest that the sample was subjected to paleotemperatures higher than present temperatures at any time after deposition. Note, however, that the AFTA track length data suggests a very recent increase in present temperatures which may mask evidence of higher paleotemperatures, which would be allowed within specified limits.
668-157 1669 m	No 89°C	No [Mean track length is only broadly controlled but is similar to that predicted from the Default Thermal History].	No [Pooled fission track age is significantly older than that predicted on the basis of the Default Thermal History]	No direct evidence to suggest that the sample was subjected to paleotemperatures higher than present temperatures at any time after deposition, although the data would allow higher paleotemperatures within specified limits.

Note: Interpretation of AFTA data is based on comparison of measured AFTA parameters with values predicted from "Default Thermal History" (Section 1.6); i.e., assuming that each sample is now at its maximum temperature since deposition. The predicted values for each sample are summarised in Table 5.1, and refer only to tracks formed after deposition. Samples may also contain tracks inherited from sediment provenance areas, which must be allowed for in interpreting the data. Calculations refer to apatites with the compositional range appropriate to each sample, as explained in Appendix A.

Table 5.2 (cont.): Tirrawarra-1

Sample number	Do AFTA data require any revision of present temperature?	Evidence of higher temperatures in the past from length data?	Evidence of higher temperatures in the past from fission track age data?	Conclusion
668-158 1827 m	No 96°C	No [Mean track length is only broadly controlled but is similar to that predicted from the Default Thermal History].	No [Central fission track age and all but one single grain age are similar to, or significantly older than, those predicted on the basis of the Default Thermal History]	No direct evidence to suggest that the sample was subjected to paleotemperatures higher than present temperatures at any time after deposition, although the data would allow higher paleotemperatures within specified limits.
668-160 2010 m	No 103°C	No [Mean track length is only broadly controlled but is similar to that predicted from the Default Thermal History].	No [Central fission track age and most single grain ages are similar to, or significantly older than, those predicted on the basis of the Default Thermal History]	No direct evidence to suggest that the sample was subjected to paleotemperatures higher than present temperatures at any time after deposition, although the data would allow higher paleotemperatures within specified limits.

Note: Interpretation of AFTA data is based on comparison of measured AFTA parameters with values predicted from "Default Thermal History" (Section 1.6); i.e., assuming that each sample is now at its maximum temperature since deposition. The predicted values for each sample are summarised in Table 5.1, and refer only to tracks formed after deposition. Samples may also contain tracks inherited from sediment provenance areas, which must be allowed for in interpreting the data. Calculations refer to apatites with the compositional range appropriate to each sample, as explained in Appendix A.

Table 5.3: Estimates of timing and magnitude of elevated paleotemperatures from AFTA data in samples from the Tirrawarra-1 well, Cooper-Eromanga Basin, South Australia (Geotrack Report #668)

Sample number	Stratigraphic Age	Present temperature	Early episode		Late episode		Comments
			Maximum paleo-temperature	Onset of cooling	Peak paleo-temperature	Duration of heating	
GC	(Ma)	(°C)	(°C)	(Ma)	(°C)	(Ma)	
668-152 407 m	97-90 Early Cretaceous	37	<105	post-deposition	No constraint		The AFTA data show no definite requirement for post-depositional paleotemperatures any higher than the present temperature of 37°C, but would allow higher paleotemperatures within the specified limits. The data show no evidence for the present temperature increasing to the present level recently as required by AFTA in sample GC668-156, but would allow this. The AFTA results predict a *maximum* possible VR level of ~0.61% based on the maximum allowed paleotemperature of 105°C at any time after deposition. No measured VR data are available for comparison with the AFTA estimate.
668-156 1586 m	117.5-100 Early Cretaceous	86	<105	post-deposition	<75	2	The data show clear evidence for the present temperature increasing to the present level recently. Evidence from the AFTA data suggest that this sample cannot have resided near the present temperature of 86°C for more than ~2 Ma, compared to ~90 Ma inferred from the preserved stratigraphy. Modelling suggests that a maximum possible temperature of 75°C is allowed for a heating duration of 2 Ma. The AFTA data show no definite requirement for post-depositional paleotemperatures any higher than the present temperature of 37°C, but would allow paleotemperatures as high as 105°C at any time after deposition. The AFTA results predict a *maximum* possible VR level of ~0.61% based on the maximum allowed paleotemperature of 105°C. No measured VR data are available for comparison with the AFTA estimate.

Note: **Brackets** surrounding italicised time/temperature constraints indicate that the AFTA results allow, but *do not* require a discrete event at this time.

*1 Based on measured present-day geothermal gradient of 41.5°C/km and a surface temperature of 20°C. As discussed in this table AFTA indicates that this is a recent developed transient thermal regime, and that lower temperatures must have persisted until this recent increase.

Table 5.3 (cont.): Tirrawarra-1 (Geotrack Report #668)

Sample number GC	Stratigraphic Age (Ma)	Present*1 temperature (°C)	Early episode Maximum paleo-temperature (°C)	Early episode Onset of cooling (Ma)	Late episode Peak paleo-temperature (°C)	Late episode Duration of Heating (Ma)	Comments
668-157 1669 m	135-117.5 Early Cretaceous	89	<110	post-depn.	No constraint		The AFTA data show no definite requirement for post-depositional paleotemperatures any higher than the present temperature of 89°C, but would allow higher paleotemperatures within the specified limits. The data show no evidence for the present temperature increasing to the present level recently as required by AFTA in sample GC668-156, but would allow this. The AFTA results predict a *maximum* possible VR level of ~0.63% based on a paleotemperature of 110°C allowed after deposition. No measured VR data are available for comparison with the AFTA estimate.
668-158 1827 m	148-145 Late Jurassic	96	<115	post-depn.	No constraint		The AFTA data show no definite requirement for post-depositional paleotemperatures any higher than the present temperature of 96°C, but would allow higher paleotemperatures within the specified limits. The data show no evidence for the present temperature increasing to the present level recently as required by AFTA in sample GC668-156, but would allow this. The AFTA results predict a *maximum* possible VR level of ~0.65% based on a paleotemperature of 115°C allowed after deposition. No measured VR data are available for comparison with the AFTA estimate.

Note: **Brackets** surrounding italicised time/temperature constraints indicate that the AFTA results allow, but *do not* require a discrete event at this time.

*1 Based on measured present-day geothermal gradient of 41.5°C/km and a surface temperature of 20°C. As discussed in this table AFTA indicates that this is a recent developed transient thermal regime, and that lower temperatures must have persisted until this recent increase.

Table 5.3 (cont.): Tirrawarra-1 (Geotrack Report #668)

Sample number GC	Stratigraphic Age (Ma)	Present*1 temperature (°C)	Early episode Maximum paleo-temperature (°C)	Early episode Onset of cooling (Ma)	Late episode Peak paleo-temperature (°C)	Late episode Duration of Heating (Ma)	Comments
668-160 2010 m	157-150 Late Jurassic	103	<125	post-deposition	No constraint		The AFTA data show no definite requirement for post-depositional paleotemperatures any higher than the present temperature of 103°C, but would allow higher paleotemperatures within the specified limits. The data show no evidence for the present temperature increasing to the present level recently as required by AFTA in sample GC668-156, but would allow this. The AFTA results predict a *maximum* possible VR level of ~0.71% based on a paleotemperature of 125°C allowed after deposition. This is consistent with a measured VR level at around this depth of 0.60%.

Note: **Brackets** surrounding italicised time/temperature constraints indicate that the AFTA results allow, but *do not* require a discrete event at this time.

*1 Based on measured present-day geothermal gradient of 41.5°C/km and a surface temperature of 20°C. As discussed in this table AFTA indicates that this is a recent developed transient thermal regime, and that lower temperatures must have persisted until this recent increase.

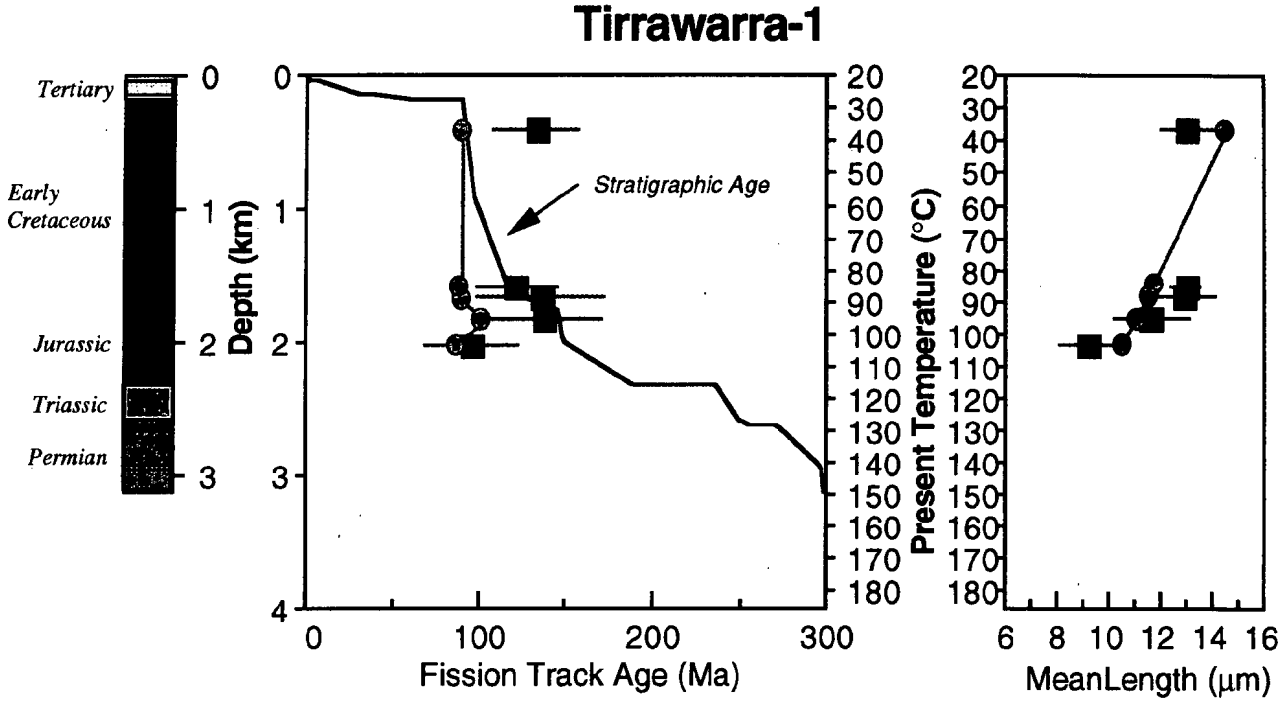

Figure 5.1: AFTA parameters plotted against sample depth and present temperature for samples from the **Tirrawarra-1 well, Cooper-Eromanga Basin.** Reprocessed data in solid blue; un-reprocessed data in grey (all data in Table 5.1). Round symbols are AFTA parameters predicted from the Default History. Comparison of the Default History parameters with the measured data suggests tenatative evidence for a minor increase in the present temperatures in the recent geological past. The variation of stratigraphic age with depth is also shown, as the solid line in the central panel.

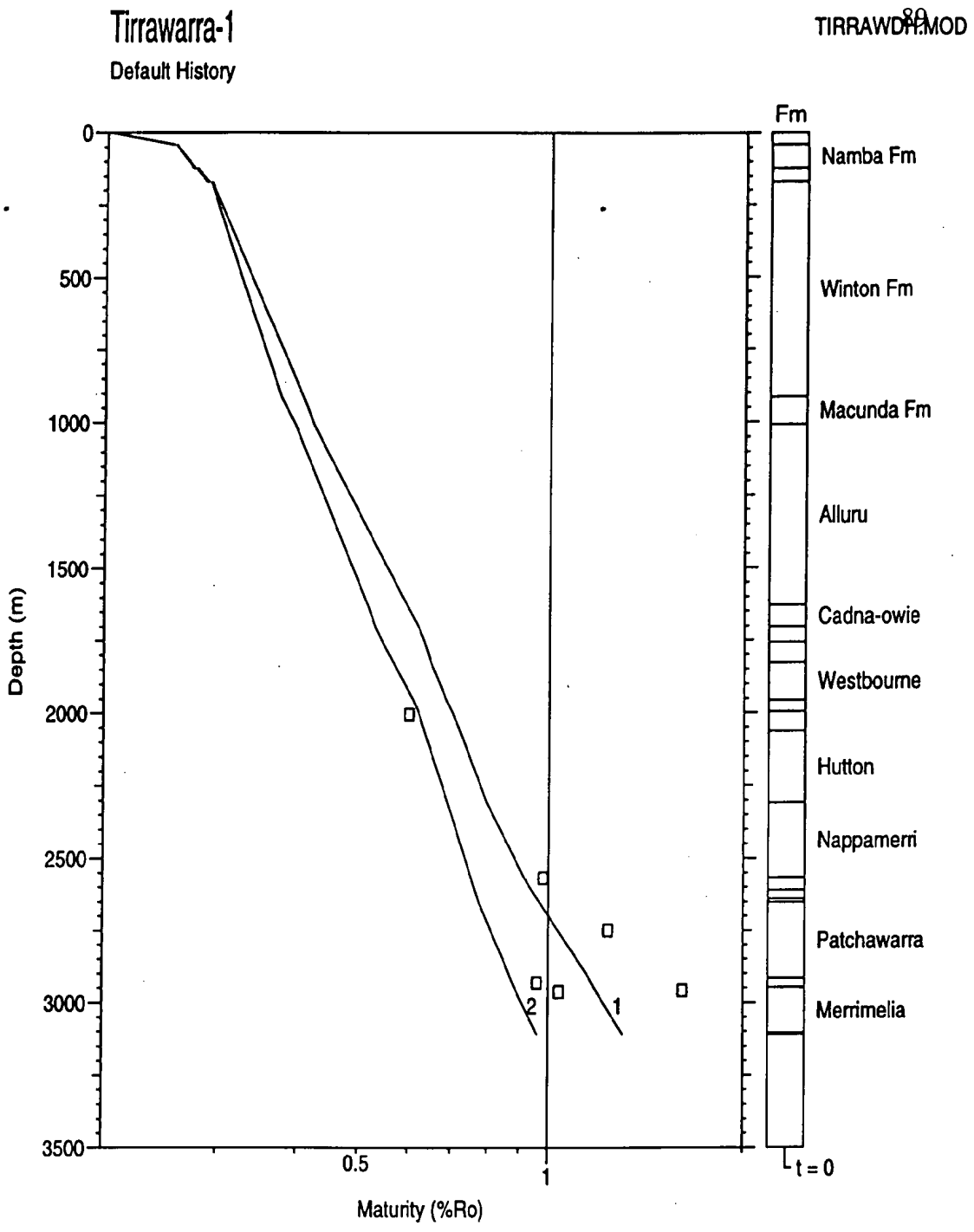

Figure 5.2: Measured vitrinite reflectance data in samples from the **Tirrawarra-1, -2, 16 & 17 wells, Cooper-Eromanga Basin** plotted against depth (with respect to KB). A VR profile (Profile 1) predicted from the "Default History" (Section 1.6) is also shown, i.e., the profile expected if samples throughout the section are currently at their maximum temperature since deposition (based on a *measured* present-day geothermal gradient of 41.5°C/km, and a constant surface temperature of 20°C - Appendix A). Also shown is a second predicted profile (Profile 2) based on the *AFTA-revised* (steady-state) present-day geothermal gradient of 35°C/km (see text). The majority of the measured VR results fall above the AFTA-revised predicted profile, more so deeper in the section, suggesting that the sampled section was subjected to maximum paleotemperature significantly higher than present temperatures after deposition. See text for details.

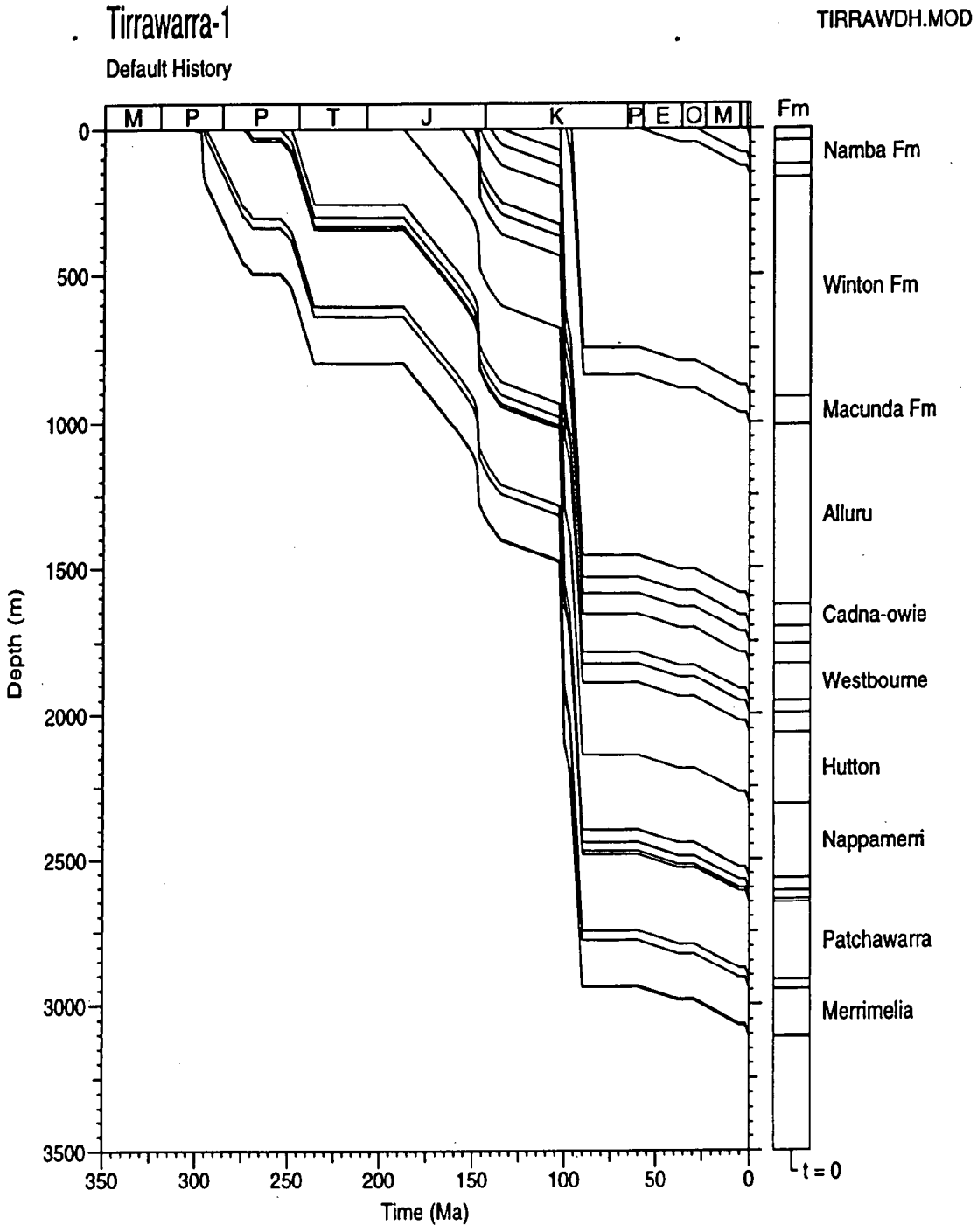

Figure 5.3: Default Burial History for the **Tirrawarra-1 well, Cooper-Eromanga Basin**, derived from the preserved section which, combined with the present-day thermal conditions, is used in predicting the VR profiles shown in Figure 5.2.

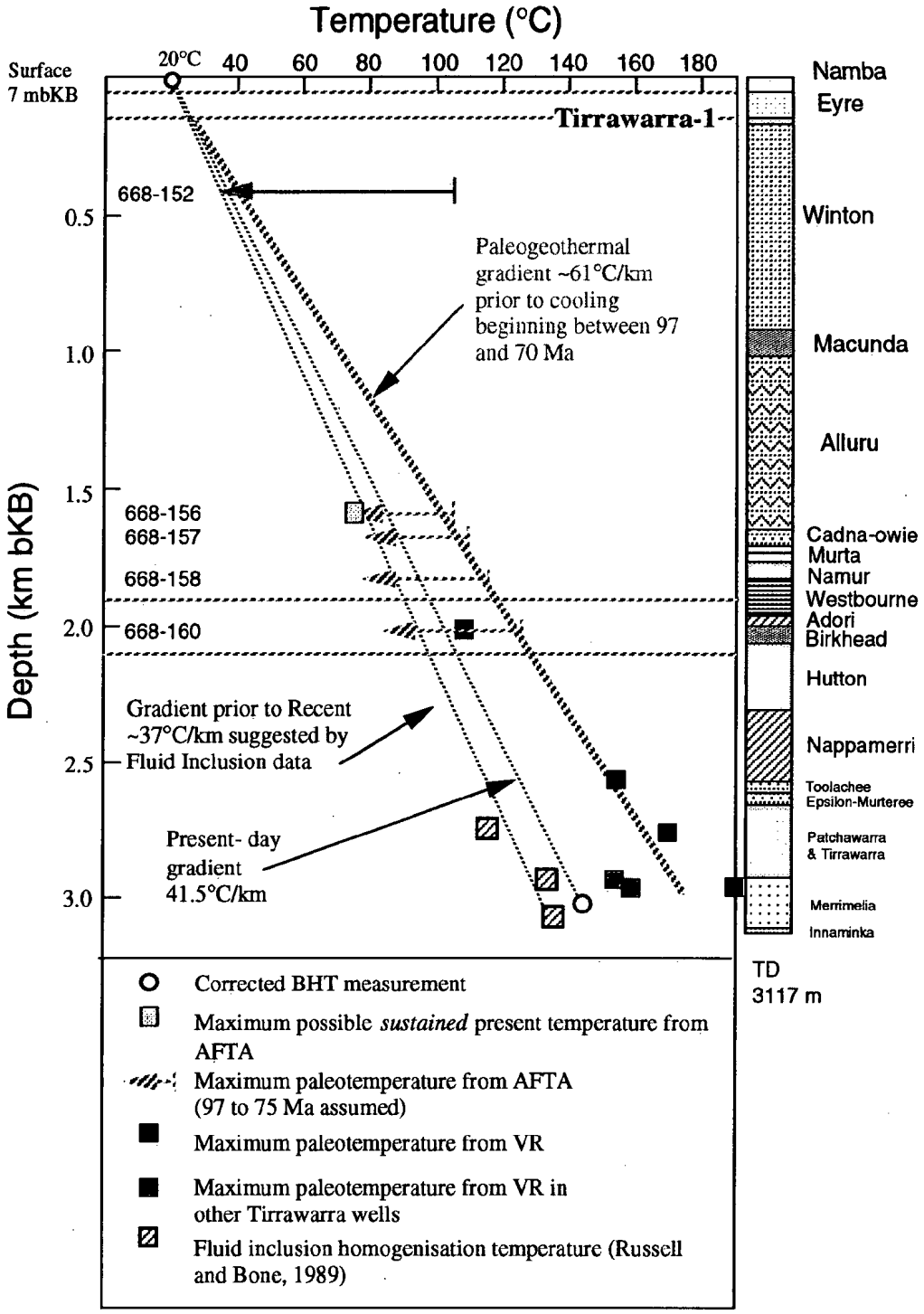

Figure 5.4: Plot of paleotemperatures derived from AFTA and VR data in the **Tirrawarra-1 well, Eromanga Basin**, against sample depth and the estimated present temperature profile for this well (see Appendix A).

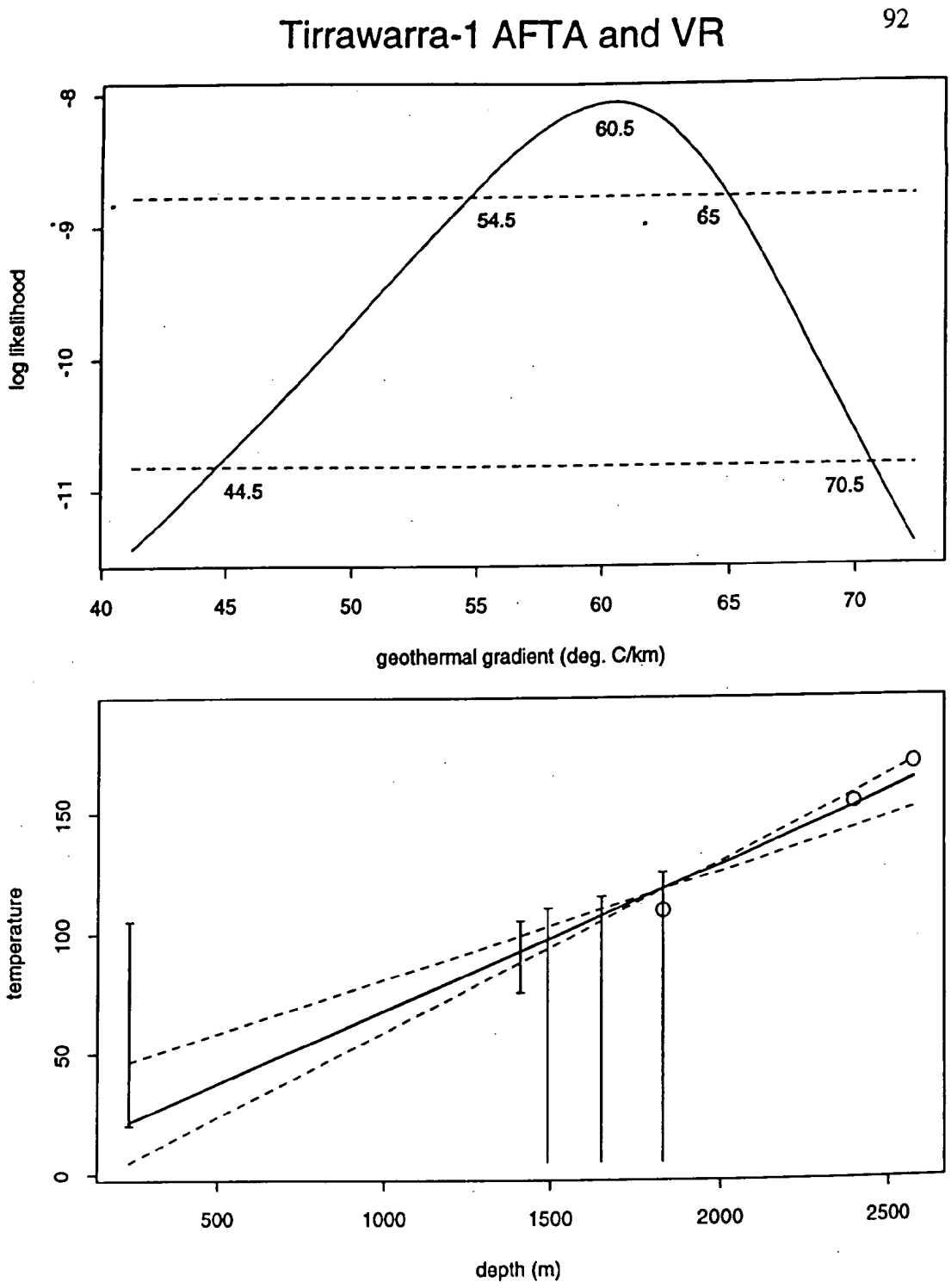

Figure 5.5: Upper: Maximum likelihood profile of linear paleogeothermal gradient fitted to the Cretaceous - Tertiary (~97 to 75 Ma) paleotemperature estimates from the AFTA and VR results in the **Tirrawarra-1 well**. The profile shows good quadratic behaviour suggesting a well constrained value, with upper and lower 95% confidence limits of 70.5 and 44.5°C/km, respectively, and a best-fit value of 60.5°C/km. The methodology employed in deriving this profile is outlined in Appendix C.

Lower: Maximum paleotemperature estimates from AFTA and VR in the **Tirrawarra-1 well**, with fitted profile (solid line) and lines (dashed) representing upper and lower 95% confidence limits.

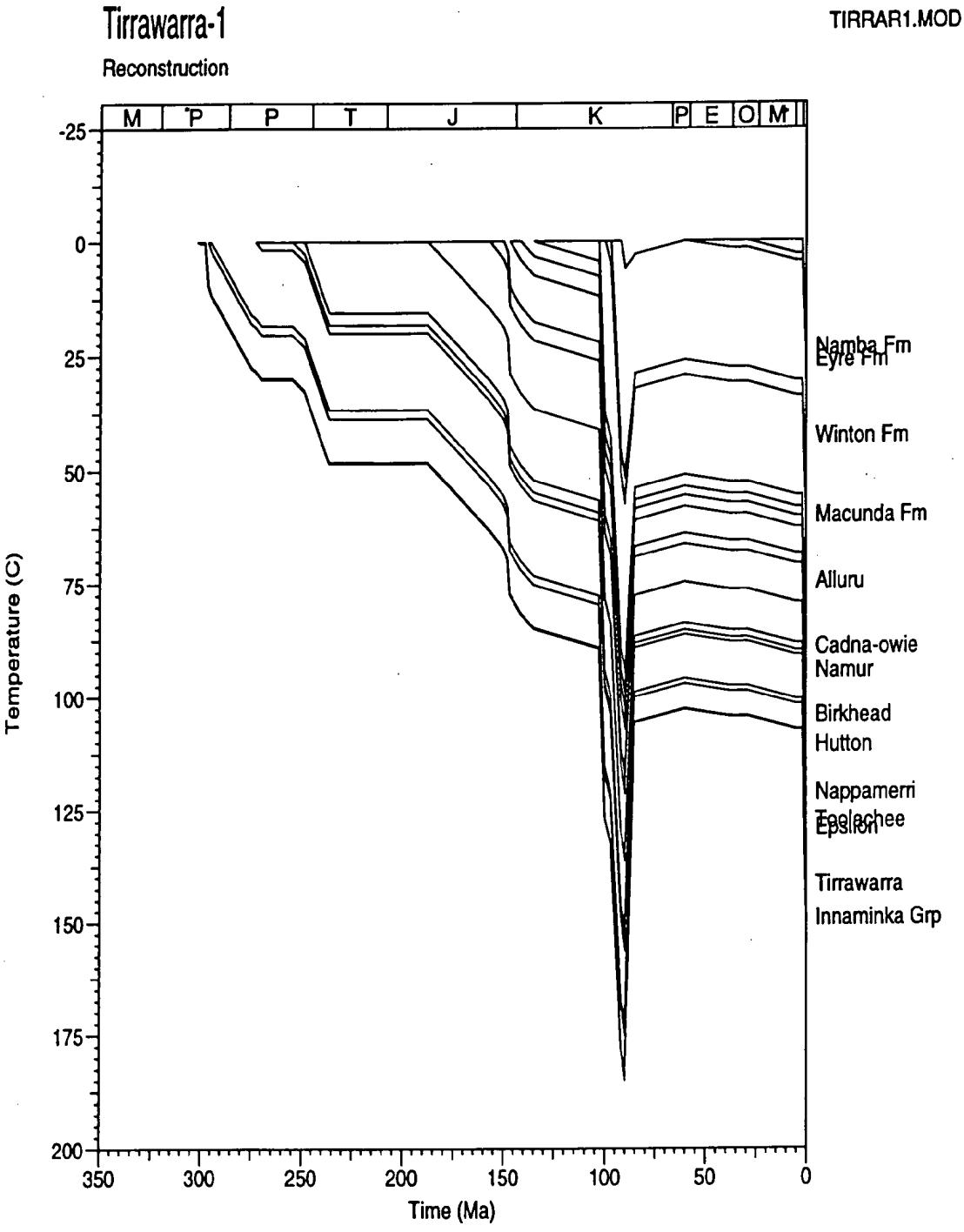

Figure 5.6: Reconstructed thermal history for **Tirrawarra-1** derived from the AFTA and VR results. Based on a paleogeothermal gradient of 60.5°C/km up until cooling began at 90 Ma (within the range from 97 to 75 Ma), at which point it declined to 35°C/km (from AFTA), rising to 41.5°C/km at 2 Ma (from AFTA). The surface temperature at 90 Ma is interpreted to have been 0°C (the results are not sensitive to the paleo-surface temperature but reconstruction of the burial history was based on this assumption in order to get a positive intercept at the top of the Winton Fm unconformity. The paleo-surface temperature is assumed to have risen to 20°C in the late Tertiary.

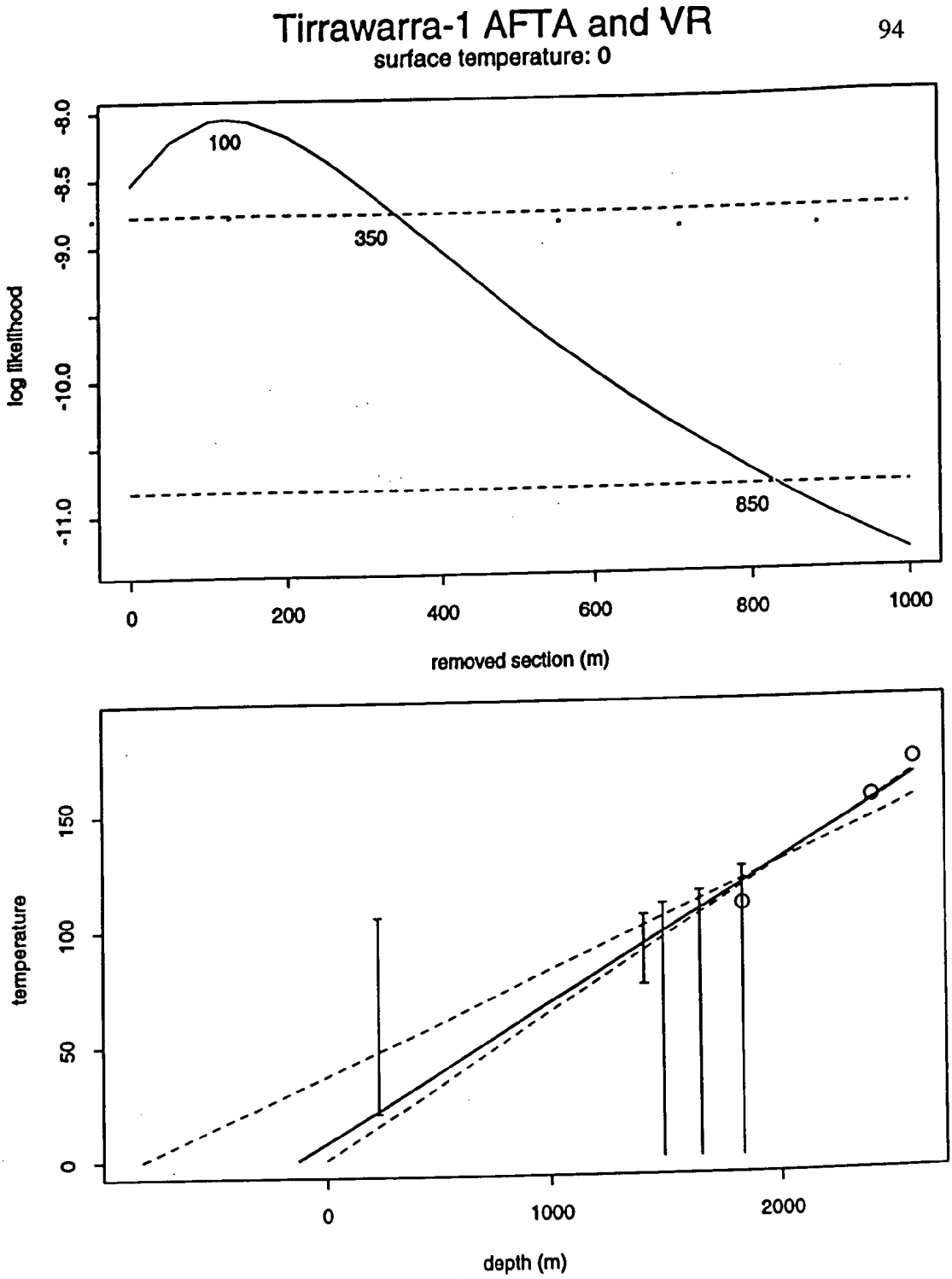

Figure 5.7: Upper: Maximum likelihood profile of estimated *total* section removed by uplift and erosion at the level of the unconformity at the top Winton Formation (~176.5 mTVD bKB) since the Cretaceous-Tertiary heating episode (~97 to 75 Ma) in the **Tirrawarra-1 well**, derived from the AFTA and VR constrained paleogeothermal gradient shown in Figure 5.5, assuming a paleo-surface temperature of 0°C. The profile gives lower and upper 95% confidence limits of 0 and 850 metres, respectively, and a well defined best-fit value of 100 metres. The methodology employed in deriving this profile is outlined in Appendix C.

Lower: Maximum paleotemperature estimates from AFTA and VR data in the **Tirrawarra-1 well**, with fitted profile (solid line) and lines (dashed) representing upper and lower 95% confidence limits, extrapolated to the assumed paleo-surface temperature of 0°C.

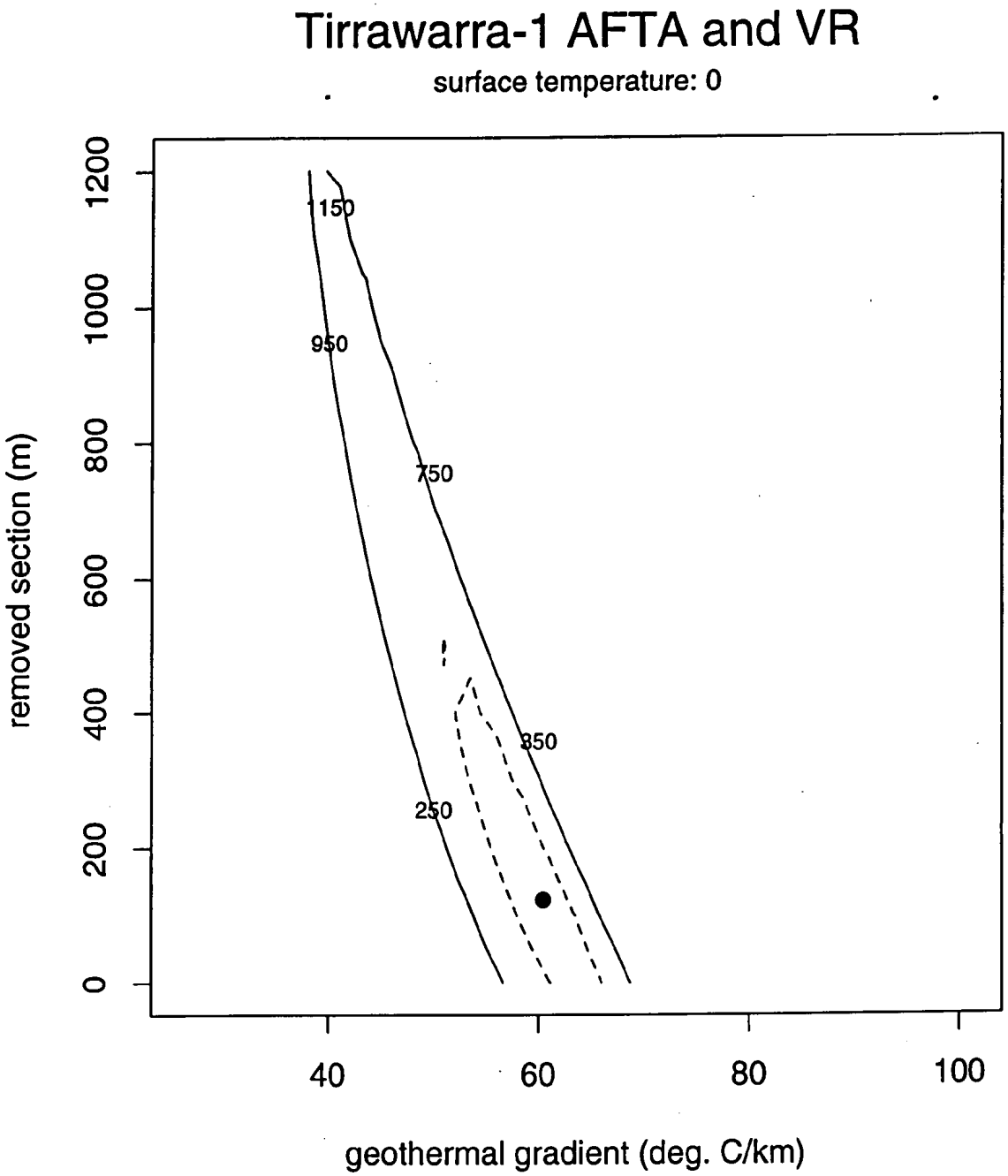

Figure 5.8: Crossplot of total removed section with respect to the level of the unconformity at the top Winton Formation (~176.5 mTVD bKB) since the Cretaceous-Tertiary heating episode (~97 to 75 Ma) in the **Tirrawarra-1 well**, showing the range of values (within the contoured region) compatible with the maximum paleotemperatures derived from the AFTA and VR data at the 95% confidence level. In effect, the thermal history reconstruction requires only very minor erosion on the top Winton Fm unconformity, with the identified cooling almost entirely attributable to decline in paleogeothermal gradient.

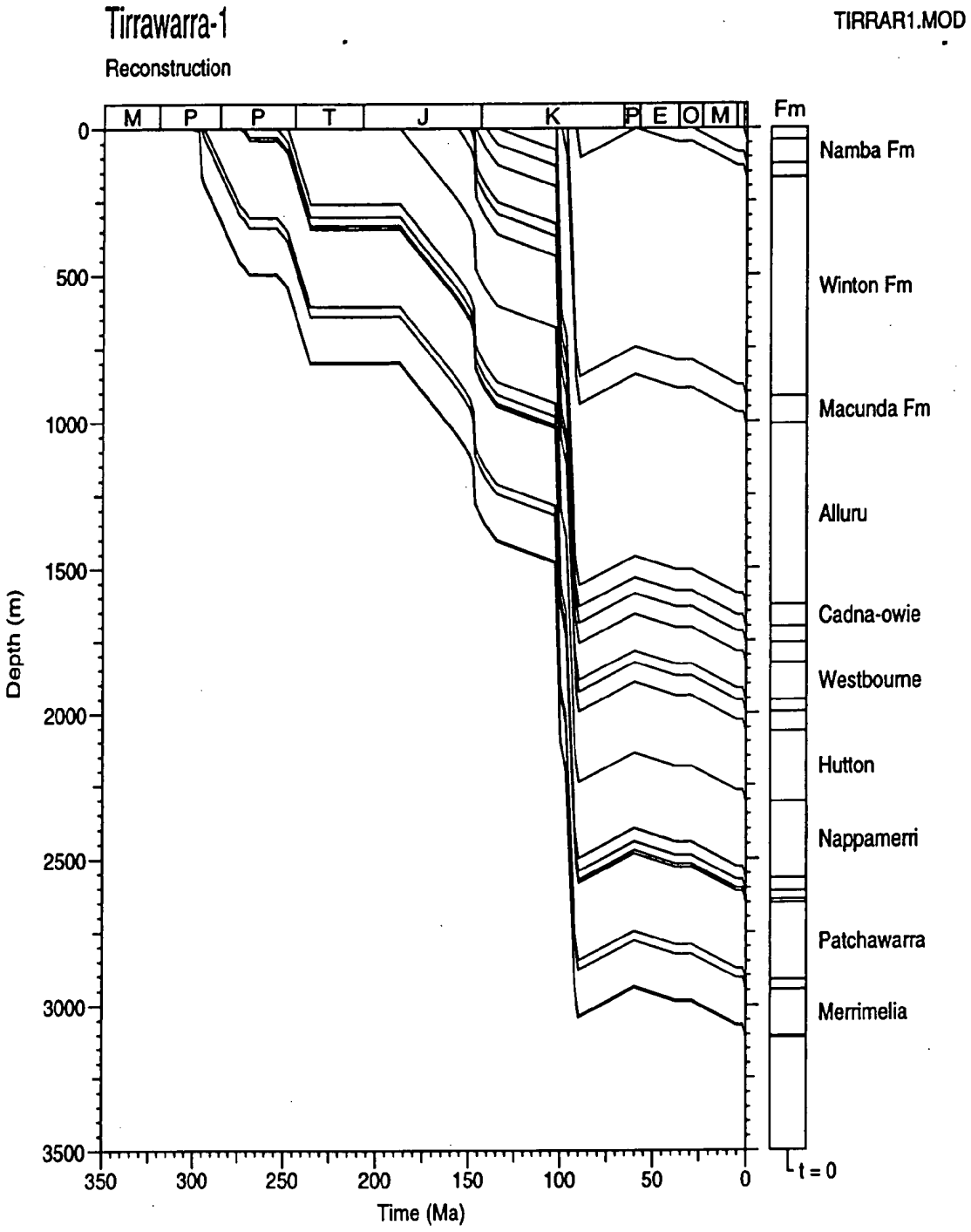

Figure 5.9: Possible burial history consistent with the thermal history reconstruction in the **Tirrawarra-1 well**. The history involves cooling from maximum paleotemperatures at 90 Ma (97 to 75 Ma allowed by the integrated thermal history results) with 100 m of uplift and erosion beginning at 90 Ma. See text for details.

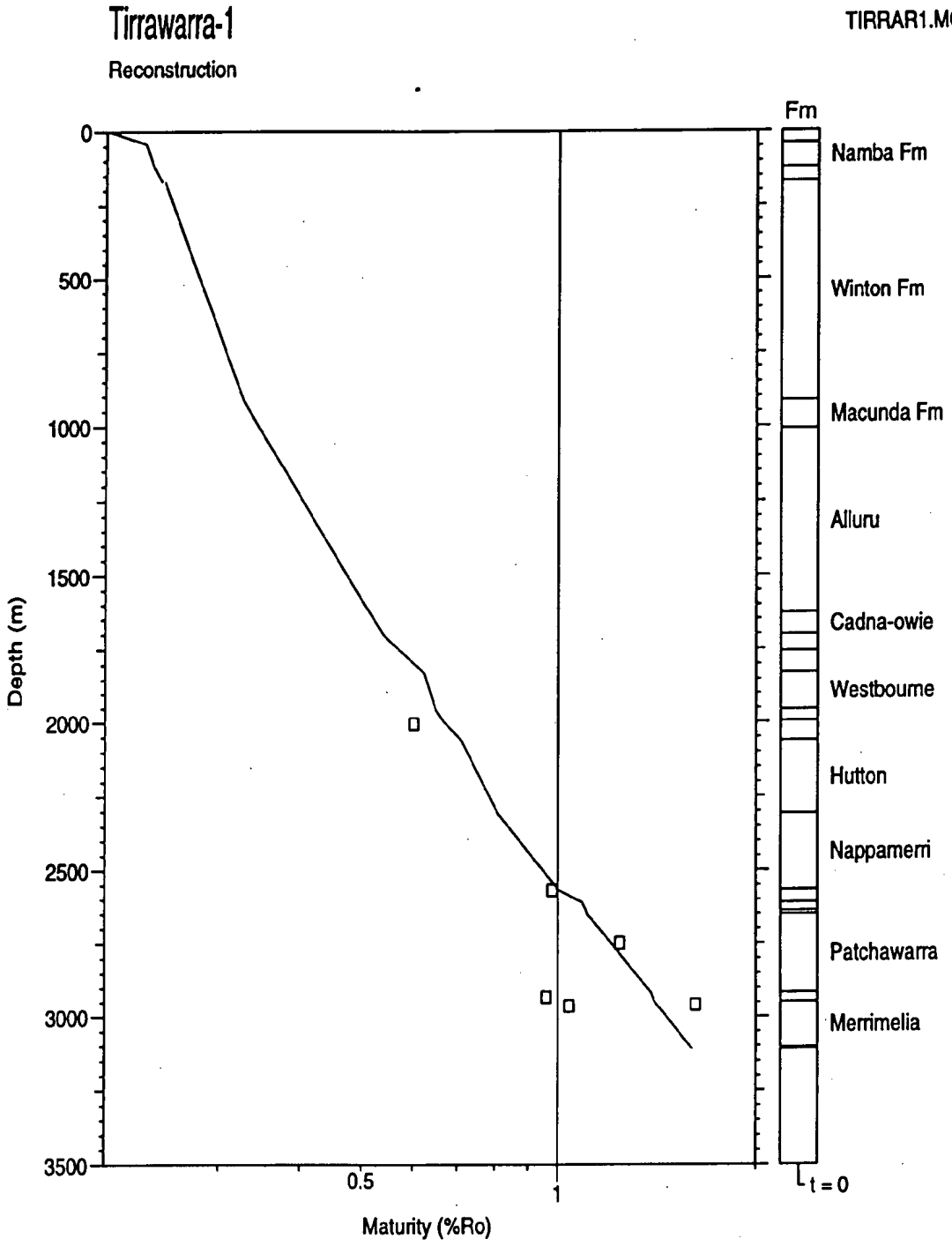

Figure 5.10: Measured vitrinite reflectance data in the **Tirrawarra-1 well,** and the VR profile with depth predicted from the reconstructed thermal history. The majority of the measured vitrinite values shows a very good match to the predicted profile throughout most of the section. The thermal history results show that the maturity values measured at the present-day reached these levels in the Cretaceous - Tertiary as illustrated in Figure 5.6. See text for further details.

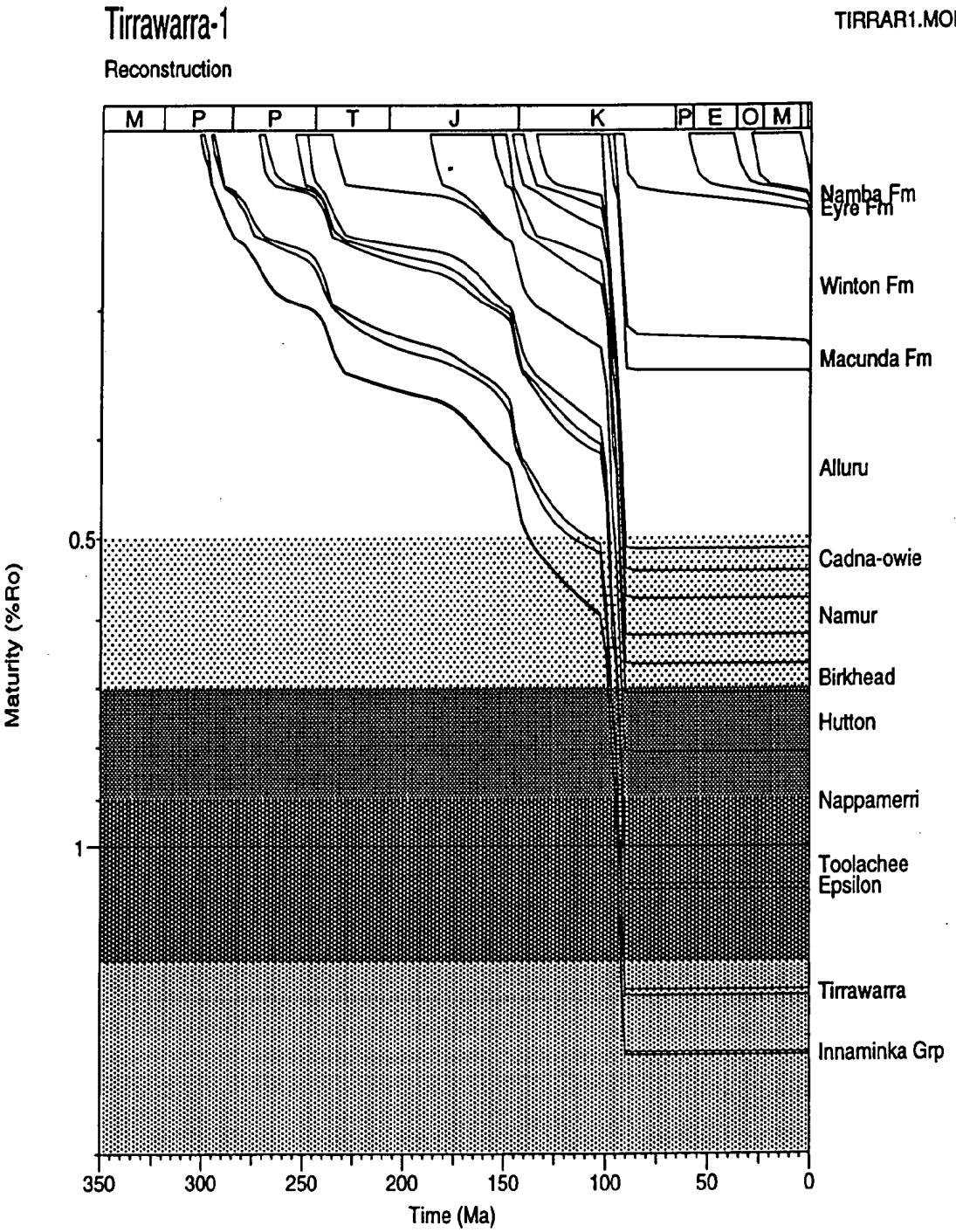

Figure 5.11: Predicted development of maturity with time (using Burnham and Sweeney, 1989) in the **Tirrawarra-1 well,** controlled by the AFTA results. Maximum maturity is shown as being reached at the 90 Ma (97 to 75 Ma), after progressive heating resulting from burial through the Early Cretaceous. This reconstruction illustrates that maximum maturity in most of the drilled section was reached at 90 Ma (97 to 75 Ma allowed), immediately prior to decline in paleogeothermal gradient and minor uplift and erosion (100 m) that commenced at this time. The reconstructed history predicts a minor increase in maturity in the upper part of the section over the last 90 Ma, but only at maturities less than that required for significant oil generation. No significant maturation can be attributed to the recent increase in geothermal gradient over the last ~2 Ma

6. Concluding remarks: geological history of the Cooper-Eromanga Basin

6.1 Comments on Recent heating - hot fluid flow

Comparison of AFTA, and VR paleotemperatures and fluid inclusion homogenisation temperatures suggests an episode of Recent heating, initiated at some time within the last 2 Ma, has affected most, if not all, of the drilled section in the wells studied.

This recent heating episode appears to have resulted in a relatively uniform geothermal gradient, although a lack of BHT measurements throughout the drilled sections makes this interpretation tentative. Work by Pitt (1986) shows some evidence for dog-leg present-day geothermal gradients, with the break in slope typically falling close to aquifer zones at around the Cretaceous - Jurassic boundary. Thus one explanation of the recent increase in gradient may be hot fluid flow in shallow aquifer horizons initiated by the uplift of the aquifer recharge areas with the last 2 Ma (eg Ziagos and Blackwell, 1986). Collection of fluid inclusion homogenisation temperatures from these shallow aquifer horizons may assist in making further progress in understanding this phenomena.

6.2 Comments on elevated heat flow in the Mid-Cretaceous

Mid-Cretaceous (~97 to 75 Ma) paleogeothermal gradients defined by the AFTA and VR maximum paleotemperature estimates are significantly higher (most 20°C/km or more higher) than either the "steady state" or recently increased present-day geothermal gradients. Absolute values in Tirrawarra-1, Toolachee-1 and Burley-2 wells are consistent between 75 and 80°C/km, values typical of high heat flow in a rift environment. Similar values have been recorded at the same time in the Cretaceous basins of Southern Australia (Otway, Gippsland, Duntroon), immediately prior to the opening of the Southern Ocean (Duddy, 1997; Geotrack report #569 to MESA, 1995). The Eromanga Basin has other similarities to these southern margin basins, particularly the dominant contemporaneous volcanogenic source of the detritus making up the Early Cretaceous section (Duddy, 1988) and the style of the burial history during this time.

Thus, one speculative interpretation of the thermal history is that it represents an aborted Cretaceous rifting episode coeval with successful episode on what now form the southern (and eastern) continental margin.

6.3 Comments on Mid-Cretaceous uplift and erosion

The results from the four wells suggest that additional burial at the top of the Winton Formation makes only a minor contribution to the observed mid-Cretaceous heating episode. Best-fit uplift and erosion estimates for the four values vary from zero m (Burley-2) to 500 m (Beanbush-1). With estimates from three wells being as low as zero metres and the fourth as low as 150 m at 95% confidence limits (Table vi).

All of these values are near the lowest limit of resolution of the thermal history techniques, representing only a few degrees of cooling, at most, at the top of the Winton Formation.

Importantly, the occurrence of cooling from elevated heat flow without significant uplift and erosion, has important implications for the underlying heating mechanism and the structural and tectonic setting.

7. Further work which would significantly improve knowledge of the geological history of the region

7.1 Time of maturation of Mesozoic and Paleozoic source rocks

Additional ZFTA sampling in key wells where VR results are around 5% or greater would greatly assist in refining the time of maturation in the Basin. At these levels the zircon fission track data should be able to directly reveal the time at which these high maturities were reached. As it stands, the currently available results from Burley-2 and McLeod-1 point strongly to a mid-Cretaceous timing, but samples which were slightly hotter should provide better evidence for this timing.

References

Burnham, A. K. and Sweeney, J. J. (1989). A chemical kinetic model of vitrinite reflectance maturation. *Geochimica et Cosmochimica Acta.*, 53, 2649-2657.

Bray, R. J., Green, P. T. and Duddy, I. R., (1992). Thermal History Reconstruction using apatite fission track analysis and vitrinite reflectance: a case study from the UK East Midlands and the Southern North Sea. In: Hardman, R.F.P. (ed), Exploration Britain: Into the next decade. *Geological Society Special Publication*, 67, 3-25.

Corrigan, J. D. (1991). Thermal anomalies in the Central Indian Ocean: Evidence for de-watering of the Bengal Fan. *Journal of Geophysical Research*, 96, 14263 - 14275.

Duddy, I.R., (1988). Fission Track Thermal History assessment of the Eromanga-Cooper Basin: an initial apatite study. In, End of Grant Technical report NERDDC Project 720, Assessment of hydrocarbon resource potential in Australian sedimentary basins: development of fission track techniques.

Duddy, I.R. (1997). Focussing exploration in the Otway Basin : Understanding timing of source rock maturation. APPEA Journal, 37, pt 1, 178-191.

Duddy, I. R., Green, P. F., Hegarty, K. A. and Bray, R. J. (1991). Reconstruction of thermal history in basin modelling using Apatite Fission Track Analysis: what is really possible. Proceedings of the First Offshore Australia Conference (Melbourne). III-49 - III-61.

Geotrack Report #569, (1995). AFTA and VR Thermal History interpretation of the Vivone-1 and Borda-1 wells, Duntroon Basin, SA. for MESA.

Green, P. F., Duddy, I. R., Gleadow, A. J. W., Tingate, P. R. and Laslett, G. M. (1985). Fission track annealing in apatite: Track length measurements and the form of the Arrhenius Plot. *Nuclear Tracks*, 10, 323-328.

Pitt, G.M. (1986). Geothermal gradients, geothermal histories and the timing of thermal maturation in the Eromanga-Cooper Basins. *In,* Contributions to the Geology and Hydrocarbon Potential of the Eromanga Basin (Gravestock et al. eds). Geol. Soc. Australia, Spec. Publ. 12, 323-351.

Sweeney, J. J. and Burnham, A. K. (1990). Evaluation of a simple model of vitrinite reflectance based on chemical kinetics. *The American Association of Petroleum Geologists' Bulletin,* 74, 1559 - 1570.

Waples, D. W., Kamata, H. and Suizu, M. (1992). The art of maturity modelling. Part 1: Finding a satisfactory geologic model. *The American Association of Petroleum Geologists' Bulletin*, 76, 31 - 46.

Ziagos, J.P. and Blackwell, D.D. (1986). A Model for the transient temperature geothermal systems. *Journal of Volcanology and Geothermal Research*, 27, 371-397.

APPENDIX A

Sample Details and Geological Data

A.1 Sample details

A total of 15 samples from the **Cooper-Eromanga Basin wells Burley-2, Toolachee-1, Beanbush-1 and Tirrawarra-1,** originally provided by Mines and Energy Resources, South Australia, as a part of a NERDDC study (1988) are re-processed here using Geotrack's proprietary multi-compositional Apatite Fission Track Analysis (AFTA®) technology. ZFTA™ Zircon Fission Track Analysis results from five samples from the **Burley-1, McLeod-1 and Dullingari-1** are also included in the study as a part of an investigation of the timing of the high organic maturation levels observed in some of the deeper parts of the Cooper Basin sequence.

Details of all AFTA samples, including depths (TVD), stratigraphic ages and estimates of present temperature for each sample, are provided in Table A.1. ZFTA sample details are provided in Table A.2.

No new vitrinite reflectance samples were processed in the current study, but VR data was provided from AFTA for each well, along with additional data from the **Tirrawarra-2, 16 and 17** wells and these are reproduced in Table D.2 (Appendix D).

A.2 Stratigraphic details

Details of the preserved stratigraphy in **each well** were provided by **MERSA** and are summarised in Table A.3. Formations and Groups were assigned numerical stratigraphic ages (Ma) by reference to Harland (1989). All depths are quoted as TVDrKB unless otherwise stated. Stratigraphic ages of the AFTA and ZFTA samples derived from the supplied information are shown in Tables A.1 and A.2.

A.3 Present temperatures

In the application of any technique involving estimation of paleotemperatures, it is critical to control the present temperature profile, since estimation of maximum paleotemperatures proceeds from assessing how much of the observed effect could be explained by the magnitude of present temperatures.

Temperature data were supplied for each well as either a linear geothermal gradient or uncorrected log temperatures from a single depth. Raw BHT data were corrected using a simplified correction procedure adapted from that of Andrews-Speed et al. (1984) and shown in numerous Geotrack studies to give results very similar to those obtained from the Horner-correction procedure. (Also see Oxburgh and Andrews-Speed, 1981.) In this procedure, the quoted BHT data were corrected by increasing the difference between the surface temperature (assumed to be 20°C) and the uncorrected BHT by 20% for uncorrected temperatures below 66°C (150°F), and by 25% for uncorrected temperatures above 66°C (see Table A.3). Note that where more than one measurement is available at any one depth, the value with the shortest time since circulation was used.

Temperature data and geothermal gradients are presented in Table A.4. Present-day temperatures of each AFTA, ZFTA and VR sample estimated using the geothermal gradient values are given in Tables A.1, A.2 and D.2, respectively.

A.4 Apatite yields and data quality

In general, excellent yields of detrital apatite were obtained after mineral separation of the 15 AFTA samples (Table A.1). Of the 15 samples, 11 samples gave an excellent or good yield, 3 samples gave a fair yield and 1 sample gave a poor yield. Nine additional samples, 6 from the Toolachee-1 well and 3 from the Beanbush-1 well contained various amounts of apatite but were not reprocessed for this study (Table A.1). Reprocessed apatite fission track age and length data are provided in Tables B.1 and B.2.

The quality of the etched surfaces of the apatites obtained for analysis was generally very good. Overall, the data set has provided the basis of a reliable interpretation and good control on the thermal history solutions.

A.5 Zircon yields and data quality

Four of the 5 samples gave excellent yields of zircon (10 or more grains) suitable for counting while the remaining sample gave a very good yield (9 grains) as shown in Table A.2.

The quality of the etched surfaces of the zircons obtained for analysis was generally very good and even though track densities in some grains are very high and near the upper limit of reliable counting (~3 x E^7 cm^{-2}), the results obtained are considered reliable. Zircon fission track age data are provided in Table B.3.

A.6 Apatite grain morphologies

Apatite grains obtained from the majority of Mesozoic samples are characterised by well developed euhedral forms, and combined with the fission track ages results and the apatite compositional data are considered to be highly characteristic of a dominant volcanogenic source (see Section A.7 below). Those units with a dominant input of contemporaneous volcanogenic detritus include the Cretaceous Winton, Alluru, Wallumbilla Formations, the Murta Member of the Mooga Formation and the Jurassic Birkhead Formations. More rounded grains, characteristic of recycled basement sources occur in the quartz-rich sandstones of the Namur and Hutton Sandstones, and the majority of samples analysed from the Permian and older sections.

These observations are very similar to those made earlier from preliminary data of Cooper-Eromanga Basin samples reported by Duddy (1988), and point a major control on reservoir quality in the basin by contemporaneous volcanism.

A.7 Apatite compositions

The annealing kinetics of fission tracks in apatite are affected by chemical composition, specifically the Cl content, as explained in more detail in Appendix C. In all samples collected for this study, Cl contents were measured in all apatite grains analysed (i.e. for both fission track age determination and track length measurement).

Chlorine contents were measured using a fully automated Jeol JXA-5A electron microprobe equipped with a computer controlled X-Y-Z stage and three computer controlled wavelength dispersive crystal spectrometers, with an accelerating voltage of 15kV and beam current of 25nA. The beam was defocussed to 20 μm diameter to avoid problems associated with apatite decomposition, which occur under a fully focussed 1 μm - 2 μm beam. The X-Y co-ordinates of dated grains within the grain mount were transferred from the Autoscan Fission Track Stage to a file suitable for direct input into the electron microprobe. The identification of each grain was verified optically prior to analysis. Cl count rates from the analysed grains were converted to wt% Cl by reference to those from a Durango apatite standard (Melbourne University Standard APT151), analysed at regular intervals. This approach implicitly takes into account atomic number absorption and fluorescence matrix effects, which are normally calculated explicitly when analysing for all elements. A value of 0.43 wt% Cl was used for the Durango standard, based on repeated measurements on the same single fragment using pure rock salt (NaCl) as a standard for chlorine. This approach gives essentially identical results to Cl contents determined from full compositional measurements, but has the advantage of reducing analytical time by a factor of ten or more.

Cl contents in individual grains are listed in the fission track age data sheets in Appendix B, and plots of fission track age against Cl content are shown in Figures B.5a to d (Appendix B). Table B.3 contains fission track age and length data grouped into 0.1 wt% Cl intervals on the basis of chlorine contents of the grains from which the data are derived. Histograms of Cl contents in individual samples are shown in Figure A.2.

The histograms in Figures A.2a to d show that most apatite grains from the samples analysed in this study contain a very broad spread of chlorine contents, with only a small number of grains having Cl contents between 0 and 0.1 wt%, with a larger number of grains giving values greater than ~0.5 wt%. Numerous grains give Cl contents between 1 and 2 wt% with several grains >2 wt%. In our experience, this pattern is typical of detritus from mixed volcanogenic sources. (Compare results from individual samples in Figures A.2a to d with Figure C.4c in Appendix C.). Also, for those samples presently at low temperatures (<80°C), inspection of the apatite fission track age data from individual samples in relation to the chlorine content (Figure B.6 a to d) shows that the fission track age overlaps with the stratigraphic age, consistent with a contemporaneous volcanogenic source.

Lower limits of detection for chlorine content have been calculated for typical analytical conditions (beam current, counting time, etc.) and are listed in Table A.5. Errors in wt% composition are given as a percentage and quoted at 1σ for chlorine determinations. A generalised summary of error values for various values of wt% chlorine is presented in Table A.6.

In all these samples, the measured distribution of compositions has been employed in interpreting the AFTA data, using methods outlined in Appendix C.

References:

Andrews-Speed, C.P., Oxburgh, E.R. and Cooper, B.A. (198). Temperatures and depth-dependent heat flow in western North Sea, *AAPG Bulletin*, 68, 1764 - 1784.

Duddy, I.R., (1988). Part 3: Fission Track Thermal History Analysis - Cooper Eromanga Basin. **In,** End of Grant Technical Report, NERDDC Project No. 720.

Harland, W.B., Armstrong, R.L., Cox, A.V., Craig, L.E., Smith, A.G. and Smith, D.G. (1989). A geologic time scale 1989, Cambridge University Press.

Oxburgh, E.R. and Andrews-Speed, C.P. (1981). Temperature, thermal gradients and heat flow in the southwestern North Sea, In: Illing, L. V. & Hobson, G.D. (eds.) The petroleum geology of the continental shelf of NW Europe, London, Institute of Petroleum 141 - 151.

Table A.1: Details of AFTA samples and apatite yields - well samples from Cooper - Eromanga Basin (Geotrack Report #668)

Sample number	Depth (m)	Sample type	Stratigraphic subdivision	Stratigraphic age (Ma)	Present temperature *1 (°C)	Apatite yield *2
Burley-2						
8642-168	539-567 *(1770-1860')*	cuttings	Winton	97-90	53	Excellent
8642-169	741-768 *(2430-2520')*	cuttings	Winton	97-90	66	Excellent
8642-170	1042-1070 *(3420-3510')*	cuttings	Alluru	103-100	84	Excellent
8642-171	1253-1280 *(4110-4200')*	cuttings	Toolebuc	106-103	97	Good
8642-172	1743-1753 *(5720-5750')*	cuttings	Murta	141.5-135	126	Excellent
8642-174	1972-1981 *(6470-6500')*	cuttings	Westbourne	148-147	140	Good
Toolachee-1						
8642-221	1311-1338 *(4300-4390')*	cuttings	Cadna owie	135-117.5	87	Not Processed
8642-222	1554-1615 *(5100-5300')*	cuttings	Namur	150-145	100	Not Processed
8642-223	1628-1664 *(5340-5460')*	cuttings	Namur - Birkhead	157-145	104	Fair
8642-224	1676-1734 *(5500-5690')*	cuttings	Hutton - Poolawanna	236.6-157	107	Poor
8642-225	1753-1786 *(5750-5860')*	cuttings	Nappamerri	249-236.6	110	Not Processed
8642-226	1911-1969 *(6270-6460')*	cuttings	Daralingie - Roseneath	270-262	119	Not Processed
8642-227	1978-2027 *(6490-6650')*	cuttings	Epsilon	273-270	122	Not Processed
8642-228	2164-2194 *(7100-7200')*	cuttings	Dullingari	304-300	131	Not Processed

Table A.1: Continued

Sample number	Depth (m)	Sample type	Stratigraphic subdivision	Stratigraphic age (Ma)	Present temperature *1 (°C)	Apatite yield *2
Beanbush-1						
8642-229	398 *(1306')*	cuttings	Winton	97-90	35	Not Processed
8642-233	1189 *(3901')*	cuttings	Macunda	100-97	66	Not Processed
8642-236	1797 *(5896')*	cuttings	Wallumbilla	117.5-106	89	Not Processed
8642-238	2051 *(6729')*	cuttings	Murta	145-135	99	Good
8642-240	2356 *(7730')*	cuttings	Birkhead	157-150	110	Excellent
Tirrawarra-1						
8642-152	384-430 *(1260-1410')*	cuttings	Winton	97-90	37	Fair
8642-156	1564-1609 *(5130-5280')*	cuttings	Alluru	117.5-100	86	Excellent
8642-157	1646-1692 *(5400-5550')*	cuttings	Cadna owie	135-117.5	89	Fair
8642-158	1810-1844 *(5940-6050')*	cuttings	Namur - Westbourne	148-145	96	Excellent
8642-160	2002-2018 *(6570-6620')*	cuttings	Birkhead	157-150	103	Excellent

*1 See Appendix A for discussion of present temperature data.

*2 Yield based on quantity of mineral suitable for age determination. Excellent: >20 grains; Very Good: ~20 grains; Good: 15-20 grains; Fair: 10-15 grains; Poor: 5-10 grains; Very Poor: <5 grains.

Note: All depths quoted are TVD with respect to KB.

Table A.2: Details of ZFTA samples and zircon yields - well samples from Cooper-Eromanga Basin wells (Geotrack Report #668)

Sample number	Depth (m)	Sample type	Stratigraphic subdivsion	Stratigraphic Age (Ma)	Present temperature*1 (°C)	Raw weight (g)	Washed weight (g)	Zircon yield*2
Burley-1								
8642-23	2803	core	Toolachee Fm	255-249	181	NR	NR	Excellent
8642-25	3109	core	Patchawarra Fm	273-270	199	NR	NR	Excellent
McLeod-1								
8642-26	3584	core	Tirrawarra Fm	297-296	221	NR	NR	Excellent
8642-27	3746	core	Granite basement	302-300	230	NR	NR	Very Good
Dullingari-1								
8642-53	2948	core	Dullingari Fm	320-310	171	NR	NR	Excellent

NR: Not recorded

*1 See Appendix A for discussion of present temperature data.

*2 Yield based on quantity of mineral suitable for age determination. Excellent: >10 grains; Very Good: ~10 grains; Good: 7-10 grains; Fair: 3-7 grains; Poor: <3 grains

Table A.3: Summary of stratigraphy - wells from the Cooper - Eromanga Basin (Geotrack Report #668)

	KB elevation (mAMSL)	Ground level (m)	Stratigraphic Interval	Age of Top (Ma)	Depth of Top TVD rKB (m)
Burley-2					
	?	6.7	Recent	0	6.7
			Unconformity	2	38.4
			Namba	5.3	38.4
			Unconformity	29.3	57.9
			Eyre	38	57.9
			Unconformity	60	108.5
			Winton	90	108.5
			Macunda	97	883.9
			Alluru Mdst	100	976
			Toolebuc	103	1250.9
			Wallumbilla	106	1256.1
			Cadna-owie	117.5	1649.6
			Murta	135	1739.8
			Mc Kinlay	141.5	1796.5
			Namur	145	1805.0
			Westbourne	147	1874.5
			Adori	148	2011.4
			Birkhead	150	2052.5
			Hutton	157	2118.4
			Unconformity	188	2280.5
			Nappamerri	236.5	2280.5
			Toolachee	249	2672.5
			Unconformity	255	2829.5
			Daralingie	262	2829.5
			Rosneath	267	2918.8
			Epsilon	270	2978.2
			Murteree	273	3117.8
			Patchawarra	275	3196.4
			Tirrawarra	295	3589.9
			Merrimelia	296.5	3613.1
			Granite Basement	298	3661.6
			Total Depth	300	3705.8

Table A.3: Continued

	KB elevation (mAMSL)	Ground level (m)	Stratigraphic Interval	Age of Top (Ma)	Depth of Top TVD rKB (m)
Toolachee-1					
	?	7	Recent	0	7
			Unconformity	2	22
			Namba	5.3	22
			Unconformity	29.3	41.5
			Eyre	38	41.5
			Unconformity	60	108.2
			Winton	90	108.2
			Macunda	97	675.4
			Oodnadatta	100	759.6
			Coorikiana	106.5	1003.4
			Bulldog Sh	108	1018
			Cadna-owie	117.5	1285.7
			Murta	135	1358.2
			Mc Kinlay	141.5	1408.5
			Namur	145	1416.1
			Birkhead	150	1636.2
			Hutton	157	1668.5
			Poolawanna	186	1688
			Nappamerri	236.5	1750.2
			Toolachee	249	1791
			Unconformity	255	1902
			Daralingie	262	1902
			Rosneath	267	1933
			Epsilon	270	1963.8
			Murteree	273	2033
			Patchawarra	275	2082.4
			Unconformity	295	2130.6
			Dullingari Gp	300	2130.6
			Total Depth	304	2202.8

Table A.3: Continued

	KB elevation (mAMSL)	Ground level (m)	Stratigraphic Interval	Age of Top (Ma)	Depth of Top TVD rKB (m)
Beanbush-1					
	?	7	Recent	0	7
			Unconformity	2	45.7
			Namba	5.3	45.7
			Unconformity	29.3	164.6
			Eyre	38	164.6
			Unconformity	60	242.9
			Winton	90	242.9
			Macunda	97	1155.8
			Alluru Mdst	100	1273.5
			Toolebuc	103	1472.5
			Wallumbilla	106	1493.5
			T		1601.4
			W		1617
			Cadna-owie	117.5	1947
			Murta	135	2024
			Namur	145	2088
			Westbourne	147	2149
			Adori	148	2301
			Birkhead	150	2322
			Hutton	157	2414
			Unconformity	188	2712
			Nappamerri	236.5	2712
			Toolachee	249	3202
			Unconformity	255	3202
			Epsilon	270	3259
			Murteree	273	3277
			Patchawarra	275	3297
			Tirrawarra	295	3555
			Merrimelia	296.5	3574
			Innaminka	298	3615
			Total Depth	300	3699.7

Table A.3: Continued

	KB elevation (mAMSL)	Ground level (m)	Stratigraphic Interval	Age of Top (Ma)	Depth of Top TVD rKB (m)
Tirrawarra-1					
	?	7	Recent	0	7
			Unconformity	2	47.9
			Namba	5.3	47.9
			Unconformity	29.3	130.5
			Eyre	38	130.5
			Unconformity	60	176.5
			Winton	90	176.5
			Macunda	97	922.3
			Alluru Mdst	100	1015.6
			Cadna-owie	117.5	1635.3
			Murta	135	1709.6
			Namur	145	1764.8
			Westbourne	147	1834.9
			Adori	148	1962.3
			Birkhead	150	2002.5
			Hutton	157	2069.9
			Unconformity	188	2315.3
			Nappamerri	236.5	2315.3
			Toolachee	249	2573.7
			Unconformity	255	2617.9
			Epsilon	270	2617.9
			Murteree	273	2646.9
			Patchawarra	275	2658.2
			Tirrawarra	295	2922.7
			Merrimelia	296.5	2955.3
			Innaminka	298	3112.0
			Total Depth	300?	3116.9

All depths quoted are with respect to KB, except where otherwise stated.

Table A.4: Summary of present temperature measurements - wells from the Cooper - Eromanga Basin (Geotrack Report #668)

Ground level (ft)	Ground level (m)	Depth (log) (ft)	Uncorrected temperature (°F)	Uncorrected temperature (°C)	Time since circulation (hrs)	Depth (m)	Corrected temperature (°C)	Geothermal gradient (°C/km)
Burley-2								62.0
Toolachee-1								51.0
Beanbush-1								
23	7	12136	272	133.3	-	3699.1	161.6	38.4
Tirrawarra-1								
23	7	9908	248	120.0	4.5	3020.0	145.0	41.5

Quoted BHT values have been corrected by increasing the difference between surface temperature and measured BHT by 20% for measured temperatures <150°F (<66°C) and by 25% for temperatures >150°F (>66°C). A surface temperature of 20°C has been assumed. All depths quoted are with respect to KB, except where otherwise stated.

Table A.5: Lower Limits of Detection for Apatite Analyses (Geotrack Report #668)

Element	LLD (95% c.l.)		LLD (99% c.l.)	
	(wt%)	(ppm)	(wt%)	(ppm)
Cl	0.01	126	0.02	182

Table A.6 Per cent errors in chlorine content (Geotrack Report #668)

Chlorine content (wt%)	Error (%)
0.01	9.3
0.02	8.7
0.05	7.3
0.10	6.1
0.20	4.7
0.50	3.2
1.00	2.3
1.50	1.9
2.00	1.7
2.50	1.5
3.00	1.4

Errors quoted are at 1σ. See Appendix A for more details.

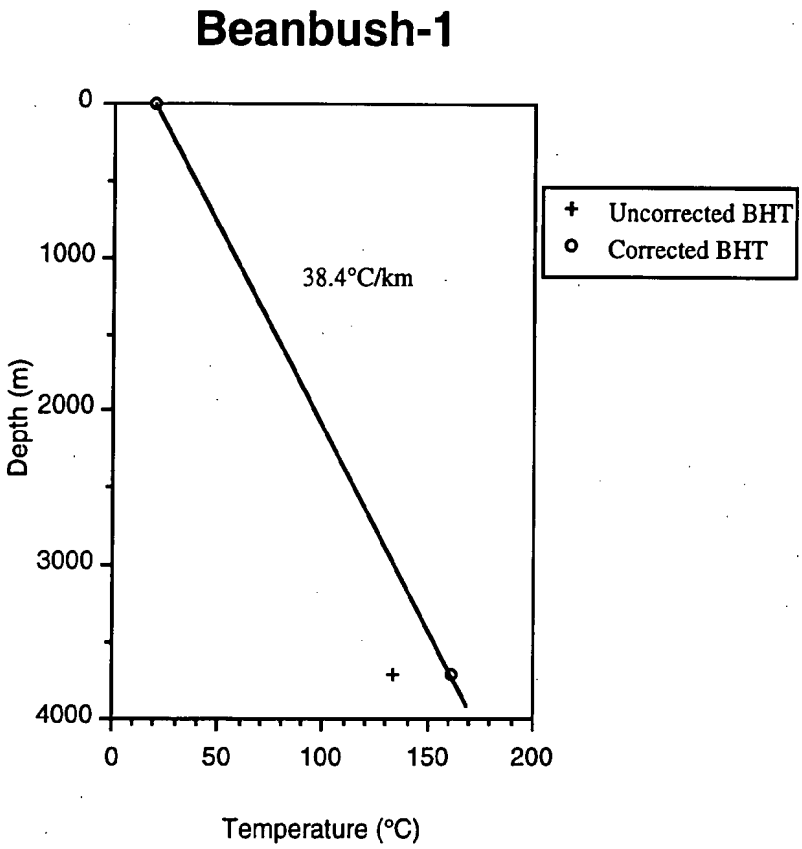

Figure A.1a: Present temperature profile calculated for **well Beanbush-1, Cooper - Eromanga Basin.** See Table A.4 and Appendix A for more detail.

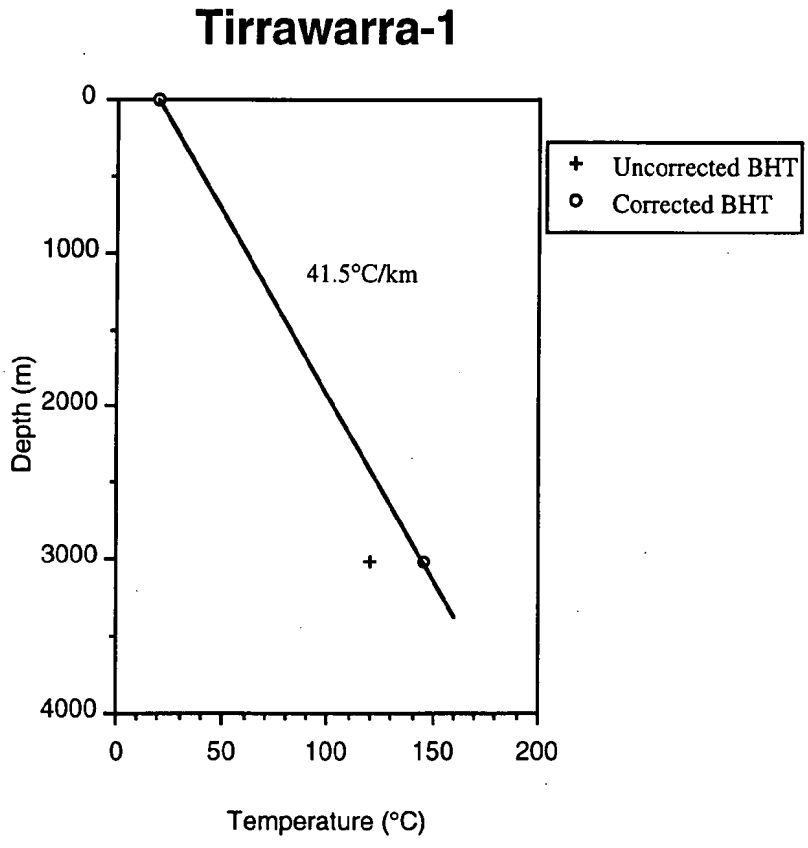

Figure A.1b: Present temperature profile calculated for **well Tirrawarra-1, Cooper - Eromanga Basin.** See Table A.4 and Appendix A for more detail.

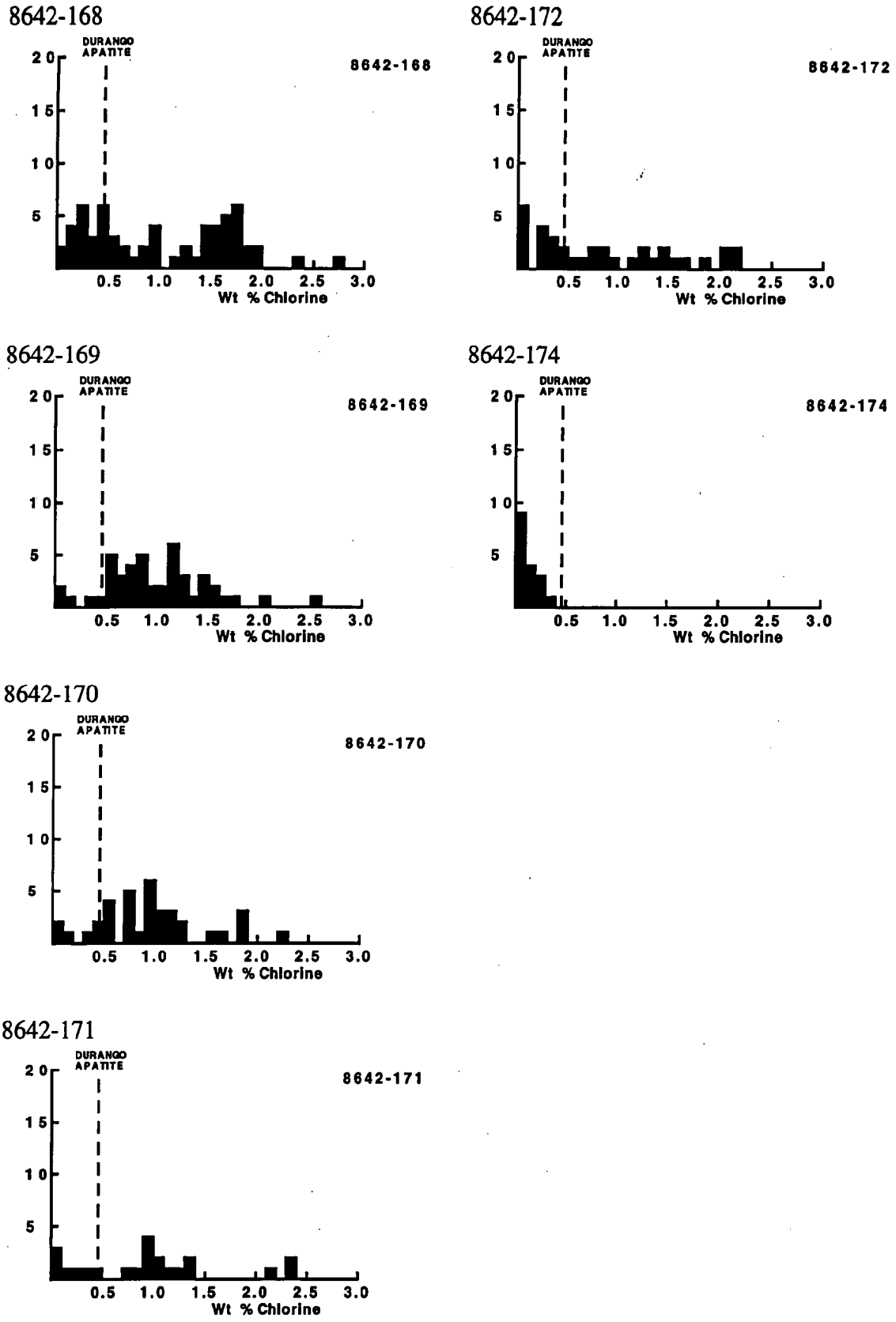

Figure A.2a: Distributions of chlorine content in samples from **well Burley-2, Cooper - Eromanga Basin.**

8642-223

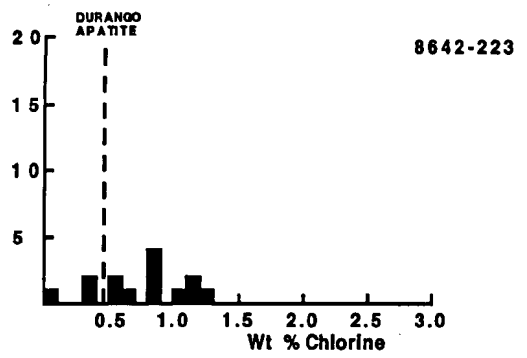

8642-224

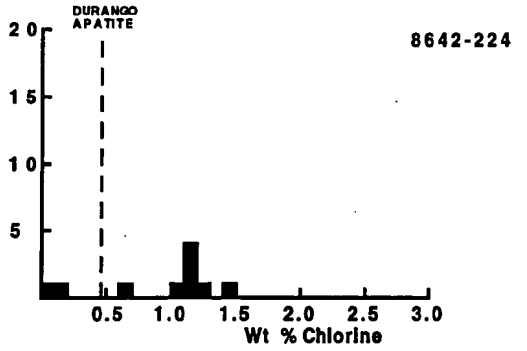

Figure A.2b: Distributions of chlorine content in samples from **well Toolachee-1, Cooper - Eromanga Basin.**

8642-238

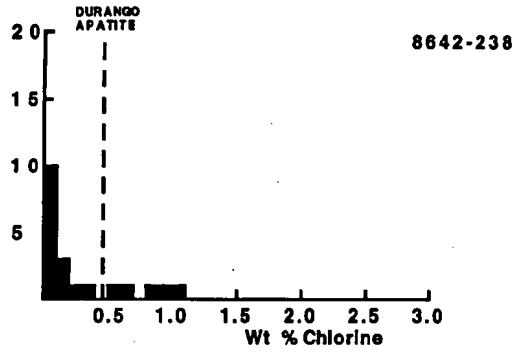

8642-240

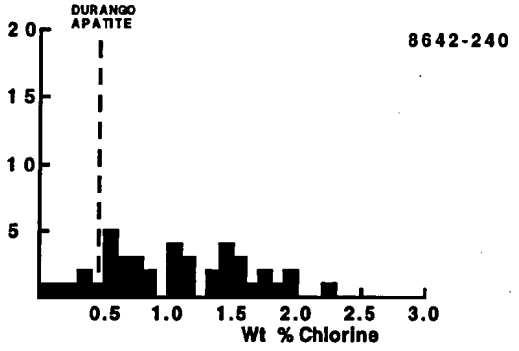

Figure A.2c: Distributions of chlorine content in samples from **well Beanbush-1, Cooper - Eromanga Basin.**

8642-152

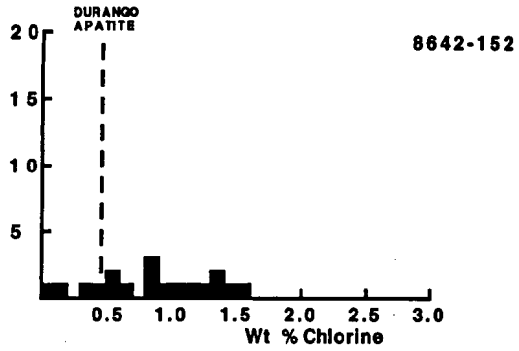

8642-160

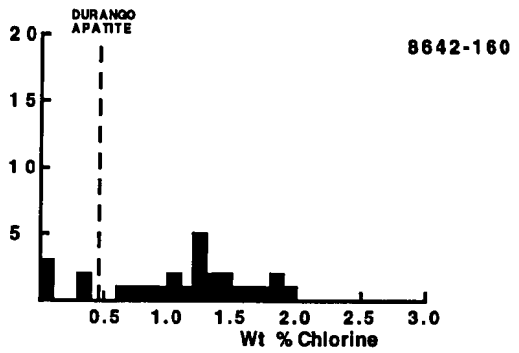

8642-156

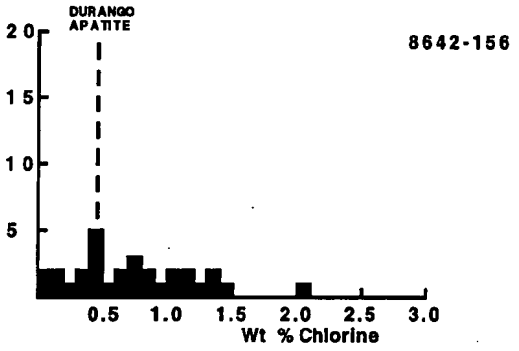

8642-157

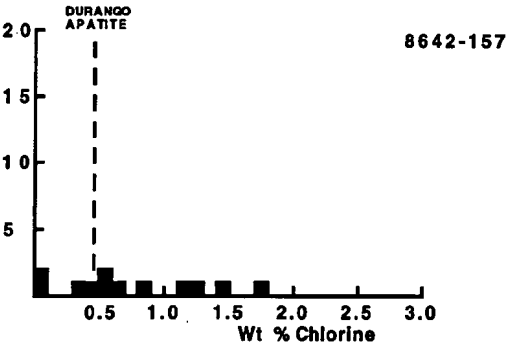

8642-158

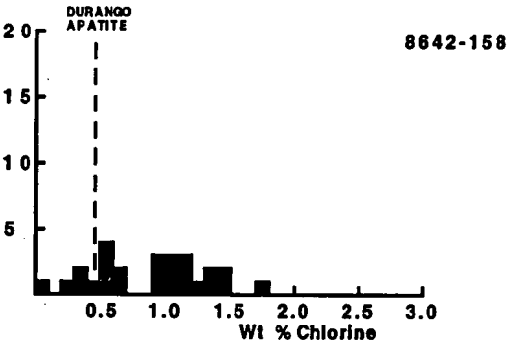

Figure A.2d: Distributions of chlorine content in samples from well **Tirrawarra-1, Cooper - Eromanga Basin.**

APPENDIX B

Sample Preparation, Analytical Details and Data Presentation

B.1 Sample Preparation

Core and outcrop samples are crushed in a jaw crusher and then ground to sand grade in a rotary disc mill. Cuttings samples are washed and dried before grinding to sand grade. The ground material is then washed to remove dust, dried and processed by conventional heavy liquid and magnetic separation techniques to recover heavy minerals.

Apatite grains are mounted in epoxy resin on glass slides, polished and etched for 20 sec in 5M HNO_3 at 20°C to reveal the fossil fission tracks. Zircon grains were embedded in FEP Teflon between heated microscope slides on a hot plate, then polished and etched in a molten KOH:NaOH eutectic mixture at ~220°C (Gleadow et al., 1976), for an appropriate time (typically between 10 and 100 hours) to reveal properly etched fission tracks in a high proportion of the grains present.

After etching, all mounts are cut down to 1.5 x 1 cm, and cleaned in detergent, alcohol and distilled water. The mounts are then sealed in intimate contact with low-uranium muscovite detectors within heat-shrink plastic film. Each batch of mounts is stacked between two pieces of uranium standard glass, which has been prepared in similar fashion. The stack is then inserted into an aluminium can for irradiation.

After irradiation, the mica detectors are removed from the grain mounts and standard glasses and etched in hydrofluoric acid to reveal the fission tracks produced by induced fission of ^{235}U in the apatite and standard glass.

B.2 Analytical Details

Fission track ages

Fission track ages are determined by the external detector method or EDM (Gleadow, 1981). The EDM has the advantage of allowing fission track ages to be determined on single grains. In apatite, tracks are counted in 20 grains from each mount wherever possible. In zircon, 10 grains are normally analysed. In those samples where the desired number is not present, all available grains are counted, the actual number depending on the availability of suitably etched and oriented grains. Only grains oriented with surfaces parallel to the crystallographic c-axis are analysed. Such grains can be identified on the basis of the etching characteristics, as well as from morphological evidence in euhedral grains. The grain mount is scanned sequentially, and for apatite the first 20 suitably

oriented grains identified are analysed, while for zircon the first 10 suitable grains are used.

Fission track ages are calculated using the standard fission track age equation using the zeta calibration method (equation five of Hurford and Green, 1983), viz:

$$\text{F.T. AGE} = \frac{1}{\lambda_D} \ln \left[1 + \left(\frac{\zeta \lambda_D \rho_s g \rho_D}{\rho_i} \right) \right] \qquad \text{B.1}$$

where:
- λ_D = Total decay constant of ^{238}U (= 1.55125 x 10^{-10})
- ζ = Zeta calibration factor
- ρ_s = Spontaneous track density
- ρ_i = Induced track density
- ρ_D = Track density from uranium standard glass
- g = A geometry factor (= 0.5)

Tracks are counted within an eyepiece graticule divided into 100 grid squares. In each grain, the number of spontaneous tracks (N_s) within a certain number of grid squares (N_a) is recorded. The number of induced tracks (N_i) in the corresponding location within the mica external detector is then counted. Spontaneous and induced track densities (ρ_s and ρ_i, respectively) are calculated by dividing the track counts by the total area counted, given by the product of Na and the area or each grid square (determined by calibration against a ruled stage graticule or diffraction grating). Fission track ages may be calculated by substituting track counts (N_s and N_i) for track densities (ρ_s and ρ_i) in equation B.1, since the areas cancel in the ratio.

Translation between apatite grains in the grain mount and external detector locations corresponding to each grain is carried out using Autoscan™ microcomputer-controlled automatic stages (Smith and Leigh Jones, 1985). This system allows repeated movement between grain and detector, and all grain locations are stored for later reference if required.

Neutron irradiations are carried out in a well-thermalised flux (X-7 facility; Cd ratio for Au ~98) in the Australian Atomic Energy Commission's HIFAR research reactor. Total neutron fluence is monitored by counting tracks in mica external detectors attached to two pieces of Corning Glass Works standard glass (CN5 containing ~11 ppm uranium for apatite, and U3 containing ~55 ppm uranium for zircon) included in the irradiation canister at each end of the sample stack. In determining track densities in external detectors irradiated adjacent to uranium standard glasses, 25 fields are normally counted in each detector. The total track count (N_D) is divided by the total area counted to obtain the track density (ρ_D). The positions of the counted fields are arranged in a 5 X 5 grid

covering the whole area of the detector. For typical track densities of between ~5 X 10^5 and 5 X 10^6, this is a convenient arrangement to sample across the detector while gathering sufficient counts to achieve a precision of ~±2% in a reasonable time.

A small flux gradient is often present in the irradiation facility over the length of the sample package. If a detectable gradient is present, the track count in the external detector adjacent to each standard glass is converted to a track density ρ_D and a value for each mount in the stack is calculated by linear interpolation. When no detectable gradient is present, the track counts in the two external detectors are pooled to give a single value of ρ_D which is used to calculate fission track ages for each sample.

A Zeta calibration factor (ζ) has been determined empirically for each observer by analysing a set of carefully chosen age standards with independently known K-Ar ages, following the methods outlined by Hurford and Green (1983) and Green (1985).

All track counting is carried out using Zeiss(R) Axioplan microscopes, with an overall linear magnification of 1068 x using dry objectives.

For further details and background information on practical aspects of fission track age determination, see e.g. Fleischer, Price and Walker (1975), Naeser (1979) and Hurford (1986).

Track length measurements

For track length studies in apatite, the full lengths of "confined" fission tracks are measured. Confined tracks are those which do not intersect the polished surface but have been etched from other tracks or fractures, so that the whole length of the track is etched. Confined track lengths are measured using a digitising tablet connected to a microcomputer, superimposed on the microscope field of view via a projection tube. With this system, calibrated against a stage graticule ruled in 2 μm divisions, individual tracks can be measured to a precision of ± 0.2 μm. Tracks are measured only in prismatic grains, characterised by sharp polishing scratches with well-etched tracks of narrow cone angle in all orientations, because of the anisotropy of annealing of fission tracks in apatite (as discussed by Green et al. 1986). Tracks are also measured following the recommendations of Laslett et al. (1982), the most important of which is that only horizontal tracks should be measured. One hundred tracks are measured whenever possible. In apatite samples with low track density, or in those samples in which only a small number of apatite grains are obtained, fewer confined tracks may be available. In such cases, the whole mount is scanned to measure as many confined tracks as possible.

Integrated fission track age and length measurement

Fission track age determination and length measurement are now made in a single pass of the grain mount, in an integrated approach. The location of each grain in which tracks are either counted or measured is recorded for future reference. Thus, track length measurements can be tied to age determination in individual grains. As a routine procedure we do not measure the age of every grain in which lengths are determined, as this would be much too time-consuming. Likewise we do not only measure ages in grain in which lengths are measured, as this would bias the age data against low track density grains. Nevertheless, the ability to determine the fission track age of certain grains from which length data originate can be a particularly useful aid to interpretation in some cases. Grain location data are not provided in this report, but are available on request.

B.3 Data Presentation

Fission track age data

Data sheets summarising the fission track age data for both apatite and zircon, including full details of fission track age data for individual grains in each sample, together with the primary counting results and statistical data, are given in the following pages. Individual grain fission track ages are calculated from the ratio of spontaneous to induced fission track counts for each grain using equation B.1, and errors in the single grain ages are calculated using Poissonian statistics, as explained in more detail by Galbraith (1981) and Green (1981). All errors are quoted as $\pm 1\sigma$ throughout this report, unless otherwise stated.

The variability of fission track ages between individual apatite grains within each sample can be assessed using a chi-squared (χ^2) statistic (Galbraith, 1981), the results of which are summarised for each sample in the data sheets. If all the grains counted belong to a single age population, the probability of obtaining the observed χ^2 value, for ν degrees of freedom (where ν = number of crystals -1), is listed in the data sheets as $P(\chi^2)$ or P(chi squared).

A $P(\chi^2)$ value greater than 5% can be taken as evidence that all grains are consistent with a single population of fission track age. In this case, the best estimate of the fission track age of the sample is given by the "pooled age", calculated from the ratio of the total spontaneous and induced track counts in all grains analysed. Errors for the pooled age are calculated using the "conventional" technique outlined by Green (1981), based on the total number of tracks counted for each track density measurement (see also Galbraith, 1981).

A $P(\chi^2)$ value of less than 5% denotes a significant spread of single grain ages, suggesting real differences exist between the fission track ages of individual apatite grains. A significant spread in grain ages can result either from inheritance of detrital grains from mixed source areas (in sedimentary rocks), or from differential annealing in apatite grains of different composition, within a narrow range of temperature.

Calculation of the pooled age inherently assumes that only a single population of ages is present, and is thus not appropriate to samples containing a significant spread of fission track ages. In such cases, Galbraith has recently devised a means of estimating the modal age of a distribution of single grain fission track ages which is referred to as the "central age". Calculation of the central age assumes that all single grain ages belong to a Normal distribution of ages, with a standard deviation (σ) known as the "age dispersion". An iterative algorithm (as yet unpublished) is used to provide estimates of the central age with its associated error, and the age dispersion, which are all quoted in the data sheets. Note that this treatment replaces use of the "mean age", which has used been in the past for those samples in which $P(\chi^2)<5\%$. For samples in which $P(\chi^2)>5\%$, the central age and the pooled age should be equal, and the age dispersion should be less than ~10%.

Table B.1 summarises the fission track age data in apatite from each sample analysed, while Table B.3 summarises similar data for zircon in each sample analysed.

Construction of radial plots of single grain age data

Single grain age data are best represented in the form of radial plot diagrams (Galbraith, 1988, 1990). As illustrated in Figure B.1, these plots display the variation of individual grain ages in a plot of y against x, where:

$$y = (z_j - z_o)/\sigma_i \qquad x = 1/\sigma_j \qquad \text{B.2}$$

and;
z_j = Fission track age of grain j
z_o = A reference age
σ_j = Error in age for grain j

In this plot, all points on a straight line from the origin define a single value of fission track age, and, at any point, the value of x is a measure of the precision of each individual grain age. Therefore, precise individual grain ages fall to the right of the plot (small error, high x), which is useful, for example, in enabling precise, young grains to be identified. The age scale is shown radially around the perimeter of the plot (in Ma). If all grains belong to a single age population, all data should scatter between y = +2 and y = -2, equivalent to scatter within $\pm 2\sigma$. Scatter outside these boundaries shows a significant spread of individual grain ages, as also reflected in the values of $P(\chi^2)$ and age dispersion.

In detail, rather than using the fission track age for each grain as in equation B.2, we use:

$$z_j = \frac{N_{sj}}{N_{ij}} \qquad \sigma_j = \{ 1/N_{sj} + 1/N_{ij} \} \qquad \text{B.3}$$

as we are interested in displaying the scatter within the data from each sample in comparison with that allowed by the Poissonian uncertainty in track counts, without the additional terms which are involved in determination of the fission track age (ρ_D, ζ, etc).

Zero ages cannot be displayed in such a plot. This can be achieved using a modified plot, (Galbraith, 1990) with:

$$z_j = \text{arc sin} \sqrt{\left\{ \frac{N_{sj}+3/8}{N_{sj} + N_{ij} + 3/4} \right\}} \qquad \sigma_j = \frac{1}{2} \sqrt{\left\{ \frac{1}{N_{sj} + N_{ij}} \right\}} \qquad \text{B.4}$$

Note that the numerical terms in the equation for z_j are standard terms, introduced for statistical reasons. Using this arc-sin transformation, zero ages plot on a diagonal line which slopes from upper left to lower right. Note that this line does not go through the origin. Figure B.2 illustrates this difference between conventional and arc-sin radial plots, and also provides a simple guide to the structure of radial plots.

Use of arc-sin radial plots is particularly useful in assessing the relative importance of zero ages. For instance, grains with $N_s = 0$, $N_i = 1$ are compatible with ages up to ~900 Ma (at the 95% confidence level), whereas grains with $N_s = 0$, $N_i = 50$ are only compatible with ages up to ~14 Ma. The two data would readily be distinguishable on the radial plot as the 0,50 datum would plot well to the right (high x) compared to the 0,1 datum.

In this report the value of z corresponding to the stratigraphic age of each sample (or the midpoint of the range where appropriate) is adopted as the reference value, z_o. This allows rapid assessment of the fission track age of individual grains in relation to the stratigraphic age, which is a key component in the interpretation of AFTA data, as explained in more detail in Appendix C.

Note that the x axis of the radial plot is normally not labelled, as this would obscure the age scale around the plot. In general labelling is not considered necessary, as we are concerned only with relative variation within the data, rather than absolute values of precision.

Radial plots of the single grain age data from each sample analysed in this report are shown in Figure B.3 for apatite and Figure B.5 for zircon. Use of radial plots to provide thermal history information is explained in Appendix C and Figure C.7.

Smoothed probability distributions

The single grain ages within each sample are also shown in Figures B.3 and B.5 in histogram form and also as smoothed probability distributions (Hurford et al., 1984). In constructing these distributions, each grain is represented by a normal probability curve, with mean equal to the single grain age, standard deviation given by the error on the single grain age and the contributions from all grains analysed in each sample are summed to produce the plotted curve. These distributions are generally not as informative as the radial plot presentation of single grain age data as they convey little assessment of the relative precision of the fission track ages of different grains. However, they can be useful for portraying the general form of the distribution of ages within a sample.

Track length data

Distributions of confined track lengths in apatite from each sample are shown as simple histograms in Figure B.4. For every track length measurement, the length is recorded to the nearest 0.1 μm, but the measurements have been grouped into 1 μm intervals in the histograms in Figure B.4. Each distribution has been normalised to 100 tracks for each sample to facilitate comparison. A summary of the length distribution in each sample is presented in Table B.2, which also shows the mean track length in each sample and its associated error, the standard deviation of each distribution and the number of tracks (N) measured in each sample. The angle which each confined track makes with the crystallographic c-axis is also routinely recorded, as is the width of each fracture within which tracks are revealed. These data are not provided in this report, but can be supplied on request. Track length data is not routinely collected in zircon.

Breakdown of data into compositional groups

In Table B.4, AFTA data are grouped into compositional intervals of 0.1 wt% Cl width. Parameters for each interval represent the data from all grains with Cl contents within each interval. Also shown are the parameters for each compositional interval predicted from the Default Thermal History (see Section 2.1). These data form the basis of interpretation of the AFTA data, which takes full account of the influence of Cl content on annealing kinetics, as described in Appendix C.

Plots of fission track age against Cl content for individual apatite grains

In Figure B.6, fission track ages of single apatite grains within individual samples are plotted against the Cl content of each grain. These plots are useful in assessing the degree of annealing, as expressed by the fission track age data. For example, if grains with a range of Cl contents from zero to some upper limit all give similar fission track ages which are significantly less than the stratigraphic age, then grains with these compositions

must have been totally annealed. Alternatively, if fission track age falls rapidly with decreasing Cl content, the sample displays a high degree of partial annealing.

B.4 A note on terminology

Note that throughout this report, the term "fission track age" is understood to denote the parameter calculated from the fission track age equation, using the observed spontaneous and induced track counts (either pooled for all grains or for individual grains). The resulting number (with units of Ma) should not be taken as possessing any significance in terms of events taking place at the time indicated by the measured fission track age, but should rather be regarded as a measure of the integrated thermal history of the sample, and should be interpreted in that light using the principles outlined in Appendix C. Use of the term "apparent age" is not considered to be useful in this regard, as almost every fission track age should be regarded as an apparent age, in the classic sense, and repeated use becomes cumbersome.

References

Fleischer, R.L., Price, P.B., and Walker, R.M. (1975) Nuclear tracks in solids, University of California Press, Berkeley.

Galbraith, R.F. (1981) On statistical models for fission-track counts. *Mathematical Geology*, 13, 471-488.

Galbraith, R.F. (1988) Graphical display of estimates having differing standard errors. *Technometrics*, 30, 271-281.

Galbraith, R.F. (1990) The radial plot: graphical assessment of spread in ages. *Nuclear tracks*, 17, 207-214.

Gleadow, A.J.W. (1981) Fission track dating methods; what are the real alternatives? *Nuclear Tracks*, 5, 3-14.

Green, P.F. (1981) A new look at statistics in fission track dating. *Nuclear Tracks 5*, 77-86.

Green, P.F. (1985) A comparison of zeta calibration baselines in zircon, sphene and apatite. *Chem. Geol. (Isot. Geol. Sect.)*, 58, 1-22.

Green, P.F., Duddy, I.R., Gleadow, A.J.W., Tingate, P.R. and Laslett, G.M. (1986) Thermal annealing of fission tracks in apatite 1. A qualitative description. *Chem. Geol. (Isot. Geosci. Sect.)*, 59, 237-253.

Hurford, A.J. (1986) Application of the fission track dating method to young sediments: Principles, methodology and Examples. *In:* Hurford, A.J., Jäger, E. and Ten Cate, J.A.M. (*eds*), Dating young sediments, CCOP Technical Publication 16, CCOP Technical Secretariat, Bangkok, Thailand.

Hurford, A.J., Fitch, F.J. and Clarke, A. (1984) Resolution of the age structure of the detrital zircon populations of two Lower Cretaceous sandstones from the Weald of England by fission track dating. *Geological Magazine*, 121, 269-396.

Hurford, A.J. and Green, P.F. (1982) A user's guide to fission track dating calibration. *Earth. Planet. Sci Lett.* 59, 343-354.

Hurford, A.J. and Green, P.F. (1983) The zeta age calibration of fission track dating. *Isotope Geoscience* 1, 285-317.

Laslett, G.M., Kendall, W.S., Gleadow, A.J.W. and Duddy, I.R. (1982) Bias in measurement of fission track length distributions. *Nuclear Tracks*, 6, 79-85.

Naeser, C.W. (1979) Fission track dating and geologic annealing of fission tracks. *In:* Jäger, E. and Hunziker, J.C. (*eds*), Lectures in Isotope Geology, Springer Verlag, Berlin.

Smith, M.J. and Leigh-Jones, P. (1985) An automated microscope scanning stage for fission-track dating. *Nuclear Tracks*, 10, 395-400.

Table B.1: Apatite fission track analytical results - well samples from Cooper - Eromanga Basin (Geotrack Report #668)

Sample number	Number of grains	Rho D x10 ^{6} (ND)	Rho S x10 ^{6} (Ns)	Rho I x10 ^{6} (Ni)	Uranium content (ppm)	P(chi squared) (%)	Age dispersion (%)	Fission track age (Ma)
Burley-2								
8642-168	30	1.562 (2455)	0.672 (814)	1.835 (2224)	15	<1	46	102.2 ± 5.0 *115.5 ± 12.1**
8642-169	21	1.559 (2455)	0.438 (326)	1.075 (800)	9	<1	30	113.4 ± 8.1 *117.5 ± 12.4**
8642-170	23	1.555 (2455)	0.488 (331)	1.089 (739)	9	<1	36	124.3 ± 8.9 *108.5 ± 12.4**
8642-171	17	1.552 (2455)	0.342 (155)	0.887 (402)	7	8	28	106.9 ± 10.5
8642-172	29	1.549 (2455)	0.203 (168)	1.124 (929)	9	<1	84	50.3 ± 4.4 *42.0 ± 8.4**
8642-174	15	1.545 (2455)	0.016 (6)	3.631 (1380)	29	<1	167	1.2 ± 0.5 *2.1 ± 1.3**
Toolachee-1								
8642-223	11	1.273 (1889)	0.213 (60)	0.512 (144)	5	74	<1	94.9 ± 14.8
8642-224	7	1.257 (1889)	0.319 (68)	0.745 (159)	7	68	<1	96.1 ± 14.2
Beanbush-1								
8642-238	16	1.128 (1889)	0.392 (212)	2.000 (1081)	22	<1	37	39.7 ± 3.2 *38.0 ± 5.1**
8642-240	20	1.112 (1889)	0.263 (187)	0.921 (655)	10	<1	54	56.9 ± 5.0 *81.4 ± 13.1**
Tirrawarra-1								
8642-152	13	1.579 (2455)	0.303 (181)	0.645 (385)	5	61	<1	132.4 ± 12.5
8642-156	20	1.576 (2455)	0.407 (170)	0.944 (394)	7	26	21	121.3 ± 11.6
8642-157	11	1.572 (2455)	0.195 (84)	0.404 (174)	3	7	32	135.3 ± 18.4
8642-158	21	1.569 (2455)	0.350 (245)	0.638 (447)	5	<1	35	153.1 ± 12.9 *136.7 ± 17.0**
8642-160	22	1.565 (2455)	0.448 (271)	1.926 (1166)	15	<1	48	65.2 ± 4.8 *96.1 ± 13.5**

Rho S = spontaneous track density; Rho I = induced track density; Rho D = track density in glass standard external detector.
All track densities quoted in units of 1000000 tracks per square cm. Brackets show number of tracks counted.
Rho D and Rho I measured in mica external detectors; Rho S measured in internal surfaces.
* Central age, used where sample contains a significant spread of single grain ages—P(chi squared)<5%. Errors quoted at ±1 sigma.
Ages calculated using dosimeter glass CN5, with a zeta of 392.9±7.4 (M. Moore)

Table B.2: Length distribution summary data - well samples from Cooper - Eromanga Basin (Geotrack Report #668)

Sample number	Mean track length (µm)	Standard deviation (µm)	Number of tracks (N)	Number of Tracks in Length Intervals (µm) 1	2	3	4	5	6	7	8	9	10	11	12	13	14	15	16	17	18	19	20
Burley-2																							
8642-168	13.27 ± 0.19	2.00	114	-	-	1	-	-	-	1	1	1	3	2	13	19	28	32	10	3	-	-	-
8642-169	13.15 ± 0.23	1.66	52	-	-	-	-	-	-	-	1	1	-	3	1	22	8	12	3	1	-	-	-
8642-170	12.04 ± 0.38	2.49	42	-	-	-	-	1	-	1	1	1	3	5	7	6	7	8	1	-	1	-	-
8642-171	12.49 ± 0.78	3.21	17	-	-	1	-	-	-	-	-	-	2	-	3	1	4	3	2	1	-	-	-
8642-172	11.40 ± 0.73	2.81	15	-	-	-	-	1	-	1	-	-	1	1	2	5	3	1	-	-	-	-	-
8642-174	11.29 ± 1.28	1.81	2	-	-	-	-	-	-	-	-	-	-	1	-	1	-	-	-	-	-	-	-
Toolachee-1																							
8642-223	12.34 ± 0.75	2.13	8	-	-	-	-	-	-	-	-	1	-	1	1	2	1	1	1	-	-	-	-
8642-224	12.90 ± 0.54	2.01	14	-	-	-	-	-	-	-	-	-	1	2	-	5	1	4	-	-	1	-	-
Beanbush-1																							
8642-238	9.51 ± 0.57	2.54	20	-	-	-	-	2	1	1	-	2	2	5	4	3	-	-	-	-	-	-	-
8642-240	11.28 ± 0.33	2.49	58	-	-	-	-	1	1	2	1	5	8	7	7	14	5	4	1	1	1	-	-
Tirrawarra-1																							
8642-152	12.99 ± 0.50	1.72	12	-	-	-	-	-	-	-	-	-	-	3	2	-	2	4	1	-	-	-	-
8642-156	12.96 ± 0.26	1.09	17	-	-	-	-	-	-	-	-	-	-	1	3	2	10	1	-	-	-	-	-
8642-157	12.89 ± 0.62	0.87	2	-	-	-	-	-	-	-	-	-	-	-	-	1	1	-	-	-	-	-	-
8642-158	11.65 ± 0.74	3.23	19	-	-	1	-	-	-	-	1	3	-	-	3	4	2	3	2	-	-	-	-
8642-160	9.22 ± 0.56	2.83	26	-	1	-	1	-	1	2	1	4	5	4	2	4	1	-	-	-	-	-	-

Track length measurements by M. Moore

Table B.3: ZFTA™ analytical results - well samples from the Cooper-Eromanga Basin (Geotrack Report #668)

Sample number	Number of grains (m)	Rho D x 10^6 (ND)	Rho S x 10^6 (Ns)	Rho I x 10^6 (Ni)	Uranium content (ppm)	P (chi squared) (%)	Age dispersion (%)	Fission track Age (Ma)
Burley-1								
8642-23	10	2.964 (6335)	13.382 (2880)	6.328 (1362)	114	<1	33	269.1±9.7 *274.6±30.1**
8642-25	10	2.964 (6335)	18.961 (3162)	11.71 (1953)	211	≤1	34	207.1±6.7 *217.7±24.9**
McLeod-1								
8642-26	13	2.964 (6335)	16.372 (4286)	8.270 (2165)	149	<1	24	252.3±7.7 *250.6±18.9**
8642-27	9	2.964 (6335)	36.968 (1675)	29.66 (1344)	533	<1	28	160.3±6.3 *159.8±16.2**
Dullingari-1								
8642-53	10	2.964 (6335)	23.599 (1396)	9.399 (556)	169	2	15	318.3±16.7 *319.5±22.9**

Rho S = spontaneous track density; Rho I = induced track density; Rho D = track density in glass standard external detector. All track densities quoted in units of millions of tracks per square cm. Brackets show numbers of tracks counted. Rho D and Rho I are measured in mica external detectors; Rho S measured in internal surfaces of the mineral. Ages calculated using dosimeter glass U3, with a zeta of 87.7±0.8 (Analyst: P.F. Green).
*Central fission track age quoted (in italics) where sample contains a significant spread of single grain ages - P (chi squared) < 5%. Errors quoted at ± 1 sigma.

Estimates	z_i
Standard errors	σ_i
Reference value	z_o
Standardised estimates	$y_i = (z_i - z_o) / \sigma_i$
Precision	$x_i = 1 / \sigma_i$

PLOT y_i against x_i

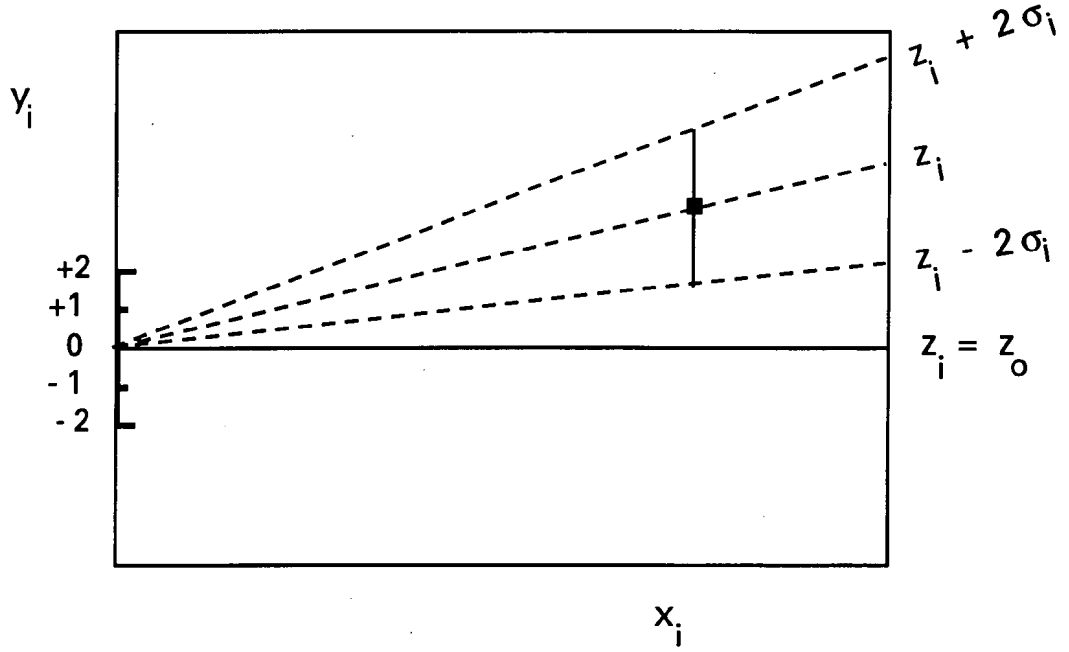

Slope of line from origin through data point $= y_i / x_i$

$= \{(z_i - z_o)/\sigma_i\} / \{1/\sigma_i\}$

$= z_i - z_o$

Key Points:

Radial lines emanating from the origin correspond to fixed values of z

Data points with higher values of x_i have greater precision.

Error bars on all points are the same size in this plot.

Figure B.1 Basic construction of a radial plot. In AFTA, the estimates z_i correspond to the fission track age values for individual apatite grains. Any convenient value of age can be chosen as the reference value corresponding to the horizontal in the radial plot. Radial lines emanating from the origin with positive slopes correspond to fission track ages greater than the reference value. Lines with negative slopes correspond to fission track ages less than the reference value.

Normal radial plot (equations B.2 and B.3)

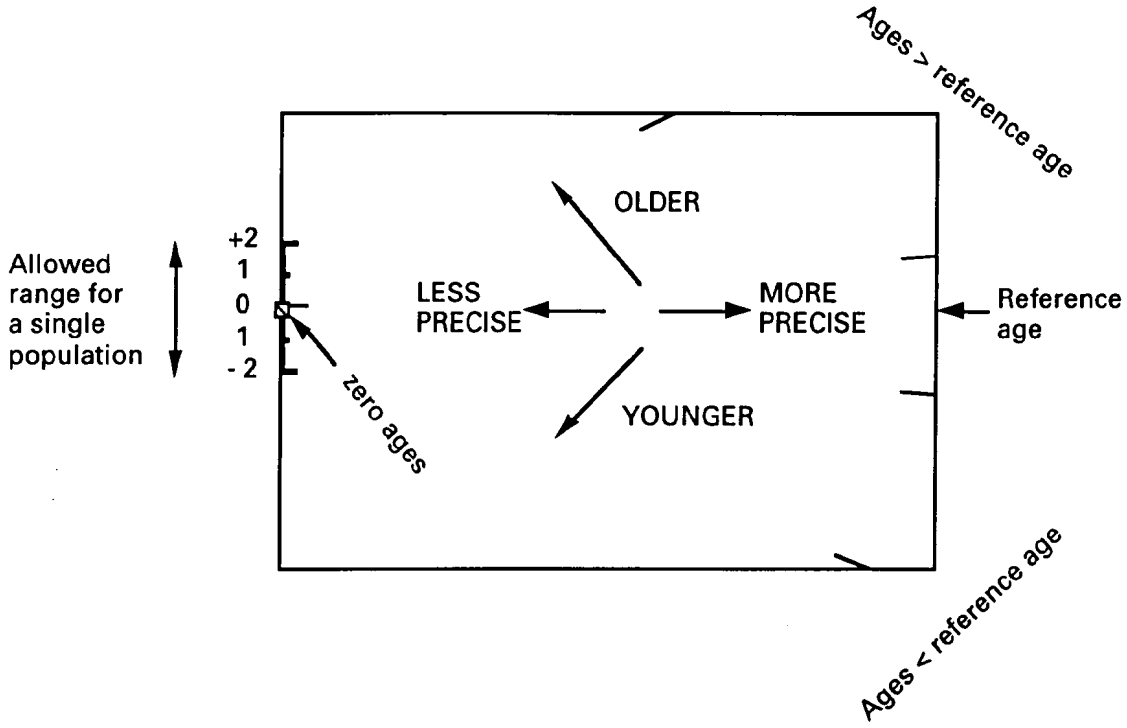

Arc-sin radial plot (equations B.2 and B.4)

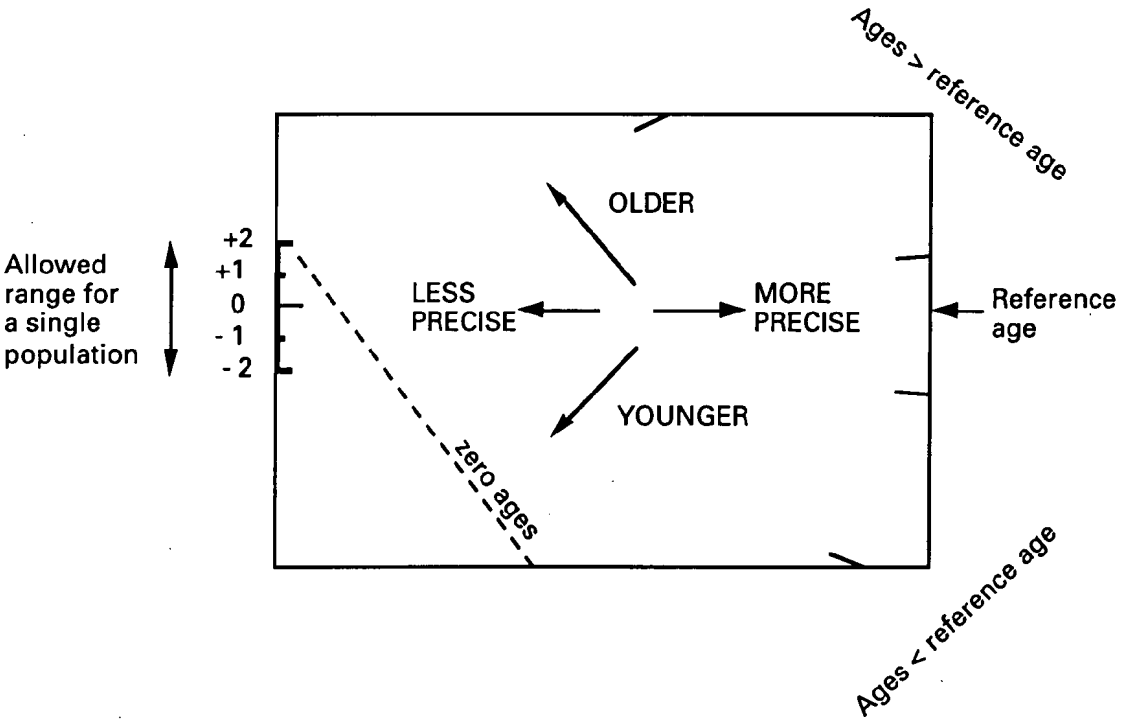

Figure B.2 Simplified structure of Normal and Arc-sin radial plots.

8642-168

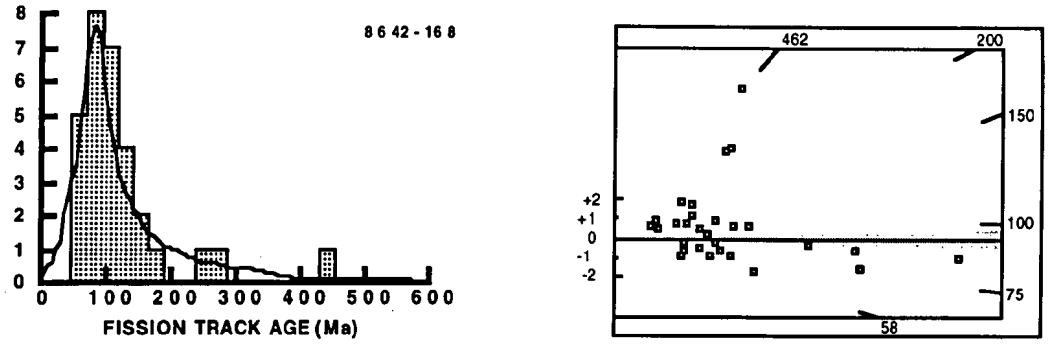

8642-169

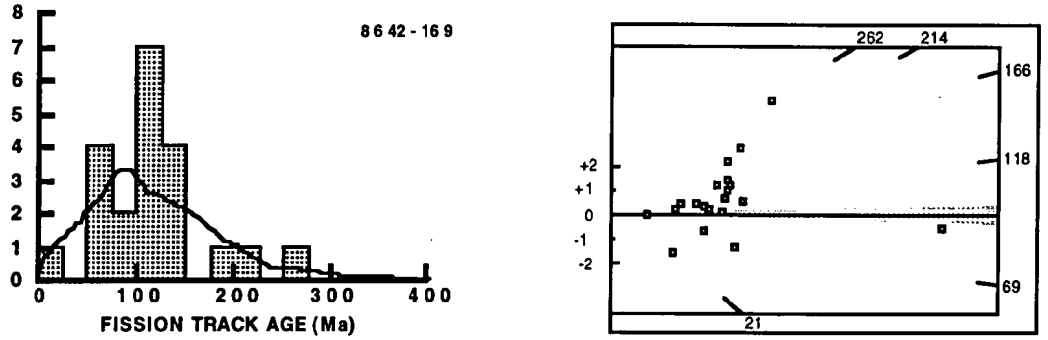

8642-170

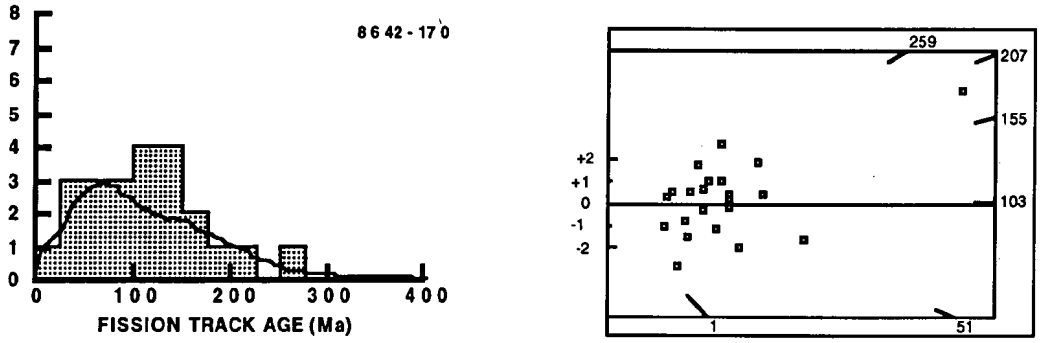

8642-171

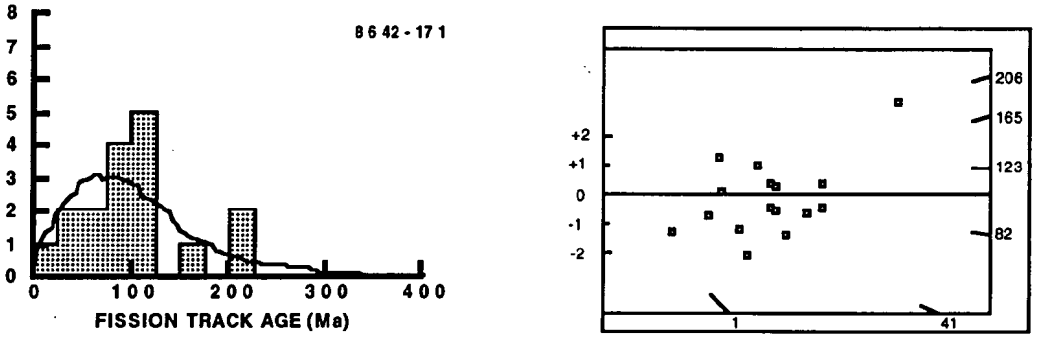

Figure B.3a: Single grain age figures for samples from **well Burley-2, Cooper - Eromanga Basin.** The horizontal line or shaded area in the radial plot diagrams shows the stratigraphic age. See Appendix B for further details.

8642-172

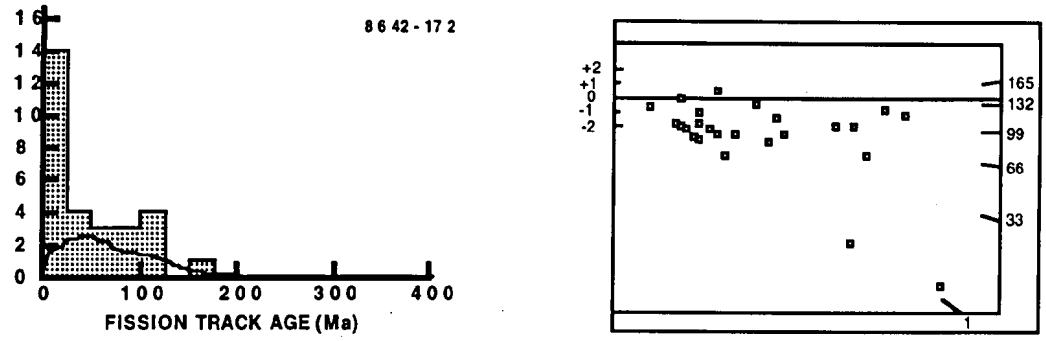

8642-174

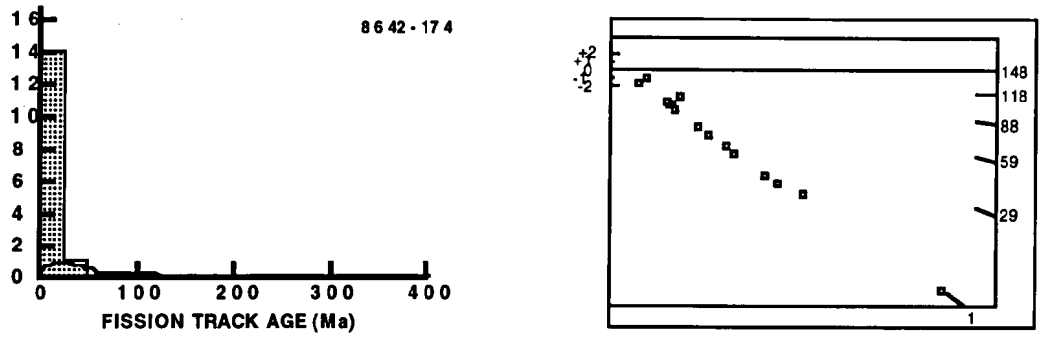

Figure B.3a: Continued.

8642-223

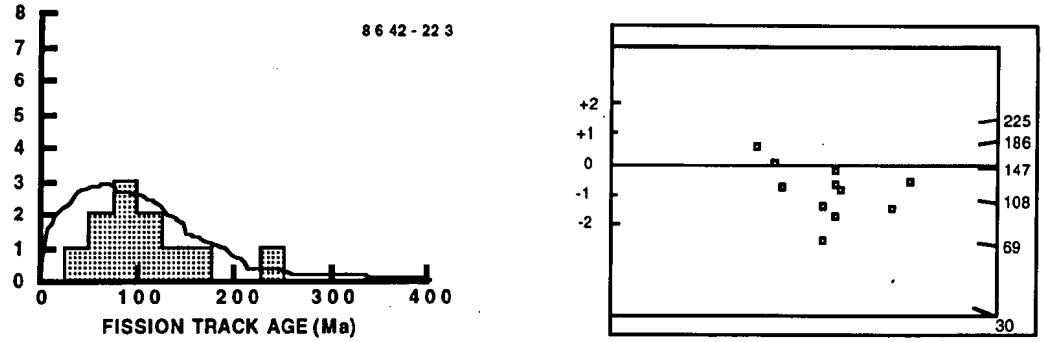

8642-224

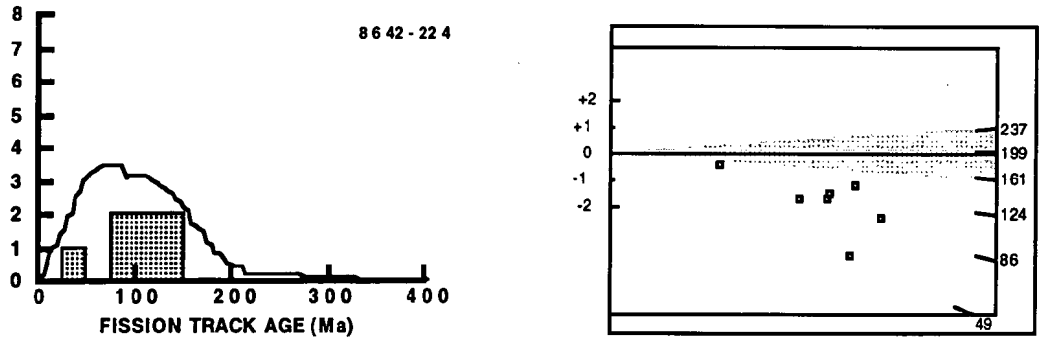

Figure B.3b: Single grain age figures for samples from **well Toolachee-1, Cooper - Eromanga Basin.** The horizontal line or shaded area in the radial plot diagrams shows the stratigraphic age. See Appendix B for further details.

8642-238

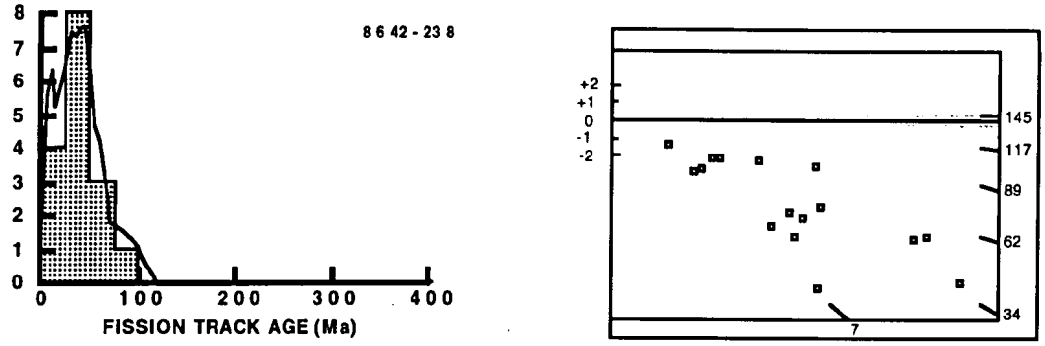

8642-240

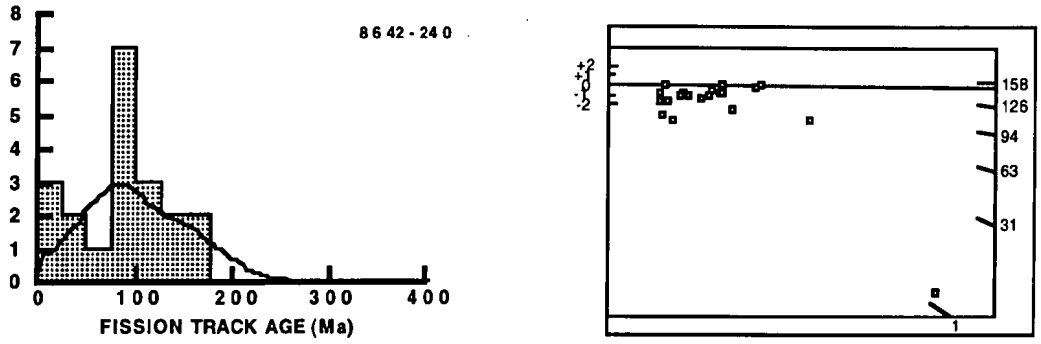

Figure B.3c: Single grain age figures for samples from **well Beanbush-1, Cooper - Eromanga Basin.** The horizontal line or shaded area in the radial plot diagrams shows the stratigraphic age. See Appendix B for further details.

8642-152

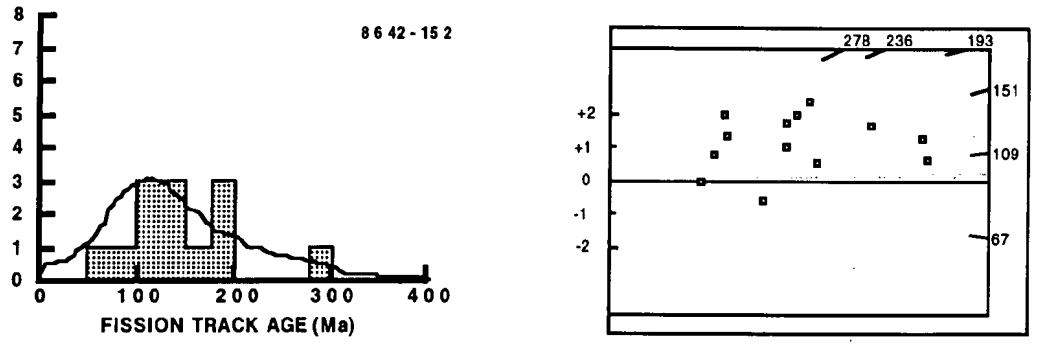

8642-156

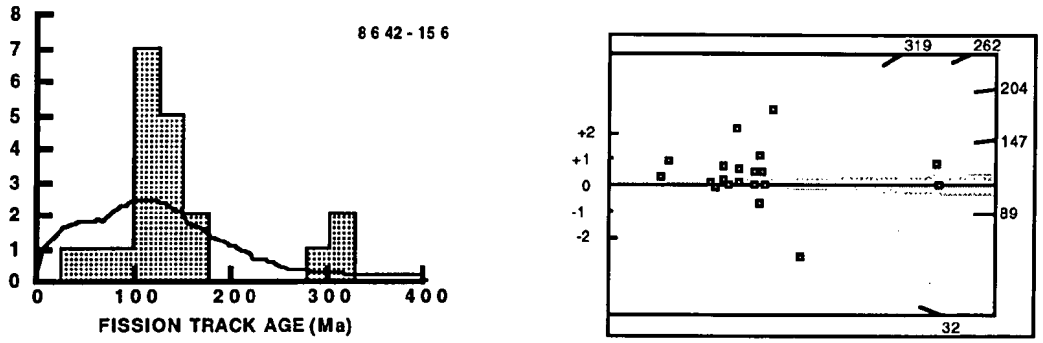

8642-157

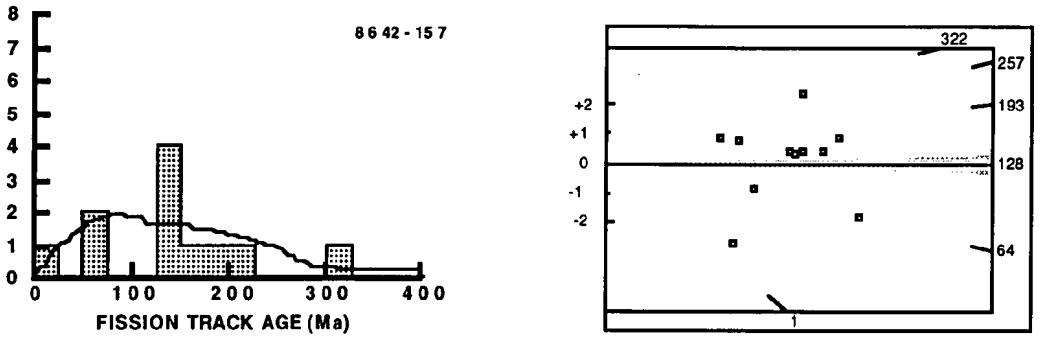

8642-158

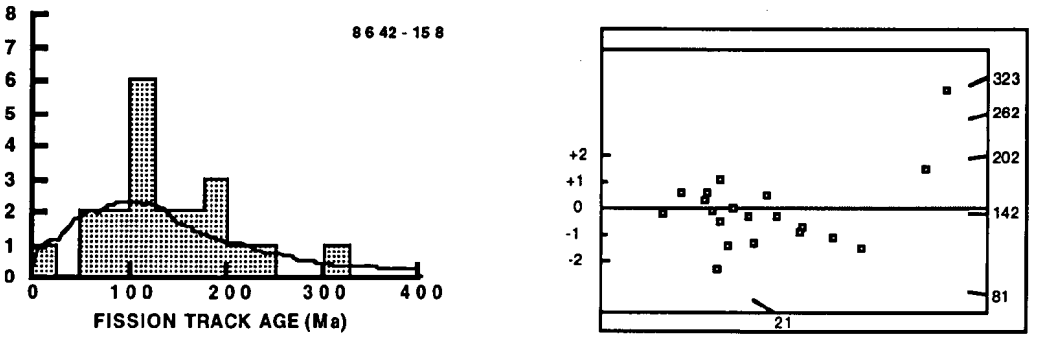

Figure B.3d: Single grain age figures for samples from **well Tirrawarra-1, Cooper - Eromanga Basin.** The horizontal line or shaded area in the radial plot diagrams shows the stratigraphic age. See Appendix B for further details.

8642-160

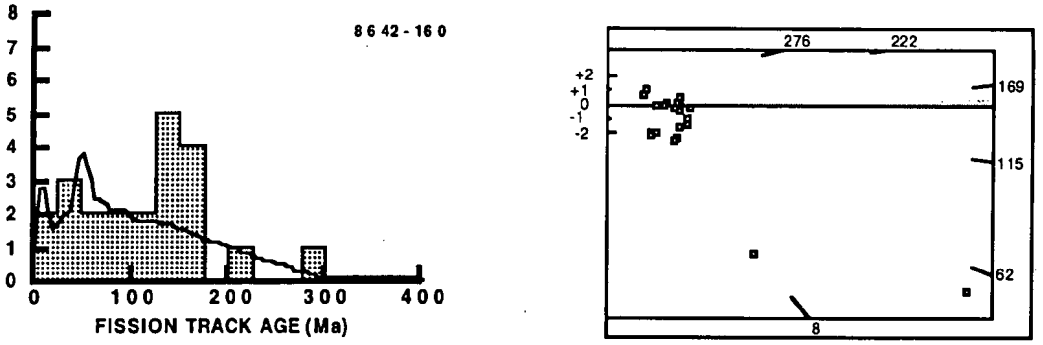

Figure B.3d: Continued.

8642-168

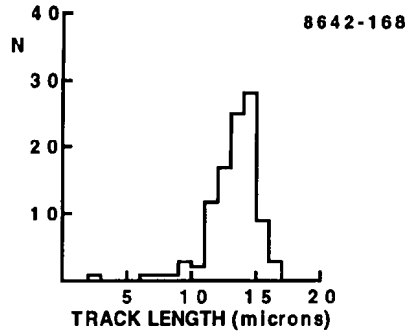

8642-172

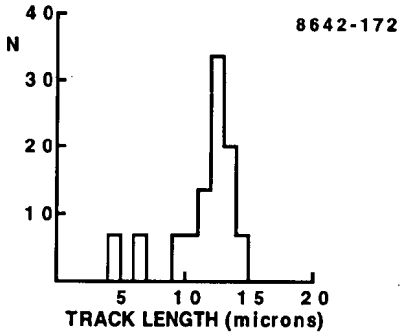

8642-169

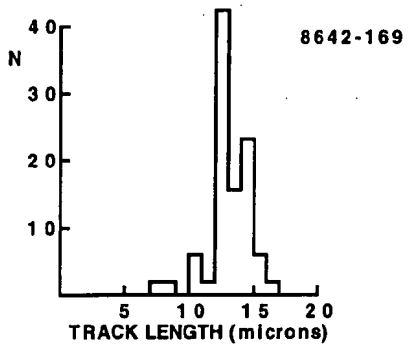

8642-174

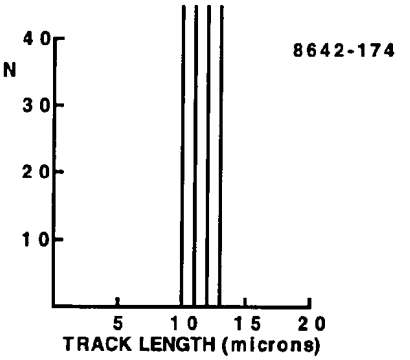

8642-170

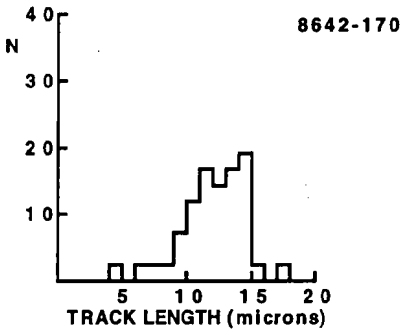

8642-171

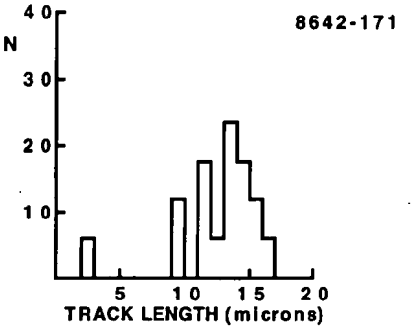

Figure B.4a: Distributions of confined track lengths in samples from **well Burley-2, Cooper - Eromanga Basin.**

8642-223

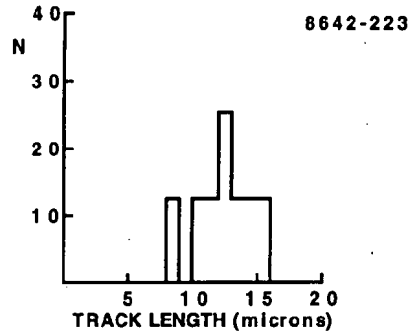

8642-224

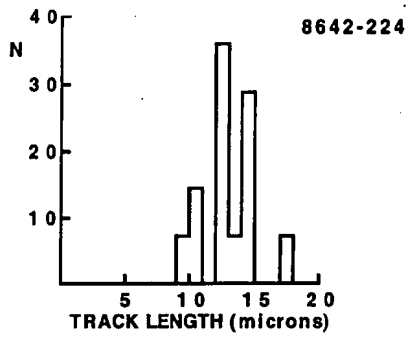

Figure B.4b: Distributions of confined track lengths in samples from **well Toolachee-1, Cooper - Eromanga Basin.**

8642-238

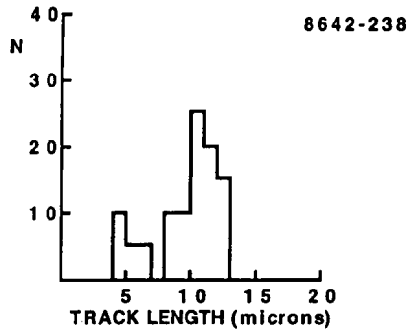

8642-240

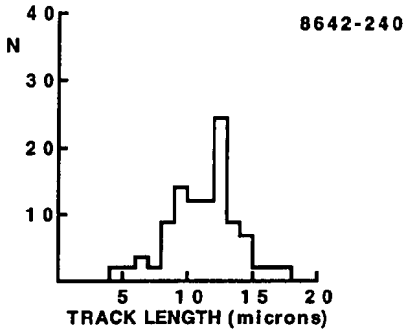

Figure B.4c: Distributions of confined track lengths in samples from **well Beanbush-1, Cooper - Eromanga Basin.**

8642-152

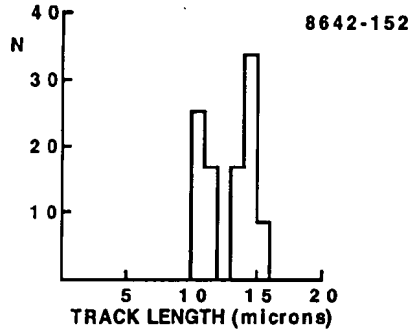

8642-160

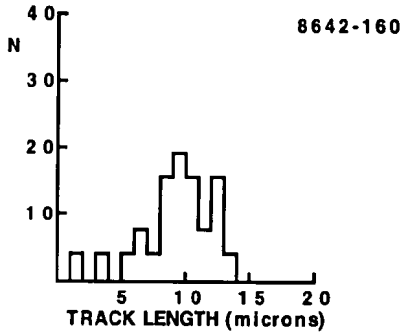

8642-156

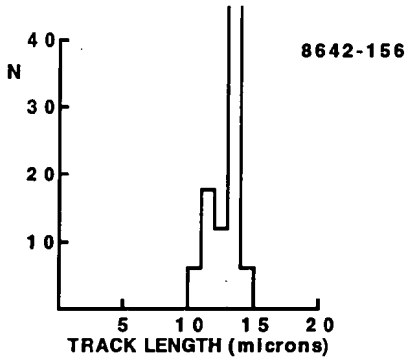

8642-157

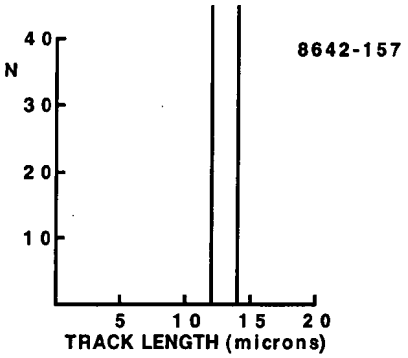

8642-158

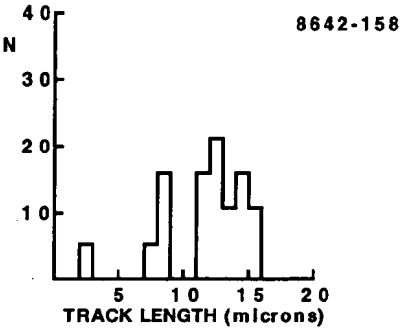

Figure B.4d: Distributions of confined track lengths in samples from **well Tirrawarra-1, Cooper - Eromanga Basin.**

8642-23

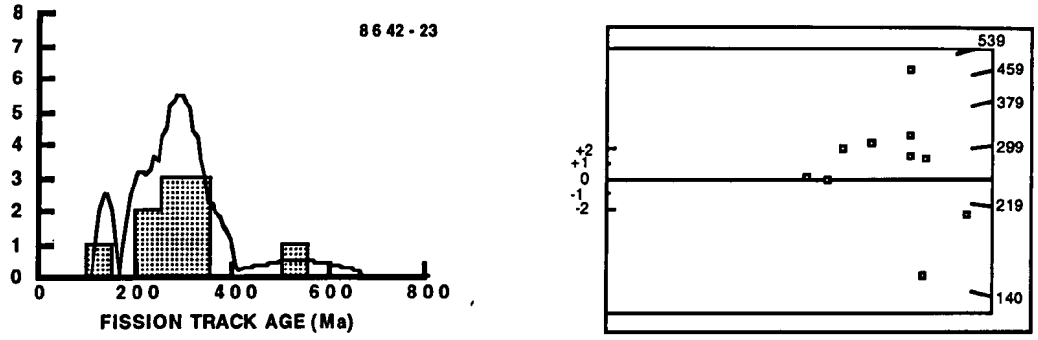

8642-25

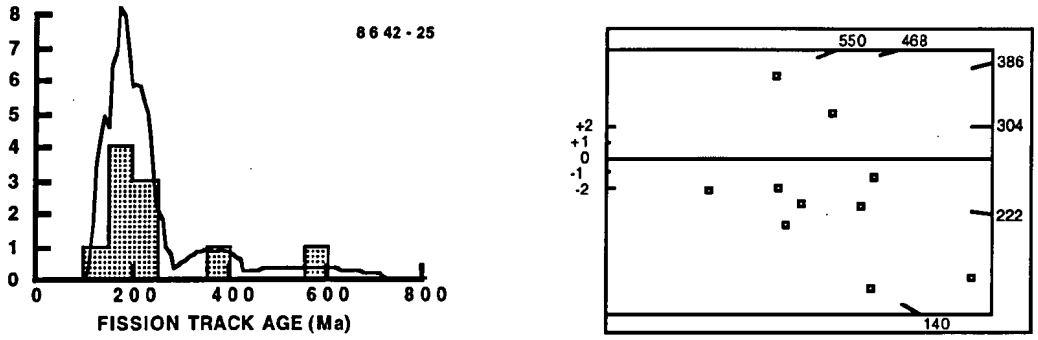

8642-26

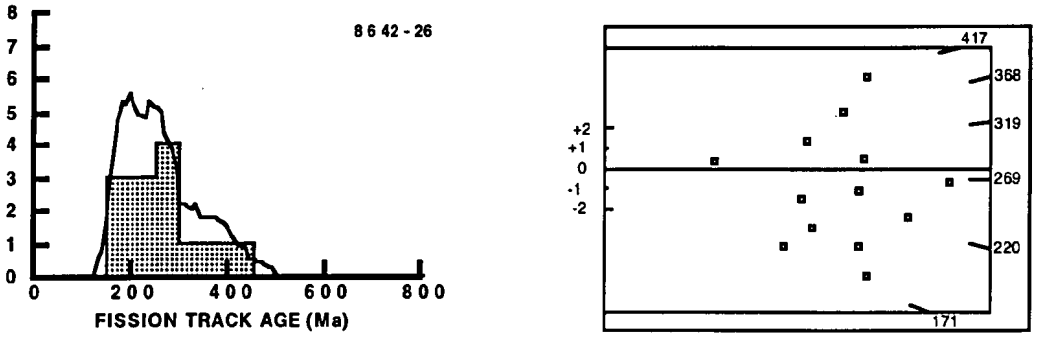

8642-27

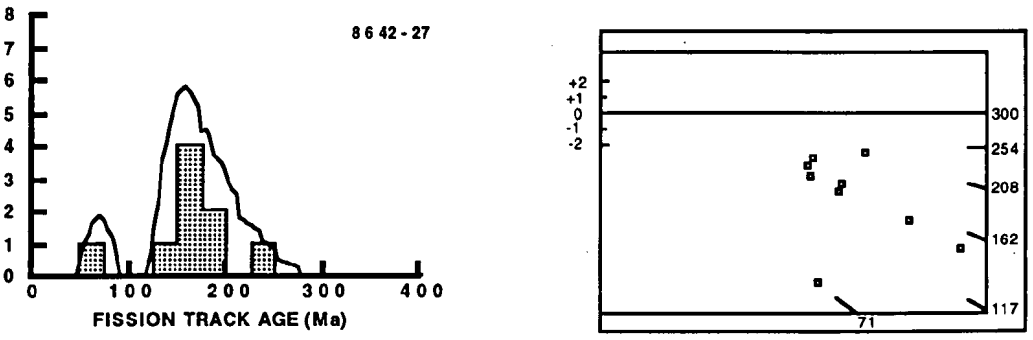

Figure B.5: Single grain age figures for samples from **Cooper/Eromanga Basin wells.** The horizontal line or shaded area in the radial plot diagrams shows the stratigraphic age. See Appendix B for further details.

8642-53

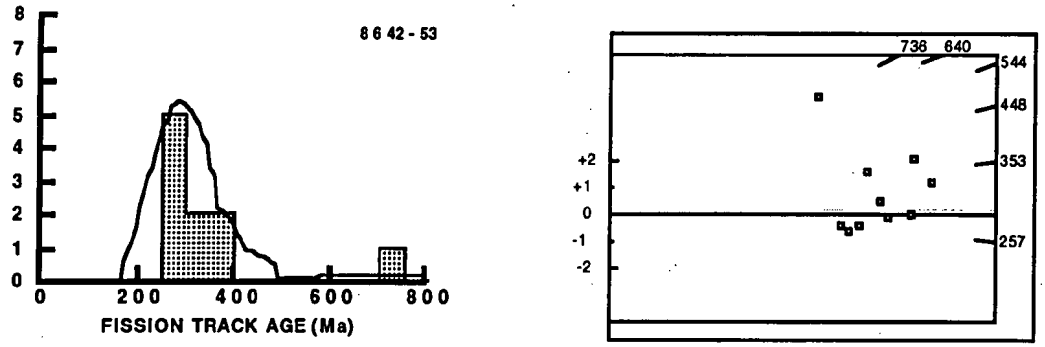

Figure B.5: Continued.

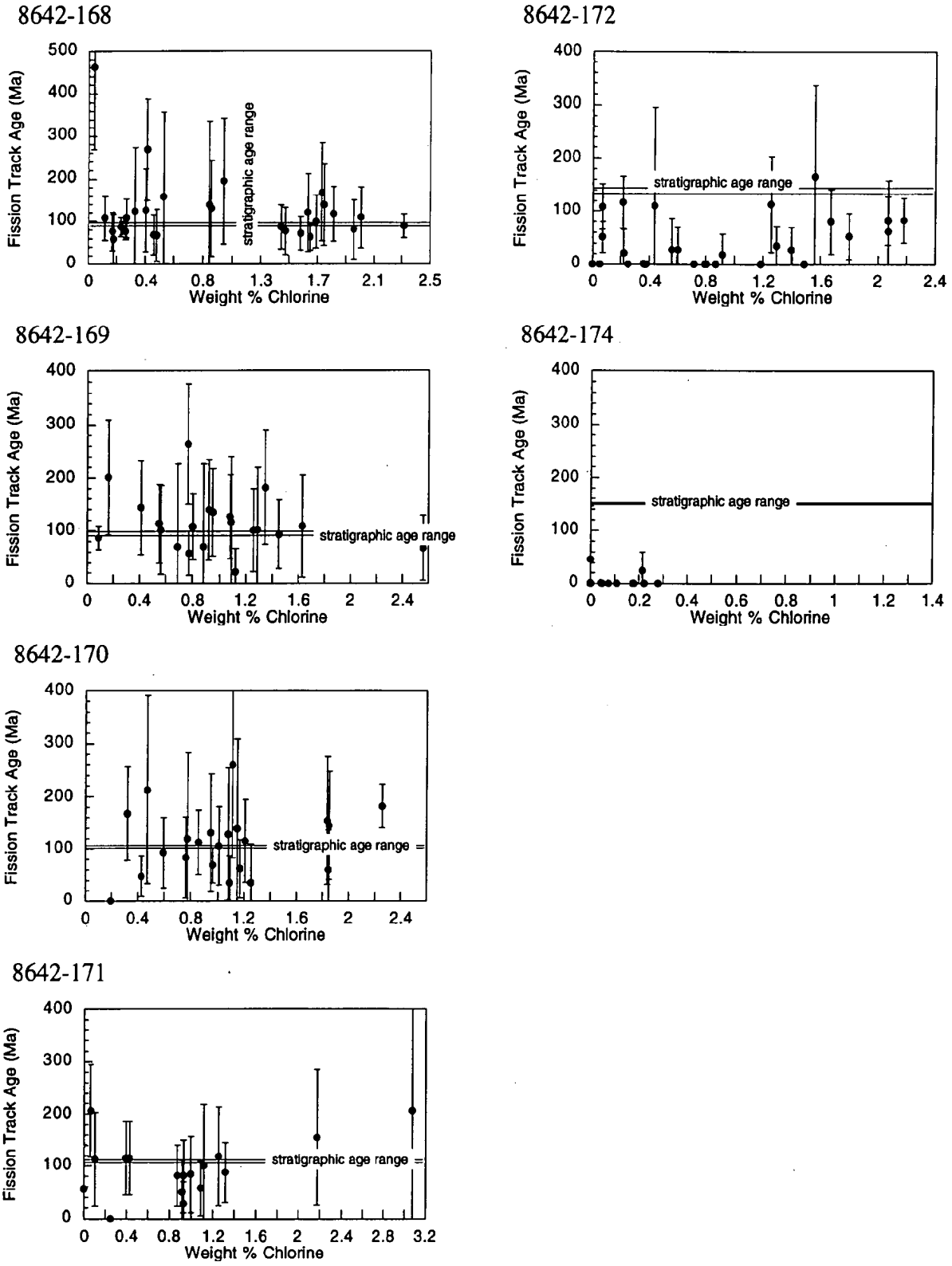

Figure B.6a: Plots of single grain age against weight percent chlorine for samples from **well Burley-2, Cooper - Eromanga Basin.**

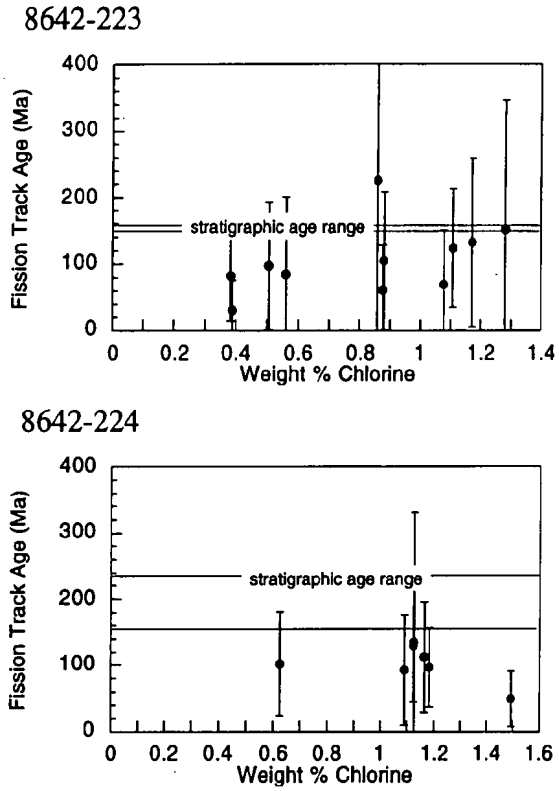

Figure B.6b: Plots of single grain age against weight percent chlorine for samples from **well Toolachee-1, Cooper - Eromanga Basin.**

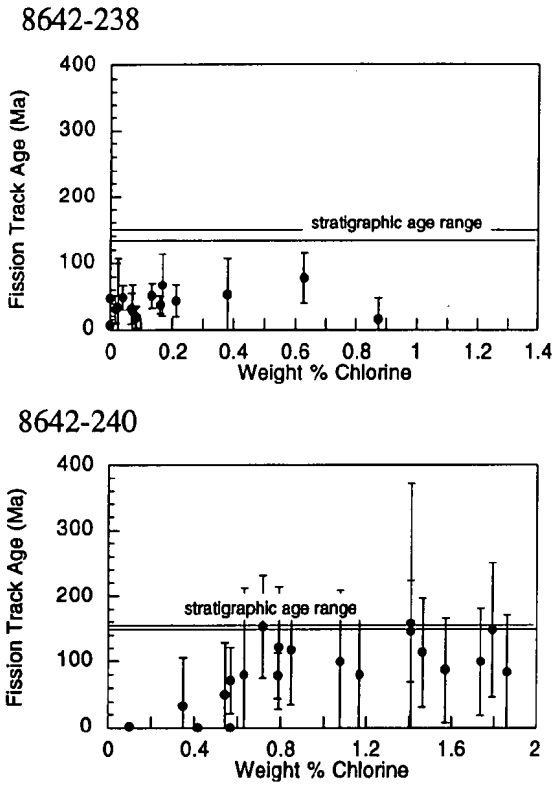

Figure B.6c: Plots of single grain age against weight percent chlorine for samples from **well Beanbush-1, Cooper - Eromanga Basin.**

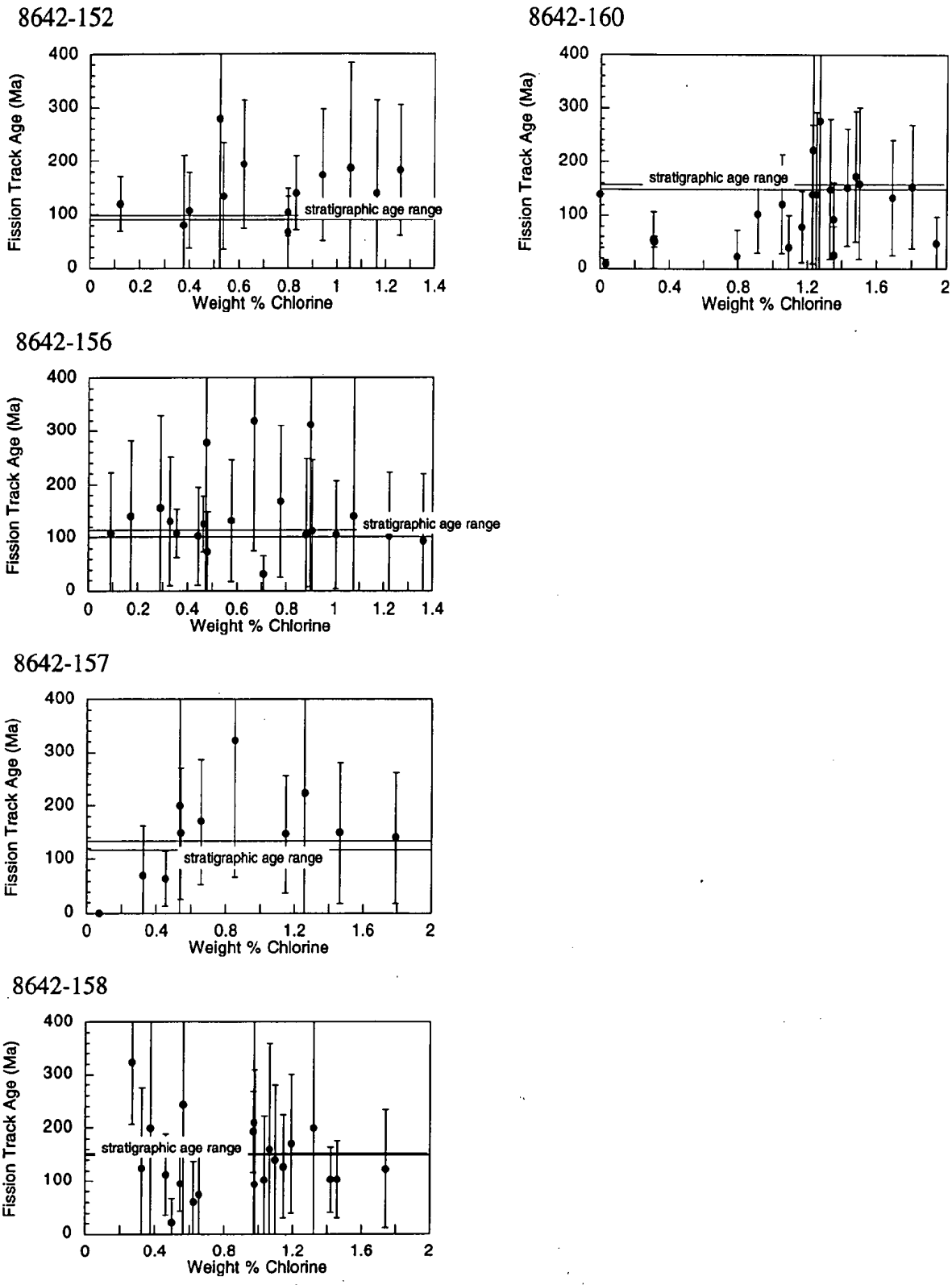

Figure B.6d: Plots of single grain age against weight percent chlorine for samples from **well Tirrawarra-1, Cooper - Eromanga Basin.**

Fission Track Age Data Sheets - Glossary

Ns	=	Number of spontaneous tracks in Na grid squares
Ni	=	Number of induced tracks in Na grid squares
Na	=	Number of grid squares counted in each grain
RATIO	=	Ns/Ni
U (ppm)	=	Uranium content of each grain (= U content of standard glass * $\rho i/\rho_D$)
Cl (wt%)	=	Weight percent chlorine content of each grain
RHOs	=	Spontaneous track density (ρs) = Ns/ (Na*area of basic unit)
RHOi	=	Induced track density (ρi) = Ni/(Na*area of basic unit)
F.T. AGE	=	Fission track age, calculated using equation B.1
Area of basic unit	=	Area of one grid square
Chi squared	=	χ^2 parameter, used to assess variation of single grain ages within the sample
P(chi squared)	=	Probability of obtaining observed χ^2 value for the relevant number of degrees of freedom, if all grains belong to a single population
Correlation coefficient	=	Correlation coefficient between Ns and Ni
Variance of SQR(Ns)	=	Variance of square root of Ns values - should be ~ 0.25 for Poisson distribution; greater if additional variation present
Variance of SQR(Ni)	=	Variance of square root of Ni values - should be ~ 0.25 for Poisson distribution; greater if additional variation present
Age Dispersion	=	% variation in single grain ages - see discussion in text re "Central age"
Ns/Ni	=	Pooled ratio, total spontaneous tracks divided by total induced tracks for all grains
Mean ratio	=	Mean of (Ns/Ni) for individual grains
Zeta	=	Calibration constant, determined empirically for each observer
RhoD	=	Track density (ρ_D) from uranium standard glass (interpolated from values at each end of stack)
ND	=	Total number of tracks counted for determining ρ_D
POOLED AGE	=	Fission track age calculated from pooled ratio Ns/Ni. Valid only when $\chi^2 > 5\%$
CENTRAL AGE	=	Alternative to pooled age when $\chi^2 < 5\%$

8642-23 ZIRCON

IRRADIATION PT816
SLIDE NUMBER 13
COUNTED BY: PFG

Current grain no.	Ns	Ni	Na	RHOs	RHOi	RATIO	U (ppm)	F.T. AGE (Ma)
1	209	81	40	8.303E+06	3.218E+06	2.580	57.9	326.9 ± 43.1
2	410	253	30	2.172E+07	1.340E+07	1.621	241.0	207.3 ± 16.9
3	385	89	36	1.699E+07	3.929E+06	4.326	70.6	539.1 ± 63.9
4	363	162	30	1.923E+07	8.581E+06	2.241	154.3	284.8 ± 27.3
5	138	69	36	6.091E+06	3.046E+06	2.000	54.8	254.8 ± 37.8
6	263	101	24	1.741E+07	6.687E+06	2.604	120.3	329.9 ± 38.9
7	346	131	30	1.833E+07	6.939E+06	2.641	124.8	334.5 ± 34.7
8	166	85	36	7.327E+06	3.752E+06	1.953	67.5	249.0 ± 33.4
9	332	145	40	1.319E+07	5.760E+06	2.290	103.6	290.9 ± 29.3
10	268	246	40	1.065E+07	9.773E+06	1.089	175.7	140.1 ± 12.5
	2880	1362		1.338E+07	6.328E+06		113.8	

Area of basic unit = 6.293E-07 cm-2

Chi Squared = 120.024 with 9 degrees of freedom
P(chi squared) = 0.0 %
Correlation Coefficient = 0.549
Variance of SQR(Ns) = 8.56
Variance of SQR(Ni) = 7.40
Age Dispersion = 32.543 %

Ns/Ni = 2.115 ± 0.070
Mean Ratio = 2.334 ± 0.269

Ages calculated using a zeta of 87.7 ± 0.8 for U3 glass
Rho D = 2.964E+06cm-2; ND = 6335

POOLED AGE = 269.1 ± 9.7 Ma
CENTRAL AGE = 274.6 ± 30.1 Ma

8642-25 ZIRCON

IRRADIATION PT816
SLIDE NUMBER 15
COUNTED BY: PFG

Current grain no.	Ns	Ni	Na	RHOs	RHOi	RATIO	U (ppm)	F.T. AGE (Ma)
1	737	542	70	1.673E+07	1.230E+07	1.360	221.3	174.4 ± 10.2
2	450	234	40	1.788E+07	9.296E+06	1.923	167.2	245.2 ± 20.1
3	177	139	16	1.758E+07	1.380E+07	1.273	248.2	163.4 ± 18.7
4	224	145	24	1.483E+07	9.601E+06	1.545	172.6	197.7 ± 21.3
5	387	236	20	3.075E+07	1.875E+07	1.640	337.2	209.7 ± 17.6
6	60	44	10	9.534E+06	6.992E+06	1.364	125.7	174.8 ± 34.8
7	353	324	30	1.870E+07	1.716E+07	1.090	308.6	140.1 ± 11.0
8	230	52	21	1.740E+07	3.935E+06	4.423	70.8	550.7 ± 85.0
9	364	129	20	2.892E+07	1.025E+07	2.822	184.3	356.7 ± 36.9
10	180	108	14	2.043E+07	1.226E+07	1.667	220.4	213.1 ± 26.1
	3162	1953		1.896E+07	1.171E+07		210.6	

Area of basic unit = 6.293E-07 cm-2

Chi Squared = 123.219 with 9 degrees of freedom
P(chi squared) = 0.0 %
Correlation Coefficient = 0.906
Variance of SQR(Ns) = 28.33
Variance of SQR(Ni) = 25.25
Age Dispersion = 34.116 %

Ns/Ni = 1.619 ± 0.047
Mean Ratio = 1.911 ± 0.318

Ages calculated using a zeta of 87.7 ± 0.8 for U3 glass
Rho D = 2.964E+06cm-2; ND = 6335

POOLED AGE = 207.1 ± 6.7 Ma
CENTRAL AGE = 217.7 ± 24.9 Ma

8642-26 ZIRCON

IRRADIATION PT816
SLIDE NUMBER 16
COUNTED BY: PFG

Current grain no.	Ns	Ni	Na	RHOs	RHOi	RATIO	U (ppm)	F.T. AGE (Ma)
1	357	181	20	2.836E+07	1.438E+07	1.972	258.6	251.4 ± 23.3
2	393	173	30	2.082E+07	9.164E+06	2.272	164.8	288.7 ± 26.7
3	325	212	40	1.291E+07	8.422E+06	1.533	151.4	196.2 ± 17.6
4	445	134	30	2.357E+07	7.098E+06	3.321	127.6	417.8 ± 41.7
5	494	274	30	2.617E+07	1.451E+07	1.803	261.0	230.2 ± 17.7
6	156	117	20	1.239E+07	9.296E+06	1.333	167.2	171.0 ± 21.1
7	215	117	16	2.135E+07	1.162E+07	1.838	209.0	234.5 ± 27.2
8	355	123	20	2.821E+07	9.773E+06	2.886	175.7	364.6 ± 38.5
9	74	32	20	5.880E+06	2.542E+06	2.312	45.7	293.8 ± 62.3
10	251	98	30	1.330E+07	5.191E+06	2.561	93.3	324.6 ± 39.0
11	330	241	30	1.748E+07	1.277E+07	1.369	229.6	175.6 ± 15.1
12	224	142	30	1.186E+07	7.522E+06	1.577	135.3	201.8 ± 21.9
13	667	321	100	1.060E+07	5.101E+06	2.078	91.7	264.6 ± 18.4
	4286	2165		1.637E+07	8.270E+06		148.7	

Area of basic unit = 6.293E-07 cm-2

Chi Squared = 93.970 with 12 degrees of freedom
P(chi squared) = 0.0 %
Correlation Coefficient = 0.838
Variance of SQR(Ns) = 19.64
Variance of SQR(Ni) = 10.24
Age Dispersion = 24.434 %

Ns/Ni = 1.980 ± 0.052
Mean Ratio = 2.066 ± 0.165

Ages calculated using a zeta of 87.7 ± 0.8 for U3 glass
Rho D = 2.964E+06cm-2; ND = 6335

POOLED AGE = 252.3 ± 7.7 Ma
CENTRAL AGE = 250.6 ± 18.9 Ma

8642-27 ZIRCON

IRRADIATION PT816
SLIDE NUMBER 17
COUNTED BY: PFG

Current grain no.	Ns	Ni	Na	RHOs	RHOi	RATIO	U (ppm)	F.T. AGE (Ma)
1	356	307	16	3.536E+07	3.049E+07	1.160	548.3	149.0 ± 11.8
2	86	156	6	2.278E+07	4.132E+07	0.551	743.0	71.3 ± 9.6
3	268	219	10	4.259E+07	3.480E+07	1.224	625.8	157.1 ± 14.5
4	162	128	6	4.290E+07	3.390E+07	1.266	609.6	162.4 ± 19.4
5	142	91	4	5.641E+07	3.615E+07	1.560	650.1	199.7 ± 27.0
6	128	97	6	3.390E+07	2.569E+07	1.320	462.0	169.3 ± 22.9
7	131	90	8	2.602E+07	1.788E+07	1.456	321.5	186.5 ± 25.7
8	231	130	7	5.244E+07	2.951E+07	1.777	530.7	226.9 ± 25.1
9	171	126	9	3.019E+07	2.225E+07	1.357	400.1	174.0 ± 20.6
	1675	1344		3.697E+07	2.966E+07		533.4	

Area of basic unit = 6.293E-07 cm-2

Chi Squared = 55.276 with 8 degrees of freedom
P(chi squared) = 0.0 %
Correlation Coefficient = 0.846
Variance of SQR(Ns) = 8.74
Variance of SQR(Ni) = 7.12
Age Dispersion = 27.846 %

Ns/Ni = 1.246 ± 0.046
Mean Ratio = 1.297 ± 0.112

Ages calculated using a zeta of 87.7 ± 0.8 for U3 glass
Rho D = 2.964E+06cm-2; ND = 6335

POOLED AGE = 160.0 ± 6.3 Ma
CENTRAL AGE = 159.8 ± 16.2 Ma

8642-171 APATITE

IRRADIATION PT798
SLIDE NUMBER 9
COUNTED BY: MEM

Current grain no.	Ns	Ni	Na	RHOs	RHOi	RATIO	U (ppm)	Cl (wt%)	F.T. AGE (Ma)
3	7	24	54	2.060E+05	7.063E+05	0.292	5.7	0.93	81.0 ± 34.9
4	0	5	20	0.000E+00	3.973E+05	0.000	3.2	0.25	0.0 ± 0.0
7	39	52	20	3.099E+06	4.132E+06	0.750	33.3	0.06	206.4 ± 44.1
9	2	20	32	9.932E+04	9.932E+05	0.100	8.0	0.93	27.9 ± 20.7
11	9	21	40	3.575E+05	8.343E+05	0.429	6.7	1.25	118.7 ± 47.4
12	15	36	60	3.973E+05	9.534E+05	0.417	7.7	0.43	115.5 ± 35.6
10	7	23	30	3.708E+05	1.218E+06	0.304	9.8	1.00	84.5 ± 36.6
14	10	34	70	2.270E+05	7.718E+05	0.294	6.2	0.87	81.7 ± 29.5
16	6	8	30	3.178E+05	4.238E+05	0.750	3.4	3.08	206.4 ± 111.6
17	12	38	49	3.892E+05	1.232E+06	0.316	9.9	1.32	87.7 ± 29.1
19	3	17	30	1.589E+05	9.005E+05	0.176	7.3	0.92	49.2 ± 30.8
25	15	36	60	3.973E+05	9.534E+05	0.417	7.7	0.39	115.5 ± 35.6
26	4	11	35	1.816E+05	4.994E+05	0.364	4.0	1.12	100.9 ± 59.0
28	9	22	70	2.043E+05	4.994E+05	0.409	4.0	0.10	113.4 ± 45.0
29	2	10	25	1.271E+05	6.356E+05	0.200	5.1	0.00	55.7 ± 43.2
32	9	16	60	2.384E+05	4.238E+05	0.562	3.4	2.18	155.4 ± 64.9
34	6	29	35	2.724E+05	1.317E+06	0.207	10.6	1.09	57.6 ± 25.9
	155	402		3.421E+05	8.872E+05		7.1		

Area of basic unit = 6.293E-07 cm-2

Chi Squared = 24.678 with 16 degrees of freedom
P(chi squared) = 7.6 %
Correlation Coefficient = 0.833
Variance of SQR(Ns) = 1.78
Variance of SQR(Ni) = 1.77
Age Dispersion = 28.452 %

Ns/Ni = 0.386 ± 0.036
Mean Ratio = 0.352 ± 0.049

Ages calculated using a zeta of 360.3 ± 6.8 for SRM612 glass
Rho D = 1.552E+06cm-2; ND = 2455
Rho D interpolated between top of can; Rho D = 1.579E+06cm-2, ND = 1242
bottom of can; Rho D = 1.542E+06cm-2, ND = 1213

POOLED AGE = 106.9 ± 10.5 Ma
CENTRAL AGE = 100.8 ± 12.6 Ma

8642-172 APATITE

IRRADIATION PT798
SLIDE NUMBER 10
COUNTED BY: MEM

Current grain no.	Ns	Ni	Na	RHOs	RHOi	RATIO	U (ppm)	Cl (wt%)	F.T. AGE (Ma)
4	0	8	60	0.000E+00	2.119E+05	0.000	1.7	0.72	0.0 ± 0.0
6	6	10	70	1.362E+05	2.270E+05	0.600	1.8	1.56	165.3 ± 85.5
7	0	7	20	0.000E+00	5.562E+05	0.000	4.5	1.18	0.0 ± 0.0
8	4	32	24	2.648E+05	2.119E+06	0.125	17.1	1.29	34.8 ± 18.5
9	0	6	36	0.000E+00	2.648E+05	0.000	2.1	0.38	0.0 ± 0.0
10	2	9	20	1.589E+05	7.151E+05	0.222	5.8	2.07	61.7 ± 48.3
12	0	8	35	0.000E+00	3.632E+05	0.000	2.9	1.49	0.0 ± 0.0
13	0	8	15	0.000E+00	8.475E+05	0.000	6.8	0.80	0.0 ± 0.0
15	0	85	35	0.000E+00	3.859E+06	0.000	31.1	0.05	0.0 ± 0.0
16	2	20	60	5.297E+04	5.297E+05	0.100	4.3	0.60	27.8 ± 20.7
18	2	20	12	2.648E+05	2.648E+06	0.100	21.4	1.40	27.8 ± 20.7
19	0	19	60	0.000E+00	5.032E+05	0.000	4.1	0.81	0.0 ± 0.0
20	0	2	20	0.000E+00	1.589E+05	0.000	1.3	0.25	0.0 ± 0.0
21	1	13	25	6.356E+04	8.263E+05	0.077	6.7	0.22	21.4 ± 22.2
24	0	11	30	0.000E+00	5.827E+05	0.000	4.7	0.87	0.0 ± 0.0
25	2	5	24	1.324E+05	3.311E+05	0.400	2.7	0.44	110.6 ± 92.6
27	0	6	50	0.000E+00	1.907E+05	0.000	1.5	0.37	0.0 ± 0.0
28	1	15	49	3.243E+04	4.864E+05	0.067	3.9	0.92	18.6 ± 19.2
29	0	10	48	0.000E+00	3.311E+05	0.000	2.7	0.00	0.0 ± 0.0
30	1	10	60	2.648E+04	2.648E+05	0.100	2.1	0.56	27.8 ± 29.2
44	15	81	36	6.621E+05	3.575E+06	0.185	28.9	0.07	51.5 ± 14.5
45	33	78	64	8.194E+05	1.937E+06	0.423	15.6	0.22	117.0 ± 24.5
46	36	92	12	4.767E+06	1.218E+07	0.391	98.3	0.07	108.3 ± 21.5
48	9	22	100	1.430E+05	3.496E+05	0.409	2.8	1.26	113.1 ± 44.9
49	20	67	70	4.540E+05	1.521E+06	0.298	12.3	2.18	82.8 ± 21.2
51	7	37	48	2.317E+05	1.225E+06	0.189	9.9	1.80	52.6 ± 21.7
52	1	160	100	1.589E+04	2.542E+06	0.006	20.5	0.36	1.7 ± 1.7
54	17	57	100	2.701E+05	9.058E+05	0.298	7.3	2.07	82.7 ± 23.0
55	9	31	30	4.767E+05	1.642E+06	0.290	13.3	1.67	80.5 ± 30.6
	168	929		2.033E+05	1.124E+06		9.1		

Area of basic unit = 6.293E-07 cm-2

Chi Squared = 115.891 with 28 degrees of freedom
P(chi squared) = 0.0 %
Correlation Coefficient = 0.527
Variance of SQR(Ns) = 3.28
Variance of SQR(Ni) = 7.89
Age Dispersion = 84.019 %

Ns/Ni = 0.181 ± 0.015
Mean Ratio = 0.148 ± 0.032

Ages calculated using a zeta of 360.3 ± 6.8 for SRM612 glass
Rho D = 1.549E+06cm-2; ND = 2455
Rho D interpolated between top of can; Rho D = 1.579E+06cm-2, ND = 1242
bottom of can; Rho D = 1.542E+06cm-2, ND = 1213

POOLED AGE = 50.3 ± 4.4 Ma
CENTRAL AGE = 42.0 ± 8.4 Ma

8642-152 APATITE

IRRADIATION PT798
SLIDE NUMBER 1
COUNTED BY: MEM

Current grain no.	Ns	Ni	Na	RHOs	RHOi	RATIO	U (ppm)	Cl (wt%)	F.T. AGE (Ma)
3	18	26	70	4.086E+05	5.902E+05	0.692	4.7	0.62	194.0 ± 59.7
5	2	7	50	6.356E+04	2.225E+05	0.286	1.8	0.38	80.8 ± 64.8
12	13	21	40	5.164E+05	8.343E+05	0.619	6.6	0.94	173.7 ± 61.5
13	4	8	70	9.080E+04	1.816E+05	0.500	1.4	1.16	140.7 ± 86.2
14	25	50	100	3.973E+05	7.945E+05	0.500	6.3	0.83	140.7 ± 34.7
16	32	75	100	5.085E+05	1.192E+06	0.427	9.4	0.12	120.2 ± 25.6
19	6	9	30	3.178E+05	4.767E+05	0.667	3.8	1.05	186.9 ± 98.6
20	7	7	70	1.589E+05	1.589E+05	1.000	1.3	0.52	278.3 ± 149.0
25	13	34	70	2.951E+05	7.718E+05	0.382	6.1	0.40	107.8 ± 35.3
26	30	81	100	4.767E+05	1.287E+06	0.370	10.2	0.80	104.5 ± 22.5
27	5	21	49	1.621E+05	6.810E+05	0.238	5.4	0.80	67.4 ± 33.6
28	11	23	100	1.748E+05	3.655E+05	0.478	2.9	0.54	134.6 ± 49.5
29	15	23	100	2.384E+05	3.655E+05	0.652	2.9	1.26	182.9 ± 60.9
	181	385		3.031E+05	6.447E+05		5.1		

Area of basic unit = 6.293E-07 cm-2

Chi Squared = 10.018 with 12 degrees of freedom
P(chi squared) = 61.4 %
Correlation Coefficient = 0.944
Variance of SQR(Ns) = 1.80
Variance of SQR(Ni) = 4.55
Age Dispersion = 0.629 % (did not converge)

Ns/Ni = 0.470 ± 0.042
Mean Ratio = 0.524 ± 0.056

Ages calculated using a zeta of 360.3 ± 6.8 for SRM612 glass
Rho D = 1.579E+06cm-2; ND = 2455
Rho D interpolated between top of can; Rho D = 1.579E+06cm-2, ND = 1242
bottom of can; Rho D = 1.542E+06cm-2, ND = 1213

POOLED AGE = 132.4 ± 12.5 Ma
CENTRAL AGE = 132.4 ± 12.5 Ma

8642-174 APATITE

IRRADIATION PT798
SLIDE NUMBER 11
COUNTED BY: MEM

Current grain no.	Ns	Ni	Na	RHOs	RHOi	RATIO	U (ppm)	Cl (wt%)	F.T. AGE (Ma)
4	1	6	18	8.828E+04	5.297E+05	0.167	4.3	0.00	46.2 ± 50.0
6	0	51	48	0.000E+00	1.688E+06	0.000	13.7	0.18	0.0 ± 0.0
7	2	564	70	4.540E+04	1.280E+07	0.004	103.6	0.00	1.0 ± 0.7
8	0	20	32	0.000E+00	9.932E+05	0.000	8.0	0.28	0.0 ± 0.0
9	0	124	21	0.000E+00	9.383E+06	0.000	75.9	0.00	0.0 ± 0.0
11	0	69	50	0.000E+00	2.193E+06	0.000	17.7	0.00	0.0 ± 0.0
13	0	19	40	0.000E+00	7.548E+05	0.000	6.1	0.18	0.0 ± 0.0
16	2	23	32	9.932E+04	1.142E+06	0.087	9.2	0.22	24.2 ± 17.8
19	0	18	30	0.000E+00	9.534E+05	0.000	7.7	0.22	0.0 ± 0.0
20	0	145	42	0.000E+00	5.486E+06	0.000	44.4	0.05	0.0 ± 0.0
24	0	23	30	0.000E+00	1.218E+06	0.000	9.9	0.11	0.0 ± 0.0
25	0	5	25	0.000E+00	3.178E+05	0.000	2.6	0.00	0.0 ± 0.0
26	0	41	18	0.000E+00	3.620E+06	0.000	29.3	0.18	0.0 ± 0.0
27	1	191	100	1.589E+04	3.035E+06	0.005	24.5	0.04	1.5 ± 1.5
28	0	81	48	0.000E+00	2.682E+06	0.000	21.7	0.08	0.0 ± 0.0
	6	1380		1.579E+04	3.631E+06		29.4		

Area of basic unit = 6.293E-07 cm-2

Chi Squared = 67.086 with 14 degrees of freedom
P(chi squared) = 0.0 %
Correlation Coefficient = 0.560
Variance of SQR(Ns) = 0.32
Variance of SQR(Ni) = 31.20
Age Dispersion = 166.812 % (did not converge)

Ns/Ni = 0.004 ± 0.002
Mean Ratio = 0.017 ± 0.012

Ages calculated using a zeta of 360.3 ± 6.8 for SRM612 glass
Rho D = 1.545E+06cm-2; ND = 2455
Rho D interpolated between top of can; Rho D = 1.579E+06cm-2, ND = 1242
bottom of can; Rho D = 1.542E+06cm-2, ND = 1213

POOLED AGE = 1.2 ± 0.5 Ma
CENTRAL AGE = 2.1 ± 1.3 Ma

8642-156 APATITE

IRRADIATION PT798
SLIDE NUMBER 2
COUNTED BY: MEM

Current grain no.	Ns	Ni	Na	RHOs	RHOi	RATIO	U (ppm)	Cl (wt%)	F.T. AGE (Ma)
3	5	19	40	1.986E+05	7.548E+05	0.263	6.0	0.48	74.3 ± 37.4
4	3	9	12	3.973E+05	1.192E+06	0.333	9.5	1.36	93.9 ± 62.7
5	7	15	30	3.708E+05	7.945E+05	0.467	6.3	0.33	131.1 ± 60.1
7	4	11	28	2.270E+05	6.243E+05	0.364	5.0	1.22	102.4 ± 59.9
9	9	15	20	7.151E+05	1.192E+06	0.600	9.5	0.78	168.1 ± 71.0
11	1	2	20	7.945E+04	1.589E+05	0.500	1.3	1.08	140.4 ± 172.0
12	32	83	40	1.271E+06	3.297E+06	0.386	26.2	0.36	108.5 ± 22.8
13	2	2	25	1.271E+05	1.271E+05	1.000	1.0	0.47	277.8 ± 277.9
15	5	9	50	1.589E+05	2.860E+05	0.556	2.3	0.29	155.8 ± 87.0
16	15	13	25	9.534E+05	8.263E+05	1.154	6.6	0.67	319.5 ± 121.4
18	9	8	28	5.108E+05	4.540E+05	1.125	3.6	0.90	311.7 ± 151.7
19	4	10	36	1.766E+05	4.414E+05	0.400	3.5	0.91	112.5 ± 66.7
20	6	16	35	2.724E+05	7.264E+05	0.375	5.8	1.00	105.6 ± 50.6
24	35	78	50	1.112E+06	2.479E+06	0.449	19.7	0.46	126.1 ± 25.9
25	4	35	40	1.589E+05	1.390E+06	0.114	11.0	0.71	32.4 ± 17.1
26	3	8	16	2.980E+05	7.945E+05	0.375	6.3	0.88	105.6 ± 71.5
27	5	13	60	1.324E+05	3.443E+05	0.385	2.7	0.09	108.3 ± 57.0
28	6	12	28	3.405E+05	6.810E+05	0.500	5.4	0.17	140.4 ± 70.3
29	8	17	60	2.119E+05	4.502E+05	0.471	3.6	0.58	132.2 ± 56.8
30	7	19	20	5.562E+05	1.510E+06	0.368	12.0	0.44	103.7 ± 46.0
	170	394		4.075E+05	9.443E+05		7.5		

Area of basic unit = 6.293E-07 cm-2

Chi Squared = 22.440 with 19 degrees of freedom
P(chi squared) = 26.3 %
Correlation Coefficient = 0.914
Variance of SQR(Ns) = 1.54
Variance of SQR(Ni) = 3.86
Age Dispersion = 20.906 % (did not converge)

Ns/Ni = 0.431 ± 0.040
Mean Ratio = 0.509 ± 0.061

Ages calculated using a zeta of 360.3 ± 6.8 for SRM612 glass
Rho D = 1.576E+06cm-2; ND = 2455
Rho D interpolated between top of can; Rho D = 1.579E+06cm-2, ND = 1242
bottom of can; Rho D = 1.542E+06cm-2, ND = 1213

POOLED AGE = 121.3 ± 11.6 Ma
CENTRAL AGE = 123.3 ± 13.9 Ma

8642-157 APATITE

IRRADIATION PT798
SLIDE NUMBER 3
COUNTED BY: MEM

Current grain no.	Ns	Ni	Na	RHOs	RHOi	RATIO	U (ppm)	Cl (wt%)	F.T. AGE (Ma)
6	4	5	70	9.080E+04	1.135E+05	0.800	0.9	1.26	222.7 ± 149.5
7	14	12	40	5.562E+05	4.767E+05	1.167	3.8	0.85	322.2 ± 127.1
12	8	16	80	1.589E+05	3.178E+05	0.500	2.5	1.79	140.1 ± 60.8
15	5	7	100	7.945E+04	1.112E+05	0.714	0.9	0.54	199.2 ± 116.8
16	8	15	60	2.119E+05	3.973E+05	0.533	3.2	1.46	149.3 ± 65.5
17	9	17	100	1.430E+05	2.701E+05	0.529	2.1	0.54	148.2 ± 61.2
19	3	12	50	9.534E+04	3.814E+05	0.250	3.0	0.32	70.4 ± 45.5
20	11	21	36	4.855E+05	9.270E+05	0.524	7.4	1.15	146.7 ± 54.7
25	0	11	30	0.000E+00	5.827E+05	0.000	4.6	0.08	0.0 ± 0.0
26	14	23	48	4.635E+05	7.614E+05	0.609	6.1	0.66	170.1 ± 57.9
27	8	35	70	1.816E+05	7.945E+05	0.229	6.3	0.45	64.4 ± 25.3
	84	174		1.951E+05	4.042E+05		3.2		

Area of basic unit = 6.293E-07 cm-2

Chi Squared = 17.225 with 10 degrees of freedom
P(chi squared) = 7.0 %
Correlation Coefficient = 0.447
Variance of SQR(Ns) = 1.14
Variance of SQR(Ni) = 1.04
Age Dispersion = 31.797 %

Ns/Ni = 0.483 ± 0.064
Mean Ratio = 0.532 ± 0.094

Ages calculated using a zeta of 360.3 ± 6.8 for SRM612 glass
Rho D = 1.572E+06cm-2; ND = 2455
Rho D interpolated between top of can; Rho D = 1.579E+06cm-2, ND = 1242
bottom of can; Rho D = 1.542E+06cm-2, ND = 1213

POOLED AGE = 135.3 ± 18.4 Ma
CENTRAL AGE = 135.7 ± 22.9 Ma

8642-158 APATITE

IRRADIATION PT798
SLIDE NUMBER 4
COUNTED BY: MEM

Current grain no.	Ns	Ni	Na	RHOs	RHOi	RATIO	U (ppm)	Cl (wt%)	F.T. AGE (Ma)
3	15	41	100	2.384E+05	6.515E+05	0.366	5.2	1.42	102.6 ± 31.1
7	3	4	12	3.973E+05	5.297E+05	0.750	4.2	0.97	208.6 ± 159.4
9	5	7	30	2.648E+05	3.708E+05	0.714	3.0	1.32	198.8 ± 116.5
16	12	30	50	3.814E+05	9.534E+05	0.400	7.6	0.46	112.1 ± 38.4
17	7	16	50	2.225E+05	5.085E+05	0.438	4.1	1.74	122.5 ± 55.6
18	3	14	80	5.959E+04	2.781E+05	0.214	2.2	0.62	60.3 ± 38.4
19	11	18	40	4.370E+05	7.151E+05	0.611	5.7	1.19	170.4 ± 65.4
20	5	7	28	2.838E+05	3.973E+05	0.714	3.2	0.38	198.8 ± 116.5
21	1	3	20	7.945E+04	2.384E+05	0.333	1.9	0.98	93.5 ± 108.0
22	68	58	25	4.322E+06	3.687E+06	1.172	29.4	0.27	323.1 ± 58.4
23	1	13	60	2.648E+04	3.443E+05	0.077	2.7	0.50	21.7 ± 22.5
24	45	65	100	7.151E+05	1.033E+06	0.692	8.2	0.97	192.8 ± 37.8
26	7	8	80	1.390E+05	1.589E+05	0.875	1.3	0.56	242.7 ± 125.8
28	4	11	18	3.531E+05	9.711E+05	0.364	7.7	1.03	102.0 ± 59.6
29	4	9	20	3.178E+05	7.151E+05	0.444	5.7	0.33	124.4 ± 74.8
31	5	19	30	2.648E+05	1.006E+06	0.263	8.0	0.66	74.0 ± 37.2
34	11	30	60	2.913E+05	7.945E+05	0.367	6.3	1.46	102.8 ± 36.3
37	4	7	30	2.119E+05	3.708E+05	0.571	3.0	1.06	159.5 ± 100.1
38	10	22	100	1.589E+05	3.496E+05	0.455	2.8	1.14	127.2 ± 48.6
40	18	53	100	2.860E+05	8.422E+05	0.340	6.7	0.55	95.3 ± 26.1
41	6	12	80	1.192E+05	2.384E+05	0.500	1.9	1.10	139.8 ± 70.0
	245	447		3.498E+05	6.382E+05		5.1		

Area of basic unit = 6.293E-07 cm-2

Chi Squared = 39.872 with 20 degrees of freedom
P(chi squared) = 0.5 %
Correlation Coefficient = 0.838
Variance of SQR(Ns) = 3.03
Variance of SQR(Ni) = 3.39
Age Dispersion = 35.067 %

Ns/Ni = 0.548 ± 0.044
Mean Ratio = 0.508 ± 0.054

Ages calculated using a zeta of 360.3 ± 6.8 for SRM612 glass
Rho D = 1.569E+06cm-2; ND = 2455
Rho D interpolated between top of can; Rho D = 1.579E+06cm-2, ND = 1242
bottom of can; Rho D = 1.542E+06cm-2, ND = 1213

POOLED AGE = 153.1 ± 12.9 Ma
CENTRAL AGE = 136.7 ± 17.0 Ma

8642-160 APATITE

IRRADIATION PT798
SLIDE NUMBER 5
COUNTED BY: MEM

Current grain no.	Ns	Ni	Na	RHOs	RHOi	RATIO	U (ppm)	Cl (wt%)	F.T. AGE (Ma)
4	10	30	28	5.675E+05	1.703E+06	0.333	13.6	1.35	93.3 ± 34.2
5	10	23	60	2.648E+05	6.091E+05	0.435	4.9	1.05	121.5 ± 46.1
4	1	11	16	9.932E+04	1.092E+06	0.091	8.7	1.35	25.6 ± 26.7
10	5	10	21	3.783E+05	7.567E+05	0.500	6.0	1.25	139.5 ± 76.5
11	4	5	20	3.178E+05	3.973E+05	0.800	3.2	1.23	221.8 ± 148.9
12	7	25	50	2.225E+05	7.945E+05	0.280	6.3	1.17	78.5 ± 33.6
13	1	12	32	4.966E+04	5.959E+05	0.083	4.8	0.79	23.5 ± 24.4
14	120	668	50	3.814E+06	2.123E+07	0.180	169.5	0.31	50.5 ± 5.2
16	12	22	42	4.540E+05	8.324E+05	0.545	6.6	1.43	152.0 ± 54.7
17	2	14	50	6.356E+04	4.449E+05	0.143	3.6	1.09	40.2 ± 30.4
18	11	30	60	2.913E+05	7.945E+05	0.367	6.3	0.91	102.6 ± 36.3
19	13	21	80	2.582E+05	4.171E+05	0.619	3.3	1.48	172.3 ± 61.0
21	8	15	35	3.632E+05	6.810E+05	0.533	5.4	1.33	148.7 ± 65.2
23	9	19	30	4.767E+05	1.006E+06	0.474	8.0	1.69	132.2 ± 53.6
24	5	26	40	1.986E+05	1.033E+06	0.192	8.2	0.31	54.0 ± 26.4
25	4	130	50	1.271E+05	4.132E+06	0.031	33.0	0.04	8.7 ± 4.4
26	11	20	60	2.913E+05	5.297E+05	0.550	4.2	1.80	153.3 ± 57.7
27	8	14	70	1.816E+05	3.178E+05	0.571	2.5	1.50	159.2 ± 70.7
28	5	5	24	3.311E+05	3.311E+05	1.000	2.6	1.27	276.0 ± 174.7
31	4	24	42	1.513E+05	9.080E+05	0.167	7.2	1.94	46.8 ± 25.3
32	7	14	42	2.648E+05	5.297E+05	0.500	4.2	1.23	139.5 ± 64.7
33	14	28	60	3.708E+05	7.416E+05	0.500	5.9	0.00	139.5 ± 45.8
	271	1166		4.476E+05	1.926E+06		15.4		

Area of basic unit = 6.293E-07 cm-2

Chi Squared = 89.695 with 21 degrees of freedom
P(chi squared) = 0.0 %
Correlation Coefficient = 0.972
Variance of SQR(Ns) = 3.82
Variance of SQR(Ni) = 23.88
Age Dispersion = 47.794 %

Ns/Ni = 0.232 ± 0.016
Mean Ratio = 0.404 ± 0.052

Ages calculated using a zeta of 360.3 ± 6.8 for SRM612 glass
Rho D = 1.565E+06cm-2; ND = 2455
Rho D interpolated between top of can; Rho D = 1.579E+06cm-2, ND = 1242
bottom of can; Rho D = 1.542E+06cm-2, ND = 1213

POOLED AGE = 65.2 ± 4.8 Ma
CENTRAL AGE = 96.1 ± 13.5 Ma

8642-168 APATITE

IRRADIATION PT798
SLIDE NUMBER 6
COUNTED BY: MEM

Current grain no.	Ns	Ni	Na	RHOs	RHOi	RATIO	U (ppm)	Cl (wt%)	F.T. AGE (Ma)
1	41	42	80	8.144E+05	8.343E+05	0.976	6.7	0.43	269.0 ± 59.5
3	4	7	30	2.119E+05	3.708E+05	0.571	3.0	0.55	158.8 ± 99.7
4	7	24	80	1.390E+05	4.767E+05	0.292	3.8	1.93	81.6 ± 35.1
6	12	17	60	3.178E+05	4.502E+05	0.706	3.6	0.98	195.6 ± 74.0
7	4	9	50	1.271E+05	2.860E+05	0.444	2.3	0.34	123.9 ± 74.5
10	14	23	40	5.562E+05	9.137E+05	0.609	7.3	1.70	169.1 ± 57.5
12	14	39	100	2.225E+05	6.197E+05	0.359	5.0	1.66	100.2 ± 31.4
13	13	33	60	3.443E+05	8.740E+05	0.394	7.0	1.99	109.9 ± 36.1
14	56	175	24	3.708E+06	1.159E+07	0.320	92.7	2.31	89.4 ± 14.0
15	6	25	100	9.534E+04	3.973E+05	0.240	3.2	0.50	67.2 ± 30.6
17	11	45	80	2.185E+05	8.938E+05	0.244	7.2	0.48	68.4 ± 23.1
18	22	97	80	4.370E+05	1.927E+06	0.227	15.4	1.62	63.5 ± 15.1
23	19	45	70	4.313E+05	1.022E+06	0.422	8.2	1.78	117.7 ± 32.4
24	3	6	56	8.513E+04	1.703E+05	0.500	1.4	0.88	139.2 ± 98.5
25	10	36	90	1.766E+05	6.356E+05	0.278	5.1	1.43	77.7 ± 27.9
26	17	66	100	2.701E+05	1.049E+06	0.258	8.4	1.54	72.1 ± 19.7
27	10	23	80	1.986E+05	4.569E+05	0.435	3.7	1.60	121.2 ± 46.0
28	13	26	80	2.582E+05	5.164E+05	0.500	4.1	1.72	139.2 ± 47.4
29	8	17	28	4.540E+05	9.648E+05	0.471	7.7	0.89	131.1 ± 56.3
30	15	48	70	3.405E+05	1.090E+06	0.312	8.7	1.40	87.3 ± 26.0
37	38	37	80	7.548E+05	7.349E+05	1.027	5.9	2.72	282.7 ± 65.8
43	10	22	80	1.986E+05	4.370E+05	0.455	3.5	0.42	126.7 ± 48.4
49	15	55	70	3.405E+05	1.249E+06	0.273	10.0	0.18	76.3 ± 22.3
51	5	24	36	2.207E+05	1.059E+06	0.208	8.5	0.19	58.4 ± 28.7
52	24	62	60	6.356E+05	1.642E+06	0.387	13.1	0.12	108.0 ± 26.1
53	31	80	56	8.797E+05	2.270E+06	0.388	18.2	0.28	108.1 ± 23.1
54	83	267	42	3.140E+06	1.010E+07	0.311	80.8	0.24	86.9 ± 11.2
56	167	548	64	4.146E+06	1.361E+07	0.305	108.9	0.24	85.2 ± 7.9
77	79	289	40	3.138E+06	1.148E+07	0.273	91.9	0.27	76.5 ± 9.9
91	63	37	40	2.503E+06	1.470E+06	1.703	11.8	0.04	462.2 ± 96.6
	814	2224		6.716E+05	1.835E+06		14.7		

Area of basic unit = 6.293E-07 cm-2

Chi Squared = 142.522 with 29 degrees of freedom
P(chi squared) = 0.0 %
Correlation Coefficient = 0.941
Variance of SQR(Ns) = 6.45
Variance of SQR(Ni) = 21.22
Age Dispersion = 46.028 %

Ns/Ni = 0.366 ± 0.015
Mean Ratio = 0.463 ± 0.056

Ages calculated using a zeta of 360.3 ± 6.8 for SRM612 glass
Rho D = 1.562E+06cm-2; ND = 2455
Rho D interpolated between top of can; Rho D = 1.579E+06cm-2, ND = 1242
bottom of can; Rho D = 1.542E+06cm-2, ND = 1213

POOLED AGE = 102.2 ± 5.0 Ma
CENTRAL AGE = 115.5 ± 12.1 Ma

8642-169 APATITE

IRRADIATION PT798
SLIDE NUMBER 7
COUNTED BY: MEM

Current grain no.	Ns	Ni	Na	RHOs	RHOi	RATIO	U (ppm)	Cl (wt%)	F.T. AGE (Ma)
4	1	4	28	5.675E+04	2.270E+05	0.250	1.8	0.69	69.8 ± 78.1
5	16	33	60	4.238E+05	8.740E+05	0.485	7.0	0.95	134.7 ± 41.2
8	17	44	70	3.859E+05	9.988E+05	0.386	8.0	0.80	107.6 ± 30.9
10	13	32	100	2.066E+05	5.085E+05	0.406	4.1	0.55	113.1 ± 37.3
11	16	31	36	7.063E+05	1.368E+06	0.516	11.0	0.41	143.3 ± 44.3
12	7	18	40	2.781E+05	7.151E+05	0.389	5.7	1.63	108.3 ± 48.3
13	4	11	49	1.297E+05	3.567E+05	0.364	2.9	1.29	101.3 ± 59.2
14	6	25	48	1.986E+05	8.276E+05	0.240	6.6	2.56	67.0 ± 30.5
15	9	25	64	2.235E+05	6.207E+05	0.360	5.0	1.26	100.3 ± 39.1
16	19	29	100	3.019E+05	4.608E+05	0.655	3.7	1.35	181.4 ± 53.8
18	15	33	60	3.973E+05	8.740E+05	0.455	7.0	1.08	126.4 ± 39.5
20	43	45	100	6.833E+05	7.151E+05	0.956	5.7	0.77	262.9 ± 56.5
21	1	13	36	4.414E+04	5.738E+05	0.077	4.6	1.12	21.6 ± 22.4
22	8	22	48	2.648E+05	7.283E+05	0.364	5.8	0.56	101.3 ± 41.9
23	13	26	60	3.443E+05	6.886E+05	0.500	5.5	0.92	138.9 ± 47.3
24	5	12	30	2.648E+05	6.356E+05	0.417	5.1	1.09	116.0 ± 61.8
25	11	33	80	2.185E+05	6.555E+05	0.333	5.3	1.45	92.9 ± 32.5
26	24	33	42	9.080E+05	1.249E+06	0.727	10.0	0.16	201.1 ± 54.2
28	1	4	30	5.297E+04	2.119E+05	0.250	1.7	0.88	69.8 ± 78.1
29	9	44	42	3.405E+05	1.665E+06	0.205	13.3	0.77	57.2 ± 21.0
40	88	283	60	2.331E+06	7.495E+06	0.311	60.1	0.09	86.7 ± 10.9
	326	800		4.379E+05	1.075E+06		8.6		

Area of basic unit = 6.293E-07 cm-2

Chi Squared = 40.041 with 20 degrees of freedom
P(chi squared) = 0.5 %
Correlation Coefficient = 0.927
Variance of SQR(Ns) = 3.65
Variance of SQR(Ni) = 8.62
Age Dispersion = 29.738 %

Ns/Ni = 0.408 ± 0.027
Mean Ratio = 0.412 ± 0.042

Ages calculated using a zeta of 360.3 ± 6.8 for SRM612 glass
Rho D = 1.559E+06cm-2; ND = 2455
Rho D interpolated between top of can; Rho D = 1.579E+06cm-2, ND = 1242
bottom of can; Rho D = 1.542E+06cm-2, ND = 1213

POOLED AGE = 113.4 ± 8.1 Ma
CENTRAL AGE = 117.5 ± 12.4 Ma

8642-170 APATITE

IRRADIATION PT798
SLIDE NUMBER 8
COUNTED BY: MEM

Current grain no.	Ns	Ni	Na	RHOs	RHOi	RATIO	U (ppm)	Cl (wt%)	F.T. AGE (Ma)
3	11	29	100	1.748E+05	4.608E+05	0.379	3.7	1.01	105.4 ± 37.4
5	3	14	15	3.178E+05	1.483E+06	0.214	11.9	1.84	59.8 ± 38.1
6	2	16	36	8.828E+04	7.063E+05	0.125	5.7	1.09	34.9 ± 26.2
7	1	8	35	4.540E+04	3.632E+05	0.125	2.9	1.25	34.9 ± 37.1
9	0	14	60	0.000E+00	3.708E+05	0.000	3.0	0.20	0.0 ± 0.0
11	6	20	30	3.178E+05	1.059E+06	0.300	8.5	0.76	83.5 ± 38.9
13	10	30	28	5.675E+05	1.703E+06	0.333	13.7	0.60	92.7 ± 34.0
14	12	23	50	3.814E+05	7.310E+05	0.522	5.9	1.85	144.6 ± 51.6
15	12	29	60	3.178E+05	7.680E+05	0.414	6.2	1.21	114.9 ± 39.6
16	8	17	42	3.027E+05	6.432E+05	0.471	5.2	0.95	130.5 ± 56.1
17	6	20	21	4.540E+05	1.513E+06	0.300	12.2	0.76	83.5 ± 38.9
18	6	13	48	1.986E+05	4.304E+05	0.462	3.5	1.08	128.0 ± 63.3
20	19	47	100	3.019E+05	7.469E+05	0.404	6.0	0.86	112.3 ± 30.7
21	7	41	64	1.738E+05	1.018E+06	0.171	8.2	0.43	47.7 ± 19.5
26	3	7	20	2.384E+05	5.562E+05	0.429	4.5	0.78	119.0 ± 82.2
32	17	18	48	5.628E+05	5.959E+05	0.944	4.8	1.11	259.4 ± 88.0
33	4	8	40	1.589E+05	3.178E+05	0.500	2.6	1.15	138.6 ± 85.0
34	10	18	42	3.783E+05	6.810E+05	0.556	5.5	1.83	153.8 ± 60.8
35	6	27	70	1.362E+05	6.129E+05	0.222	4.9	1.17	62.0 ± 28.0
36	10	13	30	5.297E+05	6.886E+05	0.769	5.5	0.47	212.0 ± 89.4
55	21	85	35	9.534E+05	3.859E+06	0.247	31.0	0.96	68.9 ± 16.9
56	134	204	56	3.802E+06	5.789E+06	0.657	46.5	2.26	181.5 ± 20.8
61	23	38	48	7.614E+05	1.258E+06	0.605	10.1	0.32	167.4 ± 44.5
	331	739		4.879E+05	1.089E+06		8.8		

Area of basic unit = 6.293E-07 cm-2

Chi Squared = 50.515 with 22 degrees of freedom
P(chi squared) = 0.0 %
Correlation Coefficient = 0.955
Variance of SQR(Ns) = 4.71
Variance of SQR(Ni) = 6.21
Age Dispersion = 35.613 %

Ns/Ni = 0.448 ± 0.030
Mean Ratio = 0.398 ± 0.046

Ages calculated using a zeta of 360.3 ± 6.8 for SRM612 glass
Rho D = 1.555E+06cm-2; ND = 2455
Rho D interpolated between top of can; Rho D = 1.579E+06cm-2, ND = 1242
bottom of can; Rho D = 1.542E+06cm-2, ND = 1213

POOLED AGE = 124.3 ± 8.9 Ma
CENTRAL AGE = 108.5 ± 12.4 Ma

8642-238 APATITE

IRRADIATION PT838
SLIDE NUMBER 12
COUNTED BY: MEM

Current grain no.	Ns	Ni	Na	RHOs	RHOi	RATIO	U (ppm)	Cl (wt%)	F.T. AGE (Ma)
3	9	57	70	2.043E+05	1.294E+06	0.158	14.3	0.07	32.0 ± 11.5
4	4	49	45	1.412E+05	1.730E+06	0.082	19.2	0.08	16.6 ± 8.6
7	10	65	70	2.270E+05	1.476E+06	0.154	16.4	0.02	31.2 ± 10.6
8	11	33	32	5.462E+05	1.639E+06	0.333	18.2	0.17	67.4 ± 23.5
9	1	6	9	1.766E+05	1.059E+06	0.167	11.7	0.03	33.8 ± 36.5
10	4	17	49	1.297E+05	5.513E+05	0.235	6.1	0.00	47.6 ± 26.5
11	39	209	60	1.033E+06	5.535E+06	0.187	61.3	0.16	37.8 ± 6.7
12	1	13	50	3.178E+04	4.132E+05	0.077	4.6	0.87	15.6 ± 16.2
14	2	15	15	2.119E+05	1.589E+06	0.133	17.6	0.07	27.0 ± 20.4
16	3	85	40	1.192E+05	3.377E+06	0.035	37.4	0.00	7.2 ± 4.2
18	6	64	100	9.534E+04	1.017E+06	0.094	11.3	0.09	19.0 ± 8.1
19	24	62	40	9.534E+05	2.463E+06	0.387	27.3	0.63	78.2 ± 18.9
20	5	19	49	1.621E+05	6.162E+05	0.263	6.8	0.38	53.3 ± 26.8
23	16	74	100	2.542E+05	1.176E+06	0.216	13.0	0.21	43.8 ± 12.1
24	36	151	30	1.907E+06	7.998E+06	0.238	88.6	0.04	48.3 ± 9.1
25	41	162	100	6.515E+05	2.574E+06	0.253	28.5	0.14	51.2 ± 9.1
	212	1081		3.922E+05	2.000E+06		22.2		

Area of basic unit = 6.293E-07 cm-2

Chi Squared = 33.625 with 15 degrees of freedom
P(chi squared) = 0.4 %
Correlation Coefficient = 0.900
Variance of SQR(Ns) = 3.36
Variance of SQR(Ni) = 12.13
Age Dispersion = 37.332 %

Ns/Ni = 0.196 ± 0.015
Mean Ratio = 0.188 ± 0.024

Ages calculated using a zeta of 360.3 ± 6.8 for SRM612 glass
Rho D = 1.128E+06cm-2; ND = 1889
Rho D interpolated between top of can; Rho D = 1.306E+06cm-2, ND = 1027
bottom of can; Rho D = 1.096E+06cm-2, ND = 862

POOLED AGE = 39.7 ± 3.2 Ma
CENTRAL AGE = 38.0 ± 5.1 Ma

8642-240 APATITE

IRRADIATION PT838
SLIDE NUMBER 13
COUNTED BY: MEM

Current grain no.	Ns	Ni	Na	RHOs	RHOi	RATIO	U (ppm)	Cl (wt%)	F.T. AGE (Ma)
3	11	18	80	2.185E+05	3.575E+05	0.611	4.0	0.79	121.3 ± 46.6
6	31	79	25	1.970E+06	5.021E+06	0.392	56.4	0.79	78.1 ± 16.7
9	7	16	70	1.589E+05	3.632E+05	0.438	4.1	1.57	87.0 ± 39.5
11	27	35	49	8.756E+05	1.135E+06	0.771	12.8	0.72	152.7 ± 39.4
12	5	12	54	1.471E+05	3.531E+05	0.417	4.0	1.86	82.9 ± 44.2
13	12	21	72	2.648E+05	4.635E+05	0.571	5.2	1.46	113.5 ± 41.2
14	0	11	35	0.000E+00	4.994E+05	0.000	5.6	0.42	0.0 ± 0.0
15	5	10	70	1.135E+05	2.270E+05	0.500	2.6	1.08	99.4 ± 54.5
20	4	10	35	1.816E+05	4.540E+05	0.400	5.1	1.17	79.6 ± 47.2
21	2	8	48	6.621E+04	2.648E+05	0.250	3.0	0.54	49.9 ± 39.5
23	2	5	40	7.945E+04	1.986E+05	0.400	2.2	0.63	79.6 ± 66.7
24	13	22	42	4.919E+05	8.324E+05	0.591	9.4	0.85	117.3 ± 41.2
26	9	18	56	2.554E+05	5.108E+05	0.500	5.7	1.74	99.4 ± 40.7
27	4	5	28	2.270E+05	2.838E+05	0.800	3.2	1.41	158.3 ± 106.3
28	11	31	100	1.748E+05	4.926E+05	0.355	5.5	0.57	70.7 ± 24.9
29	25	34	70	5.675E+05	7.718E+05	0.735	8.7	1.41	145.6 ± 38.6
30	15	20	70	3.405E+05	4.540E+05	0.750	5.1	1.79	148.5 ± 50.9
33	3	286	100	4.767E+04	4.545E+06	0.010	51.1	0.10	2.1 ± 1.2
34	0	8	30	0.000E+00	4.238E+05	0.000	4.8	0.57	0.0 ± 0.0
35	1	6	56	2.838E+04	1.703E+05	0.167	1.9	0.35	33.3 ± 36.0
	187	655		2.630E+05	9.211E+05		10.4		

Area of basic unit = 6.293E-07 cm-2

Chi Squared = 142.184 with 19 degrees of freedom
P(chi squared) = 0.0 %
Correlation Coefficient = 0.078
Variance of SQR(Ns) = 2.44
Variance of SQR(Ni) = 10.71
Age Dispersion = 54.173 %

Ns/Ni = 0.285 ± 0.024
Mean Ratio = 0.433 ± 0.056

Ages calculated using a zeta of 360.3 ± 6.8 for SRM612 glass
Rho D = 1.112E+06cm-2; ND = 1889
Rho D interpolated between top of can; Rho D = 1.306E+06cm-2, ND = 1027
bottom of can; Rho D = 1.096E+06cm-2, ND = 862

POOLED AGE = 56.9 ± 5.0 Ma
CENTRAL AGE = 81.4 ± 13.1 Ma

8642-223 APATITE

IRRADIATION PT838
SLIDE NUMBER 3
COUNTED BY: MEM

Current grain no.	Ns	Ni	Na	RHOs	RHOi	RATIO	U (ppm)	Cl (wt%)	F.T. AGE (Ma)
3	3	8	35	1.362E+05	3.632E+05	0.375	3.6	0.56	85.4 ± 57.9
5	4	4	25	2.542E+05	2.542E+05	1.000	2.5	0.86	225.4 ± 159.5
7	4	13	30	2.119E+05	6.886E+05	0.308	6.8	1.08	70.2 ± 40.2
8	7	12	20	5.562E+05	9.534E+05	0.583	9.4	1.17	132.4 ± 63.1
10	2	15	25	1.271E+05	9.534E+05	0.133	9.4	0.39	30.5 ± 23.0
11	6	14	90	1.059E+05	2.472E+05	0.429	2.4	0.50	97.6 ± 47.7
12	4	15	60	1.059E+05	3.973E+05	0.267	3.9	0.88	60.9 ± 34.3
13	6	13	49	1.946E+05	4.216E+05	0.462	4.1	0.88	105.0 ± 51.9
14	8	22	35	3.632E+05	9.988E+05	0.364	9.8	0.38	82.9 ± 34.3
15	4	6	28	2.270E+05	3.405E+05	0.667	3.3	1.28	151.1 ± 97.7
18	12	22	50	3.814E+05	6.992E+05	0.545	6.9	1.11	123.9 ± 44.6
	60	144		2.133E+05	5.119E+05		5.0		

Area of basic unit = 6.293E-07 cm-2

Chi Squared = 6.898 with 10 degrees of freedom
P(chi squared) = 73.5 %
Correlation Coefficient = 0.664
Variance of SQR(Ns) = 0.33
Variance of SQR(Ni) = 0.70
Age Dispersion = 0.088 % (did not converge)

Ns/Ni = 0.417 ± 0.064
Mean Ratio = 0.467 ± 0.070

Ages calculated using a zeta of 360.3 ± 6.8 for SRM612 glass
Rho D = 1.273E+06cm-2; ND = 1889
Rho D interpolated between top of can; Rho D = 1.306E+06cm-2, ND = 1027
bottom of can; Rho D = 1.096E+06cm-2, ND = 862

POOLED AGE = 94.9 ± 14.8 Ma
CENTRAL AGE = 94.9 ± 14.8 Ma

8642-224 APATITE

IRRADIATION PT838
SLIDE NUMBER 4
COUNTED BY: MEM

Current grain no.	Ns	Ni	Na	RHOs	RHOi	RATIO	U (ppm)	Cl (wt%)	F.T. AGE (Ma)
3	7	17	35	3.178E+05	7.718E+05	0.412	7.7	1.08	92.6 ± 41.7
5	11	22	32	5.462E+05	1.092E+06	0.500	10.9	1.16	112.3 ± 41.6
8	15	35	100	2.384E+05	5.562E+05	0.429	5.5	1.18	96.3 ± 29.9
9	15	26	40	5.959E+05	1.033E+06	0.577	10.3	1.12	129.4 ± 42.1
10	3	5	20	2.384E+05	3.973E+05	0.600	4.0	1.12	134.5 ± 98.3
11	10	22	42	3.783E+05	8.324E+05	0.455	8.3	0.62	102.1 ± 39.1
13	7	32	70	1.589E+05	7.264E+05	0.219	7.2	1.49	49.4 ± 20.6
	68	159		3.188E+05	7.453E+05		7.4		

Area of basic unit = 6.293E-07 cm-2

Chi Squared = 3.968 with 6 degrees of freedom
P(chi squared) = 68.1 %
Correlation Coefficient = 0.720
Variance of SQR(Ns) = 0.58
Variance of SQR(Ni) = 1.49
Age Dispersion = 0.280 % (did not converge)

Ns/Ni = 0.428 ± 0.062
Mean Ratio = 0.456 ± 0.048

Ages calculated using a zeta of 360.3 ± 6.8 for SRM612 glass
Rho D = 1.257E+06cm-2; ND = 1889
Rho D interpolated between top of can; Rho D = 1.306E+06cm-2, ND = 1027
bottom of can; Rho D = 1.096E+06cm-2, ND = 862

POOLED AGE = 96.1 ± 14.2 Ma
CENTRAL AGE = 96.1 ± 14.2 Ma

APPENDIX C

Principles of Interpretation of AFTA and ZFTA Data in Sedimentary Basins

C.1 Introduction

In this Appendix, we set out some basic aspects of the processes underlying the AFTA and ZFTA techniques, and explain the principles involved in determining thermal history parameters from AFTA and ZFTA data. As the processes involved in AFTA are understood in considerably more detail than for ZFTA, the discussion is centred on AFTA, with some additional comments on ZFTA provided at the end of the Appendix.

Detrital apatite grains are incorporated into sedimentary rocks from three dominant sources - crystalline basement rocks, older sediments and contemporaneous volcanism. Apatites derived from the first two sources will, in general, contain fission tracks when they are deposited, with AFTA parameters characteristic of the source regions. However, apatites derived from contemporaneous volcanism, or from rapidly uplifted basement, will contain no tracks when they are deposited. For now, we will restrict discussion to this situation, and generalise at a later point to cover the case of apatites which contain tracks that have been inherited from source regions.

C.2 Basic principles of Apatite Fission Track Analysis

Fission tracks are trails of radiation damage, which are produced within apatite grains at a more or less constant rate through geological time, as a result of the spontaneous fission of ^{238}U impurity atoms. Therefore, the number of fission events which occur within an apatite grain during a fixed time interval depends on the magnitude of the time interval and the uranium content of the grain. Each fission event leads to the formation of a single fission track, and the proportion of tracks which can intersect a polished surface of an apatite grain depends on the length of the tracks. Therefore, the number of tracks which are etched in unit area of the surface of an apatite grain (the "spontaneous track density") depends on three factors - (i) The time over which tracks have been accumulating; (ii) The uranium content of the apatite grain; and, (iii) The distribution of track lengths in the grain. In sedimentary rocks which have not been subjected to temperatures greater than ~50°C since deposition, spontaneous fission tracks have a characteristic distribution of confined track lengths, with a mean length in the range 14-15 μm and a standard deviation of ~1 μm. In such samples, by

measuring the spontaneous track density and the uranium content of a collection of apatite grains, a "fission track age" can be calculated which will be equal to the time over which tracks have been accumulating. The technique is calibrated against other isotopic systems using age standards which also have this type of length distribution (see Appendix B).

In samples which have been subjected to temperatures greater than ~50°C after deposition, fission tracks are shortened because of the gradual repair of the radiation damage which constitutes the unetched tracks. In effect, the tracks shrink from each end, in a process which is known as fission track "annealing". The final length of each individual track is essentially determined by the maximum temperature which that track has experienced. A time difference of an order of magnitude produces a change in fission track parameters which is equivalent to a temperature change of only ~10°C, so temperature is by far the dominant factor in determining the final fission track parameters. As temperature increases, all existing tracks shorten to a length determined by the prevailing temperature, regardless of when they were formed. After the temperature has subsequently decreased, all tracks formed prior to the thermal maximum are "frozen" at the degree of length reduction they attained at that time. Thus, the length of each track can be thought of as a maximum-reading thermometer, recording the maximum temperature to which it has been subjected.

Therefore, in samples for which the present temperature is maximum, all tracks have much the same length, resulting in a narrow, symmetric distribution. The degree of shortening will depend on the temperature, with the mean track length falling progressively from ~14 μm at 50°C, to zero at around 110°-120°C - the precise temperature depending on the timescale of heating and the composition of the apatites present in the sample (see below). Values quoted here relate to times of the order of 10^7 years (heating rates around 1 to 10°C/Ma) and average apatite composition. If the effective timescale of heating is shorter than 10^7 years, the temperature responsible for a given degree of track shortening will be higher, depending in detail on the kinetics of the annealing process (Green et al., 1986; Laslett et al., 1987; Duddy et al., 1988; Green et al., 1989b). Shortening of tracks produces an accompanying reduction in the fission track age, because of the reduced proportion of tracks which can intersect the polished surface. Therefore, the fission track age is also highly temperature dependent, falling to zero at around 120°C due to total erasure of all tracks.

Samples which have been heated to a maximum paleotemperature less than ~120°C at some time in the past and subsequently cooled will contain two populations of tracks, and will show a more complex distribution of lengths and ages. If the maximum paleotemperature was less than ~50°C then the two components will not be resolvable, but for maximum paleotemperatures between ~50° and 120°C the presence of two components can readily be identified. Tracks formed prior to the thermal maximum will all be shortened to approximately the same degree (the precise value depending on the maximum

paleotemperature), while those formed during and after cooling will be longer, due to the lower prevailing temperatures. The length distribution in such samples will be broader than in the simple case, consisting of a shorter and a longer component, and the fission track age will reflect the amount of length reduction shown by the shorter component (determined by the maximum paleotemperature).

If the maximum paleotemperature was sufficient to shorten tracks to between 9 and 11 μm, and cooling to temperatures of ~50°C or less was sufficiently rapid, tracks formed after cooling will have lengths of 14-15 μm and the resulting track length distribution will show a characteristic bimodal form. If the maximum paleotemperature was greater than ~110 to 120°C, all pre-existing tracks will be erased, and all tracks now present will have formed after the onset of cooling. The fission track age in such samples relates directly to the time of cooling.

In thermal history scenarios in which a heating episode is followed by cooling and then temperature increases again, the tracks formed during the second heating phase will undergo progressive shortening. The tracks formed prior to the initial cooling, which were shortened in the first heating episode, will not undergo further shortening until the temperature exceeds the maximum temperature reached in the earlier heating episode. (In practice, differences in timescale of heating can complicate this simple description. In detail, it is the integrated time-temperature effect of the two heating episodes which should be considered.) If the maximum and peak paleotemperatures in the two episodes are sufficiently different (>~10°C), and the later peak paleotemperature is less than the earlier maximum value, then the AFTA parameters allow determination of both episodes. As the peak paleotemperature in the later episode approaches the earlier maximum, the two generations of tracks become increasingly more difficult to resolve, and when the two paleotemperatures are the same, both components are shortened to an identical degree and all information on the earlier heating phase will be lost.

No information is preserved on the approach to maximum paleotemperature because the great majority of tracks formed up to that time have the same mean track length. Only those tracks formed in the last few per cent of the history prior to the onset of cooling are not shortened to the same degree (because temperature dominates over time in the annealing kinetics). These form a very small proportion of the total number of tracks and therefore cannot be resolved within the length distribution because of the inherent spread of several μm in the length distribution.

To summarise, AFTA allows determination of the magnitude of the maximum temperature and the time at which cooling from that maximum began. In some circumstances, determination of a subsequent peak paleotemperature and the time of cooling is also possible.

C.3 Quantitative understanding of fission track annealing in apatite

Annealing kinetics and modelling the development of AFTA parameters

Our understanding of the behaviour of fission tracks in apatite during geological thermal histories is based on study of the response of fission tracks to elevated temperatures in the laboratory (Green et al., 1986; Laslett et al., 1987; Duddy et al., 1988; Green et al., 1989b), in geological situations (Green et al. 1989a), observations of the lengths of spontaneous tracks in apatites from a wide variety of geological environments (Gleadow et al. 1986), and the relationship between track length reduction and reduction in fission track age observed in controlled laboratory experiments (Green, 1988).

These studies resulted in the capability to simulate the development of AFTA parameters resulting from geological thermal histories for an apatite of average composition (Durango apatite, ~0.43 wt% Cl). Full details of this modelling procedure have been explained in Green et al. (1989b). The following discussion presents a brief explanation of the approach.

Geological thermal histories involving temperatures varying through time are broken down into a series of isothermal steps. The progressive shortening of track length through sequential intervals is calculated using the extrapolated predictions of an empirical kinetic model fitted to laboratory annealing data. Contributions from tracks generated throughout the history (remembering that new tracks are continuously generated through time as new fissions occur) are summed to produce the final distribution of track lengths expected to result from the input history. In summing these components, care is taken to allow for various biases which affect revelation of confined tracks (Laslett et al. 1982). The final length reduction of each component of tracks is converted to a contribution of fission track age, using the relationship between track length and density reduction determined by Green (1988). These age contributions are summed to generate the final predicted fission track age.

This approach depends critically on the assumption that extrapolation of the laboratory-based kinetic model to geological timescales, over many orders of magnitude in time, is valid. This was assessed critically by Green et al. (1989b), who showed that predictions from this approach agree well with observed AFTA parameters in apatites of the appropriate composition in samples from a series of reference wells in the Otway Basin of south-east Australia (Gleadow and Duddy, 1981; Gleadow et al., 1983; Green et al., 1989a). This point is illustrated in Figure C.1. Green et al. (1989b) also quantitatively assessed the errors associated with extrapolation of the Laslett et al. (1987) model from laboratory to geological timescales (i.e. precision, as opposed to accuracy). Typical levels of precision are ~0.5 μm for mean lengths <~10 μm, and ~0.3 μm for lengths >~10 μm. These figures are equivalent to an uncertainty in estimates of maximum paleotemperature derived using this approach of

~10°C. Precision is largely independent of thermal history for any reasonable geological history. Accuracy of prediction from this model is limited principally by the effect of apatite composition on annealing kinetics, as explained in the next section.

Compositional effects

Natural apatites essentially have the composition $Ca_5(PO_4)_3(F,OH,Cl)$. Most common detrital and accessory apatites are predominantly Fluor-apatites, but may contain appreciable amounts of chlorine. The amount of chlorine in the apatite lattice exerts a subtle compositional control on the degree of annealing, with apatites richer in fluorine being more easily annealed than those richer in chlorine. The result of this effect is that in a single sample, individual apatite grains may show a spread in the degree of annealing (i.e. length reduction and fission track age reduction). This effect becomes most pronounced in the temperature range 90 - 120°C (assuming a heating timescale of ~10 Ma), and can be useful in identifying samples exposed to paleotemperatures in this range. At temperatures below ~80°C, the difference in annealing sensitivity is less marked, and compositional effects can largely be ignored.

Our original quantitative understanding of the kinetics of fission track annealing, as described above, relates to a single apatite (Durango apatite) with ~0.43 wt% Cl, on which most of our original experimental studies were carried out. Recently, we have extended this quantitative understanding to apatites with Cl contents up to ~3 wt%. This new, multi-compositional kinetic model is based both on new laboratory annealing studies on a range of apatites with different F-Cl compositions (Figure C.2), and on observations of geological annealing in apatites from a series of samples from exploration wells in which the section is currently at maximum temperature since deposition. A composite model for Durango apatite composition was first created by fitting a common model to the old laboratory data (from Green et al., 1986) and the new geological data for a similar composition. This was then extended to other compositions on the basis of the multi-compositional laboratory and geological data sets. Details of the multi-compositional model are contained in a Technical Note, available from Geotrack in Melbourne.

The multi-compositional model allows prediction of AFTA parameters for any Cl content between 0 and 3 wt%, using a similar approach to that used in our original single composition modelling, as outlined above. Then, for an assumed or measured distribution of Cl contents within a sample, the composite parameters for the sample can be predicted. The range of Cl contents from 0 to 3 wt% spans the range of compositions commonly encountered, as discussed in the next section.

Predictions of the new multi-compositional model are in good agreement with the geological constraints on annealing rates provided by the Otway Basin reference wells, as shown in

Figure C.3. However, note that the AFTA data from these Otway Basin wells were among those used in construction of the new model, so this should not be viewed as independent verification, but rather as a demonstration of the overall consistency of the model.

Distributions of Cl content in common AFTA samples

Figure C.4a shows a histogram of Cl contents, measured by electron microprobe, in apatite grains from more than 100 samples of various types. Most grains have Cl contents less than ~0.5 wt%. The majority of grains with Cl contents greater than this come from volcanic sources and basic intrusives, and contain up to ~2 wt% Cl. Figure C.4b shows the distribution of Cl contents measured in randomly selected apatite grains from 61 samples of "typical" quartzo-feldspathic sandstone. This distribution is similar to that in Figure C.4a, except for a more rapid fall-off as Cl content increases. Apatites from most common sandstones give distributions of Cl content which are very similar to that in Figure C.4b. Volcanogenic sandstones typically contain apatites with higher Cl contents, with a much flatter distribution for Cl contents up to ~1.5%, falling to zero at ~2.5 to 3 wt%, as shown in Figure C.4c. Cl contents in granitic basement samples and high-level intrusives are typically much more dominated by compositions close to end-member Fluorapatite, although many exceptions occur to this general rule.

Information about the spread of Cl contents in samples analysed in this report can be found in Appendix A.

Alternative kinetic models

Recently, both Carlson (1990) and Crowley et al. (1991) have published alternative kinetic models for fission track annealing in apatite. Carlson's model is based on our laboratory annealing data for Durango apatite (Green et al., 1986) and other (unpublished) data. In his abstract, Carlson claims that because his model is "based on explicit physical mechanisms, extrapolations of annealing rates to the lower temperatures and longer timescales required for the interpretation of natural fission track length distributions can be made with greater confidence than is the case for purely empirical relationships fitted to the experimental annealing data". As explained in detail by Green et al. (1993), all aspects of Carlson's model are in fact purely empirical, and his model is inherently no "better" for the interpretation of data than any other. In fact, detailed inspection shows that Carlson's model does not fit the laboratory data set at all well. Therefore, we recommend against use of this model to interpret AFTA data.

The approach taken by Crowley et al. (1991) is very similar to that taken by Laslett et al., (1987). They have fitted models to new annealing data in two apatites of different composition - one close to end-member Fluorapatite (B-5) and one having a relatively high Sr

content (113855). The model developed by Crowley et al. (1991) from their own annealing data for the B-5 apatite gives predictions in geological conditions which are consistently higher than measured values, as shown in Figure C.5. Corrigan (1992) reported a similar observation in volcanogenic apatites in samples from a series of West Texas wells. Since the B-5 apatite is close to end-member Fluor-apatite, while the Otway Group apatites contain apatites with Cl contents from zero up to ~3 wt% (and the West Texas apatites have up to 1 wt%), the fluorapatites should have mean lengths rather less than the measured values, which should represent a mean over the range of Cl contents present. Therefore, the predictions of the Crowley et al. (1991) B-5 model appear to be consistently high.

We attribute this to the rather restricted temperature-time conditions covered by the experiments of Crowley et al. (1991), with annealing times between one and 1000 hours, in contrast to times between 20 minutes and 500 days in the experiments of Green et al. (1986). In addition, few of the measured length values in Crowley et al.'s study fall below 11 μm (in only five out of 60 runs in which lengths were measured in apatite B-5) and their model is particularly poorly defined in this region.

Crowley et al. (1991) also fitted a new model to the annealing data for Durango apatite published by Green et al. (1986). Predictions of their fit to our data are not very much different to those from the Laslett et al. (1987) model (Figure C.6). We have not pursued the differences between their model and ours in detail because the advent of our multi-compositional model has rendered the single compositional approach obsolete.

C.4 Evidence for elevated paleotemperatures from AFTA

The basic principle involved in the interpretation of AFTA data in sedimentary basins is to determine whether the degree of annealing shown by tracks in apatite from a particular sample could have been produced if the sample has never been hotter than its present temperature at any time since deposition. To do this, the burial history derived from the stratigraphy of the preserved sedimentary section is used to calculate a thermal history for each sample using the present geothermal gradient and surface temperature (i.e. assuming these have not changed through time). This is termed the "Default Thermal History". For each sample, the AFTA parameters predicted as a result of the Default Thermal History are then compared to the measured data. If the data show a greater degree of annealing than calculated on the basis of this history, the sample must have been hotter at some time in the past. In this case, the AFTA data are analysed to provide estimates of the magnitude of the maximum paleotemperature in that sample, and the time at which cooling commenced from the thermal maximum.

The degree of annealing is assessed in two ways - from fission track age and track length data. The stratigraphic age provides a basic reference point for the interpretation of fission track age, because reduction of the fission track age below the stratigraphic age unequivocally reveals that appreciable annealing has taken place after deposition of the host sediment. Large degrees of fission track age reduction, with the pooled or central fission track age very much less than the stratigraphic age, indicate severe annealing, which requires paleotemperatures of at least ~100°C for any reasonable geological time-scale of heating (>~1 Ma). Note that this applies even when apatites contain tracks inherited from source areas. More moderate degrees of annealing can be detected by inspection of the single grain age data, as the most sensitive (fluorine-rich) grains will begin to give fission track ages significantly less than the stratigraphic age before the central or pooled age has been reduced sufficiently to give a noticeable signal. Note that this aspect of the single grain age data can also be used for apatites which have tracks inherited from source areas. If signs of moderate annealing (from single grain age reduction) or severe annealing (from the reduction in pooled or central age) are seen in samples in which the Default Thermal History predicts little or no effect, the sample must have been subjected to elevated paleotemperatures at some time in the past. Figure C.7 shows how increasing degrees of annealing are observable in radial plots of the single grain fission track age data.

Similarly, the present temperature from which a sample is taken, and the way in which this has been approached (as inferred from the preserved sedimentary section), forms a basic point of reference for track length data. The observed mean track length is compared with the mean length predicted from the Default Thermal History. If the observed degree of track shortening in a sample is greater than that expected from the Default Thermal History (i.e. the mean length is significantly less than the predicted value), either the sample must have been subjected to higher paleotemperatures at some time after deposition, or the sample contains shorter tracks which were inherited from sediment source areas at the time the sediment was deposited. If shorter tracks were inherited from source areas, the sample should still contain a component of longer tracks corresponding to the tracks formed after deposition. In general, the fission track age should be greater than the stratigraphic age. This can be assessed quantitatively using the computer models for the development of AFTA parameters described in an earlier section. If the presence of shorter tracks cannot be explained by their inheritance from source areas, the sample must have been hotter in the past.

C.5 Quantitative determination of the magnitude of maximum paleotemperature and the timing of cooling using AFTA

Values of maximum paleotemperature and timing of cooling in each sample are determined using a forward modelling approach based on the quantitative description of fission track annealing described in earlier sections. The Default Thermal History described above is used

as the basis for this forward modelling, but with the addition of episodes of elevated paleotemperatures as required to explain the data. AFTA parameters are modelled iteratively through successive thermal history scenarios in order to identify thermal histories that can account for observed parameters. The range of values of maximum paleotemperature and timing of cooling which can account for the measured AFTA parameters (fission track age and track length distribution) are defined using a maximum likelihood-based approach. In this way, best estimates ("maximum likelihood values") can be defined together with ±95% confidence limits.

In samples in which all tracks have been totally annealed at some time in the past, only a minimum estimate of maximum paleotemperature is possible. In such cases, AFTA data provide most control on the time at which the sample cooled to temperatures at which tracks could be retained. The time at which cooling began could be earlier than this time, and therefore the timing also constitutes a minimum estimate.

Comparison of the AFTA parameters predicted by the multi-compositional model with measured values in samples which are currently at their maximum temperatures since deposition shows a good degree of consistency, suggesting the uncertainty in application of the model should be less than ±10°C. This constitutes a significant improvement over earlier approaches, since the kinetic models used are constrained in both laboratory and geological conditions. It should be appreciated that relative differences in maximum paleotemperature can be identified with greater precision than absolute paleotemperatures, and it is only the estimation of absolute paleotemperature values to which the ±10°C uncertainty relates.

Cooling history

If the data are of high quality and provided that cooling from maximum paleotemperatures began sufficiently long ago (so that the history after this time is represented by a significant proportion of the total tracks in the sample), determination of the magnitude of a subsequent peak paleotemperature and the timing of cooling from that peak may also be possible (as explained in Section C.2). A similar approach to that outlined above provides best estimates and corresponding ±95% confidence limits for this episode. Such estimates may simply represent part of a protracted cooling history, and evidence for a later discrete cooling episode can only be accepted if this scenario provides a significantly improved fit to the data. Geological evidence and consistency of estimates between a series of samples can also be used to verify evidence for a second episode.

In practise, most typical AFTA datasets are only sufficient to resolve two discrete episodes of heating and cooling. One noteable exception to this is when a sample has been totally annealed in an early episode, and has then undergone two (or more) subsequent episodes with

progressively lower peak paleotemperatures in each. But in general, complex cooling histories involving a series of episodes of heating and cooling will allow resolution of only two episodes, and the results will depend on which episodes dominate the data. Typically this will be the earliest and latest episodes, but if multiple cooling episodes occur within a narrow time interval the result will represent an approximation to the actual history.

C.6 Qualitative assessment of AFTA parameters

Various aspects of thermal history can often be assessed by qualitative assessment of AFTA parameters. For example, samples which have reached maximum paleotemperatures sufficient to produce total annealing, and which only contain tracks formed after the onset of cooling, can be identified from a number of lines of evidence. In a vertical sequence of samples showing increasing degrees of annealing, the transition from rapidly decreasing fission track age with increasing depth to more or less the same age over a range of depth denotes the transition from partial to total annealing of all tracks formed prior to the thermal maximum. In samples in which all tracks have been totally annealed, the single grain age data should show that none of the individual grain fission track ages are significantly older than the time of cooling, and grains in all compositional groups should give the same fission track age unless the sample has been further disturbed by a later episode. If the sample cooled rapidly to sufficiently low temperatures, little annealing will have taken place since cooling, and all grains will give ages which are compatible with a single population around the time of cooling, as shown in Figure C.7.

Inspection of the distribution of single grain ages in partially annealed samples can often yield useful information on the time of cooling, as the most easily annealed grains (those richest in fluorine) may have been totally annealed prior to cooling, while more retentive (Cl-rich) compositions were only partially annealed (as in Figure C.7, centre). The form of the track length distribution can also provide information, from the relative proportions of tracks with different lengths. All of these aspects of the data can be used to reach a preliminary thermal history interpretation.

C.7 Allowing for tracks inherited from source areas

The effect of tracks inherited from source areas, and present at the time the apatite is deposited in the host sediment, is often posed as a potential problem for AFTA. However, this can readily be allowed for in analysing both the fission track age and length data.

In assessing fission track age data to determine the degree of annealing, the only criterion used is the comparison of fission track age with the value expected on the basis of the Default Thermal History. From this point of view, inherited tracks do not affect the conclusion: if a grain or a sample gives a fission track age which is significantly less than expected, the grain

or sample has clearly undergone a higher degree of annealing than can be accounted for by the Default Thermal History, and therefore must have been hotter in the past, whether the sample contained tracks when it was deposited or not.

The presence of inherited tracks does impose a limit on our ability to detect post-depositional annealing from age data alone, as in samples which contain a fair proportion of inherited tracks, moderate degrees of annealing may reduce the fission track age from the original value, but not to a value which is significantly less than the stratigraphic age. This is particularly noticeable in the case of Tertiary samples containing apatites derived from Paleozoic basement. In such cases, although fission track age data may show no evidence of post-depositional annealing, track length data may well show such evidence quite clearly.

The influence of track lengths inherited from source areas can be allowed for by comparison of the fission track age with the value predicted by the Default Thermal History combined with inspection of the track length distribution. If the mean length is much less than the length predicted by the Default Thermal History, either the sample has been subjected to elevated paleotemperatures, sufficient to produce the observed degree of length reduction, or else the sample contains a large proportion of shorter tracks inherited from source areas. However, in the latter case, the sample should give a pooled or central fission track age correspondingly older than the stratigraphic age, while the length distribution should contain a component of longer track lengths corresponding to the value predicted by the Default Thermal History. It is important in this regard that the length of a track depends primarily on the maximum temperature to which it has been subjected, whether in the source regions or after deposition in the sedimentary basin. Thus, any tracks retaining a provenance signature will have lengths towards the shorter end of the distribution where track lengths will not have "equilibrated" with the temperatures attained since deposition.

In general, it is only in extreme cases that inherited tracks render track length data insensitive to post-depositional annealing. For example, if practically all the tracks in a particular sample were formed prior to deposition, perhaps in a Pliocene sediment in which apatites were derived from a stable Paleozoic shield with fission track ages of ~300 Ma or more, the track length distribution will, in general, be dominated by inheritance, as only ~2% of tracks would have formed after deposition. Post-depositional heating will not be detectable as long as the maximum paleotemperature is insufficient to cause greater shortening than that which occurred in the source terrain. Even in such extreme cases, once a sample is exposed to temperatures sufficient to produce greater shortening than that inherited from source areas, the inherited tracks and those formed after deposition will all undergo the same degree of shortening, and the effects of post-depositional annealing can be recognised. In such cases, the presence of tracks inherited from source areas is actually very useful, because the number of tracks

formed after deposition is so small that little or no information would be available without the inherited tracks.

C.8 Plots of fission track age and mean track length vs depth and temperature

AFTA data from well sequences are usually plotted as shown in Figure C.8. This figure shows AFTA data for two scenarios: one in which deposition has been essentially continuous from the Carboniferous to the present and all samples are presently at their maximum paleotemperature since deposition (Figure C.8a); and, one in which the section was exposed to elevated paleotemperatures prior to cooling in the Early Tertiary (Figure C.8b).

In both figures, fission track age and mean track length are plotted against depth and present temperature. Presentation of AFTA data in this way often provides insight into the thermal history interpretation, following principles outlined earlier in this Appendix.

In Figure C.8a, for samples at temperatures below ~70°C, the fission track age is either greater than or close to the stratigraphic age, and little fission track age reduction has affected these samples. Track lengths in these samples are all greater than ~13 μm. In progressively deeper samples, both the fission track age and mean track length are progressively reduced to zero at a present temperature of around 110°C, with the precise value depending on the spread of apatite compositions present in the sample. Track length distributions in the shallowest samples would be a mixture of tracks retaining information on the thermal history of source regions, while in deeper samples, all tracks would be shortened to a length determined by the prevailing temperature. This pattern of AFTA parameters is characteristic of a sequence which is currently at maximum temperatures.

The data in Figure C.8b show a very different pattern. The fission track age data show a rapid decrease in age, with values significantly less than the stratigraphic age at temperatures of ~40 to 50°C, at which such a degree of age reduction could not be produced in any geological timescale. Below this rapid fall, the fission track ages do not change much over ~1 km (30°C). This transition from rapid fall to consistent ages is diagnostic of the transition from partial to total annealing. Samples above the "break-in slope" contain two generations of tracks: those formed prior to the thermal maximum, which have been partially annealed (shortened) to a degree which depends on the maximum paleotemperature; and, those formed after cooling, which will be longer. Samples below the break-in slope contain only one generation of tracks, formed after cooling to lower temperatures at which tracks can be retained. At greater depths, where temperatures increase to ~90°C and above, the effect of present temperatures begins to reduce the fission track ages towards zero, as in the "maximum temperatures now" case.

The track length data also reflect the changes seen in the fission track age data. At shallow depths, the presence of the partially annealed tracks shortened prior to cooling causes the mean track length to decrease progressively as the fission track age decreases. However, at depths below the break in slope in the age profile, the track length increases again as the shorter component is totally annealed and so does not contribute to the measured distribution of track lengths. At greater depths, the mean track lengths decrease progressively to zero once more due to the effects of the present temperature regime.

Examples of such data have been presented, e.g. by Green (1989) and Kamp and Green (1990).

C.9 Determining paleogeothermal gradients and amount of section removed on unconformities

Estimates of maximum paleotemperatures in samples over a range of depths in a vertical sequence provides the capability of determining the paleogeothermal gradient immediately prior to the onset of cooling from those maximum paleotemperatures. The degree to which the paleogeothermal gradient can be constrained depends on a number of factors, particularly the depth range over which samples are analysed. If samples are only analysed over ~1 km, then the paleotemperature difference over that range may be only ~20 to 30°C. Since maximum paleotemperatures can often only be determined within a ~10°C range, this introduces considerable uncertainty into the final estimate of paleogeothermal gradient (see Figure C.9)

Another important factor is the difference between maximum paleotemperatures and present temperatures ("net cooling"). If this is only ~10°C, which is similar to the uncertainty in absolute paleotemperature determination, only broad limits can be established on the paleogeothermal gradient. In general, the control on the paleogeothermal gradient improves as the amount of net cooling increases. However, if the net cooling becomes so great that many samples were totally annealed prior to the onset of cooling - so that only minimum estimates of maximum paleotemperatures are possible - constraints on the paleogeothermal gradient from AFTA come only from that part of the section in which samples were not totally annealed. In this case, integration of AFTA data with VR measurements can be particularly useful in constraining the paleo-gradient.

Having constrained the paleogeothermal gradient at the time cooling from maximum paleotemperatures began, if we assume a value for surface temperature at that time, the amount of section subsequently removed by uplift and erosion can be calculated as shown in Figure C.10. The *net* amount of section removed is obtained by dividing the difference between the paleo-surface temperature (T_S) and the intercept of the paleotemperature profile at

the present ground surface (T_i) by the estimated paleogeothermal gradient. The *total* amount of section removed is obtained by adding the thickness of section subsequently redeposited above the unconformity to the *net* amount estimated as in Figure C.10. If the analysis is performed using depths from the appropriate unconformity, then the analysis will directly yield the *total* amount of section removed.

Geotrack have developed a method of deriving estimates of both the paleogeothermal gradient and the net amount of section removed using estimated paleotemperatures derived from AFTA and VR. Perhaps more importantly, this method also provides rigorous values for upper and lower 95% confidence limits on each parameter. The method is based on maximum likelihood estimation of the paleogeothermal gradient and the surface intercept, from a table of paleotemperature and depth values. The method is able to accept ranges for paleotemperature estimates (e.g. where the maximum paleotemperature can only be constrained to between, for example, 60 and 90°C), as well as upper and lower limits (e.g. <60°C for samples which show no detectable annealing; >110°C in samples which were totally annealed). Estimates of paleotemperature from AFTA and VR may be combined or analysed separately. Some results from this method have been reported by Bray et al. (1992). Full details of the methods employed are presented in a confidential, in-house, Geotrack research report, copies of which are available on request from the Melbourne office.

Results are presented in two forms. Likelihood profiles, plotting the log-likelihood as a function of either gradient or section removed, portray the probability of a given value of gradient or section removed. The best estimate is given by the value of gradient or section removed for which the log-likelihood is maximised. Ideally, the likelihood profiles should show a quadratic form, and values of gradient or section removed at which the log-likelihood has fallen by two from the maximum value define the upper and lower 95% confidence limits on the estimates. An alternative method of portraying this information is a crossplot of gradient against section removed, in which values which fall within 95% confidence limits (in two dimensions) are contoured. Note that the confidence limits defined by this method are rather tighter than those from the likelihood profiles, as the latter only reflect variation in one parameter, whereas the contoured crossplot takes variation of both parameters into account.

It must be emphasised that this method relies on the assumption that the paleotemperature profile was linear both throughout the section analysed and through the overlying section which has been removed. While the second part of this assumption can never be confirmed independently, visual inspection of the paleotemperature estimates as a function of depth should be sufficient to verify or deny the linearity of the paleotemperature profile through the preserved section.

Results of this procedure are shown in this report if the data allow sufficiently well-defined paleotemperature estimates to justify use of the method. Where the AFTA data suggest that the section is currently at maximum temperature since deposition, or that the paleotemperature profile was non-linear, or where data are of insufficient quality to allow rigorous paleotemperature estimation, the method is not used.

C.10 Thermal history interpretation of Zircon Fission Track Age data

The understanding of the annealing characteristics of fission tracks in zircon is not as well developed as for apatite. From both laboratory and geological evidence, fission tracks in zircon are known to be less sensitive to annealing than fission tracks in apatite. Zircon fission track ages are conventionally interpreted in terms of a closure temperature, defined as the nominal temperature below which a radiogenic product, in this case fission tracks, is effectively retained. Although the closure temperature in zircon is not well constrained, geological evidence suggests values between 175° and 300°C. Based on comparison of zircon fission track ages with ages from other radiometric systems, Hurford (1986) proposed a closure temperature for fission track retention in zircon of 240° ± 50°C. A value around 240°C or possibly higher is broadly consistent with all available evidence, although the ±50°C quoted uncertainty would allow unrealistically low values, and our experience suggests a value between 220 and 300°C would be most appropriate.

In contrast, tracks in apatite begin to be retained when the mineral cools below a temperature of the order of ~110°-120°C (depending on apatite composition). Where fission track ages are available for apatite and zircon, the cooling history of a sample can be assessed because of the differing thermal sensitivities of the tracks in the minerals. In samples which have cooled rapidly from high temperatures of >240°C to less than ~50°C, the apatite and zircon fission track ages are usually concordant, as tracks in both minerals began to be retained at roughly the same time.

The type of analysis presented for apatite data is not possible in zircon, because it is not usually possible to measure track lengths in zircon due to the etching properties of the mineral. This makes it difficult to determine whether a thermally affected zircon fission track age represents partial or total annealing, and, thus, whether the fission track age can be interpreted in terms of a specific "event". Another problem with the interpretation of zircon data is posed by the lack of constraint on the temperatures required for a given degree of partial annealing. Therefore, unlike the situation with apatite, it is not possible to rigorously estimate maximum paleotemperatures on the basis of zircon data alone. On the basis of experience in a small number of sedimentary basins, it appears that significant age reduction in zircon does not normally occur below temperatures of ~200°C. However, the effects of composition on

annealing rates in zircon are not well understood, and it is possible that some particularly sensitive zircons may exist which undergo annealing at lower temperatures.

Investigation of zircon data in samples with different levels of vitrinite reflectance suggests that no significant age reduction occurs in zircon at VR levels below ~4%. VR values in excess of 5% are required in order to produce any significant age reduction. Some evidence suggests that the rock needs to reach the stage of incipient recrystallisation in order to produce observable effects in zircon.

Based on all evidence currently available, we define the following broad paleotemperature ranges which may be defined on the basis of ZFTA data:

Some age reduction	200-300°C
Appreciable age reduction	≥240°C
Total annealing of most grains	>300°C

It should be borne in mind that these paleotemperatures are only very loosely constrained, and any conclusions based thereon should be treated with caution.

References

Carlson, W.D. (1990) Mechanisms and kinetics of apatite fission-track annealing. *American Mineralogist*, 75, 1120 - 1139.

Corrigan, J. (1992) Annealing models under the microscope, *On Track*, 2, 9-11.

Crowley, K.D., Cameron, M. and Schaefer, R.L. (1991) Experimental studies of annealing of etched fission tracks in apatite. *Geochimica et Cosmochimica Acta*, 55, 1449-1465.

Duddy, I.R., Green, P.F. and Laslett G.M. (1988) Thermal annealing of fission tracks in apatite 3. Variable temperature behaviour. *Chem. Geol. (Isot. Geosci. Sect.)*, 73, 25-38.

Gleadow, A.J.W. and Duddy, I.R. (1981) A natural long-term track annealing experiment for apatite. *Nuclear Tracks*, 5, 169-174.

Gleadow, A.J.W., Duddy, I.R. and Lovering, J.F. (1983) Fission track analysis; a new tool for the evaluation of thermal histories and hydrocarbon potential. *APEA J*, 23, 93-102.

Gleadow, A.J.W., Duddy, I.R., Green, P.F. and Lovering, J.F. (1986) Confined fission track lengths in apatite - a diagnostic tool for thermal history analysis. *Contr. Min. Petr.*, 94, 405-415.

Green, P.F. (1988) The relationship between track shortening and fission track age reduction in apatite: Combined influences of inherent instability, annealing anisotropy, length bias and system calibration. *Earth Planet. Sci. Lett.*, 89, 335-352.

Green, P.F., Duddy, I.R., Gleadow, A.J.W., Tingate, P.R. and Laslett, G.M. (1986) Thermal annealing of fission tracks in apatite 1. A qualitative description. *Chem. Geol. (Isot. Geosci. Sect.)*, 59, 237-253.

Green, P.F., Duddy, I.R., Gleadow, A.J.W. and Lovering, J.F. (1989a) Apatite Fission Track Analysis as a paleotemperature indicator for hydrocarbon exploration. *In:* Naeser, N.D. and McCulloh, T. (eds.) *Thermal history of sedimentary basins - methods and case histories*, Springer-Verlag, New York, 181-195.

Green, P.F., Duddy, I.R., Laslett, G.M., Hegarty, K.A., Gleadow, A.J.W. and Lovering, J.F. (1989b) Thermal annealing of fission tracks in apatite 4. Quantitative modelling techniques and extension to geological timescales. *Chem. Geol. (Isot. Geosci. Sect.)*, 79, 155-182

Green, P.F., Laslett, G.M. and Duddy, I.R. (1993) Mechanisms and kinetics of apatite fission track annealing: Discussion. *American Mineralogist*, 78, 441-445.

Hurford, A.J. (1986) Cooling and uplift patterns in the Lepontine Alps, South Central Switzerland and an age of vertical movement on the Insubric fault line. *Contrib. Mineral. Petrol.*. 92, 413-427.

Laslett, G.M., Kendall, W.S., Gleadow, A.J.W. and Duddy, I.R. (1982) Bias in measurement of fission track length distributions. *Nuclear Tracks*, 6, 79-85.

Laslett, G.M., Green, P.F., Duddy, I.R. and Gleadow, A.J.W. (1987) Thermal annealing of fission tracks in apatite 2. A quantitative analysis. *Chem. Geol. (Isot. Geosci. Sect.)*, 65, 1-13.

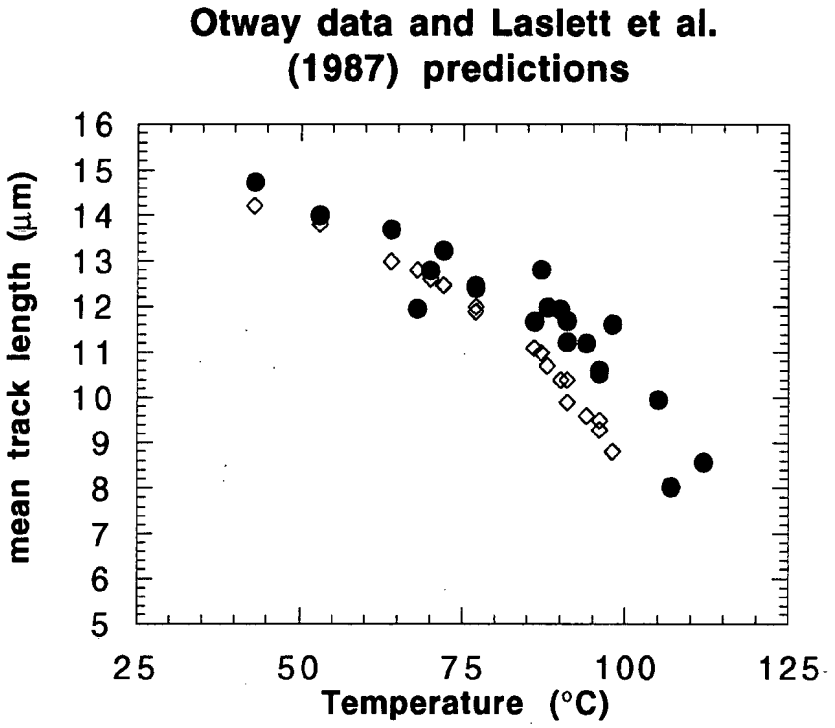

Figure C.1a Comparison of mean track length (solid circles) measured in samples from four Otway Basin reference wells (from Green et al, 1989a) and predicted mean track lengths (open diamonds) from the kinetic model of fission track annealing from Laslett et al. (1987). Although the predictions underestimate the measured values, they refer to an apatite composition that is more easily annealed than the majority of apatites in these samples, and therefore this is expected.

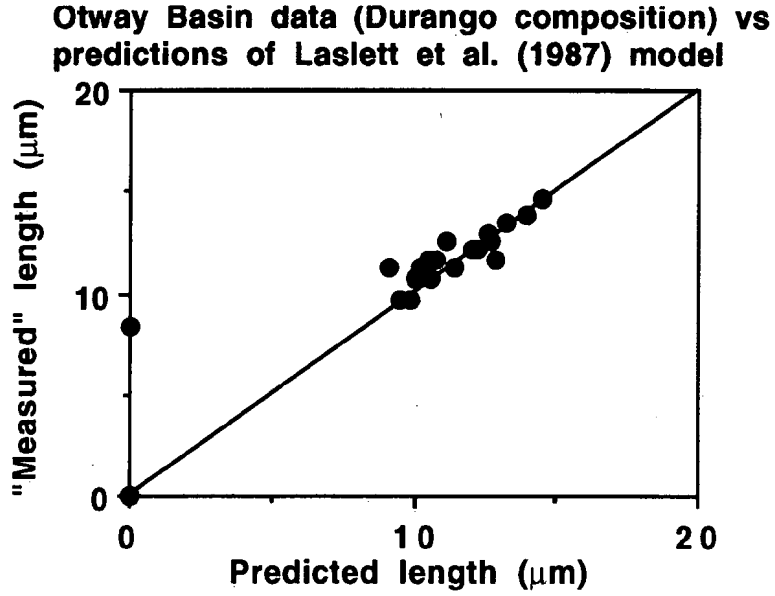

Figure C.1b Comparison of the mean track length in apatites of the same Cl content as Durango apatite from the Otway Group samples illustrated in figure C.1a, with values predicted for apatite of the same composition by the model of Laslett et al. (1987). The agreement is clearly very good except possibly at lengths below ~10 µm.

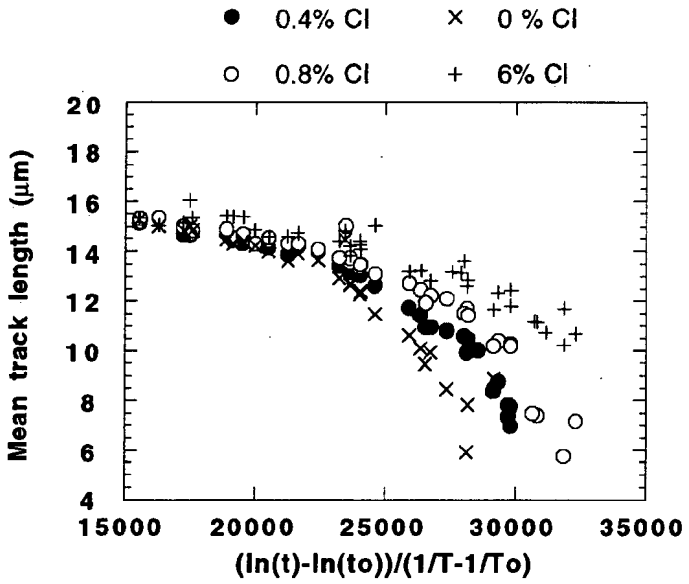

Figure C.2 Mean track length in apatites with four different chlorine contents, as a combined function of temperature and time, to reduce the data to a single scale. Fluorapatites are more easily annealed than chlorapatites, and the annealing kinetics show a progressive change with increasing Cl content.

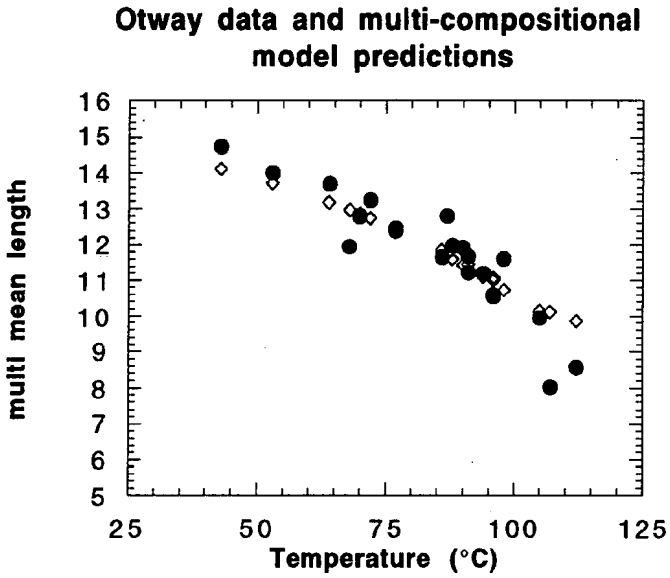

Figure C.3 Comparison of measured mean track length (solid circles) in samples from four Otway Basin reference wells (from Green et al, 1989a) and predicted mean track lengths (open diamonds) from the new multi-compositional kinetic model of fission track annealing described in Section C.3. This model takes into account the spread of Cl contents in apatites from the Otway Group samples and the influence of Cl content on annealing rate. The agreement is clearly very good over the range of the data.

All samples

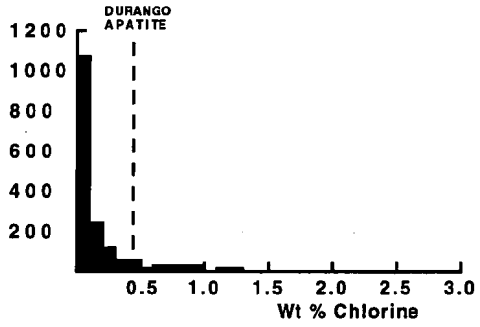

"Normal sandstones"

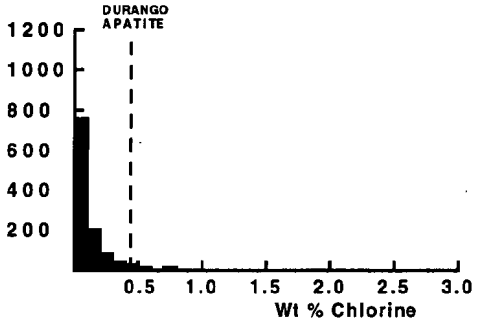

Volcanogenic sandstones

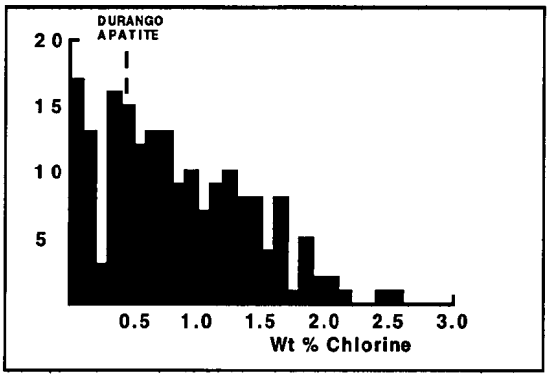

Figure C.4 **a:** Histogram of Cl contents (wt%) in over 1750 apatite grains from over 100 samples of various sedimentary and igneous rocks. Most samples give Cl contents below ~0.5 wt %, while those apatites giving higher Cl contents are characterisitic of volcanogenic sandstones and basic igneous sources.

b: Histogram of Cl contents (wt%) in 1168 apatite grains from 61 samples which can loosely be characterised as "normal sandstone". The distribution is similar to that in the upper figure, except for a lower number of grains with Cl contents greater than ~1%.

c: Histogram of Cl contents (wt%) in 188 apatite grains from 15 samples of volcanogenic sandstone. The distribution is much flatter than the other two, with much higher proportion of Cl-rich grains.

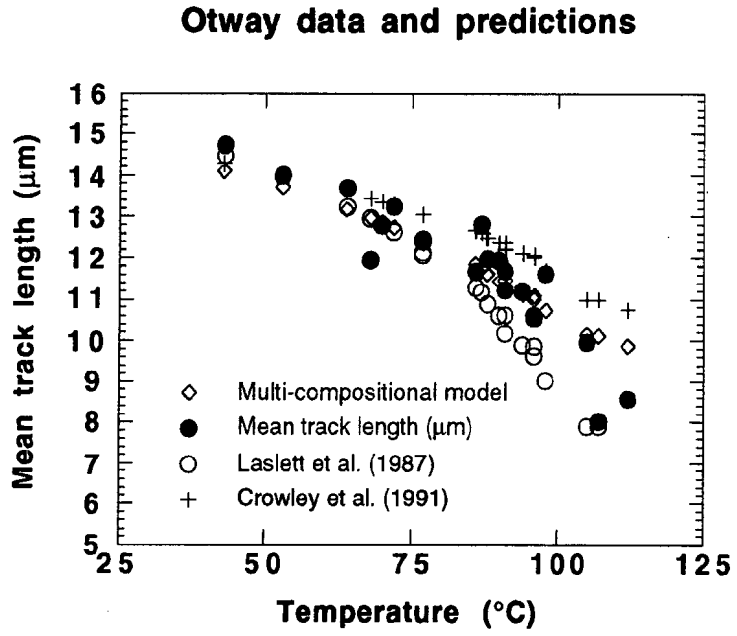

Figure C.5 Comparison of mean track length in samples from four Otway Basin reference wells (from Green et al, 1989a) and predicted mean track lengths from three kinetic models for fission track annealing. The Crowley et al. (1991) model relates to almost pure Fluorapatite (B-5), yet overpredicts mean lengths in the Otway Group samples which are dominated by Cl-rich apatites. The predictions of that model are therefore not reliable.

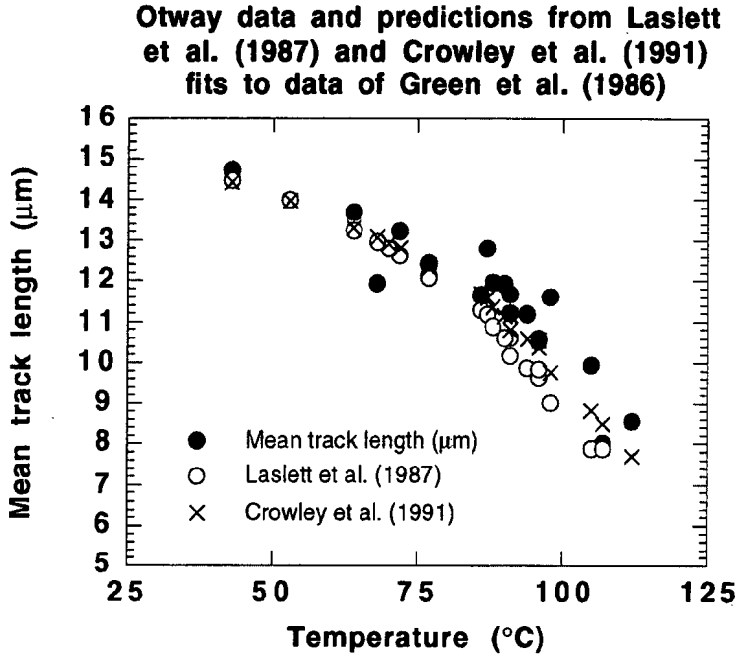

Figure C.6 Comparison of mean track length in samples from four Otway Basin reference wells with values predicted from Laslett et al. (1987) and the model fitted to the annealing data of Green et al. (1986) by Crowley et al. (1991). The predictions of the two models are not very different.

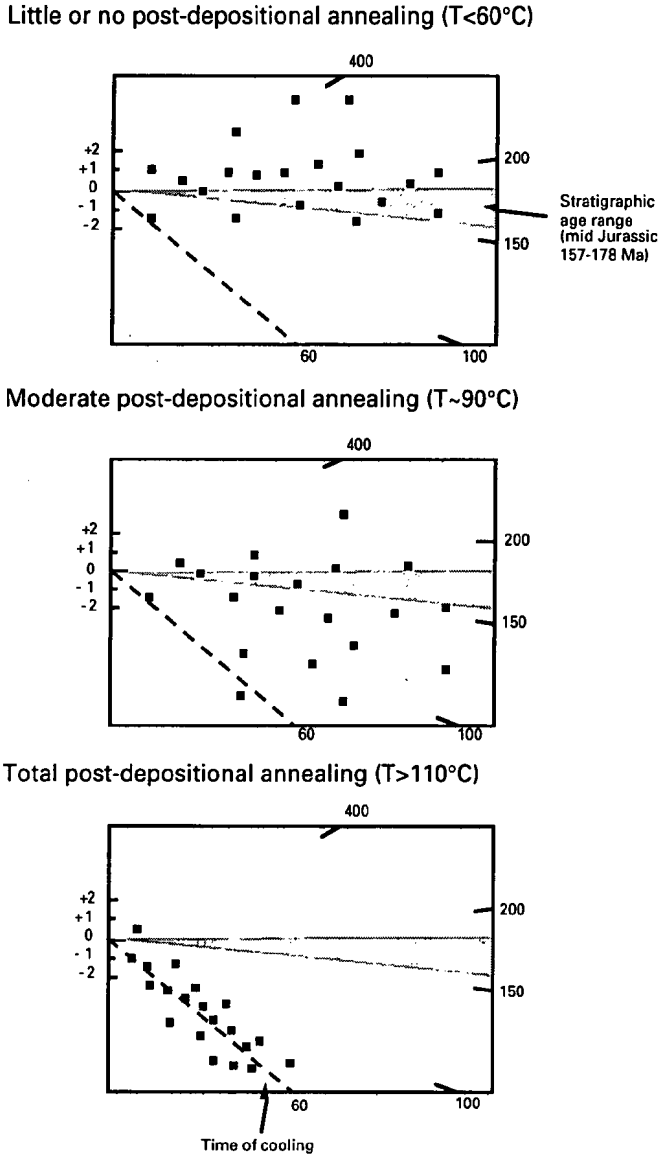

Figure C.7 Radial plots of single grain age data in three samples of mid-Jurassic sandstone that have been subjected to varying degrees of post-depositional annealing prior to cooling at ~60 Ma. The mid-point of the stratigraphic age range has been taken as the reference value (corresponding to the horizontal).

The upper diagram represents a sample which has remained at paleotemperatures less than ~60°C, and has therefore undergone little or no post-depositional annealing. All single grain ages are either compatible with the stratigraphic age (within $y = \pm 2$ in the radial plot) or older than the stratigraphic age ($y_i > 2$).

The centre diagram represents a sample which has undergone a moderate degree of post-depositional annealing, having reached a maximum paleotemperature of around ~90°C prior to cooling. While some of the individual grain ages are compatible with the stratigraphic age ($-2 < y_i < +2$) and some may be significantly greater than the stratigraphic age ($y_i > 2$), a number of grains give ages which are significantly less than the stratigraphic age ($y < 2$).

The lower diagram represents a sample in which all apatite grains were totally annealed, at paleotemperatures greater than ~110°C, prior to rapid cooling at ~60 Ma. All grains give fission track ages compatible with a fission track age of ~60 Ma (i.e., all data plot within ±2 of the radial line corresponding to an age of ~60 Ma), and most are significantly younger than the stratigraphic age.

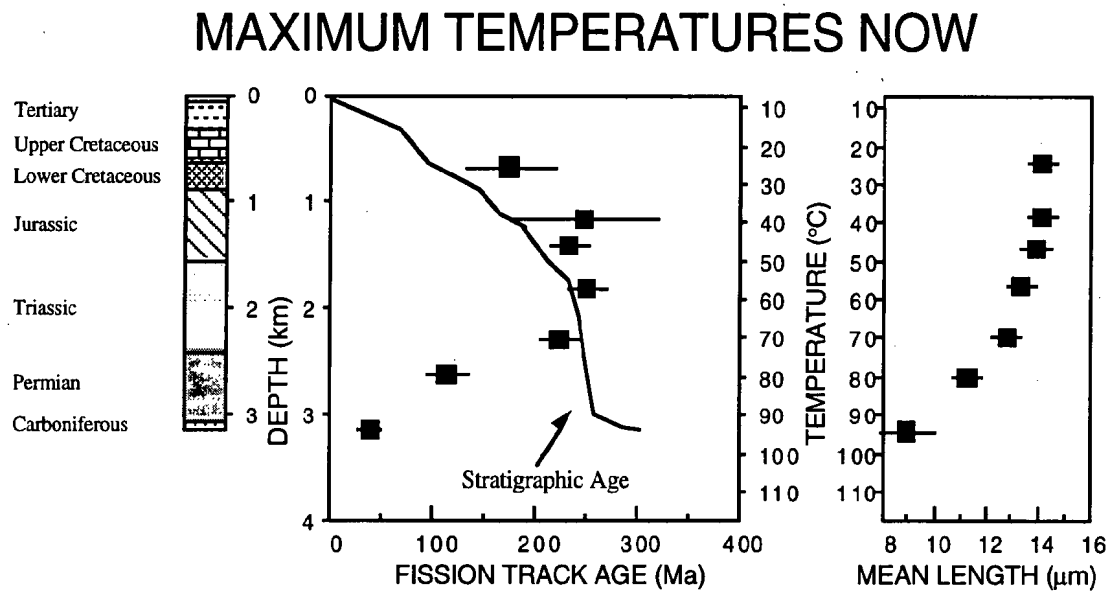

Figure C.8a Typical pattern of AFTA parameters in a well in which samples throughout the entire section are currently at their maximum temperatures since deposition. Both the fission track age and mean track length undergo progressive reduction to zero at temperatures of ~100 - 110°C, the actual value depending on the range of apatite compositions present.

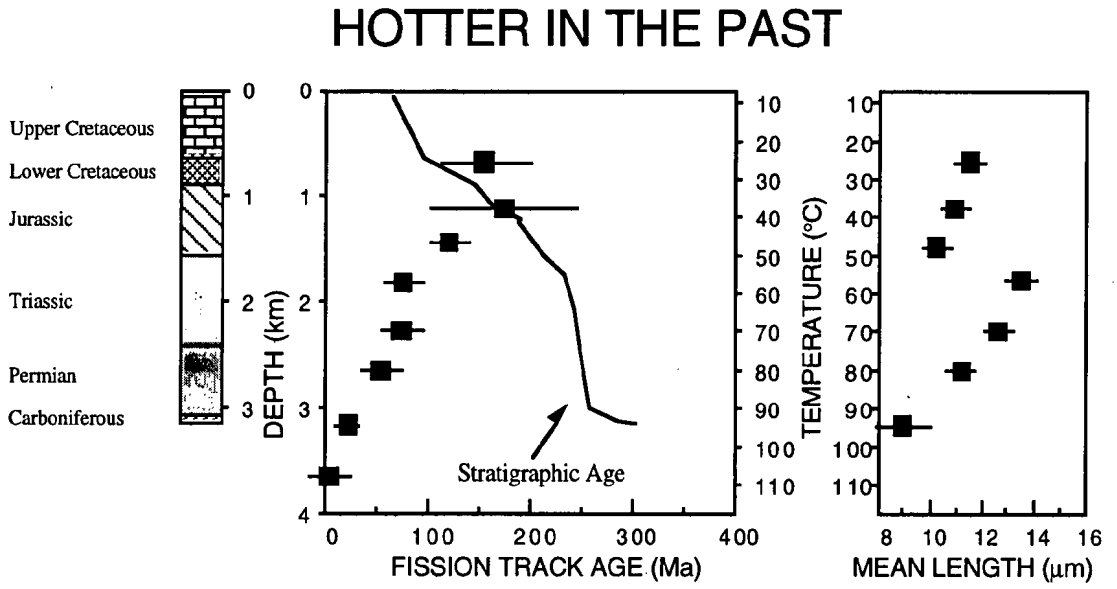

Figure C.8b Typical pattern of AFTA parameters in a well in which samples throughout the section were exposed to elevated paleotemperatures after deposition (prior to cooling in the Early Tertiary, in this case). Both the fission track age and mean track length show more reduction at temperatures of ~40 to 50°C than would be expected at such temperatures. At greater depths (higher temperatures), the constancy of fission track age and the increase in track length are both diagnostic of exposure to elevated paleotemperatures. See Appendix C for further discussion

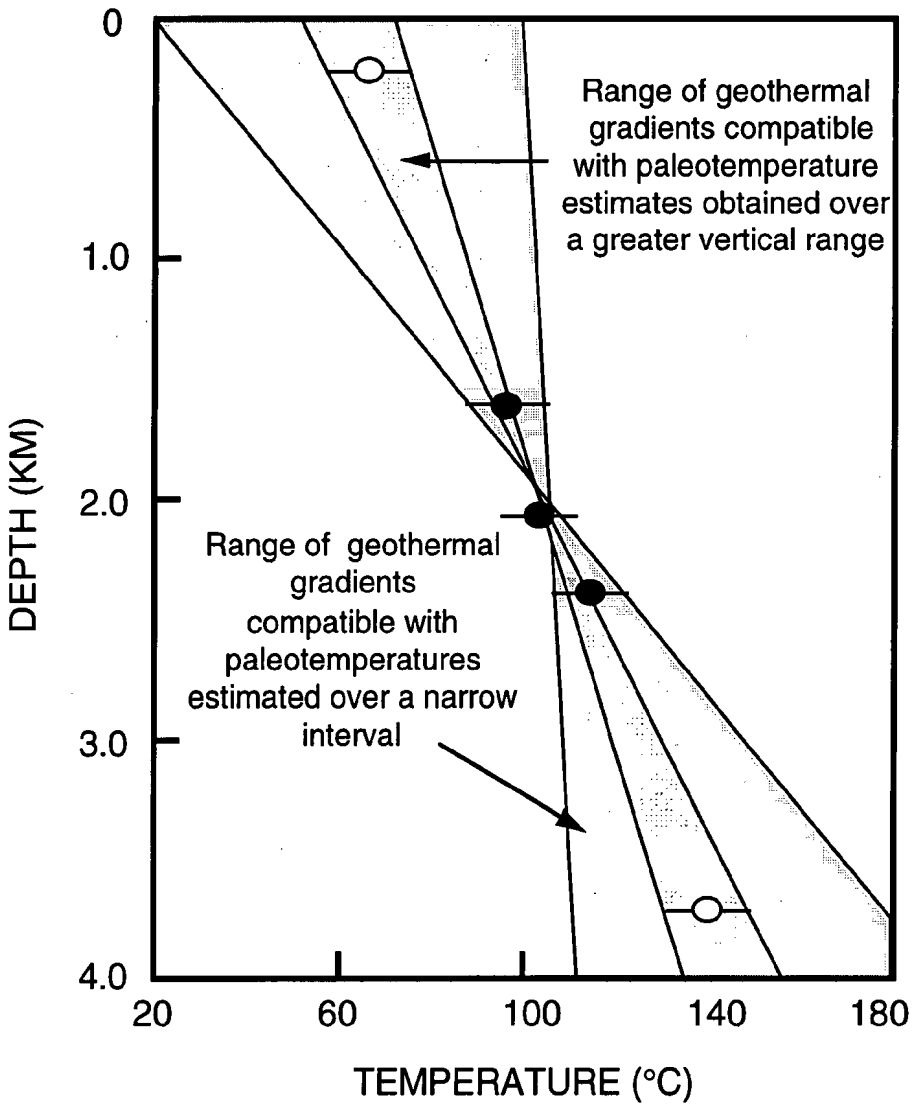

Figure C.9 It is important to obtain paleotemperature constraints over as great a range of depths as possible in order to provide a reliable estimate of paleogeothermal gradient. If paleotemperatures are only available over a narrow depth range, then the paleogeothermal gradient can only be very loosely constrained.

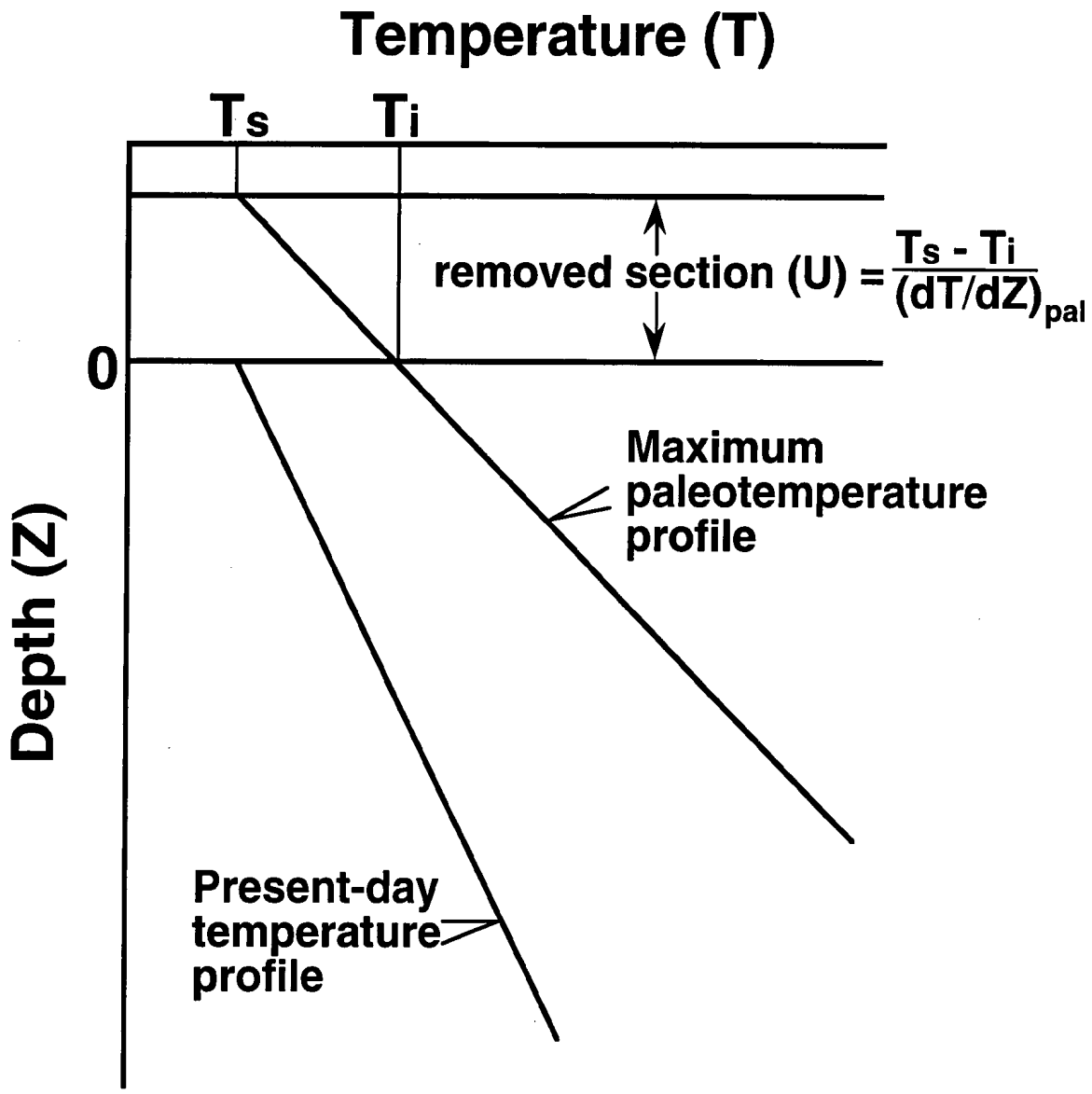

Figure C.10 If the paleogeothermal gradient can be constrained by AFTA and VR, as explained in the text, then for an assumed value of surface temperature, T_S, the amount of section removed can be estimated, as shown.

APPENDIX D

Integration of Vitrinite Reflectance Data with AFTA

Vitrinite reflectance is a time-temperature indicator governed by a kinetic response in a similar manner to the annealing of fission tracks in apatite as described in Appendix C. In this study, vitrinite reflectance data are interpreted on the basis of the distributed activation energy model describing the evolution of VR with temperature and time described by Burnham and Sweeney (1989), as implemented in the BasinMod™ software package of Platte River Associates. In a considerable number of wells from around the world, in which AFTA has been used to constrain the thermal history, we have found that the Burnham and Sweeney (1989) model gives good agreement between predicted and observed VR data, in a variety of settings.

As in the case of fission track annealing, it is clear from the chemical kinetic description embodied in equation 2 of Burham and Sweeney (1989) that temperature is more important than time in controlling the increase of vitrinite reflectance. If the Burham and Sweeney (1989) distributed activation energy model is expressed in the form of an Arrhenius plot (a plot of the logarithm of time versus inverse absolute temperature), then the slopes of lines defining contours of equal vitrinite reflectance in such a plot are very similar to those describing the kinetic description of annealing of fission tracks in Durango apatite developed by Laslett et al. (1987), which is used to interpret the AFTA data in this report. This feature of the two quite independent approaches to thermal history analysis means that for a particular sample, a given degree of fission track annealing in apatite of Durango composition will be associated with the same value of vitrinite reflectance regardless of the heating rate experienced by a sample. Thus paleotemperature estimates based on either AFTA or VR data sets should be equivalent, regardless of the duration of heating. As a guide, Table D.1 gives paleotemperature estimates for various values of VR for two different heating times.

One practical consequence of this relationship between AFTA and VR is, for example, that a VR value of 0.7% is associated with total annealing of all fission tracks in apatite of Durango composition, and that total annealing of all fission tracks in apatites of more Chlorine-rich composition is accomplished between VR values of 0.7 and ~0.9%.

Furthermore, because vitrinite reflectance continues to increase progressively with increasing temperature, VR data allow direct estimation of maximum paleotemperatures in

the range where fission tracks in apatite are totally annealed (generally above ~110°C) and where therefore AFTA only provides minimum estimates. Maximum paleotemperature estimates based on vitrinite reflectance data from a well in which most AFTA samples were totally annealed will allow constraints on the paleogeothermal gradient that would not be possible from AFTA alone. In such cases the AFTA data should allow tight constraints to be placed on the time of cooling and also the cooling history, since AFTA parameters will be dominated by the effects of tracks formed after cooling from maximum paleotemperatures. Even in situations where AFTA samples were not totally annealed, integration of AFTA and VR can allow paleotemperature control over a greater range of depth, e.g. by combining AFTA from sand-dominated units with VR from other parts of the section, thereby providing tighter constraint on the paleogeothermal gradient.

References

Burnham, A.K. and Sweeney, J.J. (1989) A chemical kinetic model of vitrinite reflectance maturation. *Geochim. et Cosmochim. Acta*, 53, 2649-2657.

Laslett, G.M., Green, P.F., Duddy, I.R. and Gleadow, A.J.W. (1987) Thermal annealing of fission tracks in apatite 2. A quantitative analysis. *Chem. Geol. (Isot. Geosci. Sect.)*, 65, 1-13.

Table D.1: Paleotemperature - vitrinite reflectance nomogram based on Equation 2 of Burnham and Sweeney (1989)

Paleotemperature (°C / °F)	Vitrinite Reflectance (%) 1 Ma Duration of heating	10 Ma Duration of heating
40 / *104*	0.29	0.32
50 / *122*	0.31	0.35
60 / *140*	0.35	0.40
70 / *158*	0.39	0.45
80 / *176*	0.43	0.52
90 / *194*	0.49	0.58
100 / *212*	0.55	0.64
110 / *230*	0.61	0.70
120 / *248*	0.66	0.78
130 / *266*	0.72	0.89
140 / *284*	0.81	1.04
150 / *302*	0.92	1.20
160 / *320*	1.07	1.35
170 / *338*	1.23	1.55
180 / *356*	1.42	1.80
190 / *374*	1.63	2.05
200 / *392*	1.86	2.33
210 / *410*	2.13	2.65
220 / *428*	2.40	2.94
230 / *446*	2.70	3.23

Table D.2: Vitrinite reflectance sample details and results open file data - wells from the Cooper-Eromanga Basin (Geotrack Report #668)

Sample number	Depth (m)	Stratigraphic subdivision	Stratigraphic age (Ma)	Present temperature*1 (°C)	RoMax (Range) (%)	N
Burley-2						
VR1	341	Winton	97-90	40	0.29 (0.23-0.32)	14
VR2	498	Winton	97-90	50	0.31 (0.27-0.36)	14
VR3	681	Winton	97-90	61	0.36 (0.28-0.47)	16
VR4	773	Winton	97-90	67	0.39 (0.31-0.52)	28
VR5	828	Winton	97-90	70	0.48 (0.41-0.62)	30
VR6	892	Macunda	100-97	74	0.46 (0.39-0.61)	30
VR7	974	Macunda	100-97	79	0.51 (0.41-0.61)	31
VR8	1038	Alluru Mdst	103-100	83	0.51 (0.41-0.61)	27
VR9	1102	Alluru Mdst	103-100	87	0.53 (0.45-0.64)	29
VR10	1253	Toolebuc	106-103	96	0.58 (0.51-0.64)	8
VR11	1376	Wallumbilla	117.5-106	104	0.57	1
VR12	1673	Cadna-owie	135-117.5	122	0.68 (0.53-0.88)	9
VR13	1760	Murta	141.5-135	127	0.69 (0.61-0.77)	14
VR14	1876	Westbourne	148-147	134	1.15 (1.07-1.24)	5
VR15	1949	Westbourne	148-147	138	1.15 (1.02-1.25)	6
VR16	2004	Westbourne	148-147	142	1.33 (1.20-1.44)	12
VR17	2083	Birkhead	157-150	147	1.52 (1.40-1.70)	30
VR18	2105	Birkhead	157-150	148	1.53 (1.37-1.72)	26
VR19	2256	Hutton	188-157	157	1.43 (1.21-1.71)	26
VR20	2269	Hutton	188-157	158	1.67 (1.34-2.50)	20
VR21	2673	Toolachee	255-249	183	3.22 (2.83-3.72)	27
VR22	2699	Toolachee	255-249	184	3.25 (2.93-3.68)	28
VR23	2737	Toolachee	255-249	187	3.25 (2.90-3.66)	27
VR24	2760	Toolachee	255-249	188	3.21 (2.79-3.59)	27
VR25	2800	Toolachee	255-249	190	3.32 (3.03-3.73)	27
VR26	2821	Toolachee	255-249	192	3.53 (3.12-3.90)	27

Table D.2: Continued

Sample number	Depth (m)	Stratigraphic subdivision	Stratigraphic age (Ma)	Present temperature*1 (°C)	RoMax (Range) (%)	N
Burley-2 Cont.						
VR27	2867	Daralingie	267-262	194	3.63 (3.16-4.10)	28
VR28	2918	Daralingie	267-262	198	3.59 (3.34-3.83)	28
VR29	3028	Epsilon	273-270	204	3.95 (3.70-4.25)	20
VR30	3092	Epsilon	273-270	208	4.05 (3.75-4.57)	26
VR31	3269	Patchawarra	295-275	219	4.75 (4.07-5.29)	30
VR32	3336	Patchawarra	295-275	223	5.12 (4.62-5.81)	28
VR33	3357	Patchawarra	295-275	224	5.72 (5.22-6.28)	27
VR34	3443	Patchawarra	295-275	230	6.27 (5.29-6.98)	27
VR35	3491	Patchawarra	295-275	233	7.00 (6.36-7.53)	26
VR36	3543	Patchawarra	295-275	236	6.58 (6.22-7.89)	28
VR37	3638	Merrimelia	298-296.5	241	6.81 (6.00-7.83)	28
VR38	3659	Merrimelia	298-296.5	243	6.70 (6.31-7.10)	28

Table D.2: Continued

Sample number	Depth (m)	Stratigraphic subdivision	Stratigraphic age (Ma)	Present temperature*1 (°C)	RoMax (Range) (%)	N
Toolachee-1						
VR39*2	663	Winton	97-90	53	0.32 (0.27-0.40)	
VR40*2	1300	Cadna-owie	135-118	86	0.50	
VR41*2	1666	Birkhead-Namur??	157-147	105	0.67 (0.52-0.74)	
VR42*2	1700	Poolawanna	237-186	106	0.70	
VR43	1849	Toolachee	255-249	114	0.77	
VR44*2	1870	Toolachee	255-249	115	0.92 (0.80-1.04)	
VR45*2	1900	Toolachee	255-249	117	0.90	
VR46*2	1913	Daralingie	267-262	117	0.95 (0.85-1.03)	
VR47*2	1983	Epsilon	273-270	121	1.02 (0.89-1.20)	
VR48*2	2035	Murteree	275-273	123	1.10 (0.92-1.20)	
VR49*2	2100	Patchawarra	295-275	127	1.10	
VR50	2107	Patchawarra	295-275	127	1.00	
VR51	2110	Patchawarra	295-275	127	1.06	
VR52*2	2123	Patchawarra	295-275	128	1.13 (1.00-1.26)	
VR53*2	2265	Dullingari	304-300	135	1.27 (1.02-1.36)	
VR54*2	2303	Dullingari	304-300	137	1.31 (1.23-1.41)	
VR55*2	2315	Dullingari	304-300	138	1.32 (1.26-1.44)	

Table D.2: Continued

Sample number	Depth (m)	Stratigraphic subdivision	Stratigraphic age (Ma)	Present temperature*1 (°C)	RoMax (Range) (%)	N
Beanbush-1						
VR56	457.2	Winton	97-90	38	0.24 (0.20-0.32)	15
VR57	914.4	Winton	97-90	55	0.40 (0.36-0.49)	20
VR58	1216	Macunda	100-97	67	0.41 (0.34-0.52)	20
VR59	1372	Alluru Mdst	103-100	73	0.42 (0.30-0.55)	20
VR60	1527	Wallumbilla	117.5-106	79	0.40 (0.34-0.46)	20
VR61	1829	Wallumbilla	117.5-106	90	0.54 (0.38-0.60)	5
VR62	1948	Cadna-owie	135-117.5	95	0.51 (0.44-0.57)	7
VR63	2020	Cadna-owie	135-117.5	98	0.65 (0.60-0.72)	4
VR64	2231	Westbourne	148-147	106	0.57 (0.46-0.67)	10
VR65	2307	Adori	150-148	109	0.64 (0.54-0.71)	12
VR66	2384	Adori	150-148	112	0.61 (0.50-0.73)	20
VR67	2442	Hutton	188-157	114	0.60 (0.30-0.58)	19
VR68	2606	Hutton	188-157	120	0.72 (0.64-0.79)	20
VR69	2665	Hutton	188-157	122	0.68 (0.59-0.76)	20
VR70	2758	Nappamerri	249-236.5	126	0.71 (0.57-0.75)	7
VR71	2987	Nappamerri	249-236.5	135	0.65 (0.50-0.74)	9
VR72	3204	Toolachee	255-249	143	1.08 (1.00-1.18)	16
VR73	3268	?Epsilon??	273-262	145	1.16 (1.04-1.24)	25
VR74	3301	Patchawarra	295-275	147	1.17 (1.11-1.30)	10
VR75	3311	Patchawarra	295-275	147	1.16 (1.07-1.36)	20
VR76	3365	Patchawarra	295-275	149	1.32 (1.19-1.44)	20
VR77	3423	Patchawarra	295-275	151	1.59 (1.43-1.78)	20
VR78	3514	Patchawarra	295-275	155	1.45 (1.36-1.47)	12
VR79	3549	Patchawarra	295-275	156	1.59 (1.53-1.67)	13
VR80	3606	Merrimelia	298-296.5	158	1.28 (1.18-1.40)	19
VR81	3608	Merrimelia	298-296.5	159	1.50 (1.40-1.58)	6

Table D.2: Continued

Sample number	Depth (m)	Stratigraphic subdivision	Stratigraphic age (Ma)	Present temperature*1 (°C)	RoMax (Range) (%)	N
Tirrawarra-1						
VR82	2012	Birkhead	157-150	103	0.60	
VR83	2575	Toolachee	255-249	127	0.98	
VR84	2756	Patchawarra	295-275	134	1.24	
Tirrawarra-16						
VR85	2939	Tirrawarra	?296.5-295	142	0.96	29
Tirrawarra-2						
VR86	2965	Merrimelia	?298-296.5	143	1.62	26
Tirrawarra-17						
VR87	2970	Merrimelia	?298-296.5	143	1.04	18

*1 See Appendix A for discussion of present temperature data.
*2 Additional results from Toolachee-9.